University of Nottingham
Biodiscovery Institute

Supported by wellcome trust

Design, Synthesis and Biological Evaluation of Novel Inhibitors of InhA from *Mycobacterium tuberculosis*

Tom Armstrong

Thesis submitted to the University of Nottingham for the degree of

Doctor of Philosophy

December 2020

Abstract

Multi-drug resistant tuberculosis (MDR-TB) represents a growing problem for global healthcare systems. The World Health Organisation reported 1.3 million deaths from tuberculosis in 2019, making the disease a leading cause of global mortality. In addition to this, there is an increasing spread of drug-resistant tuberculosis infections, with 390,000 new cases of MDR-TB recorded in 2019, these are infections resistant to Rifampicin and Isoniazid. Isoniazid is a key anti-TB drug and an inhibitor of InhA, a crucial enzyme in the cell wall biosynthesis pathway and identical in *Mycobacterium tuberculosis* and *Mycobacterium bovis*. Isoniazid is a prodrug which requires activation by the enzyme KatG, this active species then forms an adduct with the NAD^+ cofactor which then binds to InhA and prevents substrate recognition. Mutations in KatG prevent this activation and confer INH-resistance. 'Direct inhibitors' of InhA are attractive as they would circumvent the main clinically observed resistance mechanisms.

A total of 50 new compounds have been designed and synthesised as potential direct InhA inhibitors. These compounds were based on the triclosan (TCL) scaffold, which has been shown to act as a moderate, direct inhibitor of InhA. These compounds were evaluated using the GOLD molecular docking platform to interrogate their ability to bind to InhA.

The inhibitory activity of these compounds was evaluated *via* isolated enzyme assays using octenoyl CoA as the substrate. The most potent novel design strategy derivative inhibitor was di-TCL triazole compound **55** exhibiting an IC_{50} value 5.6 μM, compared to 10 μM for TCL. TCL derivatives bearing modifications to the phenolic

ring have previously been shown to be effective InhA inhibitors, the most potent derivative synthesised in this work was ether-linked **97**, exhibiting an IC_{50} of 340 nM. Whole-cell evaluation of these compounds was performed against *M. bovis*. This testing revealed a number of compounds which were potent against the whole-cell bacteria despite being only weakly active against InhA. The most potent of these compounds were triazole **64** and amines **88** and **94**, which all displayed MIC_{99} values of 13 μM against *M. bovis,* respectively. There is scope for the structure of these compounds to be optimised to further improve their potency.

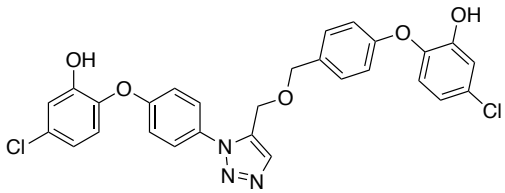

55

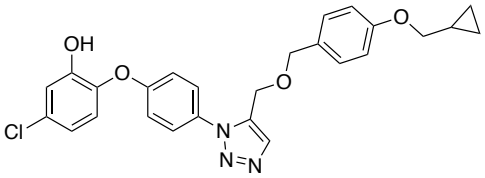

64

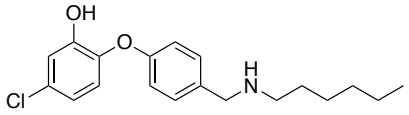

88

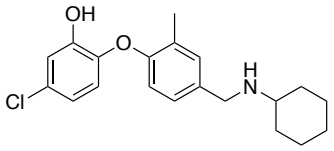

94

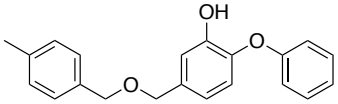

97

Acknowledgements

I would like to begin by thanking the Wellcome Trust for funding this research and its continued commitment to improving the lives of people around the world.

Thank you to my supervisor Professor Neil Thomas for his guidance and providing an interesting project. I wish to extend my gratitude to all of the analytical, technical and building staff in the Chemistry Department and the Biodiscovery Institute.

Thank you to numerous PhD students and post-docs who have taken the time to help with this project, specifically Malcolm, Parisa, Faadil, Dr David Harvey and Dr Francesco Zamberlan. Thank you to Malcolm, for his help with all aspects of protein production and running enzyme assays. I am grateful to Alice Lanne from the University of Birmingham for her work in the whole-cell evaluation aspects of this project. Thank you to the various members of the A20 and C29 offices who have made the last 4 years so enjoyable: Malcolm, James Reekes, Parisa, Faadil, Rowan, Jolanta, David, Alex Holland, Tom D'Arcy, James Krupa, Alex Wichlacz, Matt and Chris.

I am grateful for the continued support from my friends, in particular: Harry, Ben, Mike, Dylan and James.

Thank you to my uncle Mark for his time and advice in the lead-up to starting my PhD.

Finally, thank you to my mam, for everything.

This work is dedicated to my grandad, Tom Kearney.

Declaration

I herby declare that the content of this thesis has not been submitted, nor is currently being submitted for any other degree. I also declare that any work reported in this thesis is the result of my own investigation. Any work conducted by other investigators has been fully acknowledged and is clearly referenced in the text.

Tom Armstrong

Table of Contents

Abbreviations

ADMET	Adsorption, distribution, metabolism, excretion and toxicity
ADP	Adenosine diphosphate
AG	Arabinogalactan
AMR	Antimicrobial resistance
Arg	Arginine
BCN	Bicyclononyne
Boc	*tert*-Butoxycarbonyl
CADD	Computer-aided drug discovery
CCDC	Cambridge Crystallographic Data Centre
CoA	Coenzyme A
CYP	Hepatic cytochrome
CuAAC	Copper-catalysed azide alkyne cycloaddition
Da	Daltons
DBCO	Dibenzylcyclooctyne
DCC	Dicyclohexyl carbodiimde
DCE	1,2-Dichloroethane
DEL	DNA encoded library
DFT	Density functional theory
DIPEA	*N*,*N*-Diisopropylethylamine
DMAP	4-Dimethylaminopyridine
DMF	*N,N*-Dimethylformamide
DMSO	Dimethyl sulfoxide
DR-TB	Drug-resistant tuberculosis
DS-TB	Drug-susceptible tuberculosis
E. coli	*Escherichia coli*
ENR	Enoyl-acyl carrier reductase enzyme
ESI	Electrospray ionisation
Et_3N	Triethylamine
ETH	Ethambutol
FBDD	Fragment-based drug discovery
FPLC	Fast protein liquid chromatography

GA	Genetic algorithm
GalfT1	Galactofuranse Transferase Enzyme 1
GalfT2	Galactofuranse Transferase Enzyme 2
GalpM	Galactopyranose Mutase Enzyme
Gly	Glycine
GOLD	Genetic Optimisation for Ligand Docking
GSK	GlaxoSmithKline
H	Hours
H. influenza	*Haemophilus influenza*
HIV	Human immunodeficiency virus
HPLC	High-performance liquid chromatography
HPOA	Pyrazinoic acid
HR-MS	High resolution mass spectrometry
HSQC	Heteronuclear Single Quantum Coherence
HTS	High-throughput screening
IC_{50}	Half maximal inhibitory concentration
Ile	Isoleucine
Im	Imidazole
IMAC	Immobilised Metal-affinity Chromatography
INH	Isoniazid
InhA	Enoyl-acyl carrier reductase enzyme from Mycobacteria
^{i}Pr	Isopropyl
KatG	Multifunctional catalase, peroxidase enzyme from Mycobacteria
Leu	Leucine
Lys	Lysine
M. bovis	*Mycobacterium bovis*
Mtb	*Mycobacterium tuberculosis*
mAGP	Mycolic Acid, Galactofuranose and Peptidoglycan Complex
MDR-TB	Multi-drug resistant tuberculosis
Met	Methionine
MIC_{99}	Minimal inhibitory concentration
Min	Minutes

Mm	*Mycobacterium marinum*
MOM	Methoxy methyl ether
NAD^+	Nicotinamide adenine dinucleotide oxidised form
NADH	Nicotinamide adenine dinucleotide reduced form
NADP	Nicotinamide adenine dinucleotide phosphate
NAG	*N*-acetylglucosamine
NAM	*N*-acetylmuramic acid
NGMA	Non-growing, metabolically active bacteria
NMP	*N*-methyl-2-pyrrolidone
NMR	Nuclear magnetic resonance
P. falciparum	*Plasmodium falciparum*
PDB	Protein Data Bank
Phe	Phenylalanine
PZA	Pyrazinamide
r.t.	Room temperature
RCSB	Research Collaboratory for Structural Bioinformatics
RMP	Rifampicin
RMSD	Root mean squared deviation
ROS	Reactive oxygen species
RSA	Retrosynthetic Analysis
R_T	Retention time
RuAAC	Ruthenium-catalysed azide alkyne cycloaddition
S. Aureus	*Staphylococcus aureus*
SAR	Structure activity relationship
SDF	Spatial data file
SDR	Short chain reductase
SDS-PAGE	Sodium dodecyl sulfate polyacrylamide gel electrophoresis
S_NAr	Nucleophilic aromatic substitution
TB	Tuberculosis
TBAF	Tetra-*n*-butylammonium fluoride
TBDMS	*tert*-Butyldimethyl silyl
TBDPS	*tert*-Butyldiphenyl silyl

^{t}Bu	*tert*-butyl
TCL	Triclosan
TDR-TB	Totally drug-resistant tuberculosis
TFA	Trifluoroacetic acid
THF	Tetrahydrofuran
TLC	Thin layer chromatography
Tyr	Tyrosine
WHO	World Health Organisation
WT	Wild type
XDR-TB	Extensively drug-resistant tuberculosis

1. Introduction

1.1 Historical Perspective of Tuberculosis - The White Plague

Tuberculosis (TB) is a disease which has been prevalent throughout the course of human history, evidence of TB infections has been found in the remains of ancient Egyptian mummies dating back 5000 years.[1, 2] *Mycobacterium tuberculosis (Mtb)* was first identified as the causative agent of TB by Robert Koch in 1882.[3] Initially, skepticism surrounded Koch's assertion that TB was a bacterial infection, with the consensus at the time being that it was a hereditary condition. Koch's work on TB resulted in two major breakthroughs, firstly the successful staining of *Mtb* samples using methylene blue and heating to 40 °C.[4] This staining provided evidence that *Mtb* were rod-shaped organisms bearing a strong resemblance to the bacilli found in leprosy (*Mycobacterium leprae*). The second breakthrough was even more profound. Koch was able to isolate the causative bacterium and infect 4 guinea pigs before demonstrating the presence of the bacilli in culture samples taken from the animals. The transformative effect of this work earned Koch the Nobel Prize for Medicine in 1905 for his contributions to the "investigation and discoveries in relation to Tuberculosis". This work formed the basis of Koch's famous 'Postulates' which define the criteria that draw a direct link between a disease and its causative agent. Since this initial work, the issue of TB has remained a scourge and now accounts for roughly 1.3 million deaths annually.[5] This escalation has gone hand-in-hand with increasing prevalence of the Human Immunodeficiency Virus (HIV), with immunocompromised individuals being at a heightened risk of TB infection and activation of latent TB infections. This issue is further exacerbated by the emergence and spread of drug-resistant strains of the bacteria which complicate and diminish

treatment efficacy for infected individuals. This difficult landscape creates a major need for new anti-TB drugs to address the significant problems at hand.

1.2 Microbiological Characteristics

The *Mycobacterium tuberculosis* complex (*Mtb*C) consists of 10 distinct members which can causes TB in humans and other organisms: *Mycobacterium tuberculosis*, *M. africanum*, *M. canettii*, *M. bovis*, *M. microti*, *M. orygis*, *M. caprae*, *M. pinnipedii*, *M. suricattae* and *M. Mungi*.[6, 7] Of these 10 members, *M. tuberculosis*, is the primary driver of infection in humans.[8]

Mtb is characterised as an 'obligate pathogen' meaning it is found only within infected hosts and not as a free-living bacterium.[9] With a doubling time of 12-24 hours, *Mtb* exists as a slow growing, intracellular aerobic bacillus. TB is primarily a respiratory disease and is spread through airborne transmission. Transmission can be achieved by the inhalation of only a few droplets, no more 5 μm in diameter, containing as few as 1-3 bacilli.[10] The relative ease of transmission is one of the main reasons behind the high infection rates, with 10 million new infections recorded in 2019.[5] Infections which are localised to the lungs are known as pulmonary TB.[11] While airborne transmission is the most common route, it is also possible to contract extra-pulmonary TB, which is localised at other areas of the body aside from the lungs.[12] An example of extra-pulmonary infection sites would be the walls of the intestine, such infections could arise from the consumption of milk from cattle infected with TB.[13] These infections originate from *Mycobacterium bovis (M. bovis)*, the causative agent of TB in cattle.

1.3 Route to Infection: Active vs Latent TB

Pulmonary TB infections occur when airborne tubercle bacilli enter the alveoli of a host's lungs. At this point the bacteria is phagocytised by alveolar macrophages. In ~ 90% of cases this initial immune response is sufficient to isolate the bacterium and render the infection 'latent' meaning the carrier remains asymptomatic. In the event that the bacteria are able to circumvent this first line of defence, the bacteria begin to replicate within the host macrophages and also diffuse into the surrounding epithelial and endothelial tissue. Given the low replication rate, it takes several weeks for the bacterial burden to reach a high level, during which time the host remains asymptomatic. Reaching a high bacterial burden then triggers the host's adaptive immune response resulting in the production of reactive oxygen species (ROS). These species have a necrotic effect and result in the formation of granulomas. These granulomas provide an inhospitable, anoxic environment which renders cell division unfavourable, thus encasing the bacteria. However, in isolating the bacteria, these granulomas are associated with clinical diseases and in some cases can lead to serious complications.

As previously mentioned, even if the initial immunological response is able to prevent an active TB infection, the latent form of the infection carries with it the lifelong threat of reactivation.[14] This threat is significantly increased in individuals who suffer from impaired immune systems, these groups include the elderly, organ transplant recipients, cancer patients and HIV sufferers. In terms of the mechanism of 'activation' of latent TB, recent work has helped further the understanding of the process.

One theory suggests that during the latent phase, a small population of actively dividing bacteria exists. These bacteria are known as “scouts”. Typically, these scouts will be killed by the immune response and trigger the induction of T cells directed at *Mtb* antigens. These scouts are constantly replenished and killed, effectively acting as a sacrificial population for the dominant latent population. However, if, for whatever reason, the host’s immune system is unable to mount an effective response, the scout population is able to replicate uncontrollably and thus the disease enters its active form.[8]

Recent work by Manina *et al.* has also provided evidence that a, so-called, “zombie tuberculosis” is present in latent TB infections.[15] This refers to a population of bacteria which, whist being metabolically active, are not actively replicating. These populations are described as being “Non-growing but metabolically active” (NGMA). Using immunodeficient, genetically modified mice the researchers were able draw a direct link between a host’s immune response and these presence of NGMA bacteria, with the immune-deficient mice not presenting these zombie cells. This suggests that *Mtb* enters this NGMA phase as a defence mechanism when confronted by the host’s immune system.[15]

1.4 Global TB Infections

TB has proven to be a major cause of human mortality since its identification. Prior to the emergence of Covid-19, TB was the leading infectious cause of death and is responsible for more deaths worldwide than HIV. One of the main issues associated with TB is the ease with which it spreads. This ease of transmission brings with it a high infection rate, which resulted in an estimated 10 million new cases of TB in

2019.[5] This high infection rate is further complicated by the fact that TB can exists in multiple forms, both active and 'latent'. It is estimated that ~2 billion people are carriers of latent TB, which while presenting no direct health risk does carry the lifelong threat of 'activation' of the bacteria into an active form.[16] Effective surveillance of new infections and the spread of TB is significantly hampered by the nature of the countries TB is most prevalent in. TB infections are most common in less-economically developed nations such as India, Pakistan and Nigeria. These countries lack the robust healthcare systems and financial resources to properly surveil and report new infections and so it is possible that the infection rate is actually higher than thought. A map of the estimated new cases of TB in 2019 is shown in **Figure 1**.

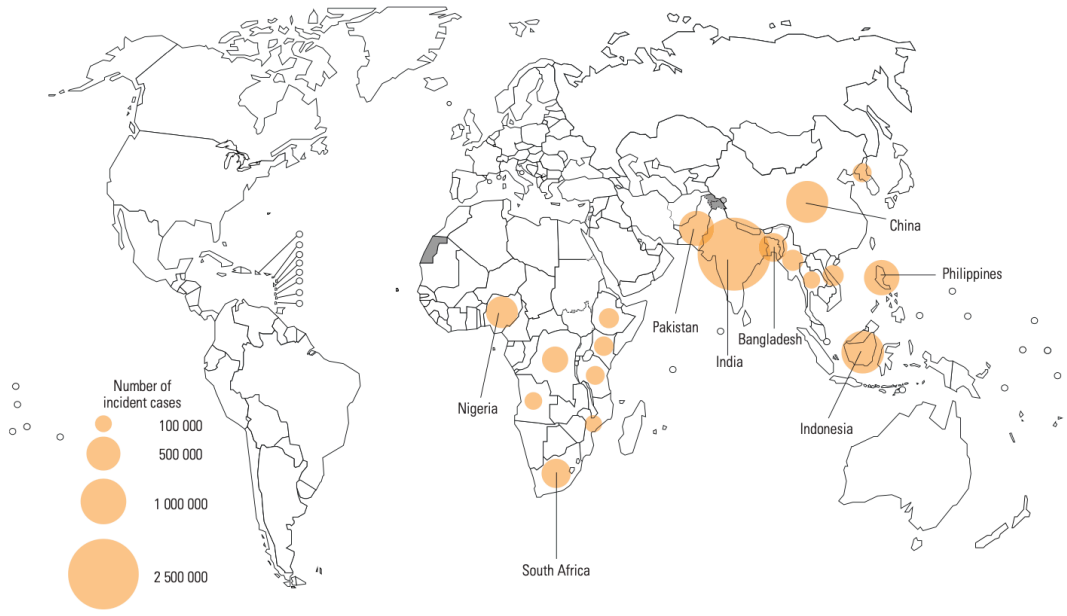

Figure 1. *Global map showing estimated new cases of TB in 2019, per country. Taken from the WHO 2020 TB Report.*[5]

As can be seen from the data in **Figure 1**, the number of estimated cases of TB is disproportionately skewed towards poorer, developing nations thus creating a deadly synergy between deprivation and disease.

1.5 Bacillus Calmette-Guérin (BCG) Vaccination

As with any disease, prevention will always be a more effective means of disease control than cure. Efforts to prevent TB infections centre around the use of the Bacillus Calmette-Guérin (BCG) vaccine. This vaccine is named after its discoverers, Albert Calmette and Camille Guérin. BCG is an attenuated strain of *M. bovis* that was originally isolated from a cow in 1903.[17] The strain was then cultured for 13 years, over which time it lost its virulence. BCG was first used in humans in 1921. Between 1953-2005 the vaccine was used for universal immunisation of school age children (13 years old) throughout the UK.

The efficacy of the vaccine remains a contentious issue. BCG has demonstrated protective effects for certain populations, however, these results are not consistently mirrored across all age groups or strains of TB. Indeed, various randomised controlled trials and observational studies have shown protective effects ranging from negative to close to 100%.[18] The reasons for the disparities in these results are unclear, and many hypotheses exist to attempt to explain the fluctuation. In 1999, the WHO provided a summary of the potential explanations for the variable efficacy, the main reasons are stated below:

1. Genetic variations between strains of BCG used in different trials
2. Genetic variations in trial populations
3. Prior exposure to non-tubercular mycobacteria
4. Interference from parasitic infections altering the immune response to the vaccine

While the factors controlling the vaccine's efficacy remain uncertain, the WHO still recommends that the vaccine be administered to children in areas with a high TB burden.[19]

1.6 Current Drug Treatments

The current treatment for drug-susceptible Tuberculosis (DS-TB) infections relies on a combination of 4 drugs (**Figure 2**): rifampicin (RIF, **1**) isoniazid (INH, **2**), pyrazinamide (PZA, **3**), ethambutol (ETH, **4**).[20]

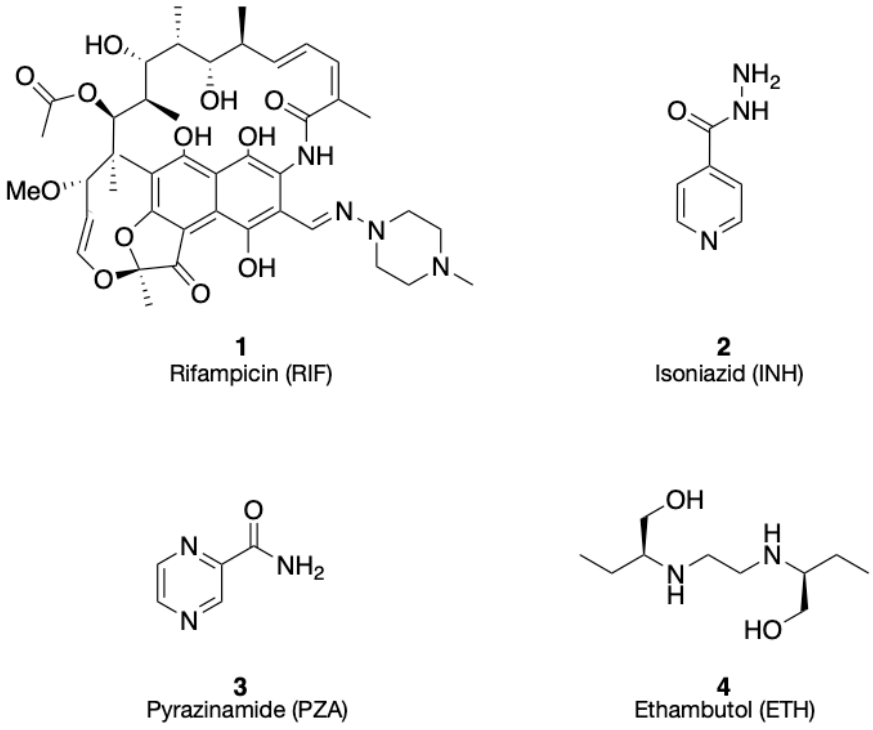

Figure 2. *The structures of the 4 drugs which form the front-line treatment regimen for DS-TB.*

Treatment of DS-TB uses a two-phase regimen. Initially a patient will take a course of all 4 antibiotics for a two month period, after which time there is a continuation phase

where only INH and RIF are used. This continuation phase usually lasts a further 4 months, but can take up to a year, depending on the extent of the infection.[21, 22]

The aim of antibiotic drug treatments is to totally eradicate the viable bacterial population in a host. In order to achieve this goal in TB infections, it is necessary to use this 4 drug regimen, some of which are bactericidal and some which are bacteriostatic. As has been previously mentioned, *Mtb* can exist as an actively replicating or as an inactive 'latent' infection. This complicates the treatment as different drugs are required to address different bacterial states.

Rifampicin (RIF) is a complex, cyclic natural product and is the only drug which shows efficacy against active and latent mycobacterial states. First introduced to the clinic in 1972, RIF mediates its biological activity through binding to the β-subunit of RNA polymerase. This binding prevents transcription, which blocks translation to protein sequences thus depriving the bacteria of its internal machinery.[23] The importance of RIF to the anti-TB regimen represents a major issue to the significant number of people co-infected with TB and HIV. This is due to the fact RIF results in an up-regulation of the hepatic cytochrome (CYP) P450 oxidase system.[24] The increased level of CYP450 results in the metabolism of many HIV protease inhibitors, so much so that even in the presence of CYP450 inhibitors, the anti-HIV drug concentration falls to a sub-therapeutic level.[25]

Isoniazid (INH) displays a strong potency against active *Mtb* populations, however, it shows significantly reduced effects against latent bacteria. INH is responsible for inhibition of the fatty acid biosynthetic (FAS) pathway, which in turn disrupts the

formation of *Mtb*'s vital, protective cell wall. This process will be discussed in greater detail later. INH represented a real breakthrough in the way TB was treated. Its discovery has been described as "one of the most extraordinary pharmaceutical coincidences of all time".[26] In 1951 INH was concurrently identified by 3 different groups working at Bayer, Squibb and Hoffman-La Roche.[27] In such situations, a lengthy patent battle for ownership of the compound would have been inevitable were it not for the fact that INH had actually been synthesised and reported almost 40 years previous, by two Czech students.[27]

INH's initial results were so promising that the April 1952 edition of *American Review of Tuberculosis* (now *American Journal of Respiratory and Critical Care Medicine*) was almost entirely dedicated to studies focusing on INH.[28-32] Initial trials suggested that INH alone could be used to combat TB infections. However, of the patients featured in these trials, almost 75% relapsed and many displayed newly INH-resistant infections, this reinforced the belief that a multi-drug treatment regimen was required to eradicate the infection from a host.[26]

Pyrazinamide (PZA) belongs to the nicotinamide class of compounds and its efficacy as an anti-TB drug was discovered somewhat fortuitously. First synthesised in 1936, it was not until 1952 that its anti-TB properties were first recognised.[33] Following the discovery that nicotinamide compounds possessed moderate activity against mycobacteria in mouse models, a range of derivatives were synthesised and PZA was found to be the most active.[34] Initial use of PZA was restricted to second-line treatment status due to hepatic toxicity caused by the high dosage it required, however subsequent studies showed impressive activity at lower doses, when

combined with INH.[35] Further work highlighted the synergistic nature of RIF and PZA when the pair were used in tandem, this allowed the treatment time to be shortened significantly.[36] Following these discoveries, PZA has been a crucial drug in the anti-TB regimen, acting as a first-line treatment since the 1970s. Despite its importance to the anti-TB regimen, PZA's mechanism of action remained enigmatic until recently.[37] This is due to the fact that PZA is primarily effective against non-replicating forms of TB.[38]

An initial proposal was that upon entry into the cell, PZA is converted to pyrazinoic acid (HPOA), this compound is a relatively strong acid and so dissociates into its charged constituents (POA^- and H^+). It was suggested POA^- then leaves the intercellular environment, predominantly by passive diffusion. Upon leaving the cell, if the surrounding environment was sufficiently acidic, the negatively charged species would be protonated to the neutral HPOA, which could then re-enter the *Mtb* cell, again *via* passive diffusion. It was thought that the accumulation of HPOA inside the bacteria would result in acidification of the cellular environment and ultimately the disruption of vital enzymes. This process is depicted in **Scheme 1**.

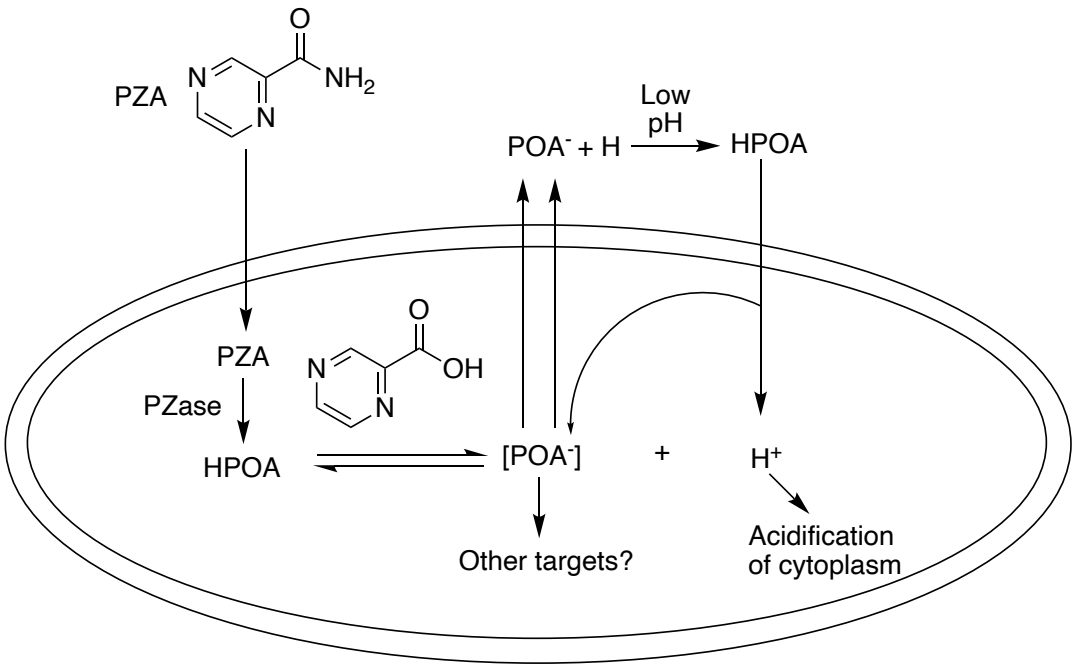

Scheme 1. *Initial postulated mechanism of action for PZA. PZA enters the cell via passive diffusion before conversion to HPOA by PZase. The acidic HPOA dissociates to POA- and H+ before POA- is transported out of the cell by passive diffusion. In the presence of an acidic environment, POA- is reprotonated to form HPOA, which can reenter the cell and cause acidification of the cellular environment. Adapted from Zhang et al.*[34]

However, recent work by Peterson *et al*. has since disproven this theory. Their work showed that PZA was able to elicit biological activity against *Mtb* in a range of extracellular environments, including both those that are neutral and basic.[39] Clearly this shows that the theory that HPOA is the active species, as a result of an acidic extracellular environment, is not accurate. Additionally, Peterson's work demonstrated that acidification of the cell membrane was not the origin of PZA's anti-TB effects. Through the use of an acid-inducible fluorescent tag, Peterson showed no significant increase in fluorescence in bacteria treated with PZA, disproving the idea that cytoplasmic acidification was responsible for PZA's activity. Shi *et al.* were the first to suggest that the actual target of PZA was the aspartate decarboxylase (PanD)

system.[40] This enzyme plays a key role in the synthesis of pantothenate, which is required for Coenzyme A production. Inhibiting this pathway disrupts a host of bacteria processes, including cell wall biosynthesis. PanD was later validated as a target of PZA by Gopal *et al*. in 2017.[41]

The final frontline therapeutic agent is Ethambutol (ETH). First described in 1961, ETH is a bacteriostatic compound which has been used in the clinic since 1966.[20] ETH is thought to inhibit a range of different processes within the cell and the specific site(s) of action remains unknown. ETH is believed to primarily target cell wall biosynthesis and production of the arabinogalactan (AG) component of the *Mtb* cell wall.[42] Work by Deng *et al*., demonstrated that ETH disrupts the entire AG, which in turn also makes the cell more permeable to entry from other drug compounds, something which is a major stumbling block in anti-TB treatment.[43] Electron microscopy studies support the notion that ETH targets the cell wall composition as Kilburn and Greenberg demonstrated that treatment with ETH causes the usually rod-like *Mycobacteria* to adopt a more spherical shape, increased de-clumping has also been seen to accompany these morphological changes.[44]

For individuals who do not respond to the first round of treatments, there exists a number of second and third-line treatment options. However, these are typically antibiotics which are not designed for anti-TB treatment and can carry with them significant side effects. In 2016, the WHO sought to clarify the best-practice for treatment of drug-resistant TB (DR-TB) infections and reclassified the fallback options (**Table 1**).[45]

Table 1. *WHO classification for drugs used to treat TB infections which do not respond to the front line drugs.*

Group	Example	Biological Target
A	Levofloxacin	DNA gyrase
	Moxifloxacin	DNA gyrase
	Gatifloxacin	DNA gyrase
B (injectable)	Kanamycin	Protein synthesis
	Capreomycin	Protein synthesis
	Amikacin	Protein synthesis
C	Ethionamide	Mycolic acid biosynthesis
	Cycloserine	Cell wall biosynthesis
	Linezolid	Protein synthesis
	Clofazimine	Electron transfer chain
D	Bedaquiline	Electron transfer chain
	Delamanid	Mycolic acid biosynthesis
	p-Aminosalicylic acid	Folic acid synthesis
	Meropenem	Cell wall biosynthesis
	Iminipenem-calistatin	Cell wall biosynthesis
	Amoxicillin–clavulanate	Cell wall biosynthesis
	Thioacetazone	Mycolic acid biosynthesis

One thing that is evident when looking at the second and third-line compounds is that many are broad spectrum antibiotics and are not designed for use against *Mtb*, this often leads to sub-optimal therapeutic conditions and protracted treatment times.

1.7 Emergence of Drug-Resistant TB

As has been witnessed across the spectrum of bacterial infections, there has been a steady increase in the prevalence of DR-TB infections. These strains can be classified as multi-drug resistant (MDR-TB) extensively-drug resistant (XDR-TB) and totally-drug resistant (TDR-TB).

MDR-TB infections are classified as infections which display resistance to INH and RIF, the two strongest drugs in the anti-TB regimen.[46] In 2019, the WHO reported an estimated 390,000 new cases of MDR-TB.[5] Part of the difficultly associated with effective surveillance of these infections is that they predominantly occur in less economically developed nations, where access to good medical and testing facilities is severely limited. Individuals diagnosed with such infections are treated with a fluoroquinolone antibiotic (**Table 1,** Group A), however, recent data suggests only around 54% of these treatments are successful, with 16% of patients dying.[47] Typically MDR-TB infections can arise through incomplete treatment of a previously drug-susceptible infection. The WHO has attempted to combat the issue of non-compliance by introducing Directly Observed Therapy (DOTS) whereby drug dosing is supervised to ensure adherence. This is particularly important considering a treatment course for DS-TB can typically last up to 12 months, increasing to at least 18 months and requiring up to 8 different drugs in the case of DR-TB infections.[48, 49]

XDR-TB infections are defined as being resistant to one fluoroquinolones (**Table 1,** Group A) and at least one of the injectable aminoglycosides (**Table 1,** Group B), in addition to RIF and INH. Due to XDR-TB's resistance to the most effective anti-TB drugs, the outlook for XDR patients is incredibly bleak, with treatment success falling

to 34%.[49] Treatment is composed mainly of drugs not originally intended for use against TB, so their efficacy is reduced and many produce negative side effects. Of the 390,000 new MDR-TB cases reported in 2019, over 12,000 were defined as XDR-TB, with such infections being reported in over 130 countries.[5]

TDR-TB remains much less clearly defined and is still lacking an official WHO recognition. TDR-TB, in theory, represents infections that are totally non-responsive to any drugs. Such infections have reportedly been identified in India, Italy and Iran.[50-52] In order to archive specimens of TDR-TB, the United Nations set up the TDR Tuberculosis Specimen Bank in 2010, which is designed to help support the development of diagnostic tools.[53] Part of the reason that TDR-TB is currently so poorly documented and ill-defined is because most countries do not test samples against a sufficiently broad range of drugs. Clearly any infections which are 'totally resistant' to current treatments represent an effective death sentence for the sufferer, the emergence of such infections only serves to heighten the need for new anti-TB drugs.

1.8 The Composition of the *Mtb* Cell Wall

One of the main reasons that TB infections are so difficult to treat is *Mtb's* uniquely dense and hydrophobic cell wall.[54] The composition of the cell wall can be broken down into three main components (**Figure 3**).

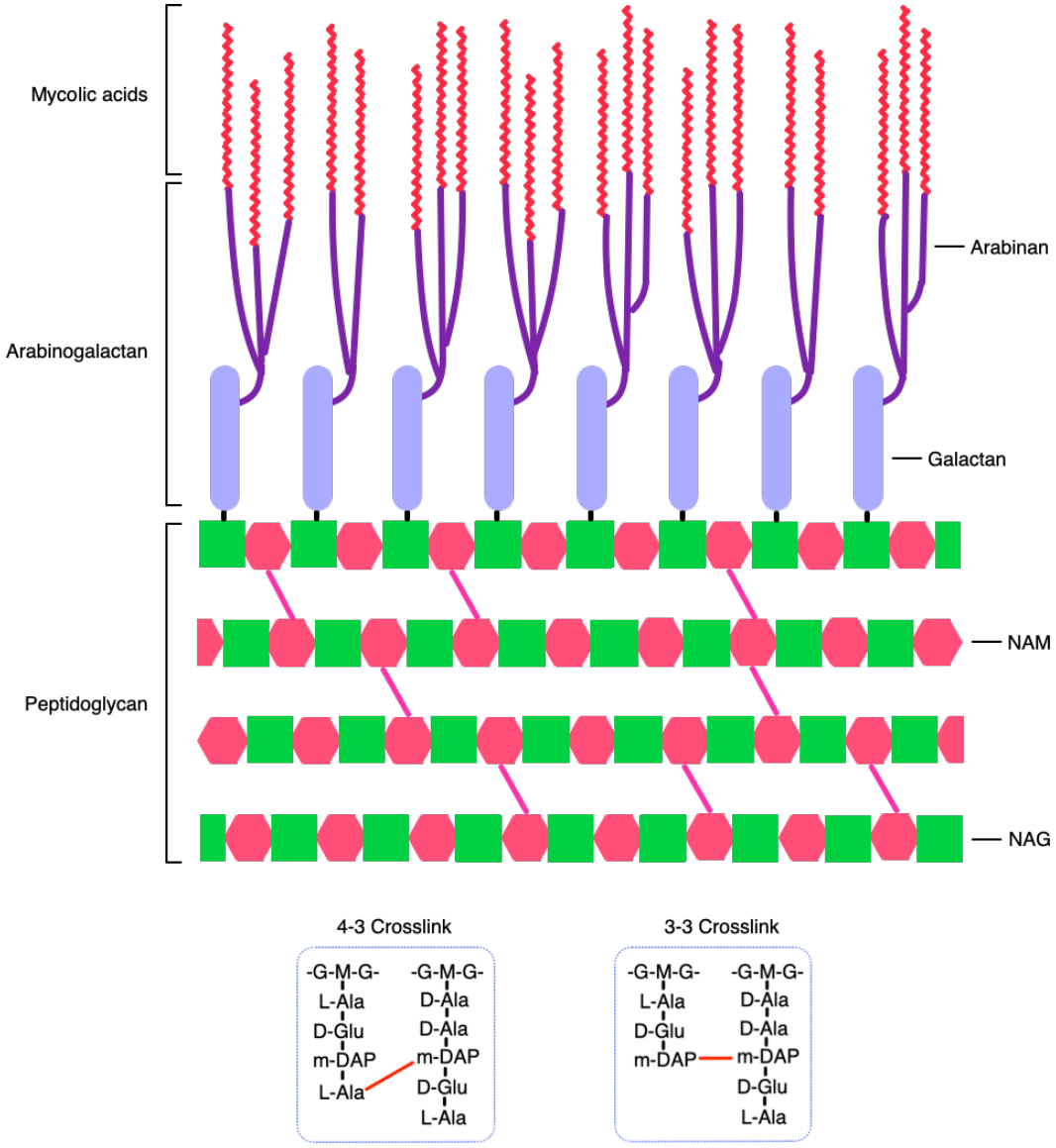

Figure 3. *Structure of the Mycobacterium tuberculosis cell wall, showing the three main components: peptidoglycan, arabinogalactan and mycolic acid layers. Also shown are the 4-3 and 3-3 crosslinkages in the peptidoglycan layer. G is N-acetyl glucosamine, M is N-acetyl-muramic, m-DAP is meso-diaminopimelic acid. Adapted from Kieser and Rubin.*[54]

The peptidoglycan layer directly surrounds the plasma membrane and is made up long repeating *N*-acetyl glucosamine–*N*-acetyl-muramic acid (NAG–NAM) polymer units, connected by peptide linkages. This layer is highly cross-linked, which provides significant structural integrity to the cell wall.[55, 56] The cross-linkages in the

peptidoglycan layer are predominantly 3-3 crosslinks, the formation of these linkages is catalysed by L,D-transpeptidase enzymes. This explains why standard penicillins are ineffective against *Mtb*, as they target specifically D-transpeptidases.[57, 58] Carbapenems and cephalosporins show greater activity against the L,D-transpeptidases but have to be administered with a β-lactamase inhibitor (**Table 1**, Group D) to combat the mycobacterial BlaC enzyme.[58]

On top of the peptidoglycan layer is the arabinogalactan (AG) layer. This layer consists of alternating β-1,5 and β-1,6 D-galactan units, which are synthesised by galactopyranose mutase (Gal*p*M) and galactofuranosyl transferases (Gal*f*T1 and Gal*f*T2). This layer composed of ~30 repeating galactofuranose moieties. The AG then forms the anchor point for the mycolic acid layer.[59]

The mycolic acid layer is ligated to the AG and accounts for the bulk of the cell walls' dry weight. This waxy barrier consists of long chain (~$C_{50\text{-}90}$) α-branched, β-hydroxylated fatty acids. This layer forms an incredibly dense, hydrophobic envelope surrounding the cell, which significantly reduces its permeability to small molecules. The unique glycolipid cell wall provides substantial protection from the cellular environment, including ROS and 'masks' it from the immune system.[59, 60]

Collectively, the Mycolic Acid, Arabinogalactan and Peptidoglycan components of the *Mtb* cell wall are referred to as mAGP. Due to its intrinsic importance to the organism and the fact that the arabinogalactan and mycolic acid layers are unique to *Mycobacteria*, the cell wall biosynthetic pathways represent attractive anti-TB drug targets.[61]

1.9. Development of New Anti-TB Drugs

The anti-TB drug landscape has seen relatively little change over the last five decades. Indeed, until very recently the 'newest' anti-TB drug was introduced in the 1970s. At the time of writing, there have been 3 'recently' approved anti-TB drugs which have helped ease the burden of DR-TB (**Figure 4**).

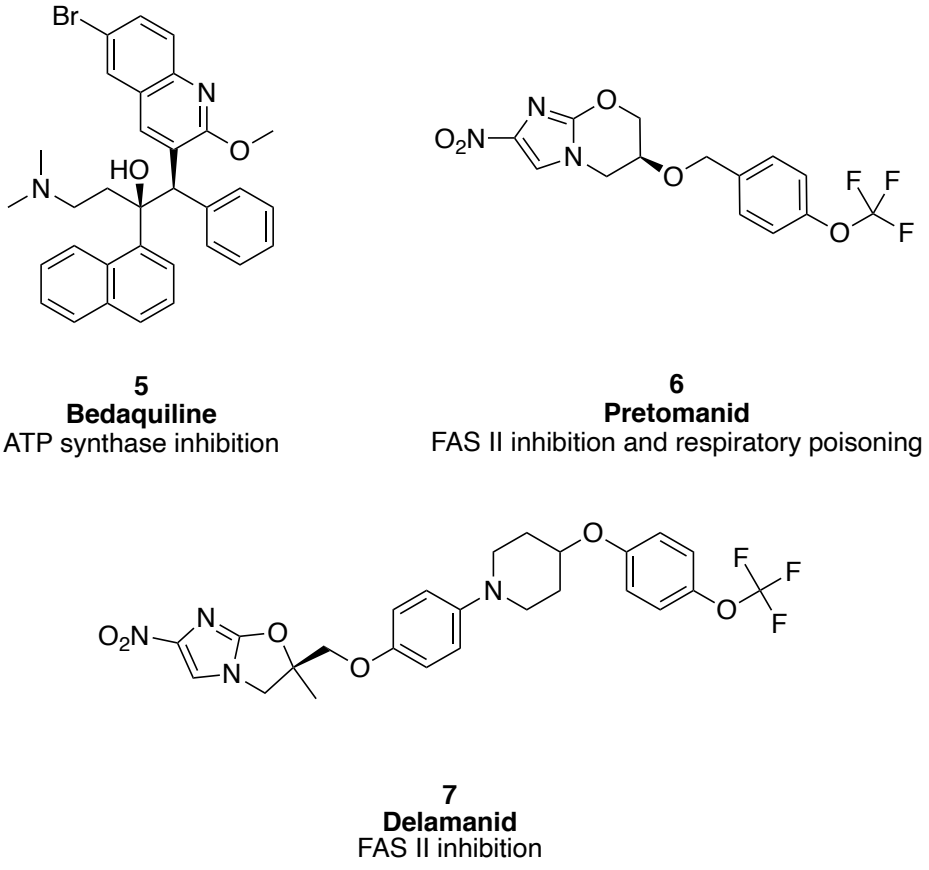

5
Bedaquiline
ATP synthase inhibition

6
Pretomanid
FAS II inhibition and respiratory poisoning

7
Delamanid
FAS II inhibition

Figure 4. *The structures of 3 recently approved drugs for treatment of DR-TB: Bedaquiline, Pretomanid and Delamanid.*

Bedaquiline (**5**) was first approved for use in the USA by the Food and Drug Administration (FDA) in 2012.[62] Bedaquiline acts as an ATP synthase inhibitor, blocking the production of ATP. Given the fundamental importance of ATP to living organisms, this inhibition effectively starves the bacteria of the energy it requires to

carry out biological processes, which ultimately leads to cell death.[63] Due to the ubiquitous nature of ATP-dependent processes, bedaquiline is active against both replicating and non-replicating bacteria, further highlighting its utility as an anti-TB drug. The diarylquinoline compound shows potency against both MDR and XDR-TB, for this reason the WHO has advised that its use be restricted to individuals presenting DR-TB in order to shield against the potential acquisition of resistance. Bedaquiline has been shown to result in a prolongation of QT interval in the cardiac cycle, for this reason its use is contraindicated in individuals who suffer from coronary complications such as arrhythmia or coronary artery disease.[64]

The other two compounds, pretomanid (**6**) and delamanid (**7**) both belong to the nitroimidazole class of compounds. Delamanid was first approved for use in Europe in 2014 and has since been recognised by the WHO as one of its 'Essential Medicines'. Similar to INH, Delamanid is a pro-drug, which elicits its biological effects upon activation by a nitroreductase enzyme (Rv3547).[65] This reactive intermediate is then able to prevent the synthesis of mycolic acids resulting in cell death. As with bedaquiline, delamanid demonstrates activity against both replicating and non-replicating forms of *Mtb*.[66] This activity towards both active and latent inflections suggests further targets beyond just mycolic acid synthesis, as evidenced by INH's inactivity against latent TB.

Pretomanid was approved for use in the US in 2019.[67] Similar to delamanid, mycolic acid biosynthesis is the primary target in the replicating form of the infection, however, a second mode of action has also been identified.[68] A combination of transcriptional profiling and metabolite screening suggests that pretomanid's ability to

act as a nitric oxide (NO) donor is crucial to its activity against non-replicating cells. NO has been shown to have a range of targets in *Mycobacterium*, with as many as 29 enzymes implicated. Work by Manjunatha *et al.* showed the transcriptional response of anaerobic *Mtb* treated with pretomanid was similar to that of *Mtb* treated with potassium cyanide, resulting in the upregulation of various genes involved in respiration.[69] This suggests that pretomanid is able to address multiple enzymatic targets through a single compound. Given its structural similarity, it is possible that delamanid can also operate through similar routes though no such data is available to support this theory. The power of pretomanid is best illustrated by the potency of the recently reported three-drug regimen BPaL. Consisting of bedaquiline, pretomanid and linezolid, a trial of the drug cocktail showed a 96% cure rate for individuals infected with XDR-TB.[70] This success represents a potentially transformative step forward in the treatment of DR-TB and could prevent thousands of deaths each year going forward.

1.10 Mycobacterial Fatty Acid Biosynthesis

As has previously been discussed, the mycolic acid layer is of fundamental importance to *Mtb*. Due to its significance, disruption of the mycolic acid biosynthesis represents an attractive target from a drug discovery perspective. The *Mtb* fatty acid biosynthetic pathway consists of two discrete multi-step enzymatic cycles. These two cycles are defined as Fatty Acid Synthase I and II (FASI and II). These cycles, and their relationship is summarised in **Scheme 2**.[71, 72]

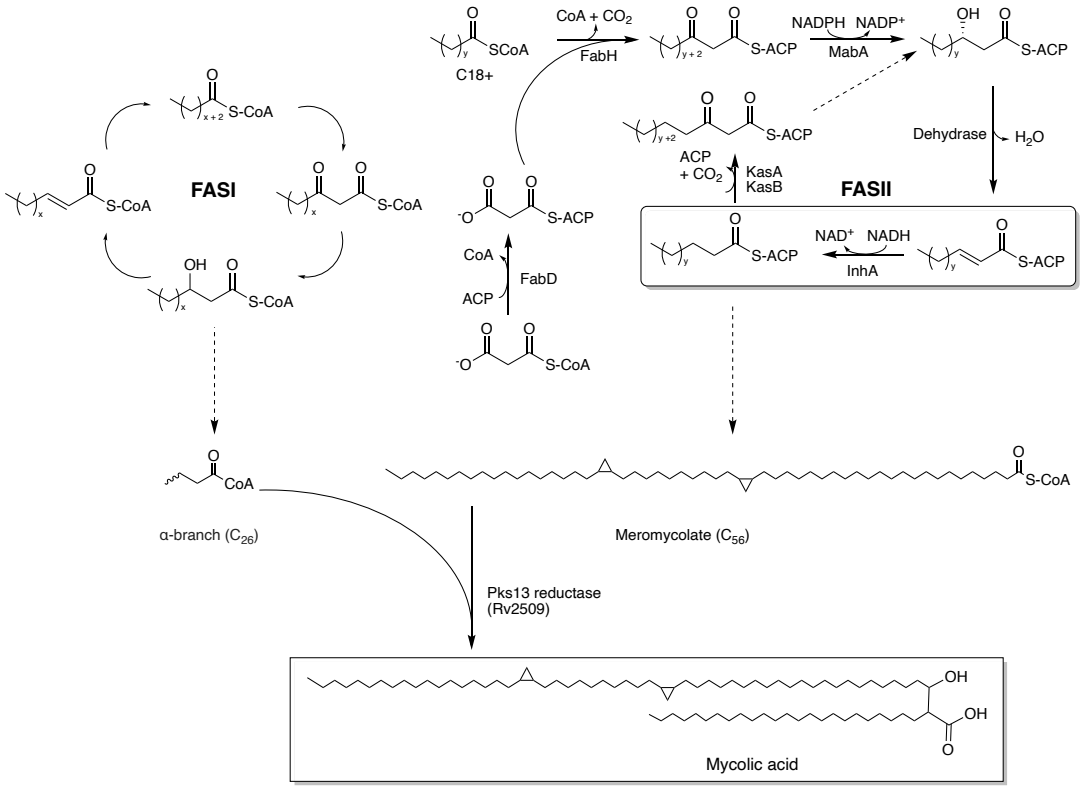

Scheme 2. *Representation of the FAS I and II cycles involved in the synthesis of mycolic acids in Mtb, the role of InhA and the structure of the final Mycolic acid are highlighted. Adapted from Abrahams and Besra.*[72]

The FASI system is responsible for the production of two sets of fatty acid chains, the first being a C18 unit which is fed into the FASII pathway, and the second being the C26 branch which is later transferred to a meromycolate unit to form the final mycolic acid structure. The FASI cycle is carried out by a large, multifunctional fatty acid synthase enzyme that is found in a variety of eukaryotes and advanced prokaryotes.

The role of the FASII cycle is to elongate the fatty acid chains produced by the FASI system. This elongation process generates the long chain mycolic acids which are so

characteristic of the *Mtb* cell wall. The link between the FASI and II systems is proposed to be the enzyme FabH. This enzyme generates the dicarbonyl-AcP component *via* the condensation of two acetyl-CoA precursors. MabA is a reductase which converts the γ-carbonyl to its corresponding alcohol. This is then converted to an unsaturated 1,4 system by an unknown dehydrase enzyme. This newly formed alkene is then reduced by the enoyl-acyl carrier protein reductase (ENR), InhA, which results in saturation of the C=C double bond. This chain is then extended by the enzyme KasA through condensation with acyl-AcpM. This newly extended chain is then fed back into the FASII system, allowing for subsequent extensions. KasB is responsible for the final elongation step to produce the full length mycolate. Finally, the C_{26} branch and meromycolate are combined through the polyketide synthase (Pks13) enzyme. This gives a full length α-branched-β-hydroxylated fatty acid which is characteristic of the *Mtb* cell wall. Recent work by Tahiri *et al.* demonstrated the first chemical total synthesis of a mycolic acid unit from *Mtb*.[73]

Unlike the FASI cycle, the FASII system is not present in eukaryotes and is instead found more commonly in plants, bacteria and parasites. For this reason, enzymes within the FASII system represent an attractive 'silver bullet' drug target, whereby inhibition will have no negative side effects for the human host.

1.11 InhA

As previously mentioned, InhA plays a crucial role in the FASII system. InhA belongs to the ENR class of enzymes and is also sometimes referred to as Fatty Acid Biosynthase I (FabI). Homologous enzymes have been characterised in a range of different bacterial species: *Escheria coli* (*E. coli*), *Haemophilus influenza* (*H.*

influenza) *Plasmodium falciparum* (*P. falciparum*), and *Staphylococcus aureus* (*S. aureus*).

InhA is reliant upon its nicotinamide adenine dinucleotide (NADH) cofactor in order to carry out its biological function. As such it is capable of binding NADH and NAD^+, additionally the enzyme can bind to nicotinamide adenine dinucleotide phosphate ($NADP^+$). In performing its biological function, InhA utilises NADH to deliver a hydride to its substrate in order to carry out the alkene reduction (**Scheme 3**).

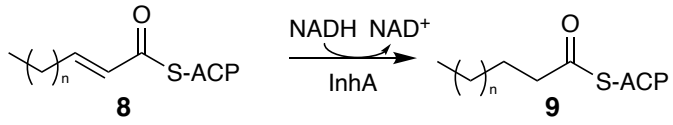

Scheme 3. *Catalytic reduction of C=C double bond carried out by InhA.*

InhA, and its structural homologues, belongs to the short chain dehydrogenase/ reductase (SDR) class of enzymes. The residues Phe149, Tyr158 and Lys165 are integral to the catalytic activity of InhA. Work by Parikh *et al*., helped to elucidate the functions of the latter two residues.[74] Rather than being a proton donor, Tyr158 was shown to stabilise the enolate intermediate formed by the initial hydride addition. Mutagenesis studies on the Lys165 residues indicated that its primary role is in binding to the NADH cofactor. The NADH cofactor is responsible for the delivery of a single hydride to the double bond, it is thought that the second proton is obtained from a water molecule. Phe149 is believed to act as a steric blocker, preventing reduction of the carbonyl with hydride delivery instead directed to the less hindered alkene.

1.11.1 The Structure of InhA

InhA is a homotetrameric protein, with each of the 4 subunits consisting of a single domain, these domains possess a Rossmann fold which harbours the NADH binding site.[75] Stretching beyond this binding site, several α-helices and β-sheets extend to create a groove for the fatty acid substrate. Within this groove is the substrate binding loop, comprising 23 residues (196-219).[76] This substrate binding loop is composed of two adjacent α-helices which are comprise mostly hydrophobic residues. InhA's binding loop is longer than those found in its homologues, reflecting the larger size of its substrate. The binding loop of InhA is significantly disordered in the apo-form of the enzyme, with substrate binding promoting loop ordering (**Figure 5**).[75, 76]

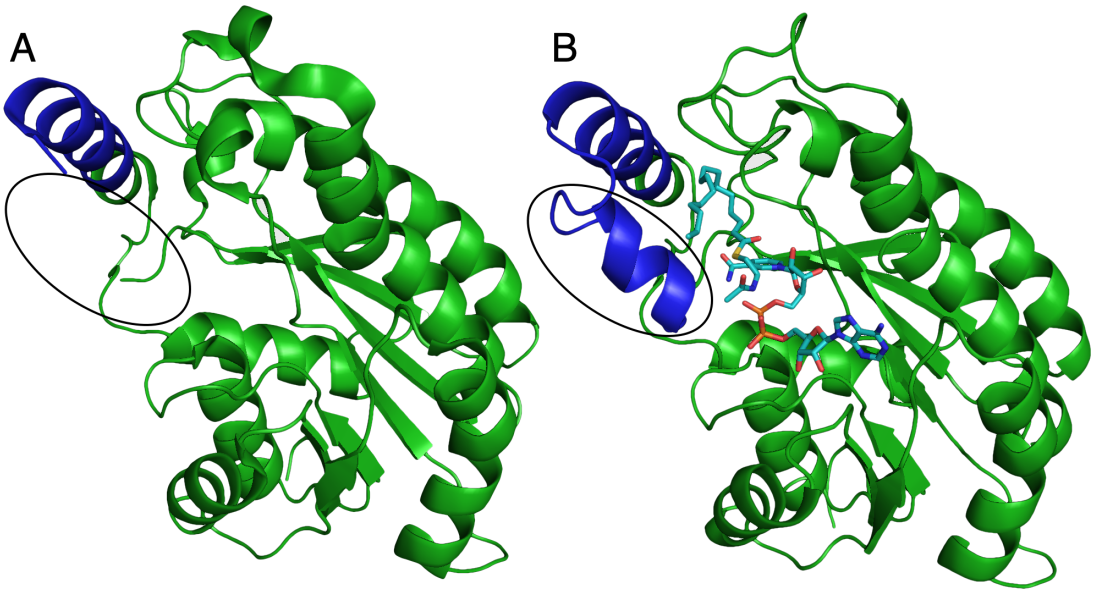

Figure 5. *A) Apo form of InhA, substrate binding loop (blue) is disordered (PDB: 4TRM, 1.8 Å). B) Crystal structure of InhA bound to a substrate mimetic (trans-2-hexadeconyl-(N-acetyl-cysteamine)-thioester) (PDB: 1BVR, 2.8 Å) showing ordering of the substrate binding loop, highlighted by a red circle.*[75, 76]

The crystal structure of InhA bound to a C16 fatty acyl substrate mimetic revealed a "U-shaped" binding mode for the InhA substrate, with the long carbon chain looping back on itself in order to engage the substrate binding loop. The protein-ligand interactions are depicted below (**Figure 6**).

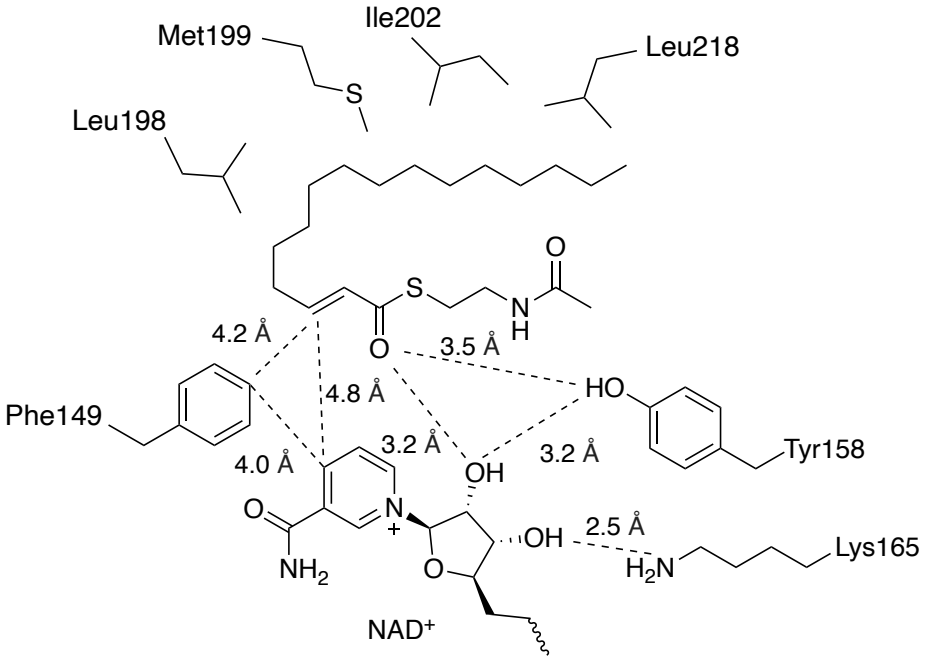

Figure 6. *Binding mode of the C16 fatty acyl substrate mimetic in complex with InhA. Key interactions are shown by dashed lines, with inter-molecular distances displayed. Adapted from Rozwarski et al.*[75]

This work also confirmed the hydrogen bonding interaction between the Tyr158 and the thioester carbonyl of the substrate, supporting the idea that Tyr158's primary role is stabilisation of an enolate intermediate.

1.11.2 InhA and Isoniazid

InhA is the accepted clinical target of the front-line drug INH, eliciting its biological effects through disruption of the vital mycolic acid layer of the *Mtb* cell wall.[77]

Subsequent work has revealed that INH is actually a pro-drug which requires activation before it can elicit its biological effect.[78] This activation comes from the enzyme KatG, a multi-functional peroxidase which also displays other enzymatic activities including NADH oxidase and peroxynitritase.[79] The primary biological role of KatG is to protect the cell from the host's immune system, through catalytic degradation of ROS. This enzyme converts INH to an isonicotinic acyl radical species which is able to covalently bind to an NAD^+ molecule (**Scheme 4**).[80]

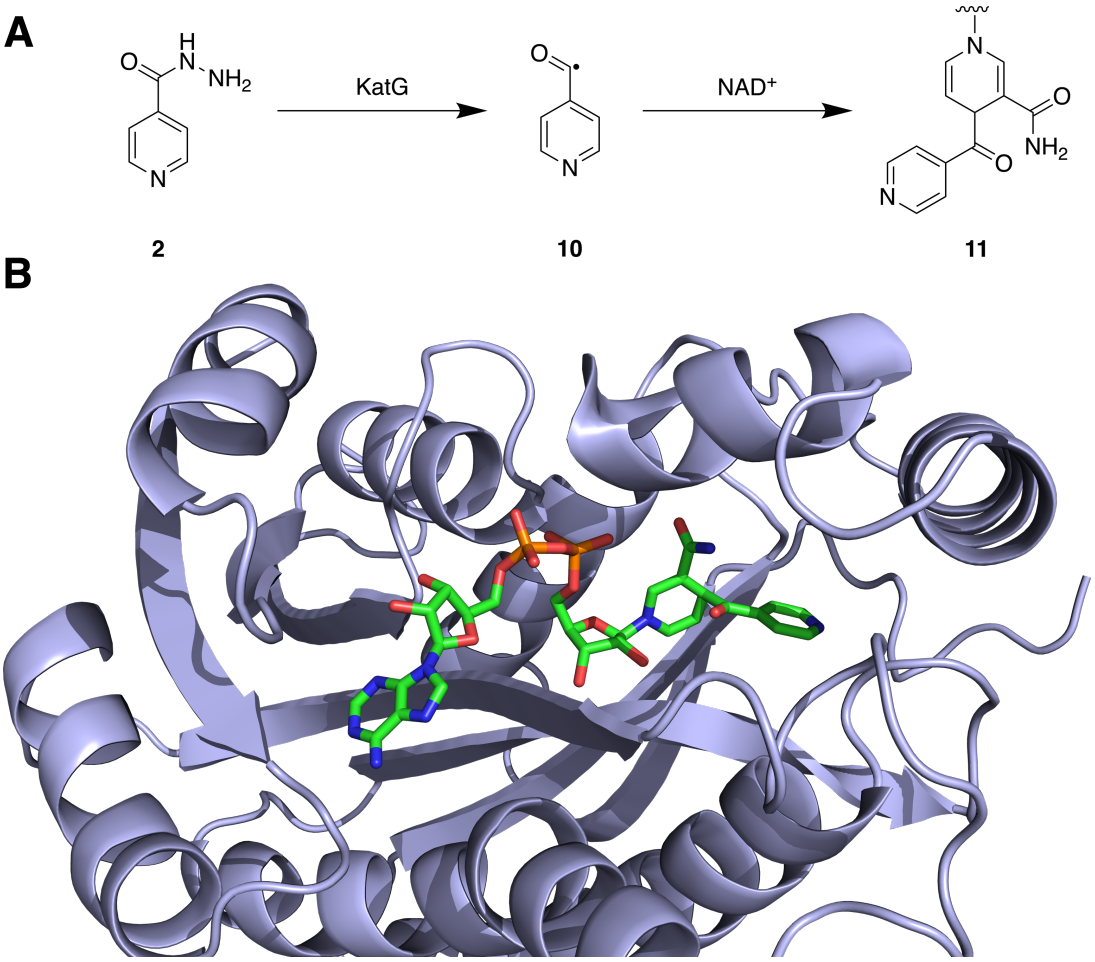

Scheme 4. *A) The pathway through which INH is able to inhibit InhA. First INH is converted an isonicotinic acyl radical (**10**) by KatG. This radical then forms an INH-NAD^+ adduct via a Minisci addition reaction, this radical cation is terminated by delivery of a hydride ion INH-NAD (**11**). B) Crystal structure showing the INH-NAD adduct bound to InhA (PDB: 1ZID).*[80]

Work by Marcinkeviciene and Magliozzo showed that KatG converts Mn^{2+} to Mn^{3+} this species is then reduced by INH through the donation of an electron, regenerating the Mn^{2+} and forming the isonicotinic acyl radical **10**.[81] In order to oxidise Mn^{2+} to Mn^{3+}, there must be an oxidant present, this explains why INH is primarily active against aerobic, dividing bacteria and lacks efficacy against latent TB.

Conjugation of INH to NAD results in a blocking of the InhA substrate binding site, meaning its long chain fatty acid substrate is sterically occluded (**Scheme 4**, Part B). This in turn means the FASII cycle breaks down and the long chain mycolic acid component of the *Mtb* cell wall remains unsynthesised.[82] This deficiency undermines the structural integrity of the cell ultimately leading cell lysis. The INH-NAD adduct has also been demonstrated to further disrupt the FASII cycle through binding to MabA and dihydrofolate reductase, though InhA is its primary site of action.[83-85]

1.11.3 Isoniazid Resistance in TB

The majority of INH resistance can be attributed to mutations in the KatG which prevent activation of the pro-drug.[86] Specifically, mutation of a single amino acid residue, S315T, has been found to be a major driver of INH resistance. This mutation has been implicated in up to 95% of the clinically isolated, INH-resistant infections.[87-90] Solution of the S315T crystal structure shows that this mutation narrows the access channel to the oxidising pocket, from 6 to 4.7 Å, thus restricting INH's entry and reducing conversion to its active form.[91] In addition to providing a survival advantage to the host, this mutation does not significantly impede KatG's ability to carry out its biological functions and so carries a low fitness cost.

While INH resistance primarily comes from the aforementioned mutation in KatG, there is evidence that mutations in InhA can also confer resistance. Specifically, the S94A mutation has been shown to significantly reduce the effectiveness of INH. This mutation disrupts the co-factor binding pocket, such that the binding affinity of the INH-NAD adduct is significantly reduced. Work by Vilchèze *et al*. demonstrated that the S94A mutant of InhA was 17 times more resistant to INH than the wild type enzyme.[92] This work also helped to confirm that InhA was the primary active target of INH. Mutations in the promoter region of the InhA gene have also been shown to result in an over-expression of the enzyme which reduces the efficacy of INH.[93] While these two mutations do account for some of the drug resistance observed in clinical isolates, the vast majority of INH-resistances originates from the mutations in KatG.

1.11.4 Reported Direct InhA Inhibitors

Given that INH activation is significantly hampered by KatG mutations, it is desirable to identify compounds which are capable of acting as 'direct inhibitors' of InhA. The term 'direct inhibitors' refers to compounds which can inhibit InhA's biological function without requiring prior activation. Mutations that confer resistance against such compounds would likely carry a significantly higher fitness cost than the KatG mutation required to provide INH resistance.

Diazaborines were first reported as covalent inhibitors of enoyl-acyl carrier reductases in 1996, by Baldock *et al*.[94] Following this work, Davis *et al*. synthesised a small library of such compounds for evaluation against *Mtb*.[95] While evaluation was only performed against whole-cell bacteria, these compounds likely represent the first

compounds which deliberately targeted InhA in *Mtb*. Diazaborines have been shown to bind covalently to the NAD cofactor *via* the 2'-OH of the ribose unit to produce an adduct which blocks substrate binding, in a similar fashion to the INH-NAD adduct (**Figure 7**).

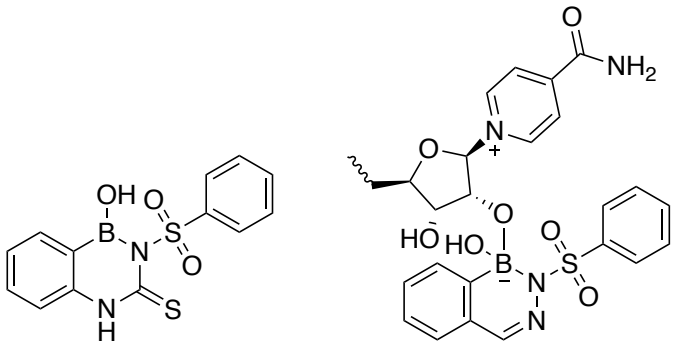

12
MIC = 33 μM

13

Figure 7. *The structure of **13** the first reported direct inhibitor of InhA and the adduct it forms with NAD+.*[95]

The first attempt to rationally design inhibitors of InhA was reported by Broussy *et al*. in the form of **14 (Figure 8)**.[96] This compound sought to merge an INH and nicotinamide fragment attached to a ribose moiety. The aim of this strategy was to mimic the INH-NAD adduct formed *in situ* upon activation of INH. This initial compound showed little effect towards InhA in isolated enzyme assays (**Figure 8**). This work was subsequently advanced by Bonnac *et al*. who demonstrated the importance of the ADP unit for InhA inhibition with **15**.[97]

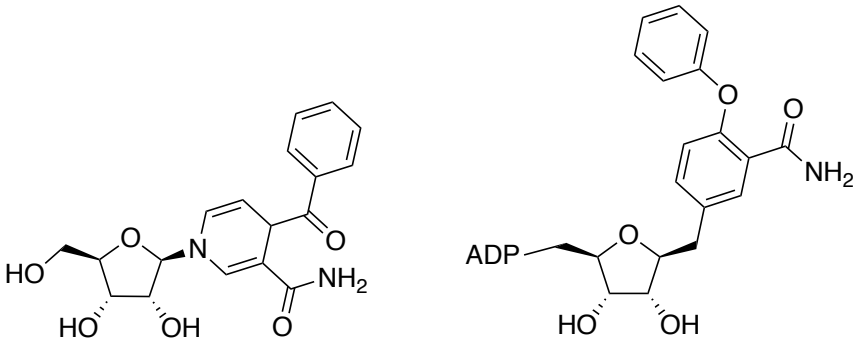

14
IC_{50} 100 μM <<

15
IC_{50} = 27 μM

Figure 8. *Structures of two direct InhA inhibitors designed to mimic the INH-NAD adduct.*[96, 97]

Since the identification of these basic inhibitors there has been significant progress in the field, with several groups identifying highly potent, direct inhibitors of InhA.[98] High-throughput screening (HTS) represents one of the most commonly used drug discovery techniques. HTS entails assaying large libraries of compounds for biological activity against a specific enzyme target, or whole-cell organism. Promising compounds can then be treated as 'hits' for further optimisation. The first direct InhA inhibitors (**16** and **18, Figure 9**) identified through HTS were reported by Kuo *et al.* in 2003. The aryl amide compound class was subsequently optimised by He *et al.* in 2007 (**19**, **Figure 9**).[99, 100]

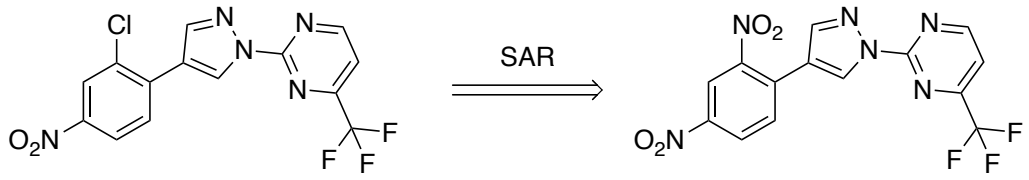

16
Inhibition: 82% (40 μM)
MIC = Not Reported

17
IC_{50} = 2.40 μM
MIC = 2.50 μM

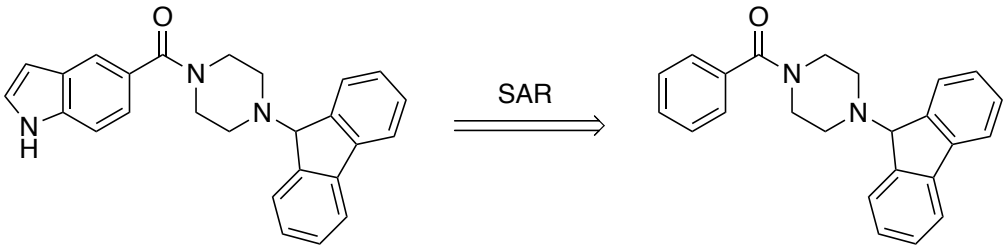

18
IC_{50} = 0.16 μM
MIC = > 30 μM

19
IC_{50} = 0.09 μM
MIC = > 125 μM

Figure 9. *The structures of two hit compounds **16** and **18** and the optimised structures **17** and **19**, respectively, including their biological activities.*[99, 100]

Compound **18** showed particularly promising activity against purified InhA, with an IC_{50} of 160 nM, however, this potency was not replicated in whole-cell assays with the MIC rising to > 30 μM. This reduced activity was attributed to poor cellular uptake of the molecule. Further optimisation of the arylamide scaffold **18** produced **19,** an InhA inhibitor with an IC_{50} of 90 nM, however, as with the its predecessor, the MIC value was disappointingly high, in excess of 125 μM. Compounds based on the pyrazole scaffold (**16**) showed the reverse trend. Despite having a relatively modest IC_{50} profile against purified InhA, **17** showed good activity in whole-cell assays, with MIC values ranging from 1.25-30 μM against a range of clinical isolates (2.50 μM vs

H37Rv). Interestingly, the lowest MIC value was obtained against an INH and RIF resistant strain (1.25 μM vs TN5038).

In 2006, He *et al.* reported the pyrrolidine carboxamides as a novel class of direct InhA inhibitors (**Figure 10**).[101]

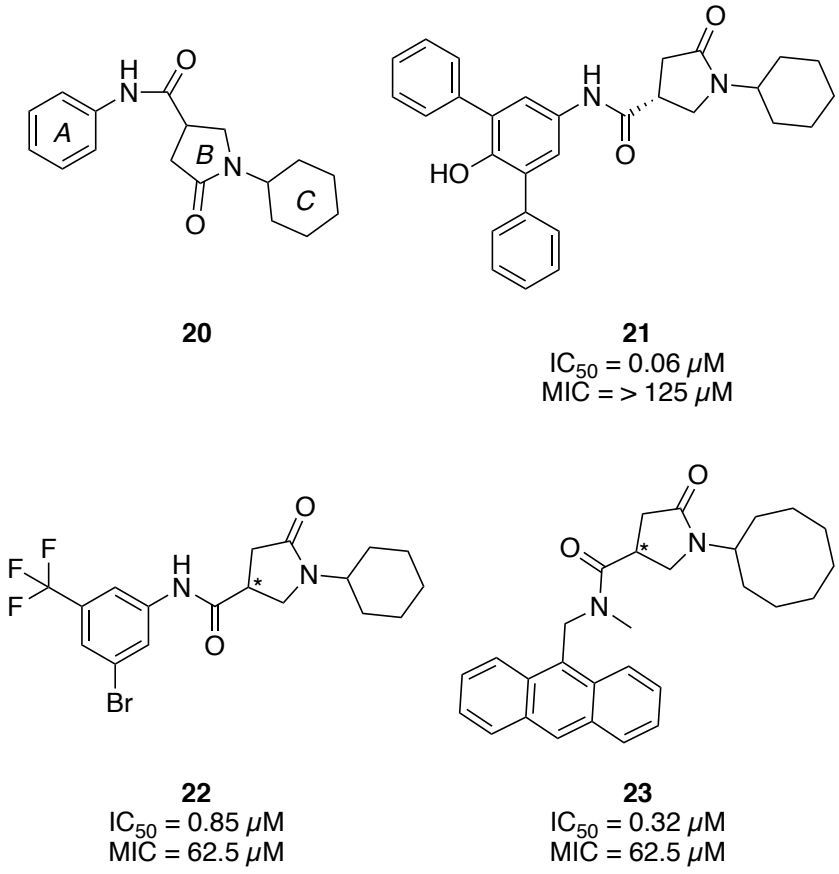

Figure 10. *General structure for the pyrrolidine carboxamide scaffold and optimisation against InhA. Asterisks denote compounds evaluated as racemic mixtures.*[101]

Following identification of a hit compound (general structure **20**) subsequent SAR explorations were untaken in order to increase potency. The most potent compound in the series was **21**, with an IC_{50} of 62 nM in isolated enzyme assays. Resolution of the two enantiomers showed that only the (*R)*-enantiomer was active against InhA. However, this inhibition failed to translate into *in vivo* activity, as the compound had

an MIC of greater than 125 μM. The compounds showing the greatest activity in whole-cell screening were **22** and **23**, with both compounds showing MICs of 62.5 μM, chiral resolution of these compounds was not performed. This highlights one of the major issues with anti-TB drug design, with the relationship between activity in isolated enzyme assays and whole-cell potency rarely being straightforward one.

Triclosan (TCL) is a small molecule, broad spectrum antibiotic (**Figure 11**). It has been used in a range of different products including soaps, detergents and shampoos. TCL has been identified as an inhibitor of InhA and its bacterial homologues. TCL binds preferentially to the NAD^+ bound form of InhA and does so in a slow, reversible manner.[102]

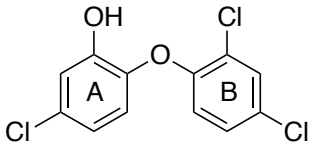

24
TCL
IC_{50} = 10.0 μM
MIC = 69.1 μM

Figure 11. *Structure of TCL with the 'A' and 'B' rings labelled.*[102]

While only a moderate inhibitor of InhA (IC_{50} = 10 μM), TCL has been shown to be a potent inhibitor of the InhA homologue, FabI, found in *E. coli*.[103] This increased potency likely reflects the smaller cavity of the FabI active site, which results in tighter binding of TCL.[104] InhA has a significantly large active site in order to accommodate for its long-chain substrate.

While TCL represents a promising starting point for discovery of InhA inhibitors, it is not without its issues, namely its high hydrophobicity (logP 4.89) limits bioavailability and it is relatively weak inhibitor (IC_{50} 10 μM). Additionally, whole-cell screening has

revealed that exposure to TCL causes an up-regulation in the rv3160-rv3161c genes. These genes encode for deoxygenase enzymes which metabolises aromatic compounds to non-aromatic *cis*-diols. As well as effectively promoting its own metabolism, TCL also causes an up-regulation efflux pumps which remove the compound from the cytoplasm.

A recent review by Vosátka *et al*. provides a very good summary of the various strategies which have been applied to the design of various TCL derivatives as anti-TB agents.[105, 106] The most significant InhA inhibitors will be highlighted here (**Figure 12**).

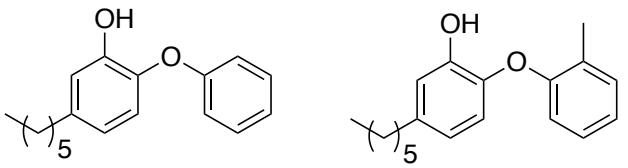

25
6PP
IC_{50} = 11.0 nM
MIC = 7.7 μM

26
PT70
IC_{50} = 50.7 nM
MIC = 10.9 μM

Figure 12. *Structures of two optimised TCL-derivatives, showing potent inhibition of InhA.*[105, 107]

Much of the area of TCL derivatives as InhA inhibitors has been pioneered by Tonge and colleagues.[105, 107] Compounds **25** and **26** were designed to exploit the hydrophobic binding site occupied by InhA's natural long chain substrate. Both compounds displayed potent inhibition of isolated InhA and reasonable whole-cell potency. Compound **26** showed an impressive binding profile, with a residence time of 24 minutes within the active site of the enzyme. This residence time was particularly notable, given that it is 14,000 times higher than that of **25** (0.1 second). The introduction of an *ortho* methyl substituent to the B-ring of TCL is believed to increase residence time as it reduces the conformational freedom around the ether

linkage and thus there is a reduced entropic penalty to binding. The hexyl chain of the A-ring mimics the long carbon chain of the InhA substrate, engaging and stabilising the substrate binding loop. This loop ordering is associated with increased residence time for InhA inhibitors.

In 2010 GlaxoSmithKline (GSK) patented the use of thiadiazole compounds as anti-TB agents (**Figure 13**).[108, 109] Following the disclosure of this scaffold, the compound class was simultaneously explored by researchers at both AstraZeneca and GSK.

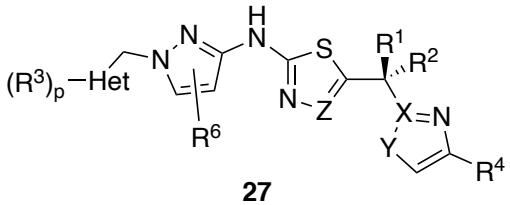

27
Patented Scaffold

X = N or C
Y = CR^5 or S
Z = N or CH
$\mathbf{R^1}$ = H or Me
$\mathbf{R^2}$ = H, OH, OMe or Me
$\mathbf{R^3}$ = Para: Alkyl, halogen, CF_3 or NH_2
$\mathbf{R^4}$ = Me, CF_3, NO_2, CHF_2
$\mathbf{R^5}$ = H, Me, CHF_2
$\mathbf{R^6}$ = H or Me

Figure 13. *The methyl thiazole anti-TB scaffold originally patented by GSK in 2010.*[108]

First published in 2013, AstraZeneca's compound **28** (**Figure 14**) demonstrated significant potency in both isolated and whole-cell assays.[110] However, the most significant findings of this work came in the collection of a crystal structure which demonstrated that the methyl thiazole inhibitor class has a previously unseen binding mode (**Figure 14**).

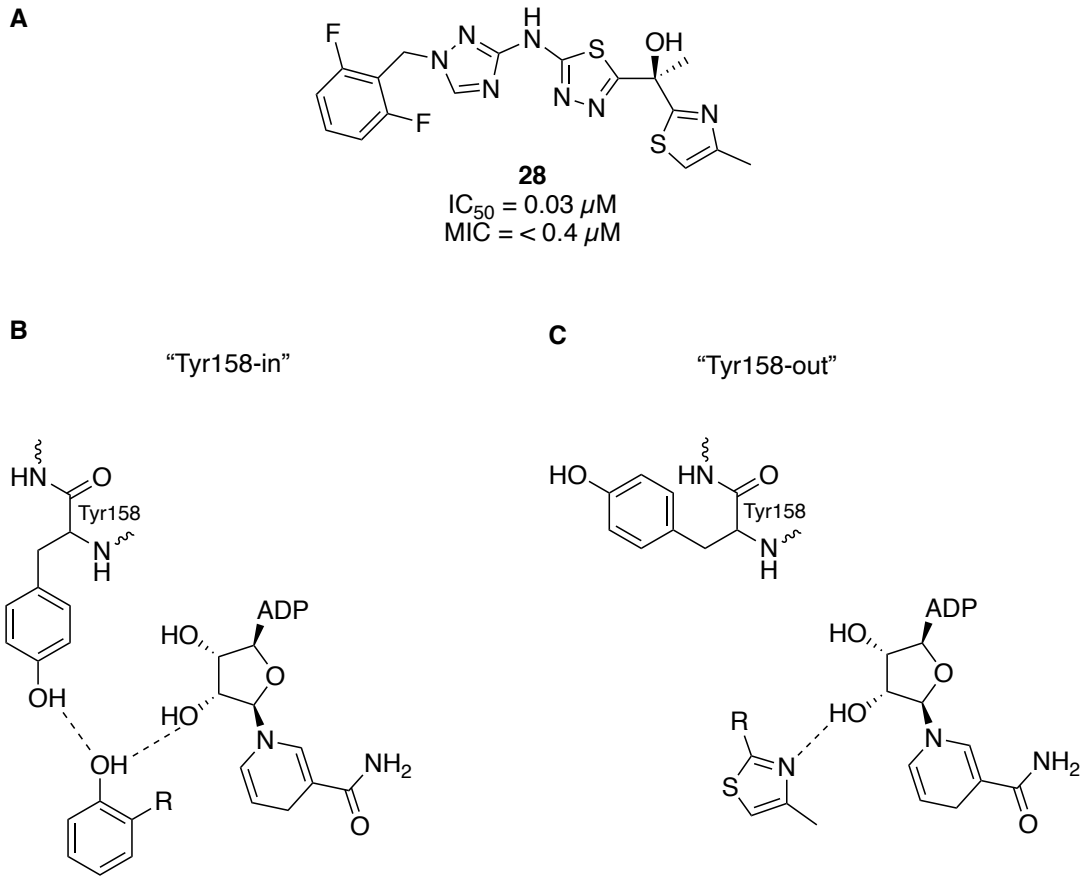

Figure 14. ***A****) Structure of AstraZeneca's optimised methyl thiazole* ***28*** *and representation of the Tyr158-in and out binding modes.* ***B)*** *shows the Tyr residue engaging the inhibitor through an H-bond in the 'in' configuration.* ***C)*** *shows the binding mode of the methyl thiazole compound class, with the Tyr residue pointing 'out' and not making an H-bond with the inhibitor.*[110]

The crystal structure of one of the AstraZeneca's methyl thiazole derivative revealed that, unlike in previously disclosed InhA inhibitors, the Tyr158 residue was in an 'out' configuration and did not engage the inhibitor through a hydrogen bond. This represents a novel binding mode and is something that could be further exploited by other novel scaffolds.

In 2016, GSK reported the optimisation of their original scaffold, ultimately arriving at **GSK693** as their lead compound (**Figure 15**).[111]

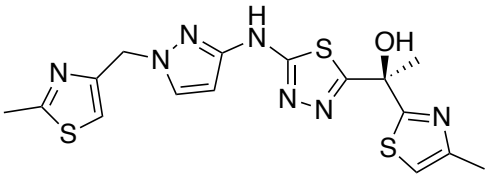

29
GSK693
Mol.Wt.: 419.6 g mol^{-1}
cLog P: 0.71
Aqueous Solubility: 413 μM
IC_{50} = 0.007 μM
MIC = 0.2 μM

Figure 15. *Structure of **GSK693**, along with its potency and various drug-like properties.*[111]

This compound displayed excellent activity in isolated enzyme assays. Of considerable importance was the fact that **GSK693** retained its activity in whole-cell assays, demonstrating an MIC of 0.2 μM. This whole-cell activity is comparable to that of INH. **GSK693** was subject to extensive adsorption, distribution, metabolism, excretion and toxicity (ADMET) testing, showing a pleasing safety profile across the board. Further investigation showed that **GSK693** retained its activity against both wild type (WT) and KatG-deficient strains of *Mtb*, reinforcing the KatG-independent nature of its inhibition. This lead compound represents a promising avenue as a potentially clinically viable compound.

In 2015, Manjunatha *et al.*, reported the discovery and development of the 4-hydroxy-2-pyridones scaffold as a novel class of potent InhA inhibitors (**Figure 16**).[112]

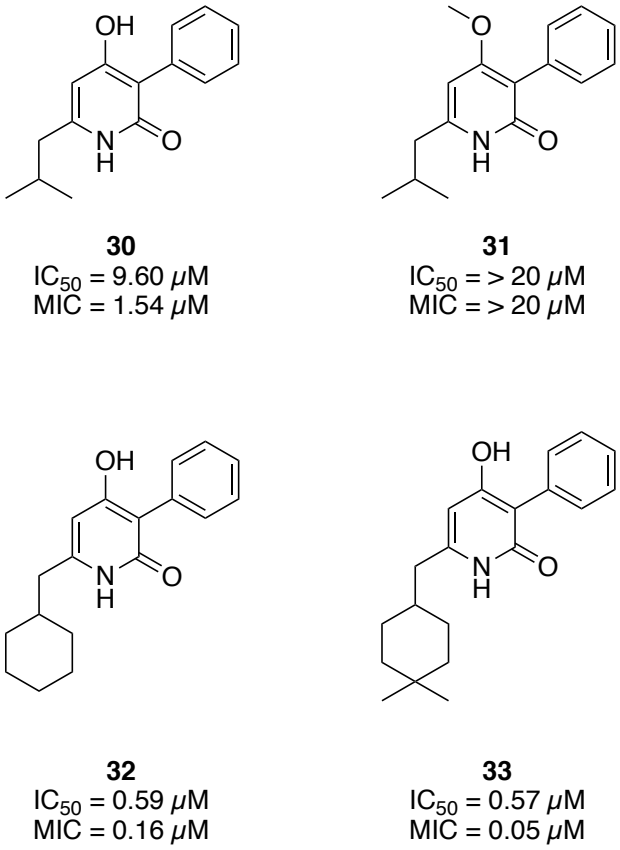

30
IC_{50} = 9.60 μM
MIC = 1.54 μM

31
IC_{50} = > 20 μM
MIC = > 20 μM

32
IC_{50} = 0.59 μM
MIC = 0.16 μM

33
IC_{50} = 0.57 μM
MIC = 0.05 μM

Figure 16. *Structures of several 4-hydroxy-2-pyridones reported as direct inhibitors of InhA.*[112]

The best compound, **33**, showed good activity against a range of drug-resistant strains of *Mtb*, including XDR-TB isolates resistant to moxifloxacin. Interestingly there is a three-fold disparity between the MIC values for **32** and **33** despite their very similar IC_{50} values. This difference was attributed to the higher logP value of **33**, which better facilitates its passage through the dense bacterial cell wall. It can be seen that there is a disparity between the MIC and IC_{50} values, with the MIC values being lower, this suggests that there are other enzymes, in addition to InhA, which are targeted by this class of compounds.

In 2016, Slepikas *et al*. reported the use of Rhodanine derivatives as direct inhibitors of InhA.[113] Rhodanines represent a biologically privileged architecture, displaying

activity against a range of biological targets, including cell-wall assembly enzymes in *Mtb*.[114-116] Based on the 4-thiazolidinone scaffold (**34**), Slepikas' work represented their first use as InhA inhibitors (**Figure 17**).

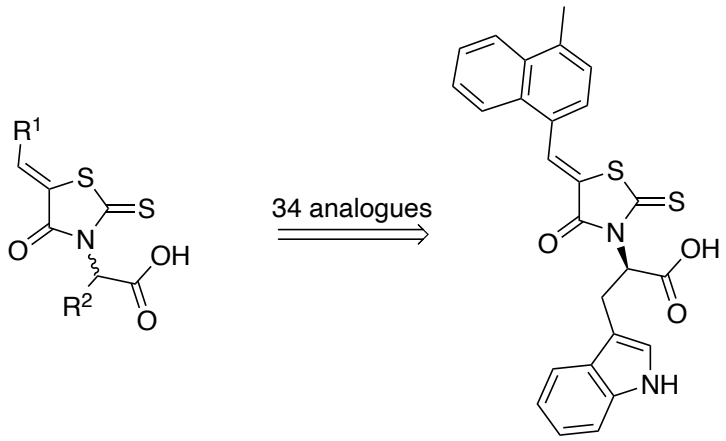

34

35
IC_{50} = 8.7 μM
MIC = 0.21 μM

Figure 17. *General Rhodanine structure **34** and the optimised structure of InhA inhibitor, **35**.*[113]

This work led to the identification of **35**. This compound demonstrated an encouraging IC_{50} of 8.7 μM against InhA. Whole-cell evaluation showed an MIC of 0.21 μM, however, it should be noted that whole-cell evaluation was performed against *Mycobacterium marinum* (*Mm*). The *Mm*-InhA sequence does not share 100% sequence identity with *Mtb*-InhA, so this leaves some ambiguity regarding the actual whole-cell target, as isolated enzyme testing was performed against *Mtb*-InhA, rather than *Mm*-InhA. It should also be noted that there is a significant disparity between **35**'s IC_{50} (8.7 μM) and MIC (0.21 μM). This suggests that **35** has other intracellular targets, in addition to InhA, or has a greater affinity for *Mm*-InhA than *Mtb*-InhA.

In addition to HTS, a number of InhA inhibitors have been discovered using more contemporary methods, including fragment-based drug discovery (FBDD) and through the use of DNA encoded libraries (DELs).

FBDD entails screening libraries of small 'fragments' of compounds, typically < 150 mw, and assaying for biological activity.[117] Due to the small nature of the compounds being investigated, fragments 'hits' typically display much lower activity than hits detected through HTS. Fragments can then be linked, merged or grown with the aim of improving potency. Several authoritative reviews on the use of FBDD as a general drug discovery technique are available.[117-119]

In 2018, Prati *et al.* reported the first published FBDD study towards the discovery of direct InhA inhibitors (**Figure 18**).[120] Through the use of 4 diverse libraries, including one containing fragments from known InhA inhibitors, several potent InhA inhibitors were obtained.

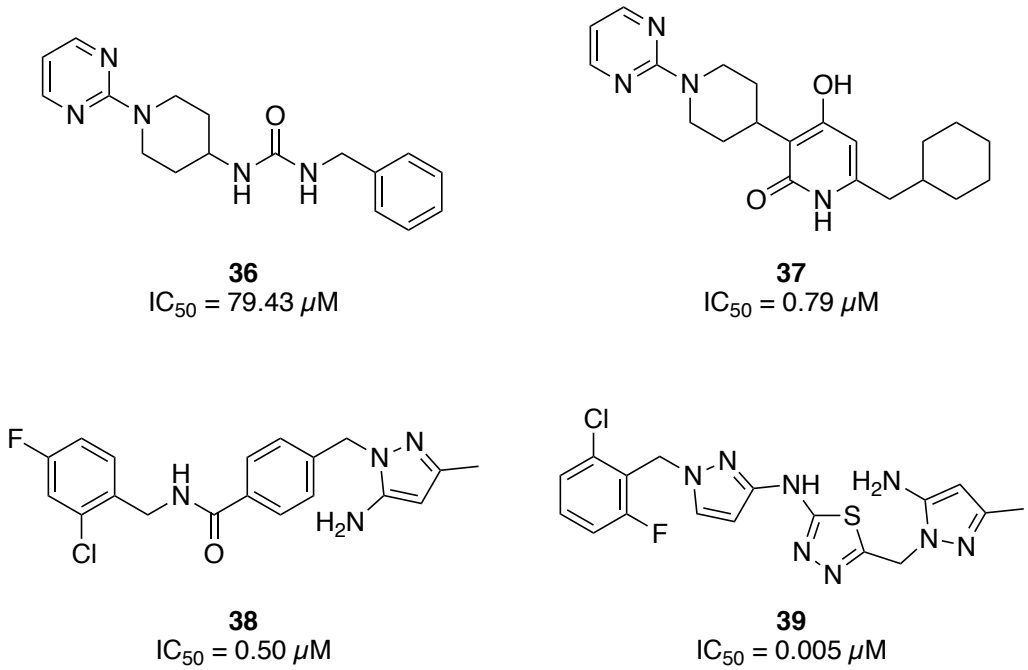

Figure 18. *The structures of several potent InhA inhibitors identified using FBDD.*[120]

As can be seen from their structures, these compounds are reliant on fragments found in previously disclosed inhibitors, namely thiadiazoles (**29** [**Figure 15**] vs **39**) and 4-hydroxy-2-pyridones (**32** [**Figure 16**] vs **37**). Of these compounds, **39** shows particularly potent inhibition of InhA, though this compound is very close to the chemical space covered in the original GSK patent mentioned previously. In their initial 2018 disclosure of these compounds, the authors promised future publication of the additional optimisation and whole-cell efficacy of these compounds, however, at the time of writing, no such data has been published.

A second FBDD investigation into InhA inhibitors was recently reported by Sabbah *et al.*, this study identified a number of hit fragments, initially based on the melting point of InhA:ligand crystals.[121] These hits were subsequently followed up by X-Ray crystallography. A lead fragment (**40**) was chosen and subject to iterative rounds of fragment growing and medicinal chemistry optimisation (**Figure 19**)

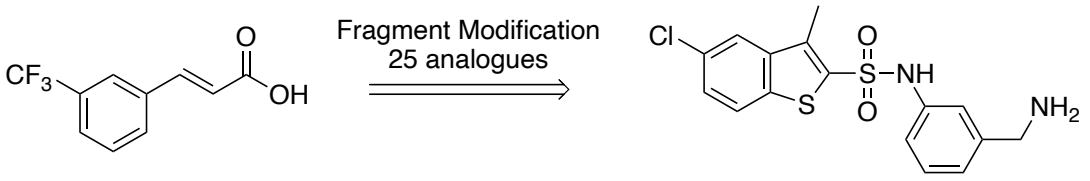

40
Initial Fragment Hit
IC_{50} = > 2 mM

41
IC_{50} = 310 nM
MIC = > 200 μM

Figure 19. *The structure of Sabbah's initial fragment hit **40** and the optimised compound **41**.*[121]

The carboxylic acid was initially replaced with an isosteric sulfonamide which acted as a linker between two variable groups. Optimisation yielded **41**, which displayed an IC_{50} of 310 nM against InhA. Unfortunately, despite this good enzyme inhibition, the whole-cell potency was much lower with only 30% growth inhibition observed at 200 μM. This indicates that either the compound was unable to permeate the *Mtb* cell wall, or it was rapidly metabolised/eliminated upon reaching the intracellular environment.

Along with FBDD and HTS, the use of a DEL has demonstrated its ability to identify potent InhA inhibitors. DELs work through attachment of a small molecule to a strand of DNA before rapid and thorough derivatisation with each new compound being 'tagged' to allow for its characterisation. Several general reviews of this technique are available.[122, 123] The first reported curation of a DEL claimed to have made a library with in excess of 800 million unique chemical entities.[124] Clearly this represents an attractive means to assemble a chemically diverse library to fully probe the chemical space of an enzyme's active site and as such DELs have been used to identify several potent inhibitors for various targets.[125-127]

In 2014, researchers at GSK reported the first use of a DEL to identify an InhA inhibitor. Starting from a putative hit based on the aminoproline scaffold (**42**), over 16 million new compounds were synthesised resulting in the identification of **43** (**Figure 20**).[128]

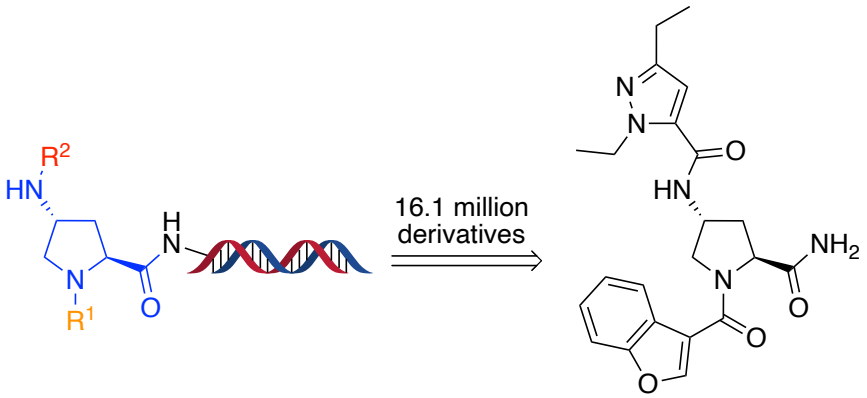

Figure 20. *Aminoproline hit **42** and optimised structure **43.***[128]

Despite showing encouraging performance in both isolated enzyme and whole-cell assays **43** was shown to be ineffective in the treatment of mice infected with TB. This was particularly disappointing given the compound showed acceptable ADMET and stability results. This result serves to underline the difficulty in TB drug discovery, despite the fact **43** demonstrated a low nanomolar IC_{50} and a nanomolar MIC this did not translate into *in vivo* efficacy in the acute mouse models used.

Natural products also represent a rich reservoir of biologically active compounds from which medicinal chemist can draw inspiration. The most notable natural product inhibitor of InhA is pyridomycin, a cyclic compound isolated from *Dactylosporangium fulvum* (**Figure 21**).

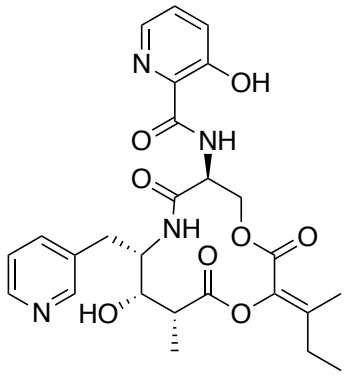

44
Pyridomycin
MIC = 1.1 μM

Figure 21. *Pyridomycin, **44**, a natural product InhA inhibitor.*[130]

Pyridomycin has been shown to exhibit an MIC of 1.1 μM against wild-type *Mtb*. Through genetic sequencing of pyridomycin-resistant strains of *Mtb*, Hartkoorn *et al*. were able to identify InhA as Pyridomycin's the primary target.[129] While no IC_{50} value was reported for the compound, the group did resolve the crystal structure of pyridomycin bound to InhA, which revealed a hitherto unseen binding trait, pyridomycin occupies both the substrate and NADH binding sites (**Figure 22**).[130]

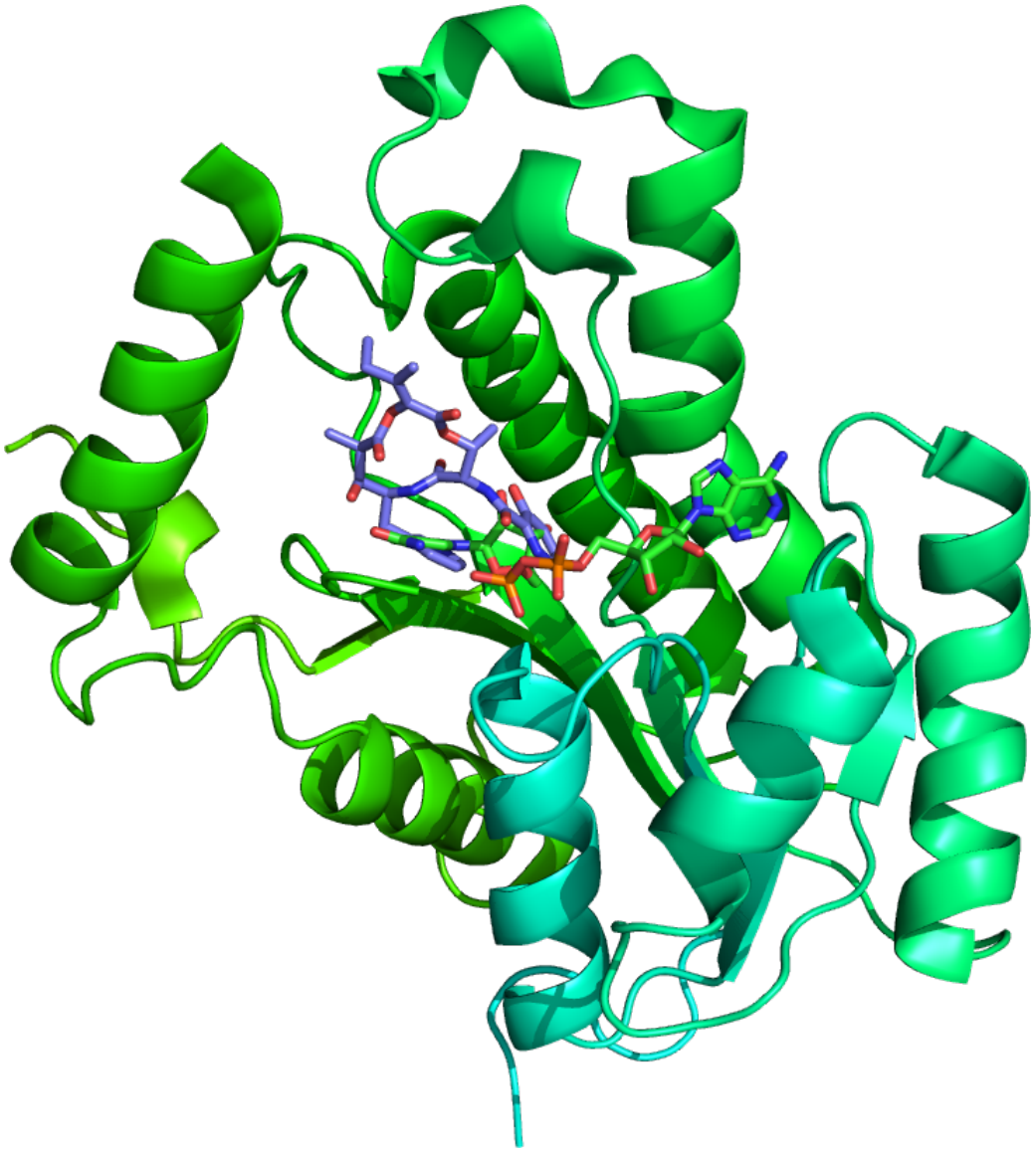

Figure 22. *Crystal structure of pyridomycin bound to InhA, showing the overlap between pyridomycin and the NADH binding site. Pyridomycin shown with blue carbons, NAD^+ shown with yellow carbons. (PDB: 4BII, 1.95 Å).*[130]

All previously disclosed direct inhibitors of InhA have only occupied the substrate binding site, whereas pyridomycin provided the first evidence that multiple different binding site are possible for InhA inhibitors. This could potentially lead to the identification of further inhibitors which break from the traditional binding mode.[130]

Clearly the area of direct InhA inhibitors represents a viable and attractive avenue for drug discovery, however there are as yet no such compounds being used in a clinical setting. This highlights the need for further work to identify more novel compounds which are able to inhibit the function of InhA.

1.12 Aims of the Work Presented in This Thesis

There is a significant need for novel compounds with anti-TB properties. InhA represents a clinically validated target which has been drugged in the clinic. This project aims to exploit InhA's large active site to design TCL-derivatives which are structurally larger, in an attempt to increase their selectively for InhA over other off-target protein. This work will focus on the synthesis of 4 series of compounds: triazole derivatives, ether-linked derivatives, amine-linked derivatives and A-ring modified ethers. The structure of these compounds will be informed by the use of *in silico* modelling. The Genetic Optimisation of Ligand Docking (GOLD) software package will be used to assess the potential binding modes of these compounds. Following their synthesis, biological evaluation will be performed using both isolated enzyme and whole-cell assays. This will provide a clear picture of the activities of all synthesised compounds and help elucidate further SAR information.

2. *In Silico* Drug Design

2.1. Computer-aided Drug Design

The ever-increasing availability of high-performance computers and expanded capabilities in protein structure determination techniques have brought with them major advances in drug discovery.[131, 132] Computer-aided Drug Design (CADD) lies at the intersection of these two disciplines. CADD techniques allow a streamlining of the long and complicated drug discovery process, particularly in the early stages.[133, 134] CADD plays 3 major roles in the drug discovery process:

1. Virtual screening of large compound libraries in order to filter out unsuitable compounds before experimental evaluation
2. Optimisation of lead molecule properties such as ADMET
3. Homology modelling and protein structure prediction

2.2 Genetic Optimisation for Ligand Docking (GOLD)

The Genetic Optimisation for Ligand Docking (GOLD) platform, from the Cambridge Crystallographic Data Centre (CCDC) was chosen as the lead docking platform.[135] GOLD has been extensively validated and proven successful at identifying inhibitors against a range of enzyme targets.[136-141]

GOLD interrogates the binding poses of small molecules within a defined binding site, this is done using a genetic algorithm (GA) for sampling conformational space. The GA is an algorithm which mimics evolution, this is due to the fact that starting poses are assigned as ‘chromosomes’ and each structural manipulation is referred to as a ‘mutation’.

GOLD explores the full conformational flexibility of each ligand it docks. In addition to ligand flexibility, GOLD assigns rational flexibility to the protein structure, allowing for rotational flexibility within selected protein hydrogens and hydroxyl groups in order to allow the arrangement of a hydrogen bonding network.

GOLD offers a significant degree of control and customisation for the end user, one way this manifests itself is in the form of the various scoring functions available. These scoring functions are responsible for the ranking of the predicted binding modes. The scoring functions available in GOLD are: GoldScore, ChemScore, Astex Statistical Potential (ASP) and PieceWise Linear Potential (PLP).

The GoldScore fitness function is the default scoring function for the GOLD platform. As part of the scoring function, GoldScore contains terms for hydrogen bonding interactions, hydrophobic binding energy and a molecular mechanics term which considered the internal energy of the ligand. The equation for this scoring function is given below in **Equation 1**.

$$GoldScore = (hb\_ext) + 1.375(vdw\_ext) + (hb\_\mathrm{int}) + (\mathrm{int})$$

Where:
(hb_ext) is the sum of the protein-ligand hydrogen bonding interactions
(vdw_ext) is the sum of the protein-ligand van der Waals interactions energy
(hb_int) is the sum of the intramolecular hydrogen bonding energy
(int) is the sum of the internal torsional energy and the internal vdw energy

Equation 1. *Formula used to calculate the GoldScore Fitness Score.*[135]

2.3 Validation of GOLD With Known InhA:Inhibitor Structures

In advance of using *in silico* drug discovery methods, it is necessary to validate the docking software that is to be used. This means assessing whether the software is able to recreate experimentally obtained ligand binding poses. If a software package is unable to accurately recreate an experimental binding pose, it would be unsuitable for further docking studies as it cannot accurately calculate the interactions occurring within the enzyme's active site. The standard method of assessing the quality of a binding pose is by calculating its root-mean square deviation (RMSD) compared to an experimental structure.[142] RMSD calculations can performed using the Maestro software package.[143, 144]

To assess to the quality of GOLD as an InhA docking platform, 6 structures were taken from the Research Collaboratory for Structure Bioinformatics (RCSB) database. Of these 6 structures, 4 contained small molecule inhibitors and 2 contained larger, more complex structures (NAD^+ and NAD-INH adduct). This was undertaken to test GOLD's ability to accurately interrogate the InhA active site with both small and large ligands. The structures of the validation ligands are shown in **Figure 23**.

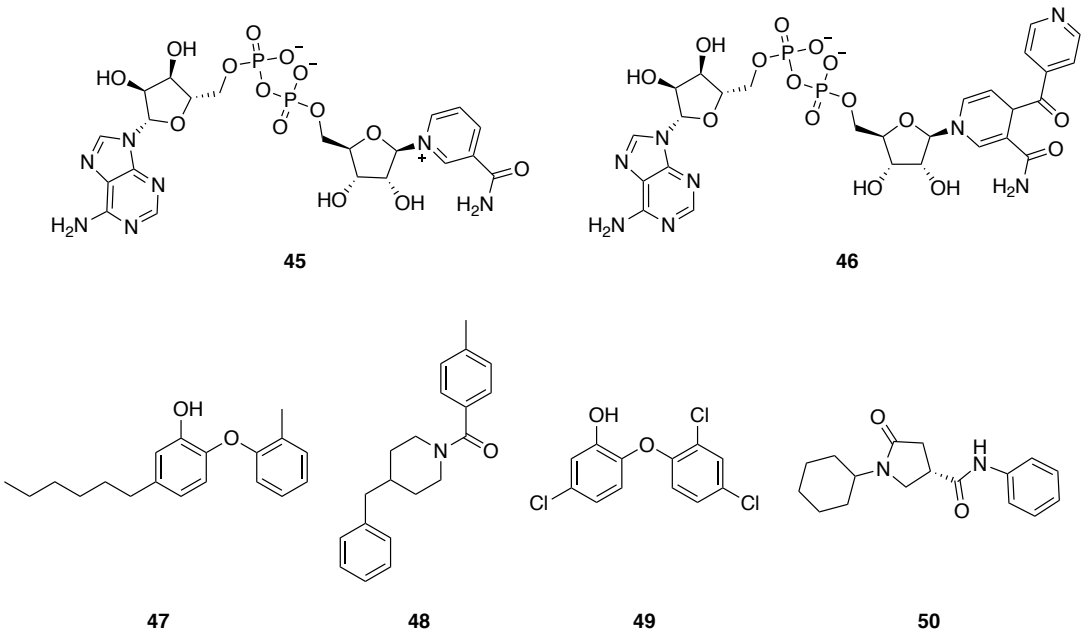

Figure 23. *The structures of the 6 ligands used in the validation studies for the GOLD docking platform.*

Before docking, all crystal structures were subject to preparation using the Maestro Protein Preparation tool. This highlights amino acid residues which display multiple occupancy, as well as highlighting residues with unexpected vacancies and missing side chains. Following this the crystal structures were subject to energetic minimisation and optimisation to reconstruct their hydrogen bonding networks. The co-crystalised ligands were extracted and re-docked into their respective crystal structures in order to investigate how well GOLD was able to recreate experimentally observed binding poses. An average RMSD value was calculated for each protein:ligand complex. The results are shown in **Table 2**.

Table 2. *RMSD calculations for docking solutions generated by GOLD for 6 different InhA:Ligand complexes*

PDB Accession Code	Resolution / Å	Ligand	Number of Poses Generated	Average RMSD / Å
1ENY	2.2	**45**	10	4.69
1ZID	2.7	**46**	10	4.13
2X23	1.8	**47**	9	1.54
2NSD	1.9	**48**	9	1.56
1P45	2.6	**49**	3	0.87
4U0J	1.6	**50**	3	0.80

Typically an RMSD value of ~ 2 Å indicates an accurate recreation of an experimentally determined binding pose. The average RMSD for the larger compounds (**45** and **46**) falls outside of the accepted range, with average values of 4.69 and 4.13. This is likely due to the greater complexity of the NAD^+ and NAD-INH structures meaning it is harder to recreate their binding poses. However, these two structures (**45** and **46**) are significantly larger than molecules typically explored during the drug discovery process. As can be seen from the data in **Table 2**, GOLD is able to recreate binding poses well within the 2 Å limit for the small molecules being interrogated (**47**-**50**). The overlay images of the experimental and calculated binding poses are shown in **Figure 24**.

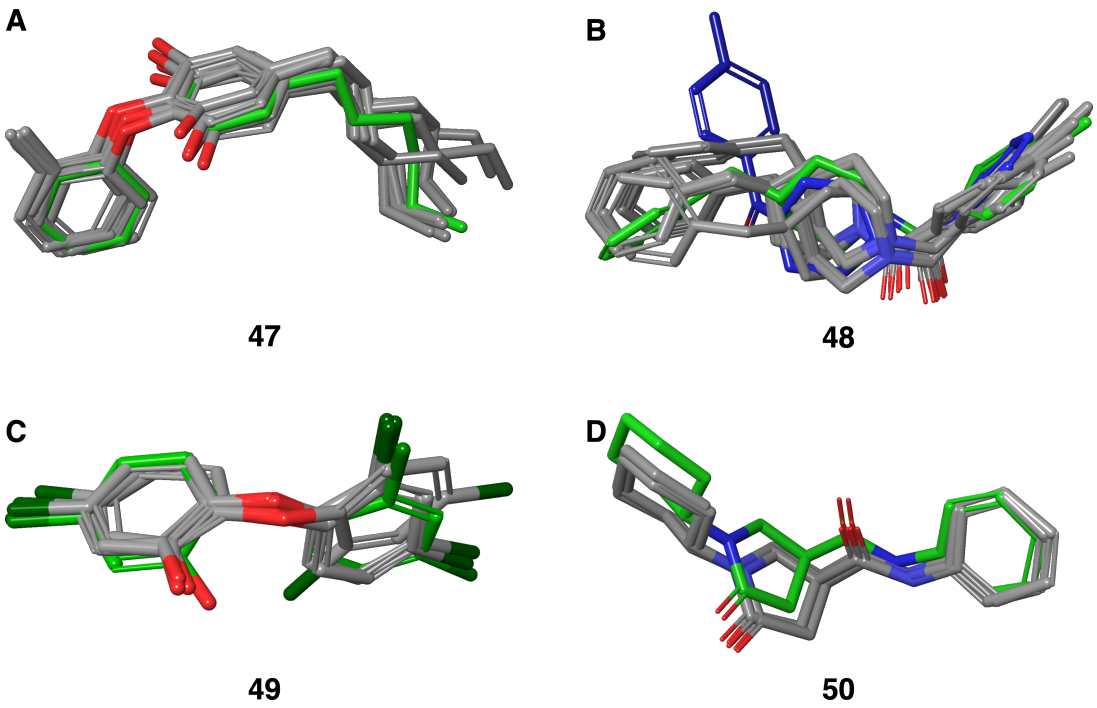

Figure 24. *The docking poses generated for 4 small-molecule InhA inhibitors overlaid on top of the experimentally observed binding poses. Experimental structures are shown with green carbons, 'good' calculated structures shown with grey carbons, 'bad' calculated structures shown with blue carbons.*

For **47**, **49** and **50**, in all cases the predicted binding mode showed a very good similarity to the experimental modes, retaining the key interactions. In the case of **48**, one of the predicted structures deviated significantly from the experimental structure (shown in blue). However, GOLD produced a further 8 poses which had a very similar orientation as the experimentally observed structure. These results show GOLD is robust and accurate at reproducing the structures of small molecule inhibitors of InhA and thus is a valid platform for designing novel InhA inhibitors.

2.4 The TCL:InhA Complex

The use of TCL derivatives as InhA inhibitors has previously been discussed (**Section 1.11.4**).

Solution of the TCL:InhA crystal structure revealed a unique binding trait with two molecules of TCL are capable of binding to the InhA active site (**Figure 25**). This is in contrast to the single TCL molecules observed in the active site of various InhA homologues.[145-147] InhA's ability to accommodate two TCL molecules likely reflects the increased volume of its active site, required to facilitate its large natural substrate. Further inspection of the 1P45 crystal structure also reveals that the two TCL molecules lie only 4.1 Å from one another.

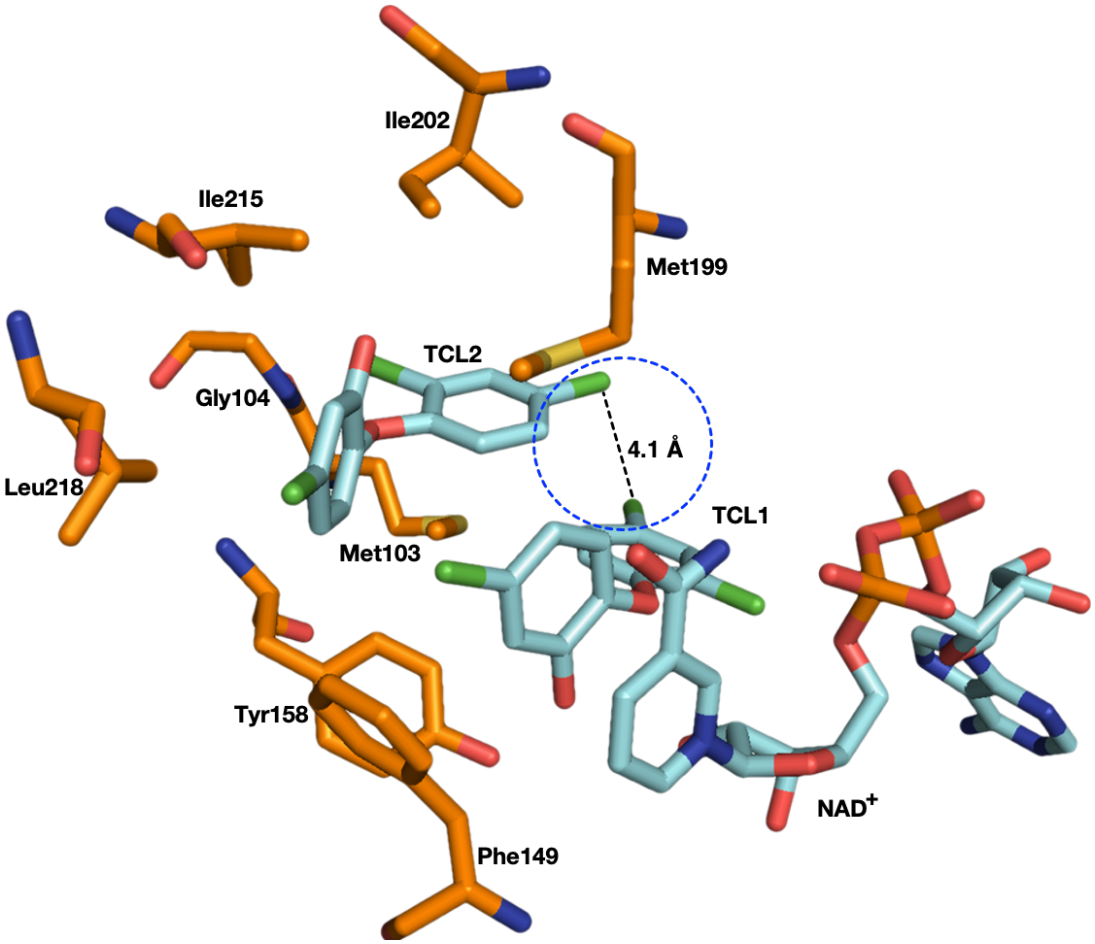

Figure 25. *Crystal structure of two TCL molecules in the InhA active site, showing the distance between the Cl atoms as 4.1 Å. TCL molecules and NAD+ shown with grey carbons, select protein residues shown with orange carbons. (PDB: 1P45, 2.6 Å).*[99]

The full protein:ligand interactions are shown in **Figure 26**. Briefly, the phenolate group engages in a hydrogen bonding network with Tyr158 and the ribose moiety of the NAD^+ co-factor. It is believed that the phenolate group allows TCL to mimic the enolate intermediate generated during the InhA catalytic cycle.[145] Additional π-π stacking interactions are observed between the A-ring and the pyrimidine ring and Phe149. Analysis of the second TCL molecule reveals its binding is driven purely by hydrophobic interactions with residues in the substrate binding loop.

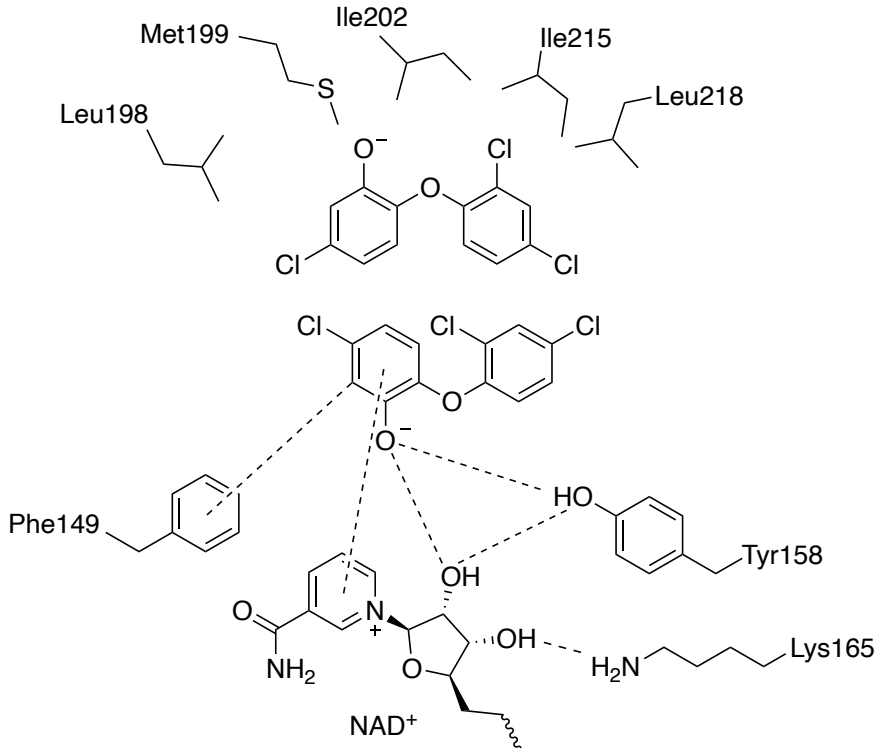

Figure 26. *Binding mode of both TCL observed in the InhA active site, key interactions are shown with dashed lines.*

This raises the concept of designing di-TCL or di-TCL-like molecules which contain two TCL-like fragments which could occupy both of these binding sites. This approach could hold the dual benefit of increasing compound potency through stronger protein binding, but also increasing the specificity of the inhibitors. Due to TCL's relatively small size, it is capable of binding to a range of proteins in a various different bacteria. The specific design of di-TCL should result in compounds which are too large to bind to off-target proteins, this could increase their specificity for InhA and thus potency towards *Mtb*.

2.5 Design of di-TCL Derivatives

In order for any di-TCL derivatives to engage both of binding sites, a suitable linker must be selected join the two fragments. To this end, two different linker strategies were selected for investigation: rigid linkers and flexible linkers. The rigid linker strategy was designed to attempt to provide a fixed geometry that would force the second TCL fragment into the rear binding site, thus engaging the substrate binding loop. The flexible linker strategy focused on allowing a greater deal of conformational freedom to the attached fragment, which would allow it to explore not only the second binding site, but also the rest of the active site. These two strategies are summarised in **Figure 27**.

Rigid Linker

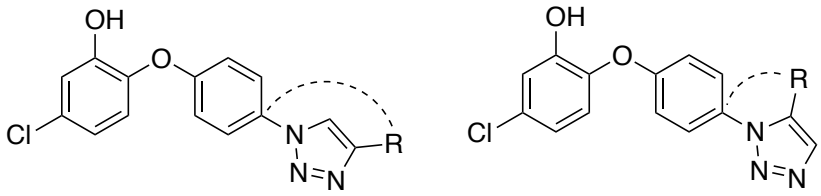

51 **52**

Geometry dictated by rigid triazole ring

Flexible Linker

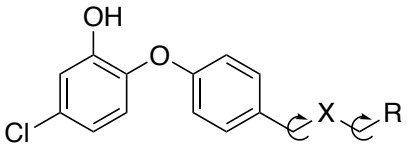

53

Free rotation along the chain
X = O or NH

Figure 27. *Structures summarising the difference between the rigid and flexible linker approaches to di-TCL compounds.*

Figure 27 shows how, when linked through a 1,2,3-disubstituted triazole ring (**51** and **52**), the geometry between benzene carbon atom and the R group is dictated by the nature of the triazole, indicated by the dashed lines. Triazole **51** shows how the 1,5 geometry directs the R back towards the TCL unit. On the other hand, the 1,4-triazole, **52**, has a much flatter relationship with the biaryl ring system. The flexible linkers, **53**, do not have the same geometric constraints as the triazole rings, with free rotation possible throughout the linear chains. This difference between the **51** and **52** triazoles was further inspected using the Maestro software package to measure the C-N-R angle (**Figure 28**).

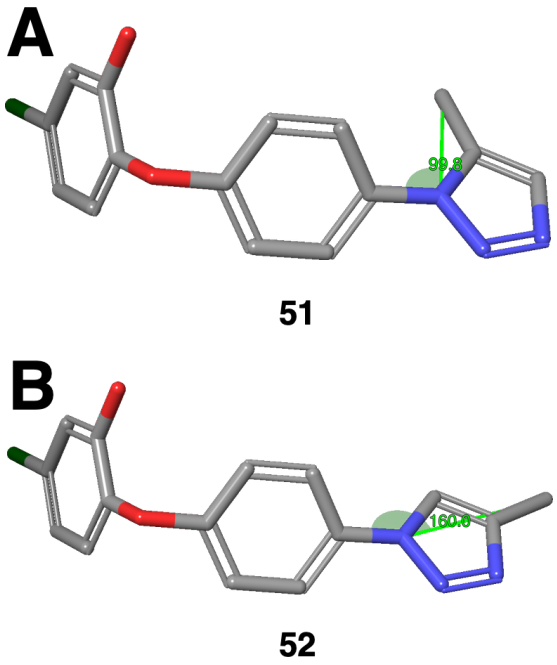

Figure 28. *Comparison of the C-N-R bond angle between **51** and **52**, showing the influence of the triazole geometry.*

For the 1,5-triazole, the C-N-R angle was calculated to be 99.8° compared to 160.0° in the 1,4-triazole. This shows the subtle but important difference between the suitability of the 1,4 and 1,5-triazole rings as rigid directing moieties.

2.6 Docking of Chlorinated-Triazole Derivatives

Next, the GOLD docking platform was used to probe the possible differences between the binding modes of the 1,4 and 1,5-triazole derivatives. Two di-TCL derivatives were designed, fusing two TCL moieties through a 1,4 and 1,5-triazole. These compounds were then docked into 1P45 crystal structure in order to investigate their predicted binding modes and how they compared to the experimentally observed TCL:InhA complex (**Figure 29**).

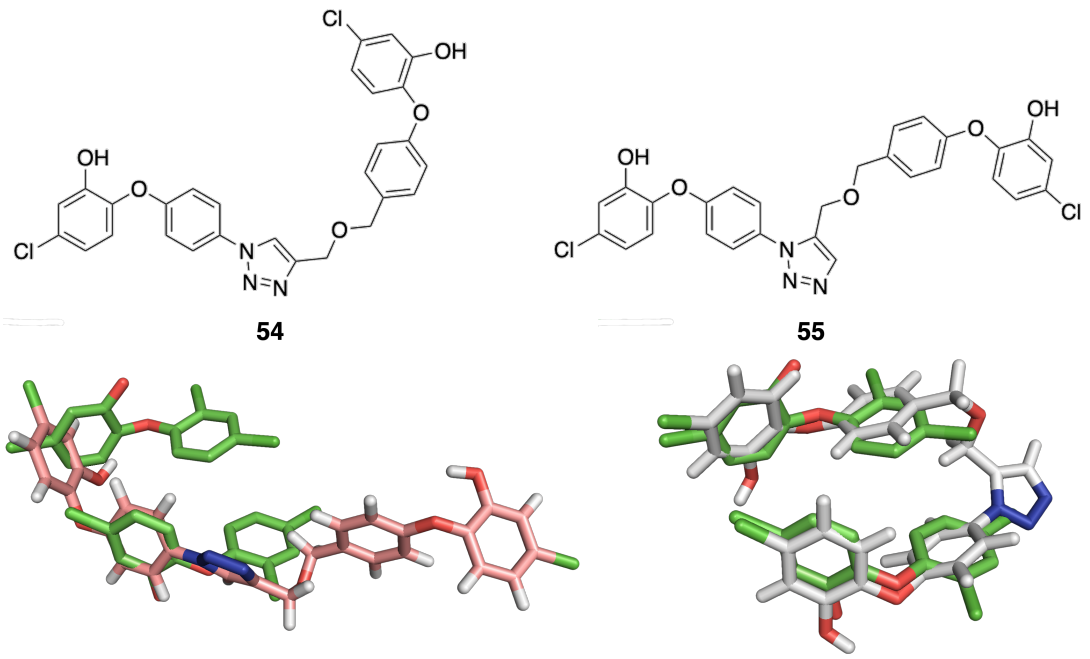

Figure 29. *Comparison of the calculated binding poses for **54** and **55**, showing the overlap with the two TCL molecules in the InhA binding site. TCL molecules shown with orange carbons. Calculated structures shown with grey carbon. PDB: 1P45.*

As can be seen by these docking poses, the 1,4-triazole **54** shows a perturbation of the experimentally determined TCL binding mode. The second TCL fragment was not predicted to occupy the substrate binding loop region of the active site. This suggests that the 1,4-triazole motif is not an appropriate linker for the intended purposes. Conversely, the binding pose of **55** shows a very good overlap with both of the experimentally observed TCLs. In addition to occupying both binding sites, the 1,5-triazole motif also retained the key hydrogen bonding arrangement that is observed in a variety of potent, direct InhA inhibitors.

Based on these results, a range of truncated di-TCL derivates were designed. These compounds had only a single aryl ring attached to the TCL-triazole, *in lieu* of a biaryl ether scaffold. Both of Cl atoms were removed from B-ring, in-line with Sivaraman's

findings that they are not required for potent InhA inhibition.[101] These compounds are shown in **Figure 30**.

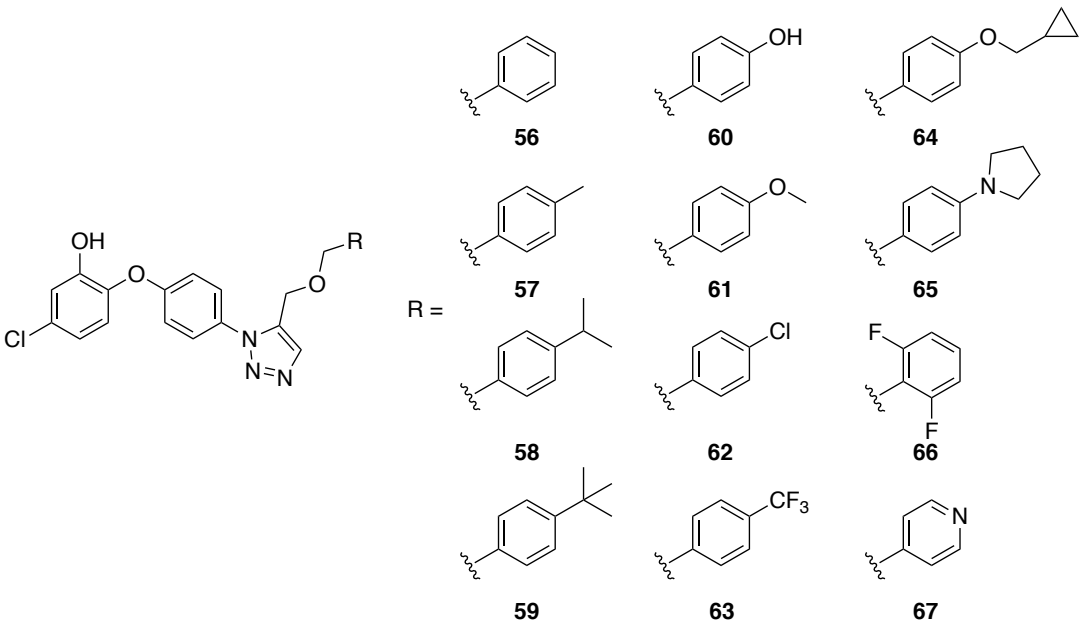

Figure 30. *Structures of a range of 1,5-triazoles designed as potential InhA inhibitors.*

The compounds were then docked into the InhA 1P45 crystal structure to assess their ability to bind to InhA (**Table 3**).

Table 3. *Docking scores and key interactions for compounds **54-67**.*

Compound	GOLD Fitness Score	NAD^+ Hydrogen Bond	Phe149 π-π stacking	Other Interactions
54	75.7	×	✓	Arg43 Ile215
55	87.7	✓	✓	×
56	65.2	✓	×	Lys165
57	73.5	✓	×	×
58	77.8	✓	✓	×
59	74.0	✓	×	Lys165
60	69.0	✓	×	Lys165
61	76.7	✓	✓	×
62	73.2	✓	×	Met98
63	75.6	✓	×	Met98
64	80.7	✓	✓	×
65	83.6	✓	✓	×
66	71.0	✓	✓	×
67	71.3	✓	✓	×

Pleasingly, all of the designed 1,5-triazoles showed a similar predicted binding mode as **55**, that is to say the two linked fragments anchored into each of the observed binding sites. Importantly, the 1,5 derivatives all engaged in a H-bonding interaction with the ribose unit of the NAD^+ cofactor. This is a key interaction for both the InhA natural substrate and the vast majority of published inhibitors. Beyond the ribose interaction, a number of compounds were predicted to engage in a π—π stacking interaction with Phe 149. Interestingly, when R was an electron withdrawing group (**62** or **63**) a further interaction was made with Met98. A review of the literature shows that this interaction is also observed in the methyl thiazole class of InhA inhibitors (**Section 1.11.4**, **Figure 14**).[110] An electrostatic interaction between the A-ring phenolate and Lys165 was also predicated for **56**, **59** and **60**, this interaction seemed

to be at the expense of the π—π stacking with Phe149, as this was lost in all instances. The 1,4-triazole, **54**, was the only compound to show a unique binding mode and did not occupy both TCL binding sites. This binding mode allowed it to engage in a number of interactions not observed in the 1,5 derivatives. Arg43 was predicted to engage the ligand in a cation-π interaction, as well as an H-bond interaction with the phenol group. A halogen bonding interaction was also predicted between the Ile215 backbone carbonyl and the ligand's Cl atom.

In terms of fitness scoring, **55** showed the highest score, suggesting it is well designed to bind to InhA. Scores seem to loosely suggest that increasing hydrophobicity of the R group results in increased binding, however there do seem to be some steric limitations. Moving from H -> ^{i}Pr (**56** -> **58**) an increase in fitness score is seen, however, when R is ^{t}Bu, the docking score falls, suggesting that particularly bulky groups are may be poorly tolerated. The important balance between size and hydrophobicity is further supported by the encouraging score of **64** (R = methyl cylcopropyl), this compound showed a score of 83.6, the second highest behind **55**.

A number of representative docking poses and interactions are shown in **Figure 31**.

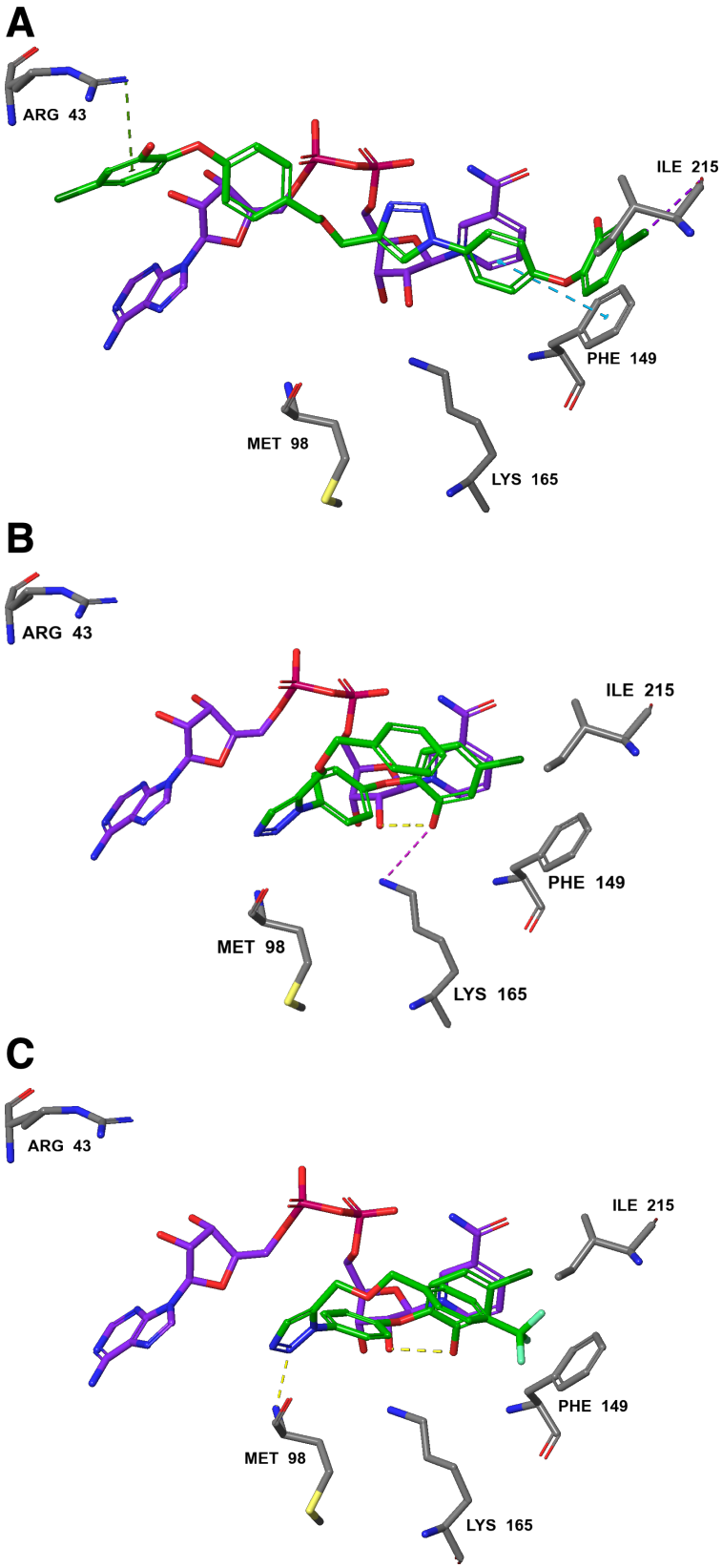

Figure 31. *Binding poses and key interactions for A)* ***54****. B)* ***56****. C)* ***63.*** *Hydrogen bonds shown in yellow, electrostatics in blue, π-π stacking in light blue, cation-π in orange.*

As previously demonstrated in **Figure 29**, when a 1,4-triazole unit links two TCL fragments, the second fragment occupies an unexpected binding region. This allows **54** to interact with the peripheral Arg43 residue, through a cation-π interaction. **56** shows retention of the desired being binding mode, consistent with all the 1,5-triazoles, with overlap into both TCL sites being predicted. An electrostatic interaction can be seen through Lys165 and the phenolate group on the A-ring. For the **63** it can be seen that the triazole unit extends far enough to engage the Met98 residue through an H-bonding interaction with the protein backbone.

2.7 Docking of *n*-Propylated-Triazole Derivatives

As previously discussed in section **1.11.4**, A-ring modifications have been well explored for TCL derivatives targeting InhA.[106] With this in mind, a series of 1,5-triazoles bearing an *n*-propyl chain *in lieu* of the A-ring Cl atom were designed (**Figure 32**).

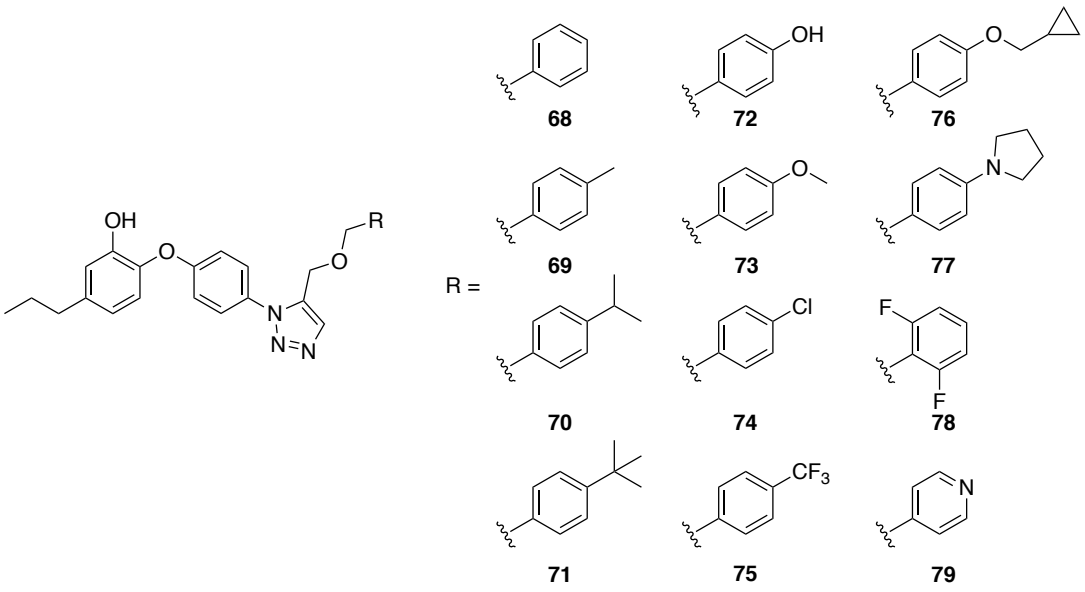

Figure 32. *Structures of a range of 1,5-triazoles designed as potential InhA inhibitors.*

These compounds shared the same R group as the chlorinated derivatives and were designed to exploit the hydrophobic pocket into which the A-ring Cl atom points. The binding potential of these compounds was evaluated in GOLD, scores and interactions are shown in **Table 4**.

Table 4. *Docking scores and key interactions for compounds **68-79**.*

Compound	GOLD Fitness Score	NAD^+ Hydrogen Bond	Phe149 π-π stacking	Other Interactions
68	82.7	✓	✓	×
69	83.0	✓	✓	×
70	79.7	✓	×	×
71	80.0	✓	✓	×
72	80.4	✓	✓	×
73	84.6	✓	✓	×
74	81.6	✓	✓	×
75	83.0	✓	×	×
76	78.0	✓	✓	×
77	82.2	✓	✓	×
78	82.2	✓	✓	×
79	82.3	✓	✓	Tyr158

In comparison to the chlorinated derivatives (**Table 3**) the propylated derivatives show higher fitness scores. As had been predicted, the propyl chain directs into the hydrophobic cleft, resulting in higher binding scores. Interestingly, where a chlorinated derivatives showed extra interactions (Met98, Lys165, Arg43, Ile215) the propyl chain compounds do not show any such additional interactions. Only **79** engages in an addition interaction, an H-bond with Tyr158. Interestingly, **70** and **75** showed no other interactions other than the H-bond with the co-factor, suggesting

their binding was largely driven by hydrophobic interactions. Two representative binding modes are shown in **Figure 33**.

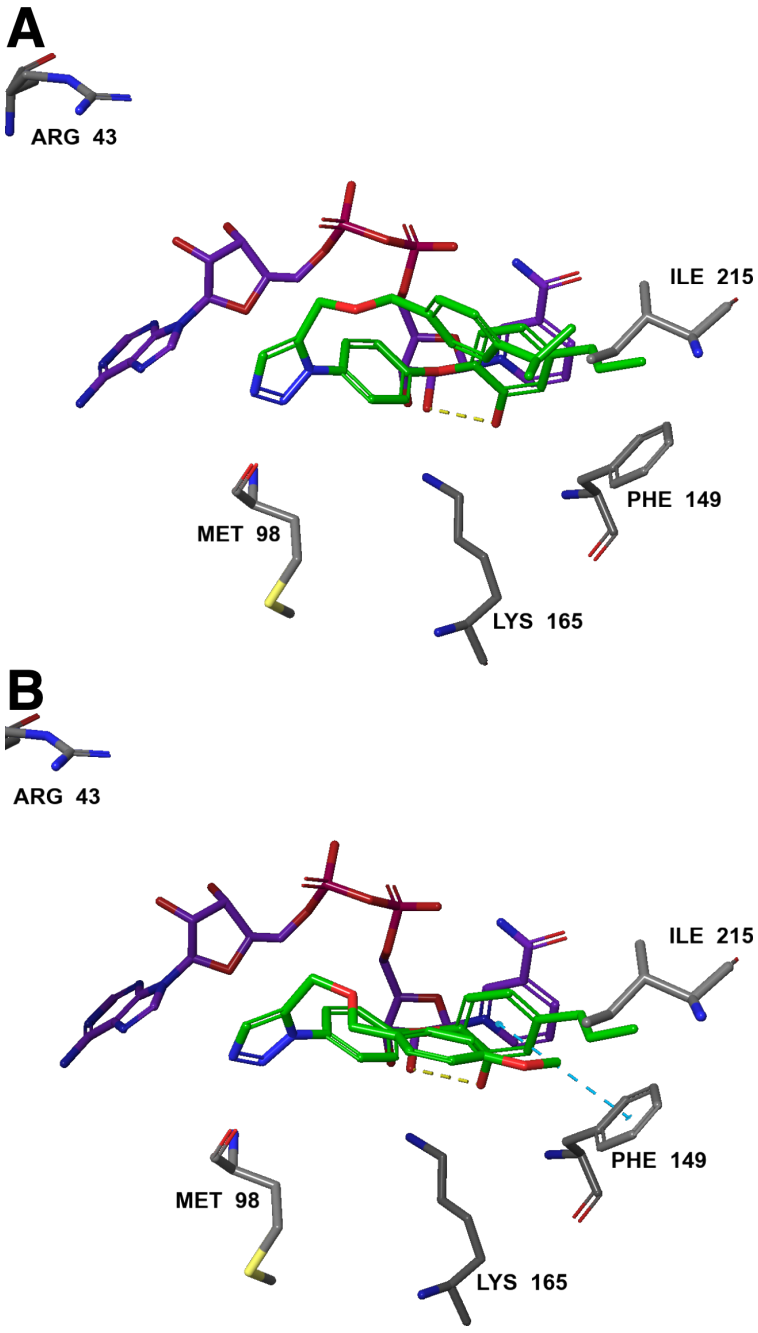

Figure 33. *Binding poses and key interactions for A) **70**. B) **73**. Hydrogen bonds shown in yellow, π—π stacking in light blue.*

The binding mode for all of the propylated 1,5-triazoles was consistent with the chlorinated derivatives (**Figure 31**), with overlap observed in both of the desired binding sites for all compounds.

2.8 Docking of Ether Derivative Target Molecules

In order to explore the potential of 'flexible' linker TCL derivatives, a range of ether-linked of compounds were designed (**Figure 34**).

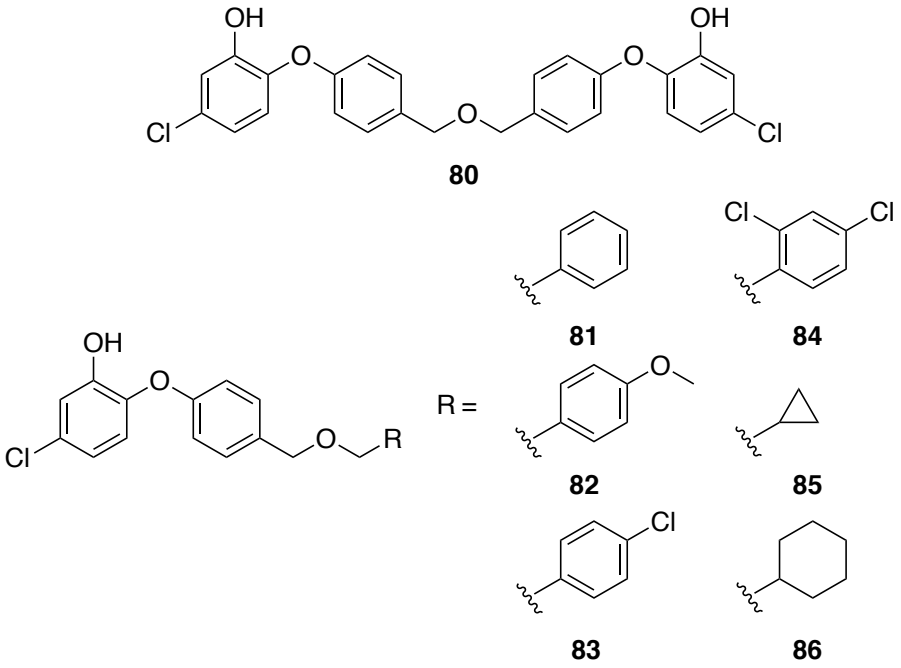

Figure 34. *Structure of a range of ether-linked compounds designed as potential InhA inhibitors.*

These compounds were then evaluated in GOLD in order to assess their ability to bind to InhA (**Table 5**).

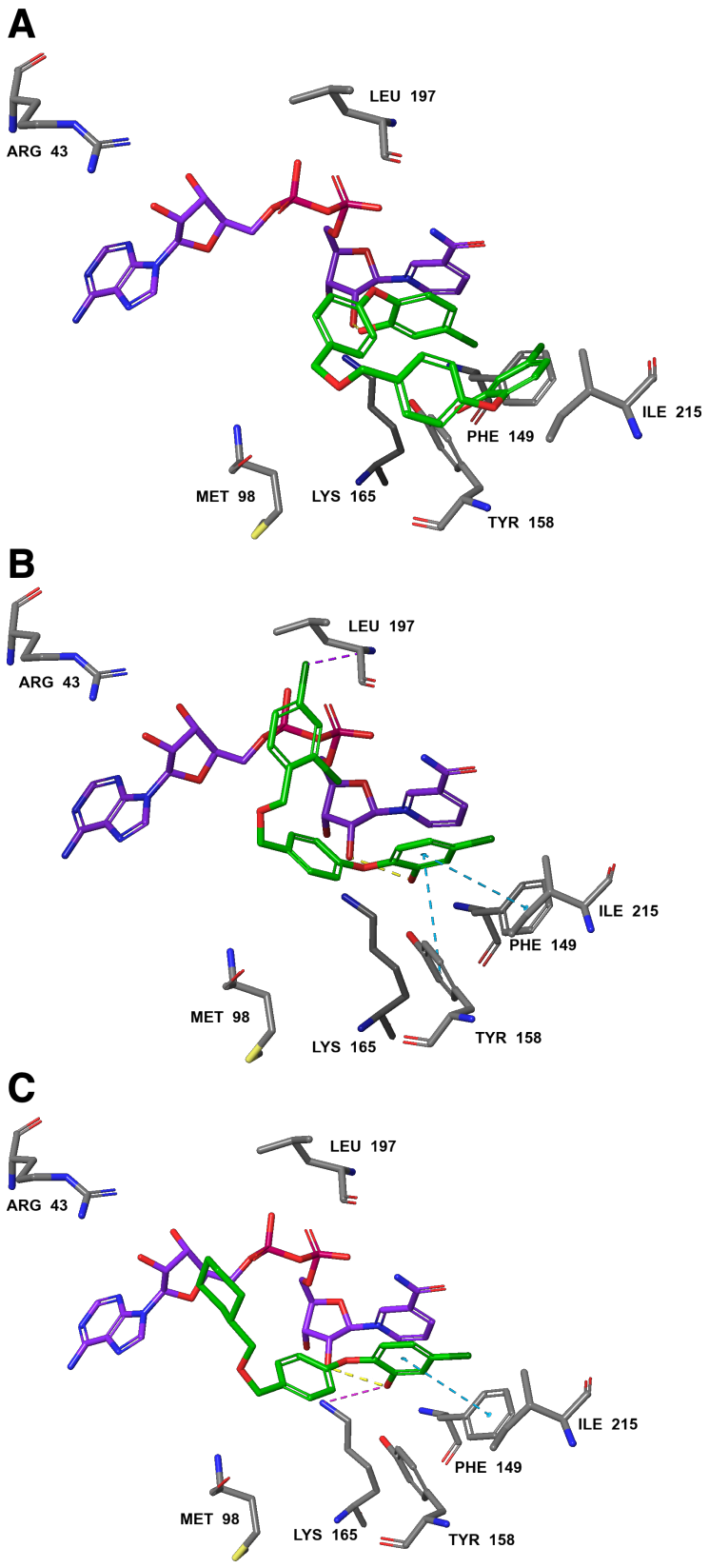

Figure 35. *Binding poses and key interactions for A) **80**. B) **84**. C) **86**. Hydrogen bonds shown in yellow, electrostatics in blue, π-π stacking in light blue, cation-π in orange.*

Table 5. *Docking scores and key interactions for compounds **80-86**.*

Compound	GOLD Fitness Score	NAD^+ Hydrogen Bond	Phe149 π-π stacking	Other Interactions
80	65.3	✓	×	×
81	64.5	✓	✓	×
82	67.4	✓	✓	×
83	70.8	✓	✓	Leu197
84	72.0	✓	✓	Leu197 Tyr158
85	61.2	✓	✓	×
86	59.6	✓	✓	Lys165

While the fitness scores for these compounds are lower than the triazole derivatives, they are still encouraging. Broadly it seems that aromatic rings are preferred, with substituted aryl rings showing the highest fitness scores. Importantly, the binding modes showed retention of the key H-bond interaction with the NAD^+ co-factor. All compounds, bar **80**, engaged Phe149 in an edge-face π—π stacking interaction. The two chlorinated molecules (**83** and **84**) also benefited from halogen bonding with the Leu197 backbone. An additional electrostatic interaction was observed between the **86** phenolate and that catalytically relevant Lys165 residue. A number of representative binding modes are shown in Figure **35**.

It is interesting to note that both **84** and **86** show a different binding mode to **80**. Rather than looping directly back into the second TCL binding region, the R groups point almost perpendicular to the biphenyl ether. This supports the notion that the greater conformation freedom of the ether linkage will allow for interrogation of a greater range of space within the InhA active site.

2.9 Docking of Amine Derivative Target Molecules

In order to explore the potential effects of charge state on the flexible linker derivatives, a number of amine linked compounds were designed. It was thought that the presence of an ammonium ion, at physiological pH, could result in additional interactions, possibly with the pyrophosphate moiety of the NAD(H) cofactor. The designed amine linked compounds are shown in **Figure 36**.

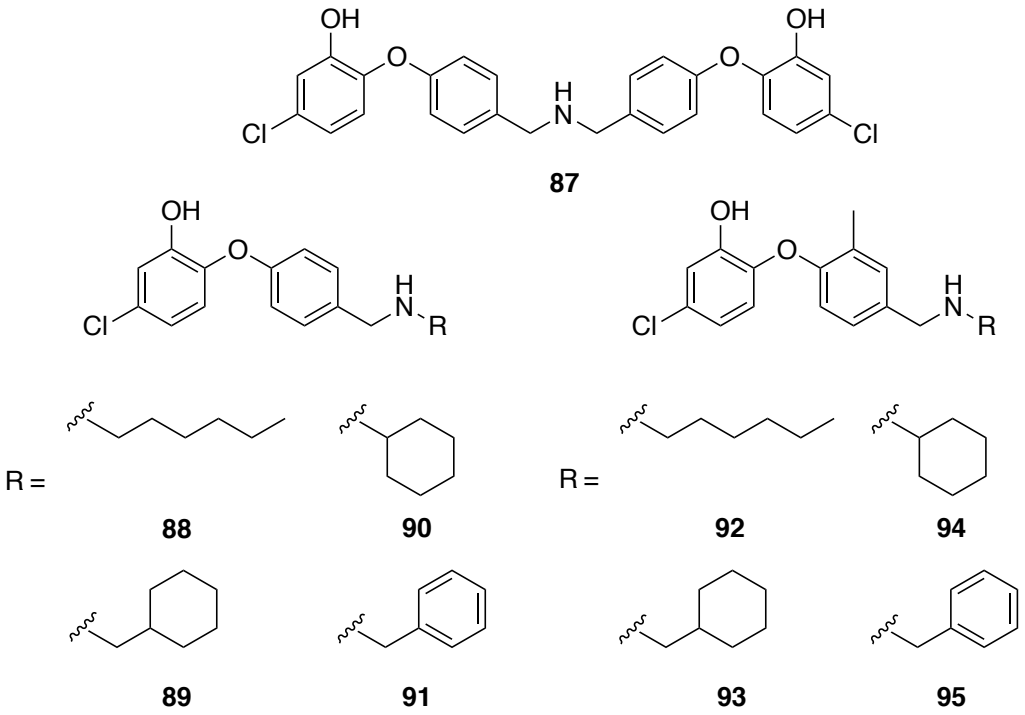

Figure 36. *Structure of a range of amine-linked compounds designed as potential InhA inhibitors.*

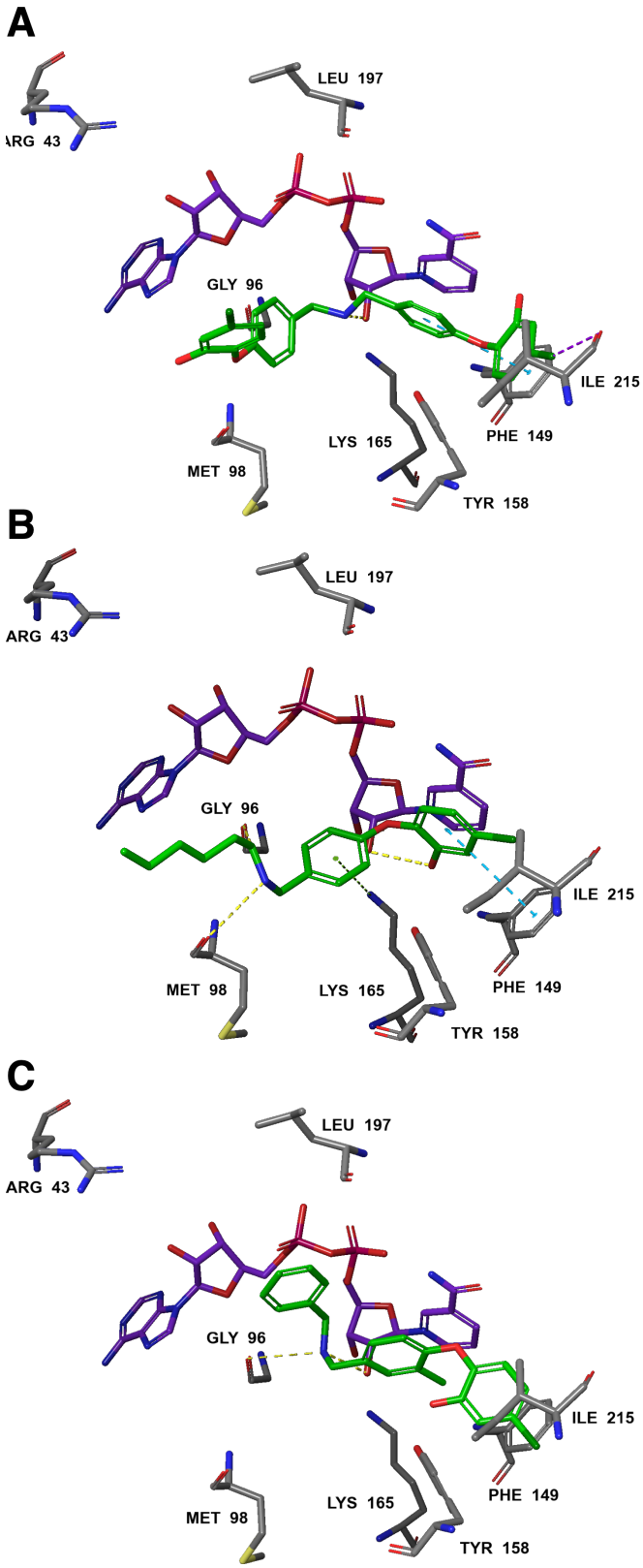

Figure 37. *Binding poses and key interactions for A) **87**. B) **88**. C) **91**. Hydrogen bonds shown in yellow, electrostatics in blue, π-π stacking in light blue, cation-π in orange.*

The rationale behind the introduction of an *ortho* methyl substituent on the B-ring (**92**-**95**) comes from the previous work of Luckner *et al*.[107] During their studies, they demonstrated that introduction of a methyl group to the *ortho* position of the B-ring resulted in a significantly increased residence time for their inhibitor within the InhA active site. This increased residence time is likely down to the methyl group reducing the rotational freedom around the biaryl ether bond, this in turn results in a lower entropic penalty upon organisation within the InhA active site. Docking scores for the amine-linked derivatives are shown in **Table 6**.

Table 6. *Docking scores and key interactions for compounds **87-95**.*

Compound	GOLD Fitness Score	NAD^+ Hydrogen Bond	Phe149 π-π stacking	Other Interactions
87	81.3	✓	✓	Ile215
88	72.4	✓	✓	Met98 Lys165
89	70.3	✓	✓	Ile215
90	71.2	✓	✓	Gly96
91	64.7	✓	✓	×
92	77.7	✓	✓	Met98 Lys165
93	69.0	✓	×	Arg43
94	71.4	✓	✓	Met98 Lys165
95	70.5	✓	×	Gly96

Again, all compounds were able to engage the ribose moiety with an H-bond. Two compounds, **90** and **95** were predicted to engage in a further H-bonding interaction with the Gly96 backbone. A number of compounds (**88**, **92**, **94**) demonstrated cation-π interactions with Lys165, in addition to H-bonding interactions with Met98. Representative docking poses and interactions are shown in **Figure 37**.

Unlike the triazole and ether linked compounds, the amine derivatives showed a number of different binding poses. As can be seen for **87**, the amine linking the two fragments engages the ribose unit to make the crucial hydrogen bonding interaction. This sees one of TCL units shifted up into the substrate binding loop, which facilitates a halogen bonding interaction with Ile215. Compound **88** retains the experimentally observed binding mode, with the phenolate being responsible for the key H-bonding interaction, however, a number of additional interactions are also predicted. Firstly, a cation-π interaction is predicted between Lys165 and the B-ring, at the same time an H-bonding network between Met98 and the amine-linker is also expected. Finally, for **91**, the ribose unit interacts with amine group, which also engages the Gly96 backbone through an H-bond. As with **87**, the biaryl ether unit in **91** moves further up into the substrate binding loop.

2.10 Docking of A-Ring Derivative Target Molecules

In addition to the B-ring modified compounds discussed above, a number of more 'traditional' A-ring modified TCL derivatives were explored. Such compounds have previously demonstrated their potency as InhA inhibitors and this series of derivatives was designed to further expand the scope of A-ring modification SAR. These compounds are shown in **Figure 38**.

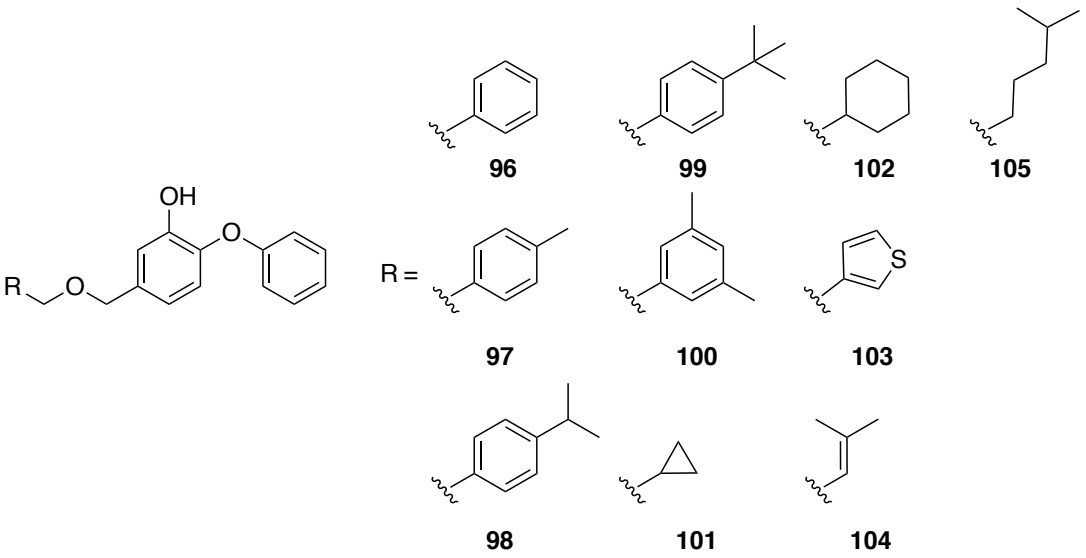

Figure 38. *Structure of a range of A-ring derivative compounds designed as potential InhA inhibitors*

The GOLD docking scores for **96**-**105** are shown in **Table 7**.

Table 7. *Docking scores and key interactions for compounds **96-105**.*

Compound	GOLD Fitness Score	NAD^+ Hydrogen Bond	Phe149 π-π stacking	Other Interactions
96	68.0	✓	✓	×
97	69.5	✓	✓	×
98	72.5	✓	✓	×
99	70.1	✓	✓	Tyr158
100	74.2	✓	✓	Tyr158
101	64.0	✓	✓	Tyr158 Lys165
102	67.3	✓	✓	×
103	70.9	✓	✓	Tyr158
104	68.1	✓	✓	Tyr158
105	70.5	✓	✓	×

Broadly speaking, fitness score tends to increase with the hydrophobicity of the R group, this is reasonable to expect as this group is pointing into a known hydrophobic cavity.

Representative binding modes for these compounds are shown in **Figure 39**.

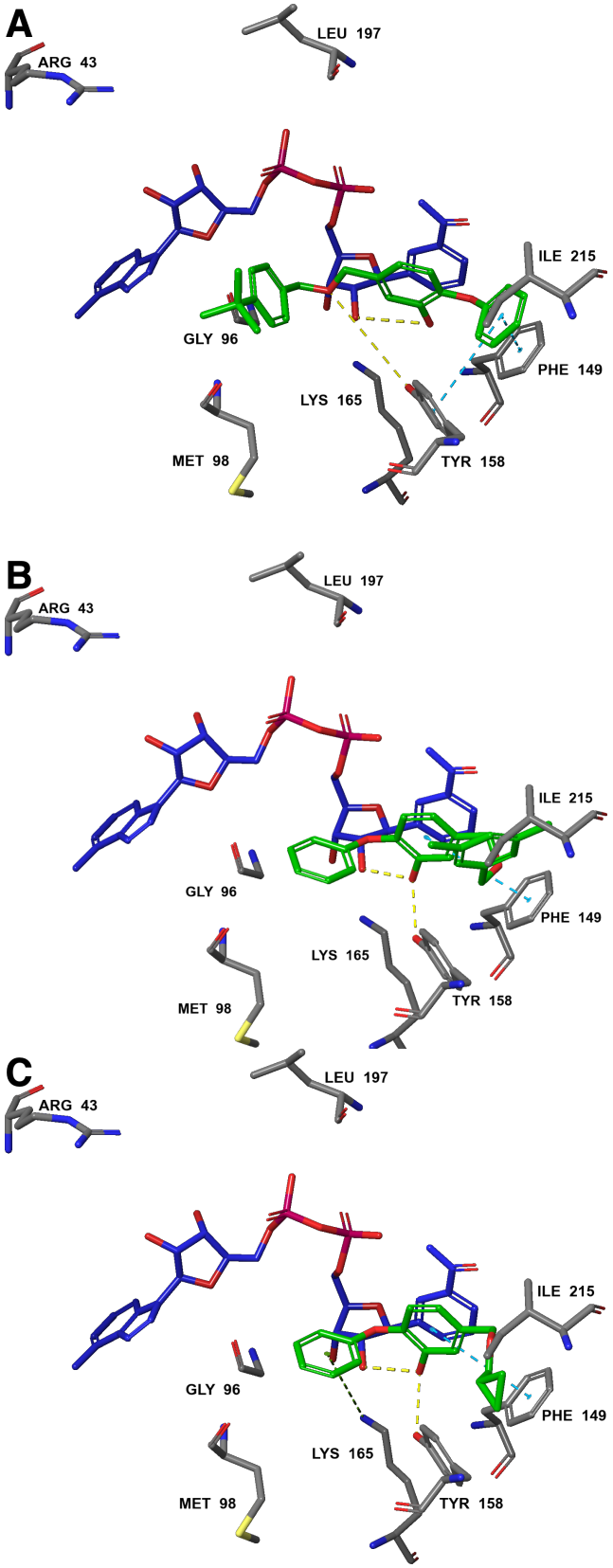

Figure 39. *Binding poses and key interactions for A)* ***99****. B)* ***100*** *C)* ***101*** *Hydrogen bonds shown in yellow, π-π stacking in light blue, cation-π in orange.*

Of the 10 compounds, only **99** showed a unique binding mode. Compound **99** shows an inversion of the expected binding mode, with the B-ring directing into the hydrophobic pocket. This inverted binding mode allows the B-ring to engage both Phe149 and Tyr158 in π-π stacking interactions. Tyr158 also forms an H-bond with the biaryl ether. The A-ring substituent occupies a space roughly parallel to the NAD^+ cofactor. Compound **100** shows a binding mode consistent with previously published A-ring modified TCL derivatives.[106] The phenolic oxygen on the A-ring engages in an H-bonding network with both the cofactor and Tyr158. An addition to a π—π stacking interaction between the A-ring and Phe149 is also observed, the R group points upwards towards the hydrophobic substrate binding loop. **101** shows a similar binding mode to **100**, however an additional cation-π interaction is seen between Lys165 and the B-ring on the biaryl ether.

3. Synthesis

3.1 Synthesis of Chlorinated-Triazole Target Molecules

The first series of target molecules were the chlorinated-triazoles. The docking studies (**Section 2.6**) suggested that these compounds were possibly promising candidates as InhA inhibitors. The 1,5-triazoles were of particular interest as these structures maintained the experimentally observed binding mode and showed encouraging docking scores. The structures of the first two target molecules are shown in **Figure 40**.

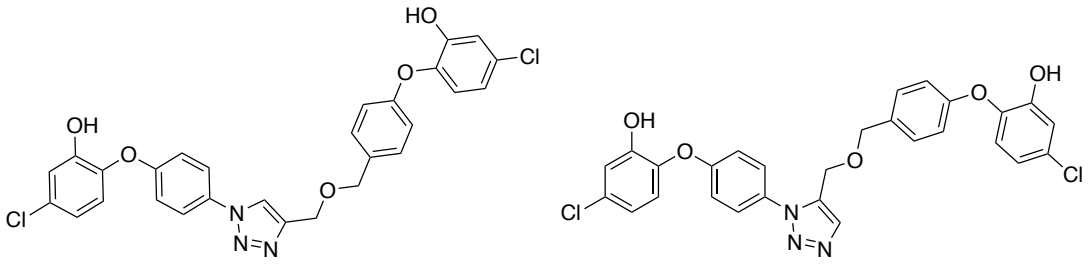

Figure 40. *The structures of the triazole target molecules **54** and **55**.*

A retrosynthetic analysis for target **55** is shown in **Scheme 5**.

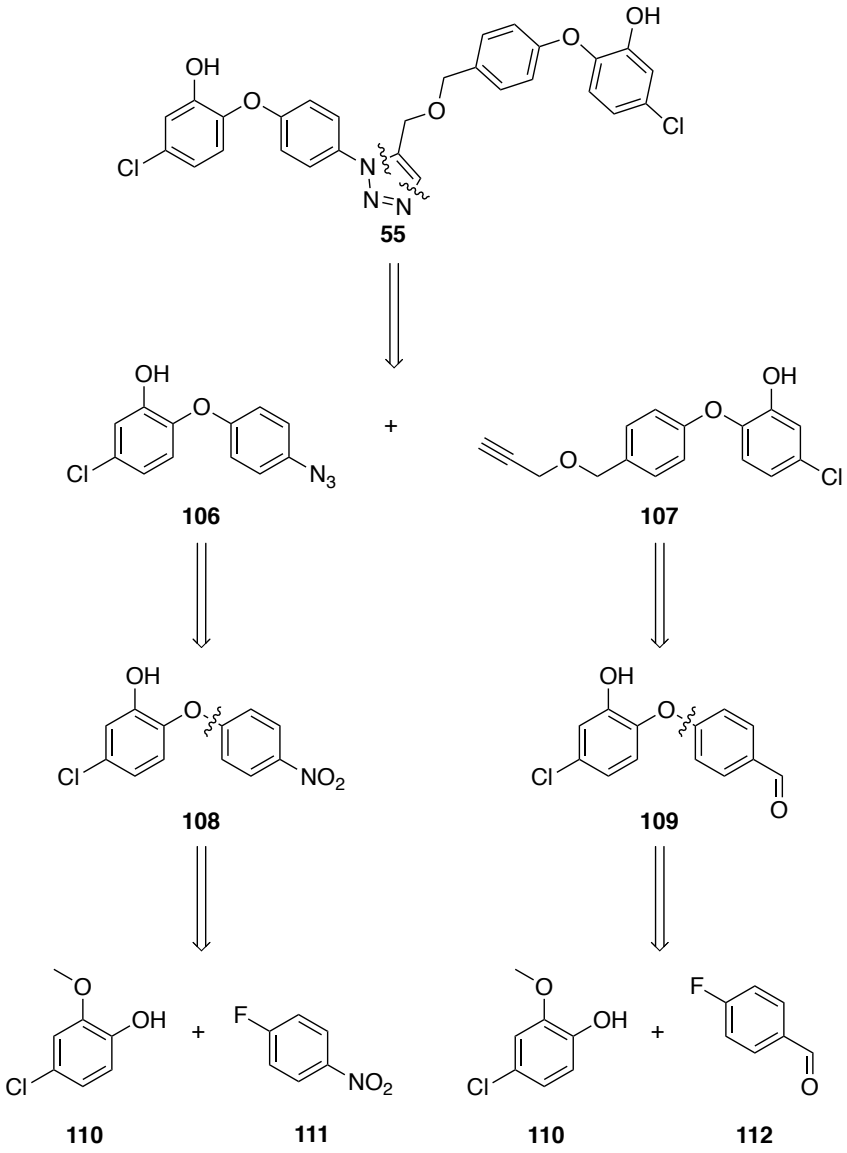

Scheme 5. *RSA of Triazole Target **55**.*

It was envisioned that the triazole structure would be assembled through a [1+3] dipolar cycloaddition 'Click Reaction' from fragments **106** and **107**. The required aryl azide would be obtained through functional group interconversion of the corresponding nitro derivative **108**. Alkyne fragment **107** could be accessed from aldehyde **109**. The basic biphenyl ether scaffolds would be assembled from the commercially available **110**, **111** and **112**. **108** and **109** share phenol **110** as a

common starting material. The forward synthesis of aniline **114** is shown in **Scheme 6**.

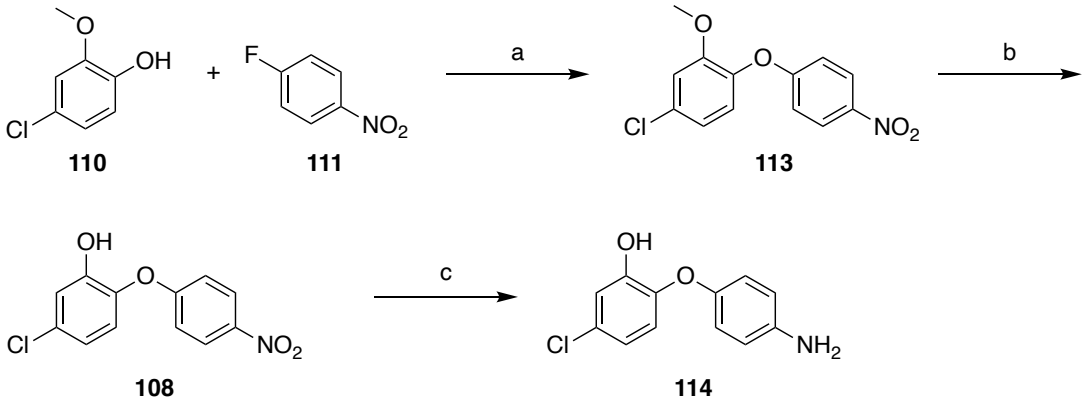

Scheme 6. *Forward synthesis of aniline **114**. a) K_2CO_3, DMF, 130 °C, 18 h, 93%. b) BBr_3, CH_2Cl_2, 0 °C → r.t., N_2 3 h, 86%. c) Zn, NH_4Cl, MeOH, r.t., 18 h, quant.*

Initial formation of the biphenyl ether scaffold proceeded smoothly using K_2CO_3 in DMF at an elevated temperature, furnishing the desired product in a good yield. Following this, BBr_3 mediated demethylation was carried out to unveil the phenol group. Reduction of the nitro group to the corresponding amine was performed using Zn dust and NH_4Cl, generating the desired product in excellent yield over 3 steps. The attempted conversion of aniline **114** to its corresponding aryl azide is shown in **Scheme 7**.

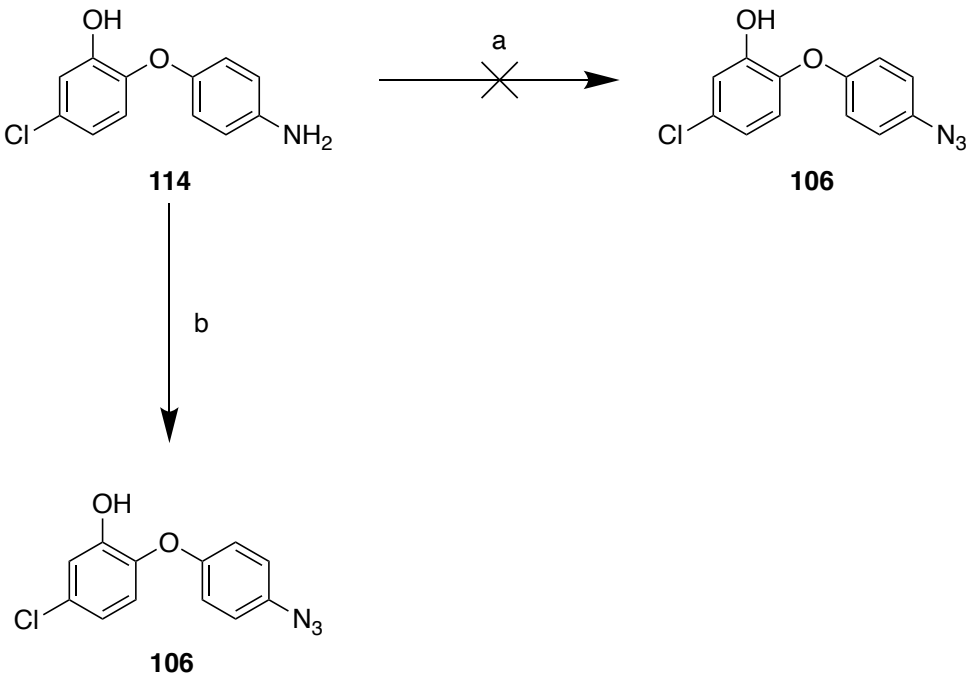

Scheme 7. *Conversion of aniline derivative **114** to aryl azide **106**. a) $NaNO_2$, NaN_3, HCl (aq), 0 °C → r.t., 3 h. b) ^tBuONO, $TMSN_3$, ACN, 0 °C → r.t. 3h, 80%.*

Initially, conversion of **114** to its corresponding aryl azide **106** was attempted using the standard $NaNO_2/NaN_3$ diazotisation method.[148] Unfortunately, this failed to generate the desired product despite complete consumption of the starting material, as judged by TLC. A review of the literature suggested that ^tBuONO and $TMSN_3$ can be used to provide efficient access to aryl azides.[149] These conditions generated the target compound in a good yield, with a single produced by mass spec, 260.0234 *m/z* (corresponding to the $[M-H]^-$ ion). An additional benefit of these reaction conditions was the elimination of the use of large quantities of NaN_3 (6 equiv). Not only is the use of excess NaN_3 wasteful, there are also significant safety ramifications accompanying the large-scale use of inorganic azides, including the requirement for effective quenching and disposal (*via* copper drainage pipes) after the reaction is complete. With the azide fragment in hand, focus turned to the synthesis of the

alkyne-bearing TCL fragment **107**. The synthesis of benzaldehyde **109** is shown in **Scheme 8**.

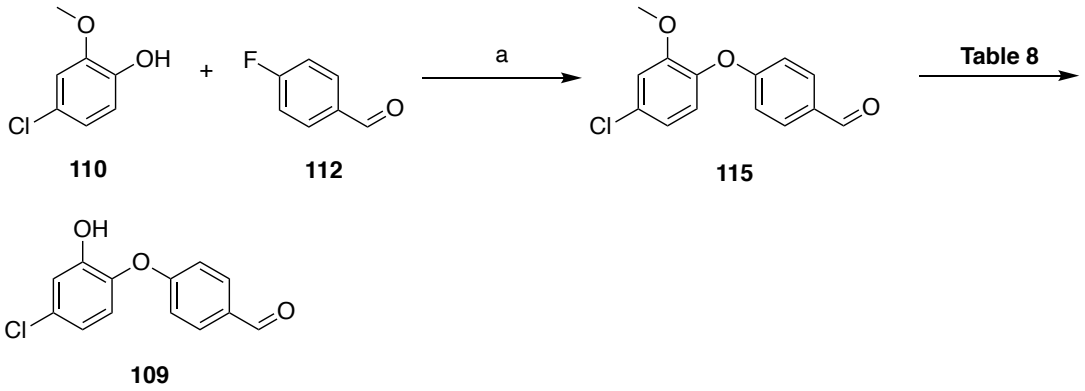

Scheme 8. *Synthesis of benzaldehyde **109**. a) K_2CO_3, DMF, 130 °C, 18 h, 93%. b) **Table 8***

The biaryl ether motif was assembled using the same conditions as previously discussed for nitrobenzene derivative **113**, again providing the desired compound in an excellent yield. Demethylation of the phenol group proved significantly more difficult than in the synthesis of the azide containing fragment, and a number of reagents were explored to identify the optimal reaction conditions (**Table 8**).

Table 8. *Reaction conditions attempted for demethylation of **115** to **109**.*

Reagents	Solvent	Temperature / °C	Time / h	Yield / %
BBr_3	CH_2Cl_2	25	3	NA
Thiophenol K_2CO_3 (cat)	NMP	190	0.5	10
Dodecanthiol NaOH	NMP	130	0.5	N/A
Cyclohexyl Iodide	DMF	120	18	N/A
Pyridinium Hydrochloride	Neat	180	18	N/A
HBr	AcOH	130	8	18
HBr	AcOH	130	18	38
HBr	AcOH	130	72	25

Initial deprotection was attempted using BBr_3, which is the standard route to aryl methyl ether cleavage.[150] Disappointingly the reaction failed to yield any of the desired product. This was surprising as a review of the literature suggested that the reaction should be feasible. However, Lansinger and Ronald have reported the sensitivity of benzaldehyde groups to BBr_3.[151] Their work showed that disruption of the carbonyl group proceeds quicker than the demethylation reaction, resulting in formation of a benzal bromide. The NMR data from the crude reaction mixture was consistent with the loss of the benzaldehyde group, indicated by the disappearance of the characteristic ^1H signal (~10.0 ppm). This suggests the reaction produced the corresponding benzal bromide, although this was not unambiguously confirmed.

Following this observation, it was apparent that an alternate set of conditions would be required to unveil the phenol group. Initial investigations focused on the use of nucleophilic cleavage to remove the methoxy group. Work in the literature shows that methoxy groups can be cleaved in the presence of hard thiol nucleophiles, such as potassium thiophenolate.[152] Demethylation was attempted using thiophenol in the presence of a catalytic amount of K_2CO_3 at 190 °C in *N*-methyl-2-pyrrolidone (NMP). While this did produce the desired product, the yield for this reaction was poor and the complex mixture of products required laborious purification, rendering scale up of the reaction infeasible. Slightly encouraged by this, demethylation was attempted using an odourless thiol reagent, dodecanthiol, with NaOH at a milder temperature of 130 °C.[153] Unfortunately, this reaction failed to generate any product and so the thiolate mediated demethylation strategy was abandoned.

The use of excess cyclohexyl iodide (10 equiv.) was investigated as a means to perform the demethylation.[154] This reaction works through the *in situ* generation of HI which protonates the etheric oxygen, followed by iodide attack at the methyl group, producing MeI and unmasking the phenol. Again, no product formation was detected by MS for this reaction and the starting material was still present on TLC.

The use of molten pyridinium hydrochloride (180 °C) has previously been reported in the literature for large scale demethylation reactions.[155] Demethylation of **115** was attempted under these conditions but the reaction yielded only a complex mixture of products with none of the desired phenol detected.

Cinu *et al.* have previously reported the demethylation of a similar aryl ether using HBr and AcOH at elevated temperatures, in a 60% yield.[156] This reaction was initially attempted using identical conditions (8 hours, 130 °C), while this reaction did provide the desired product, it did so in a considerably lower yield than reported (18%). It was observed by TLC that the reaction mixture contained only two components, the desired phenol and the original starting material. Encouraged by this finding, the reaction time was extended to 18 h, this generated the desired product in a better yield (38%), though starting material was still observed by TLC. Unfortunately, further extension of the reaction time (72 h) resulted in a lower yield, presumably through decomposition of the product, as the formation of an unknown third product was observed by TLC.

Following the demethylation reaction, it was necessary to reprotect the phenol functional group with a protecting group that could be easily removed at the end of

the synthesis. The first protecting group chosen was the *tert*-butyldimethylsilyl (TBDMS) group. These groups can be readily installed and then easily cleaved using *tetra*-butylammonium fluoride (TBAF). This synthetic strategy is outlined in **Scheme 9**.

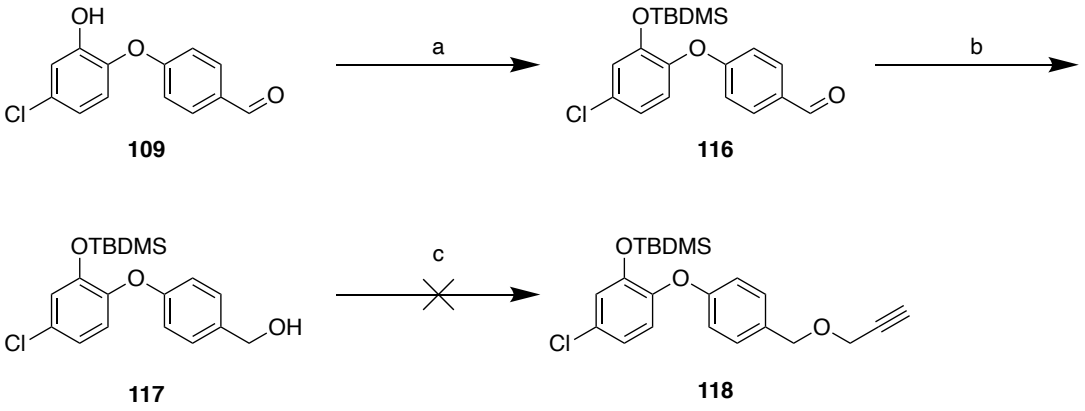

Scheme 9. Attempted synthesis of alkyne **118**. *a) TBDMSCl, Im, DMF, 0 °C r.t., 18 h, 89%. b) $NaBH_4$, MeOH, 0 °C → r.t., 3 h, 38%. c) NaH, propargyl bromide, DMF, 0 °C → r.t., 18 h*

Protection of the phenol **109** using TBDMSCl and imidazole in DMF furnished the desired product in an excellent yield. The aldehyde was subsequently reduced using $NaBH_4$ providing the corresponding primary alcohol **117** in a lower than anticipated yield. At this point, propargylation of the alcohol functionality was attempted using NaH and propargyl bromide in DMF. Disappointingly this reaction failed to yield the desired target **118** and instead generated a complex mixture of products. The reaction was repeated a second time, again yielding a complex mixture. This suggests that the TBDMS group was labile under the reaction conditions. This was somewhat surprising but could be attributed to the increased acidity of phenol groups, making their liberation more likely under highly basic conditions. In their systematic review of protecting groups in organic chemistry, Greene *et al.* reported

the half-life of phenolic TBDMS ethers at a basic pH to be as low as 3.5 minutes, depending on substituent groups.[157]

Following this result an alternate protecting group strategy was required. The next protecting group investigate was the methoxy methyl ether (MOM) group. These protecting groups are notably resistant to basic cleavage, requiring strong acids to remove them. This synthetic strategy is outlined in **Scheme 10**.

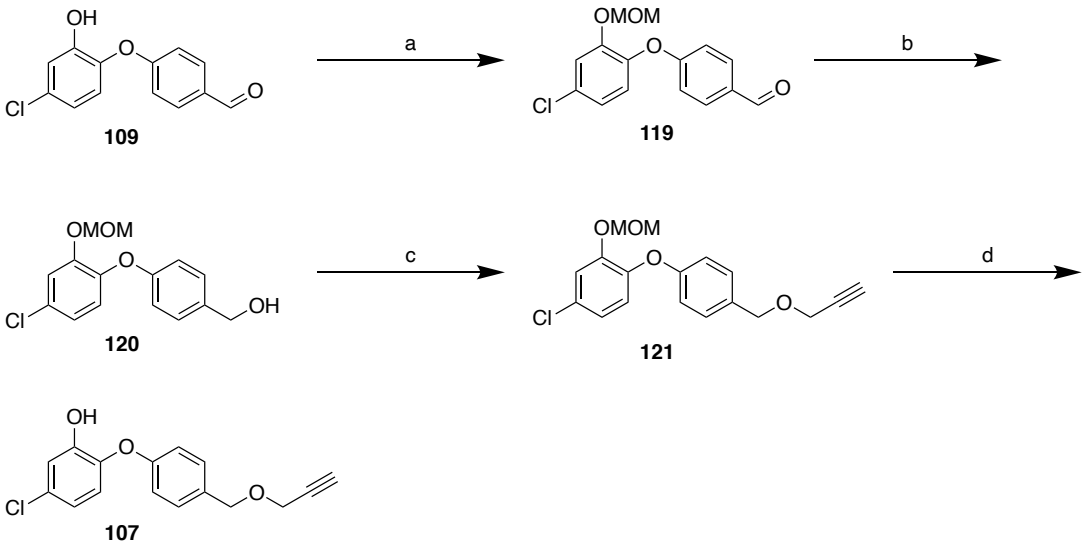

Scheme 10. *Forward synthesis of alkyne **107**. a) MOMCl, DIPEA, CH_2Cl_2, r.t., 18 h, 85%. b) $NaBH_4$, MeOH 0 °C → r.t., 4 h, 95%. c) NaH, Propargyl bromide, DMF, 0 °C → r.t., 18 h, 75%. d) 6 M HCl, MeOH, 70 °C, 2 h, 91%.*

The phenol functionality was protected using MOMCl and DIPEA, providing ether **119** in a good yield. Reduction of the aldehyde group proceeded smoothly and generated **120**, this time in a much improved yield over the TBDMS-protected derivative. Pleasingly propargylation of the primary alcohol provided **121** in an acceptable yield, using the same conditions which had failed to generate the desired TBDMS-

protected product. The phenol functionality was then revealed using 6 M HCl in methanol at reflux, furnishing the target **107** in a good yield.

The use of copper-catalysed azide alkyne cycloaddition (CuACC) to construct 1,2,3 triazoles has been widely documented and extensively explored since its disclosure in 2002.[158-161] However, this reaction delivers exclusively the 1,4 disubstituted product, whereas the desired product was the 1,5 configuration. The use of thermally promoted [1+3] cycloaddition reactions is one method to synthesise 1,5-triazoles, however this reaction produces a mixture of both 1,4 and 1,5 products which then require time-consuming HPLC separation.

It was not until 2005 that the first report of ruthenium-catalysed azide alkyne cycloaddition (RuAAC) was published.[162, 163] Importantly, it was observed that the use of the Ru catalyst led exclusively to the formation of the 1,5 product. Since this time, various different catalysts have been developed to selectively produce 1,5-triazoles, two of the most commonly used are shown in **Figure 41**.[164]

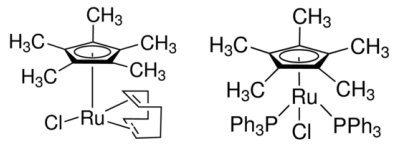

122 **123**

Figure 41. *The structure of two ruthenium catalysts used for RuAAC 'Click Chemistry'.*[164]

The proposed catalytic cycle for RuAAC is depicted below in **Scheme 11**.[165]

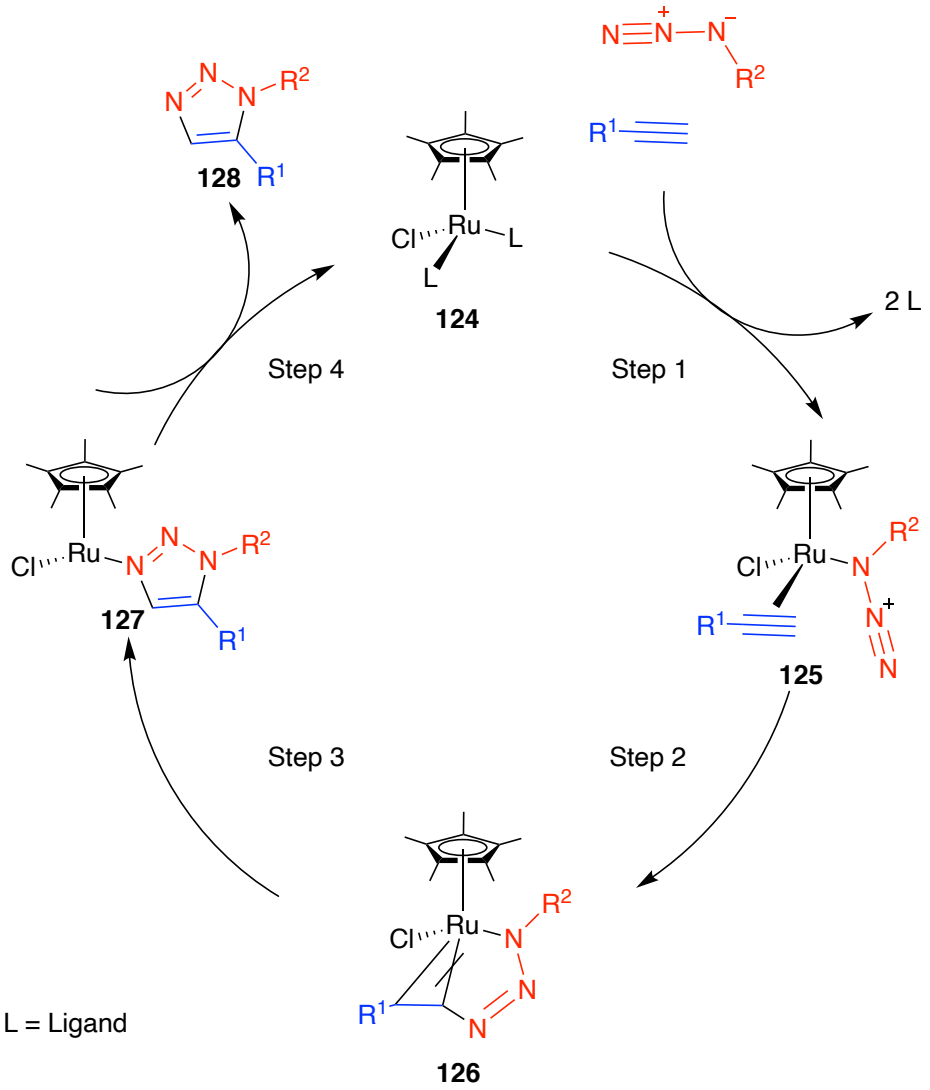

Scheme 11. *The proposed catalytic cycle and intermediates involved in the RuAAC formation of 1,5-triazoles. Adapted from Boren et al.*[165]

Briefly, in step 1, displacement of the spectator ligand(s) by the alkyne and azide leads to the formation of the activated Ru(II) complex **125**. This is followed by an oxidative coupling of the alkyne and azide components to form a ruthenacycle intermediate **126**. It should be noted that it is this step that imparts the regioselectivity on the process. Density functional theory (DFT) modelling has shown that the specific orientation of the alkyne, with respect to the azide, in complex **125** is the

lowest energy orientation and so is favoured. The C-N bond formed by this process is between the least sterically encumbered carbon and the terminal nitrogen of the azide. Ruthenacycle **126** then collapses in on itself, forming the triazole structure. The resulting metallacycle **127** then undergoes reductive elimination to release the newly formed triazole, regenerating the catalyst.

Through the use of Ru catalyst **123**, the cycloaddition reaction was conducted in 1,4-dioxane at 60 °C under a nitrogen atmosphere. These conditions furnished the desired product in a moderate yield after HPLC purification (**Scheme 12**).

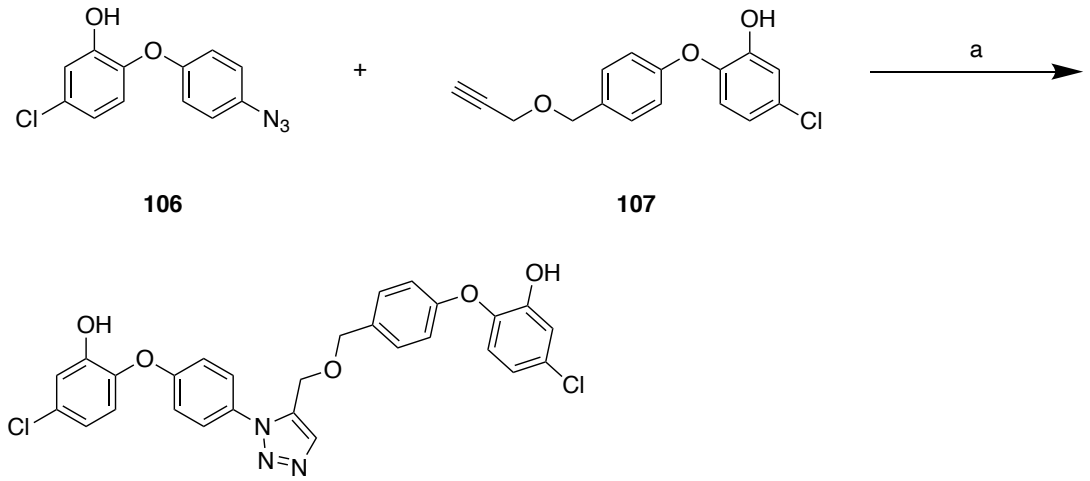

Scheme 12. *Forward synthesis of **55** using ruthenium catalysed 'Click Chemistry'. a) Ru Cat. **123**, 1,4-dioxane, 60 °C, N_2, 18 h, 17%*

The regioselectivity of this reaction can be confirmed through the use of ^{13}C-NMR, on the basis of the possible resonance structures of 1,4 and 1,5-triazoles, as previously reported by Creary *et al.* (**Scheme 13**).[166]

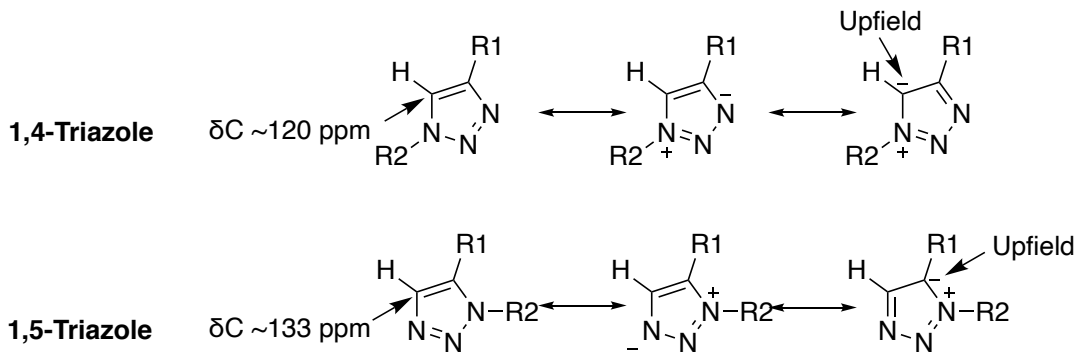

Scheme 13. *Resonance structures of 1,4 and 1,5-triazoles, showing how the chemical shift of the CH alkene carbon changes depending on the regioisomer.*

This shows how in 1,4-triazoles, a negative charge can be delocalised onto the CH of the triazole. This negative charge results in increased shielding of the nuclei, so it experiences a weaker magnetic field, resulting in its chemical shift being further upfield (δ_C = ~ 120 ppm). The reverse is true for the 1,5 regioisomer. In this case, no charge can be delocalised onto the CH and therefore it experiences less shielding than the 1,4 counterpart, resulting in a carbon signal that is further downfield (δ_C = ~ 133 ppm).

Through the use of Heteronuclear Single Quantum Coherence (HSQC) spectroscopy it was possible to unambiguously characterise **55** as a 1,5-triazole, using the distinctive signal from the triazole proton (**Figure 42**).

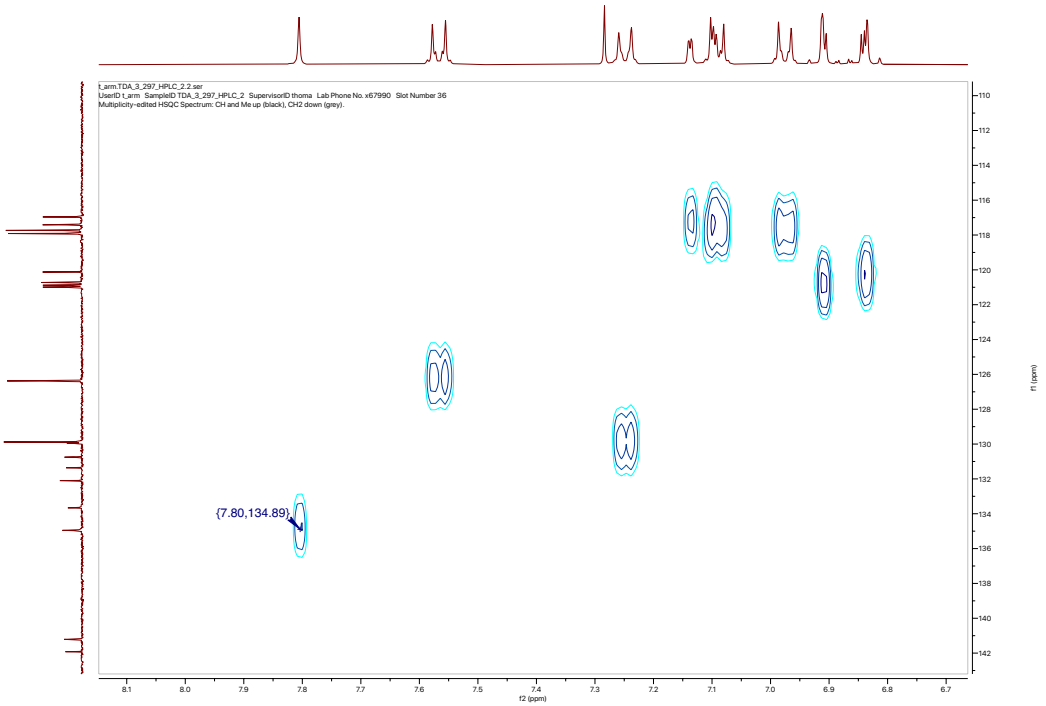

Figure 42. *The aromatic region of the HSQC spectrum recorded for **55**, showing the correlation between the proton signal at 7.80 ppm and the carbon environment at 134.9 ppm.*

The spectrum in **Figure 42** shows the correlation between the triazole ^{1}H (7.80 ppm) and a carbon at 134.9 ppm. This result is consistent with Creary's observation that 1,5-triazoles should have a ^{13}C shift of ~133 ppm In order to probe the importance of the 1,5-triazole geometry, the corresponding 1,4 regioisomer was also synthesised using traditional CuAAC methods (**Scheme 14**).[158]

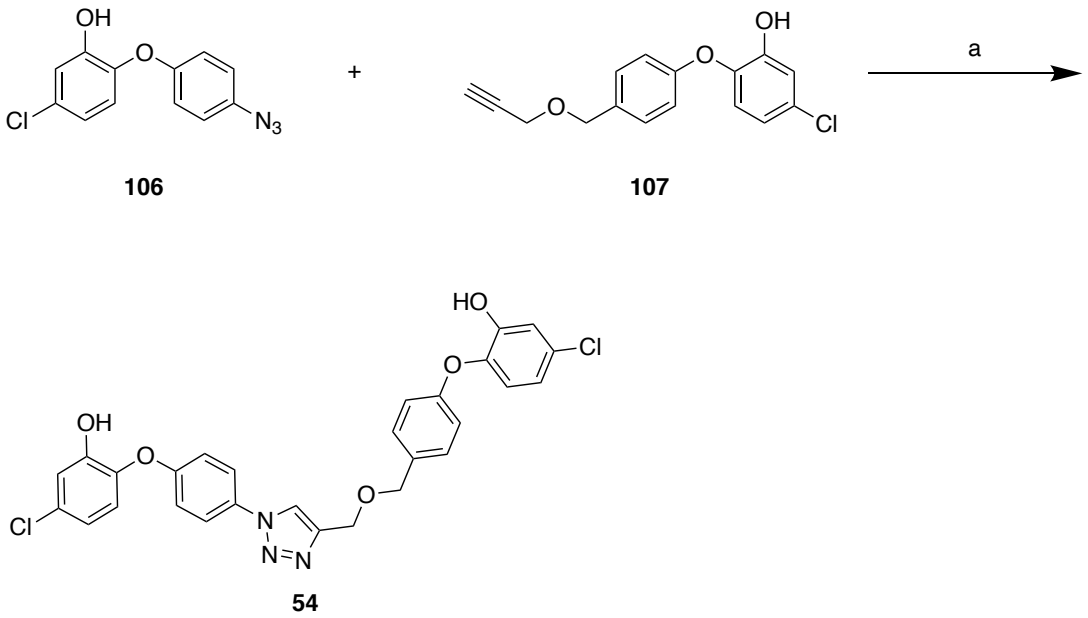

Scheme 14. *Forward synthesis of **54** using copper-catalysed 'Click Chemistry'. a) $CuSO_4.5H_2O$, Sodium ascorbate, r.t., 18 h, 25%*

This reaction generated the desired compound in a good yield. The 1,4 geometry was confirmed using the same 2D NMR methods previously discussed for **55**. The correlation between the triazole proton and its corresponding carbon atom is shown in **Figure 43**.

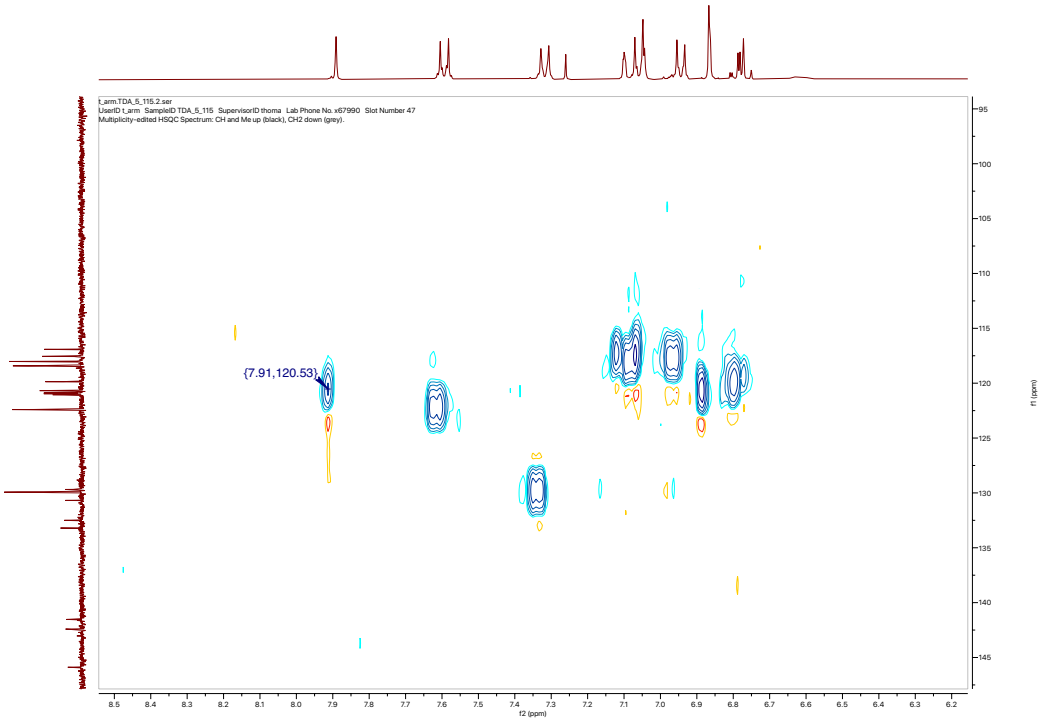

Figure 43. *The aromatic region of the HSQC spectrum recorded for **54**, showing the correlation between the proton signal at 7.91 ppm and the carbon environment at 120.5 ppm.*

This shows the correlation between the triazole proton with a carbon resonance at the lower shift of 120.5 ppm, compared to 134.8 for **55** (*vide supra*), indicating the formation of the 1,4 scaffold.

To explore the SAR of this series of compounds, a range of derivatives were designed **Figure 44**.

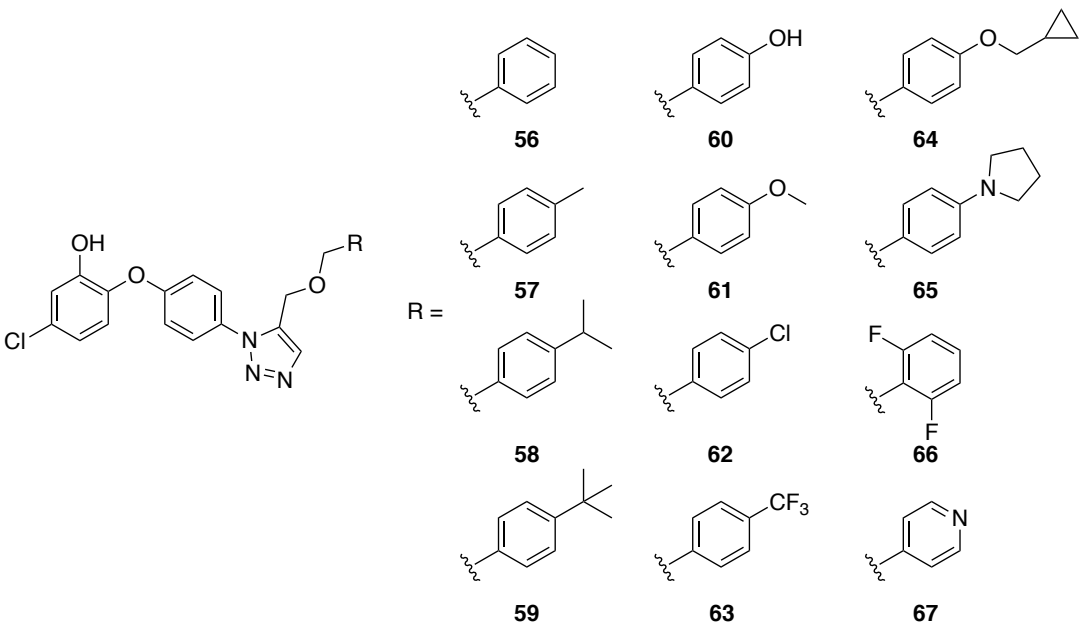

Figure 44. *The structures of a library of 1,5-triazole compounds designed to explore SAR.*

While these triazoles can all be assembled from azide fragment **106**, each requires a specific alkyne fragment. The 12 alkyne fragments required to assemble the desired triazole motifs are shown in **Figure 45**.

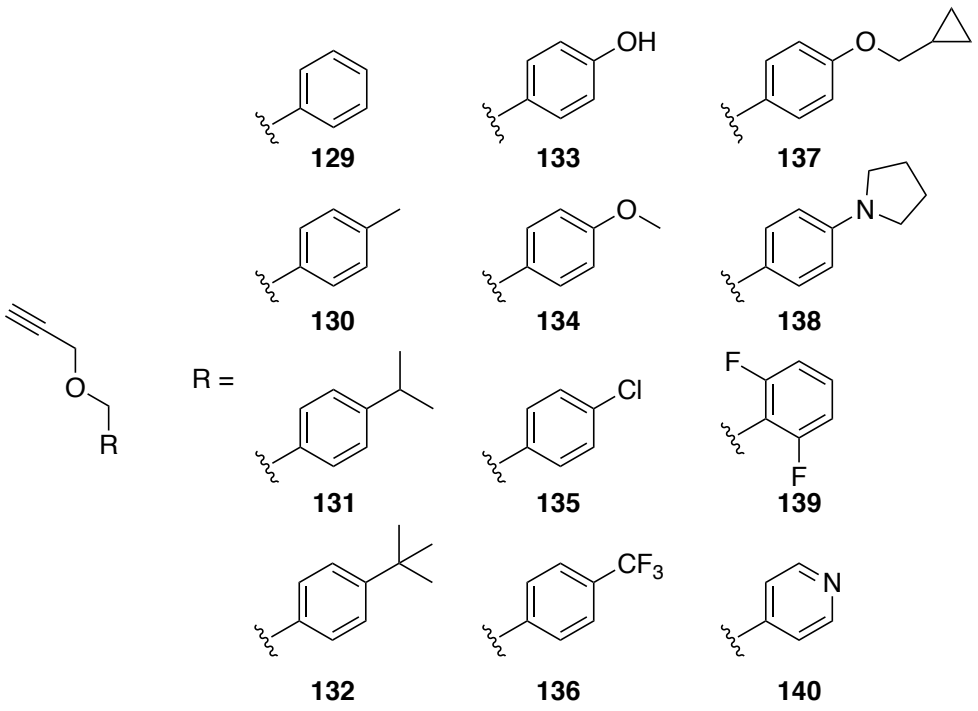

Figure 45. *Alkyne fragments required for the synthesis of the library of 1,5-triazoles.*

In each instance, the necessary alkyne fragment was synthesised from its corresponding alcohol, benzyl chloride or benzaldehyde, depending on commercial availability. Five alkynes were synthesised from their corresponding primary alcohols using NaH and propargyl bromides (**Scheme 15**).

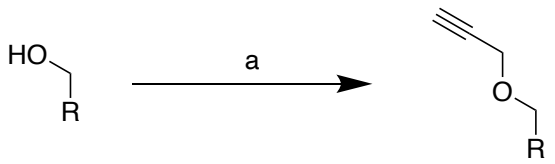

129
135-6
139-40

Scheme 15. *Forward synthesis of alkyne fragments **129**, **135-6** and **138-9** from their corresponding primary alcohols. a) NaH, Propargyl bromide, DMF, 0 °C → r.t., 18 h*

Yields for these reactions are shown in **Table 9**.

Table 9. *Yields for the reactions shown in **Scheme 15**.*

Compound	R	Yield / %
129	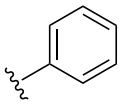	73
135	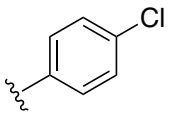	81
136	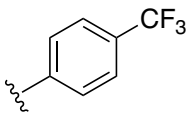	83
139	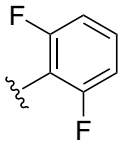	67
140	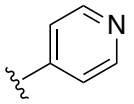	90

All products were obtained in reasonable-to-good yields.

A further 4 alkynes were synthesised from their corresponding benzyl chlorides, using propargyl alcohol and NaH (**Scheme 16**).

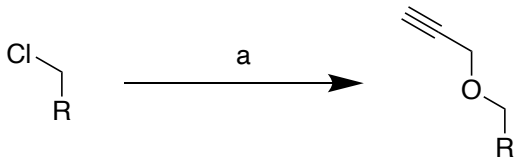

130-132, 134

Scheme 16. *Forward synthesis of alkyne fragments **130-32** and **134** from their corresponding benzyl halides. a) Propargyl alcohol, NaH, DMF, 0 °C → r.t., 18 h*

Yields for the reactions are shown in **Table 10**.

Table 10. *Yields for the reactions shown in* ***Scheme 16****.*

Compound	R	Yield / %
130	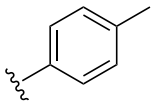	83
131	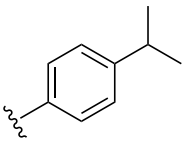	84
132	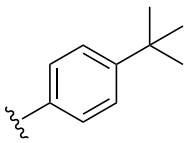	86
134	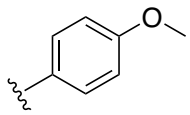	86

The 4 target compounds were all generated in excellent yields.

Pyrrolidine derivative **138** was synthesised from its benzaldehyde precursor (**Scheme 17**).

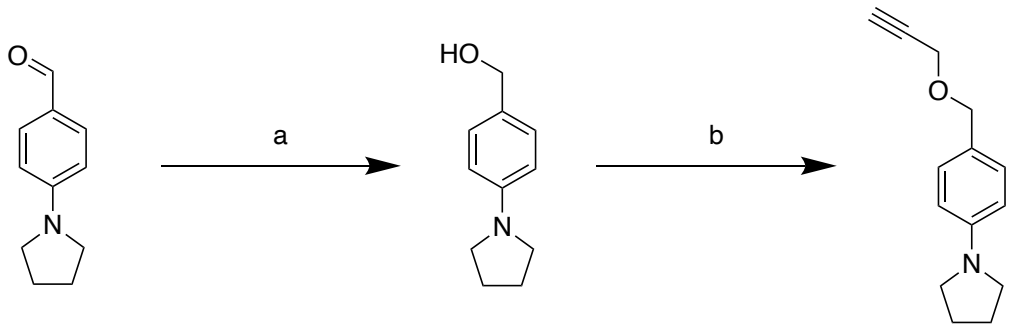

141 **142** **138**

Scheme 17. *Synthesis of alkyne* ***138****. a) $NaBH_4$, MeOH, 0 °C → r.t., 4 h, 76%. b) NaH, Propargyl bromide, 0 → r.t., 18 h, 81%.*

$NaBH_4$ mediated benzaldehyde reduction proceeded smoothly, furnishing benzyl alcohol **142** in a moderate yield. Propargylation of the resulting primary alcohol provided the desired alkyne **138** in good yields over two steps.

Alkyne fragment **137** was synthesised from 4-hydroxybenzaldehyde (**Scheme 18**).

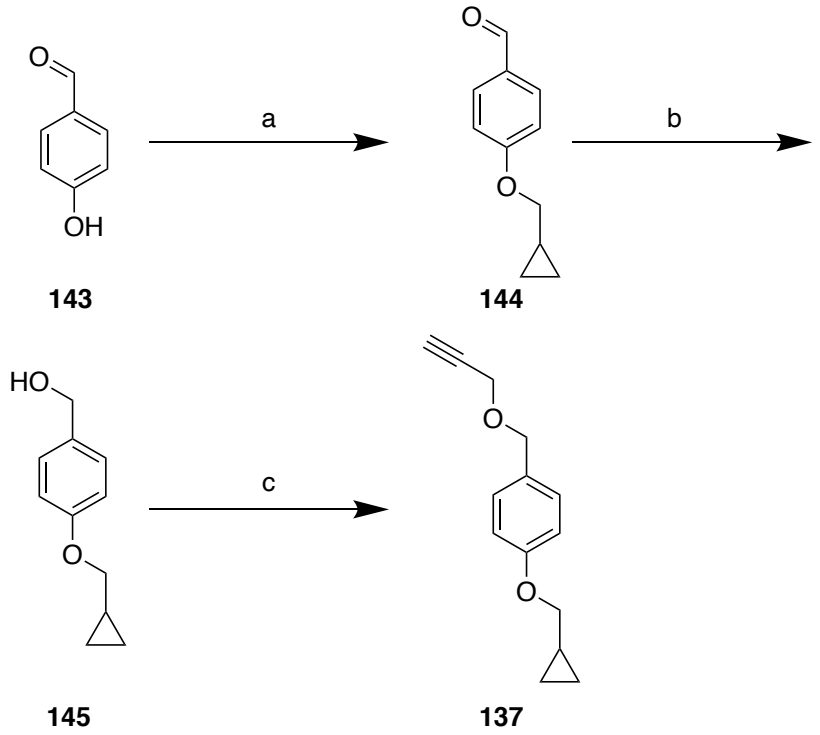

Scheme 18. *Synthesis of alkyne **137**. a) (Bromomethyl)cyclopropane, K_2CO_3, DMF, 130 °C, 69%. b) $NaBH_4$, MeOH, 0 → r.t., 4 h, 64%. c) NaH, Propargyl bromide, 0 → r.t., 18 h, 68%.*

The methylcyclopropyl moiety was installed using (bromomethyl)cyclopropane and K_2CO_3 at elevated temperatures, generating the desired product in a modest yield. Subsequent benzaldehyde reduction and propargylation provided the target alkyne **137** in an acceptable yield over three steps.

The synthesis of the phenolic fragment **133** is shown in **Scheme 19**.

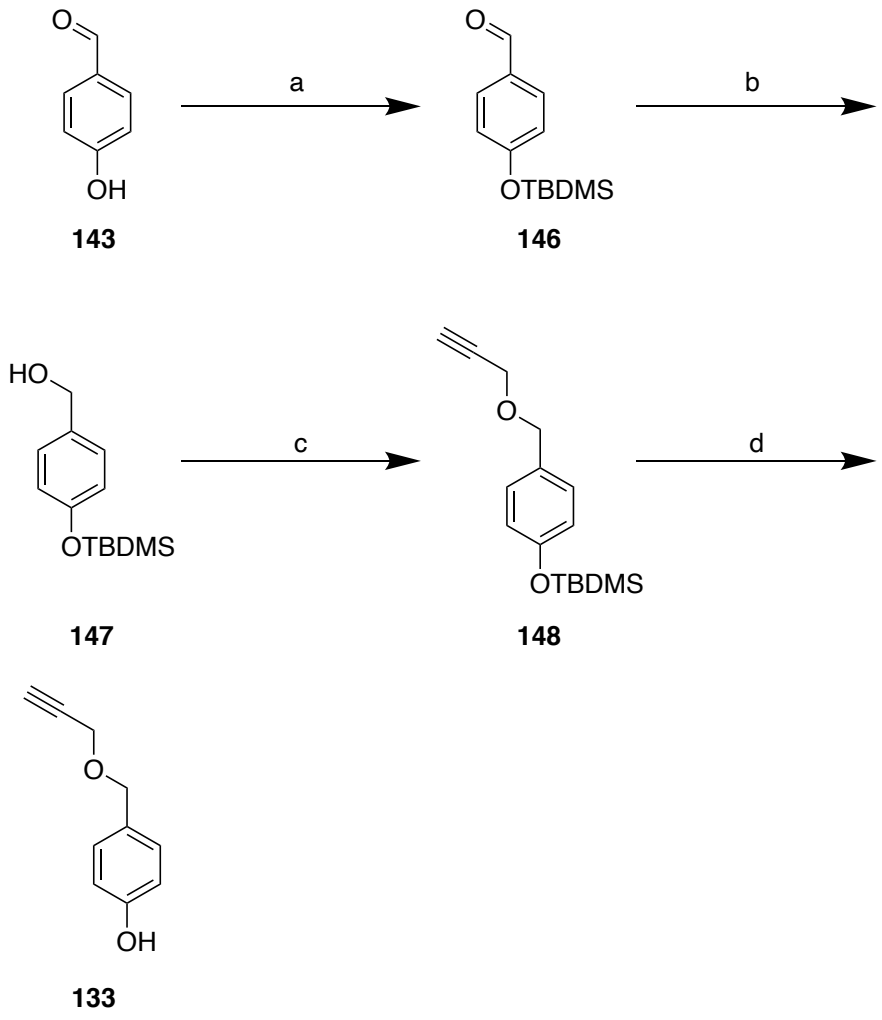

143 **146** **147** **148** **133**

Scheme 19. *Synthesis of alkyne **133**. a) TBDMSCl, Et_3N, CH_2Cl_2, r.t., 3 h, 85%. b) $NaBH_4$, MeOH, 0 → r.t., 4 h, 91%. c) NaH, Propargyl bromide, 0 → r.t., 18 h, 74%. d) TBAF, THF, r.t., 18 h, 72%*

The phenol functionality was initially masked using the TBDMS protecting group, generating silyl ether **146** in a good yield. This allowed for the reduction and selective propargylation of the benzaldehyde moiety giving ether **148** in a 68% yield over two steps. Removal of the silyl protecting group, furnishing the desired alkyne **133** in a good yield over 4 steps.

With the required alkyne fragments in hand, a library of 1,5-triazoles was assembled through RuAAC (**Scheme 20**).

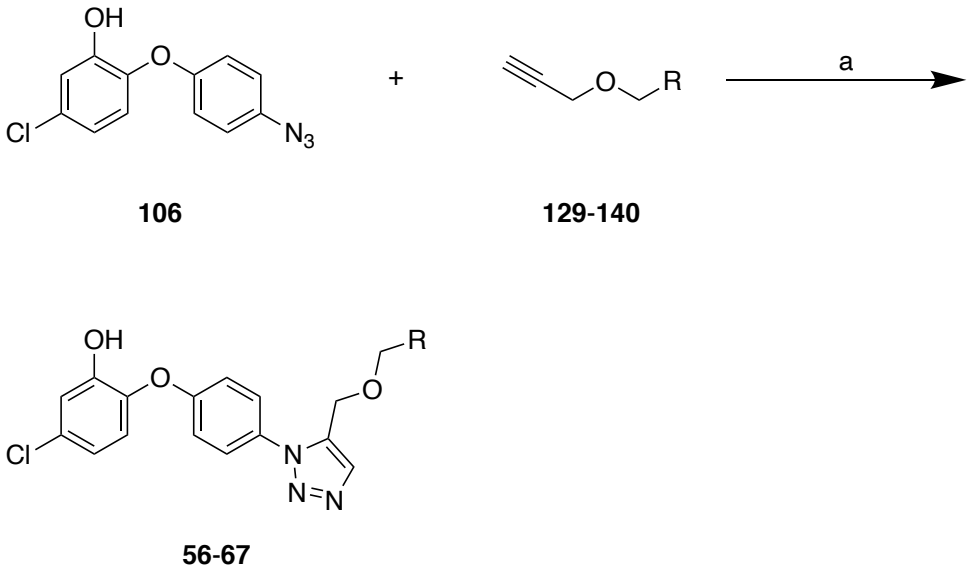

Scheme 20. *General reaction scheme for the forward synthesis of the chlorinated triazole library. a) Ru Cat.* ***123****, 1,4-dioxane, 60 °C,* N_2*, 18 h*

The yield of this reaction for each target molecule is shown in **Table 11**.

Table 11. *Yields for the reactions shown in* ***Scheme 20***.

Compound	R	Yield / %
56	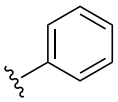	10
57	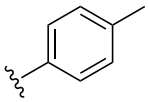	11
58	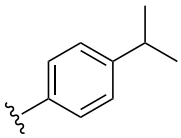	28
59	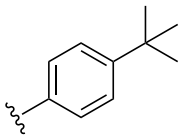	33
60	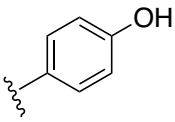	6
61	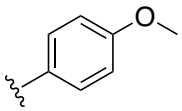	16
62	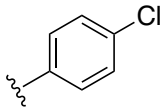	12
63	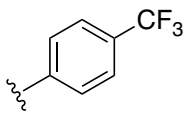	24
64	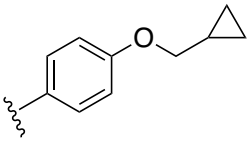	5
65	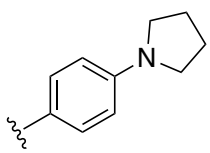	5
66	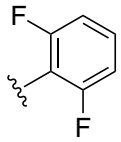	17
67	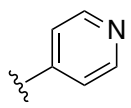	N/A

The RuAAC reaction proved itself to be relatively robust and tolerant to a range of R groups present on the alkyne. While the reported yields are moderate to low, these yields are after HPLC purification and are consistent with those reported in the literature.[167-170] The only compound which could not be synthesised using this route was **67**, where R was a pyridine ring. It was thought that this could be due to coordination of the pyridine to the ruthenium metal centre, which could have deactivated the catalyst.

3.2 Synthesis of *n*-Propylated-Triazole Target Molecules

In order to explore SAR at the A ring, a range of triazoles bearing a propyl chain instead of a Cl atom were synthesised. Synthesis of the propylated aryl azide fragment is shown in **Scheme 21**.

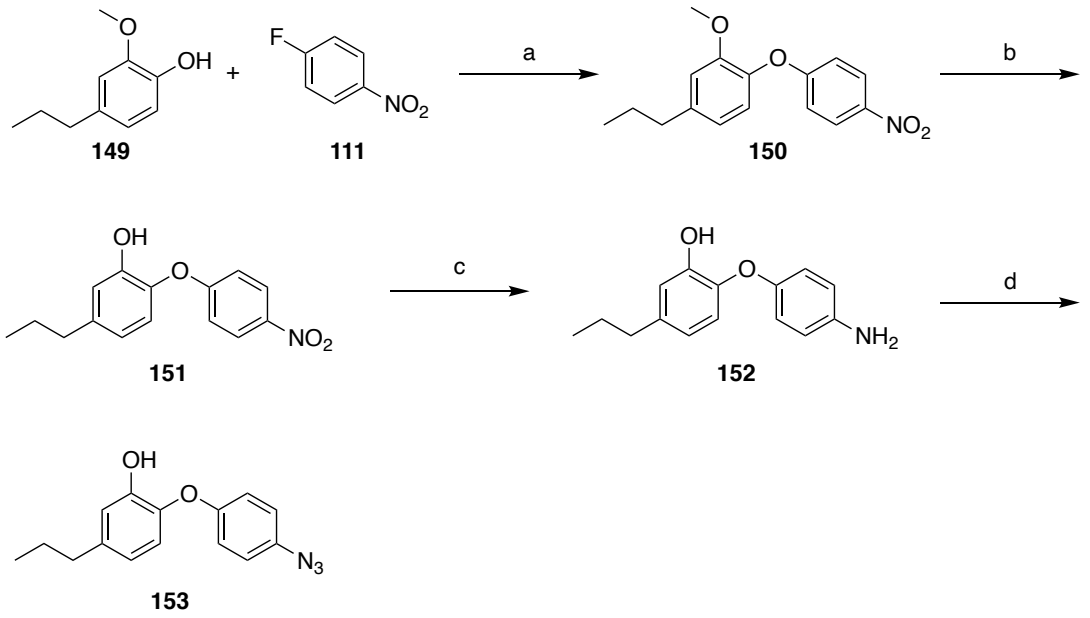

Scheme 21. *Synthesis of azide **153**. a) K_2CO_3, DMF, 130 °C, 18 h, 80%. b) BBr_3, CH_2Cl_2, 0 °C → r.t., N_2 3 h, 88%. c) Zn, NH_4Cl, MeOH, r.t., 18 h, 75%. d) ^tBuONO, $TMSN_3$, ACN, 0 °C → r.t. 3h, 82%.*

Synthesis was performed in the same fashion as previously discussed for the **112** (**Scheme 6** and **7**). Substitution of 4-fluoronitrobenzene with the commercially available 4-propyl-2-methoxyphenol afforded **150** in a good yield. Subsequent ether cleavage and nitro reduction furnished the aniline **152** in 66% yield over two steps. Functional group interconversion then generated the desired azide **153** in a good yield. Following the synthesis of azide **153**, the previously synthesised alkyne fragments were used to generate an expanded library of 1,5-triazole compounds (**Scheme 22**).

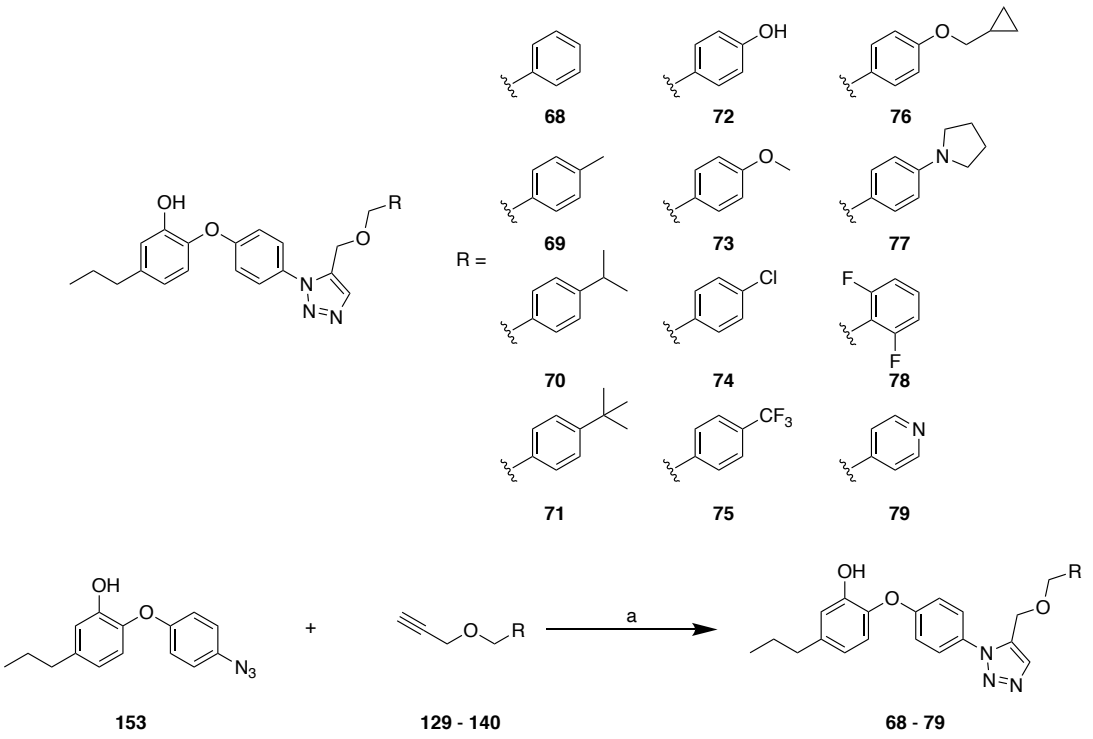

Scheme 22. *The structures and synthesis of a library of propylated triazole compounds. a) Ru Cat.* ***123****, 1,4-dioxane, 60 °C, N_2, 18 h.*

The yield for each final compound is shown in **Table 12**.

Table 12. *Yields for the reactions shown in* ***Scheme 22***

Compound	R	Yield / %
68	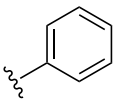	15
69	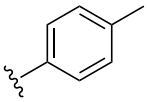	5
70	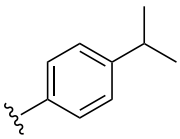	26
71	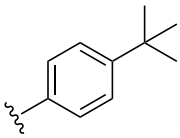	25
72	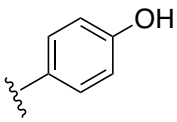	24
73	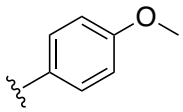	20
74	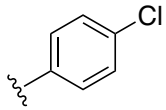	17
75	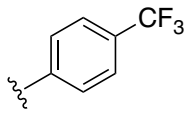	19
76	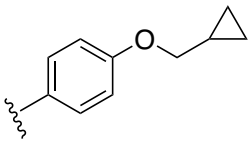	14
77	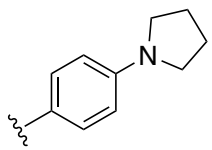	8
78	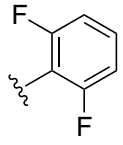	19
79	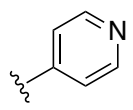	N/A

Yields for these reactions were broadly similar to the chlorinated derivatives (**Table 11**), with each reaction providing a moderate yield following HPLC purification. Again, it was not possible to assemble the pyridine analogue **79**, further reinforcing the idea that the pyridine ring is incompatible with the reaction. These syntheses allowed the rapid construction of a library of 24 triazole compounds, allowing the exploration of SAR at two positions in the structures.

3.3 Synthesis of Ether Derivative Target Molecules

The structures of the ether linked target molecules are shown below in **Figure 46**.

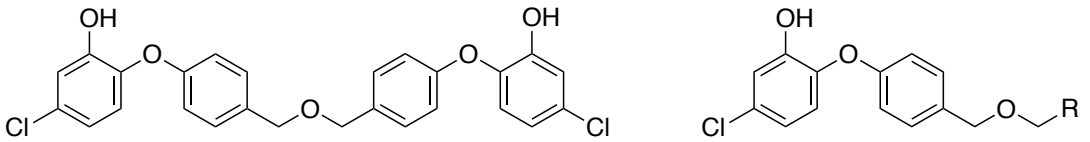

80 **81-86**

Figure 46. *The general structures of ether linked target compounds.*

Compound **80** had been the focus of a previous PhD student's work.[171] Unfortunately, they were unable to complete the synthesis. They were able to synthesise the methoxy protected derivative (**154**, **Figure 47**), but attempts to demethylate this compound were unsuccessful, with cleavage of the benzyl ethers being the main issue.

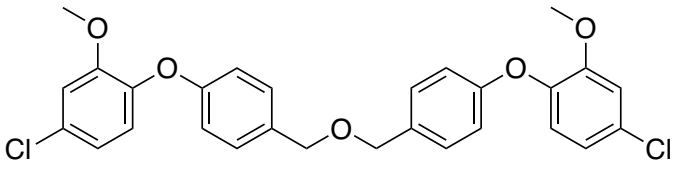

154

Figure 47. *Structure of the compound synthesised by Chetty.*[164]

With this in mind, it was clear that a new synthetic route was required, one in which the methyl protecting group would be replaced by a different protecting group which was ultimately more amenable to removal. The RSA shown in **Scheme 23** was devised.

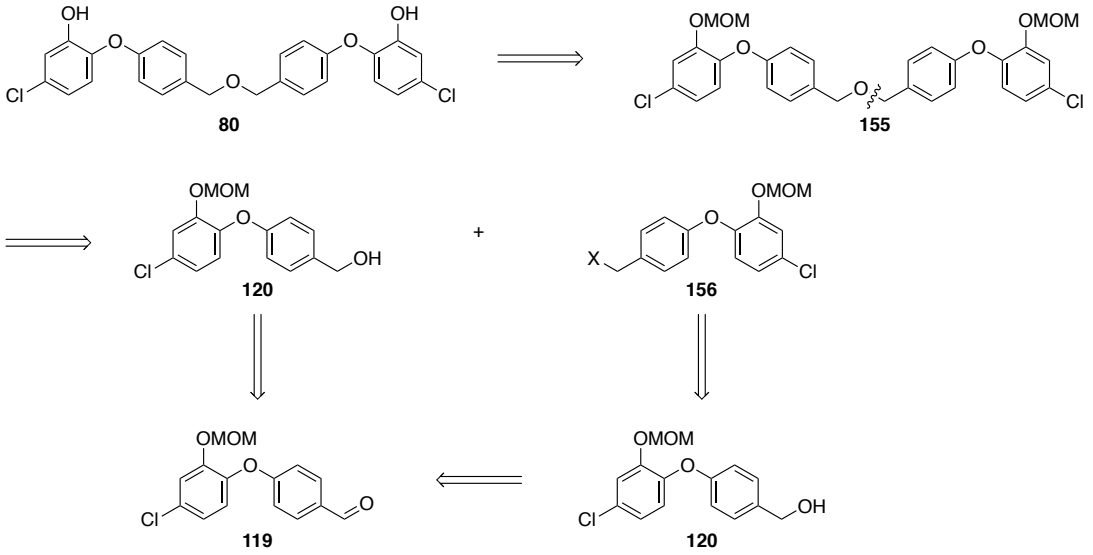

X = Leaving group

Scheme 23. *RSA for target compound **80**.*

It was envisioned that **80** would be unveiled following global deprotection of **155**. The di-TCL scaffold would be constructed through unification of alcohol **120** and an activated alcohol derivative **156**. Both of these compounds could be access *via* the previously synthesised MOM protected benzaldehyde derivative **119**.

Primary alcohol **120** was resynthesised in accordance to the synthetic methods previously discussed (**Scheme 8** and **10**). With the required primary alcohol in hand, it was necessary to activate the alcohol in the form of a leaving group to allow unification of the two fragments. Initial attempts focused on the conversion of the primary alcohol into its corresponding benzyl bromide (**Scheme 24**).

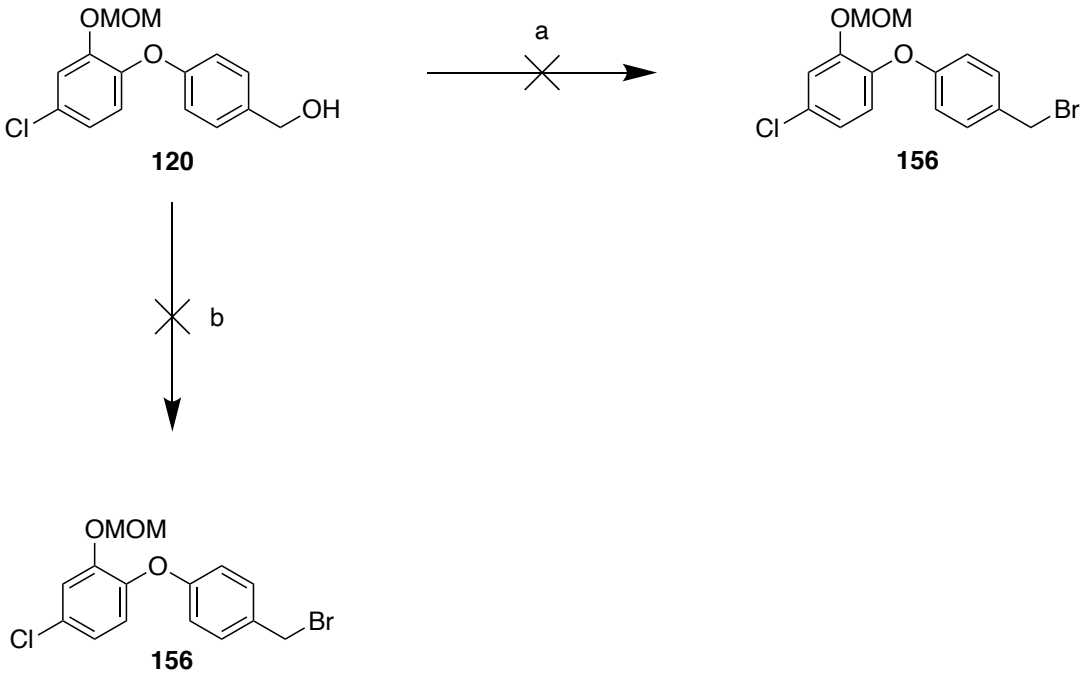

Scheme 24. *Attempted bromination of alcohol **120**. a) CBr_4, PPh_3, CH_2Cl_2, r.t., 1 h. b) PBr_3, CH_2Cl_2, r.t., 3 h.*

Initial bromination efforts focused on the use of Appel reaction conditions to substitute the alcohol with a bromine atom.[172] Surprisingly this reaction failed to generate the desired product. Complete consumption of the starting material and the formation of a less polar product was observed by TLC, however, the desired product was not detected by MS. The decision was taken to purify the reaction product and fully characterise it to elucidate the structure (**Figure 48**).

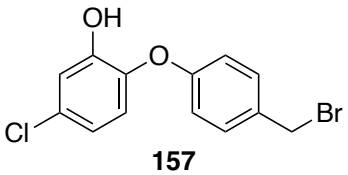

Figure 48. *The structure of the reaction product obtained by the attempted Appel bromination of alcohol **120**.*

The ^{1}H NMR spectrum showed the disappearance of a broad singlet at ~ 2.47 ppm, this was coupled with the upfield shift of the methylene group from ~ 64.6 to ~ 45.9 ppm in the ^{13}C spectrum. These two pieces of evidence supported the conversion of the alcohol into the desired alkyl bromide. However, the peaks corresponding with the MOM protecting group were no longer present. Reevaluation of the MS results supported the idea that the MOM group had been removed during the reaction, with a major peak at 310.9475 *m/z*, which also corresponded to the mass of compound **157**. This result was surprising as MOM groups are only typically cleaved under highly acidic conditions. A review of the literature found a report detailing the use of Appel conditions to remove phenolic MOM ethers.[173] Combined, this evidence showed that an alternate strategy would be required to brominate the alcohol.

PBr_3 is another reagent which can be used to convert alcohols into bromides. Unfortunately, when this reaction was attempted a complex mixture of products was generated and the desired product could not be observed *via* MS and so this route was abandoned.

Following the failure to generate bromide **156**, focus shifted to converting alcohol **120** to a mesylate. Mesylates are frequently used as leaving groups and it was thought that the conditions required for their installation would be sufficiently mild enough to not disrupt the MOM protecting group. The attempted conversion of alcohol **117** to its corresponding mesylate is shown in **Scheme 25**.

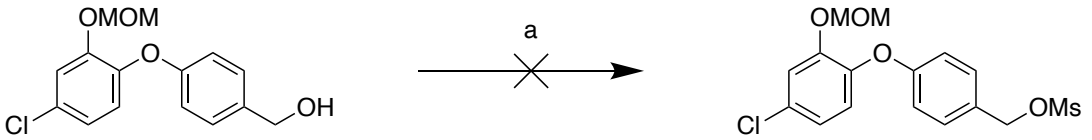

120 **158**

Scheme 25*. Attempted mesylation of alcohol **120**. a) MsCl, Et_3N, CH_2Cl_2, 0 → r.t., 1 h.*

The reaction was initiated by the addition of MsCl to the reaction mixture at 0 °C, before being allowed to warm and stir at r.t. for an hour, after which time complete consumption of the starting material was judged by TLC. It was noticed that the R_f of the product was significantly higher than expected, especially when compared to the starting alcohol. Typically, mesylates are used without purification, however, following the unexpectedly high R_f, the decision was taken to purify and full characterise the product, rather than treating it as an intermediate. This characterisation revealed the product of the reaction was actually a benzyl chloride **159**, rather than a mesylate (**Figure 49**)

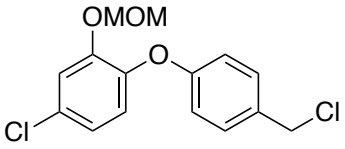

159

Figure 49. *The structure of the reaction product obtained by the attempted mesylation of alcohol **120**.*

This structure was confirmed by the absence of the mesylate CH_3 group in both the ^1H and ^{13}C NMR spectra. Additionally, the methylene group ^{13}C peak was shifted from 64.6 (in **120**) to 49.1 ppm, consistent with that of alkyl halides. A review of the literature showed that methanesulfonyl chloride and ammoniacal bases can be used to synthesise benzyl chlorides from benzyl alcohols.[174] This process is presumably

contingent on initial formation of the target mesylate which, is then displaced by a chloride ion. Following the synthesis of chloride **159**, the desired di-TCL ether was synthesised as shown in **Scheme 26**.

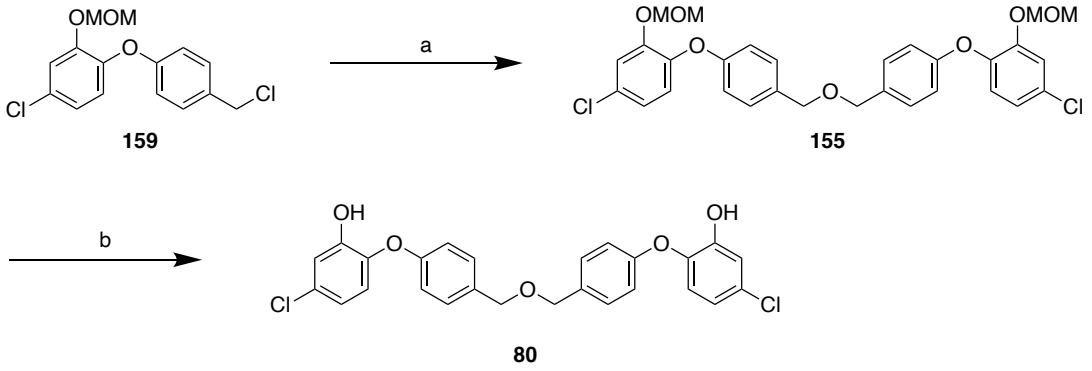

Scheme 26. Forward synthesis of **80**. *a) **120**, NaH, DMF, 0 → r.t., 18 h, 45%. b) 6 M HCl, MeOH, 70 °C, 2 h, 44%.*

The initial di-TCL scaffold was assembled from alcohol **120** and chloride **159**, using NaH as a base. Following this, global deprotection of the MOM groups furnished the desired product in a moderate yield over two steps.

Following the synthesis of **80**, a number of truncated derivatives were synthesised to explore any SAR for the library of compounds. The general structure and R groups for this scaffold are shown in **Figure 50**.

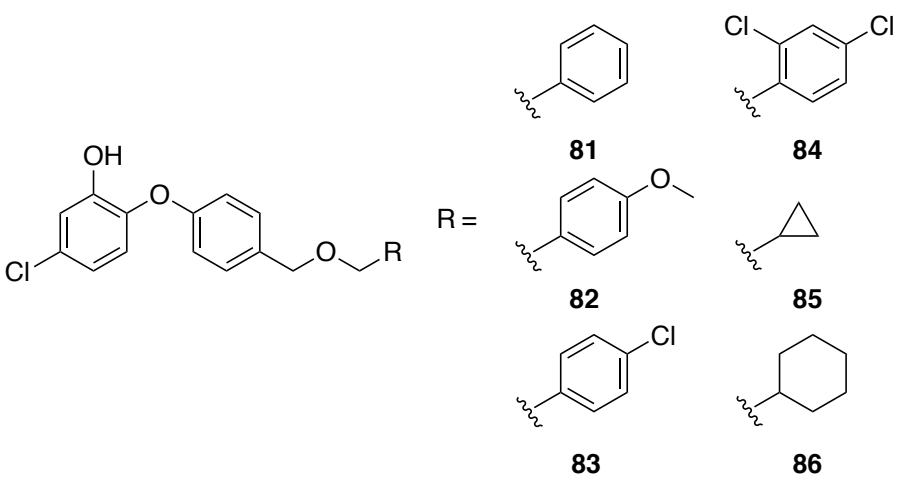

Figure 50. *Structures of target compounds **81**-**86**.*

Using alcohol **120**, the direct precursors to each target compound was synthesised as shown in **Scheme 27**.

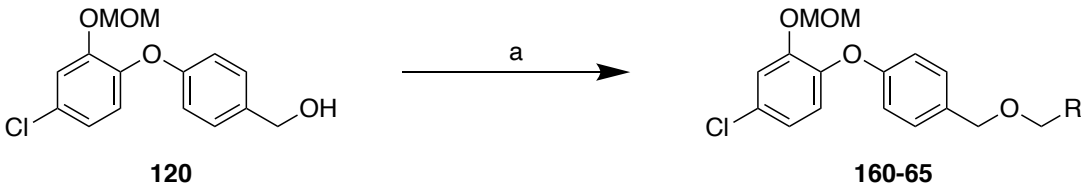

Scheme 27. *Forward synthesis of compounds **160**-**5** a) XCH_2R, NaH, DMF, 0 → r.t., 18 h.*

The yields for each reaction are shown in **Table 13**.

Table 13. *Yields for the reactions shown in* ***Scheme 27****.*

Compound	R	Yield / %
160	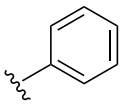	80
161	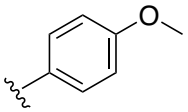	68
162	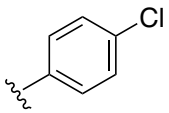	70
163	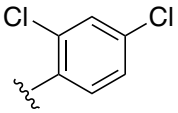	68
164		76
165	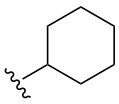	23

With the exception of the cyclohexyl derivative **165**, the reaction generated the desired products in moderate to good yields in all instances. Due to the low yield obtained for compound **165**, the reaction was repeated and again gave the target compound in a low yield. The reason for these low yields is unclear, though it could be due to a problem with the commercial (bromomethyl)cyclohexane that was used in the reaction. This could be confirmed by using a different batch of material, though this was not explored as a sufficient amount of material was obtained to continue with the synthesis.

In order to unveil desired phenol functionality, the MOM protecting group was removed using 6 M HCl in refluxing methanol (**Scheme 28**).

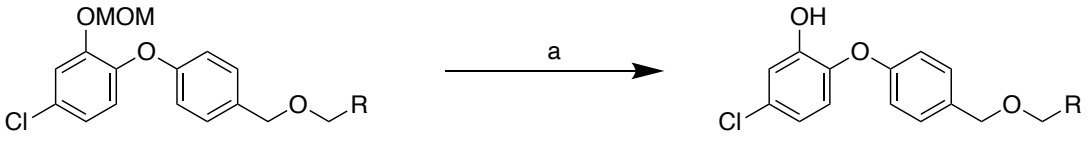

160-5 **81-86**

Scheme 28. *Deprotection of **160-5** to yield target compounds **81-6.** a) 6 M HCl, MeOH, 70 °C, 3 h.*

The yields for these reactions are shown in **Table 14**.

Table 14. *Yields for the reactions shown in **Scheme 28**.*

Compound	R	Yield / %
81	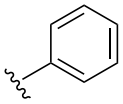	38
82	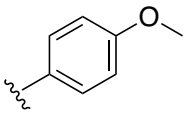	N/A
83	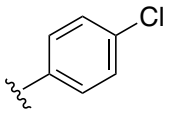	56
84	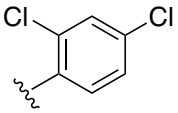	52
85		61
86	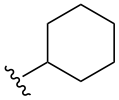	34

Moderate yields were obtained for all compounds following HPLC purification, with the exception of the *p*-methyoxybenzyl derivative **82**. In this instance, the major isolated product was observed to be **166** (**Figure 51**).

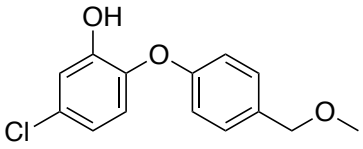

166

Figure 51. *The structure of the reaction product obtained by the attempted demethylation of* ***161****.*

The cleavage of the MOM group was confirmed by the presence of a broad singlet peak at ~5.90 ppm and the disappearance of the characteristic MOM signals in the ^{1}H NMR spectrum. However, both the ^{1}H and ^{13}C spectra showed the absence of the *p*-methoxybenzyl group. MS also showed the absence any peaks corresponding to the desired product. Both the NMR and MS data indicated that the product formed was actually ether **166**. The mechanism for this transformation remains unclear.

To deprotect the MOM group on **161,** while leaving the benzyl ether linkage intact, CBr_4 and PPh_3 were used, in line with the previous serendipitous observation that MOM groups are labile under these conditions (**Scheme 29**).

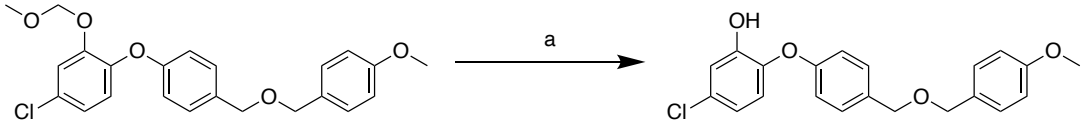

161 **82**

Scheme 29. *CBr_4 and PPh_3 mediated deprotection of* ***161****. a) CBr_4, PPh_3, DCE, 83 °C, 18 h. 62%*

This reaction furnished the desired product in a good yield, following HPLC purification. Interestingly this yield was superior to any obtained when using 6 M HCl to remove the MOM group (**Table 14**), suggesting it may be a more efficient route to performing this transformation.

3.4 Synthesis of Amine Derivative Target Molecules

The amine-linked series of compounds were designed to explore the effects of a positively charged substituent at the B-ring. The RSA for the target molecule **87** is shown in **Scheme 30**.

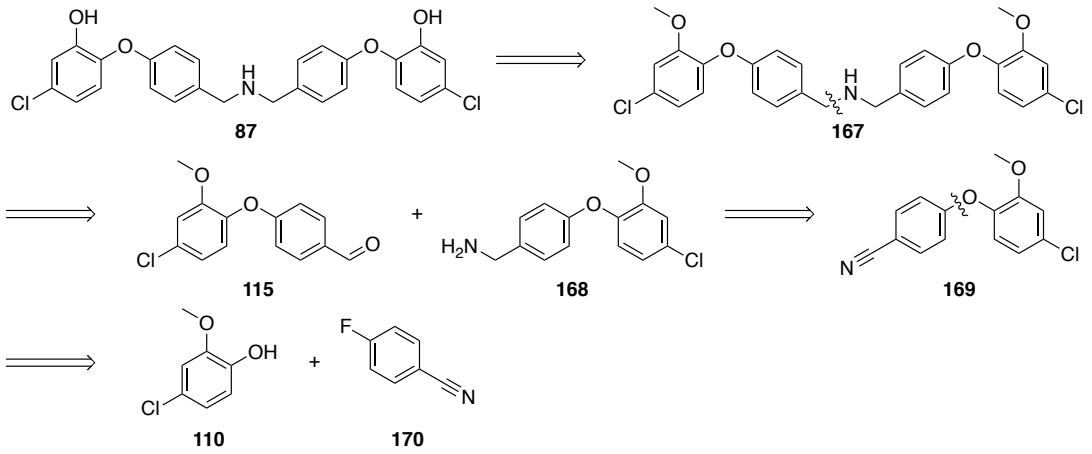

Scheme 30. *RSA for compound **87**.*

It was envisioned that **87** could be accessed through the demethylation of the corresponding protected compound, **167**. The di-TCL motif could be obtained through a reductive amination between the benzylamine derivative **168** and aldehyde **115**, (previously synthesised as part of the triazole synthesis, **Scheme 8**). The required benzylamine functionality would be unveiled through the functional group interconversion of its corresponding benzonitrile **169**, which in turn could be obtained from the readily available **110** and **170**.

The forward synthesis of **87** is shown in **Scheme 31**.

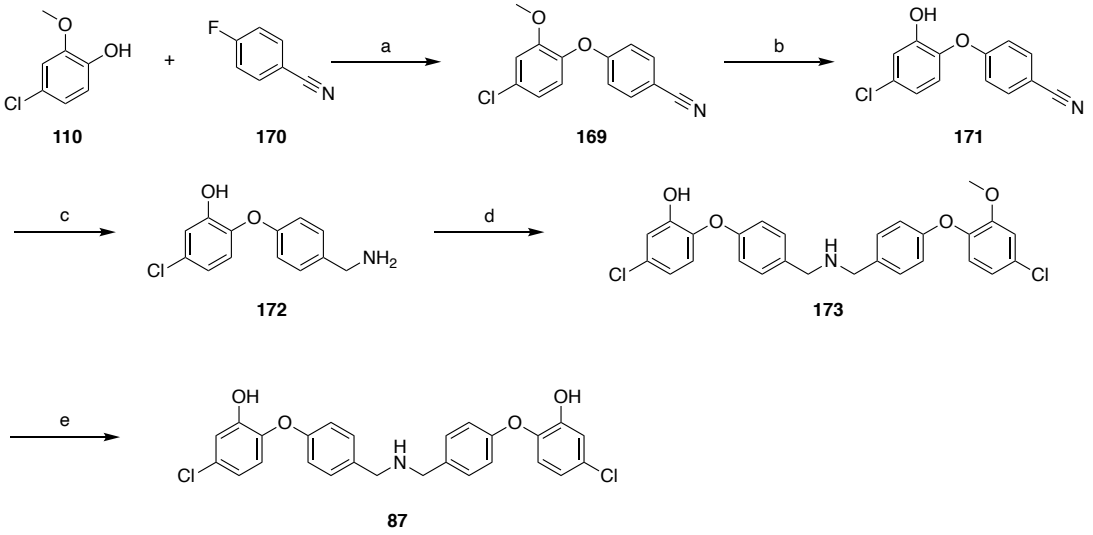

Scheme 31. *Forward synthesis of target molecule* ***87.*** *a) K_2CO_3, DMF, 130 °C, 18 h, 86%. b) BBr_3, CH_2Cl_2, 0 °C → r.t., N_2, 3 h, 83%. c) $LiAlH_4$, THF, 0 °C → r.t., N_2, 18 h, quant. d)* ***115****, $NaBH(OAc)_3$, DCE, r.t., 18 h, 76%. e) BBr_3, CH_2Cl_2, 0 °C → r.t., N_2, 3 h, 65%.*

Firstly, benzonitrile **169** was assembled *via* an S_NAr reaction, in a good yield. The phenol functionality was then unveiled using a BBr_3 mediated demethylation. Amine **172** was accessed through $LiAlH_4$ reduction of nitrile **171**, generating the desired product in a quantitative yield. With the primary amine installed, the di-TCL scaffold **173** was assembled using a reductive amination with aldehyde **115**. Finally, removal of the methyl protecting group furnished compound **87** in a moderate yield.

The structures of the other amine-linked target compounds are shown in **Figure 52**.

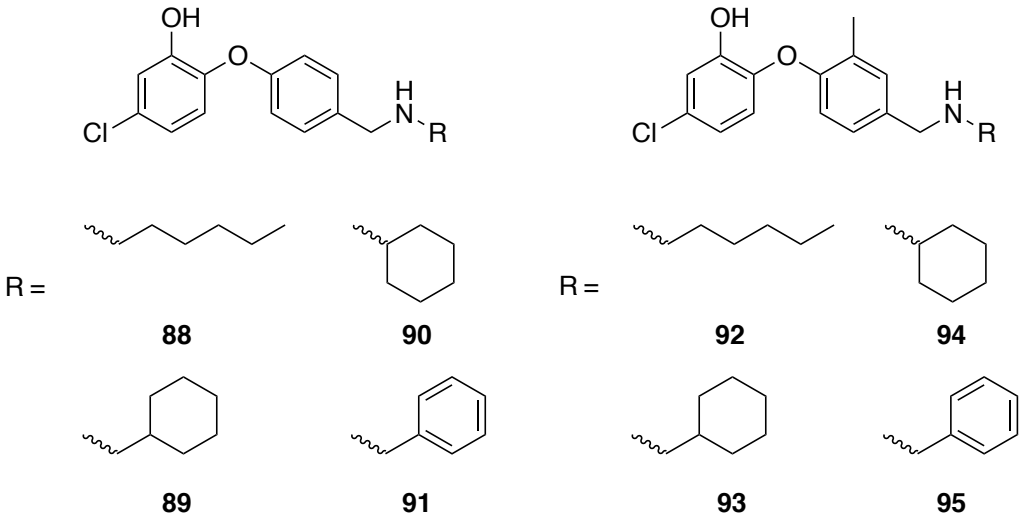

Figure 52. *Structures of the 8 amine target compounds.*

Using the previously assembled aldehyde **115**, the first four analogues could be synthesised over two steps (**Scheme 32**).

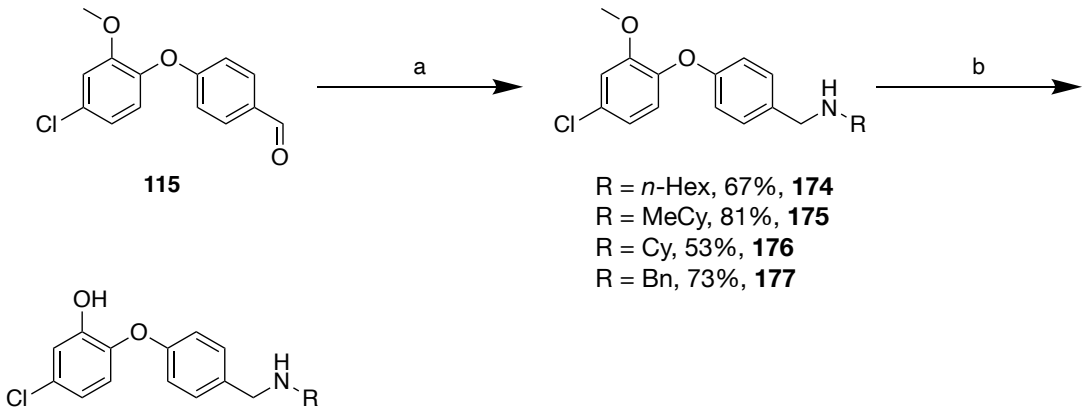

Scheme 32. *Forward synthesis of the amine-linked targets **88-91**. a) RNH_2, $NaBH(OAc)_3$, DCE, r.t., 18 h. b) BBr_3, CH_2Cl_2, 0 °C → r.t., N_2, 3 h.*

Reductive aminations of **115** was carried out in 1,2-dichloroethane (DCE) with $NaBH(OAc)_3$ as the reducing agent. These reactions furnished the desired amine in moderate-to-good yields. BBr_3 mediated demethylation was carried out under nitrogen atmosphere over the course of 3 h, providing the target compounds in acceptable yields.

Introduction of a methyl group to the ortho position of the B-ring has been shown to increase the potency of TCL derivatives. For this reason, a number of amine derivatives containing a B-ring methyl group were synthesised (**Scheme 33**).

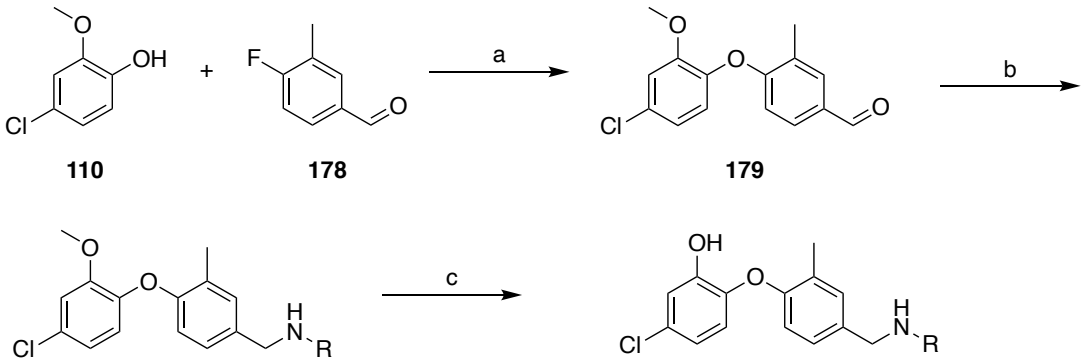

R = *n*-Hex, 72%, **180**
R = MeCy, 57%, **181**
R = Cy, 80%, **182**
R = Bn, 76%, **183**

R = *n*-Hex, 66%, **92**
R = MeCy, 61%, **93**
R = Cy, 71%, **94**
R = Bn, 59%, **95**

Scheme 33. *Forward synthesis of the amine-linked targets **92**-**95**. a) K_2CO_3, DMF, 130 °C, 18 h, 88%. b) RNH_2, $NaBH(OAc)_3$, DCE, r.t., 18 h. c) BBr_3, CH_2Cl_2, 0 → r.t., N_2, 3 h.*

Biaryl ether scaffold **179** was constructed through S_NAr fusion of two commercially available precursors, furnishing the desired compound in a good yield. Reductive aminations of **179** with the corresponding primary amines generated the target secondary amines (**180**-**83**) in good yields. Subsequent demethylation furnished a further 4 target compounds in acceptable yields.

3.5 Synthesis of A-Ring Derivative Target Molecules

In addition to the B-ring modified TCLs, a range of A-ring modified derivatives were designed to further explore SAR at the A-ring (**Figure 53**).

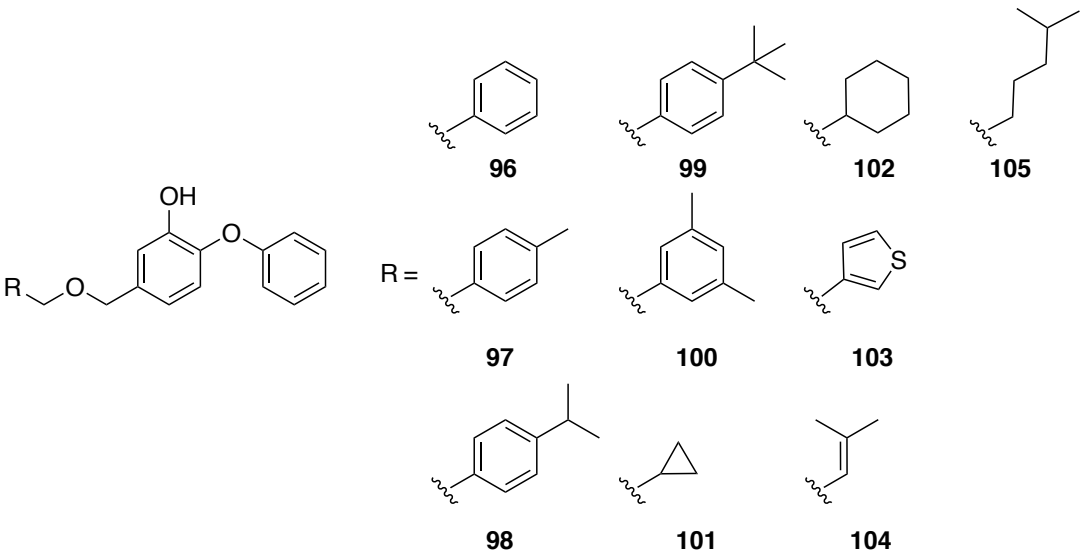

Figure 53. *Structures of the A-ring modified TCL target molecules.*

Initial assembly of the biaryl scaffold was attempted using a copper mediated Chan-Lam coupling between Vanillin and phenylboronic acid (**Scheme 34**).

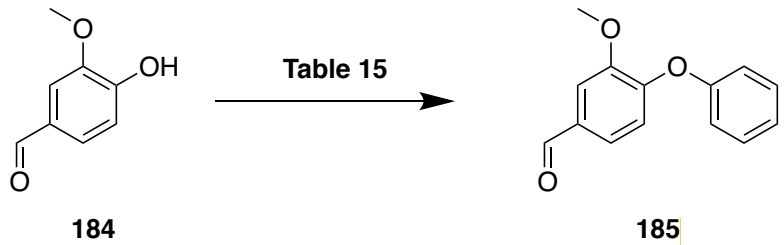

Scheme 34. *Attempted Chan-Lam cross-coupling to form **185.** Conditions shown in **Table 15.***

The conditions attempted for this reaction are shown in **Table 15**.

Table 15. *Conditions investigated for the reaction shown in* ***Scheme 34****.*

Conditions	Phenylboronic Acid / equivs	$Cu(OAc)_2$ equivs	Base (equivs)	Solvent	Time / h	Yield / %
A	2	1.1	Et_3N (5) Pyridine (5)	CH_2Cl_2	72	27
B	2	1.1	Et_3N (2.5)	CH_2Cl_2	18	30

While both reactions provided the desired compound, they did so in low yields and required laborious purification of complex mixtures of products. Following these trial reactions, the decision was taken to use the S_NAr procedure utilised in the assembly of the previously discussed biaryl scaffolds (**Scheme 35**).

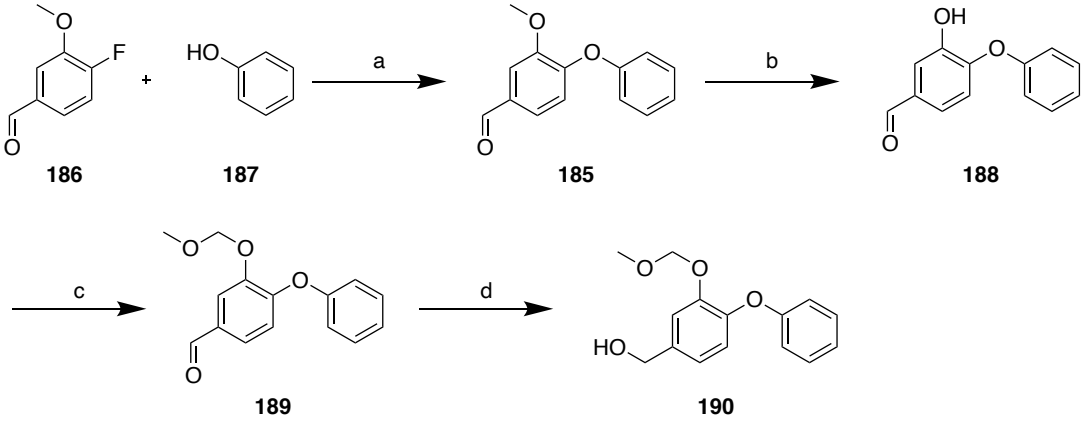

Scheme 35. *Forward synthesis of alcohol* ***190****.* a) *K_2CO_3, DMF, 130 °C, 18 h, 79%; b) AcOH, HBr, 140 °C, 18 h, 38%; c) MOMCl, DIPEA, CH_2Cl_2, r.t., 18 h, 81%; d) $NaBH_4$, MeOH, 0 → r.t., 4 h, 81%.*

The performance of these reactions was consistent with that of the reactions detailed in Scheme **8** and **10**. Following the synthesis of **190**, the alcohol group was derivatised to form the target pre-cursors (**Scheme 36**).

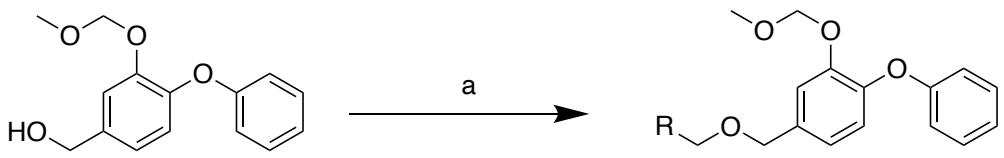

190 **191 - 200**

Scheme 36. *Forward synthesis of alcohol **191** - **200**. a) XCH_2R, NaH, DMF, 0 → r.t., 18 h.*

Yields for these reactions are reported in **Table 16.**

Table 16. *Yields for the reaction show in* ***Scheme 36****.*

Compound	R	Yield / %
191	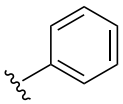	80
192	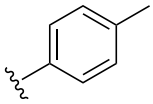	85
193	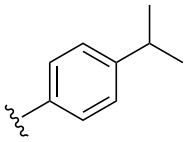	87
194	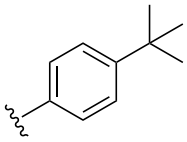	49
195	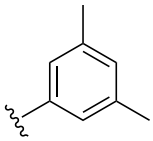	82
196		78
197	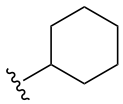	56
198	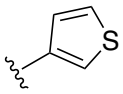	64
199	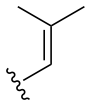	63
200	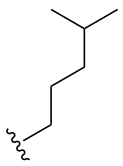	70

All compounds were obtained in reasonable yields, with the exception of **194** and **197**. The low yield of **197** is consistent with the previous observations that substitution using (bromomethyl)cyclohexane provided low yields (**Table 14**). These precursors were then subsequently deprotected to unveil the phenol functionality and generate a further 10 final compounds (**Scheme 37**).

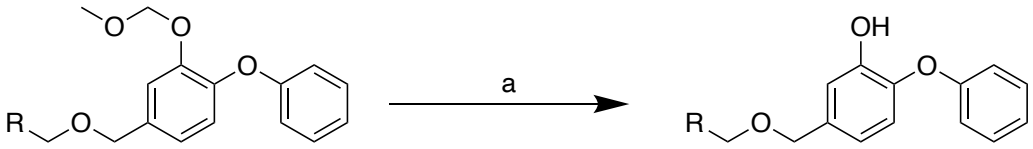

191 - 200 **96 - 105**

Scheme 37. *Deprotection of **191-200** to yield target compounds **96-105**. a) 6 M HCl, MeOH, 70 °C, 3 h.*

Yields for these reactions are shown in **Table 17**.

Table 17. *Yields for the reaction show in* ***Scheme 37****.*

Compound	R	Yield / %
96	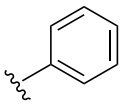	38
97	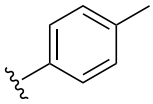	50
98	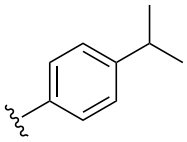	31
99	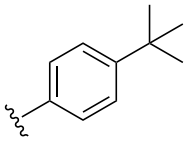	22
100	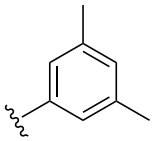	28
101		38
102	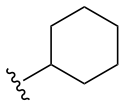	49
103	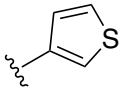	38
104	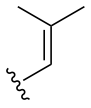	48
105	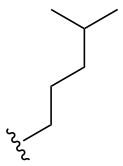	31

All compounds were obtained in a reasonable yield after HPLC purification. This completed the synthesis of a total of 50 novel compounds which could be evaluated for their potency as anti-TB molecules.

3.6 Synthesis of an InhA Substrate Mimic

An InhA substrate mimic was synthesised for use in isolated enzyme assays (**Scheme 38**). This substrate mimc replaces the acyl carrier protein of the natural substrate with a Coenzyme A (CoA) unit. This substrate, and ones with longer carbon chains have been used frequently in the literature to identify novel InhA inhibitors.[102, 111, 120]

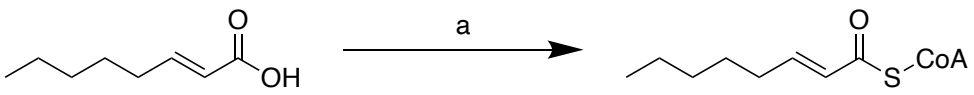

201 **202**

Scheme 38. *Synthesis of an InhA substrate mimetic,* ***202****, for use in isolated enzyme assays. a) Coenzyme A,* K_2CO_3*, PyBOP, THF:*H_2O *(1:1),* N_2*, darkness, r.t., 18 h. 27%*

Using the PyBOP coupling reagent, the desired thioester was synthesised in a modest yield following HPLC purification.[175] It should be noted that the reaction must be conducted in the absence of light as the product has previously been shown to degrade upon prolonged exposure to light. This material should be stored in solid form, at –80 °C and samples should not be reused after defrosting.

4. Biological Evaluation

4.1 Isolated Enzyme Assay Overview

The activity of InhA can be assessed using a UV-based assay which monitors the consumption of NADH by the enzyme as it reduces its substrate (**Scheme 39**).[176, 177]

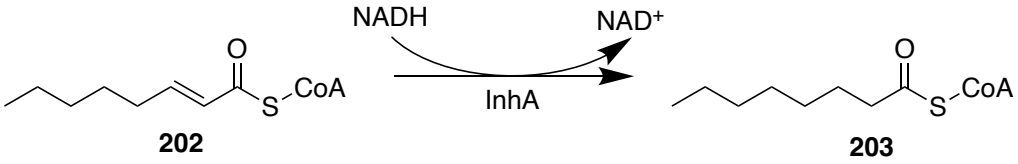

202 **203**

Scheme 39. *InhA catalysed reduction of a 2-trans-octenoyl CoA substrate mimic.*

While both NADH and NAD^+ have a λ_{max} at 259 nm, NADH shows a second strong absorbance peak at 340 nm (ε = 6.22 mM^{-1} cm^{-1}) which is not present in the oxidised form. Importantly, the soluble InhA protein also shows minimal absorbance at 340 nm, this means that the activity of the enzyme can be gauged by monitoring absorbance at this wavelength. An active enzyme will convert NADH to its oxidised form, thus resulting in a decrease in absorbance at 340 nm. Alternatively, if the enzyme's function is inhibited, the NADH signal will reduce at slower rate, or not at all in the case of total inhibition.

4.2 Protein Expression and Purification

The InhA:Pet15a plasmid construct was kindly provided by Prof. Peter Tonge.[74] This plasmid vector has previously been used for expression of InhA within the Thomas group, so pre-existing methods were available for expression and purification of the protein.[171, 178, 179]

InhA protein expression and purification studies were conducted in collaboration with Malcolm Lamont, a BBSRC-funded PhD student in the Thomas group. Isopropyl β-

D-1-thiogalactopyranoside (IPTG) was used to induce protein expression in an overnight culture of *E. coli.* (BL21 strain) inoculated with the plasmid. The soluble protein contained an N-terminal histidine tag to facilitate its purification by immobilised metal-affinity chromatography (IMAC). The IMAC trace obtained during purification of the crude extract is shown in **Figure 54.**

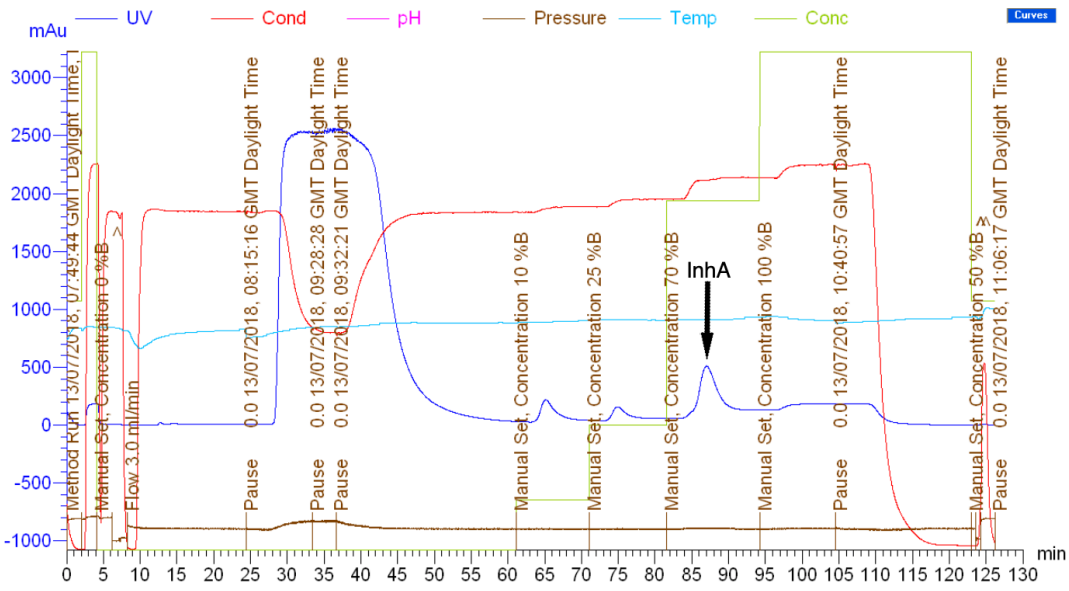

Figure 54. *Typical IMAC trace obtained during purification of soluble InhA protein from the crude cell extract. InhA elution peak at 85-90 mins. Image captured by Malcom Lamont.*

The purity of the isolated protein was confirmed using sodium dodecyl sulfate polyacrylamide gel electrophoresis (SDS-PAGE), the resulting gel is shown in **Figure 55**.

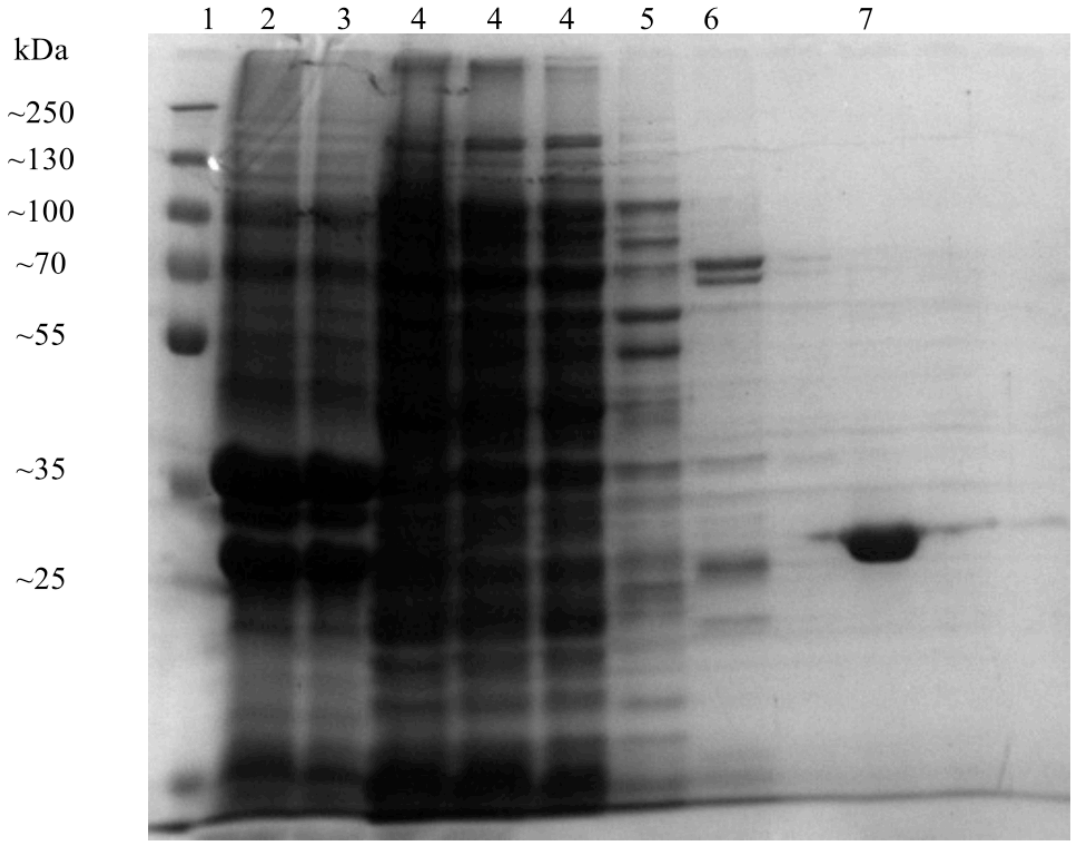

Figure 55. *SDS-PAGE gel showing the purity of the isolated InhA protein. Numbering: 1-Protein ladder, 2-Insoluble fraction, 3-soluble fraction, 4-FPLC flow-through, 5-FPLC peak at 10% imidazole, 6-FPLC peak at 25% imidazole, 7-FPLC peak at 70% imidazole, corresponding to the expected mass of the InhA protein. Image prepared by Malcolm Lamont.*

The gel shown in **Figure 55** shows that the desired protein was isolated with a high degree of purity from the crude mixture. The mass of the isolated protein was also confirmed using protein mass spectrometry. The mass spectrum for the isolated InhA protein was recorded by Malcolm Lamont and Jedd Bellamy-Carter and is shown in **Figure 56**.

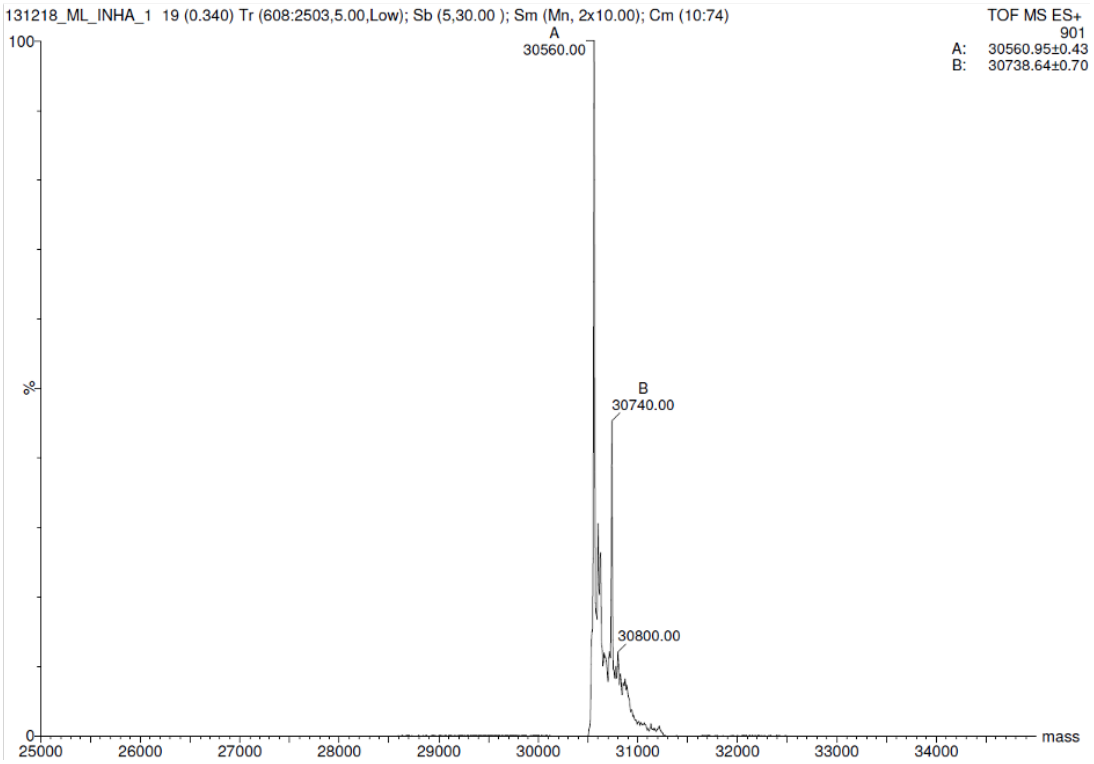

Figure 56. *Mass spectrometry spectra of purified InhA protein. Target mass 30,559.97 Da. Secondary peak at 30,740.00 Da consistent with partial alpha-N-6-phosphogluconylation of his-tag.*

Combined, this data confirms the purification of the soluble InhA protein which could be used in isolated enzyme studies. The pure protein was obtained in a yield of 13 mg L^{-1}.

4.3 Enzyme Assay Validation

Prior to using the isolated protein to assess the activity of the synthesised inhibitors, work was conducted by Malcolm Lamont in order to assess the InhA enzyme kinetics to obtain the optimal assay conditions.

In order to confirm the function and activity of the enzyme, K_M values were calculated for both NADH and the substrate. The Michaelis-Menton saturation curves for InhA is shown in **Figure 57**.

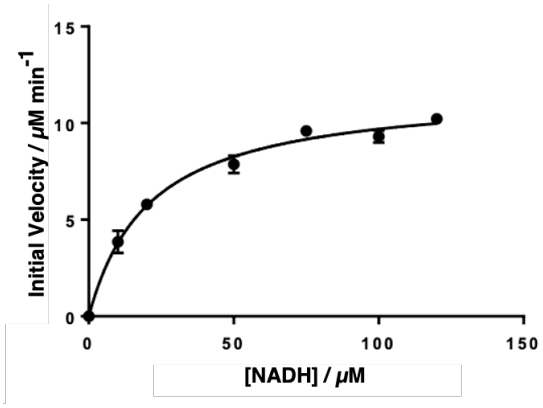

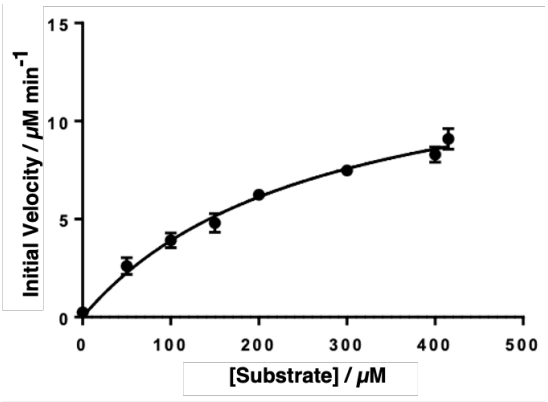

[NADH] / μM	Average initial velocity ± SD / μM min^{-1}
0	0
10	3.86 ± 0.22
20	5.79 ± 0.06
50	7.87 ± 0.17
75	9.59 ± 0.10
100	9.30 ± 0.12
120	10.22 ± 0.09

[Substrate] / μM	Average initial velocity ± SD / μM min^{-1}
0	0.24 ± 0.10
50	2.61 ± 0.16
100	3.92 ± 0.14
150	4.81 ± 0.18
200	6.24 ± 0.10
300	7.48 ± 0.08
400	8.29 ± 0.15
415	9.09 ± 0.20

Figure 57. *Kinetic studies for NADH and enzyme substrate in the standard InhA reaction. Data obtained by Malcolm Lamont.*

These kinetic studies gave a K_M values of 21 ± 1.3 and 267 ± 23.6 μM for NADH and the substrate, respectively. These values are consistent with those reported in previous studies and so the function and activity of the enzyme was deemed sufficient to proceed to biological testing of inhibitors.

4.4 Biological Evaluation Using an Isolated Enzyme Assay

All of the compounds tested using the isolated enzyme assay are shown below in **Figure 58-60**. All compounds were purified to >95%, as calculated by analytical HPLC, before evaluation, a representative analytical HPLC trace is included in **Section 9.3**.

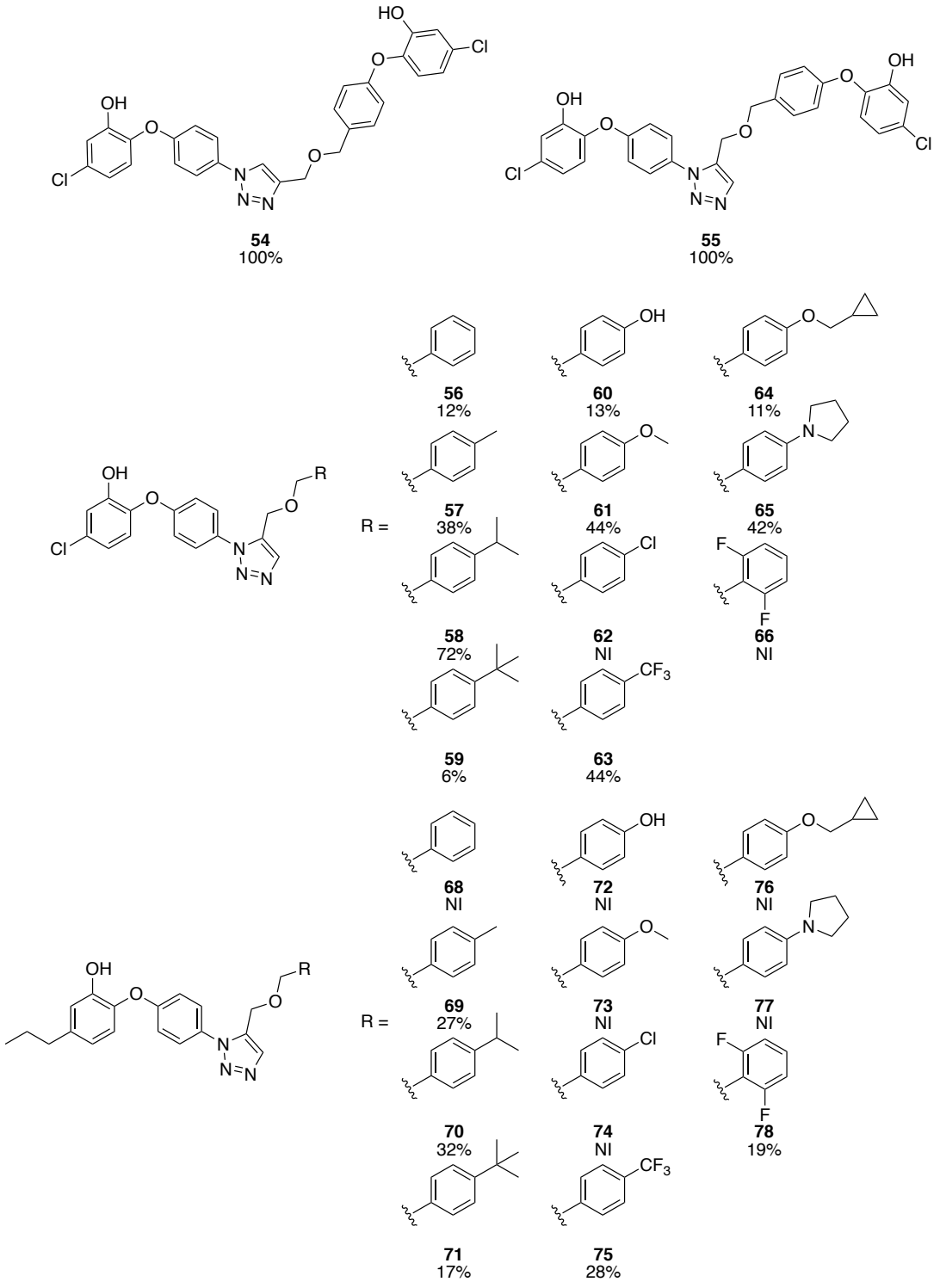

Figure 58. *The structures of all triazole compounds synthesised for evaluation as InhA inhibitors and percentage inhibition of InhA at 50 μM.*

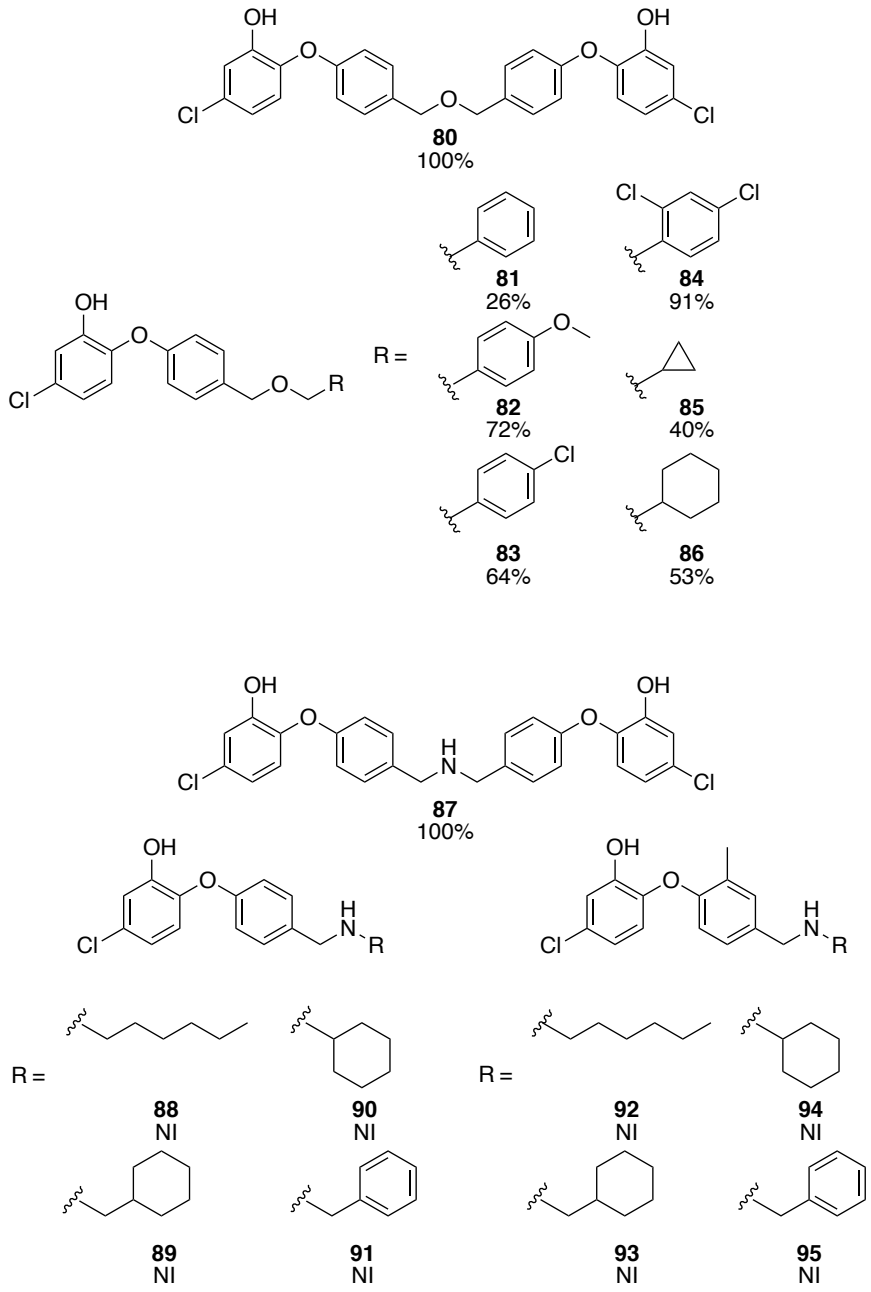

Figure 59. *The structures of all ether and amine-linked compounds synthesised for evaluation as InhA inhibitors and percentage inhibition of InhA at 50 μM.*

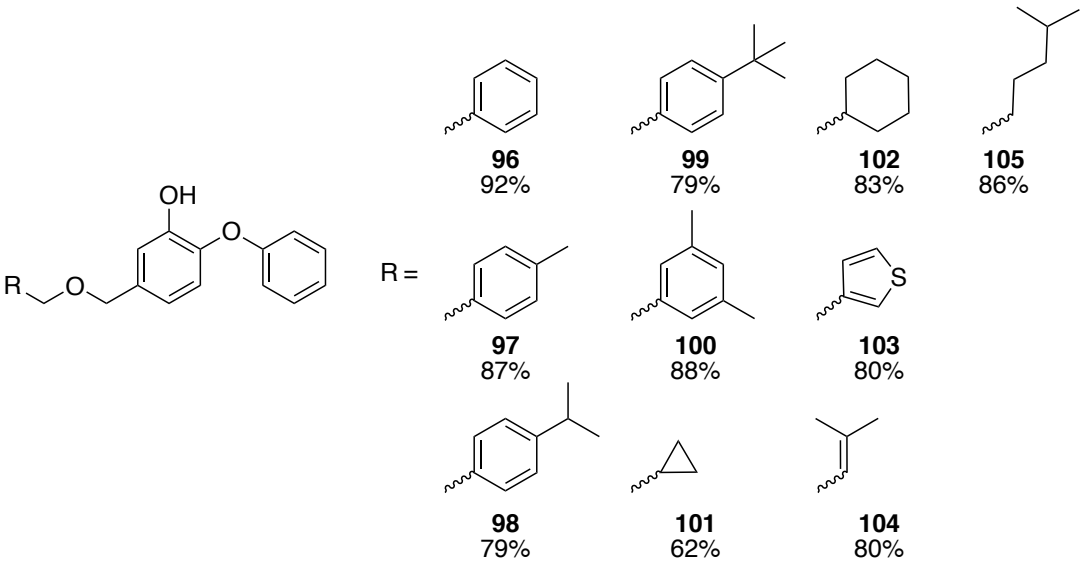

Figure 60. *The structures of all A-ring derivatives synthesised for evaluation as InhA inhibitors and percentage inhibition of InhA at 10 μM.*

4.4.1 Evaluation of Chlorinated-Triazole Derivatives Against InhA

All initial enzyme inhibition studies were conducted at 30 ºC, at a final concentration of Inhibitor (50 μM, 0.5% NaOH), PIPES (30 mM, pH 6.8), OCoA (400 μM), NADH (100 μM) and InhA (150 nM). Experiments were conducted in duplicate and results were taken as an average of the two assays. The InhA inhibition data for the chlorinated triazole derivatives is shown in **Table 18**.

Table 18. *InhA inhibition data for compounds **54**-**66**.*

Compound	R	GOLD Fitness Score	Inhibition / %	S.E.M / %
54 *(1,4 isomer)*	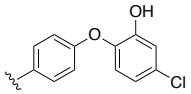	74.7	100	-
55 *(1,5 isomer)*	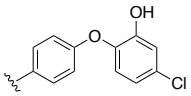	87.7	100	-
56	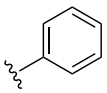	65.2	12	1
57	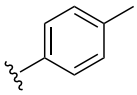	73.5	38	3
58	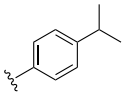	77.8	72	10
59	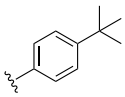	74.0	6	2
60	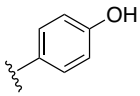	69.0	13	4
61	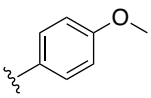	76.7	44	1
62	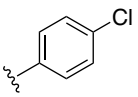	73.2	NI	2
63	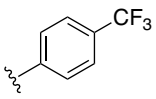	75.6	44	3
64	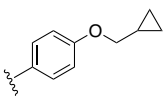	80.7	11	3
65	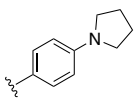	83.6	42	6
66		71.0	NI	1
TCL	**-**	68.4	92	10

Two compounds, **54** and **55** showed total inhibition of enzyme activity at 50 μM. **55** is the 1,5-triazole which was predicted to show complete overlap with both TCL molecules observed in the 1P45 crystal structure. Interestingly, **54**, the 1,4-triazole also showed complete inhibition of enzyme activity at 50 μM, this is despite the docking simulations suggesting it occupied a disfavoured binding pose which resulted in the loss of the key hydrogen bonding network. It is possible that his predicted binding mode is wrong, or the molecule shows a novel binding mode where the H-bonding network is not vital.

In terms of SAR, moving from H->Me->*i*Pr (**56**->**58**) results in increased inhibition with increasing hydrophobicity, however, the introduction of a *t*Bu (**59**) group results in a significant reduction in enzyme inhibition. This suggests that such a bulky group results in major clashes with the protein. These results correlate with the fitness scores, with compound **59** showing a lower fitness score than **58**. The possibility that this region is size sensitive is further supported by the fact that **61**, **63** and **54**, all of which bear relatively small R groups, show moderate inhibition. Further evaluation of **54** and **55** was performed to calculate the IC_{50} of each compounds (**Figure 61**).

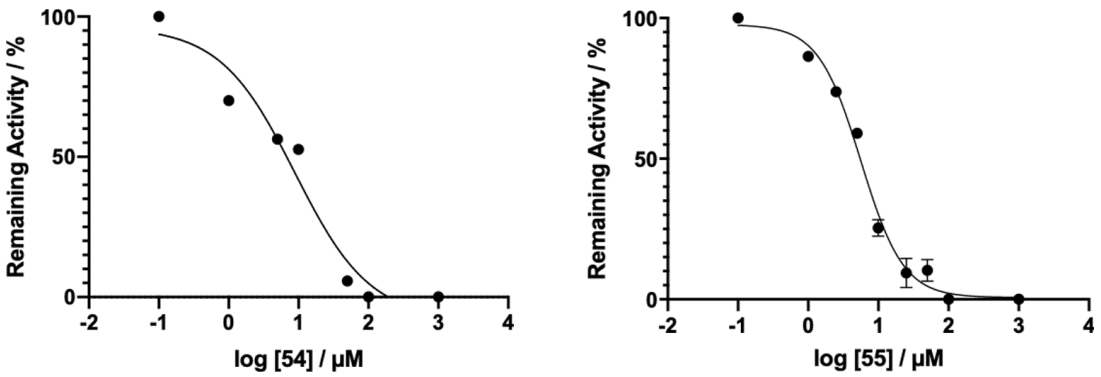

Figure 61. *IC_{50} curves for compounds **54** and **55**.*

Compound **54** exhibited an IC_{50} of 9.2 ± 3.4 μM (n = 3), whereas **55** achieved 50% inhibition at 5.6 ± 0.8 μM (n = 3). Interestingly, this suggests that the 1,5-triazole architecture does improve inhibition but not as much as might have been expected based on the predicted binding modes (**Section 2.6, Figure 29**). The result for **55** represents a modest improvement over TCL (IC_{50} = 9.2 ± 1.3 μM, n = 2, data included in **Section 8.6**) which was obtained in experiments conducted in parallel. This IC_{50} value for TCL is also consistent with those previously reported in the literature.[113]

4.4.2 Evaluation of *n*-Propylated-Triazole Derivatives Against InhA

To explore the effects of substitution on the A-ring, the propylated-triazole derivatives were screened for their activity against InhA. The results of these experiments are shown in **Table 19**.

Table 19. *InhA inhibition data for compounds **68**-**78**.*

Compound	R	GOLD Fitness Score	Inhibition / %	S.E.M / %
68	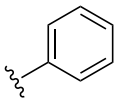	82.7	NI	-
69	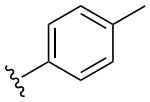	83.0	27	1
70	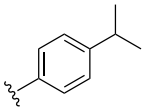	79.7	32	5
71	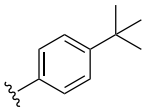	80.0	17	2
72	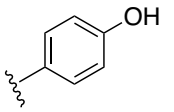	80.4	NI	-
73	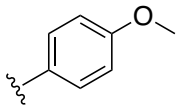	84.6	NI	-
74	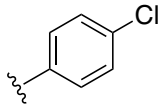	81.6	NI	-
75	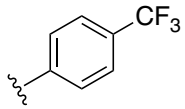	83.0	28	3
76	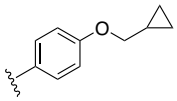	83.1	NI	-
77	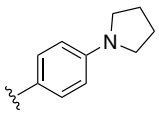	82.2	NI	-
78	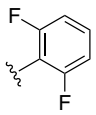	82.2	19	2
TCL	**-**	68.4	92	10

Despite having encouraging docking scores, the *n*-propyl-triazole derivatives showed disappointing inhibition of InhA. No SAR can be derived for the effects of the varying R group, however it can be concluded that *n*-propylation of the A-ring is deleterious to the potency of these compounds as in every instance the chlorinated analogues showed greater enzyme inhibition.

4.4.3 Evaluation of Ether Derivatives Against InhA

The isolated enzyme inhibition data for the ether-linked series of compounds is shown in **Table 20**.

Table 20. *InhA inhibition data for compounds **80**-**86**.*

Compound	R	GOLD Fitness Score	Inhibition / %	S.E.M / %
80	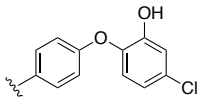	65.3	100	-
81		64.5	26	4
82	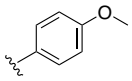	67.4	72	3
83	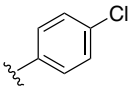	70.8	64	8
84	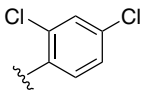	72.0	91	3
85		61.2	40	6
86	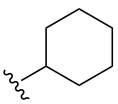	59.6	33	5
TCL	-	68.4	92	10

The most potent compound was **80**, showing total enzyme inhibition at 50 μM. **82**, **83** and **84** showed moderate enzyme inhibition, with results suggesting that increasing hydrophobicity results in greater inhibition. The aliphatic derivatives (**85**/**86**) showed relatively low inhibition, this suggests that substituted-aromatic substituents are more effective as an R group. While an IC_{50} for **80** was not determined, its potency at lower concentrations was investigated. **80** showed 44% inhibition at 25 μM and 12% at 10 μM, suggesting an IC_{50} in the range of 25 - 30 μM, a roughly 3 fold increase compared to TCL.

4.4.4 Evaluation of Amine Derivatives Against InhA

The isolated enzyme inhibition data for the amine-linked series of compounds is shown in **Table 21**.

Table 21. *InhA inhibition data for compounds **87**-**95**.*

Compound	R	GOLD Fitness Score	Inhibition / %	Standard Error of Mean / %
87	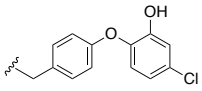	81.3	99	2
88	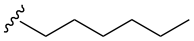	72.4	NI	-
89	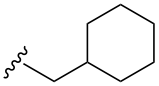	70.3	NI	-
90	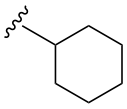	71.2	NI	-
91	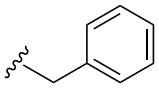	64.7	NI	-
92 *(Methylated B-Ring)*	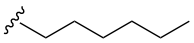	77.7	NI	-
93 *(Methylated B-Ring)*	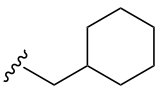	67.3	NI	-
94 *(Methylated B-Ring)*	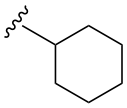	71.4	NI	-
95 *(Methylated B-Ring)*	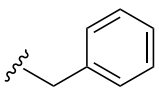	66.8	NI	-
TCL	-	68.4	92	10

Disappointingly, only compound **87** showed any inhibition of InhA activity at 50 μM. This suggests that addition of the positively charged nitrogen group to the B-ring is significantly deleterious to enzyme inhibition. Compound **87** is awaiting further evaluation to establish its IC_{50}.

4.3.5 Evaluation of A-Ring Derivatives Against InhA

The isolated enzyme inhibition data for the A-ring derivatives is shown in **Table 22**. Given the literature precedent surrounding A-Ring modified TCL derivatives, these compounds were tested at a final concentration of 10 μM, rather than 50 μM.

Table 22. *InhA inhibition data for ether-linked compounds **96**-**105** at 10 μM*

Compound	R	GOLD Fitness Score	Inhibition / %	S.E.M / %
96	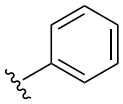	68.0	92	2
97	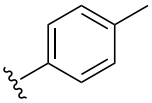	69.5	87	2
98	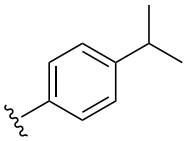	72.5	79	13
99	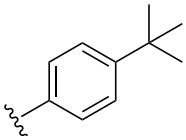	70.1	79	6
100	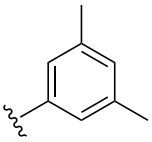	74.2	88	2
101		64.0	62	4
102	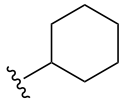	67.3	83	11
103	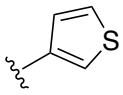	70.9	80	10
104	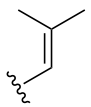	68.1	80	15
105	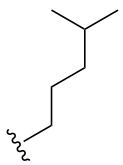	68.4	86	11

In line with data previously recorded in the literature, these A-ring modified derivatives showed significant potency, with all compounds, except the **101** (R = cyclopropyl) showing ~80% inhibition at 10 μM. The lower inhibition observed by **101** is to be excepted due to the relatively small size of the cyclopropyl group, resulting in a weaker engagement with the substrate binding loop. Additional evaluation was undertaken at 1 μM to further investigate the potency of these compounds (**Table 23**).

Table 23. *InhA inhibition data for ether-linked compounds **96**-**105** at 1 μM*

Compound	R	Inhibition / %	S.E.M / %
96	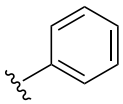	67	10
97	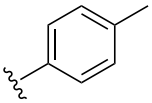	70	23
98	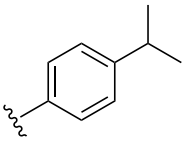	52	5
99	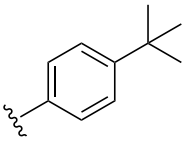	22	10
100	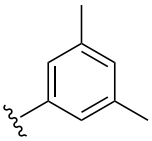	59	8
101		47	8
102	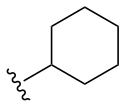	41	4
103	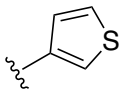	57	9
104	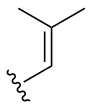	44	12
105	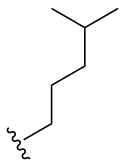	66	30

All compounds retained moderate inhibition at 1 μM, with the exception of **99**. Interestingly, compound **99** shows a significant reduction in inhibition, this is surprising as it was thought that the ^{t}Bu group would facilitate hydrophobic contacts with the substrate binding loop. It is possible that the bulky ^{t}Bu group results in steric clashes which negate the benefits of any hydrophobic contacts. It should also be noted that **99** showed a unique binding mode compared to the other A-ring derivatives (**Figure 39**, panel A), this could be responsible for the significant drop in potency observed. Compounds **96**, **97**, **100**, **103** and **105** also showed greater than 55% inhibition at 1 μM, further evaluation of these compounds was undertaken at 500 nM to investigate their inhibition in the nanomolar concentration range (**Table 24**).

Table 24. *InhA inhibition data for select ether-linked compounds at 500 nM.*

Compound	R	Inhibition / %	Standard Error of Mean / %
96	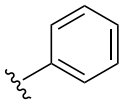	48	17
97	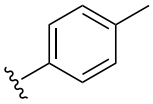	62	23
98	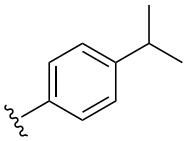	53	3
100	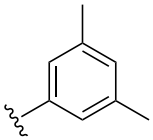	26	7
103	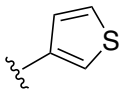	33	3
105	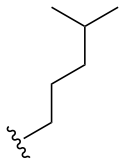	48	28

The data in **Table 24** shows that, at 500 nM, compound **96**, **100**, **103** and **105** fell below 50% inhibition of purified InhA. However, compound **97** retained a significant degree of potency towards the enzyme. This compound was then subject to IC_{50} determination to further evaluate its potency (**Figure 62**).

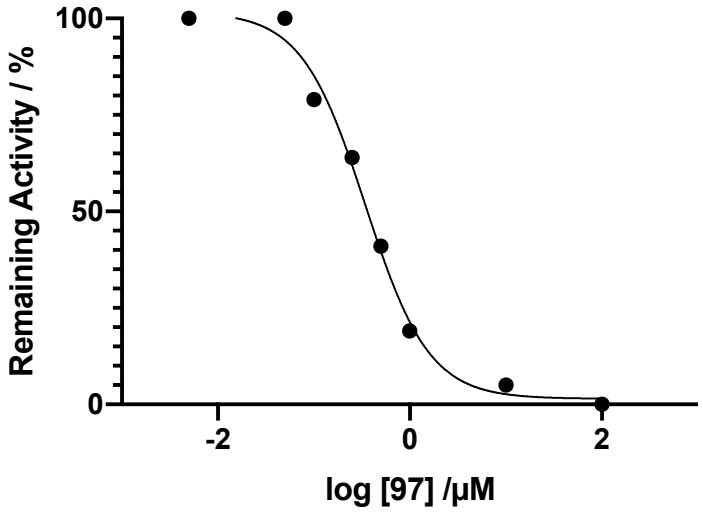

Figure 62. IC_{50} curve for **97**

IC_{50} determination for compound **97** showed half maximal inhibition at 340 ± 102 nM (n = 3), representing potent inhibition of InhA. This compound, and structural analogues, are worthy of further evaluation in attempts to improve enzyme inhibition.

4.5 Biological Evaluation Using Whole-Cell Screening Against *Mycobacterium bovis*

Following the isolated-enzyme assays, compounds were subject to whole-cell evaluation against *M. bovis,* a less pathogenic strain of Mycobacteria*. M. bovis* was chosen as its InhA protein shares an identical sequence as *Mtb*, this is not the case for all Mycobacteria, for example *Mycobacterium smegmatis* has a different InhA sequence to *Mtb*. Whole-cell evaluation was performed by Alice Lanne in the Alderwick group at the University of Birmingham. Initial screening was performed at a final inhibitor concentration of 40 μM. Bacteria were then incubated for 7 days at 37 ºC and 5% CO_2. After 7 days, resazurin was added and the plates were incubated for a further 24 hours before the resulting fluorescence was used to determine cell

viability. Experiments were conducted in triplicate and results are shown as an average.

4.5.1 Evaluation of Chlorinated-Triazole Derivatives Against *Mycobacterium bovis*

To evaluate the potency of the chlorinated 1,5-triazole derivatives whole-cell screening was performed against *M. bovis*. Growth inhibition data is shown in **Table 25**.

Table 25. *Whole-cell growth inhibition data for compounds **54**-**66**.*

Compound	R	Growth Inhibition / %	S.E.M / %	cLogP
54 *(1,4 isomer)*	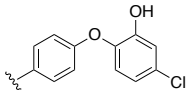	-	-	5.80
55 *(1,5 isomer)*	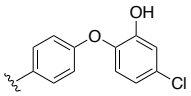	20	2	5.80
56	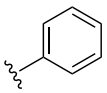	3	10	5.11
57	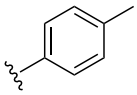	6	5	5.43
58	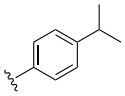	15	5	5.89
59	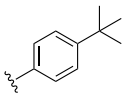	20	3	6.11
60	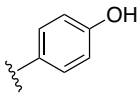	0	17	4.37
61	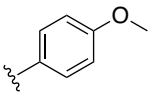	40	3	5.03
62	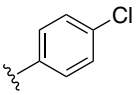	0	21	5.71
63	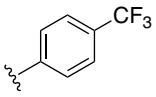	19	3	6.09
64	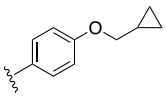	99	1	6.07
65	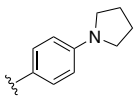	23	3	5.95
66		4	7	5.28
TCL	**-**	70	10	4.98

Of the compounds tested, only **64** showed significant growth inhibition at 40 μM. While the results for **60** and **62** have a relatively high standard deviation, the error is not enough to warrant further investigation. Disappointing, there appears to be little relationship between whole-cell activity and cLogP. Given the dense, hydrophobic nature of the mycobacterial cell wall, it was expected that compounds with greater hydrophobicity would be better suited to diffusing through the cell wall. At the time of writing, **54** is still awaiting whole-cell evaluation, this will be performed in due course. Further evaluation was undertaken to establish the MIC value for **64**, the MIC_{99} curve is shown below (**Figure 63**).

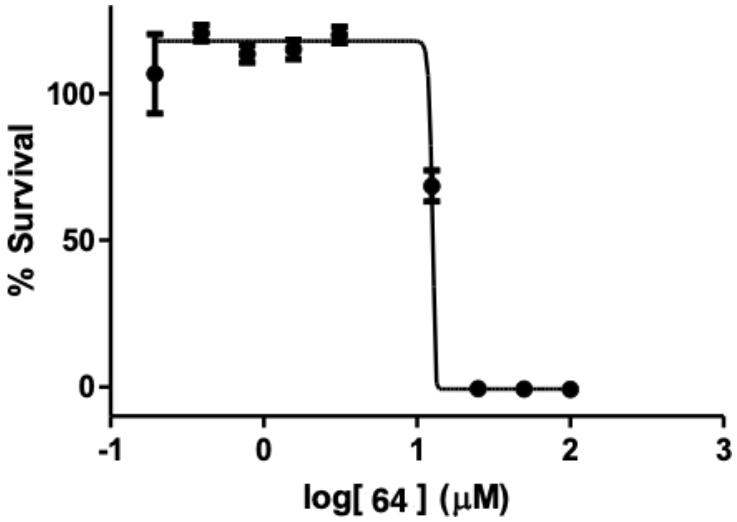

Figure 63. *MIC_{99} curves for **64**.*

Compound **64** displayed an MIC_{99} of 13.00 ± 5.03 μM (n = 3) which equates to 6.2 ± 2.4 μg mL^{-1}. Given that **64** showed only 11% InhA inhibition at 50 μM, it is obvious that this compound must have an alternate intracellular target(s) in order to demonstrate such high potency in the whole-cell assay. Additional work will be required to elucidate this target. A major limitation of this data is the lack of a distinct curve in the % survival. This makes calculating an MIC_{99} value somewhat

speculative, this could be overcame by testing a greater range of concentrations in the range where % survival begins to fall. This work was unable to be carried out due to COVID-19 and the restricted access to the required facilities. The lack of distinct curves on MIC_{99} plots is something which is apparent in several of the plots contained within this section.

4.5.2 Evaluation of *n*-Propylated-Triazole Derivatives Against *Mycobacterium bovis*

To evaluate the effects of *n*-propylation of the A-ring, the 1,5-triazole derivatives were screened for their activity against whole-cell *M. bovis*. Growth inhibition data is shown in **Table 26**.

Table 26. *Whole-cell growth inhibition data for compounds **68**-**78**.*

Compound	R	Growth Inhibition / %	S.E.M / %	cLogP
68	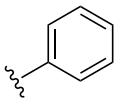	22	2	5.56
69	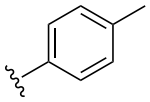	10	5	5.76
70	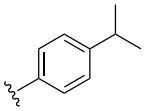	15	3	6.34
71	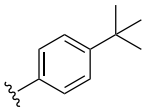	29	5	6.71
72	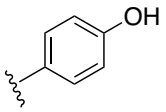	7	1	4.69
73	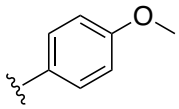	20	1	5.47
74	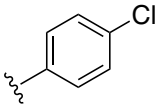	18	5	6.06
75	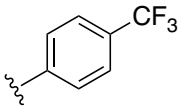	12	2	6.60
76	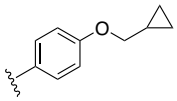	21	4	6.55
77	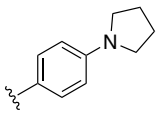	30	2	6.25
78	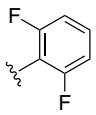	12	4	5.87
TCL	**-**	70	10	4.98

As with the chlorinated triazoles, the *n*-propylated derivatives showed only modest growth inhibition at 40 μM. Interestingly, the *n*-propyl derivatives are broadly more potent against whole-cell *M. bovis* than the chlorinated analogues (except **73**, **74** and **76**). This suggest that the propyl chain improves the ability of the compounds to pass through the mycobacterial cell wall, resulting in a slightly higher intracellular concentration of the inhibitors.

4.5.3 Evaluation of Ether Derivatives Against *Mycobacterium bovis*

The whole-cell potency of the ether linked compounds was evaluated against *M. bovis.* Growth inhibition data is shown in **Table 27**.

Table 27. *Whole-cell growth inhibition data for compounds **80-86**.*

Compound	R	Growth Inhibition / %	S.E.M / %	cLogP
80	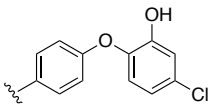	14	1	6.62
81	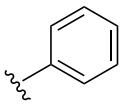	NI	17	5.32
82	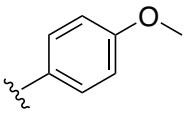	20	15	5.37
83	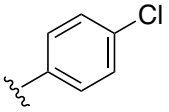	86	3	5.82
84	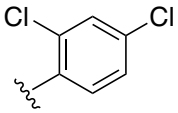	NI	39	6.11
85		NI	13	4.51
86	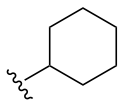	NI	24	5.40
TCL	-	70	10	4.89

Disappointingly these compounds demonstrated only modest growth inhibition at 40 μM. The most potent compound was **83**, which showed an 86% reduction in bacterial growth, given this compound did not achieve full growth inhibition it was not chosen for further MIC evaluation.

4.5.4 Evaluation of Amine Derivatives Against *Mycobacterium bovis*

The whole-cell potency of the amine derivative compounds was evaluated against *M. bovis*. Growth inhibition data for the 9 amine derivatives is shown in **Table 28**.

Table 28. *Whole-cell growth inhibition data for compounds **87**-**95**.*

Compound	R	Growth Inhibition / %	S.E.M / %	cLogP
87	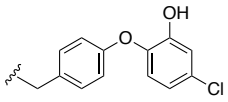	24	17	5.86
88	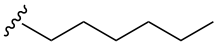	99	1	4.66
89	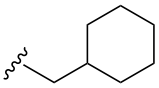	-	-	4.79
90	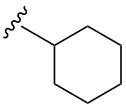	98	1	4.38
91	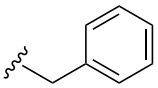	73*	23	4.56
92 *(Methylated B-Ring)*	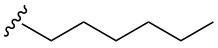	5	2	4.93
93 *(Methylated B-Ring)*	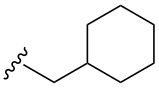	100	1	5.04
94 *(Methylated B-Ring)*	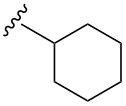	99	1	4.64
95 *(Methylated B-Ring)*	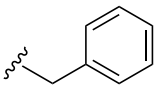	54*	42	4.99
TCL	-	70	17	4.89

**Results had standard deviation high enough to reach > 95% inhibition*

Interestingly, despite showing poor activity against InhA in isolated assays, the amine derivative compounds showed significant potency against the whole-cell bacterium. Compounds **88**, **90**, **93**, and **94** all showed >98% growth inhibition at 40 μM. Additionally, due to the high standard deviation within their results, **91** and **95** were both subject to further evaluation to remove the error from their initial testing. Compound **89** is still awaiting whole-cell evaluation. It is interesting to note that these compounds all have a cLogP in the range of ~4.4-5.0 (except **87**) and all display encouraging activity (except **92**) compared to the more hydrophobic triazoles and ethers (**Table 23-5**), this suggests that this range may be a sweet spot for penetration of the mycobacterial cell wall. This could be further examined by synthesising triazole/ether derivatives with cLogPs within this range. Compounds **88**, **91**, **93-5** were investigated further to determine their MIC, MIC_{99} curves are shown in **Figure 64**.

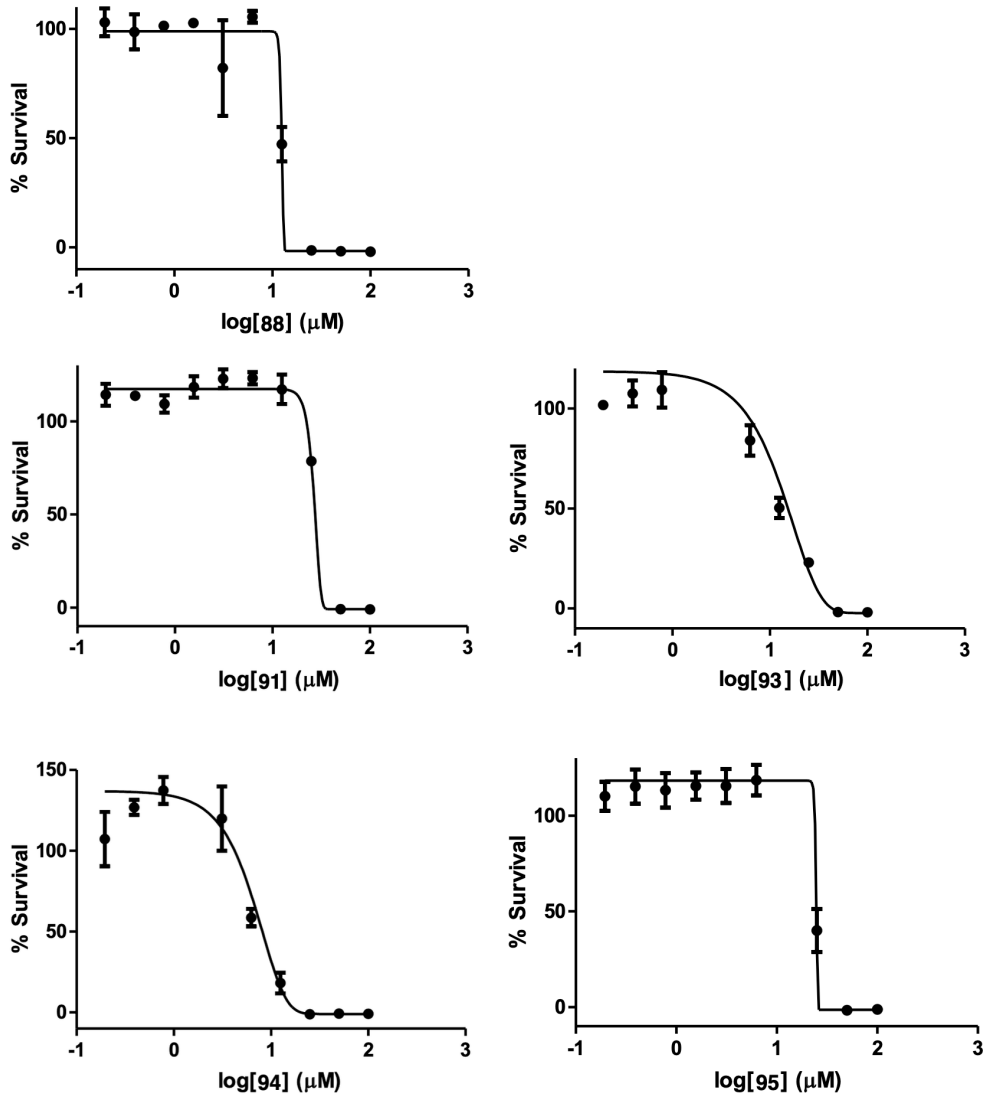

Figure 64. *MIC_{99} curves for **88**, **91**, **93-5**.*

The MIC_{99} data for the most potent amine derivatives is shown in **Table 29**.

Table 29. MIC_{99} *data for compounds* ***88, 90-5****.*

Compound	R	MIC_{99} / μM	MIC_{99} / μg mL^{-1}	cLogP
88	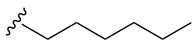	13	4.33	4.66
90	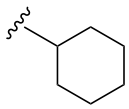	-	-	4.38
91	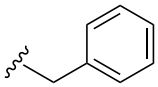	31	10.51	4.56
93 *(Methylated B-Ring)*	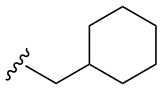	34	12.21	5.04
94 *(Methylated B-Ring)*	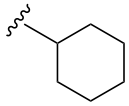	17	5.03	4.64
95 *(Methylated B-Ring)*	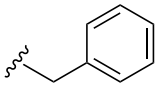	26	9.18	4.99
TCL	-	69	20	4.89

The most potent of these the compounds evaluated was **88**, with an MIC_{99} value of 13 μM (4.33 μg mL^{-1}). As with compound **62**, there is a disparity between the performance of these compounds in whole-cell vs isolated enzyme assays. None of the compounds shown in **Table 27** are inhibitors InhA, as determined in the isolated enzyme assays. This indicates that the compounds inhibit an alternate target within the bacteria, given the relative high potencies obtained, further elaboration of the amine-linked scaffold could possibly be an interesting avenue for anti-TB drug discovery. This process would of course be aided by the elucidation of the biological target of this compound class. Compound **90** is still awaiting MIC determination.

4.5.5 Evaluation of A-Ring Derivatives Against *Mycobacterium bovis*

At the time of writing, compounds **96**-**105** are awaiting evaluation against whole-cell *M. bovis*.

4.6 Observations

The data reported in this chapter serves to reinforce a major difficulty that is often encountered in anti-TB drug discovery projects; the lack of a clear link between isolated enzyme and whole-cell potency. The most potent compounds synthesised in this study, along with a number of relevant literature compounds are shown in **Figure 65**.

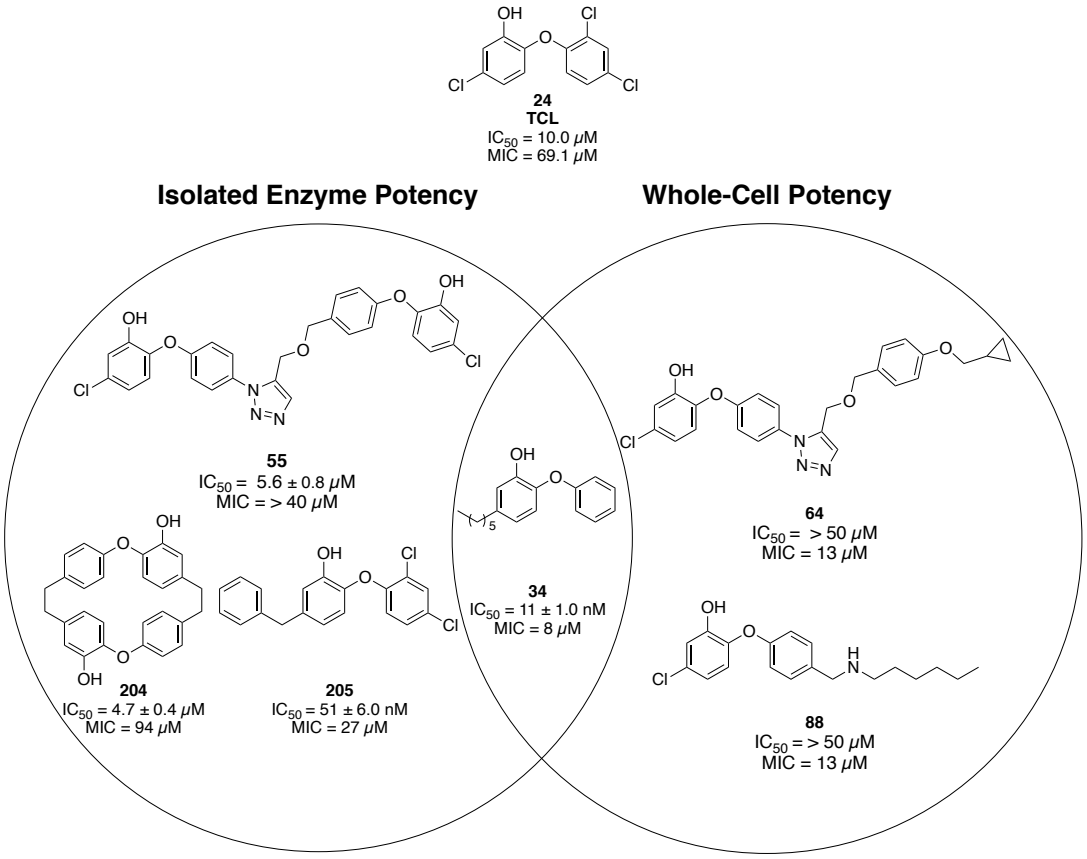

Figure 65. *The most potent compounds evaluated in both isolated enzyme and whole-cell assays as part of this work and a number of literature compounds for comparison (**34, 204 and 205**).*

The most potent InhA inhibitor synthesised in this work was di-TCL mimic **55**, this compound displayed an IC_{50} of 5.6 ± 0.8 μM, though this did not translate into whole-cell potency. During the later stages of this project Rodriguez *et al*. reported the synthesis and evaluation of **204**.[180] This compound is macrocyclic TCL derivative, which also aims to occupy both the observed binding sites from the 1P45 crystal structure. Compound **55** and **204** both have very similar IC_{50} values, indicating reasonable potency against InhA, however both suffer from significantly diminished potency against whole-cell Mycobacteria. A further example of the gap between isolated enzyme potency and whole-cell activity is compound **205**,

reported by Freundlich *et al*. This compounded showed a low nanomolar IC_{50} against InhA, but had an MIC_{99} of 27 μM against the whole-cell organism.[181] The reverse trend can be seen for **64** and **88**. These compounds have poor activity against their intended target, however they display significant potency against whole-cell *M. bovis*. Both compounds had an MIC_{99} of 13 μM, approaching that of **34** which is the most potent anti-TB TCL derivative to have been reported in the literature.[105] Taken as whole, the data shown in Figure **64** exemplify the complex nature of anti-TB drug discovery. Further evaluation will be required of the A-ring derivatives to draw a link between their isolated enzyme and whole-cell activities and so these compounds were omitted from comparison in **Figure 65**.

5.0 Synthesis of ‘Clickable’ Ligands for 4RepCT

5.1 Overview of Functionalisable 4RepCT

During the course of my PhD I also synthesised a variety of ligands for functionalisation of spider silk fibres to endow said fibres with a range of properties. This work is briefly summarised herein.

The inherent strength, biodegradability and biocompatibility of spider silk makes it an attractive scaffold for use in a biomedical context.[182, 183] To this end, the Thomas group has developed methods to site-selectively introduce azidohomoalanine residues into the sequence of the 4RepCT, a recombinant minispidron silk protein, in place of any methionine residues.[184] This allows the silk to be furnished with a variety of functional molecules through ‘Click Chemistry’ with alkyne containing ligands, using either copper catalysed azide alkyne cycloaddition (CuAAC) or strain promoted azide alkyne cycloaddition (SPAAC) reactions.

In collaboration with Dr David Harvey and Miss Jolanta Beinarovica a variety of clickable ligands were prepared for conjugation to 4RepCT^{Aha} to augment the recombinant silk with a range of functionalities (**Table 30**).

Table 30. *List of ligands generated for attachment to spider silk and their inherent functionality*

Compound	Functionality
Chloramphenicol	Antimicrobial
Ciprofloxacin	Antimicrobial
Clindamycin	Antimicrobial
Cyclic-RGDFK peptide	Cell adhesion motif
Erythromycin	Antimicrobial
Fluconazole	Antifungal
Metalated porphyrins	Antimicrobial
Methyl red	Cell viability indicator
Nitroxoline	Antimicrobial
Quaternary ammonium salts	Antimicrobial
Resazurin	Cell viability indicator
Triclosan	Antimicrobial
YIGSR peptide	Cell adhesion motif

The primary function of the majority of these compounds is as antimicrobial compounds. The potential applications of this technology could result in wound-dressing that are a hybrid of traditional materials and functionalised spider silk. Owing to the slow release of the antimicrobial payload, these bandages could provide a sterilising environment to help protect patients from possible infections following surgeries or injuries. Cell viability indicators are of interest as the colour changes they produce could can be used as an indicator of bacterial colonies growing on their surfaces, again this has potential uses in the medical industry. The interest in the exploration of cell-adhesion motifs is driven by the knowledge that spider silk can also form hydrogel. These cells could be decorated with cell adhesion motifs to provide 3D environments to model tissue formation,

additionally they could possibly be used to help promote wound repair, given spider silks biocompatibility. The synthesis of these ligands is detailed herein.

5.2 Synthesis of Antimicrobial Ligands

In order for any conjugated antimicrobial compound to elicit its biological effect, it must be attached to the spider silk through a labile, environmentally cleavable bond which can break to release the antimicrobial payload. To this end, ester bonds were selected as they are both pH labile and potentially susceptible to extracellular esterases secreted by bacteria.[185]

For simple small molecules such as triclosan, nitroxoline and fluconazole, which contain a single alcohol or phenol (**Figure 66**), alkyne functionally can be introduced in a simple one-step esterification reaction with 5-hexynoic acid.

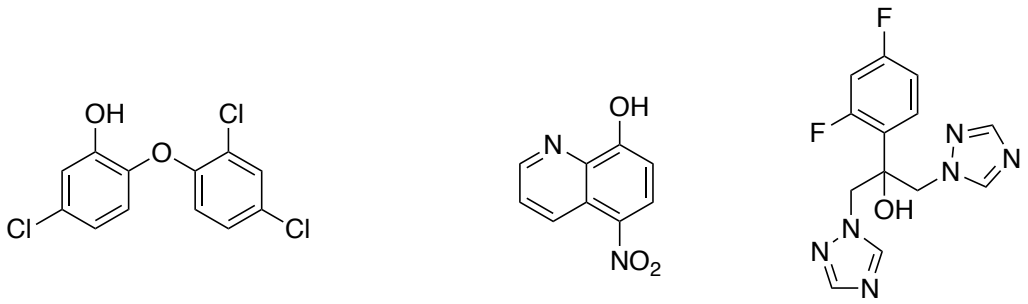

25
Triclosan

206
Nitroxoline

207
Fluconazole

Figure 66. *Structures of 3 small molecule antimicrobials, triclosan, nitroxoline and fluconazole.*

Due to the lack of any competing nucleophilic functionality within these molecules, esterification was performed directly, without the need for any protecting groups to be introduced to the molecule (**Scheme 40**)

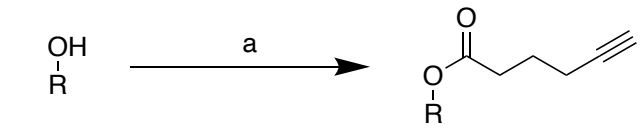

25, 206-7

208-210

208 R = Triclosan, 85%
209 R = Nitroxoline, 70%
210 R = Fluconazole, 31%

Scheme 40. *One-step esterification to form clickable triclosan, nitroxoline and fluconazole. a) 5-hexynoic acid, DCC, DMAP (5 mol%), CH_2Cl_2, r.t., 18 h.*

Esterification of **25** and **206** proceeded well, giving the target compounds in good to excellent yields. Esterification of **207** provided the desired ester in a disappointing yield. It was thought that this could be in part down to the relatively sterically encumbered tertiary alcohol being modified.

Following the synthesis of these simple ligands, the focus turned to the modification of the more complex antimicrobials: ciprofloxacin, chloramphenicol, clindamycin and erythromycin (**Figure 67**).

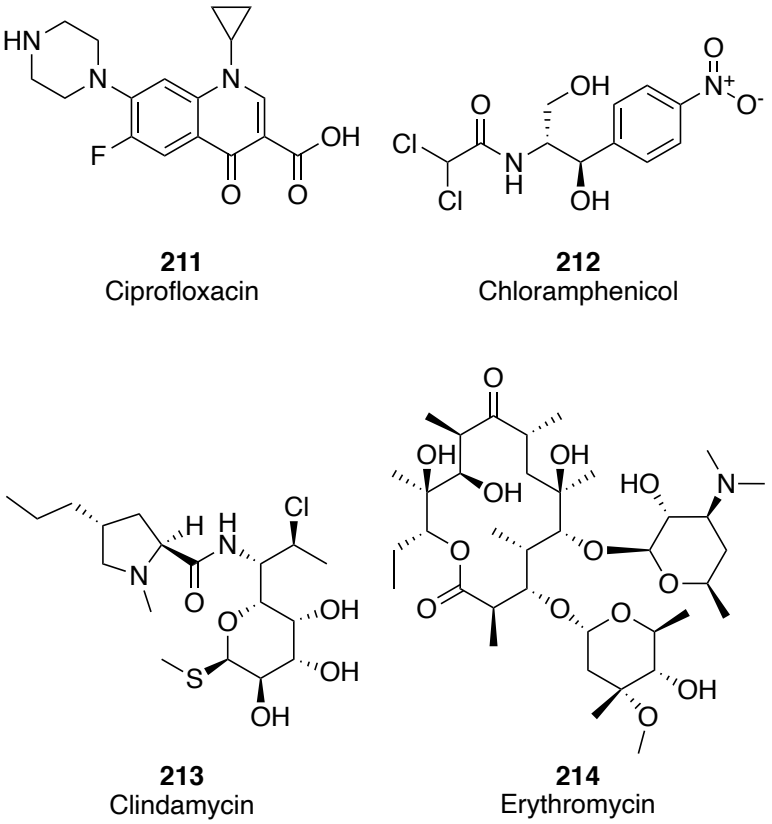

211
Ciprofloxacin

212
Chloramphenicol

213
Clindamycin

214
Erythromycin

Figure 67. *Structures of ciprofloxacin, chloramphenicol, clindamycin and erythromycin.*

Clearly these molecules contain a larger array of functional groups than the simple antimicrobials in **Figure 66**, as such these targets require multi-step synthetic pathways to selectively introduce an alkyne handle. The first compound investigated was ciprofloxacin (**Scheme 41**).

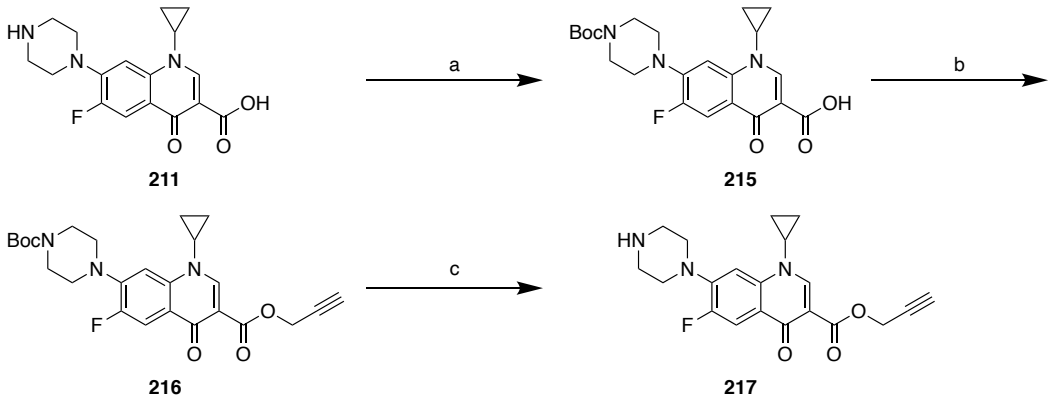

Scheme 41. *Synthesis of 'clickable' ciprofloxacin. a) $(Boc)_2O$, NaOH (aq), THF, r.t., 18 h, quant. b) Propargyl bromide, K_2CO_3, DMF, 130 ºC, 80%. c) TFA, CH_2Cl_2, r.t., 30 min, 46%*

Initially, the free amine was protected with using $(Boc)_2O$ and NaOH, furnishing carbamate **211** in a quantitive yield. This allowed the selective modification of the carboxylic acid moiety, using K_2CO_3 and propargyl bromide. Subsequent cleavage of the Boc group with TFA gave target **217** in 37% yield over 3 steps.

The modification of chlormaphenicol is shown in **Scheme 42.**

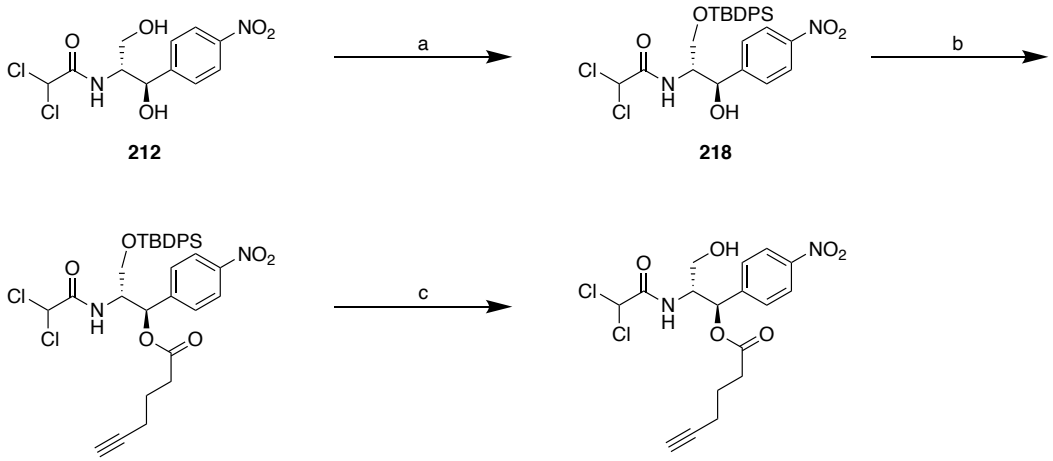

Scheme 42. *Synthesis of 'clickable' chloramphenicol. a) TBDPSCl, Imidazole, DMF, r.t., 18 h, 82%. b) 5-hexynoic acid, DCC, DMAP (5 mol%), CH_2Cl_2, r.t., 18 h, 83%. c) TBAF, THF, r.t., 18 h, 70%*

Initial protection of the primary alcohol was carried out selectively using the bulky TBDPS protecting group, affording **218** in good yield. Esterification was performed using the same DCC method as previously discussed, generating the desired ester in a good yield. The primary alcohol was then unmasked through TBAF mediated deprotection of the TBDPS group, providing **220** with a yield of 52% over three steps.

Clindamycin also required a protecting group strategy to selectively introduce the desired ester functionality (**Scheme 43**).

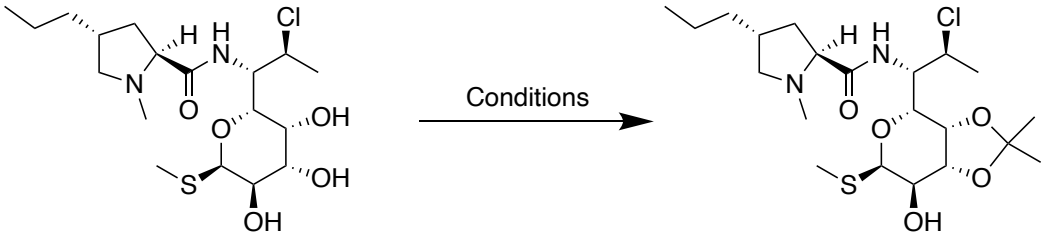

213 **221**

Scheme 43. *Selective protection of the syn-1,2 diol of clindamycin.*

Two conditions were trialed in order to generate the desired acetonide (**Table 31**).

Table 31. *Conditions attempted for the reaction shown in* ***Scheme 43****.*

Reagents	Catalyst	Temperature / °C	Time / h	Observations	Yield / %
Acetone	I_2 (0.5 equiv)	23	6	Inseparable mixture of 3 products	NA
Acetone, 2,2-dimethoxypropane	*p*TsOH.H_2O (0.1 eq)	40	18	Single product	96

Initially, the diol protection was attempted in accordance with the procedure previously reported by Bapat *et al*.[186] Whilst the target compound was identified *via* mass spec, TLC analysis of the crude reaction mixture showed 3 products which were judged to be inseparable by flash column chromatography. In their work, Bapat *et al*. claimed to have purified the product by HPLC, but provided no technical information regarding this, so this route was abandoned. The diol protection was then attempted using the conventional conditions of acetone, 2,2-dimethoxypropane and a mild acid catalyst. This afforded the desired compound as the single product of the reaction. With **221** in hand, the desired ester functionality could be selectively introduced at the remaining free alcohol (**Scheme 44**).

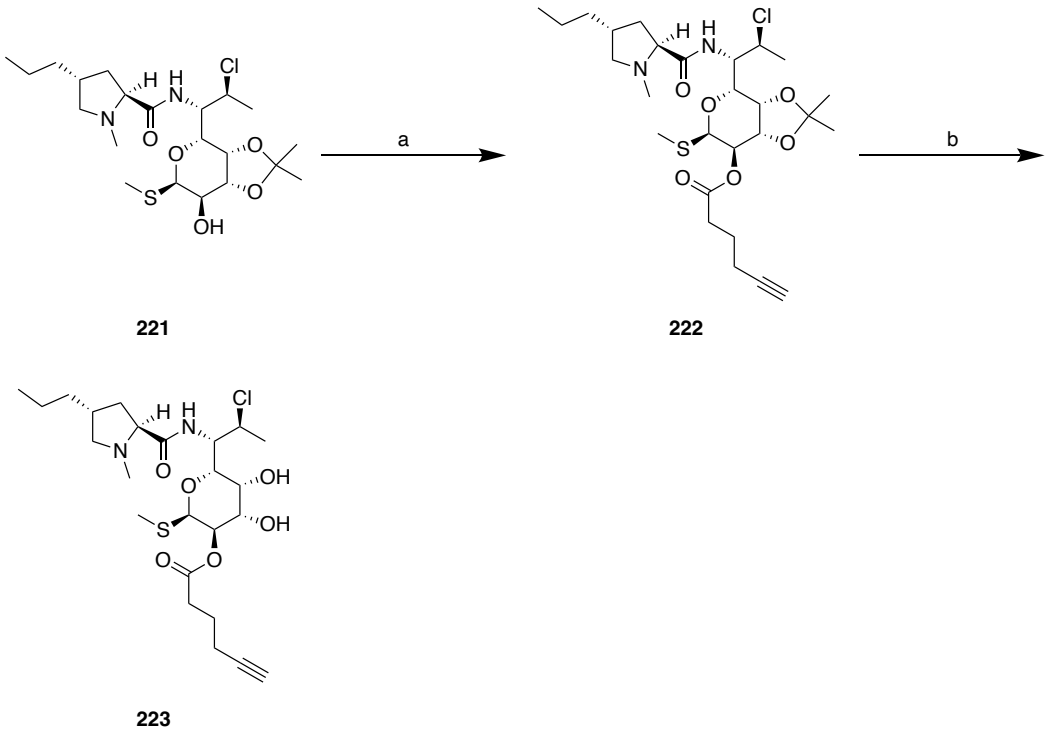

Scheme 44. *Synthesis of 'clickable' clindamycin. a) 5-hexynoic acid, DCC, DMAP (5 mol%), CH_2Cl_2, r.t., 18 h, 69%. b) 1 M HCl (aq), MeOH, 2 h, 60 °C, 83%*

The hexynoate ester functionality was installed using DCC and DMAP, in a moderate yield. The acetonide was subsequently removed using 1 M HCl in MeOH, furnishing the desired product **223** in a 55% yield over 3 steps.

Erythromycin is a complex polyketide antimicrobial which lacks as an obvious route to selectively functionalise at any of its 5 alcohols. However, work by Bosnjakovic *et al.* has elucidated the order of reactivity each alcohol unit, which in turn allows the selective functionalisation of the most reactive one.[187] Through successive acetylation, they were able to chart the reactivity and determined the 2' alcohol was the most reactive, possibly due to the effects of the dimethylamine situated in the β position to it. With this in mind, it was possible to selectively functionalise the Erythromycin scaffold (**Scheme 45**).

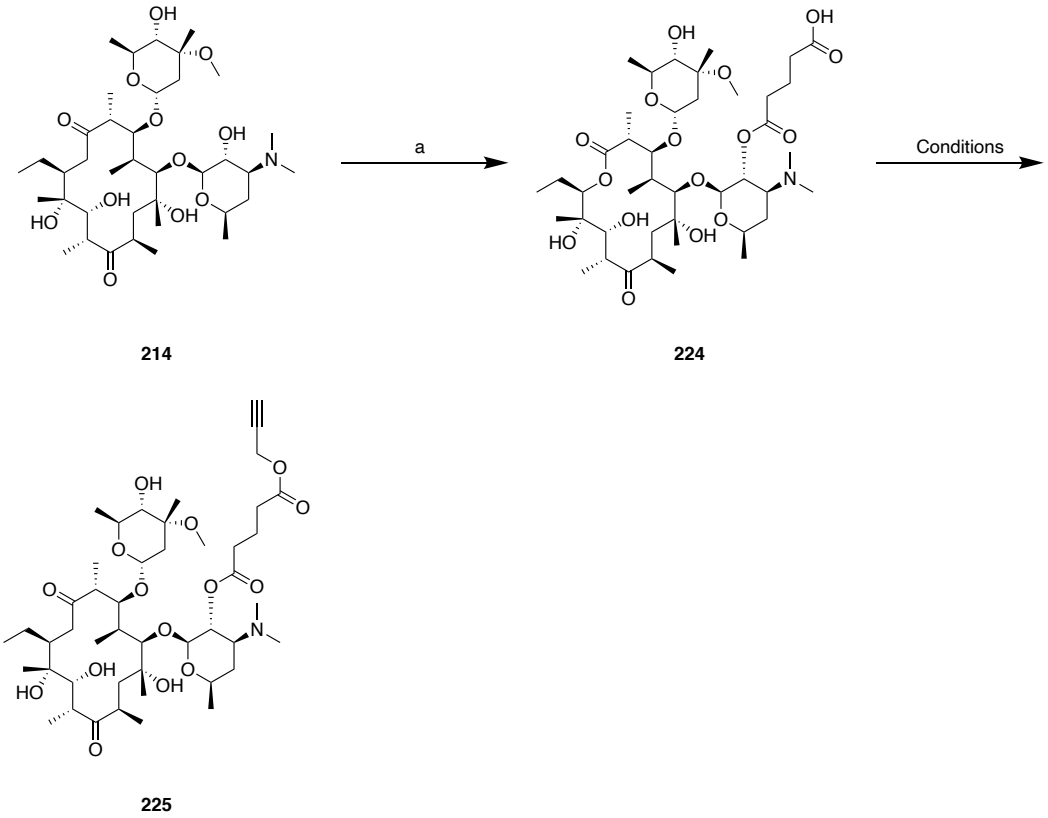

214 **224**

225

Scheme 45. *Selective functionalisation of erythromycin. a) Glutaric anhydride, Et_3N, DMF, r.t., 3 d, 75% b)* ***Table 32***

Substitution of the reactive 2' alcohol with glutaric anhydride proceeded well, delivering **224** as a single product in good yield. With the glutarate unit in place, installation of a clickable handle was attempted with a range of conditions (**Table 32**).

Table 32. *Conditions attempted for the reaction shown in* ***Scheme 44****.*

Base	Alkyne	Solvent	Temperature / °C	Time / h	Observations	Yield / %
Et_3N (4 eq)	Propargyl bromide (2 eq)	DMF	23	18	No products formed	NA
K_2CO_3 (2 eq)	Propargyl bromide (2 eq)	DMF	23	18	Multiple products formed	NA
K_2CO_3 (1.1 eq)	Propargyl bromide (1 eq)	DMF	23	18	Single product formed	88

Initial attempts to form the propargyl ester were performed in accordance with the method previously outlined by Bosnjakovic *et al*. Unfortunately, this reaction failed to generate the desired product and returned only starting material, this could be down to the significant differences in the substrate being attached at the glutarate moiety. Following this, the reaction was attempted using K_2CO_3 (2 equivs) as a base. This reaction did generate the desired product, as judged by mass spec, however the data also showed the presence of other polyfunctionalised species, owing to etherification with propargyl bromide. HPLC analysis of the crude reaction mixture proved inconclusive. To remedy this issue the reaction was repeated using an equimolar amount of propargyl bromide and a small excess of base (1.1 equiv). Pleasingly this reaction generated a single product and showed no evidence of unwanted side products.

In addition to ‘traditional’ antimicrobials, a number of more diverse compounds were synthesised for attachment to the 4RepCT protein (**Figure 68**).

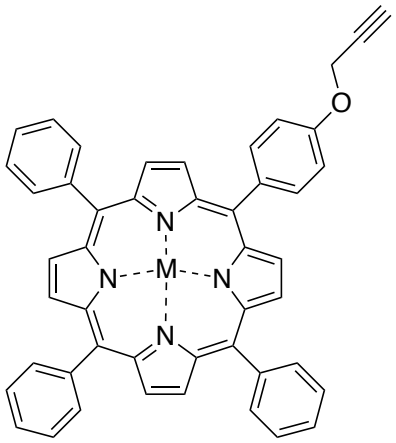

226 M = Cu^{2+}
227 M = Zn^{2+}
228 M = Fe^{3+}

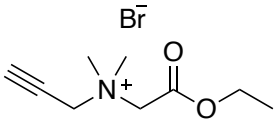

229

Figure 68. *Structures of various metalated porphyrins and quaternary ammonium salt* ***229****.*

The synthesis of the clickable porphyrin scaffold is shown in **Scheme 46**.

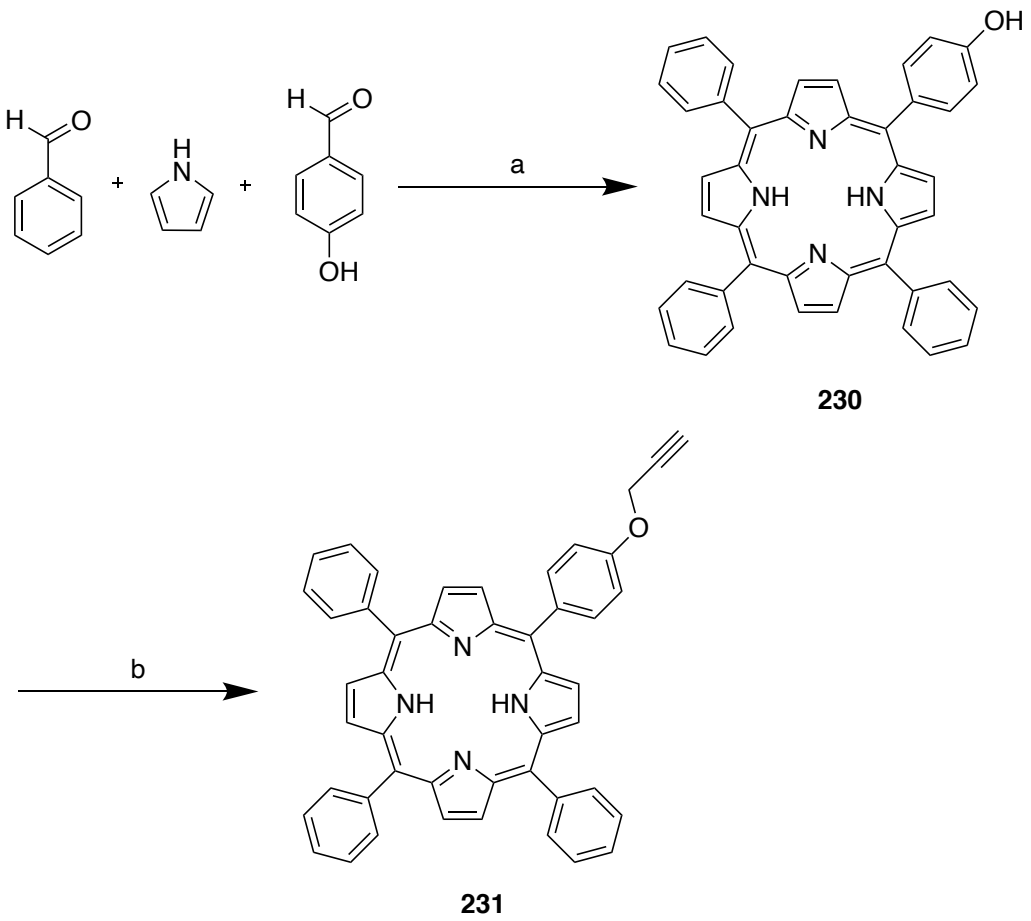

Scheme 46. *Synthesis of 'clickable' porphyrin scaffold. a) Propanoic acid, 120 → 140 °C, 1 h, 6%. b) i) NaH, 0 °C, 1 h, ii) propargyl bromide, r.t., 18 h, 82%*

The initial porphyrin scaffold was assembled through refluxing pyrrole, with the required benzaldehyde fragments, in propanoic acid. This furnished the target compound in a 6% yield, although this yield is disappointing, it is in-line with those reported in the literature for the synthesis of this compound.[188-190] The propargyl functionality was introduced using NaH and propargyl bromide, affording the desired compound in a good yield.

Encapsulation of the desired metals was performed as shown below (**Scheme 47**). Insertion of the Zn^{2+} ion into the porphyrin was performed by Dr Francesco Zamberlan.

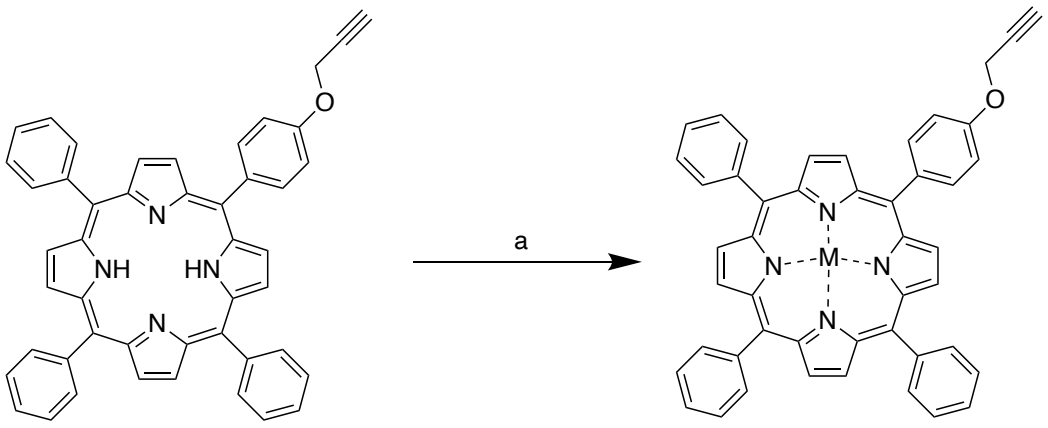

231

226 M = Cu^{2+} quant.
227 M = Zn^{2+} quant.
228 M = Fe^{3+} quant.

Scheme 47. *Metallation of 'clickable' porphyrin scaffold. a) Metal salt, $CHCl_3$:MeOH (5:2), 75 °C, 2 h*

For both the Cu^{2+} and Zn^{2+} ions, the reactions proceeded well and generated the desired product with their predicted characterisation data. However, despite the use of an Fe^{2+} precursor ($FeCl_2.4H_2O$) the characterisation data was consistent with the presence of Fe^{3+}. The ^1H NMR shows heavy peak broadening, indicative of a paramagnetic species (Fe^{3+} porphyrins are paramagnetic, whereas Fe^{2+} porphyrins diamagnetic). Additionally, the HRMS of the purified product showed an M^+ ion peak consistent with the presence of an Fe^{3+} ion. The reason for this apparent oxidation is unknown and is particularly confusing given the stable, low spin $3d^6$ configuration of Fe^{2+}.

The final antimicrobial compound synthesised was a quaternary ammonium salt bearing an alkyne handle. This was prepared as shown below (**Scheme 48**).

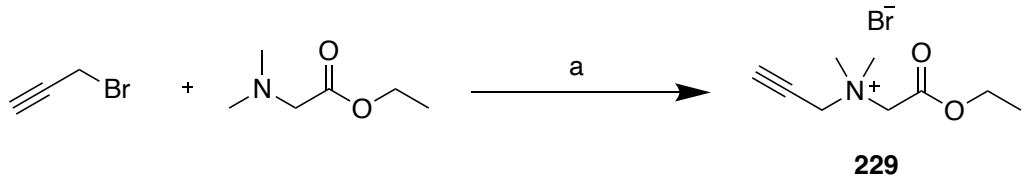

229

Scheme 48. *Synthesis of quaternary ammonium salt **229**. a) THF, r.t., 18 h, 96%*

The desired quaternary ammonium salt was synthesised in a one-step reaction between propargyl bromide and *N*,*N*-dimethylglycine ethyl ester, furnishing **229** in a near quantitative yield.

5.3 Synthesis of Clickable Cell Viability Indicators

There are a range of compounds which can be used as indicators that bacterial colonies are replicating, owing to colour changes under given conditions. Resazurin and Methyl Red are two such compounds (**Figure 69**)

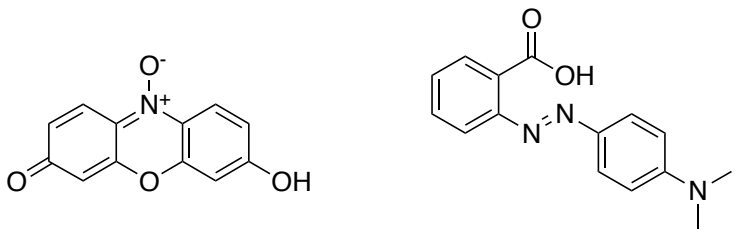

232
Resazurin

233
Methyl Red

Figure 69. *Structures of Resazurin and Methyl Red.*

Clickable Resazurin was assembled in a single step from its sodium salt and propargyl bromide (**Scheme 49**).

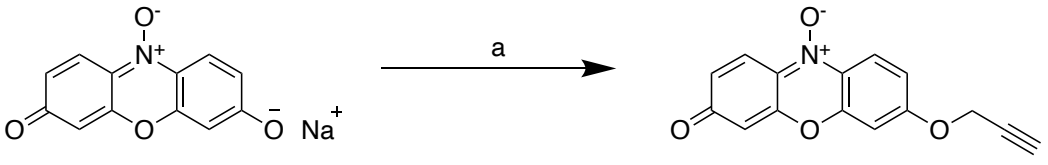

234 **235**

Scheme 49. *Synthesis of clickable resazurin **233.** a) Propargyl bromide, DMF, 60 °C, 18 h, 71%*

This reaction furnished the title compound in an acceptable yield.

A simple amine containing linker was synthesised in order to introduce the alkyne functionality to Methyl Red through a stable amide bond, which would not be cleaved by pH or esterases (**Scheme 50**).

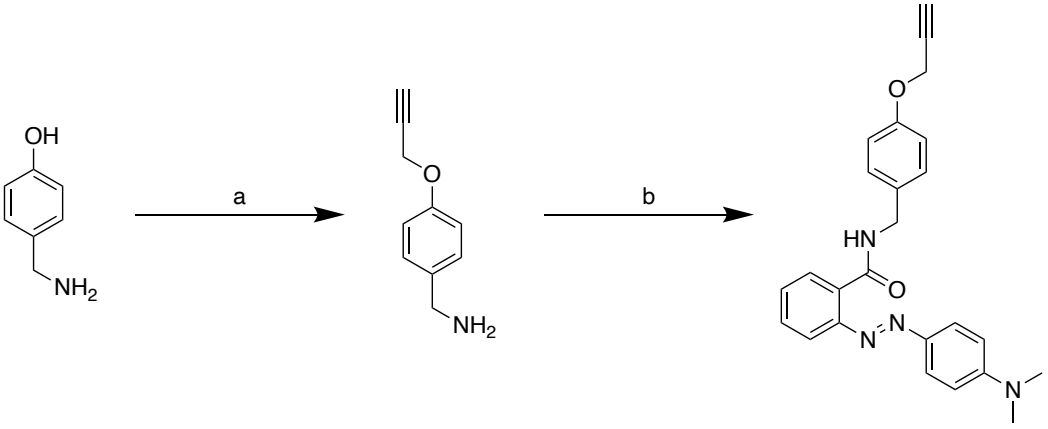

236 **237** **238**

Scheme 50. *Synthesis of clickable Methyl Red **236.** a) Propargyl bromide, K_2CO_3, DMF, 60 °C, 18 h, 65%. b) Methyl Red, DCC, DMAP, CH_2Cl_2, r.t., 18 h, 74%*

Firstly, the greater acidity of the phenolic proton was exploited to selectively form a propargyl ether, leaving the primary amine unsubstituted. Following this, DCC mediated amide bond formation was used to assemble the desired product in a reasonable yield.

5.4 Synthesis of Clickable Cell Adhesion Motifs

Within biology, a number of peptide sequences exist which can be used to facilitate cell adhesion, two such examples are the *cyclic*-RGDFK and YIGSR motifs (**Figure 70**).[191-194] Cyclic RGDFK and the modified YIGSR protein were purchased from and BioServ UK, respectively.

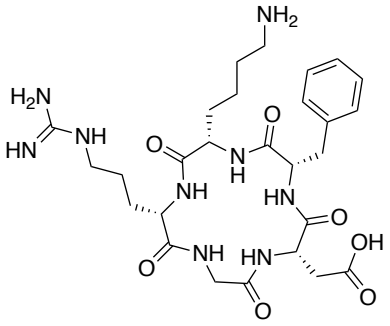

239
Cyclic-RGDFK

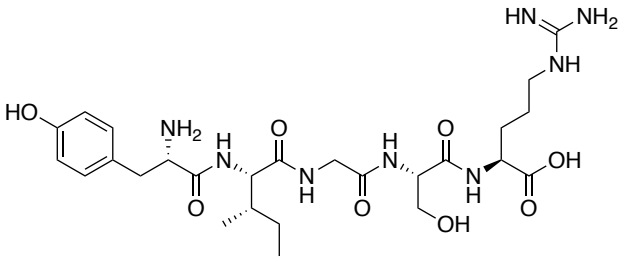

240
YIGSR

Figure 70. *The structures of two cell adhesion peptide motifs.*

In addition to copper mediated Click Chemistry, highly strained alkynes can be used to promote azide-alkyne cyclisation reactions without the need for copper catalysts. This is advantageous because residual copper requires diligent removal to prevent the cytotoxic effects of Cu (I). Two examples of SPAAC reagents are shown in **Figure 71**.

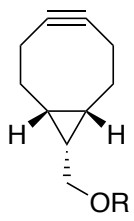

241
Bicyclononyne (BCN)

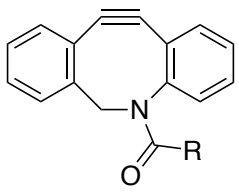

242
Dibenzylcycloctyne (DBCO)

Figure 71. *SPAAC reagents, BCN and DBCO.*

A clickable cyclic RGDFK analogue was synthesised by conjugation of BCN to the free amine of the lysine residue (**Scheme 51**).

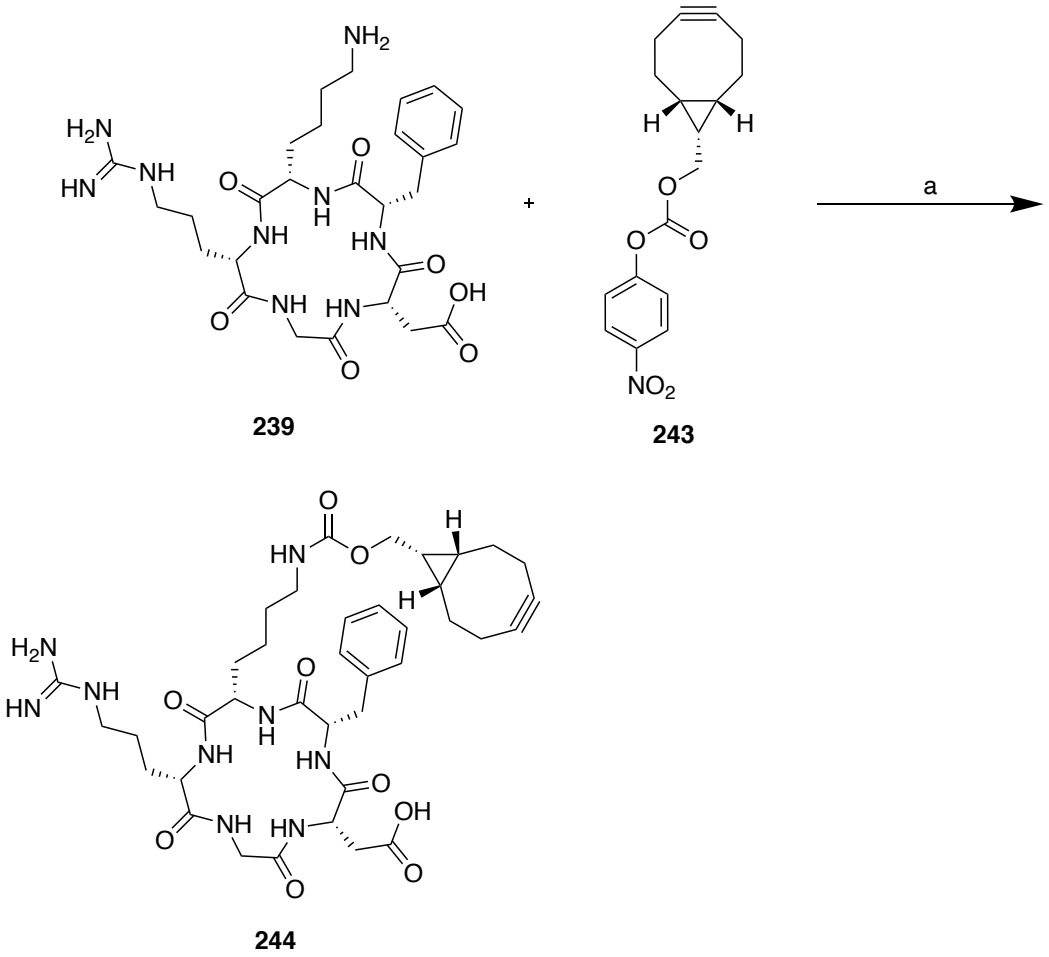

Scheme 51. *Synthesis of clickable Cyclic-RGDFK* ***238.*** *a) Et_3N, DMF, r.t., 2 h, 13%*

The reaction between cyclic RGDFK and BCN proceeded smoothly with complete consumption of the starting peptide being observed after 2 h, as judged by HR-MS. Unfortunately, HPLC purification provided the desired product in a low yield, 13%. This was attributed to the poor solubility of the crude mixture. The crude mixture only showed significant solubility at high pH, which was judged to be too harsh for the HPLC system. The crude mixture was suspended in ACN, prior to

sonication, and the remaining precipitate was removed by filtration, thus explaining the lower than expected yield.

The YIGSR peptide, with an aminohexanoic acid modification at the N-terminus, was purchased from BioServ UK. The N-modification allowed for its conjugation to BCN in the same manner as Cyclic-RGDFK (**Scheme 52**).

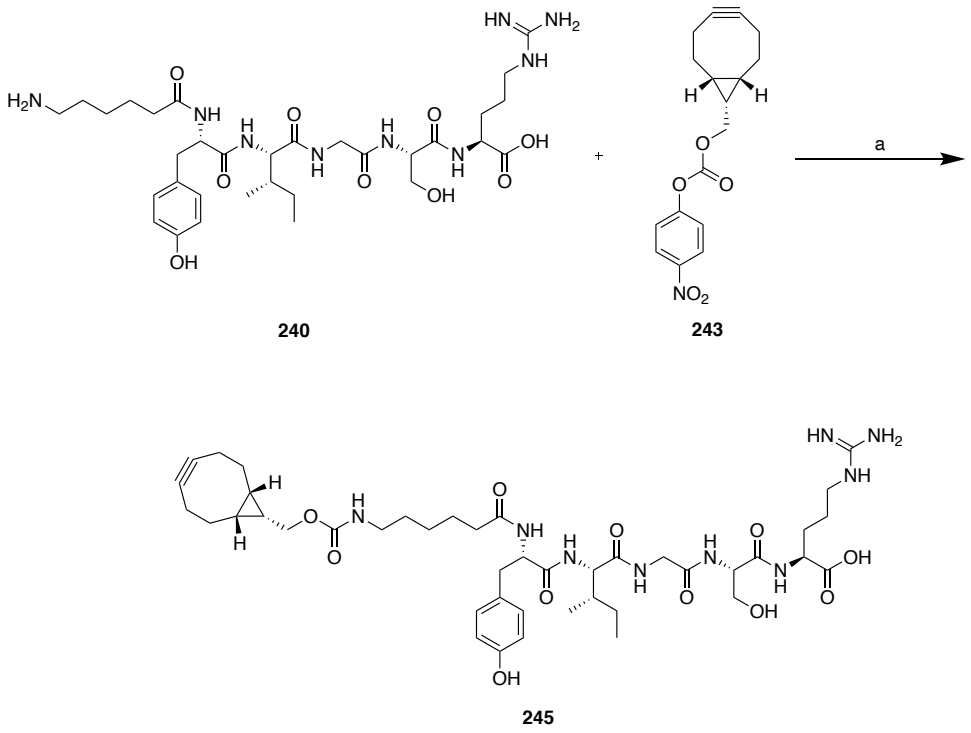

240 **243**

245

Scheme 52. *Synthesis of clickable aminohexanoic acid-YIGSR* ***245.*** *a) Et_3N, DMF, r.t., 2 h, 41%*

This reaction generated the desired product in a good yield following HPLC. The solubility issues encountered with compound **244** were not experienced with **245**, meaning its purification was more efficient.

This work has allowed the generation of a library of ligands with a range of different functionalities. Through their alkyne handles, these ligands can be attached to the 4RepCT spider silk in order to install functional activity such as antimicrobial or cell

adhesion properties to the silk fibres. These ligands opens up a range of possibilities for the exploitation of functional silk. Functionalised silk is an attractive material from a medical perspective due to its biodegradability and biocompatibility, as such this work can lay the foundation for further research into the use of modified spider silk as a functional material.

6.0 Conclusions and Future Perspectives

There remains a significant need for the identification of new anti-TB drugs in order to address the current global infections and the growing number of drug resistant infections. InhA is a clinically validated and well-understood enzyme in *Mtb* and was chosen as the target for this project. TCL was chosen as a starting point for a structure based drug design campaign, this was in part down to its well understood binding mode and the availability of high resolution protein:inhibitor crystal structures.

A range of compounds were designed to explore the potential for modification to the TCL B-ring, which has previously been relatively unexplored in the literature. In total 40 B-ring modified TCL compounds were design. In addition to this, a further 10 A-ring modified compounds were proposed to provide further modifications to the well explored A-ring. These compounds were designed to exploit InhA's uniquely large and hydrophobic active site, which has been shown to accommodate two molecules of TCL.

These 50 compounds had their binding modes interrogated *in silico* through the use of the GOLD platform. These compounds showed encouraging binding modes, all of which made the key H-bond interaction with the NAD^+ co-factor. All compounds were

subsequently synthesised, purified by HPLC and fully characterised. Additionally, an InhA substrate mimic was synthesised for the use in isolated enzyme assays.

At the same time, the *Mtb* InhA protein was expressed and purified. The activity of this enzyme was verified through kinetic assessments. All 50 compounds were tested against InhA to gauge their inhibition. Based on the data obtained, modifications to the B-ring seem to be relatively poorly tolerated. The most potent B-ring modified inhibitor was **55**, bearing two TCL moieties linked through a 1,5-triazole motif, which displayed an IC_{50} of 5.6 μM. While this is a 2 fold improvement over TCL (9.2 μM), this still only represents modest potency. The most potent A-ring derivative synthesised in this work was **97** which exhibited an IC_{50} of 340 nM, inline with previous reports that such compounds demonstrate potent InhA inhibition. Going forward it would be interesting to obtain a crystal structure for compound **55** bound to InhA. This could be used to assess whether GOLD was able to accurately predict its binding mode. This could also possibly highlight a potential novel binding mode or novel interactions, which could be useful to exploit for other scaffolds the future. Preliminary structure determination work was undertaken in collaboration with Dr Martin Walsh at the Diamond Light Source facility but has been significantly delayed following the Covid-19 outbreak.

Whole-cell growth inhibition and MIC_{99} determination was performed against *M. bovis* (the causative agent of TB in cattle), which shares an identical InhA sequence with *Mtb*. This highlighted a number of compounds which displayed significant potency against the whole-cell organism, despite being poor inhibitors of isolated, purified InhA. In particular, TCL derivatives bearing an amine group at the B-ring were

particularly potent with compound **88** showing an MIC_{99} of 13 μM (4.3 μg mL^{-1}). The A-ring derivatives are still awaiting whole-cell evaluation.

If possible, it would be useful to elucidate the biological target of the amine modified TCL compound class. While this would require a significant effort, the potency of these compounds represents a promising starting point. Upon identification of the biological target, further optimisation could be used to generate more potent compounds. If this biological target is also novel, this class of compounds becomes even more valuable, as one of the most effective ways to overcome antimicrobial resistance is through the identification and inhibition of novel enzymatic targets within the bacteria.

In summary, whilst the attempts to design a potent, novel InhA inhibitor were unsuccessful, this work has identified a scaffold which could be of interest to researchers in the hunt for novel anti-TB drugs. These compounds also posses good ‘drug-like’ qualities which will allow them to be screened against other bacteria. All compounds will be added to the Nottingham Managed Compound Collection (NMCC) to make them available to both internal and external researchers.

7.0 Experimental Methods

7.1 General Experimental

Commercial reagent grade and HPLC grade solvent were purchased from Fischer Scientific and used for all reactions. Anhydrous DMF was purchased from Sigma Aldrich. All reagents were purchased from either Sigma Aldrich, Alfa Aesar, Merck Chemicals Ltd, VWR Int, BioServ UK or Conju-Probe.

Chemical shifts (δ) are given in parts per million (ppm) and *J* values are stated in Hertz (Hz). Multiplets are designated by the following notations: singlet (s), broad singlet (bs), doublet (d), doublet of doublets (dd), apparent double of doublets (app. dd), triplet (t), apparent triplet (app. t), doublet of triplets (dt), doublet of triplet of triplets (dtt), quartet (q), heptet (hept) and multiplet (m). All ^{1}H NMR spectra were recorded on Bruker™ AV400 at 400 MHz, all spectra were recorded at ambient temperature. All spectra were recorded relative to residual solvent peaks. All ^{1}H spectra were recorded in solutions of deuterated chloroform ($CDCl_3$, δ_{solv} = 7.26) deuterated methanol (CD_3OD, δ_{solv} = 3.31), deuterated water (D2O, δ_{solv} = 4.79). All ^{13}C spectra were recorded on Bruker™ AV400 at 100 MHz, all spectra were recorded at ambient temperature. All spectra were recorded relative to residual solvent peaks. All ^{13}C spectra were recorded in solutions of deuterated chloroform ($CDCl_3$, δ_{solv} = 77.1) deuterated methanol (CD_3OD, δ_{solv} = 49.0), deuterated water (D_2O, δ_{solv} = no signal). Assignments were based on HSQC and COSY spectra.

High resolution mass spectrometry (HRMS) was recorded on a Bruker™ microTOF, an orthongal Time of Flight (TOF) instrument with electrospray ionisation (ESI, both

positive and negative). Values of mass to charge ratio (m/z) are given to four decimal places. The mass of the counter ions are H^+ 1.0078 and Na^+ 22.9898.

Thin layer chromatography was performed using Merck Kieselgel 60 F_{254} plates. Visualisation was performed by UV light and staining with $KMnO_4$ or $FeCl_3$. Flash column chromatography was perfumed using Fluorochem silica gel 60 Å, 230-400 mesh, 40-63 μm, unless otherwise stated.

All HPLC was performed on an Agilent 1200 series system. Semi-preparative HPLC was performed using an Eclipse XDB-C18 column (9.4 × 150 mm; 5 µm). Analytical HPLC was performed using an Eclipse XDB-C18 column (4.8 × 150 mm; 5 µm).

Chemical names were generated using ChemDraw Professional 19.1.

Protein crystal structures and ligand structures were prepared using the Schrodinger Maestro suite. Docking was performed using Genetic Optimisation for Ligand Docking (GOLD) version 5.6.

7.2 General Procedures

Procedure A: Biaryl ether synthesis

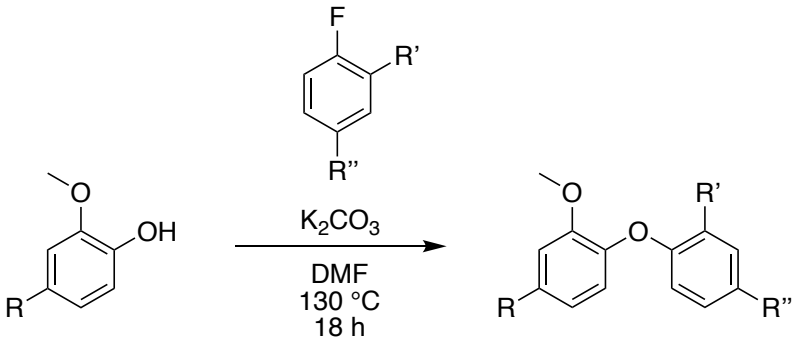

Phenol analogue (1 eq) was dissolved in DMF (0.6 mL $mmol^{-1}$) fluorobenzene analogue (1.1 eq) and K_2CO_3 (1.1 eq) were then added sequentially and the reaction mixture was heated to 130 °C and allowed to stir for 18 h. The reaction mixture was then allowed to cool to r.t. before being diluted with H_2O (30 mL) and EtOAc (30 mL). The aqueous layer was extracted with EtOAc (3 × 30 mL). The combined organic layers were then washed sequentially with saturated aqueous $NaHCO_3$, H_2O and brine (30 mL each). The organic layer was then dried over $MgSO_4$, filtered and concentrated under reduced pressure. The crude product was then purified by flash column chromatography.

Procedure B: Demethylation of phenolic ethers

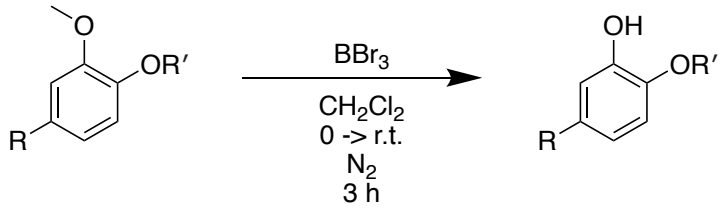

Phenyl ether derivative (1 eq) was dissolved in CH_2Cl_2, cooled to 0 °C and purged with nitrogen. BBr_3 (5 eq) was added dropwise and the reaction mixture was then allowed to warm to r.t. and stirred for 3 h. MeOH was then added dropwise until a clear solution formed and the reaction mixture was concentrated under reduced

pressure. The crude material was then diluted with saturated aqueous $NaHCO_3$ before being extracted with CH_2Cl_2 (3 × 30 mL). The combined organic layers were dried over $MgSO_4$, filtered and concentrated under reduced pressure before purification by flash column chromatography.

Procedure C: Reduction of nitrobenzene derivatives

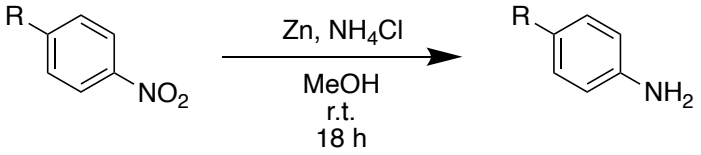

Nitrobenzene derivative (1 eq) was dissolved in MeOH (5 mL $mmol^{-1}$), zinc (6 eq) and NH_4Cl (6 eq) were added sequentially and the reaction mixture was allowed to stir for 18 h. The reaction mixture was then filtered through a pad of Celite and washed with EtOAc before being concentrated under reduced pressure and purified by flash column chromatography.

Procedure D: Aromatic azide synthesis

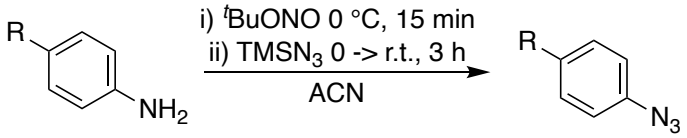

Aniline derivative (1 eq) was dissolved in anhydrous ACN (5 mL $mmol^{-1}$), the solution was then cooled to 0 °C followed by the dropwise addition of ^{t}BuONO (1.5 eq). The reaction mixture was then allowed to stir for a further 15 min before the dropwise addition of $TMSN_3$ (1.5 eq) after which point a blast-shield was erected and the reaction mixture was allowed to warm to r.t. and stirred for a further 3 h. The reaction mixture was then concentrated under reduced pressure before purification by flash column chromatography.

WARNING: Organic azides are temperature, moisture and shock sensitive. All azides were synthesised on maximum 2 g scale. Any azide that was stored was done so as a solution (200 mg mL^{-1} in 1,4-dioxane) in a vial that was purged with argon and stored at -20 °C.

Procedure E: $NaBH_4$ reduction of aldehydes

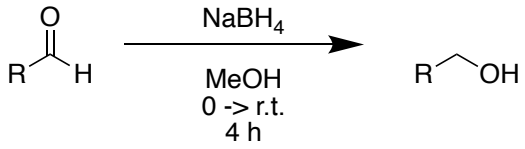

Aldehyde derivative (1 eq) was dissolved in MeOH and cooled to 0 °C followed by the portion-wise addition of $NaBH_4$ (2 eq). The reaction mixture was allowed to warm to r.t. and stirred for 4 h. The reaction mixture was then diluted with H_2O before being extracted with CH_2Cl_2 (3 × 30 mL). The combined organic layers were dried over $MgSO_4$, filtered and concentrated under reduced pressure before purification by flash column chromatography.

Procedure F: Ether synthesis

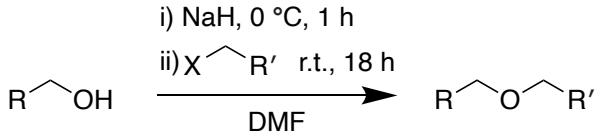

Alcohol derivative (1 eq) was dissolved in anhydrous DMF (3 mL $mmol^{-1}$) and cooled to 0 °C. NaH (60% dispersion in mineral oil, 2 eq) was added portion-wise and the reaction mixture was stirred for 1 h. Alkyl halide derivative (1.5) was added dropwise and the solution was allowed to warm to r.t. and stirred for a further 18 h. The reaction was quenched by the addition of H_2O before being extracted with EtOAc. The combined organic layers were then washed sequentially with saturated aqueous $NaHCO_3$, H_2O and brine (100 mL). The organic layer was dried over $MgSO_4$, filtered

and concentrated under reduced pressure before purification by flash column chromatography.

Procedure G: Methoxy methyl ether deprotection

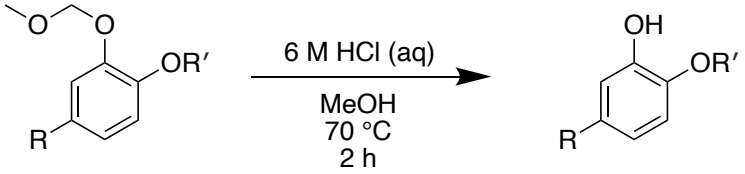

Methoxy methyl ether derivative (1 eq) was dissolved in MeOH followed by the addition of 6 M HCl (aq) (6 eq). The reaction mixture was then heated to reflux and stirred for 2 h before being allowed to cool to r.t. before being concentrated under reduced pressure. The crude material was diluted with saturated aqueous $NaHCO_3$ and then extracted with EtOAc (3 × 30 mL). The combined organic layers were then dried over $MgSO_4$, filtered and concentrated under reduced pressure before purification by semi-preparative reverse-phase high-performance liquid chromatography.

Procedure H: Ruthenium catalysed [1+3] dipolar cycloaddition

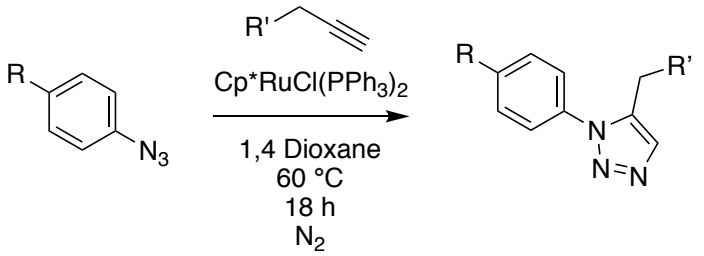

$Cp^*RuCl(PPh_3)_2$ (10 mol %) was dissolved in 1,4 Dioxane followed by the addition of alkyne derivative (1 eq) and aromatic azide (1 eq) (Note: addition was always done alkyne first). The reaction flask was then fitted with a condenser, purged with N_2 and

the reaction mixture was heated to 60 °C and stirred for 18 h. The reaction mixture was then concentrated under reduced pressure and purified by semi-preparative reverse-phase high-performance liquid chromatography.

Procedure I: Reductive animation of benzaldehyde derivatives

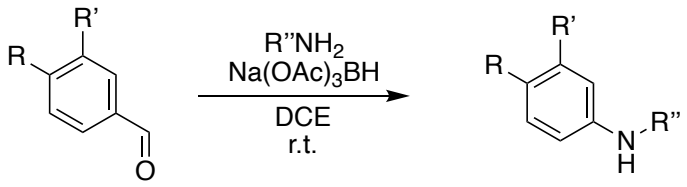

Benzaldehyde derivative (1 eq) was dissolved in anhydrous DCE (15 mL $mmol^{-1}$) followed by the addition of amine (1.1 eq) and $Na(OAc)_3BH$ (1.5 eq). The reaction mixture was allowed to stir at r.t. for 18 h (unless specified otherwise). The reaction was then quenched by the addition of saturated aqueous $NaHCO_3$ and allowed to stir for 15 min. The resultant aqueous layer was then extracted with CH_2Cl_2 (3 × 30 mL). The combined organic layers were dried over $MgSO_4$, filtered and concentrated under reduced pressure before purification by flash column chromatography.

Procedure J: Ester/Amide Coupling

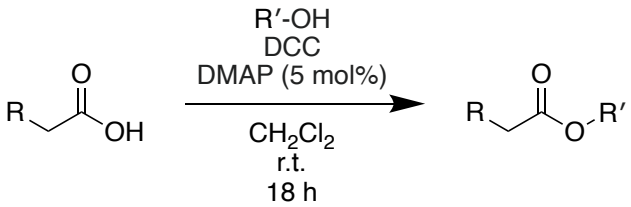

Carboxylic acid derivative (1 eq) was dissolved in CH_2Cl_2 followed by the addition of DCC (1.1 eq), the corresponding alcohol/amine (1.1 eq) and DMAP (5 mol%). The reaction mixture was stirred at r.t. for 18. The resulting precipitate was removed by

filtration and the filtrate was concentrated under reduced pressure. Purification was performed by flash column chromatography.

Procedure K: Metallation of Porphyrin

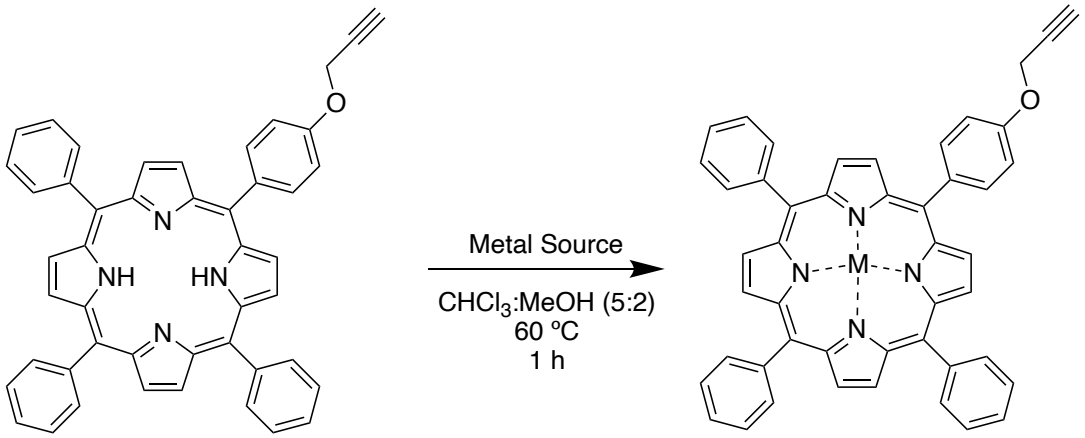

Porphyrin derivative was dissolved in $CHCl_3$:MeOH (5:2) followed by the addition of the desired metal source (2.0 equivs). The reaction mixture was heated to 60 ºC and allowed to stir for 1 h. The reaction mixture was concentrated under reduced pressure before being diluted with $CHCl_3$. The organic phase was extracted three times with H_2O before being dried over $MgSO_4$, filtered and concentrated under reduced pressure. Purification was performed by flash column chromatography.

7.3 HPLC Methods

HPLC was carried out on an Agilent 1200 series system, all columns were fitted with 5 μM pre-column column guards.

HPLC Method 1: Eclipse XDB-C18 column (9.4 × 150 mm; 5 µm) where Buffer A is 20 mM ammonium acetate pH 5.9 (adjusted with 5 M AcOH) and Buffer B is acetonitrile (neat). Flow rate 2 mL min^{-1}. Percentage is given as composition of buffer A. Variable wavelength detector set at 254 nm

0 – 1 mins (100%), 1 – 2 mins (90%), 2 – 5 mins (80%), 5 – 15 mins (75 –> 70%), 15 – 17 mins (70 –> 5%), 17 – 18 mins (5%), 18 – 19 mins (5 – 100%), 19 – 21 mins (100%).

HPLC Method 2: Eclipse XDB-C18 column (9.4 × 150 mm; 5 µm) where Buffer A is H_2O (0.1% formic acid) and Buffer B is Acetonitrile. Flow rate 2 mL min^{-1}. Percentage is given as a composition of Buffer B. Variable wavelength detector set at 254 nm

0 - 20 mins (70 –> 100%)

HPLC Method 3: Eclipse XDB-C18 column (9.4 × 150 mm; 5 µm) where Buffer A is H_2O (0.1% formic acid) and Buffer B is Acetonitrile. Flow rate 2 mL min^{-1}. Percentage is given as a composition of Buffer B. Variable wavelength detector set at 254 nm

0 - 20 mins (60 –> 100%)

HPLC Method 4: Eclipse XDB-C18 column (9.4 × 150 mm; 5 µm) where Buffer A is H_2O (0.1% formic acid) and Buffer B is Acetonitrile. Flow rate 2 mL min^{-1}. Percentage is given as a composition of Buffer B. Variable wavelength detector set at 254 nm

0 - 20 mins (40 –> 100%)

HPLC Method 5: Eclipse XDB-C18 column (9.4 × 150 mm; 5 µm) where Buffer A is H_2O (0.1% formic acid) and Buffer B is Acetonitrile. Flow rate 2 mL min^{-1}. Percentage is given as a composition of Buffer B. Variable wavelength detector set at 254 nm

0 - 20 mins (50 –> 100%)

HPLC Method 6: Eclipse XDB-C18 column (4.6 × 150 mm; 5 µm) where Buffer A is H_2O (0.1% formic acid) and Buffer B is Acetonitrile. Flow rate 2 mL min^{-1}. Percentage is given as a composition of Buffer B. Variable wavelength detector set at 254 nm.

0 - 20 mins (30 -> 100%)

7.4 LC-MS Methods

LC-MS was carried out on a Shimadzu Prominence LC-20AD XR system twinned with a LC-MS-2020 mass spectrometer. Injection volumes were 10 μL.

LC-MS Method 1: Gemini NX-C18 column (2 × 50 mm; 3 μm) where buffer A is H_2O and Buffer B is Acetonitrile. Flow rate 1 mL min^{-1}. Percentage is given as a composition of Buffer B. Variable wavelength detector set at 254 nm.

0 - 5 mins (5 -> 100%)

7.5 Chemical Methods

4-Chloro-2-methoxy-1-(4-nitrophenoxy)benzene (113)

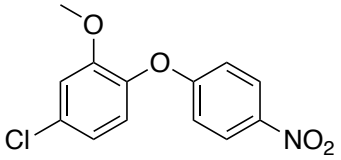

The title compound was synthesised according to General Procedure A from 4-chloro-2-methoxy phenol (2.00 g, 12.60 mmol), 4-fluoro-1-nitrobenzene (1.86 g, 13.23 mmol) and K_2CO_3 (1.74 g, 12.60 mmol). Purification was performed by flash column chromatography (Hexane/EtOAc, 2:1) to yield the title compound as a dense orange oil (2.81 g, 80%). ^{1}H NMR (400 MHz, $CDCl_3$) δ 8.21 – 8.14 (m, 2H, ArH), 7.07 – 6.97 (m, 3H, ArH), 6.96 – 6.89 (m, 2H, ArH), 3.78 (s, 3H, OCH_3). ^{13}C NMR (101 MHz, $CDCl_3$) δ 163.2 (ArC), 152.1 (ArC), 142.6 (ArC), 141.2 (ArC), 131.9 (ArC), 125.8 (ArC), 123.4 (ArC), 121.3 (ArC), 115.8 (ArC), 113.8 (ArC), 56.1 (OCH_3). HRMS (ESI) *m/z* calcd for $C_{13}H_{11}{}^{35}ClNO_4$ $[M + H]^+$, 280.0371, found 280.0377. Analytical data consistent with those reported in the literature.[195]

5-Chloro-2-(4-nitrophenoxy)phenol (108)

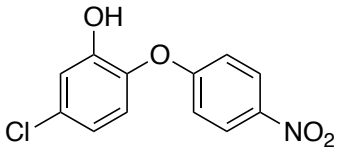

The title compound was synthesised according to General Procedure B from compound **113** (1.05 g, 3.76 mmol) and BBr_3 (1 M in CH_2Cl_2), 15 mL, 15 mmol). Purification was performed by flash column chromatography (Hexane/EtOAc, 3:1) to yield the title compound as a yellow solid (0.86 g, 87%). ^{1}H NMR (400 MHz, MeOD) δ 8.16 – 8.10 (m, 2H, ArH), 7.02 – 6.93 (m, 4H, ArH), 6.85 (dd, *J* = 8.6, 2.4 Hz, 1H,

ArH), 4.94 (s, 1H, OH). ^{13}C NMR (101 MHz, MeOD) δ 163.2 (ArC), 150.2 (ArC), 142.3 (ArC), 140.4 (ArC), 131.2 (ArC), 125.4 (ArC), 123.3 (ArC), 119.9 (ArC), 117.3 (ArC), 115.7 (ArC). HRMS (ESI) *m*/*z* calcd for $C_{12}H_8{}^{35}ClNO_4Na$ $[M + Na]^+$, 288.0034, found 288.0038. Analytical data consistent with those reported in the literature.[196]

2-(4-Aminophenoxy)-5-chlorophenol (114)

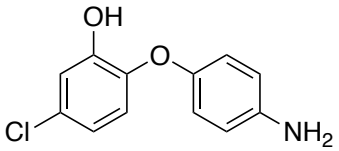

The title compound was synthesised according to General Procedure C from compound **108** (0.60 g, 2.26 mmol), zinc (0.89 g, 13.50 mmol) and NH_4Cl (0.73 g, 13.50 mmol). Purification was performed by flash column chromatography (CH_2Cl_2:MeOH, 95:5) to yield the title compound as a pale-brown solid (0.52 g, quant.). ^{1}H NMR (400 MHz, MeOD) δ 6.90 (d, *J* = 2.3 Hz, 1H, ArH), 6.82 – 6.78 (m, 2H, ArH), 6.77 – 6.73 (m, 2H, ArH), 6.72 – 6.66 (m, 2H, ArH). ^{13}C NMR (101 MHz, MeOD) δ 149.0 (ArC), 148.8 (ArC), 145.0 (ArC), 143.3 (ArC), 127.5 (ArC), 119.3 (ArC), 119.0 (ArC), 118.7 (ArC), 116.4 (ArC), 116.3 (ArC). HRMS (ESI) *m*/*z* calcd for $C_{12}H_{11}{}^{35}ClNO_2$ $[M + H]^+$, 236.0473, found 236.0472. Analytical data consistent with those reported in the literature.[197]

2-(4-Azidophenoxy)-5-chlorophenol (106)

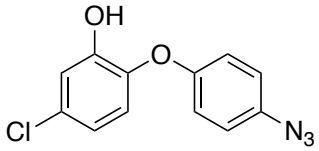

The title compound was synthesised according to General Procedure D from compound **114** (0.12 g, 0.51 mmol), ^{t}BuONO (77 mg, 0.75 mmol) and $TMSN_3$ (86

mg, 0.75 mmol). Purification was performed by flash column chromatography (Hexane/EtOAc, 0 -> 10%) to yield the title compound as a dense brown oil (0.10 g, 75%). ^{1}H NMR (400 MHz, $CDCl_3$) δ 7.07 (d, *J* = 2.4 Hz, 1H, ArH), 7.03 (s, 4H ArH), 6.84 (dd, *J* = 8.6, 2.4 Hz, 1H, ArH), 6.77 (d, J = 8.7 Hz, 1H. ArH), 5.78 (s, 1H, OH). ^{13}C NMR (101 MHz, $CDCl_3$) δ 153.4 (ArC), 147.9 (ArC), 142.6 (ArC), 135.8 (ArC), 129.6 (ArC), 120.7 (ArC), 120.5 (ArC), 119.6 (ArC), 119.1 (ArC), 116.8 (ArC). HRMS (ESI) *m*/*z* calcd for $C_{12}H_7{}^{35}ClN_3O_2$ $[M - H]^-$, 260.0232, found 260.0234.

4-(4-Chloro-2-methoxyphenoxy)benzaldehyde (115)

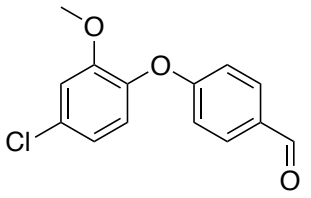

The title compound was synthesised according to General Procedure A from 4-chloro-2-methoxyphenol (5.00 g, 31.50 mmol, 4-fluorobenzaldehyde (4.30 g, 34.60 mmol) and K_2CO_3 (4.79 g, 34.60 mmol. Purification by flash column chromatography (Hexane/EtOAc, 3:1) gave the title compound as a dense orange oil (7.31 g, 89%) ^{1}H NMR (400 MHz, $CDCl_3$) δ 9.82 (s, 1H, CHO), 7.80 – 7.64 (m, 2H, ArH), 6.96 – 6.93 (m, 2H, ArH), 6.91 – 6.86 (m, 3H, ArH), 3.69 (s, 3H, CH_3). ^{13}C NMR (101 MHz, $CDCl_3$) δ 190.7 (CHO), 163.2 (ArC), 152.4 (ArC), 141.6 (ArC), 131.9 (ArC), 131.4 (ArC), 131.2 (ArC), 123.3 (ArC), 121.2 (ArC), 116.2 (ArC), 113.7 (ArC), 56.1 (CH_3). HRMS (ESI) *m*/*z* calcd for $C_{14}H_{12}{}^{35}ClO_3$ $[M + H]^+$, 263.0469, found 263.0469. Analytical data consistent with those reported in the literature.[198]

4-(4-Chloro-2-hydroxyphenoxy)benzaldehyde (109)

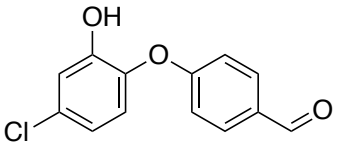

Compound **115** (8.00 g. 30.50 mmol) was dissolved in a solution of AcOH (30 ml, 0.52 mol) followed by the addition of 47% HBr (aq) (12 mL, 0.10 mol). The reaction mixture was then heated to 110 °C and stirred for 18 h. The reaction was allowed to cool to r.t. before being concentrated under reduced pressure, the mixture was then neutralised by careful addition of saturated aqueous $NaHCO_3$ before being diluted in H_2O (100 mL) and extracted with EtOAc (3 × 100 mL). The combined organic layers were then dried over $MgSO_4$ and concentrated under reduced pressure. Purification by flash column chromatography (Hexane/EtOAc, 0 -> 21%) gave the title compound as a pale-yellow solid (2.20 g, 29%). ^{1}H NMR (400 MHz, MeOD) δ 9.81 (s, 1H, CHO), 7.85 – 7.78 (m, 2H, ArH), 7.03 – 6.94 (m, 4H, ArH), 6.85 (dd, J = 8.6, 2.5 Hz, 1H, ArH). ^{13}C NMR (101 MHz, MeOD) δ 191.5 (CHO), 163.4 (ArC), 150.3 (ArC), 140.7 (ArC), 131.7 (ArC), 131.1 (ArC), 130.8 (ArC), 123.2 (ArC), 119.9 (ArC), 117.3 (ArC), 116.0 (ArC). HRMS (ESI) *m/z* calcd for $C_{13}H_8O_3{}^{35}Cl$ $[M - H]^-$, 247.0167, found 247.0175.

4-(2-((*tert*-Butyldimethylsilyl)oxy)-4-chlorophenoxy)benzaldehyde (116)

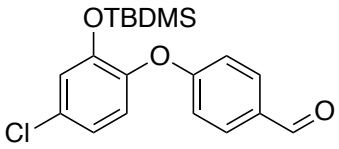

Compound **109** (0.35 g, 1.41 mmol) was dissolved in DMF (10 mL) and cooled to 0 °C. TBDMSCl (0.26 g, 1.70 mmol) and imidazole (0.12 g, 1.70 mmol) were added sequentially and the reaction mixture was allowed to warm to r.t. before being stirred

for a further 18 h. The reaction mixture was then diluted with H_2O (20 mL) before being extracted with CH_2Cl_2 (3 × 30 mL). The combined organic layer was dried over $MgSO_4$, filtered and concentrated under reduced pressure. Purification was performed by flash column chromatography (Hexane:EtOAc, 2:1) to yield the title compound as a pale-yellow oil (450 mg, 89%). ^{1}H NMR (400 MHz, $CDCl_3$) δ 9.87 (s, 1H, CHO), 7.81 – 7.77 (m, 2H, ArH), 7.01 (d, J = 9.2 Hz, 1H, ArH), 6.97 – 6.90 (m, 4H, ArH), 0.76 (s, 9H, $(CH_3)_3$), 0.11 (s, 6H, $Si(CH_3)_2$). ^{13}C NMR (101 MHz, $CDCl_3$) δ 190.64 (CHO), 162.92 (ArC), 148.53 (ArC), 143.69 (ArC), 131.86 (ArC), 131.04 (ArC), 131.00 (ArC), 123.67 (ArC), 122.33 (ArC), 121.91 (ArC), 116.03 (ArC), 25.29 ($(CH_3)_3$), 18.00 (C), -4.58 ($Si(CH_3)_2$). HRMS (ESI) *m/z* calcd for $C_{19}H_{23}O_3{}^{35}ClSiNa$ [M + Na]$^+$, 385.0997, found 385.1006.

(4-(2-((*tert*-Butyldimethylsilyl)oxy)-4-chlorophenoxy)phenyl)methanol (117)

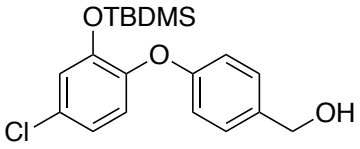

The title compound was synthesised according to General Procedure E from **116** (0.48 g, 1.33 mmol) and $NaBH_4$ (0.08 g, 1.98 mmol). Purification by flash column chromatography (Hexane/EtOAc, 3:1) gave the title compound as a pale-yellow oil (0.18 g, 38%). ^{1}H NMR (400 MHz, $CDCl_3$) δ 7.28 – 7.23 (m, 2H, ArH), 6.96 (dd, J = 1.8, 1.0 Hz, 1H, ArH), 6.91 – 6.89 (m, 2H, ArH), 6.89 – 6.84 (m, 2H, ArH), 4.58 (s, 2H, CH_2), 2.42 (bs, 1H, OH), 0.88 (s, 9H, $(CH_3)_3$), 0.16 (s, 6H, $Si(CH_3)_2$). ^{13}C NMR (101 MHz, $CDCl_3$) δ 157.11 (ArC), 148.24 (ArC), 145.61 (ArC), 135.08 (ArC), 129.39 (ArC), 128.62 (ArC), 122.22 (ArC), 122.05 (ArC), 122.03 (ArC), 116.86 (ArC), 64.74

(CH_2), 25.51 ((CH_3)$_3$), 18.22 (C), -4.52 (Si(CH_3)$_2$). HRMS (ESI) *m/z* calcd for $C_{19}H_{25}O_3{}^{35}ClSiNa$ $[M + Na]^+$, 387.1154, found 387.1142.

4-(4-(4-Chloro-2-(methoxymethoxy)phenoxy)benzaldehyde (119)

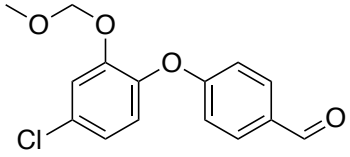

Compound **109** (2.20 g, 8.90 mmol) was dissolved in CH_2Cl_2 (40 mL) under a nitrogen atmosphere. DIPEA (3.43 g, 26.54 mmol) and MOMCl (1.07 g, 13.29 mmol) were added sequentially and the reaction mixture was allowed to stir for 18 h. The reaction mixture was then diluted with saturated NH_4Cl (aq) solution (40 mL) and extracted with EtOAc (3 × 50 mL). The combined organic layers were then dried over $MgSO_4$ and concentrated under reduced pressure. Purification by flash column chromatography (Hexane/EtOAc, 3:1) gave the title compound as a pale-yellow oil (2.41 g, 92%). ^{1}H NMR (400 MHz, $CDCl_3$) δ 9.77 (s, 1H, CHO), 7.75 – 7.63 (m, 2H, ArH), 7.17 (dd, *J* = 2.1, 0.5 Hz, 1H, ArH), 6.94 – 6.81 (m, 4H, ArH), 4.98 (s, 2H, CH_2), 3.22 (s, 3H, CH_3). ^{13}C NMR (101 MHz, $CDCl_3$) δ 190.1 (CHO), 163.1 (ArC), 149.8 (ArC), 142.4 (ArC), 131.8 (ArC), 131.3 (ArC), 131.2 (ArC), 123.5 (ArC), 122.7 (ArC), 117.6 (ArC), 116.2 (ArC), 95.0 (CH_2), 56.3 (CH_3). HRMS (ESI) *m/z* calcd for $C_{15}H_{13}O_4{}^{35}ClNa$ $[M + Na]^+$, 315.0395, found 315.0398.

(4-(4-Chloro-2-(methoxymethoxy)phenoxy)phenyl)methanol (120)

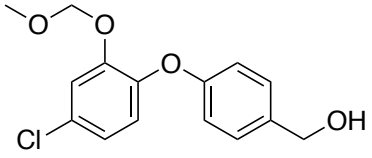

The title compound was synthesised according to General Procedure E from **119** (2.41 g, 8.25 mmol) and $NaBH_4$ (0.47 g, 12.38 mmol). Purification by flash column

chromatography (Hexane/EtOAc, 3:1) gave the title compound as a pale-yellow oil (2.30 g, 95%). ^{1}H NMR (400 MHz, $CDCl_3$) δ 7.30 – 7.07 (m, 3H, ArH), 6.88 (dd, *J* = 8.6, 2.4 Hz, 1H, ArH), 6.85 – 6.80 (m, 3H, ArH), 5.05 (s, 2H, CH_2), 4.52 (s, 2H, C*H*$_2$OH), 3.32 (s, 3H, CH_3), 2.47 (bs, 1H, OH). ^{13}C NMR (101 MHz, $CDCl_3$) δ 157.1 (ArC), 149.4 (ArC), 144.6 (ArC), 135.6 (ArC), 129.6 (ArC), 128.5 (ArC), 122.6 (ArC), 122.0 (ArC), 117.9 (ArC), 117.1 (ArC), 95.3 (CH_2), 64.6 (CH_2OH), 56.3 (CH_3). HRMS (ESI) *m*/*z* calcd for $C_{15}H_{15}O_4{}^{35}ClNa$ $[M + Na]^+$, 317.0551, found 317.0558.

4-Chloro-2-(methoxymethoxy)-1-(4-((prop-2-yn-1-yloxy)methyl)phenoxy)benzene (121)

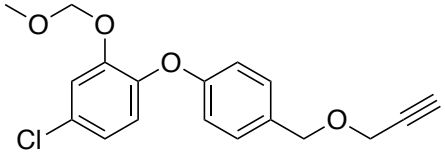

The title compound was synthesised according to General Procedure F from **120** (0.50 g, 1.70 mmol), NaH (60% dispersion in mineral oil, 0.13 g, 3.40 mmol) and propargyl bromide (0.30 g, 2.55 mmol). Purification was performed by flash column chromatography (Hexane/EtOAc, 0 -> 20%) to yield the title compound as a pale-yellow oil (0.38 g, 67%). ^{1}H NMR (400 MHz, $CDCl_3$) δ 7.34 – 7.30 (m, 2H, ArH), 7.29 – 7.27 (m, 1H, ArH), 6.99 (dd, *J* = 8.6, 2.4 Hz, 1H), 6.95 – 6.91 (m, 3H, ArH, ArH), 5.17 (s, 2H, OC*H*$_2$O), 4.58 (s, 2H, ArC*H*$_2$), 4.19 (d, *J* = 2.4 Hz, 2H, C*H*$_2$CCH), 3.44 (s, 3H, CH_3), 2.49 (t, J = 2.4 Hz, 1H, CH). ^{13}C NMR (101 MHz, $CDCl_3$) δ 157.5 (ArC), 149.5 (ArC), 144.5 (ArC), 131.7 (ArC), 129.8 (ArC), 129.7 (ArC), 122.6 (ArC), 122.2 (ArC), 117.8 (ArC), 117.0 (ArC), 95.3 (CH_3OCH_2), 79.6 (C), 74.7 (CH), 71.1 (Ar*C*H$_2$), 57.0 (*C*H$_2$CCH), 56.4 (CH_3). HRMS (ESI) *m*/*z* calcd for $C_{18}H_{17}O_4{}^{35}ClNa$ $[M + Na]^+$, 355.0708, found 355.0711.

4-Chloro-2-(methoxymethoxy)-1-(4-((prop-2-yn-1-yloxy)methyl)phenoxy)benzene (107)

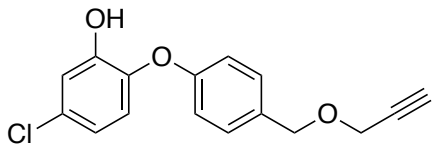

The title compound was synthesised according to General Procedure G from **121** (0.38 g, 1.14 mmol) and 6 M HCl (aq) (1.14 mL, 6.86 mmol). Purification was performed by flash column chromatography (Hexane/EtOAc, 0 -> 20%) to yield the title compound as a pale-yellow oil (0.29 g, 90%). ^{1}H NMR (400 MHz, $CDCl_3$) δ 7.40 – 7.35 (m, 2H, ArH), 7.07 (d, *J* = 2.2 Hz, 1H, ArH), 7.04 – 6.99 (m, 2H, ArH), 6.85 – 6.78 (m, 2H, ArH), 5.71 (s, 1H, OH), 4.61 (s, 2H, CH_2), 4.21 (d, *J* = 2.4 Hz, 2H, CH_2CCH), 2.50 (t, *J* = 2.4 Hz, 1H, CH). ^{13}C NMR (101 MHz, $CDCl_3$) δ 156.2 (ArC), 148.0 (ArC), 142.4 (ArC), 133.0 (ArC), 130.0 (ArC), 129.5 (ArC), 120.6 (ArC), 119.5 (ArC), 118.0 (ArC), 116.7 (ArC), 79.5 (C), 74.8 (CH), 70.9 ($ArCH_2$), 57.2 (CH_2). HRMS (ESI) m/z calcd for $C_{14}H_{18}ONa$ $[M + Na]^+$, 311.0445, found 311.0443

5-Chloro-2-(4-(4-(((4-(4-chloro-2-hydroxyphenoxy)benzyl)oxy)methyl)-1*H*-1,2,3-triazol-1-yl)phenoxy)phenol (54)

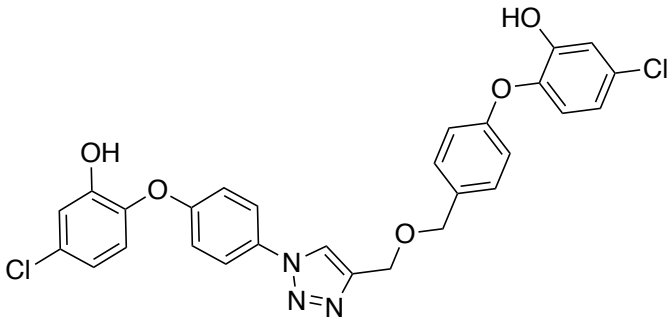

Compound **107** (147 mg, 0.51 mmol) was dissolved in H_2O:^{t}BuOH (10 mL, 1:1). Compound **106** (133 mg, 0.51 mmol), $CuSO_4.5H_2O$ (10 mg, 10 mol%) and sodium

ascorbate (50 mg, 0.26 mmol) were added sequentially and the reaction mixture was allowed to stir at r.t. for 18 h. The reaction mixture was then diluted with H_2O (20 mL) before being extracted with EtOAc (3 × 20 mL). The combined organic layers were dried over $MgSO_4$, filtered and concentrated under reduced pressure. Purification was performed by reverse-phase high-performance liquid chromatography (Method 2) to yield the title compound as a white solid (70 mg, 25%) 1H NMR (400 MHz, $CDCl_3$) δ 7.89 (s, 1H, CH), 7.64 – 7.55 (m, 2H, ArH), 7.38 – 7.28 (m, 2H, ArH), 7.11 – 7.09 (m, 1H, ArH), 7.06 (dd, *J* = 8.7, 2.1 Hz, 3H, ArH), 6.98 – 6.92 (m, 2H, ArH), 6.88 – 6.85 (m, 2H, ArH), 6.81 – 6.75 (m, 2H, ArH), 6.62 (bs, 1H, OH), 6.12 (bs, 1H, OH), 4.73 (s, 2H, CH_2), 4.59 (s, 2H, CH_2). 13C NMR (101 MHz, CDCl3) δ 157.30 (ArC), 156.30 (ArC), 148.66 (ArC), 148.24 (ArC), 145.77 (ArC), 142.29 (ArC), 141.41 (ArC), 133.09 (ArC), 132.38 (ArC), 130.57 (ArC), 129.82 (ArC), 129.57 (ArC), 122.29 (ArC), 120.93 (ArC), 120.84 (ArC), 120.77 (ArC), 120.56 (CH), 119.74 (ArC), 118.30 (ArC), 117.90 (ArC), 117.44 (ArC), 116.80 (ArC), 72.16 (CH_2), 63.44 (CH_2). HPLC R_T ~ 12 min (Method 2). HRMS (ESI) *m/z* calcd for $C_{28}H_{20}O_5N_3{}^{35}Cl_2$ $[M + H]^+$, 550.0931, found 550.0940.

5-Chloro-2-(4-(5-(((4-(4-chloro-2-hydroxyphenoxy)benzyl)oxy)methyl)-1*H*-1,2,3-triazol-1-yl)phenoxy)phenol (55)

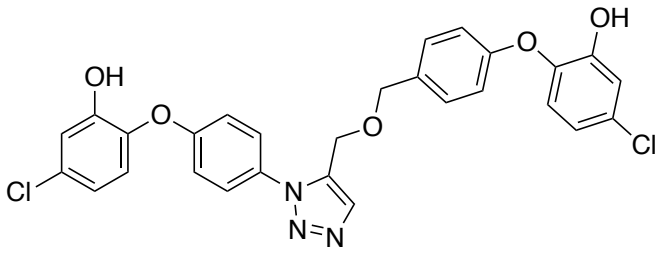

The title compound was synthesised according to General Procedure H from **107** (0.19 g, 0.73 mmol), **106** (0.19 g, 0.66 mmol) and Cp*RuCl(PPh_3)$_2$ (25 mg, 5 mol%).

Purification was performed by semi-preparative reverse-phase high-performance liquid chromatography (Method 2) to yield the title compound as a white solid (62.7 mg, 17%). ^{1}H NMR (400 MHz, $CDCl_3$) δ 7.78 (s, 1H, CH), 7.57 – 7.50 (m, 2H, ArH), 7.26 – 7.20 (m, 2H, ArH), 7.13 (d, *J* = 2.2 Hz, 1H, ArH), 7.09 – 7.04 (m, 3H, ArH), 6.98 – 6.94 (m, 2H, ArH), 6.92 – 6.89 (m, 2H, ArH), 6.84 – 6.82 (m, 2H, ArH), 4.52 (s, 2H, CH_2), 4.50 (s, 2H, CH_2). ^{13}C NMR (101 MHz, $CDCl_3$) δ 158.0 (ArC), 156.8 (ArC), 148.8 (ArC), 148.5 (ArC), 142.0 (ArC), 141.2 (ArC), 134.8 (CH), 133.8 (ArC), 131.9 (ArC), 131.1 (ArC), 130.8 (ArC), 129.9 (ArC), 129.9 (ArC), 126.3 (ArC), 121.2 (ArC), 120.9 (ArC), 120.7 (ArC), 120.3 (ArC), 117.8 (ArC), 117.7 (ArC), 117.5 (ArC), 117.1 (ArC), 72.0 (CH_2), 59.4 (CH_2). HPLC R_T ~ 13 min (Method 2). HRMS (ESI) *m/z* calcd for $C_{28}H_{20}O_5N_3{}^{35}Cl_2$ $[M - H]^-$, 548.0785, found 548.0798.

((Prop-2-yn-1-yloxy)methyl)benzene (129)

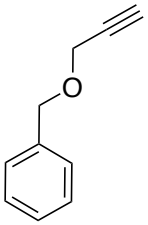

The title compound was synthesised according to General Procedure F from propargyl alcohol (1.25 g, 20.00 mmol) NaH (60% dispersion in mineral oil, 1.59 g, 40.00 mmol) and benzyl chloride (3.79 g, 30.00 mmol). Purification was performed by flash column chromatography (Hexane/EtOAc, 0 -> 20%) to yield the title compound as a pale-yellow oil (2.13 g, 73%). ^{1}H NMR (400 MHz, $CDCl_3$) δ 7.44 – 7.29 (m, 5H, ArH), 4.63 (s, 2H, $ArCH_2O$), 4.19 (d, *J* = 2.4 Hz, 2H, CH2), 2.48 (t, *J* = 2.4 Hz, 1H, CH). ^{13}C NMR (101 MHz, $CDCl_3$) δ 137.3 (ArC), 128.5 (ArC), 128.2 (ArC), 128.0 (ArC), 79.7 (C), 74.7 (CH), 71.6 ($ArCH_2O$), 57.1 (CH_2). Parent ion not observed in

HR-MS, this is likely due to the low MW of the compound. Analytical data consistent with those reported in the literature.[199]

1-Methyl-4-((prop-2-yn-1-yloxy)methyl)benzene (130)

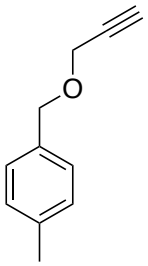

The title compound was synthesised according to General Procedure F from propargyl alcohol (0.38 g, 6.87 mmol) NaH (60% dispersion in mineral oil, 0.55 g, 13.74 mmol) and 4-methylbenzyl chloride (1.01 g, 7.21 mmol). Purification was performed by flash column chromatography (Hexane/EtOAc, 0 -> 20%) to yield the title compound as a pale-yellow oil (0.91 g, 83%). ^{1}H NMR (400 MHz, $CDCl_3$) δ 7.33 – 7.27 (m, 2H, ArH), 7.20 (d, J = 7.8 Hz, 2H, ArH), 4.61 (s, 2H, $ArCH_2$), 4.18 (d, *J* = 2.4 Hz, 2H, CH_2CCH), 2.49 (t, *J* = 2.4 Hz, 1H, CH), 2.38 (s, 3H, CH_3). ^{13}C NMR (101 MHz, $CDCl_3$) δ 137.7 (ArC), 134.2 (ArC), 129.2 (ArC), 128.3 (ArC), 79.8 (C), 74.5 (CH), 71.4 ($ArCH_2$), 56.9 (CH_2CCH), 21.2 (CH_3). HRMS (ESI^+) *m/z* calcd for $C_{11}H_{12}ONa$ $[M + Na]^+$, 183.0780 found 183.0776. Analytical data consistent with those reported in the literature.[200]

1-Isopropyl-4-((prop-2-yn-1-yloxy)methyl)benzene (131)

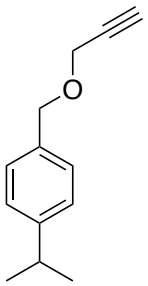

The title compound was synthesised according to General Procedure F from propargyl alcohol (0.38 g, 6.87 mmol) NaH (60% dispersion in mineral oil, 0.55 g, 13.74 mmol) and 4-isopropylbenzyl chloride (1.21 g, 7.21 mmol). Purification was performed by flash column chromatography (Hexane/EtOAc, 0 -> 20%) to yield the title compound as a pale-yellow oil (1.11 g, 84%). ^{1}H NMR (400 MHz, $CDCl_3$) δ 7.33 – 7.27 (m, 2H, ArH), 7.23 (d, J = 8.1 Hz, 2H, ArH), 4.59 (s, 2H, $ArCH_2$), 4.17 (d, *J* = 2.4 Hz, 2H, OCH_2), 2.92 (hept, *J* = 6.9 Hz, 1H, CH), 2.47 (t, *J* = 2.4 Hz, 1H, CH), 1.26 (d, *J* = 7.0 Hz, 6H, CH_3). ^{13}C NMR (101 MHz, $CDCl_3$) δ 148.9 (ArC), 134.7 (ArC), 128.4 (ArC), 126.7 (ArC), 79.9 (C), 74.7 (CH), 71.6 (*C*H_2CCH), 57.1 ($ArCH_2$), 34.0 (CH), 24.1 (CH_3). HRMS (ESI$^+$) *m/z* calcd for $C_{13}H_{16}NaO$ $[M + Na]^+$, 211.1093 found 211.1089. Analytical data consistent with those reported in the literature.[201]

1-(*tert*-Butyl)-4-((prop-2-yn-1-yloxy)methyl)benzene (132)

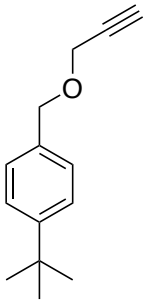

The title compound was synthesised according to General Procedure F from propargyl alcohol (0.99 g, 18.00 mmol) NaH (60% dispersion in mineral oil, 1.43 g, 24.00 mmol) and 4-*tert*-butylbenzyl chloride (2.20 g, 12.00 mmol). Purification was performed by flash column chromatography (Hexane/EtOAc, 0 -> 20%) to yield the title compound as a pale-yellow oil (3.12 g, 86%). ^{1}H NMR (400 MHz, $CDCl_3$) δ 7.44 – 7.39 (m, 2H, ArH), 7.36 – 7.31 (m, 2H, ArH), 4.61 (s, 2H, CH_2), 4.20 (d, *J* = 2.4 Hz, 2H, C*H*$_2$CCH), 2.49 (t, *J* = 2.4 Hz, 1H, CH), 1.35 (s, 9H, $(CH_3)_3$). ^{13}C NMR (101 MHz, $CDCl_3$) δ 151.0 (ArC), 134.2 (ArC), 128.0 (ArC), 125.4 (ArC), 79.8 (*C*CH), 74.5 (CH), 71.4 (Ar*C*H$_2$O), 57.0 (CH_2), 34.6 (C), 31.4 $(CH_3)_3$). HRMS (ESI) m/z calcd for $C_{14}H_{18}ONa$ $[M + Na]^+$, 225.1250, found 225.1245.

4-((*tert*-Butyldimethylsilyl)oxy)benzaldehyde (146)

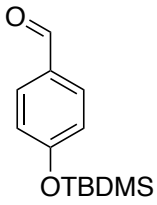

4-Hydroxybenzalehyde (3.70 g, 30.30 mmol) and Et_3N (4.57 g, 45.20 mmol) were dissolved in CH_2Cl_2 (50 mL) followed by the portion-wise addition of TBDMSCl (6.80 g, 45.12 mmol) and the reaction mixture was stirred for 3 h. The reaction mixture was then diluted with H_2O (50 mL) and extracted with CH_2Cl_2 (3 × 50 mL). The combined

organic layers were then dried over $MgSO_4$, filtered and concentrated under reduced pressure. Purification was performed by flash column chromatography (Hexane/ EtOAc, 0 -> 20%) to yield the title compound as a pale-yellow oil (6.10 g, 85%). ^{1}H NMR (400 MHz, $CDCl_3$) δ 9.79 (s, 1H, CHO), 7.84 – 7.58 (m, 2H, ArH), 6.92 – 6.74 (m, 2H, ArH), 0.90 (s, 9H, $(CH_3)_3$), 0.15 (s, 6H, $(CH_3)_2$). ^{13}C NMR (101 MHz, $CDCl_3$) δ 191.4 (CHO), 162.0 (ArC), 132.4 (ArC), 130.9 (ArC), 120.9 (ArC), 26.0 $(CH_3)_3$), 18.7 (C), -3.9 ($Si(CH_3)_2$). HRMS (ESI) *m/z* calcd for $C_{13}H_{21}O_2Si$ $[M + H]^+$, 237.1305, found 237.1302. Analytical data consistent with those reported in the literature.[202]

(4-((*tert*-Butyldimethylsilyl)oxy)phenyl)methanol (147)

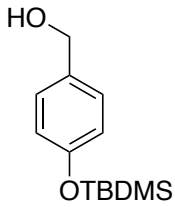

The title compound was synthesised according to General Procedure E from **146** (6.10 g, 25.83 mmol) and $NaBH_4$ (1.92 g, 37.83 mmol). Purification was performed by flash column chromatography (Hexane/EtOAc, 0 -> 20%) to yield the title compound as a pale-yellow oil (5.71 g, 91%). ^{1}H NMR (400 MHz, $CDCl_3$) δ 7.04 – 6.96 (m, 2H, ArH), 6.67 – 6.58 (m, 2H, ArH), 4.34 (s, 2H. CH_2), 2.10 (bs, 1H, OH), 0.80 (s, 9H, $(CH_3)_3$), -0.00 (s, 6H, $(CH_3)_2$). ^{13}C NMR (101 MHz, $CDCl_3$) δ 155.2 (ArC), 133.8 (ArC), 128.6 (ArC), 120.1 (ArC), 64.5 (CH_2), 25.7 $(CH_3)_3$), 18.2 (C), -4.4 ($Si(CH_3)_2$). HRMS (ESI) *m/z* calcd for $C_{13}H_{22}O_2SiNa$ $[M + Na]^+$, 261.1281, found 261.1274. Analytical data consistent with those reported in the literature.[203]

tert-Butyldimethyl(4-((prop-2-yn-1-yloxy)methyl)phenoxy)silane (148)

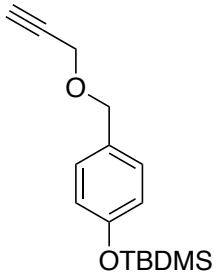

The title compound was synthesised according to General Procedure F from **147** (2.38 g, 10.00 mmol) NaH (60% dispersion in mineral oil, 0.46 g, 11.00 mmol) and propargyl bromide (1.30 g, 11.00 mmol). Purification was performed by flash column chromatography (Hexane/EtOAc, 0 -> 20%) to yield the title compound as a pale-yellow oil (2.03 g, 74%). ^{1}H NMR (400 MHz, $CDCl_3$) δ 7.26 – 7.07 (m, 2H, ArH), 6.92 – 6.79 (m, 2H, ArH), 4.62 – 4.51 (m, 4H, 2 × CH_2), 2.41 (t, *J* = 2.4 Hz, 1H, CH), 0.84 (s, 9H, $(CH_3)_3$), 0.00 (s, 6H, $(CH_3)_2$). ^{13}C NMR (101 MHz, $CDCl_3$) δ 156.6 (ArC), 134.6 (ArC), 127.5 (ArC), 114.7 (ArC), 78.7 (CCH), 75.4 (CH), 64.6 ($ArCH_2$), 55.9 (CH_2), 26.0 $(CH_3)_3$), 18.5 (Si*C*$(CH_3)_3$), -5.2 (Si$(CH_3)_2$). HRMS (ESI) *m*/*z* calcd for $C_{16}H_{24}O_2SiNa$ $[M + Na]^+$, 299.1438, found 299.1442.

4-((Prop-2-yn-1-yloxy)methyl)phenol (133)

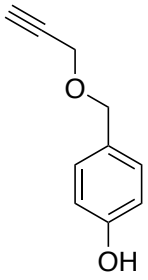

Compound **148** (2.00 g, 7.24 mmol) was dissolved in anhydrous THF (25 mL) followed by dropwise addition of TBAF (1 M solution in THF, 10.00 mL, 10.00 mmol). The reaction mixture was stirred for 18 h before being diluted with H_2O (25 mL) and

extracted with EtOAc (3 × 50 mL). The combined organic layers were dried over $MgSO_4$, filtered and concentrated under reduced pressure. Purification was performed by flash column chromatography (Hexane/EtOAc, 0 -> 40%) to yield the title compound as a pale-yellow oil (0.85 g, 72%) ^{1}H NMR (400 MHz, $CDCl_3$) δ 7.24 – 7.20 (m, 2H, ArH), 6.91 – 6.85 (m, 2H, ArH), 4.60 (d, *J* = 2.4 Hz, 2H, C*H*$_2$CCH), 4.53 (d, *J* = 5.1 Hz, 2H, CH_2), 2.44 (t, *J* = 2.4 Hz, 1H, CH). ^{13}C NMR (101 MHz, $CDCl_3$) δ 157.0 (ArC), 134.3 (ArC), 128.6 (ArC), 114.9 (ArC), 78.6 (*C*CH), 75.6 (CH), 64.8 ($ArCH_2$), 55.9 (CH_2). HRMS (ESI) *m/z* calcd for $C_{10}H_{10}O_2SiNa$ $[M + Na]^+$, 185.0573, found 185.0571.

1-Methoxy-4-((prop-2-yn-1-yloxy)methyl)benzene (134)

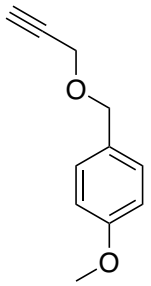

The title compound was synthesised according to General Procedure F from propargyl alcohol (0.38 g, 6.87 mmol) NaH (60% dispersion in mineral oil, 0.41 g, 10.60 mmol) and 4-methoxybenzyl chloride (1.13 g, 7.21 mmol). Purification was performed by flash column chromatography (Hexane/EtOAc, 0 -> 20%) to yield the title compound as a pale-yellow oil (0.79 g, 66%). ^{1}H NMR (400 MHz, $CDCl_3$) δ 7.33 – 7.27 (m, 2H, ArH), 6.92 – 6.86 (m, 2H, ArH), 4.55 (s, 2H, OCH_2), 4.14 (d, *J* = 2.4 Hz, 2H, OCH_2), 3.81 (s, 3H, OCH_3), 2.47 (t, *J* = 2.4 Hz, 1H, CH). ^{13}C NMR (101 MHz, $CDCl_3$) δ 159.5 (ArC), 129.9 (ArC), 129.4 (ArC), 113.9 (ArC), 79.9 (C), 74.6 (CH), 71.2 (OCH_2), 56.8 (OCH_2), 55.4 (OCH_3). HRMS (ESI^+) calcd for $C_{11}H_{12}NaO_2$ *m/z* 199.0730 found

199.0728 [M + Na]$^+$. Analytical data consistent with those reported in the literature.[204]

1-Chloro-4-((prop-2-yn-1-yloxy)methyl)benzene (135)

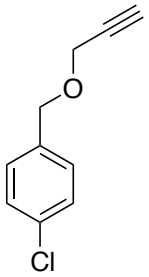

The title compound was synthesised according to General Procedure F from 4-Chlorobenzyl alcohol (0.75 g, 5.28 mmol) NaH (60% dispersion in mineral oil, 0.41 g, 10.60 mmol) and propargyl bromide (0.95 g, 7.95 mmol). Purification was performed by flash column chromatography (Hexane/EtOAc, 0 -> 20%) to yield the title compound as a pale-yellow oil (0.77 g, 81%). ^{1}H NMR (400 MHz, $CDCl_3$) δ 7.37 – 7.33 (m, 2H, ArH), 7.33 – 7.30 (m, 2H, ArH), 4.60 (s, 2H, $ArCH_2$), 4.20 (d, *J* = 2.4 Hz, 2H, CH_2CCH), 2.50 (t, *J* = 2.4 Hz, 1H, CH). ^{13}C NMR (101 MHz, $CDCl_3$) δ 135.9 (ArC), 133.7 (ArC), 129.4 (ArC), 128.6 (ArC), 79.4 (*C*CH), 74.9 (CH), 70.7 ($ArCH_2$), 57.2 (CH_2). Parent ion not observed in HR-MS, this is likely due to the low MW of the compound. Analytical data consistent with those reported in the literature.[205]

1-((Prop-2-yn-1-yloxy)methyl)-4-(trifluoromethyl)benzene (136)

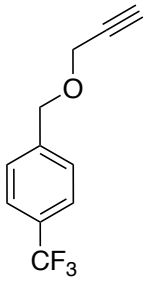

The title compound was synthesised according to General Procedure F from 4-(Trifluoromethyl)benzyl alcohol (1.00 g, 5.68 mmol) NaH (60% dispersion in mineral oil, 0.45 g, 11.36 mmol) and propargyl bromide (0.99 g, 8.32 mmol). Purification was performed by flash column chromatography (Hexane/EtOAc, 0 -> 20%) to yield the title compound as a pale-yellow oil (1.00 g, 83%). ^{1}H NMR (400 MHz, $CDCl_3$) δ 7.64 (d, J = 8.1 Hz, 2H), 7.53 – 7.46 (m, 2H), 4.69 (s, 2H), 4.24 (d, *J* = 2.4 Hz, 2H), 2.51 (t, *J* = 2.4 Hz, 1H). ^{13}C NMR (101 MHz, $CDCl_3$) δ 141.5 (ArC), 130.1 (q, J = 32.3 Hz), 127.9, 125.4 (q, J = 3.8 Hz), 122.8, 79.2 (*C*CH), 75.0 (CH), 70.7 ($ArCH_2$), 57.6 (CH_2). ^{19}F NMR (376 MHz, $CDCl_3$) δ -62.6. Parent ion not observed in HR-MS, this is likely due to the low MW of the compound.

4-(Cyclopropylmethoxy)benzaldehyde (144)

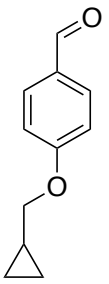

4-Hydroxybenzalehyde (2.00 g, 16.37 mmol) was dissolved in anhydrous DMF (50 mL) followed by the sequential addition of K_2CO_3 (4.46 g, 32.27 mmol) and (bromomethyl)cyclopropane (3.30 g, 24.44 mmol). The reaction mixture was then

heated to 130 °C and stirred for 18 h before being allowed to cool to r.t.. The reaction mixture was diluted with H_2O (50 mL) and extracted with EtOAc (3 × 50 mL). The combined organic layers were dried over $MgSO_4$, filtered and concentrated under reduced pressure. Purification was performed by flash column chromatography (Hexane/EtOAc, 3:1) to yield the title compound as a yellow oil (2.00 g, 69%). ^{1}H NMR (400 MHz, $CDCl_3$) δ 9.87 (s, 1H, CHO), 7.89 – 7.75 (m, 2H, ArH), 7.06 – 6.92 (m, 2H, ArH), 3.88 (d, *J* = 7.0 Hz, 2H, OCH_2), 1.37 – 1.18 (m, 1H, CH), 0.72 – 0.62 (m, 2H, CH_2), 0.43 – 0.32 (m, 2H, CH_2). ^{13}C NMR (101 MHz, $CDCl_3$) δ 190.8 (CHO), 164.1 (ArC), 132.0 (ArC), 129.8 (ArC), 114.8 (ArC), 73.1 (OCH_2), 10.1 (CH), 3.3 (CH_2). HRMS (ESI) *m/z* calcd for $C_{11}H_{13}O_2$ $[M + H]^+$, 177.0910, found 177.0931. Analytical data consistent with those reported in the literature.[206]

(4-(Cyclopropylmethoxy)phenyl)methanol (145)

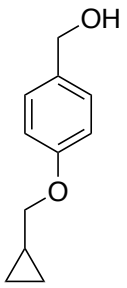

The title compound was synthesised according to General Procedure E from **144** (2.00 g, 11.36 mmol) and $NaBH_4$ (0.65 g, 17.04 mmol). Purification was performed by flash column chromatography (Hexane/EtOAc, 0 -> 20%) to yield the title compound as a pale-yellow oil (1.30 g, 64%). ^{1}H NMR (400 MHz, $CDCl_3$) δ 7.32 – 7.27 (m, 2H, ArH), 6.94 – 6.89 (m, 2H, ArH), 4.63 (s, 2H, CH_2), 3.82 (d, *J* = 6.9 Hz, 2H, OC*H*$_2$CH), 1.78 (s, 1H, OH), 1.35 – 1.24 (m, 1H, CH), 0.70 – 0.64 (m, 2H, CH_2), 0.40 – 0.35 (m, 2H, CH_2). ^{13}C NMR (101 MHz, $CDCl_3$) δ 158.7 (ArC), 133.1 (ArC), 128.7 (ArC), 114.7 (ArC), 72.9 (CH_2OH), 65.1 (OCH_2), 10.3 (CH), 3.2 (CH_2). HRMS (ESI) *m/z* calcd for

$C_{11}H_{14}O_2Na$ [M + Na]$^+$, 201.0886, found 201.0890. Analytical data consistent with those reported in the literature.[206]

1-(Cyclopropylmethoxy)-4-((prop-2-yn-1-yloxy)methyl)benzene (137)

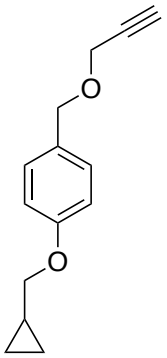

The title compound was synthesised according to General Procedure F from **145** (1.00 g, 5.61 mmol) NaH (60% dispersion in mineral oil, 0.34 g, 8.42 mmol) and propargyl bromide (1.33 g, 11.22 mmol). Purification was performed by flash column chromatography (Hexane/EtOAc, 0 -> 20%) to yield the title compound as a pale-yellow oil (0.83 g, 68%). ^{1}H NMR (400 MHz, $CDCl_3$) δ 7.35 – 7.25 (m, 2H, ArH), 6.97 – 6.83 (m, 2H, ArH), 4.56 (s, 2H $ArCH_2O$), 4.16 (d, J = 2.4 Hz, 2H, C*H*$_2$CCH), 3.82 (d, *J* = 6.9 Hz, 2H, C*H*$_2$CH), 2.48 (t, *J* = 2.4 Hz, 1H, CH_2CCH), 1.35 – 1.24 (m, 1H, CH_2CH), 0.70 – 0.62 (m, 2H, CH_2), 0.40 – 0.34 (m, 2H, CH_2). ^{13}C NMR (101 MHz, $CDCl_3$) δ 158.9 (ArC), 129.8 (ArC), 129.3 (ArC), 114.6 (ArC), 79.8 (*C*CH), 74.5 (C*C*H), 72.8 (*C*H_2CCH), 71.2 ($ArCH_2$), 56.7 (Ar*C*H_2C), 10.3 (CH_2CH), 3.2 (CH_2). HRMS (ESI) *m/z* calcd for $C_{11}H_{14}O_2Na$ [M + Na]$^+$, 239.1043, found 239.1044.

(4-(Pyrrolidin-1-yl)phenyl)methanol (142)

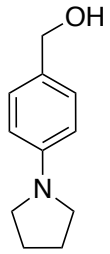

The title compound was synthesised according to General Procedure E from 4-(1-pyrrolidino)benzaldehyde (1.00 g, 5.71 mmol) and $NaBH_4$ (0.32 g, 8.53 mmol). Purification was performed by flash column chromatography (Hexane/EtOAc, 0 -> 20%) to yield the title compound as a pale-yellow oil (0.75 g, 76%). ^{1}H NMR (400 MHz, $CDCl_3$) δ 7.28 – 7.22 (m, 2H, ArH), 6.62 – 6.54 (m, 2H, ArH), 4.57 (s, 2H, CH_2OH), 3.36 – 3.26 (m, 4H, 2 × CH_2NH), 2.06 – 1.99 (m, 4H, 2 × CH_2), 1.72 (s, 1H, OH). ^{13}C NMR (101 MHz, $CDCl_3$) δ 147.8 (ArC), 128.9 (ArC), 127.7 (ArC), 111.7 (ArC), 65.6 (CH_2OH), 47.7 (CH_2NH), 25.5 (CH_2). HRMS (ESI) *m*/*z* calcd for $C_{11}H_{16}NO$ $[M + H]^+$, 176.1226, found 176.1240.

1-(4-((Prop-2-yn-1-yloxy)methyl)phenyl)pyrrolidine (138)

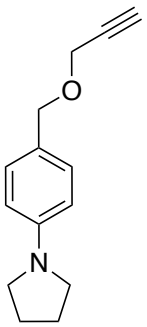

The title compound was synthesised according to General Procedure F from **142** (0.74 g, 4.17 mmol) NaH (60% dispersion in mineral oil, 0.33 g, 8.34 mmol) and propargyl bromide (0.74 g, 6.25 mmol). Purification was performed by flash column chromatography (Hexane/EtOAc, 0 -> 20%) to yield the title compound as a pale-

yellow oil (0.82 g, 81%). ^{1}H NMR (400 MHz, $CDCl_3$) δ 7.27 – 7.21 (m, 2H), 6.62 – 6.54 (m, 2H), 4.54 (s, 2H), 4.13 (d, *J* = 2.4 Hz, 2H), 3.34 – 3.26 (m, 4H), 2.46 (t, *J* = 2.4 Hz, 1H), 2.05 – 2.00 (m, 4H). ^{13}C NMR (101 MHz, $CDCl_3$) δ 147.9 (ArC), 130.0 (ArC), 123.5 (ArC), 111.5 (ArC), 80.2 (CCH), 74.2 (CH), 71.6 ($ArCH_2$), 56.1 (CH_2), 47.6 (CH_2NH), 25.5 (CH_2). HRMS (ESI) *m/z* calcd for $C_{14}H_{18}NO$ $[M + H]^+$, 216.1383, found 216.1383.

1,3-Difluoro-2-((prop-2-yn-1-yloxy)methyl)benzene (139)

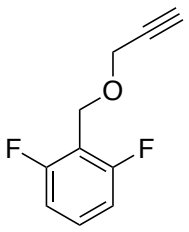

The title compound was synthesised according to General Procedure F from compound 2,6-difluorobenzyl alcohol (0.50 g, 3.50 mmol), NaH (60% dispersion in mineral oil, 0.28 g, 7.00 mmol) and propargyl bromide (0.62 g, 5.25 mmol). Purification was performed by flash column chromatography (Hexane/EtOAc, 0 -> 20%) to yield the title compound as a pale-yellow oil (0.43, 67%). ^{1}H NMR (400 MHz, $CDCl_3$) δ 7.36 – 7.25 (m, 1H, ArH), 6.97 – 6.89 (m, 2H, ArH), 4.72 (d, J = 1.5 Hz, 2H, $ArCH_2$), 4.22 (d, *J* = 2.4 Hz, 2H, C*H*$_2$CCH), 2.50 (t, *J* = 2.4 Hz, 1H, CH). ^{13}C NMR (101 MHz, $CDCl_3$) δ 162.1 (dd, J = 250.6, 8.0 Hz, ArCF), 130.5 (t, *J* = 10.5 Hz, ArCH), 113.1 (t, *J* = 19.5 Hz, ArC), 111.5 – 111.1 (m, ArCH), 79.3 (C), 74.7 (CH), 58.9 (t, J = 3.5 Hz, $ArCH_2$), 57.7 (CH_2CCH).^{19}F NMR (376 MHz, $CDCl_3$) δ -114.9 (ArF). Parent ion not observed in HR-MS.

4-((Prop-2-yn-1-yloxy)methyl)pyridine (140)

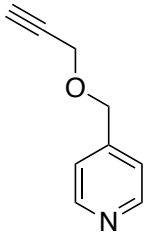

The title compound was synthesised according to General Procedure F from pyridine-4-methanol (1.00 g, 9.16 mmol), NaH (60% dispersion in mineral oil, 0.73 g, 18.32 mmol) and propargyl bromide (1.63 g, 13.74 mmol). Purification was performed by flash column chromatography (Hexane/EtOAc, 0 -> 75%) to yield the title compound as a pale-yellow oil (1.21, 90%). ^{1}H NMR (400 MHz, $CDCl_3$) δ 8.63 – 8.49 (m, 2H, ArH), 7.28 – 7.23 (m, 2H, ArH), 4.62 (s, 2H, $ArCH_2$), 4.23 (d, *J* = 2.4 Hz, 2H, CH_2CCH), 2.50 (t, *J* = 2.4 Hz, 1H, CH). ^{13}C NMR (101 MHz, $CDCl_3$) δ 149.9 (ArC), 146.6 (ArC), 122.0 (ArC), 79.0 (*C*CH), 75.3 (*C*H), 69.8 ($ArCH_2$), 57.9 (CH_2C). HRMS (ESI) *m*/*z* calcd for C_9H_9ONNa [M + Na]$^+$, 170.0576, found 170.0584.

2-(4-(5-((Benzyloxy)methyl)-1*H*-1,2,3-triazol-1-yl)phenoxy)-5-chlorophenol (56)

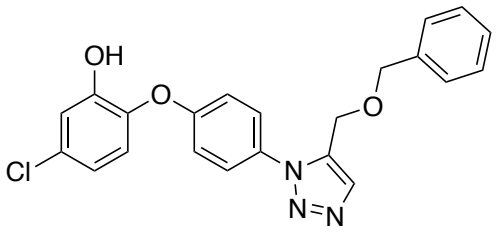

The title compound was synthesised according to General Procedure H from **106** (0.10 g, 0.38 mmol), **129** (0.06 g, 0.38 mmol) and Cp*RuCl(PPh_3)$_2$ (15 mg, 5 mol %). Purification was performed by reverse-phase high-performance liquid chromatography (Method 2) to yield the title compound as a white solid (15 mg, 10%). ^{1}H NMR (400 MHz, $CDCl_3$) δ 7.80 (s, 1H, CH), 7.57 – 7.51 (m, 2H, ArH), 7.39

– 7.26 (m, 5H, ArH), 7.15 (d, *J* = 2.2 Hz, 1H, ArH), 7.09 – 7.03 (m, 2H, ArH), 6.94 – 6.87 (m, 2H, ArH), 4.55 (s, 2H, CH_2), 4.53 (s, 2H, CH_2). ^{13}C NMR (101 MHz, $CDCl_3$) δ 158.1 (ArC), 149.1 (ArC), 141.3 (ArC), 136.7 (ArC), 134.8 (CH), 133.9 (ArC), 131.1 (ArC), 130.6 (ArC), 128.7 (ArC), 128.3 (ArC), 128.0 (ArC), 126.3 (ArC), 121.3 (ArC), 120.7 (ArC), 117.8 (ArC), 117.6 (ArC), 72.6 (CH_2), 59.5 (CH_2). HPLC R_T ~ 14 min (Method 4). HRMS (ESI) *m*/*z* calcd for $C_{22}H_{19}{}^{35}ClN_3O_3$ $[M + H]^+$, 408.1109, found 408.1116.

5-Chloro-2-(4-(5-(((4-methylbenzyl)oxy)methyl)-1*H*-1,2,3-triazol-1-yl)phenoxy)phenol (57)

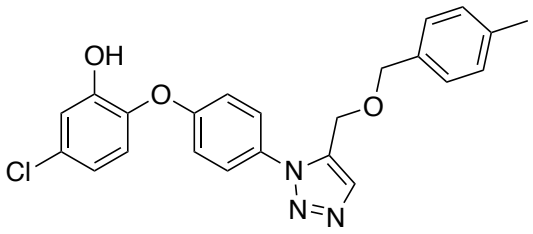

The title compound was synthesised according to General Procedure H from **106** (0.20 g, 0.76 mmol)**, 130** (0.12 g, 0.76 mmol) and Cp*RuCl(PPh_3)$_2$ (30 mg, 5 mol %)**.** Purification was performed by semi-preparative reverse-phase high-performance liquid chromatography (Method 2) to yield the title compound as a white solid (35 mg, 11%). ^{1}H NMR (400 MHz, $CDCl_3$) δ 7.78 (s, 1H, CH), 7.61 – 7.54 (m, 2H, ArH), 7.15 (s, 4H, ArH), 7.13 – 7.05 (m, 3H, ArH), 6.88 (d, *J* = 2.0 Hz, 2H, ArH), 4.50 (s, 2H, CH_2), 4.49 (s, 2H, CH_2), 2.34 (s, 3H, CH_3). ^{13}C NMR (101 MHz, $CDCl_3$) δ 157.7 (ArC), 148.6 (ArC), 141.4 (ArC), 138.1 (ArC), 135.0 (CH), 133.8 (ArC), 133.7 (ArC), 131.5 (ArC), 130.6, 129.3 (ArC), 128.1 (ArC), 126.4 (ArC), 120.9 (ArC), 120.8 (ArC), 118.0 (ArC), 117.4 (ArC), 72.4 (CH_2), 59.3 (CH_2), 21.2 (CH_3). HPLC R_T ~ 8 min (Method 2) HRMS (ESI) *m/z* calcd for $C_{23}H_{19}O_3N_3{}^{35}Cl$ [M - H]$^-$, 420.1120, found 420.1108.

5-Chloro-2-(4-(5-(((4-isopropylbenzyl)oxy)methyl)-1*H*-1,2,3-triazol-1-yl)phenoxy)phenol (58)

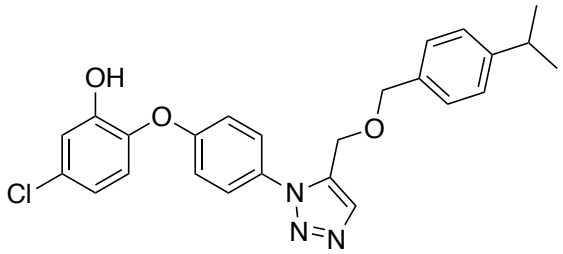

The title compound was synthesised according to General Procedure H from **106** (0.20 g, 0.76 mmol), **131** (0.14 g, 0.76 mmol) and Cp*RuCl(PPh_3)$_2$ (30 mg, 5 mol %). Purification was performed by semi-preparative reverse-phase high-performance liquid chromatography (Method 2) to yield the title compound as a white solid (97 mg, 28%). ^{1}H NMR (400 MHz, $CDCl_3$) δ 7.79 (s, 1H, CH), 7.63 – 7.51 (m, 2H, ArH), 7.23 – 7.15 (m, 4H, ArH), 7.13 – 7.05 (m, 3H, ArH), 6.92 – 6.82 (m, 2H, ArH), 4.51 (s, 2H, CH_2), 4.50 (s, 2H, CH_2), 2.90 (hept, *J* = 6.9 Hz, 1H, CH), 1.24 (d, *J* = 6.9 Hz, 6H, CH_3). ^{13}C NMR (101 MHz, $CDCl_3$) δ 157.7 (ArC), 149.1 (ArC), 148.6 (ArC), 141.4 (ArC), 135.0 (CH), 134.1 (ArC), 133.8 (ArC), 131.5 (ArC), 130.6 (ArC), 128.2 (ArC), 126.7 (ArC), 126.4 (ArC), 120.9 (ArC), 120.7 (ArC), 118.0 (ArC), 117.4 (ArC), 72.4 (CH_2), 59.4 (CH_2), 33.9 (*C*H(CH_3)$_2$), 24.0 (CH_3). HPLC R_T. ~ 10 min (Method 2). HRMS (ESI) *m*/*z* calcd for $C_{25}H_{23}O_3N_3{}^{35}Cl$ $[M - H]^-$, 448.1433, found 448.1426.

2-(4-(5-(((4-(*tert*-Butyl)benzyl)oxy)methyl)-1*H*-1,2,3-triazol-1-yl)phenoxy)-5-chlorophenol (59)

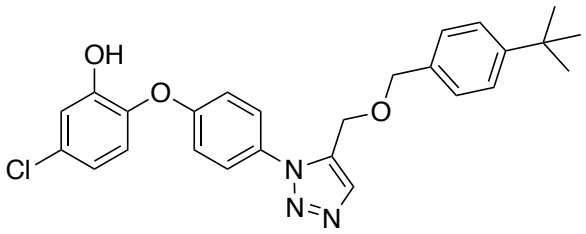

The title compound was synthesised according to General Procedure H from **106** (0.17 g, 0.68 mmol), **132** (0.13 g, 0.68 mmol) and Cp*RuCl(PPh_3)$_2$ (26 mg, 5 mol %). Purification was performed by semi-preparative reverse-phase high-performance liquid chromatography (Method 2) to yield the title compound as a white solid (104 mg, 33%). ^{1}H NMR (400 MHz, $CDCl_3$) δ 7.80 (s, 1H, CH), 7.65 – 7.57 (m, 2H, ArH), 7.41 – 7.35 (m, 2H, ArH), 7.25 – 7.18 (m, 2H, ArH), 7.15 – 7.06 (m, 3H, ArH), 6.89 (d, *J* = 1.9 Hz, 2H, ArH), 5.91 (s, 1H, OH), 4.53 (s, 2H, CH_2), 4.51 (s, 2H, CH_2), 1.32 (s, 9H, $(CH_3)_3$). ^{13}C NMR (101 MHz, $CDCl_3$) δ 158.2 (ArC), 151.4 (ArC), 149.2 (*C*CH), 141.4 (ArC), 134.8 (ArC), 134.0 (CH), 133.7 (ArC), 131.0 (ArC), 130.6 (ArC), 127.9 (ArC), 126.2 (ArC), 125.6 (ArC), 121.4 (ArC), 120.6 (ArC), 117.7 (ArC), 117.7 (ArC), 72.4 (CH_2), 59.5 (CH_2), 34.6 (C), 31.3 ((CH_3)$_3$). HPLC R_T. ~ 11 min (Method 2). HRMS (ESI) *m*/*z* calcd for $C_{26}H_{26}O_3N_3{}^{35}Cl$ [M - H]$^-$, 462.1590, found 462.1576.

5-Chloro-2-(4-(5-(((4-hydroxybenzyl)oxy)methyl)-1*H*-1,2,3-triazol-1-yl)phenoxy)phenol (60)

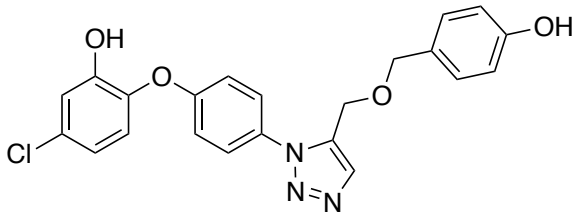

The title compound was synthesised according to General Procedure H from **106** (0.21 g, 0.80 mmol), **133** (0.13 g, 0.80 mmol) and Cp*RuCl(PPh_3)$_2$ (35 mg, 5 mol %). Purification was performed by semi-preparative reverse-phase high-performance liquid chromatography (Method 2) to yield the title compound as a white solid (19 mg, 6%). ^{1}H NMR (400 MHz, $CDCl_3$) δ 7.72 (s, 1H, CH), 7.40 – 7.33 (m, 2H, ArH), 7.18 – 7.11 (m, 3H, ArH), 6.94 (d, *J* = 2.3 Hz, 1H, ArH), 6.93 – 6.89 (m, 2H, ArH), 6.77 (d, *J* = 8.5 Hz, 1H, ArH), 6.75 – 6.66 (m, 3H, ArH), 4.89 (s, 2H, CH_2), 4.49 (s, 2H, (CH_2)). ^{13}C NMR (101 MHz, $CDCl_3$) δ 158.3 (ArC), 157.0 (ArC), 148.9 (ArC), 141.1 (ArC), 134.9 (ArC), 134.5 (CH), 133.1 (ArC), 130.8 (ArC), 128.9 (ArC), 126.5 (ArC), 121.4 (ArC), 120.8 (ArC), 117.8 (ArC), 117.5 (ArC), 115.5 (ArC), 115.0 (ArC), 64.7 (CH_2), 58.4 (CH_2). HPLC R_T. ~ 7 min (Method 5). HRMS (ESI) *m*/*z* calcd for $C_{22}H_{19}O_4N_3{}^{35}Cl$ [M - H]$^-$, 424.1059, found 424.1066.

5-Chloro-2-(4-(5-(((4-methoxybenzyl)oxy)methyl)-1*H*-1,2,3-triazol-1-yl)phenoxy)phenol (61)

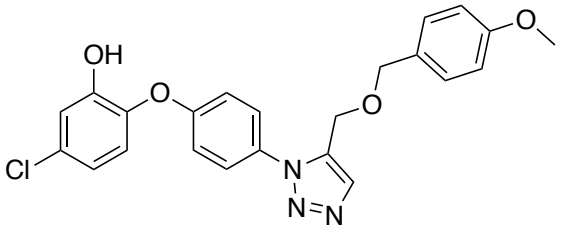

The title compound was synthesised according to General Procedure H from **106** (0.18 g, 0.69 mmol), **134** (0.12 g, 0.69 mmol) and Cp*RuCl(PPh_3)$_2$ (28 mg, 5 mol %). Purification was performed by semi-preparative reverse-phase high-performance liquid chromatography (Method 2) to yield the title compound as a white solid (48 mg, 16%). ^{1}H NMR (400 MHz, $CDCl_3$) δ 7.79 (s, 1H, CH), 7.62 – 7.49 (m, 2H, ArH), 7.23 – 7.15 (m, 2H, ArH), 7.11 (t, *J* = 1.3 Hz, 1H, ArH), 7.10 – 7.02 (m, 2H, ArH), 6.95 – 6.81 (m, 4H, ArH), 4.48 (s, 2H, CH_2), 4.46 (s, 2H, CH_2), 3.81 (s, 3H, OCH_3). ^{13}C NMR (101 MHz, $CDCl_3$) δ 159.6 (ArC), 157.8 (ArC), 148.6 (ArC), 141.4 (ArC), 135.0 (CH), 133.8 (ArC), 131.5 (ArC), 130.6 (ArC), 129.8 (ArC), 128.8 (ArC), 126.4 (ArC), 120.9 (ArC), 120.8 (ArC), 118.0 (ArC), 117.4 (ArC), 114.0 (ArC), 72.2 (CH_2), 59.0 (CH_2), 55.4 (OCH_3). HPLC R_T. ~ 18 min (Method 3). HRMS (ESI) *m*/*z* calcd for $C_{23}H_{19}O_4N_3{}^{35}Cl$ $[M - H]^-$, 436.1070, found 436.1075.

5-Chloro-2-(4-(5-(((4-chlorobenzyl)oxy)methyl)-1*H*-1,2,3-triazol-1-yl)phenoxy)phenol (62)

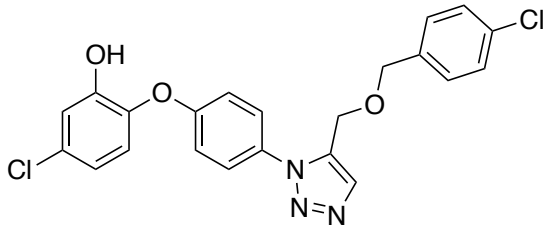

The title compound was synthesised according to General Procedure H from **106** (0.20 g, 0.77 mmol), **135** (0.13 g, 0.77 mmol) and Cp*RuCl(PPh_3)$_2$ (30 mg, 5 mol %). Purification was performed by semi-preparative reverse-phase high-performance liquid chromatography (Method 2) to yield the title compound as a white solid (42 mg, 12%). ^{1}H NMR (400 MHz, $CDCl_3$) δ 7.81 (s, 1H, CH), 7.60 – 7.54 (m, 2H, ArH), 7.36 – 7.32 (m, 2H, ArH), 7.24 – 7.19 (m, 2H, ArH), 7.14 (dd, *J* = 2.0, 0.8 Hz, 1H, ArH), 7.13 – 7.09 (m, 2H, ArH), 6.91 (d, J = 2.1 Hz, 2H, ArH), 4.54 (s, 2H, CH_2), 4.52 (s, 2H, CH_2). ^{13}C NMR (101 MHz, $CDCl_3$) δ 157.93 (ArC), 148.70 (ArC), 141.27 (ArC), 135.27 (CH), 134.93 (ArC), 134.03 (ArC), 133.57 (ArC), 131.33 (ArC), 130.69 (ArC), 129.22 (ArC), 128.81 (ArC), 126.37 (ArC), 120.92 (ArC), 120.90 (ArC), 117.94 (ArC), 117.42 (ArC), 71.69 (CH_2), 59.63 (CH_2). HPLC r.t. ~ 7 min (Method 2). HRMS (ESI) *m*/*z* calcd for $C_{22}H_{16}O_3N_3{}^{35}Cl_2$ [M - H]$^-$, 440.0574, found 440.0591.

5-Chloro-2-(4-(5-(((4-(trifluoromethyl)benzyl)oxy)methyl)-1*H*-1,2,3-triazol-1-yl)phenoxy)phenol (63)

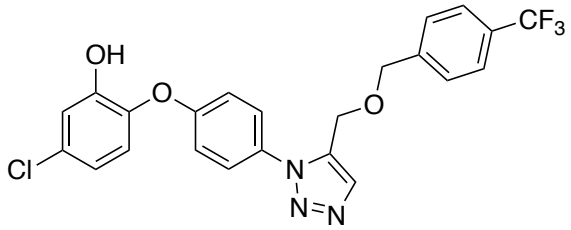

The title compound was synthesised according to General Procedure H from **106** (0.21 g, 0.84 mmol), **136** (0.17 g, 0.84 mmol) and Cp*RuCl(PPh_3)$_2$ (30 mg, 5 mol %). Purification was performed by semi-preparative reverse-phase high-performance liquid chromatography (Method 2) to yield the title compound as a white solid (96 g, 24%). ^{1}H NMR (400 MHz, $CDCl_3$) δ 7.78 (s, 1H, CH), 7.59 (d, *J* = 8.0 Hz, 2H, ArH), 7.51 – 7.47 (m, 2H, ArH), 7.36 (d, *J* = 8.0 Hz, 2H, ArH), 7.11 (d, *J* = 2.4 Hz, 1H, ArH), 7.08 – 7.01 (m, 2H, ArH), 6.90 (d, *J* = 8.6 Hz, 1H, ArH), 6.85 (dd, *J* = 8.6, 2.4 Hz, 1H, ArH), 4.57 (s, 2H, CH_2), 4.55 (s, 2H, CH_2). ^{13}C NMR (101 MHz, $CDCl_3$) δ 158.4 (ArC), 149.3 (ArC), 141.2 (ArC), 140.9 (ArC), 134.7 (CH), 133.7 (ArC), 130.8 (ArC), 130.7 (ArC), 130.3 (d, *J* = 32.5 Hz), 127.8 (ArC), 126.3 (ArC), 125.6 (q, *J* = 3.7 Hz), 122.7 (ArC), 121.6 (ArC), 120.6 (ArC), 117.7 (ArC), 117.7 (ArC), 71.7 (CH_2), 60.0 (CH_2). ^{19}F NMR (376 MHz, $CDCl_3$) δ -62.52 (CF_3). HPLC R_T. ~ 11 min (Method 3). HRMS (ESI) *m/z* calcd for $C_{23}H_{16}O_3N_3{}^{35}ClF_3$ $[M - H]^-$, 474.0838, found 474.0850.

5-Chloro-2-(4-(5-(((4-(cyclopropylmethoxy)benzyl)oxy)methyl)-1*H*-1,2,3-triazol-1-yl)phenoxy)phenol (64)

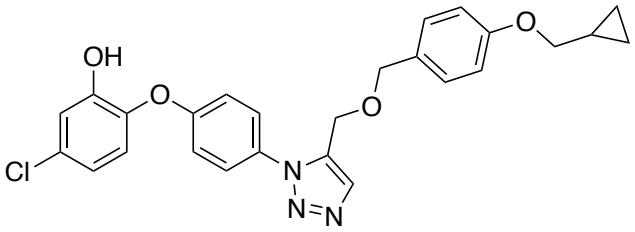

The title compound was synthesised according to General Procedure H from **106** (0.23 g, 0.88 mmol), **137** (0.19 g, 0.88 mmol) and Cp*RuCl(PPh_3)$_2$ (35 mg, 5 mol %). Purification was performed by semi-preparative reverse-phase high-performance liquid chromatography (Method 2) to yield the title compound as a white solid (21 mg, 5%). ^{1}H NMR (400 MHz, $CDCl_3$) δ 7.77 (s, 1H, CH), 7.56 – 7.47 (m, 2H, ArH), 7.21 – 7.10 (m, 3H, ArH), 7.10 – 6.98 (m, 2H, ArH), 6.98 – 6.70 (m, 4H, ArH), 4.46 (s, 2H, CH_2), 4.44 (s, 2H, CH_2), 3.80 (d, *J* = 6.9 Hz, 2H (OC*H*$_2$CH), 1.27 (dtt, *J* = 11.7, 7.0, 1.7 Hz, 1H, CH), 0.74 – 0.58 (m, 2H, CH_2), 0.46 – 0.27 (m, 2H, CH_2). ^{13}C NMR (101 MHz, $CDCl_3$) δ 159.0 (ArC), 157.9 (ArC), 148.8 (ArC), 141.3 (ArC), 134.9 (CH), 133.9 (ArC), 131.3 (ArC), 130.6 (ArC), 129.8 (ArC), 128.7 (ArC), 126.4 (ArC), 121.0 (ArC), 120.8 (ArC), 117.8 (ArC), 117.5 (ArC), 114.7 (ArC), 73.0 (O*C*H$_2$CH), 72.2 (ArCH$_2$), 58.9 (ArCH$_2$), 10.2 (CH), 3.3 (CH_2). HPLC R_T. ~ 16 min (Method 5). HRMS (ESI) *m*/*z* calcd for $C_{26}H_{24}O_4N_3{}^{35}Cl$ [M - H]$^-$, 476.1383, found 476.1376.

5-Chloro-2-(4-(5-(((4-(pyrrolidin-1-yl)benzyl)oxy)methyl)-1*H*-1,2,3-triazol-1-yl)phenoxy)phenol (65)

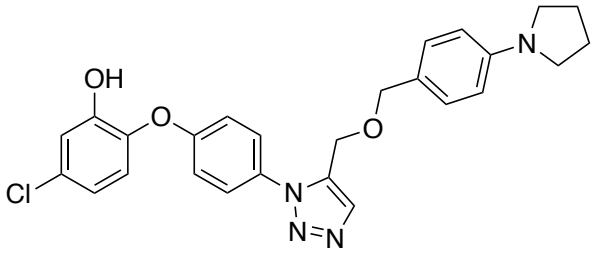

The title compound was synthesised according to General Procedure H from **106** (0.23 g, 0.88 mmol), **138** (0.19 g, 0.88 mmol) and Cp*RuCl(PPh_3)$_2$ (35 mg, 5 mol %). Purification was performed by semi-preparative reverse-phase high-performance liquid chromatography (Method 2) to yield the title compound as a white solid (20 mg, 5%). ^{1}H NMR (400 MHz, $CDCl_3$) δ 7.67 (s, 1H, CH), 7.51 – 7.43 (m, 2H, ArH), 7.05 – 6.93 (m, 5H, ArH), 6.81 – 6.75 (m, 2H, ArH), 6.45 – 6.38 (m, 2H, ArH), 4.35 (s, 2H, $ArCH_2$), 4.33 (s, 2H ($ArCH_2$), 3.24 – 3.11 (m, 4H, NCH_2), 1.96 – 1.84 (m, 4H, CH_2). ^{13}C NMR (101 MHz, $CDCl_3$) δ 157.7 (ArC), 148.8 (ArC), 148.0 (ArC), 141.5 (ArC), 134.9 (CH), 134.1 (ArC), 131.5 (ArC), 130.5 (ArC), 129.9 (ArC), 126.3, 123.0 (ArC), 120.8 (ArC), 120.8 (ArC), 118.0 (ArC), 117.4 (ArC), 111.6 (ArC), 72.7 ($ArCH_2$), 58.6 ($ArCH_2$), 47.7 (NCH_2), 25.4 (CH_2). HPLC R_T. ~ 10 min (Method 2). HRMS (ESI) *m/z* calcd for $C_{26}H_{26}O_3N_4{}^{35}Cl$ $[M + H]^+$, 477.1688, found 477.1689.

5-Chloro-2-(4-(5-(((2,6-difluorobenzyl)oxy)methyl)-1*H*-1,2,3-triazol-1-yl)phenoxy)phenol (66)

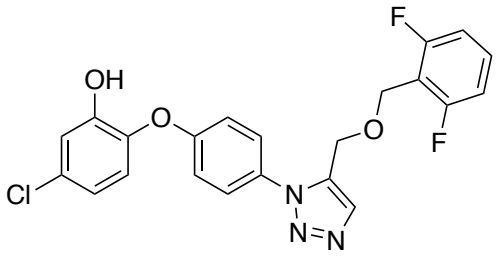

The title compound was synthesised according to General Procedure H from **106** (0.20 g, 0.77 mmol)**, 139** (0.13 g, 0.77 mmol) and Cp*RuCl(PPh_3)$_2$ (30 mg, 5 mol %)**.** Purification was performed by semi-preparative reverse-phase high-performance liquid chromatography to yield the title compound as a white solid (58 mg, 17%). ^{1}H NMR (400 MHz, $CDCl_3$) δ 7.86 (s, 1H), 7.64 – 7.59 (m, 2H, ArH), 7.38 – 7.30 (m, 1H, ArH), 7.14 (d, J = 1.7 Hz, 1H, ArH), 7.12 – 7.08 (m, 2H, ArH), 6.94 (d, J = 7.6 Hz, 2H, ArH), 6.91 (s, 2H, ArH), 4.67 (s, 2H, CH_2), 4.56 (s, 2H, CH_2). ^{13}C NMR (101 MHz, $CDCl_3$) δ 163.1 (ArC), 160.6 (ArC), 157.6 (ArC), 148.5 (ArC), 141.4 (ArC), 135.24 (CH), 133.3 (ArC), 131.5 (ArC), 130.9 (d, J = 10.6 Hz, ArCF), 130.5 (ArC), 126.4 (ArC), 120.9 (ArC), 120.6 (ArC), 118.1 (ArC), 117.3 (ArC), 111.7 – 111.2 (m), 59.6 ($ArCH_2$), 59.5 ($ArCH_2$). ^{19}F NMR (376 MHz, $CDCl_3$) δ -114.96 (app. t, *J* = 6.8 Hz). HPLC R_T. ~ 9 min (Method 3). HRMS (ESI) *m/z* calcd for $C_{22}H_{15}O_3N_3{}^{35}ClF_2$ [M - H]$^-$, 442.0775, found 442.0781.

2-Methoxy-1-(4-nitrophenoxy)-4-propylbenzene (150)

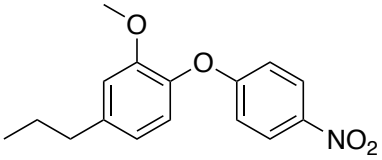

The title compound was synthesised according to General Procedure A from 4-propyl-2-methoxy phenol (5.00 g, 30.00 mmol), 4-fluoro-1-nitrobenzene (4.23 g, 30.00 mmol) and K_2CO_3 (4.57 g, 33.00 mmol). Purification was performed by flash column chromatography (Hexane/EtOAc, 2:1) to yield the title compound as a dense orange oil (7.40 g, 80%). ^{1}H NMR (400 MHz, $CDCl_3$) δ 8.21 – 8.16 (m, 2H, ArH), 7.02 (d, *J* = 8.0 Hz, 1H, ArH), 6.98 – 6.91 (m, 2H, ArH), 6.89 – 6.81 (m, 2H, ArH), 3.79 (s, 3H, OCH_3), 2.64 (t, J = 8.6, 2H, CH_2), 1.77 – 1.65 (m, 2H, CH_2), 1.01 (t, *J* = 7.3 Hz, 3H, CH_3). ^{13}C NMR (101 MHz, $CDCl_3$) δ 163.9 (ArC), 151.2 (ArC), 142.2 (ArC), 141.9 (ArC), 140.4 (ArC), 125.8 (ArC), 122.2 (ArC), 121.2 (ArC), 115.7 (ArC), 113.2 (ArC), 55.8 (OCH_3), 38.0 (CH_2), 24.6 (CH_2), 13.9 (CH_3). HRMS (ESI) *m/z* calcd for $C_{16}H_{17}NO_4Na$ $[M + Na]^+$, 310.1050, found 310.1066.

2-(4-Nitrophenoxy)-5-propylphenol (151)

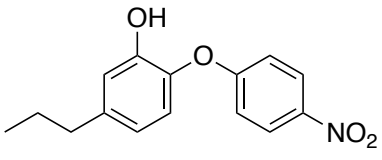

The title compound was synthesised according to General Procedure B from compound **150** (7.40 g, 25.00 mmol) and BBr_3 (1 M in CH_2Cl_2, 75 mL, 75 mmol). Purification was performed by flash column chromatography (Hexane/EtOAc, 3:1) to yield the title compound as a yellow solid (6.02 g, 88%). ^{1}H NMR (400 MHz, $CDCl_3$) δ 8.24 – 8.19 (m, 2H, ArH), 7.10 – 7.03 (m, 2H, ArH), 6.95 – 6.91 (m, 2H, ArH), 6.77 (dd, *J* = 8.3, 2.0 Hz, 1H, ArH), 2.59 (dd, *J* = 8.5, 6.7 Hz, 2H, CH_2), 1.73 – 1.63 (m,

2H, C*H*$_2$CH$_3$), 0.99 (t, *J* = 7.4 Hz, 3H, CH$_3$). ^{13}C NMR (101 MHz, CDCl$_3$) δ 162.9 (ArC), 147.4 (ArC), 143.0 (ArC), 141.9 (ArC), 139.1 (ArC), 126.0 (ArC), 121.3 (ArC), 120.6 (ArC), 117.1 (ArC), 116.6 (ArC), 37.6 (CH$_2$), 24.4 (*C*H$_2$CH$_3$), 13.8 (CH$_3$). HRMS (ESI) *m*/*z* calcd for C$_{15}$H$_{16}$O$_4$N [M + H]$^+$, 274.1074 found 274.1075.

2-(4-Aminophenoxy)-5-propylphenol (152)

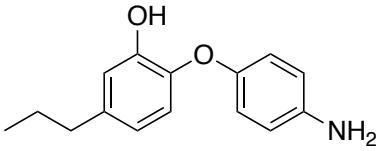

The title compound was synthesised according to General Procedure C from compound **151** (3.00 g, 10.90 mmol), zinc (5.63 g, 66.00 mmol) and NH$_4$Cl (3.53 g, 66.00 mmol). Purification was performed by flash column chromatography (CH$_2$Cl$_2$:MeOH, 95:5) to yield the title compound as a light brown solid (2.20 g, 75%). ^{1}H NMR (400 MHz, MeOD) δ 6.79 – 6.70 (m, 5H, ArH), 6.65 (d, *J* = 8.2 Hz, 1H, ArH), 6.56 (dd, *J* = 8.2, 2.1 Hz, 1H, ArH), 2.50 (dd, *J* = 8.4, 6.8 Hz, 2H, CH$_2$), 1.69 – 1.56 (m, 2H C*H*$_2$CH$_3$), 0.95 (t, *J* = 7.3 Hz, 3H, CH$_3$). ^{13}C NMR (101 MHz, MeOD) δ 150.2 (ArC), 148.0 (ArC), 143.4 (ArC), 142.4 (ArC), 138.2 (ArC), 119.2 (ArC), 118.7 (ArC), 118.3 (ArC), 116.4 (ArC), 116.4 (ArC), 37.1 (*C*H$_2$CH$_3$), 24.4 (CH$_2$), 12.7 (CH$_3$). HRMS (ESI) *m*/*z* calcd for C$_{15}$H$_{18}$O$_2$N [M + H]$^+$, 244.1332 found 244.1335.

2-(4-Azidophenoxy)-5-propylphenol (153)

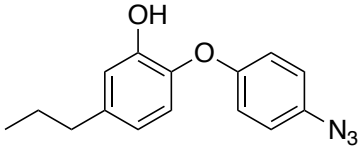

The title compound was synthesised according to General Procedure D from compound **152** (0.30 g, 1.34 mmol), ^{t}BuONO (0.19 g, 1.86 mmol) and TMSN$_3$ (0.21 g, 1.86 mmol). Purification was performed by flash column chromatography (Hexane/

EtOAc, 0 -> 10%) to yield the title compound as a dense brown oil (0.29 mg, 82%). ^{1}H NMR (400 MHz, $CDCl_3$) δ 6.60 – 6.52 (m, 4H), 6.50 – 6.39 (m, 3H), 2.30 (dd, *J* = 8.5, 6.7 Hz, 2H), 1.49 – 1.33 (m, 2H), 0.73 (t, *J* = 7.3 Hz, 3H). ^{13}C NMR (101 MHz, $CDCl_3$) δ 162.4 (ArC), 149.8 (ArC), 146.3 (ArC), 145.8 (ArC), 141.9 (ArC), 138.1 (ArC), 121.8 (ArC), 119.2 (ArC), 118.8 (ArC), 37.3 ($ArCH_2$), 24.5 (CH_2CH_3), 13.7 (CH_3). HRMS (ESI) *m/z* calcd for $C_{15}H_{14}O_2N_3$ [M - H]$^-$, 268.1091, found 268.1091.

2-(4-(5-((Benzyloxy)methyl)-1*H*-1,2,3-triazol-1-yl)phenoxy)-5-propylphenol (68)

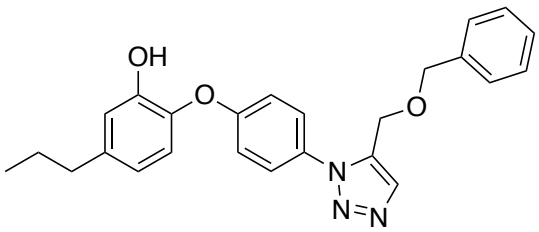

The title compound was synthesised according to General Procedure H from **153** (0.20 g, 0.75 mmol), **129** (0.12 g, 0.75 mmol) and Cp*RuCl(PPh_3)$_2$ (30 mg, 5 mol %). Purification was performed by semi-preparative reverse-phase high-performance liquid chromatography (Method 2) to yield the title compound as a white solid (46 mg, 15%). ^{1}H NMR (400 MHz, $CDCl_3$) δ 7.80 (s, 1H, CH), 7.61 – 7.50 (m, 2H, ArH), 7.38 – 7.30 (m, 3H, ArH), 7.28 (d, *J* = 1.9 Hz, 2H, ArH), 7.12 – 7.05 (m, 2H, ArH), 6.92 (d, *J* = 2.0 Hz, 1H, ArH), 6.88 (d, *J* = 8.2 Hz, 1H, ArH), 6.72 (dd, *J* = 8.2, 2.1 Hz, 1H, ArH), 4.54 (s, 2H, CH_2), 4.52 (s, 2H, CH_2), 2.57 (dd, *J* = 8.5, 6.7 Hz, 2H, C*H*$_2$CH$_2$), 1.73 – 1.56 (m, 2H, C*H*$_2$CH$_3$), 0.97 (t, *J* = 7.3 Hz, 3H, CH_3). ^{13}C NMR (101 MHz, $CDCl_3$) δ 158.4 (ArC), 147.5 (ArC), 141.0 (ArC), 140.1 (ArC), 136.8 (ArC), 135.0 (CH), 133.7 (ArC), 131.1 (ArC), 128.6 (ArC), 128.2 (ArC), 128.0 (ArC), 126.3 (ArC), 120.9 (ArC), 119.9 (ArC), 117.7 (ArC), 116.7 (ArC), 72.5 (CH_2), 59.5 (CH_2), 37.6

(*C*$H_2$$CH_2$), 24.5 (*C*$H_2$$CH_3$), 13.8 ($CH_3$). HPLC R_T. ~ 9 min (Method 2). HRMS (ESI) *m*/*z* calcd for $C_{25}H_{24}O_3N_3$ [M - H]$^-$, 414.1823, found 414.1810.

2-(4-(5-(((4-Methylbenzyl)oxy)methyl)-1*H*-1,2,3-triazol-1-yl)phenoxy)-5-propylphenol (69)

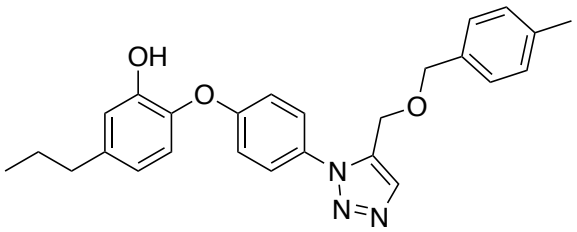

The title compound was synthesised according to General Procedure H from **153** (0.25 g, 0.95 mmol), **130** (0.15 g, 0.95 mmol) and Cp*RuCl(PPh_3)$_2$ (37 mg, 5 mol %). Purification was performed by semi-preparative reverse-phase liquid chromatography (Method 2) to yield the title compound as a white solid (20 mg, 5%). ^{1}H NMR (400 MHz, $CDCl_3$) δ 7.79 (s, 1H, CH), 7.63 – 7.50 (m, 2H, ArH), 7.16 (s, 4H, ArH), 7.12 – 7.07 (m, 2H, ArH), 6.92 (d, *J* = 2.0 Hz, 1H, ArH), 6.88 (d, *J* = 8.2 Hz, 1H, ArH), 6.72 (dd, *J* = 8.2, 2.1 Hz, 1H, ArH), 5.51 (s, 1H, OH), 4.51 (s, 2H, ArCH_2), 4.50 (s, 2H, ArCH_2), 2.57 (t, *J* = 8.5 Hz, 2H, ArC*H*$_2$$CH_2$), 2.34 (s, 3H, Ar$CH_3$), 1.71 – 1.61 (m, 2H, C*H*$_2$$CH_3$), 0.97 (t, *J* = 7.3 Hz, 3H, CH_2C*H*$_3$). ^{13}C NMR (101 MHz, $CDCl_3$) δ 158.3 (ArC), 147.4 (ArC), 140.9 (ArC), 140.1 (ArC), 138.0 (ArC), 135.0 (CH), 133.7 (ArC), 131.2 (ArC), 129.3 (ArC), 128.1 (ArC) (ArC × 2), 126.3 (ArC), 121.0 (ArC), 119.8 (ArC), 117.7 (ArC), 116.7 (ArC), 72.4 (ArCH_2), 59.3 (ArCH_2), 37.6 (Ar*C*$H_2$$CH_2$), 24.4 (*C*$H_2$$CH_3$), 21.2 (Ar$CH_3$), 13.8 ($CH_2$*C*$H_3$). HPLC R_T. ~ 11 min (Method 2). HRMS (ESI) *m*/*z* calcd for $C_{26}H_{26}O_3N_3$ [M - H]$^-$, 428.1980, found 428.1973.

2-(4-(5-(((4-Isopropylbenzyl)oxy)methyl)-1*H*-1,2,3-triazol-1-yl)phenoxy)-5-propylphenol (70)

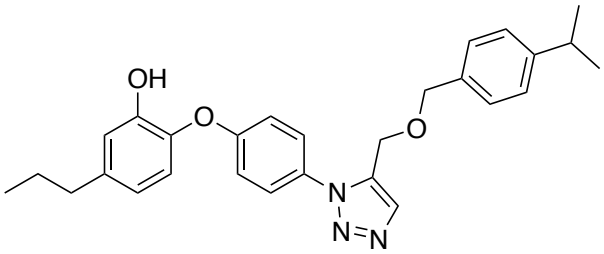

The title compound was synthesised according to General Procedure H from **153** (0.25 g, 0.95 mmol), **131** (0.18 g, 0.95 mmol) and Cp*RuCl(PPh_3)$_2$ (37 mg, 5 mol %). Purification was performed by semi-preparative reverse-phase high-performance liquid chromatography (Method 2) to yield the title compound as a white solid (111 ng, 26%). ^{1}H NMR (400 MHz, $CDCl_3$) δ 7.79 (s, 1H, CH), 7.59 – 7.54 (m, 2H, ArH), 7.21 (m, 4H, ArH), 7.12 – 7.07 (m, 2H, ArH), 6.93 – 6.86 (m, 2H, ArH), 6.72 (dd, *J* = 8.2, 2.1 Hz, 1H, ArH), 5.60 (s, 1H, OH), 4.52 (s, 2H, CH_2), 4.50 (s, 2H CH_2), 2.90 (hept, *J* = 6.9 Hz, 1H, C*H*$(CH_3)_2$), 2.61 - 2.53 (m, 2H, ArC*H*$_2$$CH_2$), 1.71 – 1.60 (m, 2H, CH_2CH_3), 1.24 (d, *J* = 6.9 Hz, 6H, $(CH_3)_2$), 0.96 (t, *J* = 7.3 Hz, 3H, CH_3). ^{13}C NMR (101 MHz, $CDCl_3$) δ 158.3 (ArC), 149.1 (ArC), 147.5 (ArC), 140.9 (ArC), 140.1 (ArC), 135.0 (CH), 134.1 (ArC), 133.8 (ArC), 131.2 (ArC), 128.2 (ArC), 126.7 (ArC), 126.3 (ArC), 120.9 (ArC), 119.8 (ArC), 117.7 (ArC), 116.7 (ArC), 72.4 ($ArCH_2$), 59.5 ($ArCH_2$), 37.6 (Ar*C*H_2CH_2), 33.9 (*C*H$(CH_3)_2$), 24.4 (CH_2CH_3), 24.0 (($CH_3)_2$), 13.8 (CH_3). HPLC R_T. ~ 13 min (Method 2). HRMS (ESI) *m*/*z* calcd for $C_{28}H_{30}O_3N_3$ [M - H]$^-$, 456.2293, found 456.2290.

2-(4-(5-(((4-(*tert*-Butyl)benzyl)oxy)methyl)-1*H*-1,2,3-triazol-1-yl)phenoxy)-5-propylphenol (71)

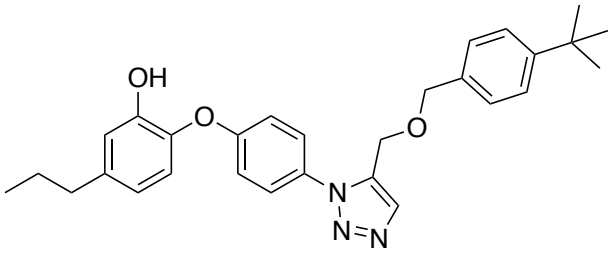

The title compound was synthesised according to General Procedure H from **153** (0.25 g, 0.95 mmol), **132** (0.19 g, 0.95 mmol) and Cp*RuCl(PPh_3)$_2$ (37 mg, 5 mol %). Purification was performed by semi-preparative reverse-phase high-performance liquid chromatography (Method 2) to yield the title compound as a white solid (99 mg, 25%). ^{1}H NMR (400 MHz, $CDCl_3$) δ 7.79 (s, 1H, CH), 7.59 – 7.50 (m, 2H, ArH), 7.41 – 7.34 (m, 2H, ArH), 7.24 – 7.18 (m, 2H, ArH), 7.12 – 7.04 (m, 2H, ArH), 6.96 - 6.86 (m, 2H, ArH), 6.72 (dd, *J* = 8.2, 2.1 Hz, 1H, ArH), 5.81 (s, 1H, OH), 4.52 (s, 2H, $ArCH_2$), 4.50 (s, 2H, $ArCH_2$), 2.56 (dd, *J* = 8.6, 6.7 Hz, 2H, ArCH_2CH_2), 1.71 – 1.59 (m, 2H, CH_2CH_3), 1.32 (s, 9H, $(CH_3)_3$), 0.96 (t, J = 7.3 Hz, 3H, CH_3). ^{13}C NMR (101 MHz, $CDCl_3$) δ 158.4 (ArC), 151.3 (ArC), 147.6 (ArC), 140.9 (ArC), 140.1 (ArC), 135.0 (CH), 133.8 (ArC), 131.1 (ArC), 127.9 (ArC), 126.3 (ArC), 125.6 (ArC), 120.9 (ArC), 119.9 (ArC), 117.7 (ArC), 116.8 (ArC), 72.3 ($ArCH_2$), 59.5 ($ArCH_2$), 37.6 (ArCH_2CH_2), 34.6 (C), 31.3 ($(CH_3)_3$), 24.4 (CH_2CH_3), 13.8 (CH_3). HPLC R_T. ~ 14 min (Method 2). HRMS (ESI) *m*/*z* calcd for $C_{29}H_{32}O_3N_3$ $[M - H]^-$, 470.2449, found 470.2445.

2-(4-(5-(((4-Hydroxybenzyl)oxy)methyl)-1*H*-1,2,3-triazol-1-yl)phenoxy)-5-propylphenol (72)

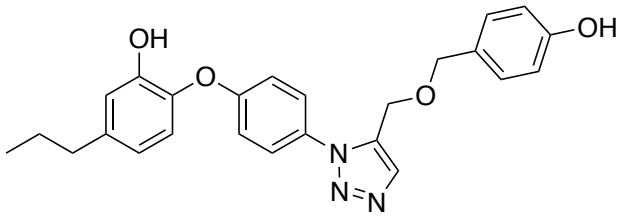

The title compound was synthesised according to General Procedure H from **153** (0.17 g, 0.63 mmol), **133** (0.10 g, 0.63 mmol) and Cp*RuCl(PPh_3)$_2$ (15 mg, 5 mol %). Purification was performed by semi-preparative reverse-phase high-performance liquid chromatography (Method 2) to yield the title compound as a white solid (65 g, 24%). ^{1}H NMR (400 MHz, $CDCl_3$) δ 7.87 (s, 1H, CH), 7.55 – 7.49 (m, 2H, ArH), 7.32 – 7.27 (m, 2H, ArH), 7.10 – 7.06 (m, 2H, ArH), 6.92 – 6.80 (m, 4H, ArH), 6.71 (dd, *J* = 8.2, 2.1 Hz, 1H, ArH), 5.04 (s, 2H, CH_2), 4.63 (s, 2H, CH_2), 2.55 (app dd, *J* = 8.6, 6.7 Hz, 2H, C*H*$_2$CH_2), 1.71 – 1.59 (m, 2H, C*H*$_2$CH_3), 0.95 (t, *J* = 7.3 Hz, 3H, CH_3). ^{13}C NMR (101 MHz, $CDCl_3$) δ 159.1 (ArC), 157.0 (ArC), 148.0 (ArC), 141.1 (ArC), 140.0 (ArC), 134.9 (CH), 134.7 (ArC), 133.2 (ArC), 130.3 (ArC), 128.8 (ArC), 126.3 (ArC), 120.8 (ArC), 120.7 (ArC), 117.5 (ArC), 117.2 (ArC), 115.0 (ArC), 64.6 (CH_2), 58.5 (CH_2), 37.6 (*C*H$_2$CH$_2$), 24.5 (*C*H$_2$CH$_3$), 13.9 (CH$_2$*C*H$_3$). HPLC R_T. ~ 6 min (Method 3). HRMS (ESI) *m*/*z* calcd for $C_{25}H_{24}O_4N_3$ [M - H]$^-$, 430.1772, found 430.1764.

2-(4-(5-(((4-Methoxybenzyl)oxy)methyl)-1*H*-1,2,3-triazol-1-yl)phenoxy)-5-propylphenol (73)

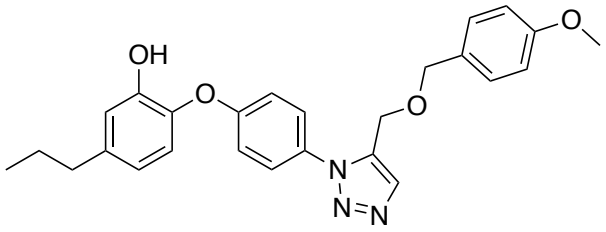

The title compound was synthesised according to General Procedure H from **153** (0.25 g, 0.95 mmol)**, 134** (0.17 g, 0.95 mmol) and Cp*RuCl(PPh_3)$_2$ (37 mg, 5 mol %)**.** Purification was performed by semi-preparative reverse-phase high-performance liquid chromatography (Method 2) to yield the title compound as a white solid (87 mg, 20%). ^{1}H NMR (400 MHz, $CDCl_3$) δ 7.78 (s, 1H, CH), 7.59 – 7.50 (m, 2H, ArH), 7.22 – 7.16 (m, 2H, ArH), 7.11 – 7.03 (m, 2H, ArH), 6.72 (dd, J = 8.2, 2.1 Hz, 1H, ArH), 5.69 (s, 1H, OH), 4.48 (s, 2H, $ArCH_2$), 4.46 (s, 2H, $ArCH_2$), 3.81 (s, 3H, OCH_3), 2.56 (app. dd, *J* = 8.5, 6.7 Hz, 2H, ArCH_2CH_2), 1.71 – 1.60 (m, 2H, CH_2CH_3), 0.96 (t, *J* = 7.3 Hz, 3H, CH_3). ^{13}C NMR (101 MHz, $CDCl_3$) δ 159.6 (ArC), 158.4 (ArC), 147.5 (ArC), 140.9 (ArC), 140.1 (ArC), 135.0 (CH), 133.8 (ArC), 131.1 (ArC), 129.7 (ArC), 128.9 (ArC), 126.3 (ArC), 120.9 (ArC), 119.9 (ArC), 117.7 (ArC), 116.7 (ArC), 114.0 (ArC), 72.1 ($ArCH_2$), 59.1 ($ArCH_2$), 55.3 (OCH_3), 37.6 (CH_2CH_2), 24.5 (CH_2CH_3), 13.8 (CH_3). HPLC R_T. ~ 8 min (Method 2). HRMS (ESI) *m/z* calcd for $C_{26}H_{26}O_4N_3$ $[M - H]^-$, 444.1929, found 444.1927.

2-(4-(5-(((4-Chlorobenzyl)oxy)methyl)-1*H*-1,2,3-triazol-1-yl)phenoxy)-5-propylphenol (74)

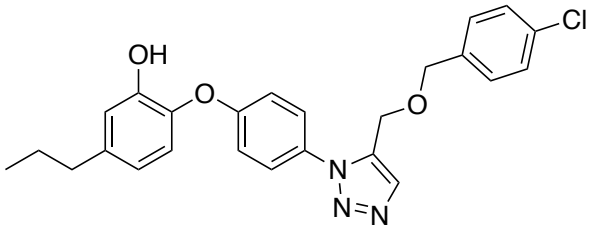

The title compound was synthesised according to General Procedure H from **153** (0.20 g, 0.75 mmol), **135** (0.15 g, 0.75 mmol) and Cp*RuCl(PPh_3)$_2$ (30 mg, 5 mol %). Purification was performed by semi-preparative reverse-phase high-performance liquid chromatography (Method 2) to yield the title compound as a white solid (60 mg, 17%). ^{1}H NMR (400 MHz, $CDCl_3$) δ 7.64 (s, 1H, CH), 7.45 – 7.33 (m, 2H, ArH), 7.20 – 7.14 (m, 2H, ArH), 7.07 – 7.02 (m, 2H, ArH), 6.99 – 6.91 (m, 2H, ArH), 6.77 (d, *J* = 2.0 Hz, 1H, ArH), 6.74 (d, *J* = 8.2 Hz, 1H, ArH), 6.58 (dd, *J* = 8.2, 2.1 Hz, 1H, ArH), 5.55 (s, 1H, OH), 4.37 (s, 2H, CH_2), 4.34 (s, 2H, CH_2), 2.42 (dd, *J* = 8.5, 6.7 Hz, 2H, C*H*$_2$CH$_2$), 1.58 – 1.41 (m, 2H, CH$_2$C*H*$_2$), 0.82 (t, *J* = 7.3 Hz, 3H, CH_3). ^{13}C NMR (101 MHz, $CDCl_3$) δ 158.5 (ArC), 147.5 (ArC), 141.0 (ArC), 140.1 (ArC), 135.3 (CH), 134.9 (ArC), 134.0 (ArC), 133.5 (ArC), 131.0 (ArC), 129.2 (ArC), 128.8 (ArC), 126.3 (ArC), 121.0 (ArC), 120.0 (ArC), 117.7 (ArC), 116.8 (ArC), 71.7 (CH_2), 59.7 (CH_2), 37.6 (*C*H$_2$CH$_2$), 24.4 (CH$_2$*C*H$_2$), 13.8 (CH_3). HPLC R_T. ~ 10 min (Method 2). HRMS (ESI) *m*/*z* calcd for $C_{25}H_{23}O_3N_3{}^{35}Cl$ [M - H]$^-$, 448.1433, found 448.1422.

5-Propyl-2-(4-(5-(((4-(trifluoromethyl)benzyl)oxy)methyl)-1*H*-1,2,3-triazol-1-yl)phenoxy)phenol (75)

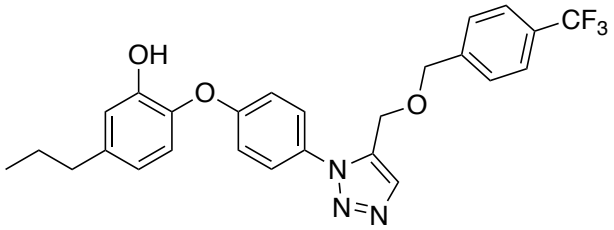

The title compound was synthesised according to General Procedure H from **153** (0.20 g, 0.75 mmol), **136** (0.12 g, 0.75 mmol) and Cp*RuCl(PPh_3)$_2$ (30 mg, 5 mol %). Purification was performed by semi-preparative reverse-phase high-performance liquid chromatography (Method 2) to yield the title compound as a white solid (70 mg, 19%). ^{1}H NMR (400 MHz, $CDCl_3$) δ 7.83 (s, 1H, CH), 7.63 (d, *J* = 8.1 Hz, 2H, ArH), 7.59 – 7.53 (m, 2H, ArH), 7.40 (d, *J* = 8.0 Hz, 2H, ArH), 7.16 – 7.10 (m, 2H, ArH), 6.94 (d, *J* = 2.0 Hz, 1H, ArH), 6.91 (d, J = 8.2 Hz, 1H, ArH), 6.74 (dd, *J* = 8.3, 2.1 Hz, 1H, ArH), 5.75 (bs, 1H, OH), 4.61 (s, 2H. $ArCH_2$), 4.59 (s, 2H, $ArCH_2$), 2.58 (dd, *J* = 8.6, 6.7 Hz, 2H, C*H*$_2$$CH_2$), 1.74 – 1.61 (m, 2H, C*H*$_2$$CH_3$), 0.98 (t, *J* = 7.3 Hz, 3H, CH_3). ^{13}C NMR (101 MHz, $CDCl_3$) δ 158.6 (ArC), 147.6 (ArC), 141.1 (ArC), 140.9 (ArC), 140.0 (ArC), 134.9 (CH), 133.4 (ArC), 130.8 (ArC), 130.5 (ArC), 127.8 (ArC), 126.3 (ArC), 125.6 (q, *J* = 3.7 Hz, CF_3), 121.0 (ArC), 120.0 (ArC), 117.7 (ArC), 116.8 (ArC), 71.6 ($ArCH_2$), 60.1 ($ArCH_2$), 37.6 (*C*$H_2$$CH_2$), 24.4 (*C*$H_2$$CH_3$), 13.8 ($CH_3$). ^{19}F NMR (376 MHz, $CDCl_3$) δ -62.57 (CF_3). HPLC R_T. ~ 11 min (Method 2). HRMS (ESI) *m*/*z* calcd for $C_{26}H_{24}O_3N_3F_3$ [M - H]$^-$, 482.1697, found 482.1698.

2-(4-(5-(((4-(Cyclopropylmethoxy)benzyl)oxy)methyl)-1*H*-1,2,3-triazol-1-yl)phenoxy)-5-propylphenol (76)

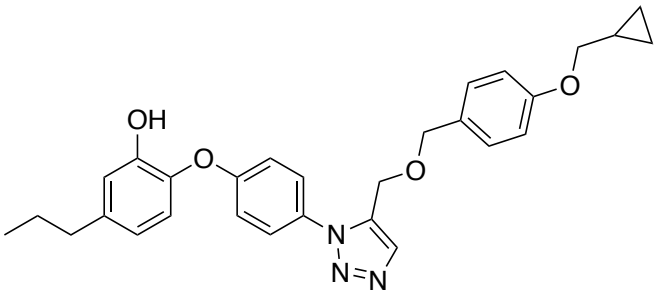

The title compound was synthesised according to General Procedure H from **153** (0.18 g, 0.67 mmol), **137** (0.14 g, 0.67 mmol) and Cp*RuCl(PPh_3)$_2$ (25 mg, 5 mol %). Purification was performed by semi-preparative reverse-phase high-performance liquid chromatography (Method 2) to yield the title compound as a white solid (45 mg, 14%). ^{1}H NMR (400 MHz, $CDCl_3$) δ 7.68 (s, 1H, CH), 7.44 – 7.39 (m, 2H, ArH), 7.10 – 7.05 (m, 2H, ArH), 6.99 – 6.93 (m, 2H, ArH), 6.85 (d, *J* = 2.0 Hz, 1H, ArH), 6.83 – 6.74 (m, 3H, ArH), 6.63 (dd, *J* = 8.2, 2.0 Hz, 1H, ArH), 6.24 (s, 1H, OH), 4.38 (s, 2H, $ArCH_2$), 4.36 (s, 2H, $ArCH_2$), 3.71 (d, *J* = 6.9 Hz, 2H, O*C*H_2CH), 2.59 – 2.52 (m, 2H, Ar*C*H_2CH_2), 1.70 – 1.60 (m, 2H, CH_2CH_3), 1.26 (q, J = 2.5, 1.3 Hz, 1H, CH), 0.96 (t, J = 7.3 Hz, 3H, CH_3), 0.67 – 0.60 (m, 2H, CH_2), 0.35 (dt, J = 6.1, 4.7 Hz, 2H, CH_2). ^{13}C NMR (101 MHz, $CDCl_3$) δ 159.0 (ArC), 158.6 (ArC), 147.8 (ArC), 140.93 (ArC), 140.1 (ArC), 134.9 (CH), 133.9 (ArC), 130.8 (ArC), 129.7 (ArC), 128.8 (ArC), 126.2 (ArC), 120.8 (ArC), 120.2 (ArC), 117.5 (ArC), 116.9 (ArC), 114.7 (ArC), 72.9 (O*C*H_2CH), 72.2 ($ArCH_2$), 59.0 ($ArCH_2$), 37.6 (Ar*C*H_2CH_2), 24.5 (C*H*$_2CH_3$), 13.8 (CH_3), 10.3 (CH), 3.2 (CH_2). HPLC R_T. ~ 14 min (Method 2). HRMS (ESI) *m*/*z* calcd for $C_{29}H_{32}O_4N_3$ [M + H]$^+$, 486.2387, found 486.2389.

5-Propyl-2-(4-(5-(((4-(pyrrolidin-1-yl)benzyl)oxy)methyl)-1*H*-1,2,3-triazol-1-yl)phenoxy)phenol (77)

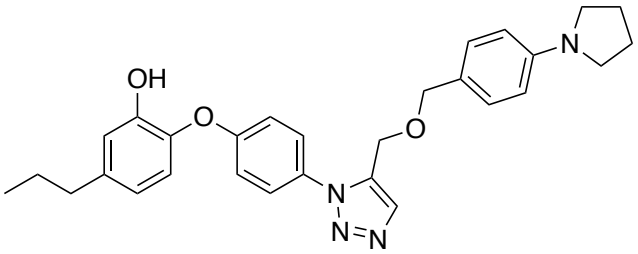

The title compound was synthesised according to General Procedure H from **153** (0.18 g, 0.67 mmol), **138** (0.14 g, 0.67 mmol) and Cp*RuCl(PPh_3)$_2$ (25 mg, 5 mol %). Purification was performed by semi-preparative reverse-phase high-performance liquid chromatography (Method 2) to yield the title compound as a white solid (27 mg, 8%). ^{1}H NMR (400 MHz, $CDCl_3$) δ 7.69 (s, 1H, CH), 7.52 – 7.45 (m, 2H, ArH), 7.09 – 6.97 (m, 4H, ArH), 6.89 – 6.77 (m, 2H, ArH), 6.64 (dd, *J* = 8.2, 2.1 Hz, 1H, ArH), 6.50 – 6.37 (m, 2H, ArH), 4.38 (s, 2H, $ArCH_2$), 4.35 (s, 2H, $ArCH_2$), 3.25 – 3.15 (m, 4H, NCH_2), 2.49 (dd, *J* = 8.5, 6.7 Hz, 2H, ArCH_2CH_2), 1.95 – 1.89 (m, 4H, CH_2), 1.64 – 1.51 (m, 2H, CH_2CH_3), 0.89 (t, *J* = 7.3 Hz, 3H, CH_3). ^{13}C NMR (101 MHz, $CDCl_3$) δ 158.2 (ArC), 148.0 (ArC), 147.5 (ArC), 140.8 (ArC), 140.2 (ArC), 135.0 (CH), 134.1 (ArC), 131.2 (ArC), 129.9 (ArC), 126.3 (ArC), 123.0 (ArC), 120.9 (ArC), 119.8 (ArC), 117.7 (ArC), 116.7 (ArC), 111.6 (ArC), 72.7 ($ArCH_2$), 58.6 ($ArCH_2$), 47.7 (NCH_2), 37.6 (ArCH_2CH_2), 25.5 (CH_2), 24.5 (CH_2CH_3), 13.8 (CH_3). HPLC R_T. ~ 13 min (Method 2). HRMS (ESI) *m*/*z* calcd for $C_{29}H_{33}O_3N_4$ $[M + H]^+$, 485.2547, found 485.2566.

2-(4-(5-(((2,6-Difluorobenzyl)oxy)methyl)-1*H*-1,2,3-triazol-1-yl)phenoxy)-5-propylphenol (78)

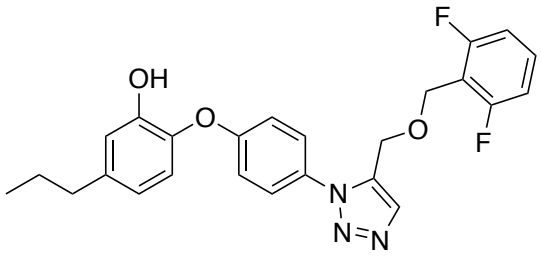

The title compound was synthesised according to General Procedure H from **153** (0.20 g, 0.75 mmol), **139** (0.15 g, 0.75 mmol) and Cp*RuCl(PPh_3)$_2$ (30 mg, 5 mol %)**.** Purification was performed by semi-preparative reverse-phase high-performance liquid chromatography to yield the title compound as a white solid (64 mg, 19%). ^{1}H NMR (400 MHz, $CDCl_3$) δ 7.82 (s, 1H, CH), 7.56 – 7.50 (m, 2H, ArH), 7.35 – 7.26 (m, 1H, ArH), 7.08 – 7.02 (m, 2H, ArH), 6.96 (d, *J* = 2.0 Hz, 1H, ArH), 6.94 – 6.86 (m, 3H, ArH), 6.73 (dd, *J* = 8.2, 2.1 Hz, 1H, ArH), 6.50 (s, 1H, OH), 4.65 (t, *J* = 1.5 Hz, 2H, ArFCH_2), 4.53 (s, 2H, ArCH_2), 2.58 (dd, *J* = 8.5, 6.7 Hz, 2H, CH_2CH_2), 1.74 – 1.62 (m, 2H, CH_2CH_3), 0.98 (t, *J* = 7.3 Hz, 3H, CH_3). ^{13}C NMR (101 MHz, $CDCl_3$) δ 161.8 (dd, *J* = 250.3, 7.6 Hz, Ar*C*CF), 158.6 (ArC), 147.8 (ArC), 140.9 (ArC), 140.2 (ArC), 135.0 (CH), 133.4 (ArC), 130.9 (t, *J* = 10.5 Hz), 130.6 (ArC), 126.1 (ArC), 120.7 (ArC), 120.2 (ArC), 117.5 (ArC), 116.9 (ArC), 112.6 (t, *J* = 19.4 Hz, ArCF), 111.7 – 111.2 (m, Ar*C*HCF), 59.6 (ArCH_2), 59.5 (t, *J* = 3.4 Hz, ArFCH_2), 37.6 (*C*H_2CH_2), 24.5 (*C*H_2CH_3), 13.8 (CH_3). ^{19}F NMR (376 MHz, $CDCl_3$) -114.9 (t, *J* = 6.8 Hz, ArF). HPLC R_T. ~ 9 min (Method 2). HRMS (ESI) *m/z* calcd for $C_{25}H_{22}O_3N_3F_2$ $[M - H]^-$, 450.1635, found 450.1637.

4-Chloro-1-(4-(chloromethyl)phenoxy)-2-(methoxymethoxy)benzene (159)

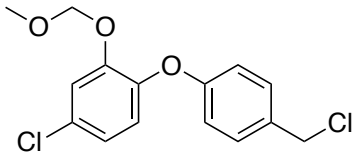

Compound **120** (0.35 g, 1.17 mmol) and Et_3N (0.24 g, 2.34 mmol) were dissolved in CH_2Cl_2 (7 mL) and cooled to 0 °C. Methanesulfonyl chloride (0.20 g, 1.75 mmol) was added dropwise to the reaction mixture and the reaction mixture was allowed to warm to r.t. and stirred for 4 h. The reaction mixture was diluted with saturated NH_4Cl (aq) solution (10 mL) and extracted with CH_2Cl_2 (3 × 10 mL). The combined organic layers were then dried over $MgSO_4$, filtered and concentrated under reduced pressure. Purification by flash column chromatography (Hexane/EtOAc, 4:1) gave a light-yellow oil (0.20 g, 56%). ^{1}H NMR (400 MHz, $CDCl_3$) δ 7.37 – 7.31 (m, 2H, ArH), 7.30 – 7.26 (m, 1H, ArH), 7.03 – 6.95 (m, 2H, ArH), 6.94 – 6.89 (m, 2H, ArH), 5.16 (s, 2H, OCH_2O), 4.59 (s, 2H, CH_2Cl), 3.42 (s, 3H, CH_3). ^{13}C NMR (101 MHz, $CDCl_3$) δ 158.0 (ArC), 149.6 (ArC), 144.0 (ArC), 131.8 (ArC), 130.1 (ArC), 122.6 (ArC), 122.6 (ArC), 117.8 (ArC), 117.0 (ArC), 95.3 (OCH_2O), 56.4 (CH_3), 45.9 (CH_2Cl). HRMS (ESI) *m/z* calcd for $C_{15}H_{14}O_3{}^{35}Cl_2Na$ $[M + Na]^+$, 335.0212, found 335.0213.

4,4'-(((Oxybis(methylene))bis(4,1-phenylene))bis(oxy))bis(1-chloro-3-(methoxymethoxy)benzene) (155)

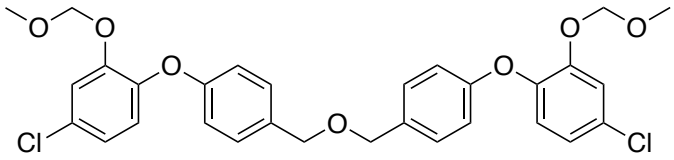

The title compound was synthesised according to General Procedure F from compound **120** (0.13 g, 0.43 mmol), compound **159** (0.20 g, 0.65 mmol) and NaH

(60% dispersion in mineral oil, 33 mg, 0.83 mmol). Purification was performed by flash column chromatography (Hexane/EtOAc, 5:1) to yield the title compound as a yellow oil (0.11 g, 45%). ^{1}H NMR (400 MHz, $CDCl_3$) δ 7.33 – 7.30 (m, 4H, ArH), 7.29 – 7.27 (m, 2H, ArH), 7.01 – 6.97 (m, 2H, ArH), 6.96 – 6.91 (m, 6H, ArH), 5.17 (s, 4H, OCH_2O), 4.52 (s, 4H, $ArCH_2$), 3.44 (s, 6H, CH_3). ^{13}C NMR (101 MHz, $CDCl_3$) δ 157.3 (ArC), 149.4 (ArC), 144.7 (ArC), 132.7 (ArC), 129.6 (ArC), 129.4 (ArC), 122.6 (ArC), 122.1 (ArC), 117.9 (ArC), 117.1 (ArC), 95.4 (OCH_2O), 71.6 ($ArCH_2$), 56.4 (CH_3). HRMS (ESI) *m/z* calcd for $C_{30}H_{28}O_7{}^{35}Cl_2Na$ $[M + Na]^+$, 593.1104, found 593.1088.

6,6'-(((Oxybis(methylene))bis(4,1-phenylene))bis(oxy))bis(3-chlorophenol) (80)

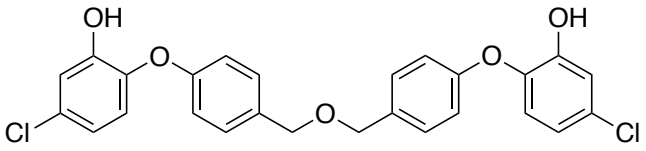

The title compound was synthesised according to General Procedure G from compound **155** (0.11 g, 0.19 mmol) and 6 M HCl (aq) (0.20 mL, 1.20 mmol). Purification was performed by semi-preparative reverse-phase high-performance liquid chromatography (Method 2) to yield the title compound as an off-white solid (0.04 g, 44%). ^{1}H NMR (400 MHz, $CDCl_3$) δ 7.40 – 7.33 (m, 4H, ArH), 7.07 (d, J = 2.2 Hz, 2H, ArH), 7.04 – 6.98 (m, 4H, ArH), 6.86 – 6.78 (m, 4H, ArH), 5.80 (s, 2H, OH), 4.56 (s, 4H, CH_2). ^{13}C NMR (101 MHz, $CDCl_3$) δ 156.1 (ArC), 148.1 (ArC), 142.4 (ArC), 133.8 (ArC), 129.7 (ArC), 129.5 (ArC), 120.6 (ArC), 119.5 (ArC), 118.0 (ArC), 116.7 (ArC), 71.6 (CH_2). HPLC R_T. ~ 17 min (Method 2) HRMS (ESI) *m/z* calcd for $C_{26}H_{20}O_5{}^{35}Cl_2Na$ $[M + Na]^+$, 505.0580, found 505.0594.

1-(4-((Benzyloxy)methyl)phenoxy)-4-chloro-2-(methoxymethoxy)benzene (160)

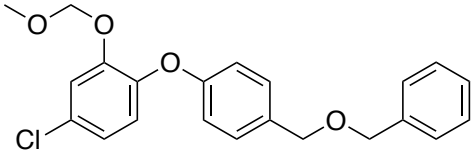

The title compound was synthesised according to General Procedure F from compound **120** (0.20 g, 0.68 mmol), benzyl chloride (0.13 g, 1.02 mmol) and NaH (60% dispersion in mineral oil, 55 mg 1.30 mmol). Purification was performed by flash column chromatography (Hexane/EtOAc, 4:1) to yield the title compound as a yellow oil (0.21 g, 80%). ^{1}H NMR (400 MHz, $CDCl_3$) δ 7.46 – 7.35 (m, 7H, ArH), 7.33 (d, *J* = 2.3 Hz, 1H, ArH), 7.04 – 6.96 (m, 4H, ArH), 5.20 (s, 2H, OCH_2O), 4.62 (s, 2H, $ArCH_2$), 4.57 (s, 2H, $ArCH_2$), 3.46 (s, 3H, OCH_3). ^{13}C NMR (101 MHz, $CDCl_3$) δ 157.4 (ArC), 149.5 (ArC), 144.7 (ArC), 138.3 (ArC), 132.8 (ArC), 129.7 (ArC), 129.4 (ArC), 128.5 (ArC), 127.9 (ArC), 127.7 (ArC), 122.6 (ArC), 122.2 (ArC), 117.9 (ArC), 117.1 (ArC), 95.4 (OCH_2O), 72.2 ($ArCH_2$), 71.7 ($ArCH_2$), 56.4 (OCH_3). HRMS (ESI) *m/z* calcd for $C_{22}H_{21}O_4{}^{35}ClNa$ $[M + Na]^+$, 407.1021, found 407.1024.

4-Chloro-1-(4-(((4-methoxybenzyl)oxy)methyl)phenoxy)-2-(methoxymethoxy)benzene (161)

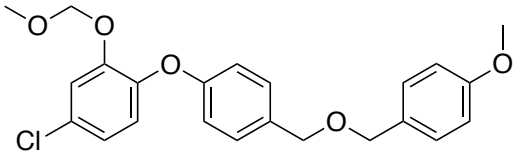

The title compound was synthesised according to General Procedure F from compound **120** (0.25 g, 0.85 mmol), 4-methoxybenzyl chloride (0.20 g, 1.28 mmol) and NaH (60% dispersion in mineral oil, 68 mg, 1.70 mmol). Purification was

performed by flash column chromatography (Hexane/EtOAc, 4:1) to yield the title compound as a yellow oil (0.24 g, 68%). ^{1}H NMR (400 MHz, $CDCl_3$) δ 7.33 – 7.27 (m, 5H, ArH), 7.01 – 6.96 (m, 1H, ArH), 6.96 – 6.89 (m, 5H, ArH), 5.17 (s, 2H, OCH_2O), 4.51 (s, 2H, $ArCH_2$), 4.50 (s, 2H, $ArCH_2$), 3.83 (s, 3H, OCH_3), 3.44 (s, 3H, CH_3OCH_2). ^{13}C NMR (101 MHz, $CDCl_3$) δ 159.3 (ArC), 157.2 (ArC), 149.4 (ArC), 144.7 (ArC), 132.9 (ArC), 130.3 (ArC), 129.6 (ArC), 129.4 (ArC), 129.4 (ArC), 122.6 (ArC), 122.0 (ArC), 117.9 (ArC), 117.1 (ArC), 113.8 (ArC), 95.4 (OCH_2O), 71.8 (CH_2), 71.3 (CH_2), 56.4 (CH_3OCH_2), 55.3 (OCH_3). HRMS (ESI) *m/z* calcd for $C_{23}H_{27}O_5{}^{35}ClN$ $[M + NH_4]^+$, 432.1572, found 432.1557.

4-Chloro-1-(4-(((4-chlorobenzyl)oxy)methyl)phenoxy)-2-(methoxymethoxy)benzene (162)

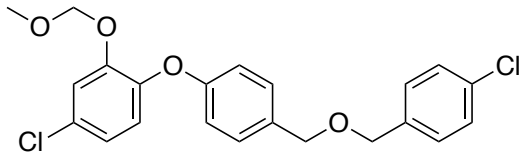

The title compound was synthesised according to General Procedure F from compound **120** (0.20 g, 0.68 mmol), 4-chlorobenzyl chloride (0.16 g, 1.02 mmol) and NaH (60% dispersion in mineral oil, 55 mg 1.30 mmol). Purification was performed by flash column chromatography (Hexane/EtOAc, 4:1) to yield the title compound as a yellow oil (0.20 g, 70%). ^{1}H NMR (400 MHz, $CDCl_3$) δ 7.40 – 7.27 (m, 7H, ArH), 7.03 – 6.91 (m, 4H, ArH), 5.18 (s, 2H, OCH_2O), 4.54 (s, 2H, $ArCH_2$), 4.53 (s, 2H, $ArCH_2$), 3.44 (s, 3H, OCH_3). ^{13}C NMR (101 MHz, $CDCl_3$) δ 157.4 (ArC), 149.5 (ArC), 144.6 (ArC), 136.8 (ArC), 133.4 (ArC), 132.4 (ArC), 129.7 (ArC), 129.4 (ArC), 129.1 (ArC), 128.6 (ArC), 122.6 (ArC), 122.1 (ArC), 117.9 (ArC), 117.1 (ArC), 95.4 (OCH_2O), 71.8 ($ArCH_2$), 71.3 ($ArCH_2$), 56.4 (OCH_3). HRMS (ESI) *m/z* calcd for $C_{22}H_{24}O_4{}^{35}Cl_2N$ $[M + NH_4]^+$, 436.1077, found 436.1058.

2,4-Dichloro-1-(((4-(4-chloro-2-(methoxymethoxy)phenoxy)benzyl)oxy)methyl)benzene (163)

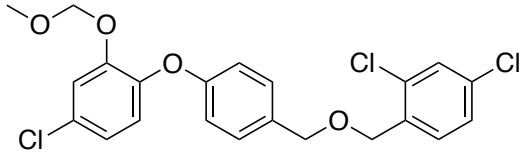

The title compound was synthesised according to General Procedure F from compound **120** (0.20 g, 0.68 mmol), 2,4-dichlorobenzyl chloride (0.20 g, 1.02 mmol) and NaH (60% dispersion in mineral oil, 55 mg 1.30 mmol). Purification was performed by flash column chromatography (Hexane/EtOAc, 4:1) to yield the title compound as a yellow oil (0.21 g, 68%). ^{1}H NMR (400 MHz, $CDCl_3$) δ 7.49 (d, *J* = 8.3 Hz, 1H, ArH), 7.39 (d, *J* = 2.1 Hz, 1H, ArH), 7.38 – 7.33 (m, 2H, ArH), 7.31 – 7.25 (m, 2H, ArH), 7.02 – 6.94 (m, 4H, ArH), 5.18 (s, 2H, OCH_2O), 4.63 (s, 2H, $ArCH_2$), 4.61 (s, 2H, $ArCH_2$), 3.44 (s, 3H, OCH_3). ^{13}C NMR (101 MHz, $CDCl_3$) δ 157.5 (ArC), 149.5 (ArC), 144.5 (ArC), 134.8 (ArC), 133.7 (ArC), 133.5 (ArC), 132.3 (ArC), 129.9 (ArC), 129.8 (ArC), 129.4 (ArC), 129.1 (ArC), 127.1 (ArC), 122.6 (ArC), 122.3 (ArC), 117.9 (ArC), 117.1 (ArC), 95.3 (OCH_2O), 72.4 ($ArCH_2$), 68.6 ($ArCH_2$), 56.4 (OCH_3). HRMS (ESI) *m/z* calcd for $C_{22}H_{19}O_4{}^{35}Cl_3Na$ $[M + Na]^+$, 475.0241, found 475.0247.

4-Chloro-1-(4-((cyclopropylmethoxy)methyl)phenoxy)-2-(methoxymethoxy)benzene (164)

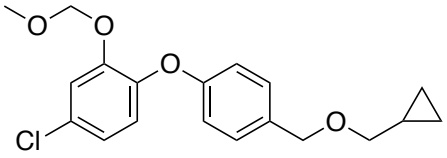

The title compound was synthesised according to General Procedure F from compound **120** (0.20 g, 0.68 mmol), bromomethyl cyclopropane (0.13 g, 1.02 mmol)

and NaH (60% dispersion in mineral oil, 55 mg 1.30 mmol). Purification was performed by flash column chromatography (Hexane/EtOAc, 4:1) to yield the title compound as a yellow oil (0.18 g, 76%). ^{1}H NMR (400 MHz, $CDCl_3$) δ 7.32 – 7.27 (m, 2H, ArH), 7.26 (d, *J* = 2.4 Hz, 1H, ArH), 6.96 (dd, *J* = 8.6, 2.3 Hz, 1H, ArH), 6.94 – 6.87 (m, 3H, ArH), 5.15 (s, 2H, OCH_2O), 4.49 (s, 2H, $ArCH_2$), 3.42 (s, 3H, OCH_3), 3.31 (d, *J* = 6.9 Hz, 2H, CH_2CH), 1.16 – 1.05 (m, 1H, CH), 0.58 – 0.51 (m, 2H, CH_2), 0.21 (dt, *J* = 6.1, 4.5 Hz, 2H, CH_2). ^{13}C NMR (101 MHz, $CDCl_3$) δ 157.2 (ArC), 149.4 (ArC), 144.7 (ArC), 133.1 (ArC), 129.5 (ArC), 129.3 (ArC), 122.6 (ArC), 122.1 (ArC), 117.8 (ArC), 117.0 (ArC), 95.3 (OCH_2O), 74.9 (CH_2CH), 72.1 ($ArCH_2$), 56.3 (OCH_3), 10.7 (CH), 3.1 (CH_2). HRMS (ESI) *m/z* calcd for $C_{19}H_{21}O_4{}^{35}ClNa$ $[M + Na]^+$, 371.1021, found 371.1015.

4-Chloro-1-(4-((cyclohexylmethoxy)methyl)phenoxy)-2-(methoxymethoxy)benzene (165)

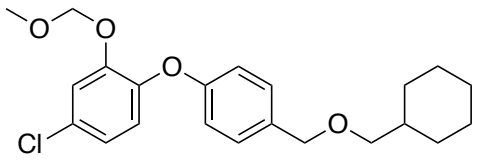

The title compound was synthesised according to General Procedure F from compound **120** (0.20 g, 0.68 mmol), bromomethyl cyclohexane (0.18 g, 1.02 mmol) and NaH (60% dispersion in mineral oil, 55 mg 1.30 mmol). Purification was performed by flash column chromatography (Hexane/EtOAc, 4:1) to yield the title compound as a yellow oil (60 mg, 23%). ^{1}H NMR (400 MHz, $CDCl_3$) δ 7.34 – 7.25 (m, 3H, ArH), 7.03 – 6.86 (m, 4H, ArH), 5.17 (s, 2H, OCH_2O), 4.46 (s, 2H, $ArCH_2$), 3.44 (s, 3H, OCH_3), 3.28 (d, *J* = 6.5 Hz, 2H, CH_2CH), 1.86 – 1.57 (m, 5H, CH_2CHCH_2), 1.34 – 1.11 (m, 4H, 2 × CH_2), 1.03 – 0.90 (m, 2H, CH_2). ^{13}C NMR (101 MHz, $CDCl_3$) δ 157.1 (ArC), 149.4 (ArC), 144.8 (ArC), 133.3 (ArC), 129.5 (ArC),

129.1 (ArC), 122.6 (ArC), 122.0 (ArC), 117.8 (ArC), 117.1 (ArC), 95.4 (OCH_2O), 76.3 (CH_2CH), 72.5 (OCH_3), 56.4 ($ArCH_2$), 38.1 (CH), 30.2 (CH_2), 26.7 (CH_2), 25.9 (CH_2). HRMS (ESI) *m*/*z* calcd for $C_{22}H_{27}O_4{}^{35}ClNa$ $[M + Na]^+$, 413.1490, found 413.1492.

2-(4-((Benzyloxy)methyl)phenoxy)-5-chlorophenol (81)

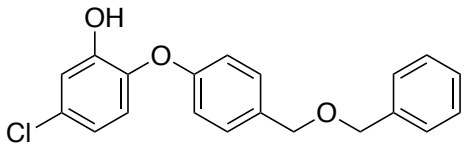

The title compound was synthesised according to General Procedure G from compound **160** (0.14 g, 0.36 mmol) and 6 M HCl (aq) (0.36 mL, 2.16 mmol). Purification was performed by semi-preparative reverse-phase high-performance liquid chromatography (Method 2) to yield the title compound as a clear oil (47 mg, 38%). ^{1}H NMR (400 MHz, $CDCl_3$) δ 7.40 – 7.28 (m, 7H, ArH), 7.05 (d, *J* = 2.2 Hz, 1H, ArH), 7.03 – 6.97 (m, 2H, ArH), 6.85 – 6.75 (m, 2H, ArH), 5.76 (s, 1H, OH), 4.58 (s, 2H, $ArCH_2$), 4.53 (s, 2H, $ArCH_2$). ^{13}C NMR (101 MHz, $CDCl_3$) δ 156.0 (ArC), 148.1 (ArC), 142.5 (ArC), 138.1 (ArC), 134.0 (ArC), 129.7 (ArC), 129.4 (ArC), 128.5 (ArC), 127.9 (ArC), 127.8 (ArC), 120.6 (ArC), 119.5 (ArC), 118.0 (ArC), 116.7 (ArC), 72.3 ($ArCH_2$), 71.5 ($ArCH_2$). HPLC R_T. ~ 9.5 min (Method 2). HRMS (ESI) *m*/*z* calcd for $C_{20}H_{16}O_3{}^{35}Cl$ $[M - H]^-$, 339.0793, found 339.0779.

5-Chloro-2-(4-(((4-methoxybenzyl)oxy)methyl)phenoxy)phenol (82)

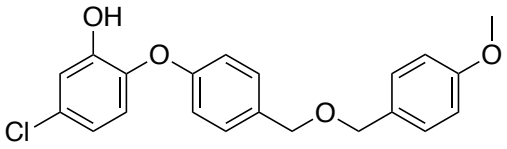

The title compound was synthesised according to General Procedure G from compound **161** (0.24 g, 0.58 mmol) and 6 M HCl (aq) (0.50 mL, 3.00 mmol).

Purification was performed by semi-preparative reverse-phase high-performance liquid chromatography (Method 2) to yield the title compound as an off-white solid (0.13 g, 62%). ^{1}H NMR (400 MHz, $CDCl_3$) δ 7.38 – 7.34 (m, 2H, ArH), 7.34 – 7.30 (m, 2H, ArH), 7.06 (d, *J* = 2.2 Hz, 1H, ArH), 7.02 – 6.98 (m, 2H, ArH), 6.95 – 6.91 (m, 2H, ArH), 6.86 – 6.79 (m, 2H, ArH), 6.03 (s, 1H, OH), 4.54 (s, 2H, CH_2), 4.52 (s, 2H, CH_2), 3.84 (s, 3H, OCH_3). ^{13}C NMR (101 MHz, $CDCl_3$) δ 159.3 (ArC), 156.0 (ArC), 148.2 (ArC), 142.5 (ArC), 134.0 (ArC), 130.1 (ArC), 129.7 (ArC), 129.5 (ArC), 129.4 (ArC), 120.6 (ArC), 119.6 (ArC), 118.0 (ArC), 116.7 (ArC), 113.9 (ArC), 71.9 (CH_2), 71.2 (CH_2), 55.3 (OCH_3). HPLC R_T. ~ 8.5 min (Method 2). HRMS (ESI) *m/z* calcd for $C_{21}H_{18}O_4{}^{35}Cl$ $[M - H]^-$, 369.0899, found 369.0897.

5-Chloro-2-(4-(((4-chlorobenzyl)oxy)methyl)phenoxy)phenol (83)

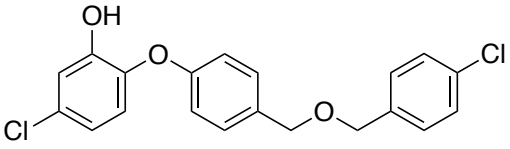

The title compound was synthesised according to General Procedure G from compound **162** (0.20 g, 0.49 mmol) and 6 M HCl (aq) (0.50 mL, 3.00 mmol). Purification was performed by semi-preparative reverse-phase high-performance liquid chromatography (Method 2) to yield the title compound as an off-white solid (0.10 g, 56%). ^{1}H NMR (400 MHz, $CDCl_3$) δ 7.38 – 7.30 (m, 6H, ArH), 7.07 (d, *J* = 2.3 Hz, 1H, ArH), 7.05 – 6.98 (m, 2H, ArH), 6.87 – 6.78 (m, 2H, ArH), 5.79 (s, 1H, OH), 4.56 (s, 2H, $ArCH_2$), 4.54 (s, 2H, $ArCH_2$). ^{13}C NMR (101 MHz, $CDCl_3$) δ 156.1 (ArC), 148.1 (ArC), 142.4 (ArC), 136.6 (ArC), 133.7 (ArC), 133.5 (ArC), 129.7 (ArC), 129.5 (ArC), 129.1 (ArC), 128.6 (ArC), 120.6 (ArC), 119.5 (ArC), 118.0 (ArC), 116.7 (ArC), 71.6 ($ArCH_2$), 71.5 ($ArCH_2$). HPLC R_T. ~ 10 min (Method 2). HRMS (ESI) *m/z* calcd for $C_{20}H_{15}O_3{}^{35}Cl_2$ $[M - H]^-$, 373.0404, found 373.0406.

5-Chloro-2-(4-(((2,4-dichlorobenzyl)oxy)methyl)phenoxy)phenol (84)

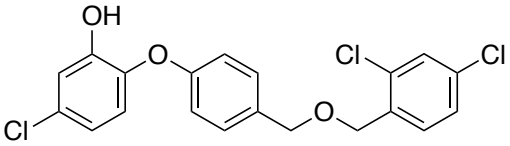

The title compound was synthesised according to General Procedure G from compound **163** (0.21 g, 0.46 mmol) and 6 M HCl (aq) (0.50 mL, 3.00 mmol). Purification was performed by semi-preparative reverse-phase high-performance liquid chromatography (Method 2) to yield the title compound as an off-white solid (0.10 g, 52%). ^{1}H NMR (400 MHz, $CDCl_3$) δ 7.48 (d, *J* = 8.2 Hz, 1H, ArH), 7.42 – 7.36 (m, 3H, ArH), 7.31 – 7.25 (m, 1H, ArH), 7.07 (d, *J* = 2.2 Hz, 1H, ArH), 7.05 – 6.95 (m, 2H, ArH), 6.88 – 6.78 (m, 2H, ArH), 5.83 (s, 1H, OH), 4.65 (s, 2H, $ArCH_2$), 4.62 (s, 2H, $ArCH_2$). ^{13}C NMR (101 MHz, $CDCl_3$) δ 156.2 (ArC), 148.1 (ArC), 142.4 (ArC), 134.6 (ArC), 133.9 (ArC), 133.6 (ArC), 133.5 (ArC), 130.9 (ArC), 129.9 (ArC), 129.7 (ArC), 129.1 (ArC), 127.2 (ArC), 120.6 (ArC), 119.6 (ArC), 118.0 (ArC), 116.7 (ArC), 72.2 ($ArCH_2$), 68.8 ($ArCH_2$). HPLC R_T. ~ 11 min (Method 2). HRMS (ESI) *m/z* calcd for $C_{20}H_{14}O_3{}^{35}Cl_3$ $[M - H]^-$, 407.0014, found 407.0016.

5-Chloro-2-(4-((cyclopropylmethoxy)methyl)phenoxy)phenol (85)

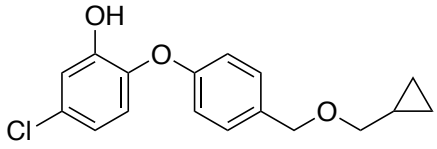

The title compound was synthesised according to General Procedure G from compound **164** (0.18 g, 0.53 mmol) and 6 M HCl (aq) (1.00 mL, 6.00 mmol). Purification was performed by semi-preparative reverse-phase high-performance liquid chromatography (Method 2) to yield the title compound as an off-white solid (0.10 g, 61%). ^{1}H NMR (400 MHz, $CDCl_3$) δ 7.39 – 7.32 (m, 2H, ArH), 7.05 (d, *J* =

2.3 Hz, 1H, ArH), 7.04 – 6.96 (m, 2H, ArH), 6.84 – 6.77 (m, 2H, ArH), 5.91 (s, 1H, OH), 4.52 (s, 2H, $ArCH_2$), 3.35 (d, *J* = 6.9 Hz, 2H, CH_2CH), 1.18 – 1.06 (m, 1H, CH), 0.61 – 0.53 (m, 2H, CH_2), 0.27 – 0.20 (m, 2H, CH_2). ^{13}C NMR (101 MHz, $CDCl_3$) δ 155.9 (ArC), 148.1 (ArC), 142.5 (ArC), 134.2 (ArC), 129.6 (ArC), 129.4 (ArC), 120.5 (ArC), 119.5 (ArC), 118.0 (ArC), 116.7 (ArC), 75.1 (*C*H_2CH), 71.9 ($ArCH_2$), 10.6 (CH), 3.1 (CH_2). HPLC R_T. ~ 6.5 min (Method 2). HRMS (ESI) *m/z* calcd for $C_{17}H_{16}O_3{}^{35}Cl$ $[M - H]^-$, 303.0793, found 303.0800.

5-Chloro-2-(4-((cyclohexylmethoxy)methyl)phenoxy)phenol (85)

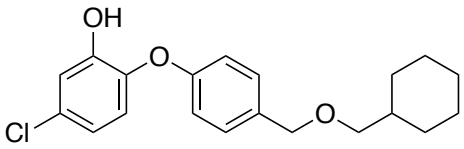

The title compound was synthesised according to General Procedure G from compound **165** (0.10 g, 0.26 mmol) and 6 M HCl (aq) (0.20 mL, 1.20 mmol). Purification was performed by semi-preparative reverse-phase high-performance liquid chromatography (Method 2) to yield the title compound as a clear oil (31 mg, 34%). ^1H NMR (400 MHz, $CDCl_3$) δ 7.37 – 7.31 (m, 2H, ArH), 7.06 (d, *J* = 2.2 Hz, 1H, ArH), 7.04 – 6.96 (m, 2H, ArH), 6.88 – 6.75 (m, 2H, ArH), 5.84 (s, 1H, OH), 4.48 (s, 2H, $ArCH_2$), 3.30 (d, *J* = 6.5 Hz, 2H, C*H*$_2$CH), 1.85 – 1.60 (m, 6H), 1.34 – 1.13 (m, 3H), 1.03 – 0.91 (m, 2H). ^{13}C NMR (101 MHz, $CDCl_3$) δ 155.8 (ArC), 148.1 (ArC), 142.5 (ArC), 134.6 (ArC), 129.3 (ArC), 120.5 (ArC), 119.4 (ArC), 118.0 (ArC), 116.6 (ArC), 76.5 (*C*H_2CH), 72.4 ($ArCH_2$), 38.1 (CH), 30.2 (CH_2), 26.6 (CH_2), 25.9 (CH_2). HPLC R_T. ~ 12 min (Method 2). $C_{20}H_{22}O_3{}^{35}Cl$ $[M - H]^-$, 345.1263, found 345.1273.

4-(4-Chloro-2-methoxyphenoxy)benzonitrile (169)

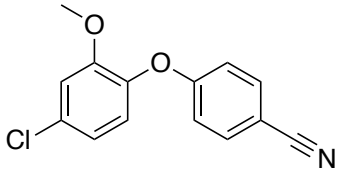

The title compound was synthesised according to General Procedure A from 4-chloro-2-methoxy phenol (2.00 g, 12.60 mmol) 4-fluorobenzonitrile (1.68 g, 13.86 mmol) and K_2CO_3 (1.74 g, 13.86 mmol). Purification was performed by flash column chromatography (Hexane/EtOAc, 2:1) to yield the title compound as a pale-yellow solid (2.91 g, 88%).^{1}H NMR (400 MHz, $CDCl_3$) δ 7.60 – 7.54 (m, 2H, ArH), 7.04 – 6.94 (m, 3H, ArH), 6.94 – 6.88 (m, 2H, ArH), 3.77 (s, 3H, OCH_3). ^{13}C NMR (101 MHz, $CDCl_3$) δ 161.6 (ArC), 152.2 (ArC), 141.3 (ArC), 134.0 (ArC), 131.7 (ArC), 123.4 (ArC), 121.3 (ArC), 118.9 (ArC), 116.5 (ArC), 113.7 (ArC), 105.6 (CN), 56.1 (OCH_3). HRMS (ESI) *m/z* calcd for $C_{14}H_{10}O_2N^{35}ClNa$ $[M + Na]^+$, 282.0292 found 282.0294.

4-(4-Chloro-2-hydroxyphenoxy)benzonitrile (171)

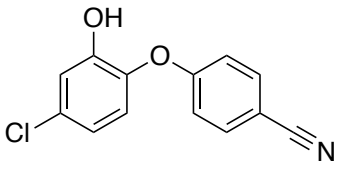

The title compound was synthesised according to General Procedure B from compound **169** (0.50 g, 2.00 mmol) and BBr_3 (1 M in CH_2Cl_2, 10.00 mL, 10.00 mmol). Purification was performed by flash column chromatography (CH_2Cl_2:MeOH, 9:1) to yield the title compound as a yellow solid (0.44 g, 90%). ^{1}H NMR (400 MHz, $CDCl_3$) δ 7.66 – 7.58 (m, 2H, ArH), 7.10 (dd, *J* = 1.9, 0.9 Hz, 1H, ArH), 7.07 – 7.03 (m, 2H, ArH), 6.92 (d, *J* = 1.9 Hz, 2H, ArH), 5.99 (bs, 1H, OH). ^{13}C NMR (101 MHz, $CDCl_3$) δ 160.8 (ArC), 148.7 (ArC), 140.2 (ArC), 134.4 (ArC), 131.4 (ArC), 121.7 (ArC), 121.2

(ArC), 118.5 (ArC), 117.7 (ArC), 117.4 (ArC), 106.5 (CN). HRMS (ESI) *m*/*z* calcd for $C_{13}H_8O_2N^{35}ClNa$ $[M + Na]^+$, 268.0136 found 268.0136.

2-(4-(Aminomethyl)phenoxy)-5-chlorophenol (172)

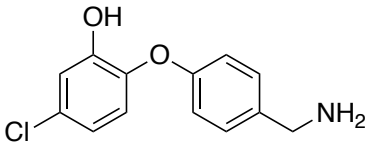

Compound **171** (0.44 g, 1.79 mmol) was dissolved in anhydrous THF (20 mL), cooled to 0 °C and placed under a nitrogen atmosphere. $LiAlH_4$ (2.4 M in THF, 2.20 mL, 5.38 mmol) was added dropwise over 2 mins and the reaction mixture was allowed to warm to r.t. before being stirred for a further 18 h. The reaction was carefully quenched by the addition of H_2O (10 mL). The reaction mixture was then filtered through Celite and washed with EtOAc before being concentrated under reduced pressure to yield a bright yellow solid (0.45 g, quant.) which was used without further purification. ^{1}H NMR (400 MHz, MeOD) δ 7.12 (d, *J* = 8.2 Hz, 2H, ArH), 6.79 – 6.72 (m, 3H, ArH), 6.64 (d, *J* = 8.5 Hz, 1H, ArH), 6.49 (dd, *J* = 8.5, 2.5 Hz, 1H, ArH), 3.66 (s, 2H, CH_2). ^{13}C NMR (101 MHz, MeOD) δ 157.8 (ArC), 153.5 (ArC), 143.4 (ArC), 132.7 (ArC), 129.4 (ArC), 129.1 (ArC), 121.5 (ArC), 118.2 (ArC), 117.1 (ArC), 116.8 (ArC), 43.9 (CH_2). HRMS (ESI) *m*/*z* calcd for $C_{13}H_{11}O_2N^{35}Cl$ $[M - H]^-$, 248.0484, found 248.0469.

5-Chloro-2-(4-(((4-(4-chloro-2-methoxyphenoxy)benzyl)amino)methyl)phenoxy)phenol (173)

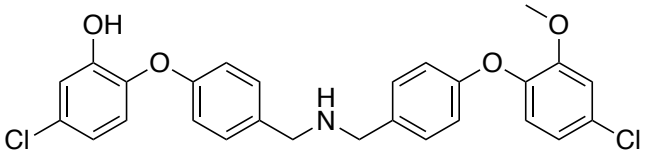

The title compound was synthesised according to General Procedure I from

compound **115** (0.35 g, 1.41 mmol) compound **172** (0.41 g, 1.55 mmol) and $NaB(OAc)_3H$ (0.59 g, 2.82 mmol). Purification was performed by flash column chromatography (CH_2Cl_2:MeOH, 9:1) to yield the title compound as a yellow solid (0.35 g, 50%). ^1H NMR (400 MHz, $CDCl_3$) δ 7.14 – 7.09 (m, 2H, ArH), 7.09 – 7.04 (m, 2H, ArH), 6.88 (d, *J* = 2.1 Hz, 1H, ArH), 6.86 – 6.83 (m, 1H, ArH), 6.79 – 6.75 (m, 4H, ArH), 6.65 (td, *J* = 4.8, 2.4 Hz, 4H, ArH), 3.71 (s, 3H, OCH_3), 3.66 (s, 2H, CH_2), 3.60 (s, 2H, CH_2). ^{13}C NMR (101 MHz, $CDCl_3$) δ 157.0 (ArC), 156.4 (ArC), 151.9 (ArC), 149.6 (ArC), 143.7 (ArC), 142.3 (ArC), 133.3 (ArC), 132.8 (ArC), 130.1 (ArC), 129.9 (ArC), 129.8 (ArC), 129.7 (ArC), 128.6 (ArC), 121.7 (ArC), 120.9 (ArC), 120.0 (ArC), 117.7 (ArC), 117.2 (ArC), 117.1 (ArC), 113.5 (ArC), 56.2 (OCH_3), 52.3 (CH_2), 52.0 (CH_2). HRMS (ESI) *m/z* calcd for $C_{27}H_{24}O_4N^{35}Cl_2$ $[M + H]^+$, 496.1077 found 496.1092.

6,6'-(((Azanediylbis(methylene))bis(4,1-phenylene))bis(oxy))bis(3-chlorophenol) (87)

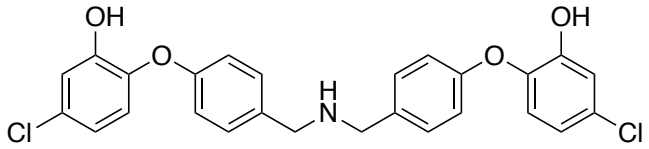

The title compound was synthesised according to general procedure B from compound **173** (80 mg, 0.12 mmol) and BBr_3 (1 M in CH_2Cl_2, 0.48 mL, 0.48 mmol). Purification was performed by flash column chromatography (CH_2Cl_2:MeOH, 9:1) to yield the title compound as a yellow solid (35 mg, 62%). ^1H NMR (500 MHz, MeOD) δ 8.54 (s, 2H, OH), 7.38 – 7.33 (m, 4H, ArH), 6.96 – 6.88 (m, 8H, ArH), 6.83 (dd, *J* = 8.6, 2.5 Hz, 2H, ArH), 4.00 (s, 4H, CH_2). ^{13}C NMR (101 MHz, MeOD) δ 159.0 (ArC), 151.7 (ArC), 143.8 (ArC), 132.0 (ArC), 131.5 (ArC), 130.8 (ArC), 123.2 (ArC), 120.6

(ArC), 118.4 (ArC), 118.1 (ArC), 52.4 (CH_2). HPLC R_T. ~ 10 min (Method 6). HRMS (ESI) *m*/*z* calcd for $C_{26}H_{20}O_4N^{35}Cl_2$ $[M - H]^-$, 480.0775, found 480.0762.

N-(4-(4-Chloro-2-methoxyphenoxy)benzyl)hexan-1-amine (174)

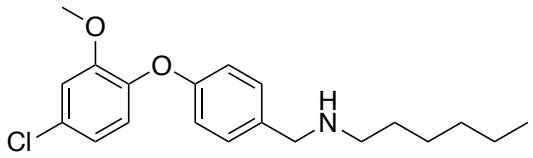

The title compound was synthesised according to a modified version General Procedure I from compound **115** (0.30 g, 1.47 mmol) hexylamine (0.16 g, 1.59 mmol) where $NaBH_4$ (0.17 g, 4.41 mmol) was added portion-wise after 18 h stirring at r.t.. Purification was performed by flash column chromatography (CH_2Cl_2:MeOH, 9:1) to yield the title compound as a yellow solid (0.34 g, 67%). ^{1}H NMR (400 MHz, $CDCl_3$) δ 7.13 (d, *J* = 8.4 Hz, 2H, ArH), 6.85 (d, *J* = 1.5 Hz, 1H ArH), 6.79 – 6.74 (m, 4H, ArH), 3.67 (s, 3H, OCH_3), 3.62 (s, 2H, CH_2NH), 2.51 (t, *J* = 7.2 Hz, 2H, CH_2), 1.38 (q, *J* = 7.0 Hz, 2H, CH_2), 1.26 – 1.11 (m, 6H, 3 × CH_2), 0.82 – 0.67 (m, 3H, CH_3). ^{13}C NMR (101 MHz, $CDCl_3$) δ 156.5 (ArC), 151.9 (ArC), 144.0 (ArC), 135.0 (ArC), 129.4 (ArC), 121.5 (ArC), 120.8 (ArC), 117.1 (ArC), 113.4 (ArC), 56.1 (OCH_3), 53.4 (CH_2NH), 49.5 (CH_2), 31.8 (CH_2), 30.0 (CH_2), 27.0 (CH_2), 22.6 (CH_2), 14.1 (CH_3). HRMS (ESI) *m*/*z* calcd for $C_{20}H_{27}O_2N^{35}Cl$ $[M + H]^+$, 348.1725, found 348.1750.

N-(4-(4-Chloro-2-methoxyphenoxy)benzyl)-1-cyclohexylmethanamine (175)

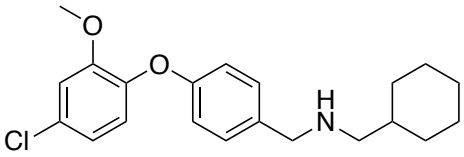

The title compound was synthesised according to General Procedure I from compound **115** (0.30 g, 1.47 mmol) cyclohexanemethylamine (0.18 g, 1.60 mmol) and $NaB(OAc)_3H$ (0.64 g, 3.00 mmol). Purification was performed by flash column chromatography (CH_2Cl_2:MeOH, 9:1) to yield the title compound as a yellow solid (0.43 g, 81%). ^1H NMR (400 MHz, MeOD) δ 7.36 – 7.30 (m, 2H, ArH), 7.04 (d, *J* = 2.2 Hz, 1H, ArH), 6.93 – 6.84 (m, 2H, ArH), 6.80 – 6.75 (m, 2H, ArH), 4.03 (s, 2H, CH_2NH), 3.63 (s, 3H, OCH_3), 2.73 (d, *J* = 6.8 Hz, 2H, $NHCH_2$), 1.73 – 1.55 (m, 8H), 1.26 – 1.05 (m, 4H), 0.96 – 0.78 (m, 3H). ^{13}C NMR (101 MHz, MeOD) δ 159.2 (ArC), 152.6 (ArC), 142.4 (ArC), 131.4 (ArC), 130.6 (ArC), 124.8 (ArC), 122.9 (ArC), 120.7 (ArC), 116.1 (ArC), 113.5 (ArC), 55.3 (OCH_3), 52.9 (CH_2NH), 50.7 ($NHCH_2$), 34.9 (CH), 30.2 (CH_2), 25.6 (CH_2), 25.2 (CH_2). HRMS (ESI) *m*/*z* calcd for $C_{21}H_{27}O_2N^{35}Cl$ $[M + H]^+$, 360.1724 found 360.1742.

N-(4-(4-Chloro-2-methoxyphenoxy)benzyl)cyclohexanamine (176)

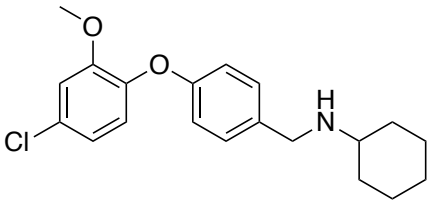

The title compound was synthesised according to General Procedure I from compound **115** (0.30 g, 1.47 mmol) cyclohexylamine (0.16 g, 1.60 mmol) and $NaB(OAc)_3H$ (0.64 g, 3.00 mmol). Purification was performed by flash column

chromatography (CH_2Cl_2:MeOH, 9:1) to yield the title compound as a yellow solid (0.27 g, 53%). ^{1}H NMR (400 MHz, $CDCl_3$) δ 7.45 – 7.37 (m, 2H, ArH), 6.99 (d, *J* = 2.3 Hz, 1H, ArH), 6.94 – 6.83 (m, 4H, ArH), 3.89 (s, 2H, CH_2NH), 3.82 (s, 3H, OCH_3), 2.67 (tt, *J* = 11.2, 3.8 Hz, 1H, CH), 2.05 (d, *J* = 12.4 Hz, 2H, CH_2), 1.79 (dd, *J* = 9.9, 4.6 Hz, 2H, CH_2), 1.68 – 1.61 (m, 1H), 1.40 (qd, *J* = 11.7, 3.6 Hz, 2H, CH_2), 1.21 (d, *J* = 7.7 Hz, 3H). ^{13}C NMR (101 MHz, $CDCl_3$) δ 157.7 (ArC), 152.0 (ArC), 143.2 (ArC), 131.0 (ArC), 130.0 (ArC), 128.6 (ArC), 122.1 (ArC), 120.9 (ArC), 117.0 (ArC), 113.5 (ArC), 56.2 (OCH_3), 55.3 (CH), 47.8 (CH_2NH), 30.6 (CH_2), 25.4 (CH_2), 24.7 (CH_2). HRMS (ESI) *m*/*z* calcd for $C_{19}H_{25}O_2N^{35}Cl$ $[M + H]^+$, 346.1568, found 346.1582.

N-Benzyl-1-(4-(4-chloro-2-methoxyphenoxy)phenyl)methanamine (177)

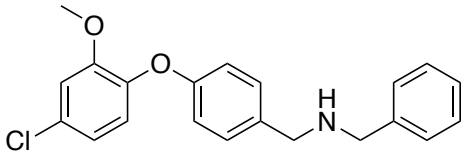

The title compound was synthesised according to General Procedure I from compound **115** (0.20 g, 0.76 mmol) benzylamine (0.11 g, 0.99 mmol) and $NaB(OAc)_3H$ (0.32 g, 1.52 mmol). Purification was performed by flash column chromatography (CH_2Cl_2:MeOH, 9:1) to yield the title compound as a yellow solid (0.19 g, 73%). ^{1}H NMR (400 MHz, $CDCl_3$) δ 7.27 – 7.21 (m, 4H, ArH), 7.19 – 7.15 (m, 3H, ArH), 6.87 (d, *J* = 2.0 Hz, 1H), 6.81 – 6.74 (m, 4H, ArH), 3.70 (s, 2H, CH_2), 3.69 (s, 3H, OCH_3), 3.67 (s, 2H, CH_2). ^{13}C NMR (101 MHz, $CDCl_3$) δ 156.9 (ArC), 151.9 (ArC), 143.8 (ArC), 138.7 (ArC), 133.2 (ArC), 129.9 (ArC), 129.7 (ArC), 128.7 (ArC), 127.9 (ArC), 127.4 (ArC), 121.7 (ArC), 120.9 (ArC), 117.2 (ArC), 113.4 (ArC), 56.2 (OCH_3), 52.5 (CH_2), 51.8 (CH_2). HRMS (ESI) *m*/*z* calcd for $C_{21}H_{21}{}^{35}ClNO_2$ $[M + H]^+$, 354.1255, found 354.1266.

5-Chloro-2-(4-((hexylamino)methyl)phenoxy)phenol (88)

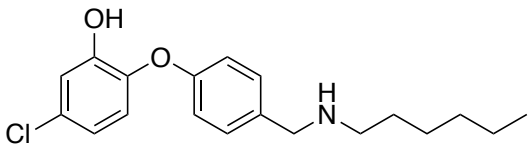

The title compound was synthesised according to general procedure B from compound **174** (0.25 g, 0.72 mmol) and BBr_3 (3.50 mL, 3.50 mmol). Purification was performed by semi-preparative reverse-phase high-performance liquid chromatography (Method 6) to yield the title compound as a white solid (0.15 g, 63%). ^{1}H NMR (500 MHz, MeOD) δ 7.41 – 7.35 (m, 2H, ArH), 6.96 – 6.88 (m, 4H, ArH), 6.80 (dd, *J* = 8.5, 2.5 Hz, 1H, ArH), 4.00 (s, 2H, CH_2), 2.90 – 2.84 (m, 2H, CH_2), 1.69 – 1.59 (m, 2H, CH_2), 1.42 – 1.27 (m, 6H, 3 × CH_2), 0.95 – 0.88 (m, 3H, CH_3). ^{13}C NMR (126 MHz, MeOD) δ 159.9 (ArC), 152.1 (ArC), 143.5 (ArC), 132.1 (ArC), 131.2 (ArC), 128.9 (ArC), 123.6 (ArC), 120.5 (ArC), 118.5 (ArC), 118.0 (ArC), 52.4 (CH_2), 48.7 (CH_2, inside solvent peak), 32.5 (CH_2), 28.1 (CH_2), 27.6 (CH_2), 23.5 (CH_2), 14.3 (CH_3). HPLC R_T ~ 7 min (Method 6). HRMS (ESI) *m/z* calcd for $C_{19}H_{25}O_2N^{35}Cl$ $[M + H]^+$, 334.1568, found 334.1577.

5-Chloro-2-(4-(((cyclohexylmethyl)amino)methyl)phenoxy)phenol (89)

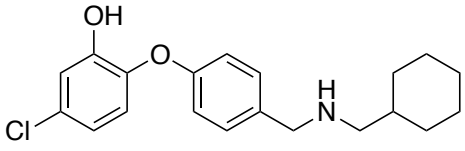

The title compound was synthesised according to general procedure B from compound **175** (0.25 g, 0.70 mmol) and BBr_3 (1 M in CH_2Cl_2, 3.50 mL, 3.50 mmol). Purification was performed by semi-preparative reverse-phase high-performance

liquid chromatography (Method 6) to yield the title compound as a white solid (80 mg, 33%). ^{1}H NMR (400 MHz, MeOD) δ 7.43 – 7.38 (m, 2H, ArH), 6.98 – 6.90 (m, 4H, ArH), 6.83 (dd, *J* = 8.5, 2.5 Hz, 1H, ArH), 4.03 (s, 2H, CH_2NH), 2.74 (d, *J* = 7.0 Hz, 2H, CH_2CH), 1.84 – 1.61 (m, 5H), 1.38 – 1.15 (m, 4H), 1.06 – 0.90 (m, 2H). ^{13}C NMR (101 MHz, MeOD) δ 158.5 (ArC), 150.6 (ArC), 142.0 (ArC), 130.8 (ArC), 129.8 (ArC), 127.3 (ArC), 122.3 (ArC), 119.2 (ArC), 117.1 (ArC), 116.6 (ArC), 53.6 (CH_2NH), 51.3 ($NHCH_2$), 35.6 (CH), 30.5 (CH_2), 25.8 (CH_2), 25.3 (CH_2). HPLC R_T ~ 12 min (Method 6). HRMS (ESI) *m*/*z* calcd for $C_{20}H_{25}O_2N^{35}Cl$ $[M + H]^+$, 346.1579 found 346.1568.

5-Chloro-2-(4-((cyclohexylamino)methyl)phenoxy)phenol (90)

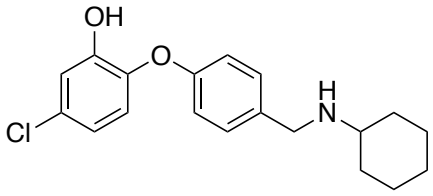

The title compound was synthesised according to general procedure B from compound **176** (0.26 g, 0.75 mmol) and BBr_3 (1 M in CH_2Cl_2, 3.00 mL, 3.00 mmol). Purification was performed by semi-preparative reverse-phase high-performance liquid chromatography (Method 6) to yield the title compound as a white solid (0.18 g, 72%). ^{1}H NMR (400 MHz, MeOD) δ 7.46 – 7.41 (m, 2H, ArH), 6.98 – 6.90 (m, 4H, ArH), 6.83 (dd, *J* = 8.5, 2.4 Hz, 1H, ArH), 4.15 (s, 2H, CH_2), 3.16 – 2.98 (m, 1H, CH), 2.23 – 2.11 (m, 2H), 1.92 – 1.84 (m, 2H), 1.75 – 1.68 (m, 1H), 1.46 – 1.18 (m, 5H). ^{13}C NMR (101 MHz, MeOD) δ 158.9 (ArC), 150.4 (ArC), 141.7 (ArC), 131.1 (ArC), 130.0 (ArC), 125.7 (ArC), 122.5 (ArC), 119.5 (ArC), 117.0 (ArC), 116.6 (ArC), 56.9 (CH), 47.5 ($NHCH_2$), 29.2 (CH_2), 24.8 (CH_2), 24.2 (CH_2). HPLC R_T ~ 11 min (Method 6). HRMS (ESI) *m*/*z* calcd for $C_{19}H_{23}O_2N^{35}Cl$ $[M + H]^+$, 332.1412, found 332.1423.

2-(4-((Benzylamino)methyl)phenoxy)-5-chlorophenol (91)

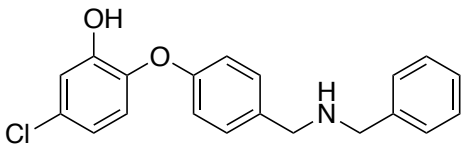

The title compound was synthesised according to general procedure B from compound **177** (0.17 g, 0.85 mmol) and BBr_3 (1 M in CH_2Cl_2, 4.2 mL, 4.2 mmol). Purification was performed by semi-preparative reverse-phase high-performance liquid chromatography (Method 6) to yield the title compound as a white solid (0.14 g, 49%). ^{1}H NMR (500 MHz, MeOD) δ 8.52 (s, 1H, OH), 7.49 – 7.37 (m, 7H, ArH), 7.00 – 6.90 (m, 4H, ArH), 6.83 (dd, *J* = 8.6, 2.5 Hz, 1H, ArH), 4.15 (s, 2H, CH_2), 4.11 (s, 2H, CH_2). ^{13}C NMR (126 MHz, MeOD) δ 170.2 (ArC), 160.2 (ArC), 151.7 (ArC), 143.1 (ArC), 133.7 (ArC), 132.5 (ArC), 130.8 (ArC), 130.3 (ArC), 130.2 (ArC), 127.3 (ArC), 123.9 (ArC), 120.9 (ArC), 118.4 (ArC), 118.0 (ArC), 52.0 (CH_2), 51.6 (CH_2). HPLC R_T ~ 10 min (Method 6). HRMS (ESI) *m/z* calcd for $C_{20}H_{19}O_2N^{35}Cl$ $[M + H]^+$, 340.1099, found 340.1098.

4-(4-Chloro-2-methoxyphenoxy)-3-methylbenzaldehyde (179)

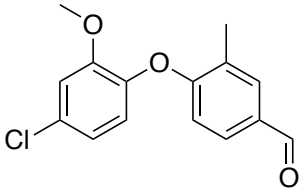

The title compound was synthesised according to General Procedure A from 4-chloro-2-methoxy phenol (1.00 g, 6.3 mmol) 4-fluoro-3-methybenzaldehyde (0.95 g, 6.9 mmol) and K_2CO_3 (0.95 g, 6.9 mmol). Purification was performed by flash column chromatography (Hexane/EtOAc, 2:1) to yield the title compound as a dense orange

oil (2.91 g, 88%). ^{1}H NMR (400 MHz, $CDCl_3$) δ 9.75 (s, 1H, CHO), 7.63 (dd, *J* = 2.1, 1.0 Hz, 1H, ArH), 7.46 (dd, *J* = 8.4, 2.1 Hz, 1H, ArH), 6.88 (t, *J* = 1.4 Hz, 1H, ArH), 6.82 (d, *J* = 1.3 Hz, 2H, ArH), 6.51 (d, J = 8.4 Hz, 1H, ArH), 3.65 (s, 3H, OCH_3), 2.29 (s, 3H, CH_3). ^{13}C NMR (101 MHz, $CDCl_3$) δ 191.1 (CHO), 161.3 (ArC), 152.0 (ArC), 142.4 (ArC), 132.5 (ArC), 131.1 (ArC), 130.9 (ArC), 129.7 (ArC), 128.4 (ArC), 122.7 (ArC), 121.1 (ArC), 114.5 (ArC), 113.7 (ArC), 56.1 (OCH_3), 16.2 ($ArCH_3$). HRMS (ESI) *m*/*z* calcd for $C_{15}H_{13}{}^{35}ClO_3Na$ $[M + Na]^+$, 299.0445, found 299.0433.

N-(4-(4-Chloro-2-methoxyphenoxy)-3-methylbenzyl)hexan-1-amine (180)

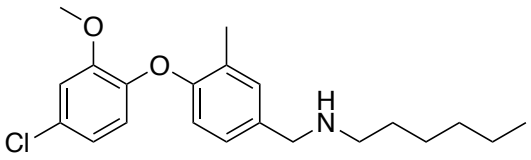

The title compound was synthesised according to General Procedure I from compound **179** (0.75 g, 2.71 mmol) hexylamine (0.30 g, 2.98 mmol) and $NaB(OAc)_3H$ (1.14 g, 5.42 mmol). Purification was performed by flash column chromatography (CH_2Cl_2:MeOH, 9:1) to yield the title compound as a yellow solid (0.71 g, 72%). ^{1}H NMR (400 MHz, $CDCl_3$) δ 7.22 (d, *J* = 2.2 Hz, 1H, ArH), 7.09 (dd, *J* = 8.2, 2.2 Hz, 1H, ArH), 6.96 (d, *J* = 2.4 Hz, 1H, ArH), 6.82 (dd, *J* = 8.6, 2.4 Hz, 1H, ArH), 6.72 (d, *J* = 8.2 Hz, 1H, ArH), 6.65 (d, *J* = 8.5 Hz, 1H, ArH), 3.85 (s, 3H, OCH_3), 3.75 (s, 2H, $ArCH_2$), 2.66 (t, *J* = 7.3 Hz, 2H, $NHCH_2$), 2.27 (s, 3H, $ArCH_3$), 1.55 (q, *J* = 7.3 Hz, 2H, CH_2), 1.39 – 1.25 (m, 6H, 3 × CH_2), 0.92 – 0.86 (m, 3H, CH_3). ^{13}C NMR (101 MHz, $CDCl_3$) δ 154.0 (ArC), 151.0 (ArC), 145.2 (ArC), 134.7 (ArC), 131.4 (ArC), 128.9 (ArC), 128.3 (ArC), 127.0 (ArC), 120.7 (ArC), 119.3 (ArC), 117.9 (ArC), 113.2 (ArC), 56.2 (OCH_3), 53.2 ($ArCH_2$), 49.3 ($NHCH_2$), 29.6 (CH_2), 27.0 (CH_2), 22.6 (CH_2), 16.1

($ArCH_3$), 14.1 (CH_3). HRMS (ESI) *m/z* calcd for $C_{21}H_{28}NO_2{}^{35}Cl$ $[M + H]^+$, 362.1882 found 362.1901.

N-(4-(4-Chloro-2-methoxyphenoxy)-3-methylbenzyl)-1-cyclohexylmethanamine (181)

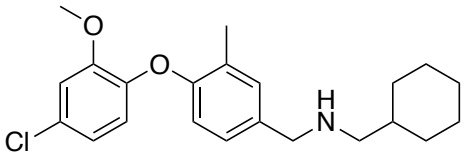

The title compound was synthesised according to General Procedure I from compound **179** (0.30 g, 1.08 mmol) cyclohexanemethylamine (0.14 g, 1.20 mmol) and $NaB(OAc)_3H$ (g, mmol). Purification was performed by flash column chromatography (CH_2Cl_2:MeOH, 9:1) to yield the title compound as a yellow solid (0.31 g, 57%). ^1H NMR (400 MHz, $CDCl_3$) δ 7.20 (d, *J* = 2.2 Hz, 1H, ArH), 7.07 (dd, *J* = 8.3, 2.2 Hz, 1H, ArH), 6.94 (d, *J* = 2.5 Hz, 1H, ArH), 6.80 (dd, *J* = 8.6, 2.4 Hz, 1H, ArH), 6.68 (d, *J* = 8.2 Hz, 1H, ArH), 6.64 (d, *J* = 8.5 Hz, 1H, ArH), 3.82 (s, 3H, OCH_3), 3.73 (s, 2H, CH_2NH), 2.48 (d, *J* = 6.8 Hz, 2H, CH_2CH), 2.25 (s, 3H, CH_3), 1.80 – 1.60 (m, 5H), 1.57 – 1.46 (m, 1H), 1.29 – 1.09 (m, 3H), 0.97 – 0.85 (m, 2H). ^{13}C NMR (101 MHz, $CDCl_3$) δ 154.1 (ArC), 151.1 (ArC), 149.8 (ArC), 145.0 (ArC), 134.3 (ArC), 131.5 (ArC), 128.8 (ArC), 128.4 (ArC), 127.1 (ArC), 120.7 (ArC), 119.4 (ArC), 117.7 (ArC), 113.2 (ArC), 56.1 (OCH_3), 55.6 (CH_2CH), 53.1 (CH_2NH), 37.4 (CH), 31.4 (CH_2), 27.0 (CH_2), 26.0 (CH_2), 16.1 (CH_3). HRMS (ESI) *m/z* calcd for $C_{22}H_{29}{}^{35}ClNO_2$ $[M + H]^+$, 374.1881, found 374.1899.

N-(4-(4-Chloro-2-methoxyphenoxy)-3-methylbenzyl)cyclohexanamine (182)

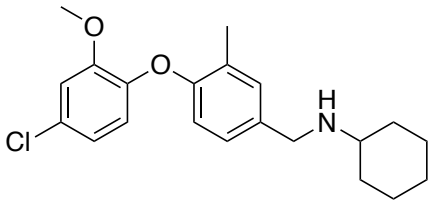

The title compound was synthesised according to General Procedure I from compound **179** (0.30 g, 1.08 mmol) cyclohexylamine (0.13 g, 1.30 mmol) and $NaB(OAc)_3H$ (0.46 g, 2.16 mmol). Purification was performed by flash column chromatography (CH_2Cl_2:MeOH, 9:1) to yield the title compound as a yellow solid (0.31 g, 80%). ^1H NMR (400 MHz, $CDCl_3$) δ 7.41 (d, *J* = 2.3 Hz, 1H, ArH), 7.27 (dd, *J* = 8.3, 2.2 Hz, 1H, ArH), 6.89 (d, *J* = 2.4 Hz, 1H, ArH), 6.76 (dd, *J* = 8.5, 2.3 Hz, 1H, ArH), 6.61 (dd, *J* = 8.6, 1.6 Hz, 1H, ArH), 6.55 (d, *J* = 8.3 Hz, 1H, ArH), 3.90 (s, 2H, C*H*$_2$NH), 3.72 (s, 3H, OCH_3), 2.76 (tt, *J* = 11.6, 3.8 Hz, 1H, CH), 2.23 (s, 3H, CH_3), 2.12 – 2.05 (m, 2H, CH_2), 1.78 – 1.69 (m, 2H, CH_2), 1.62 – 1.50 (m, 3H), 1.22 – 1.01 (m, 3H). ^{13}C NMR (101 MHz, $CDCl_3$) δ 156.4 (ArC), 151.6 (ArC), 143.7 (ArC), 133.4 (ArC), 129.6 (ArC), 129.2 (ArC), 128.8 (ArC), 124.5 (ArC), 121.1 (ArC), 120.8 (ArC), 116.4 (ArC), 113.4 (ArC), 56.1 (OCH_3), 55.2 (CH), 46.7 (CH_2NH), 29.0 (CH_2), 24.8 (CH_2), 24.5 (CH_2), 16.1 (CH_3). HRMS (ESI) *m*/*z* calcd for $C_{21}H_{27}{}^{35}ClNO_2$ $[M + H]^+$, 360.1725, found 360.1736.

_N_-Benzyl-1-(4-(4-chloro-2-methoxyphenoxy)-3-methylphenyl)methanamine (183)

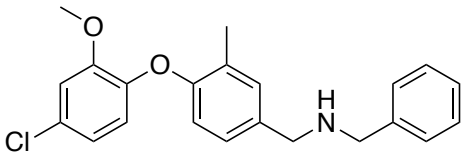

The title compound was synthesised according to General Procedure I from compound **179** (0.30 g, 1.08 mmol) benzylamine (0.15 g, 1.41 mmol) and $NaB(OAc)_3H$ (0.46 g, 2.16 mmol). Purification was performed by flash column chromatography (CH_2Cl_2:MeOH, 9:1) to yield the title compound as a yellow solid (0.30 g, 76%). ^1H NMR (400 MHz, $CDCl_3$) δ 7.24 – 7.08 (m, 6H, ArH), 6.96 (dd, *J* = 8.3, 2.2 Hz, 1H, ArH), 6.82 (d, *J* = 2.4 Hz, 1H, ArH), 6.68 (dd, *J* = 8.6, 2.4 Hz, 1H, ArH), 6.56 (d, *J* = 8.2 Hz, 1H, ArH), 6.52 (d, *J* = 8.5 Hz, 1H, ArH), 3.68 (s, 2H, CH_2), 3.66 (s, 3H, OCH_3), 3.62 (s, 2H, CH_2), 2.14 (s, 3H, CH_3). ^{13}C NMR (101 MHz, $CDCl_3$) δ 154.4 (ArC), 151.2 (ArC), 144.9 (ArC), 138.3 (ArC), 133.4 (ArC), 131.7 (ArC), 128.9 (ArC), 128.6 (ArC), 128.6 (ArC), 127.8 (ArC), 127.5 (ArC), 127.3 (ArC), 120.7 (ArC), 119.7 (ArC), 117.6 (ArC), 113.3 (ArC), 56.2 (CH_3), 52.4 (CH_2), 51.8 (CH_2), 16.2 ($ArCH_3$). HRMS (ESI) *m/z* calcd for $C_{22}H_{23}{}^{35}ClNO_2$ $[M + H]^+$, 368.1412, found 368.1421.

5-Chloro-2-(4-((hexylamino)methyl)-2-methylphenoxy)phenol (92)

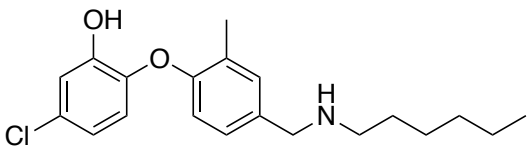

The title compound was synthesised according to general procedure B from compound **180** (0.30 g, 0.83 mmol) and BBr_3 (1 M in CH_2Cl_2, 3.30 mL, 3.30 mmol).

Purification was performed by semi-preparative reverse-phase high-performance liquid chromatography (Method 6) to yield the title compound as a white solid (0.19 g, 66%). ^{1}H NMR (500 MHz, MeOD) δ 8.55 (s, 1H, OH), 7.33 (d, *J* = 2.3 Hz, 1H, ArH), 7.18 (dd, *J* = 8.4, 2.3 Hz, 1H, ArH), 6.94 (d, *J* = 2.4 Hz, 1H, ArH), 6.78 (dd, *J* = 8.6, 2.4 Hz, 1H, ArH), 6.76 – 6.68 (m, 2H, ArH), 4.00 (s, 2H, CH_2), 2.93 – 2.86 (m, 2H, CH_2), 2.33 (s, 3H, CH_3), 1.65 (p, *J* = 7.6 Hz, 2H, CH_2), 1.41 – 1.33 (m, 6H, 3 × CH_2), 0.95 – 0.89 (m, 3H. CH_3). ^{13}C NMR (101 MHz, MeOD) δ 157.7 (ArC), 151.3 (ArC), 144.2 (ArC), 133.8 (ArC), 130.4 (ArC), 130.1 (ArC), 129.7 (ArC), 127.9 (ArC), 122.1 (ArC), 120.5 (ArC), 118.2 (ArC), 117.6 (ArC), 52.0 (CH_2), 48.7 (CH_2, inside solvent peak), 32.4 (CH_2), 27.5 (CH_2), 27.4 (CH_2), 23.4 (CH_2), 16.3 ($ArCH_3$), 14.3 (CH_3). HPLC R_T ~ 8 min (Method 6). HRMS (ESI) *m/z* calcd for $C_{20}H_{25}O_2N^{35}Cl$ $[M - H]^-$, 346.1579, found 346.1577.

5-Chloro-2-(4-(((cyclohexylmethyl)amino)methyl)-2-methylphenoxy)phenol (93)

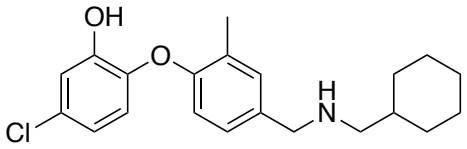

The title compound was synthesised according to general procedure B from compound **181** (0.31 g, 0.83 mmol) and BBr_3 (1 M in CH_2Cl_2, 4.14 mL, 4.14 mmol). Purification was performed by semi-preparative reverse-phase high-performance liquid chromatography (Method 6) to yield the title compound as a white solid (0.18 g, 61%). ^{1}H NMR (400 MHz, MeOD) δ 7.35 (d, *J* = 2.2 Hz, 1H, ArH), 7.20 (dd, *J* = 8.3, 2.3 Hz, 1H, ArH), 6.95 (d, *J* = 2.3 Hz, 1H, ArH), 6.74 (dd, *J* = 8.6, 2.4 Hz, 1H, ArH), 6.70 (d, *J* = 8.2 Hz, 2H, ArH), 3.96 (s, 2H, CH_2NH), 2.68 (d, *J* = 6.9 Hz, 2H, CH_2), 2.32 (s, 3H, CH_3), 1.83 – 1.61 (m, 6H), 1.37 – 1.16 (m, 3H), 1.04 – 0.92 (m, 2H). ^{13}C

NMR (101 MHz, MeOD) δ 155.8 (ArC), 150.1 (ArC), 143.3 (ArC), 132.2 (ArC), 128.8 (ArC), 128.7 (ArC), 128.6 (ArC), 128.0 (ArC), 120.3 (ArC), 118.8 (ArC), 117.0 (ArC), 116.5 (ArC), 53.8 (CH_2NH), 51.6 ($ArCH_2$), 35.8 (CH), 30.6 (CH_2), 25.9 (CH_2), 25.4 (CH_2), 15,0 (CH_3). HPLC R_T ~ 13 min (Method 6). HRMS (ESI) *m/z* calcd for $C_{21}H_{25}O_2N^{35}Cl$ $[M - H]^-$, 358.1579, found 358.1559.

5-Chloro-2-(4-((cyclohexylamino)methyl)-2-methylphenoxy)phenol (94)

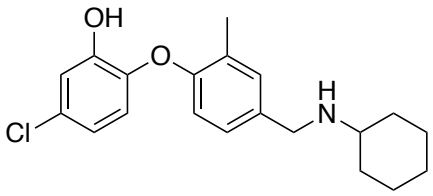

The title compound was synthesised according to general procedure B from compound **182** (0.25 g, 0.69 mmol) and BBr_3 (3.00 mL, 3.00 mmol). Purification was performed by semi-preparative reverse-phase high-performance liquid chromatography (Method 6) to yield the title compound as a white solid (0.17 g, 71%). ^{1}H NMR (400 MHz, MeOD) δ 8.59 – 8.50 (bs, 1H, OH) 7.39 (d, *J* = 2.3 Hz, 1H, ArH), 7.24 (dd, *J* = 8.4, 2.3 Hz, 1H, ArH), 6.97 (d, *J* = 2.2 Hz, 1H, ArH), 6.84 – 6.77 (m, 2H, ArH), 6.72 (d, *J* = 8.3 Hz, 1H, ArH), 4.15 (s, 2H, $ArCH_2$), 3.09 (ddd, *J* = 17.6, 8.5, 4.6 Hz, 1H, CH), 2.37 (s, 3H, $ArCH_3$), 2.19 (q, *J* = 4.7 Hz, 2H), 1.94 – 1.88 (m, 2H), 1.75 (d, *J* = 12.8 Hz, 1H), 1.46 – 1.23 (m, 5H). ^{13}C NMR (101 MHz, MeOD) δ 156.6 (ArC), 149.7 (ArC), 142.6 (ArC), 132.4 (ArC), 129.2 (ArC), 128.8 (ArC), 128.3 (ArC), 125.8 (ArC), 121.0 (ArC), 119.3 (ArC), 116.8 (ArC), 116.1 (ArC), 56.9 (CH), 47.5 ($ArCH_2$, inside solvent peak), 29.0 (CH_2), 24.7 (CH_2), 24.2 (CH_2), 14.8 (CH_3). HPLC R_T ~ 12 min (Method 6). HRMS (ESI) *m/z* calcd for $C_{20}H_{25}O_2N^{35}Cl$ $[M + H]^+$, 346.1568, found 346.1584.

2-(4-((Benzylamino)methyl)-2-methylphenoxy)-5-chlorophenol (95)

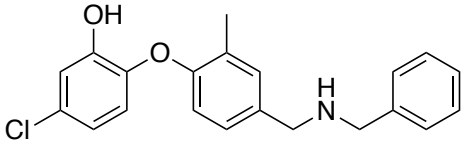

The title compound was synthesised according to general procedure B from compound **183** (0.30 g, 0.82 mmol) and BBr_3 (1 M in CH_2Cl_2, 4.10 mL, 4.10 mmol). Purification was performed by semi-preparative reverse-phase high-performance liquid chromatography (Method 6) to yield the title compound as a white solid (0.17 g, 59%). ^{1}H NMR (500 MHz, MeOD) δ 8.55 (bs, 1H, OH), 7.48 – 7.40 (m, 5H, ArH), 7.34 (d, *J* = 2.3 Hz, 1H, ArH), 7.20 (dd, *J* = 8.3, 2.3 Hz, 1H, ArH), 6.96 (d, *J* = 2.4 Hz, 1H, ArH), 6.82 – 6.70 (m, 3H, ArH), 4.10 (s, 2H, CH_2), 4.04 (s, 2H, CH_2), 2.34 (s, 3H, CH_3). ^{13}C NMR (126 MHz, MeOD) δ 170.25 (ArC), 157.43 (ArC), 150.90 (ArC), 144.28 (ArC), 134.82 (ArC), 133.68 (ArC), 130.62 (ArC), 130.34 (ArC), 130.13 (ArC), 130.07 (ArC), 129.96 (ArC), 129.52 (ArC), 121.97 (ArC), 120.68 (ArC), 118.08 (ArC), 117.76 (ArC), 52.31 (CH_2), 51.93 (CH_2), 16.25 (CH_3). HPLC R_T ~ 11 min (Method 6). HRMS (ESI) *m/z* calcd for $C_{21}H_{21}{}^{35}ClNO_2$ $[M + H]^+$, 354.1255, found 354.1263.

3-Methoxy-4-phenoxybenzaldehyde (185)

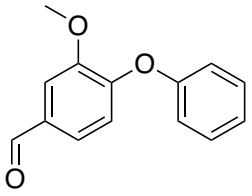

The title compound was prepared according to General Procedure A from 4-Fluoro-3-methoxybenzaldehyde (6.00 g, 38.92 mmol), Phenol (4.02 g, 42.81 mmol) and K_2CO_3 (5.92 g, 42.81 mmol). Purification was performed by flash column chromatography (Hexane/EtOAc, 0 -> 30%) to yield the title compound as a clear oil (7.00 g, 79%). ^{1}H NMR (400 MHz, $CDCl_3$) δ 9.89 (s, 1H, CHO), 7.52 (d, *J* = 1.9 Hz,

1H, ArH), 7.41 – 7.32 (m, 2H, ArH), 7.17 (td, *J* = 7.3, 1.1 Hz, 1H, ArH), 7.08 – 7.01 (m, 2H, ArH), 6.95 – 6.81 (m, 1H, ArH), 3.95 (s, 3H, CH_3). ^{13}C NMR (101 MHz, $CDCl_3$) δ 190.9 (CHO), 155.8 (ArC), 152.2 (ArC), 151.0 (ArC), 132.3 (ArC), 130.0 (ArC), 125.8 (ArC), 124.4 (ArC), 119.4 (ArC), 117.8 (ArC), 110.7 (ArC), 56.1 (CH_3). HRMS (ESI) *m*/*z* calcd for $C_{14}H_{12}{}^{35}ClO_3$ $[M + H]^+$, 229.0865, found 229.0858. Analytical data consistent with those reported in the literature.[207]

3-Hydroxy-4-phenoxybenzaldehyde (188)

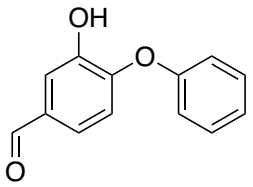

Compound **185** (7.00 g. 30.69 mmol) was dissolved in a solution of AcOH (30 ml, 0.52 mol) followed by the addition of 47% HBr (aq) (12 mL, 0.10 mol). The reaction mixture was then heated to 110 °C and stirred for 18 h. The reaction was allowed to cool to r.t. before being concentrated under reduced pressure, the mixture was then naturalised by careful addition of $NaHCO_3$ before being diluted in H_2O (100 mL) and extracted with EtOAc (3 × 100 mL). The combined organic layers were then dried over $MgSO_4$ and concentrated under reduced pressure. Purification by flash column chromatography (Hexane/EtOAc, 0 -> 15%) gave the title compound as a pale-yellow solid (2.51 g, 38%). ^1H NMR (400 MHz, $CDCl_3$) δ 9.89 (s, 1H, CHO), 7.57 (d, *J* = 1.9 Hz, 1H, ArH), 7.47 – 7.41 (m, 2H, ArH), 7.37 (dd, *J* = 8.3, 2.0 Hz, 1H, ArH), 7.31 – 7.20 (m, 1H, ArH), 7.15 – 7.09 (m, 2H, ArH), 6.89 (d, *J* = 8.3 Hz, 1H, ArH), 6.06 (s, 1H, OH). ^{13}C NMR (101 MHz, $CDCl_3$) δ 191.0 (CHO), 154.9 (ArC), 150.0 (ArC), 147.2 (ArC), 132.5 (ArC), 130.3 (ArC), 125.2 (ArC), 123.6 (ArC), 119.8 (ArC), 116.4 (ArC), 116.2 (ArC). HRMS (ESI) *m*/*z* calcd for $C_{13}H_9O_3$ $[M - H]^-$, 213.0557, found 213.0558. Analytical data consistent with those reported in the literature.[207]

3-(Methoxymethoxy)-4-phenoxybenzaldehyde (189)

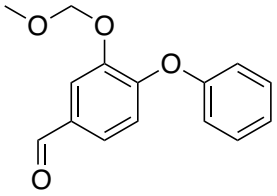

Compound **188** (1.74 g, 8.12 mmol) was dissolved in CH_2Cl_2 (40 mL) under a nitrogen atmosphere. DIPEA (3.15 g, 24.36 mmol) and MOMCl (0.98 g, 12.18 mmol) were added sequentially and the reaction mixture was allowed to stir for 18 h. The reaction mixture was then diluted with 1 M HCl (40 mL) and extracted with EtOAc (3 × 50 mL). The combined organic layers were then dried over $MgSO_4$ and concentrated under reduced pressure. Purification by flash column chromatography (Petroleum ether/EtOAc, 3:1) gave the title compound as a light-yellow oil (1.80 g, 81%). ^{1}H NMR (400 MHz, $CDCl_3$) δ 9.90 (s, 1H, CHO), 7.75 (d, *J* = 1.9 Hz, 1H, ArH), 7.48 (dd, *J* = 8.3, 1.9 Hz, 1H, ArH), 7.42 – 7.33 (m, 2H, ArH), 7.21 – 7.13 (m, 1H, ArH), 7.08 – 7.01 (m, 2H, ArH), 6.97 (d, *J* = 8.3 Hz, 1H, ArH), 5.28 (s, 2H, CH_2), 3.49 (s, 3H, CH_3). ^{13}C NMR (101 MHz, $CDCl_3$) δ 190.8 (CHO), 156.0 (ArC), 152.7 (ArC), 148.5 (ArC), 132.4 (ArC), 130.0 (ArC), 125.8 (ArC), 124.3 (ArC), 119.2 (ArC), 118.8 (ArC), 116.9 (ArC), 95.4 (CH_2), 56.5 (CH_3). HRMS (ESI) *m*/*z* calcd for $C_{15}H_{14}O_4Na$ [M + Na]$^+$, 281.0784, found 281.0784.

(3-(Methoxymethoxy)-4-phenoxyphenyl)methanol (190)

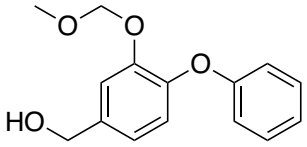

The title compound was synthesised according to General Procedure E from **189** (1.80 g, 6.61 mmol) and $NaBH_4$ (0.50 g, 13.22 mmol). Purification was performed by flash column chromatography (Hexane/EtOAc, 3:1) gave the title compound as a pale-yellow oil (1.40 g, 81%). ^{1}H NMR (400 MHz, $CDCl_3$) δ 7.34 – 7.28 (m, 3H, ArH), 7.09 – 7.04 (m, 1H, ArH), 7.01 (d, *J* = 1.3 Hz, 2H, ArH), 6.99 – 6.95 (m, 2H, ArH), 5.19 (s, 2H, CH_2), 4.69 (s, 2H, CH_2), 3.43 (s, 3H, CH_3), 1.86 (bs, 1H, OH). ^{13}C NMR (101 MHz, $CDCl_3$) δ 158.0 (ArC), 148.9 (ArC), 145.4 (ArC), 137.8 (ArC), 129.5 (ArC), 122.6 (ArC), 121.5 (ArC), 121.3 (ArC), 117.1 (ArC), 116.2 (ArC), 95.2 (OCH_2O), 65.0 (CH_2OH), 56.3 (CH_3). HRMS (ESI) *m/z* calcd for $C_{15}H1_5O_4Na$ $[M + Na]^+$, 283.0941, found 283.0951.

4-((Benzyloxy)methyl)-2-(methoxymethoxy)-1-phenoxybenzene (191)

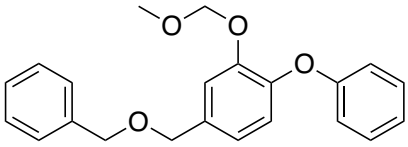

The title compound was synthesised according to General Procedure F from compound **190** (125 mg, 0.48 mmol), benzyl chloride (129 mg, 0.72 mmol) and NaH (60% dispersion in mineral oil, 48 mg, 0.96 mmol). Purification was performed by flash column chromatography (Hexane/EtOAc, 3:1) to yield the title compound as a colourless oil (84 mg, 87%). ^{1}H NMR (400 MHz, $CDCl_3$) δ 7.44 – 7.28 (m, 8H, ArH), 7.09 – 7.04 (m, 1H, ArH), 7.03 – 7.01 (m, 2H, ArH), 6.98 (dq, *J* = 7.8, 1.1 Hz, 2H,

ArH), 5.19 (s, 2H OCH_2O), 4.62 (s, 2H, CH_2), 4.55 (s, 2H, CH_2), 3.43 (s, 3H, CH_3). ^{13}C NMR (101 MHz, $CDCl_3$) δ 158.1 (ArC), 148.9 (ArC), 145.4 (ArC), 138.3 (ArC), 135.3 (ArC), 129.6 (ArC), 128.5 (ArC), 128.0 (ArC), 127.8 (ArC), 122.6 (ArC), 122.2 (ArC), 121.4 (ArC), 117.2 (ArC), 117.1 (ArC), 95.4 (OCH_2O), 72.4 ($ArCH_2$), 71.8 ($ArCH_2$), 56.3 (CH_3). HRMS (ESI) *m/z* calcd for $C_{22}H_{22}O_4Na$ $[M + Na]^+$, 373.1410, found 373.1424.

2-(Methoxymethoxy)-4-(((4-methylbenzyl)oxy)methyl)-1-phenoxybenzene (192)

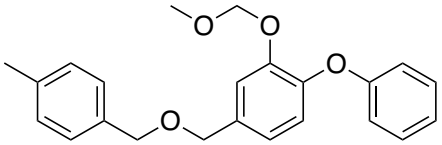

The title compound was synthesised according to General Procedure F from compound **190** (125 mg, 0.48 mmol), 4-methylbenzyl chloride (129 mg, 0.76 mmol) and NaH (60% dispersion in mineral oil, 48 mg, 0.96 mmol). Purification was performed by flash column chromatography (Hexane/EtOAc, 3:1) to yield the title compound as a colourless oil (84 mg, 87%). ^1H NMR (400 MHz, $CDCl_3$) δ 7.38 – 7.28 (m, 5H, ArH), 7.25 – 7.20 (m, 2H, ArH), 7.11 – 6.98 (m, 5H, ArH), 5.21 (s, 2H, OCH_2O), 4.59 (s, 2H, CH_2), 4.54 (s, 2H, CH_2), 3.45 (s, 3H, CH_3), 2.40 (s, 3H, $ArCH_3$). ^{13}C NMR (101 MHz, $CDCl_3$) δ 158.1 (ArC), 148.9 (ArC), 145.4 (ArC), 137.5 (ArC), 135.4 (ArC), 135.2 (ArC), 129.6 (ArC), 129.2 (ArC), 128.1 (ArC), 122.6 (ArC), 122.2 (ArC), 121.4 (ArC), 117.2 (ArC), 117.1 (ArC), 95.3 (OCH_2O), 72.3 ($ArCH_2$), 71.6 ($ArCH_2$), 56.3 (OCH_3), 21.3 ($ArCH_3$). HRMS (ESI) *m/z* calcd for $C_{23}H_{24}O_4Na$ $[M + Na]^+$, 387.1567, found 387.1583.

4-(((4-Isopropylbenzyl)oxy)methyl)-2-(methoxymethoxy)-1-phenoxybenzene (193)

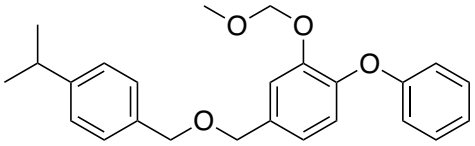

The title compound was synthesised according to General Procedure F from compound **190** (135 mg, 0.51 mmol), 4-isopropylbenzyl chloride (129 mg, 0.76 mmol) and NaH (60% dispersion in mineral oil, 42 mg, 1.02 mmol). Purification was performed by flash column chromatography (Hexane/EtOAc, 3:1) to yield the title compound as a colourless oil (174 mg, 87%). ^{1}H NMR (400 MHz, $CDCl_3$) δ 7.41 – 7.26 (m, 8H, ArH), 7.13 – 7.00 (m, 4H, ArH), 5.23 (s, 2H, OCH_2O), 4.63 (s, 2H, $ArCH_2$), 4.59 (s, 2H, $ArCH_2$), 3.47 (s, 3H, CH_3), 3.06 – 2.91 (m, 1H, CH), 1.33 (d, *J* = 6.9, Hz, 6H, CH_3). ^{13}C NMR (101 MHz, $CDCl_3$) δ 158.1 (ArC), 148.9 (ArC), 148.5 (ArC), 145.3 (ArC), 135.6 (ArC), 135.4 (ArC), 129.6 (ArC), 128.1 (ArC), 126.6 (ArC), 122.5 (ArC), 122.2 (ArC), 121.4 (ArC), 117.2 (ArC), 117.1 (ArC), 95.3 (OCH_2O), 72.3 ($ArCH_2$), 71.7 ($ArCH_2$), 56.3 (CH_3), 34.0 (CH), 24.1 ((CH_3)$_2$). HRMS (ESI) *m*/*z* calcd for $C_{25}H_{28}O_4Na$ $[M + Na]^+$, 415.1880, found 415.1887.

4-(((4-(*tert*-Butyl)benzyl)oxy)methyl)-2-(methoxymethoxy)-1-phenoxybenzene (194)

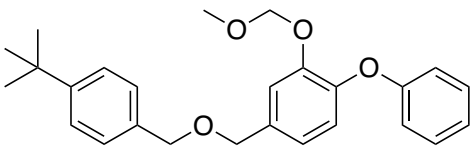

The title compound was synthesised according to General Procedure F from compound **190** (125 mg, 0.48 mmol), 4-*tert*-butylbenzyl bromide (131 mg, 0.76 mmol) and NaH (60% dispersion in mineral oil, 48 mg, 0.96 mmol). Purification was

performed by flash column chromatography (Hexane/EtOAc, 3:1) to yield the title compound as a colourless oil (95 mg, 49%). ^{1}H NMR (400 MHz, $CDCl_3$) δ 7.46 – 7.42 (m, 2H, ArH), 7.38 – 7.29 (m, 5H, ArH), 7.10 – 6.98 (m, 5H, ArH), 5.21 (s, 2H, OCH_2O), 4.60 (s, 2H, $ArCH_2$), 4.56 (s, 2H, $ArCH_2$), 3.45 (s, 3H), 1.37 (s, 9H). ^{13}C NMR (101 MHz, $CDCl_3$) δ 158.2 (ArC), 150.8 (ArC), 148.9 (ArC), 145.4 (ArC), 135.5 (ArC), 135.2 (ArC), 129.6 (ArC), 127.9 (ArC), 125.5 (ArC), 122.6 (ArC), 122.2 (ArC), 121.5 (ArC), 117.2 (ArC), 117.1 (ArC), 95.4 (OCH_2O), 72.2 ($ArCH_2$), 71.8 ($ArCH_2$), 56.4 (CH_3), 34.7 (C), 31.5 ((CH_3)$_3$). HRMS (ESI) *m*/*z* calcd for $C_{26}H_{30}O_4Na$ $[M + Na]^+$, 429.2036, found 429.2032.

4-(((3,5-Dimethylbenzyl)oxy)methyl)-2-(methoxymethoxy)-1-phenoxybenzene (195)

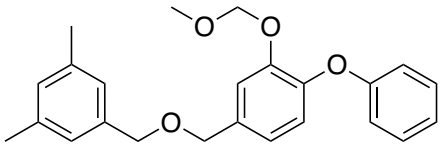

The title compound was synthesised according to General Procedure F from compound **190** (125 mg, 0.48 mmol), 3,5-dimethylbenzyl bromide (143 mg, 0.76 mmol) and NaH (60% dispersion in mineral oil, 48 mg, 0.96 mmol). Purification was performed by flash column chromatography (Hexane/EtOAc, 3:1) to yield the title compound as a colourless oil (146 mg, 82%). ^{1}H NMR (400 MHz, $CDCl_3$) δ 7.37 – 7.30 (m, 3H, ArH), 7.11 – 6.98 (m, 8H, ArH), 5.22 (s, 2H, OCH_2O), 4.57 (s, 4H, $ArCH_2$), 3.46 (s, 3H, OCH_3), 2.38 (s, 6H, (CH_3)$_2$). ^{13}C NMR (101 MHz, $CDCl_3$) δ 158.1 (ArC), 148.9 (ArC), 145.3 (ArC), 138.1 (ArC), 138.0 (ArC), 135.4 (ArC), 129.6 (ArC), 129.4 (ArC), 125.8 (ArC), 122.5 (ArC), 122.2 (ArC), 121.4 (ArC), 117.2 (ArC),

117.1 (ArC), 95.3 (OCH_2O), 72.5 ($ArCH_2$), 71.8 ($ArCH_2$), 56.3 (OCH_3), 21.4 ($ArCH_3$). HRMS (ESI) *m*/*z* calcd for $C_{24}H_{26}O_4Na$ [M + Na]$^+$, 401.1723, found 401.1725.

4-((Cyclopropylmethoxy)methyl)-2-(methoxymethoxy)-1-phenoxybenzene (196)

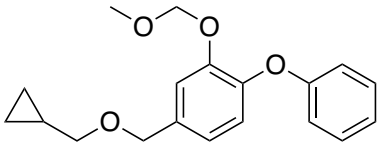

The title compound was synthesised according to General Procedure F from compound **190** (0.15 g, 0.57 mmol), (bromomethyl)cyclopropane (0.12 g, 0.85 mmol) and NaH (60% dispersion in mineral oil, 46 mg, 1.14 mmol). Purification was performed by flash column chromatography (Hexane/EtOAc, 3:1) to yield the title compound as a colourless oil (0.14 g, 78%). ^{1}H NMR (400 MHz, $CDCl_3$) δ 7.34 – 7.24 (m, 4H, ArH), 7.05 (tt, *J* = 7.2, 1.1 Hz, 1H, ArH), 7.01 – 6.99 (m, 2H, ArH), 6.98 – 6.94 (m, 2H, ArH), 5.19 (s, 2H, OCH_2O), 4.53 (s, 2H, $ArCH_2$), 3.43 (s, 3H, CH_3), 3.37 (d, *J* = 6.9 Hz, 2H, C*H*$_2$CH), 1.15 (dddd, *J* = 11.7, 8.1, 5.1, 2.1 Hz, 1H, CH), 0.63 – 0.54 (m, 2H, CH_2), 0.26 (dt, *J* = 6.0, 4.5 Hz, 2H, CH_2). ^{13}C NMR (101 MHz, $CDCl_3$) δ 158.1 (ArC), 148.9 (ArC), 145.2 (ArC), 135.6 (ArC), 129.5 (ArC), 122.4 (ArC), 122.0 (ArC), 121.4 (ArC), 117.1 (ArC), 116.9 (ArC), 95.3 (OCH_2O), 75.1 (*C*H_2CH), 72.2 ($ArCH_2$), 56.2 (CH_3), 10.7 (CH), 3.1 (CH_2). HRMS (ESI) *m*/*z* calcd for $C_{20}H_{24}O_4Na$ [M + Na]$^+$, 314.1410, found 337.1426.

4-((Cyclohexylmethoxy)methyl)-2-(methoxymethoxy)-1-phenoxybenzene (197)

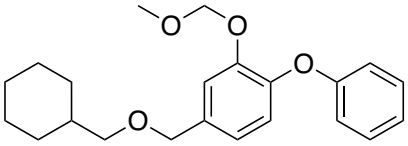

The title compound was synthesised according to General Procedure F from compound **190** (125 mg, 0.48 mmol), (bromomethyl)cyclohexane (127 mg, 0.76 mmol) and NaH (60% dispersion in mineral oil, 48 mg, 0.96 mmol). Purification was performed by flash column chromatography (Hexane/EtOAc, 3:1) to yield the title compound as a colourless oil (96 mg, 56%). ^{1}H NMR (400 MHz, $CDCl_3$) δ 7.35 – 7.27 (m, 2H, ArH), 7.24 (t, *J* = 1.1 Hz, 1H, ArH), 7.10 – 7.03 (m, 1H, ArH), 7.02 – 6.95 (m, 4H, ArH), 5.19 (s, 2H, OCH_2O), 4.49 (s, 2H, $ArCH_2$), 3.43 (s, 3H, OCH_3), 3.32 (d, *J* = 6.5 Hz, 2H, C*H*$_2$CH), 1.88 – 1.62 (m, 6H), 1.26 (dddd, *J* = 24.4, 15.3, 12.4, 9.2 Hz, 3H), 1.05 – 0.88 (m, 3H). ^{13}C NMR (101 MHz, $CDCl_3$) δ 158.1 (ArC), 148.8 (ArC), 145.1 (ArC) (ArC), 135.8 (ArC), 129.5 (ArC), 122.4 (ArC), 121.9 (ArC), 121.3 (ArC), 117.1 (ArC), 116.8 (ArC), 95.3 (OCH_2O), 76.5 (*C*H_2CH), 72.6 ($ArCH_2$), 56.2 (OCH_3), 38.1 (CH), 30.2 (CH_2), 26.7 (CH_2), 25.9 (CH_2). HRMS (ESI) *m*/*z* calcd for $C_{24}H_{26}O_4Na$ $[M + Na]^+$, 379.1880, found 379.1890.

3-(((3-(Methoxymethoxy)-4-phenoxybenzyl)oxy)methyl)thiophene (198)

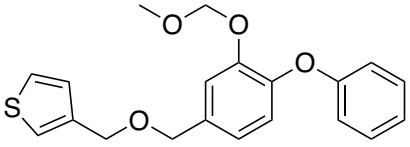

The title compound was synthesised according to General Procedure F from compound **190** (125 mg, 0.48 mmol), 3-(bromomethyl)thiophene (127 mg, 0.76

mmol) and NaH (60% dispersion in mineral oil, 48 mg, 0.96 mmol). Purification was performed by flash column chromatography (Hexane/EtOAc, 3:1) to yield the title compound as a colourless oil (110 mg, 64%). ^{1}H NMR (400 MHz, $CDCl_3$) δ 7.38 – 7.26 (m, 5H, ArH), 7.16 (dd, *J* = 5.0, 1.3 Hz, 1H, ArH), 7.11 – 7.04 (m, 1H, ArH), 7.03 – 7.00 (m, 2H, ArH), 7.00 – 6.96 (m, 2H, ArH), 5.20 (s, 2H, OCH_2O), 4.63 (s, 2H, $ArCH_2$), 4.55 (s, 2H, $ArCH_2$), 3.44 (s, 3H, CH_3). ^{13}C NMR (101 MHz, $CDCl_3$) δ 158.1 (ArC), 148.9 (ArC), 145.4 (ArC), 139.3 (ArC), 135.1 (ArC), 129.6 (ArC), 127.5 (ArC), 126.1 (ArC), 123.1 (ArC), 122.5 (ArC), 122.2 (ArC), 121.4 (ArC), 117.2 (ArC), 117.0 (ArC), 95.3 (OCH_2O), 71.7 ($ArCH_2$), 67.5 ($ArCH_2$), 56.3 (CH_3). HRMS (ESI) *m*/*z* calcd for $C_{20}H_{20}O_4SNa$ $[M + Na]^+$, 379.0975, found 379.0977.

2-(Methoxymethoxy)-4-(((3-methylbut-2-en-1-yl)oxy)methyl)-1-phenoxybenzene (199)

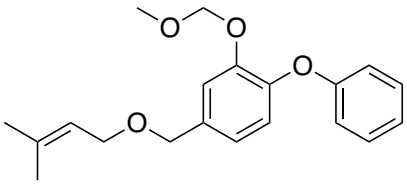

The title compound was synthesised according to General Procedure F from compound **190** (125 mg, 0.48 mmol), 3,3-dimethylallyl bromide (107 mg, 0.76 mmol) and NaH (60% dispersion in mineral oil, 48 mg, 0.96 mmol). Purification was performed by flash column chromatography (Hexane/EtOAc, 3:1) to yield the title compound as a colourless oil (100 mg, 63%). ^{1}H NMR (400 MHz, $CDCl_3$) δ 7.36 – 7.24 (m, 3H, ArH), 7.05 (tq, *J* = 8.2, 1.1 Hz, 1H, ArH), 7.02 – 6.94 (m, 4H, ArH), 5.45 (tdt, *J* = 7.0, 2.9, 1.4 Hz, 1H, CH), 5.19 (s, 2H, OCH_2O), 4.49 (s, 2H, $ArCH_2$), 4.07 (d, *J* = 6.9, Hz, 2H, CH_2), 3.43 (s, 3H, CH_3), 1.80 (d, *J* = 1.2 Hz, 3H, CH_3), 1.71 (d, *J* = 1.4 Hz, 3H). ^{13}C NMR (101 MHz, $CDCl_3$) δ 158.14 (ArC), 148.87 (ArC), 145.20 (ArC), 137.35 (C), 135.62 (ArC), 129.51 (ArC), 122.43 (ArC), 122.22 (ArC), 121.42 (ArC),

121.05 (CH), 117.05 (ArC), 117.03 (ArC), 95.26 (OCH_2O), 71.69 ($ArCH_2$), 66.75 (CH_2), 56.23 (OCH_3), 25.85 (CH_3), 18.09 (CH_3). HRMS (ESI) *m*/*z* calcd for $C_{20}H_{24}O_4Na$ $[M + Na]^+$, 351.1567, found 351.1574.

2-(Methoxymethoxy)-4-(((4-methylpentyl)oxy)methyl)-1-phenoxybenzene (200)

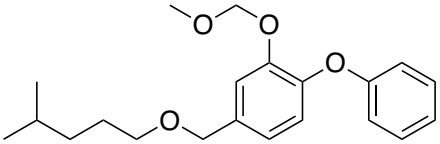

The title compound was synthesised according to General Procedure F from compound **190** (0.15 g, 0.57 mmol), 1-bromo-4-methypentane (0.12 g, 0.85 mmol) and NaH (60% dispersion in mineral oil, 46 mg, 1.14 mmol). Purification was performed by flash column chromatography (Hexane/EtOAc, 3:1) to yield the title compound as a colourless oil (0.14 g, 70%). ^1H NMR (400 MHz, $CDCl_3$) δ 7.34 – 7.28 (m, 2H, ArH), 7.27 (d, *J* = 1.5 Hz, 1H, ArH), 7.06 (td, *J* = 7.3, 1.1 Hz, 1H, ArH), 7.02 – 6.95 (m, 4H, ArH), 5.20 (s, 2H, OCH_2O), 4.50 (s, 2H, $ArCH_2$), 3.52 (t, *J* = 6.7 Hz, 2H, OCH_2), 3.43 (s, 3H, CH_3), 1.72 – 1.54 (m, 3H, CH & CH_2), 1.34 – 1.26 (m, 2H, CH_2), 0.94 (d, *J* = 6.7 Hz, 6H, $(CH_3)_2$). ^{13}C NMR (101 MHz, $CDCl_3$) δ 158.1 (ArC), 148.9 (ArC), 145.2 (ArC), 135.7 (ArC), 129.5 (ArC), 122.4 (ArC), 121.9 (ArC), 121.4 (ArC), 117.1 (ArC), 116.9 (ArC), 95.3 (OCH_2O), 72.5 ($ArCH_2$), 71.0 (OCH_2), 56.2 (CH_3), 35.4 (CH_2), 27.9 (CH), 27.7 (CH_2), 22.6 ($(CH_3)_2$). HRMS (ESI) *m*/*z* calcd for $C_{21}H_{28}O_4Na$ $[M + Na]^+$, 367.1880, found 367.1880.

5-((Benzyloxy)methyl)-2-phenoxyphenol (96)

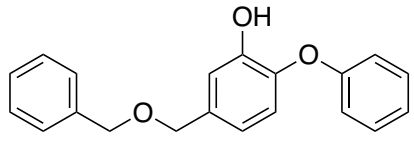

The title compound was synthesised according to General Procedure G from compound **191** (85 mg, 0.24 mmol) and 1 M HCl (aq) (1.30 mL, 1.30 mmol). Purification was performed by semi-preparative reverse-phase high-performance liquid chromatography (Method 2) to yield the title compound as a colourless solid (28 mg, 38%). ^{1}H NMR (400 MHz, $CDCl_3$) δ 7.41 – 7.28 (m, 7H, ArH), 7.16 – 7.06 (m, 2H, ArH), 7.06 – 6.99 (m, 2H, ArH), 6.86 (d, *J* = 2.1 Hz, 2H, ArH), 5.60 (bs, 1H, OH), 4.58 (s, 2H, CH_2), 4.51 (s, 2H, CH_2). ^{13}C NMR (101 MHz, $CDCl_3$) δ 156.9 (ArC), 147.6 (ArC), 143.0 (ArC), 138.3 (ArC), 135.3 (ArC), 130.0 (ArC), 128.6 (ArC), 128.0 (ArC), 127.8 (ArC), 123.7 (ArC), 120.2 (ArC), 118.9 (ArC), 118.1 (ArC), 115.8 (ArC), 72.3 (CH_2), 71.8 (CH_2). HPLC r.t. ~ 7 min (Method 2) HRMS (ESI) *m*/*z* calcd for $C_{20}H_{17}O_3$ $[M - H]^-$, 305.1183, found 305.1185.

5-(((4-Methylbenzyl)oxy)methyl)-2-phenoxyphenol (97)

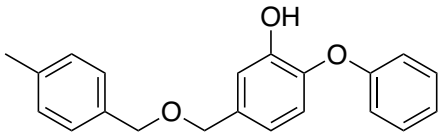

The title compound was synthesised according to General Procedure G from compound **192** (84 mg, 0.20 mmol) and 1 M HCl (aq) (1.20 mL, 1.20 mmol). Purification was performed by semi-preparative reverse-phase high-performance liquid chromatography (Method 2) to yield the title compound as a colourless solid (32 mg, 50%). ^{1}H NMR (400 MHz, $CDCl_3$) δ 7.36 – 7.29 (m, 2H, ArH), 7.24 (d, *J* = 2.2

Hz, 2H, ArH), 7.15 (d, *J* = 7.8 Hz, 2H, ArH), 7.10 (t, *J* = 7.4 Hz, 1H, ArH), 7.05 (d, *J* = 1.6 Hz, 1H, ArH), 7.03 – 6.97 (m, 2H, ArH), 6.88 – 6.78 (m, 2H, ArH), 5.56 (s, 1H, OH), 4.52 (s, 2H, CH_2), 4.46 (s, 2H, CH_2), 2.34 (s, 3H, CH_3). ^{13}C NMR (101 MHz, $CDCl_3$) δ 157.0 (ArC), 147.5 (ArC), 142.9 (ArC), 137.5 (ArC), 135.4 (ArC), 135.3 (ArC), 130.0 (ArC), 129.2 (ArC), 128.1 (ArC), 123.7 (ArC), 120.2 (ArC), 118.9 (ArC), 118.1 (ArC), 115.8 (ArC), 72.2 (CH_2), 71.5 (CH_2), 21.3 (CH_3). HPLC r.t. ~ 8 min (Method 2) HRMS (ESI) *m/z* calcd for $C_{21}H_{19}O_3$ $[M - H]^-$, 319.1340, found 319.1339.

5-(((4-Isopropylbenzyl)oxy)methyl)-2-phenoxyphenol (98)

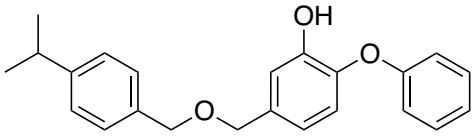

The title compound was synthesised according to General Procedure G from compound **193** (0.17 g, 0.44 mmol) and 1 M HCl (aq) (2.26 mL, 2.26 mmol). Purification was performed by semi-preparative reverse-phase high-performance liquid chromatography (Method 2) to yield the title compound as a colourless solid (48 mg, 31%). ^1H NMR (400 MHz, $CDCl_3$) δ 7.38 – 7.30 (m, 4H, ArH), 7.24 (d, *J* = 8.2 Hz, 2H, ArH), 7.16 – 7.08 (m, 2H, ArH), 7.05 – 7.01 (m, 2H, ArH), 6.87 (d, *J* = 1.5 Hz, 2H, ArH), 5.64 (s, 1H, OH), 4.56 (s, 2H, CH_2), 4.50 (s, 2H, CH_2), 2.93 (hept, *J* = 6.9 Hz, 1H, CH), 1.27 (d, *J* = 6.9 Hz, 6H, $(CH_3)_2$). ^{13}C NMR (101 MHz, $CDCl_3$) δ 157.0 (ArC), 148.6 (ArC), 147.5 (ArC), 142.9 (ArC), 135.6 (ArC), 135.4 (ArC), 130.0 (ArC), 128.1 (ArC), 126.6 (ArC), 123.7 (ArC), 120.2 (ArC), 118.9 (ArC), 118.0 (ArC), 115.8 (ArC), 72.2 (CH_2), 71.6 (CH_2), 34.0 (CH), 24.2 (CH_3). HPLC r.t. ~ 11 min (Method 2) HRMS (ESI) *m/z* calcd for $C_{23}H_{23}O_3$ $[M - H]^-$, 347.1653, found 347.1666.

5-(((4-*tert*-Butylbenzyl)oxy)methyl)-2-phenoxyphenol (99)

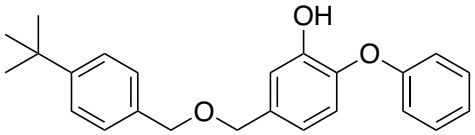

The title compound was synthesised according to General Procedure G from compound **194** (95 mg, 0.23 mmol) and 1 M HCl (aq) (1.40 mL, 1.40 mmol). Purification was performed by semi-preparative reverse-phase high-performance liquid chromatography (Method 2) to yield the title compound as a colourless solid (18 mg, 22%). ^{1}H NMR (400 MHz, $CDCl_3$) δ 7.45 – 7.28 (m, 6H, ArH), 7.16 – 7.07 (m, 2H, ArH), 7.07 – 6.98 (m, 2H, ArH), 6.86 (d, *J* = 1.6 Hz, 2H, ArH), 5.57 (s, 1H, OH), 4.55 (s, 2H, CH_2), 4.50 (s, 2H, CH_2), 1.33 (s, 9H, $(CH_3)_3$). ^{13}C NMR (101 MHz, $CDCl_3$) δ 157.0 (ArC), 150.8 (ArC), 147.6 (ArC), 142.9 (ArC), 135.5 (ArC), 135.3 (ArC), 130.0 (ArC), 127.8 (ArC), 125.5 (ArC), 123.7 (ArC), 120.2 (ArC), 118.9 (ArC), 118.1 (ArC), 115.8 (ArC), 72.1 (CH_2), 71.7 (CH_2), 34.7 (C), 31.5 (CH_3). HPLC r.t. ~ 15 min (Method 2) HRMS (ESI) *m*/*z* calcd for $C_{24}H_{25}O_3$ $[M - H]^-$, 361.1809, found 361.1809.

5-(((3,5-Dimethylbenzyl)oxy)methyl)-2-phenoxyphenol (100)

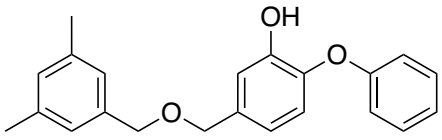

The title compound was synthesised according to General Procedure G from compound **195** (0.14 g, 0.38 mmol) and 1 M HCl (aq) (2.31 mL, 2.31 mmol). Purification was performed by semi-preparative reverse-phase high-performance liquid chromatography (Method 2) to yield the title compound as a colourless solid

(35 mg, 28%). ^{1}H NMR (400 MHz, $CDCl_3$) δ 7.40 – 7.30 (m, 2H, ArH), 7.17 – 7.09 (m, 2H, ArH), 7.06 – 6.98 (m, 4H, ArH), 6.95 (s, 1H, ArH), 6.87 (d, *J* = 1.7 Hz, 2H, ArH), 4.52 (s, 2H, CH_2), 4.51 (s, 2H, CH_2), 2.34 (s, 6H, $(CH_3)_2$). ^{13}C NMR (101 MHz, $CDCl_3$) δ 156.96 (ArC), 147.55 (ArC), 142.96 (ArC), 138.14 (ArC), 138.09 (ArC), 135.36 (ArC), 129.99 (ArC), 129.43 (ArC), 125.81 (ArC), 123.70 (ArC), 120.15 (ArC), 118.94 (ArC), 118.04 (ArC), 115.86 (ArC), 72.39 (CH_2), 71.77 (CH_2), 21.40 (CH_3). HPLC r.t. ~ 11 min (Method 2) HRMS (ESI) *m/z* calcd for $C_{22}H_{21}O_3$ [M - H]$^-$, 333.1496, found 333.1500.

5-((Cyclopropylmethoxy)methyl)-2-phenoxyphenol (101)

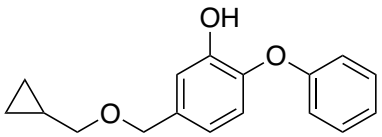

The title compound was synthesised according to General Procedure G from compound **196** (0.14 g, 0.44 mmol) and 1 M HCl (aq) (2.40 mL, 2.40 mmol). Purification was performed by semi-preparative reverse-phase high-performance liquid chromatography (Method 2) to yield the title compound as a colourless solid (45 mg, 38%). ^{1}H NMR (400 MHz, $CDCl_3$) δ 7.38 – 7.28 (m, 2H, ArH), 7.11 (ddt, *J* = 8.6, 7.3, 1.1 Hz, 1H, ArH), 7.06 (d, *J* = 1.8 Hz, 1H, ArH), 7.03 – 6.99 (m, 2H, ArH), 6.89 – 6.79 (m, 2H, ArH), 5.69 (s, 1H, OH), 4.48 (s, 2H, $ArCH_2$), 3.33 (d, *J* = 6.9 Hz, 2H, CH_2CH), 1.23 – 1.02 (m, 1H, CH), 0.61 – 0.49 (m, 2H, CH_2), 0.22 (dt, *J* = 6.0, 4.5 Hz, 2H, CH_2). ^{13}C NMR (101 MHz, $CDCl_3$) δ 157.0 (ArC), 147.6 (ArC), 142.9 (ArC), 135.6 (ArC), 130.0 (ArC), 123.6 (ArC), 120.0 (ArC), 119.0 (ArC), 118.0 (ArC), 115.8 (ArC), 75.1 (OCH_2CH), 72.2 ($ArCH_2$), 10.8 (CH), 3.2 (CH_2). HPLC r.t. ~ 8 min (Method 2) HRMS (ESI) *m/z* calcd for $C_{22}H_{21}O_3$ [M - H]$^-$, 269.1183, found 269.1190.

5-((Cyclohexylmethoxy)methyl)-2-phenoxyphenol (102)

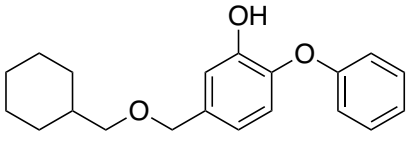

The title compound was synthesised according to General Procedure G from compound **197** (96 mg, 0.26 mmol) and 1 M HCl (aq) (1.56 mL, 1.56 mmol). Purification was performed by semi-preparative reverse-phase high-performance liquid chromatography (Method 2) to yield the title compound as a colourless solid (40 mg, 49%). ^{1}H NMR (400 MHz, $CDCl_3$) δ 7.38 – 7.29 (m, 2H, ArH), 7.11 (ddt, *J* = 8.5, 7.2, 1.1 Hz, 1H, ArH), 7.06 – 6.99 (m, 3H, ArH), 6.89 – 6.79 (m, 2H, ArH), 5.65 (s, 1H, OH), 4.44 (s, 2H, CH_2), 3.29 (d, *J* = 6.5 Hz, 2H, CH_2CH), 1.85 – 1.57 (m, 6H), 1.23 (ddtd, *J* = 24.5, 15.6, 12.6, 3.3 Hz, 3H), 0.96 (qd, *J* = 12.1, 3.1 Hz, 2H). ^{13}C NMR (101 MHz, $CDCl_3$) δ 157.0 (ArC), 147.5 (ArC), 142.8 (ArC), 135.9 (ArC), 130.0 (ArC), 123.6 (ArC), 119.8 (ArC), 118.9 (ArC), 118.0 (ArC), 115.6 (ArC), 76.5 (*C*H_2CH), 72.6 (CH_2), 38.2 (CH), 30.3 (CH_2), 26.8 (CH_2), 26.0 (CH_2). HPLC r.t. ~ 14 min (Method 2) HRMS (ESI) *m/z* calcd for $C_{20}H_{23}O_3$ $[M - H]^-$, 311.1653, found 311.1653.

2-Phenoxy-5-((thiophen-3-ylmethoxy)methyl)phenol (103)

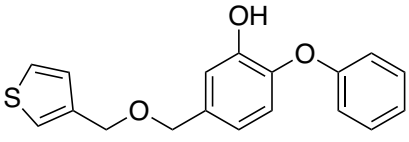

The title compound was synthesised according to General Procedure G from compound **198** (0.11 g, 0.31 mmol) and 1 M HCl (aq) (1.86 mL, 1.86 mmol). Purification was performed by semi-preparative reverse-phase high-performance liquid chromatography (Method 2) to yield the title compound as a colourless solid

(37 mg, 38%). ^{1}H NMR (400 MHz, $CDCl_3$) δ 7.39 – 7.29 (m, 3H, ArH), 7.25 (dq, *J* = 3.0, 1.0 Hz, 1H, ArH), 7.15 – 7.10 (m, 2H, ArH), 7.07 (d, *J* = 1.8 Hz, 1H, ArH), 7.05 – 7.00 (m, 2H, ArH), 6.90 – 6.80 (m, 2H, ArH), 5.63 (s, 1H, OH), 4.58 (s, 2H, CH_2), 4.49 (s, 2H, CH_2). ^{13}C NMR (101 MHz, $CDCl_3$) δ 156.9 (ArC), 147.6 (ArC), 143.0 (ArC), 139.4 (ArC), 135.2 (ArC), 130.0 (ArC), 127.5 (ArC), 126.2 (ArC), 123.7 (ArC), 123.1 (ArC), 120.2 (ArC), 118.9 (ArC), 118.1 (ArC), 115.8 (ArC), 71.6 (CH_2), 67.5 (CH_2). HPLC r.t. ~ 9 min (Method 2) HRMS (ESI) *m*/*z* calcd for $C_{18}H_{15}SO_3$ [M - H]$^-$, 311.0747, found 311.0757.

5-(((3-Methylbut-2-en-1-yl)oxy)methyl)-2-phenoxyphenol (104)

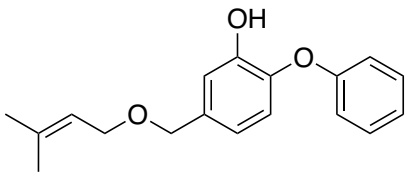

The title compound was synthesised according to General Procedure G from compound **199** (0.10 g, 0.30 mmol) and 1 M HCl (aq) (1.80 mL, 1.80 mmol). Purification was performed by semi-preparative reverse-phase high-performance liquid chromatography (Method 2) to yield the title compound as a colourless solid (41 mg, 48%). ^{1}H NMR (400 MHz, $CDCl_3$) δ 7.38 – 7.29 (m, 2H, ArH), 7.14 – 7.08 (m, 1H, ArH), 7.05 (d, *J* = 1.7 Hz, 1H, ArH), 7.04 – 6.97 (m, 2H, ArH), 6.89 – 6.80 (m, 2H, ArH), 5.58 (s, 1H, OH), 5.44 – 5.37 (m, 1H, CH), 4.44 (s, 2H, $ArCH_2$), 4.02 (d, *J* = 6.9 Hz, 2H, CH_2), 1.76 (d, *J* = 1.6 Hz, 3H, CH_3), 1.67 (d, *J* = 1.4 Hz, 3H, CH_3). ^{13}C NMR (101 MHz, $CDCl_3$) δ 157.0 (ArC), 147.5 (ArC), 142.8 (ArC), 137.4 (ArC), 135.6 (ArC), 130.0 (ArC), 123.6 (ArC), 121.1 (CH), 120.2 (ArC), 119.0 (ArC), 118.0 (ArC), 115.9 (ArC), 71.7 ($ArCH_2$), 66.7 (CH_2), 25.9 (CH_3), 18.2 (CH_3). HPLC r.t. ~ 7 min (Method 2) HRMS (ESI) *m*/*z* calcd for $C_{18}H_{19}O_3$ [M - H]$^-$, 283.1340, found 283.1344.

5-(((4-Methylpentyl)oxy)methyl)-2-phenoxyphenol (105)

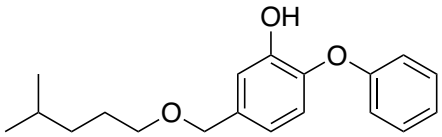

The title compound was synthesised according to General Procedure G from compound **200** (0.14 g, 0.41 mmol) and 1 M HCl (aq) (2.40 mL, 2.40 mmol). Purification was performed by semi-preparative reverse-phase high-performance liquid chromatography (Method 2) to yield the title compound as a white solid (38 mg, 31%). ^{1}H NMR (400 MHz, $CDCl_3$) δ 7.38 – 7.30 (m, 2H, ArH), 7.15 – 7.09 (m, 1H, ArH), 7.07 – 6.98 (m, 3H, ArH), 6.89 – 6.79 (m, 2H, ArH), 5.58 (s, 1H, OH), 4.44 (s, 2H, $ArCH_2$), 3.47 (t, *J* = 6.8 Hz, 2H, CH_2), 1.69 – 1.50 (m, 3H, CH_2 and CH), 1.30 – 1.21 (m, 2H, CH_2), 0.89 (d, *J* = 6.6 Hz, 6H, CH_3). ^{13}C NMR (101 MHz, $CDCl_3$) δ 156.9 (ArC), 147.4 (ArC), 142.7 (ArC), 135.6 (ArC), 129.9 (ArC), 123.6 (ArC), 119.8 (ArC), 118.8 (ArC), 117.9 (ArC), 115.5 (ArC), 72.4 ($ArCH_2$), 70.9 (CH_2), 35.3 (CH_2), 27.9 (CH_2), 27.7 (CH_2), 22.6 (CH_3). HPLC R_T. ~ 12 min (Method 2). HRMS (ESI) *m*/*z* calcd for $C_{19}H_{23}O_3$ [M - H]$^-$, 299.1653, found 299.1659.

2-*trans*-Octenoyl CoA (202)

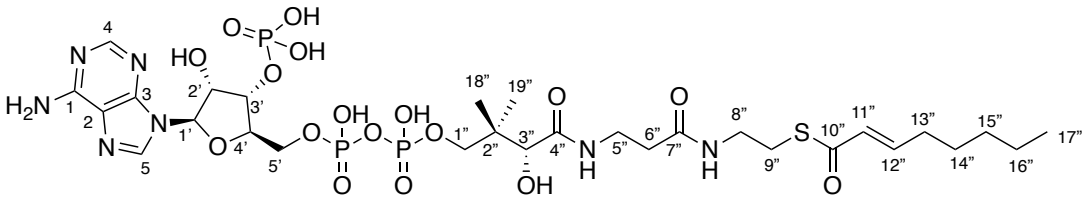

K_2CO_3 (70 mg, 480 µmol) was dissolved in water (5 mL) in a round bottom flask, **shielded from light**, and CoA.3Li salt (100 mg, 120 µmol) was added. THF (5 mL) was added followed by *trans*-2-octenoic acid (32 µL, 220 µmol) and PyBOP (99 mg, 190 µmol), the reaction vessel was then purged with nitrogen and allowed to stir **in**

the dark for 12 h at r.t.. The reaction was monitored by staining with DTNB, completion was indicated by the absence of yellow staining, at this point the organic solvent was removed under reduced pressure at **ambient temperature**, and the remaining aqueous solvent was removed by lyophilisation **in the dark** affording a white solid (271 mg). The crude material was purified by semi-preparative HPLC (method 2). The crude product was dissolved in water (5 mL, 20 mg mL^{-1} wrt CoA) and the insoluble PyBOP remnants were removed by filtration through a Minisart syringe driven PTFE-membrane (0.45 µm) prior to HPLC injection. The product-containing HPLC fractions (r.t. ~ 10 – 13.00 mins) were pooled and the organic solvent was removed under reduced pressure at **ambient temperature** before lyophilisation **in the dark**. The white solid was then lyophilised three times **in the dark**, to remove residual ammonium acetate, to yield the title compound as a fluffy white solid (29 mg, 27%) which was stored under an argon atmosphere **in the dark** at **– 20 °C** until required. ^{1}H NMR (400 MHz, D_2O) δ 8.55 (s, 1H, H-5), 8.25 (s, 1H, H-4), 6.94 (dt, J = 15.6, 6.9 Hz, 1H, H-12”), 6.20 – 6.11 (m, 2H, H-11” and H-1’), 4.86 – 4.82 (m, 2H, H-2' and H-3’ under the solvent peak), 4.59 (s, 1H, H-4’), 4.25 (dd, J = 4.9, 2.8 Hz, 2H, H-5’), 4.03 (s, 1H, H-3’), 3.85 (dd, J = 9.8, 4.9 Hz, 1H, H-1_A”), 3.57 (dd, J = 9.8, 4.8 Hz, 1H, H-1_B”), 3.44 (t, J = 6.6 Hz, 2H, H-5”), 3.36 (t, J = 6.9, 2H, H-8”), 3.04 (t, J = 6.3 Hz, 2H, H-9”), 2.43 (t, J = 6.6 Hz, 2H, H-6”), 2.17 (m, 2H, H-13”), 1.45 – 1.36 (m, 2H, H-14"), 1.30 – 1.18 (m, 4H, H-15” and 16”), 0.90 (s, 3H, H-18”), 0.84 (t, J = 6.8 Hz, 3H, H-17”), 0.76 (s, 3H, H-19”). ^{13}C NMR (101 MHz, D_2O) δ 193.7 (C-10”), 174.7 (C-4”), 173.9 (C-7”), 155.0 (C-1), 152.1 (C-4), 149.1 (C-3), 148.9 (C-12”), 140.0 (C-5), 127.7 (C-11”), 86.4 (C-1’), 83.4 (C-4’), 74.1 (C-2’ and 3”), 73.9 (d, J = 5.2 Hz, C-3’), 71.9 (d, J = 4.5 Hz, C-1”), 65.2 (C-5’), 38.7 (C-8”), 38.3 (d, J = 8.0 Hz, C-2”), 35.4 (C-5”), 35.4 (C-6”), 31.6 (C-13”), 30.6 (C-15”), 27.8 (C-9”),

26.7 (C-14”), 21.7 (C-16”), 20.9 (C-18”), 18.2 (C-19”). ^{31}P NMR (162 MHz, D_2O) δ 0.8, -10.8, -11.3. HPLC R_T. ~ 10 min (Method 1). HRMS (ESI) *m*/*z* calcd for $C_{29}H_{47}N_7O_{17}P_3S$ [M - H]$^-$, 890.1967, found 890.1917.

Appendix Experimental: Spider Silk Ligands

5-Chloro-2-(2,4-dichlorophenoxy)phenyl hex-5-ynoate (208)

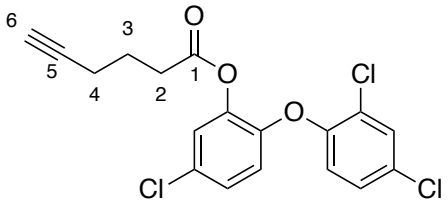

The title compound was prepared according to General Procedure J from 5-Hexynoic acid (1.00 g, 8.91 mmol), DCC (2.02 g, 9.81 mmol), triclosan (2.84 g, 9.81 mmol) and DMAP (54 mg, 5 mol%). Purification was performed by flash column chromatography (Hexane/EtOAc, 9:1) to yield the title compound as a dense, clear oil (2.90 g, 85%). ^{1}H NMR (400 MHz, $CDCl_3$) δ 7.47 (d, *J* = 2.5 Hz, 1H, ArH), 7.25 – 7.15 (m, 3H, ArH), 6.87 (dd, *J* = 8.8, 4.7 Hz, 2H, ArH), 2.66 (t, *J* = 7.4 Hz, 2H, H-2), 2.29 (td, *J* = 6.9, 2.6 Hz, 2H, H-4), 2.01 (t, *J* = 2.7 Hz, 1H, H-6), 1.89 (p, *J* = 7.1 Hz, 2H, H-3). ^{13}C NMR (101 MHz, $CDCl_3$) δ 175.7 (C-1), 151.5 (ArC), 146.1 (ArC), 141.8 (ArC), 130.5 (ArC), 129.5 (ArC), 129.3 (ArC), 128.2 (ArC), 127.0 (ArC), 125.8 (ArC), 124.4 (ArC), 120.3 (ArC), 118.4 (ArC), 83.9 (C-5), 71.4 (C-6), 32.4 (C-2), 23.4 (C-3), 17.7 (C-4). HRMS (ESI) *m*/*z* calcd for $C_{18}H_{13}O_3{}^{35}Cl3Na$ [M + Na]+, 404.9822 found 404.9818.

5-Nitroquinolin-8-yl hex-5-ynoate (209)

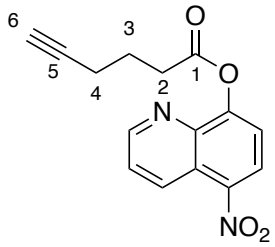

The title compound was prepared according to General Procedure J from 5-Hexynoic acid (0.64 g, 5.78 mmol), DCC (1.21 g, 5.78 mmol), nitroxoline (1.00 g, 5.26 mmol) and DMAP (32 mg, 5 mol%). Purification was performed by flash column chromatography (Hexane/EtOAc, 6:4) to yield the title compound as a yellow solid (1.05 g, 70%). ^{1}H NMR (400 MHz, $CDCl_3$) δ 9.10 (dd, *J* = 8.9, 1.6 Hz, 1H, ArH), 9.03 (dd, *J* = 4.1, 1.6 Hz, 1H, ArH), 8.47 (d, *J* = 8.5 Hz, 1H, ArH), 7.70 (dd, *J* = 8.9, 4.1 Hz, 1H, ArH), 7.57 (d, *J* = 8.5 Hz, 1H, ArH), 3.00 (t, *J* = 7.3 Hz, 2H, CH2, H-2), 2.49 (td, *J* = 6.9, 2.7 Hz, 2H, H-4), 2.16 – 2.10 (m, 2H, H-3), 2.07 (t, *J* = 2.6 Hz, 1H, H-6). ^{13}C NMR (101 MHz, $CDCl_3$) δ 171.2 (C-1), 152.8 (ArC), 151.3 (ArC), 142.9 (ArC), 140.9 (ArC), 132.4 (ArC), 125.3 (ArC), 124.5 (ArC), 122.7 (ArC), 119.8 (ArC), 83.2 (C-5), 69.4 (C-6), 32.9 (C-2), 23.7 (C-3), 17.8 (C-4). HRMS (ESI) *m*/*z* calcd for $C_{15}H_{13}N_2O_4Na$ [M + Na]+, 285.0870, found 285.0876.

2-(2,4-Difluorophenyl)-1,3-di(1*H*-1,2,4-triazol-1-yl)propan-2-yl hex-5-ynoate (210)

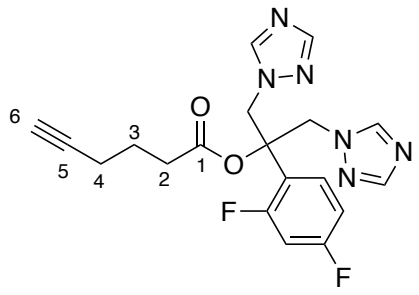

The title compound was prepared according to General Procedure J from 5-Hexynoic acid (0.36 g, 3.27 mmol), DCC (0.75 g, 3.59 mmol), fluconazole (1.00 g, 3.27 mmol) and DMAP (20 mg, 5 mol%). Purification was performed by flash column chromatography (CH_2Cl_2/MeOH, 9:1) to yield the title compound as a green solid (0.40 g, 31%). ^{1}H NMR (400 MHz, $CDCl_3$) δ 7.96 (s, 2H, CH), 7.91 (s, 2H, CH), 6.95 – 6.76 (m, 3H, ArH), 5.19 (d, *J* = 14.6 Hz, 2H, CH_2), 5.09 (d, *J* = 14.5 Hz, 2H, CH_2), 2.53 (t, *J* = 7.4 Hz, 2H, H-2), 2.30 (td, *J* = 6.9, 2.6 Hz, 2H, H-4), 2.03 (t, *J* = 2.6 Hz, 1H, H-6), 1.84 (p, *J* = 7.1 Hz, 2H, H-3). ^{13}C NMR (101 MHz, $CDCl_3$) δ 171.9 (C-1), 152.2 (CH), 144.8 (CH), 128.3 (dd, J = 9.7, 5.3 Hz, ArC), 119.9 (ArC), 112.3 (d, J = 18.0 Hz, ArC), 105.7 – 104.8 (m, ArC), 83.2 (C-5), 80.9 (C), 69.4 (C-6), 51.3 (CH_2), 51.2 (CH_2), 32.9 (C-2), 23.7 (C-3), 17.8 (C-4). ^{19}F NMR (376 MHz, $CDCl_3$) δ -107.4 (ArF), -108.8 (ArF). HRMS (ESI) *m/z* calcd for $C_{19}H_{19}O_4F_2N_6O_2$ $[M + H]^+$, 401.1532, found 401.1544.

N-Boc Ciprofloxacin (215)

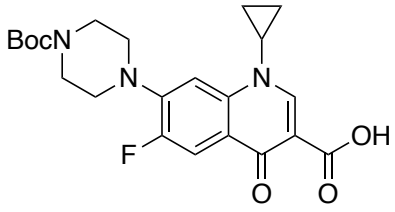

Ciprofloxacin (1.00 g, 3.02 mmol) was suspended in THF (25 mL). Upon addition of 1 M NaOH (aq) (6.00 mL, 6.00 mmol) a clear solution formed to which $(Boc)_2O$ (725 mg, 3.31 mmol) was added. The reaction mixture was then allowed to stir at r.t. for 18 h. The organic solvent was removed under reduced pressure and the resulting aqueous phase was acidified to pH 3-4 using 1 M HCl (aq). The resulting solid was isolated by filtration and washed with EtOAc before being dried under reduced pressure to yield the title compound as a white solid (1.42 g, quant.) which was used without further purification. ^{1}H NMR (400 MHz, $CDCl_3$:MeOD, 2:1) δ 9.25 (s, 1H, CH), 8.44 (d, *J* = 12.9 Hz, 1H, ArH), 7.98 – 7.91 (m, 1H, ArH), 4.20 – 4.09 (m, 5H, NCH_2), 3.87 – 3.78 (m, 4H, CH_2), 1.98 (s, 9H, $(CH_3)_3$), 1.95 – 1.89 (m, 2H, CH_2), 1.75 – 1.68 (m, 2H, CH_2). ^{13}C NMR (101 MHz, $CDCl_3$:MeOD, 2:1) δ 177.07 (CO), 167.92 (CO), 154.90 (CO), 152.49 (*C*=CH), 147.80 (CH), 145.88 (d, *J* = 10.3 Hz, ArC), 139.21 (ArC), 119.82 (d, *J* = 8.0 Hz, ArC), 112.11 (d, *J* = 23.6 Hz, ArCF), 107.35 (ArC), 105.40 (d, *J* = 3.4 Hz, ArC), 80.72 (C), 49.57 (CH_2), 35.61 (CH), 28.11 ($(CH_3)_3$), 7.99 (CH_2). ^{19}F NMR (376 MHz, $CDCl_3$:MeOD, 2:1) δ -117.05 (dd, *J* = 12.9, 7.0 Hz). HRMS (ESI) m/z calcd for $C_{22}H_{26}O_5N_3FNa$ $[M + Na]^+$, 454.1749, found 454.1760. Analytical data consistent with those reported in the literature.[208]

N-Boc Ciprofloxacin propargyl ester (216)

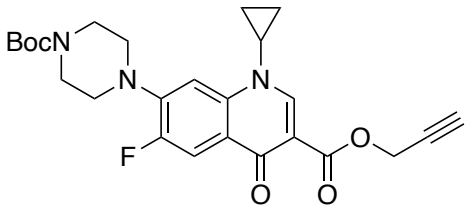

Acid **215** (400 mg, 0.93 mmol) was suspended in DMF (20 mL) followed by the sequential addition of K_2CO_3 (256 mg, 1.86 mmol) and propargyl bromide (165 mg, 1.40 mmol). The reaction mixture was heated to reflux and the resulting solution was stirred for 18 h. The reaction mixture was allowed to cool to 0 ºC and diluted with H_2O (20 mL) before being extracted with EtOAc (3 × 30 mL). The combined organic layers were then washed with saturated aqueous $NaHCO_3$, H_2O and brine (30 mL each). The organic layer was dried over $MgSO_4$, filtered and concentrated under reduced pressure. Purification was performed by flash column chromatography (Hexane/ EtOAc, 0 -> 100%) to yield the title compound as a white solid (357 mg, 80%) ^{1}H NMR (400 MHz, $CDCl_3$) δ 8.51 (s, 1H, CH), 7.97 (d, *J* = 13.1 Hz, 1H, ArH), 7.28 – 7.22 (m, 1H, ArH), 4.90 (d, *J* = 2.5 Hz, 2H, C*H*$_2$CCH), 3.68 – 3.60 (m, 4H, NCH_2), 3.42 (dt, *J* = 7.0, 3.2 Hz, 1H, CH), 3.21 (dd, *J* = 6.1, 4.0 Hz, 4H, CH_2), 2.48 (t, *J* = 2.4 Hz, 1H, CH_2CC*H*), 1.49 (s, 9H, $(CH_3)_3$), 1.36 – 1.28 (m, 2H, CH_2), 1.18 – 1.11 (m, 2H, CH_2). ^{13}C NMR (101 MHz, CDCl3) δ 172.8 (CO), 164.6 (CO), 154.6 (CO), 148.6 (CH), 144.4 (ArC), 137.9 (ArC), 113.4 (d, J = 22.8 Hz, ArCF), 109.4 (ArC), 105.1 (ArC), 80.2 (C), 78.1 (C), 74.8 (CH_2), 52.1 (CH), 49.9 (CH_2), 34.7 (CH), 28.4 ($(CH_3)_3$), 8.2 (CH_2). ^{19}F NMR (376 MHz, $CDCl_3$) δ -123.50 (dd, *J* = 13.1, 7.0 Hz). HRMS (ESI) m/z calcd for $C_{25}H_{28}O_5N_3F^3Na$ $[M + Na]^+$, 492.1905, found 492.1915

Ciprofloxacin propargyl ester (217)

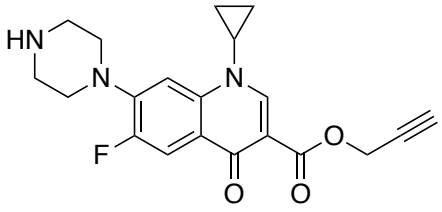

Carbamate **216** (47 mg, 0.10 mmol) was dissolved in a 9:1 mixture of CH_2Cl_2:TFA (20 mL). The reaction mixture was allowed to stir for 30 min before being concentrated under reduced pressure. The residue was suspended in saturated aqueous $NaHCO_3$ and the resulting solid was isolated by filtration to yield the title compound as an off-white solid (17 mg, 46%). ^{1}H NMR (400 MHz, $CDCl_3$) δ 8.53 (s, 1H, CH), 7.99 (d, *J* = 13.3 Hz, 1H, ArH), 7.25 (d, *J* = 6.9 Hz, 2H, ArH, under solvent peak), 4.90 (d, *J* = 2.4 Hz, 2H, CH_2), 3.43 (tt, *J* = 7.1, 4.0 Hz, 1H, CH), 3.31 – 3.20 (m, 4H, CH_2), 3.09 (dd, *J* = 6.3, 3.4 Hz, 4H, CH_2), 2.48 (t, *J* = 2.4 Hz, 1H, CH), 1.35 – 1.29 (m, 2H, CH_2), 1.17 – 1.11 (m, 2H, CH_2). ^{13}C NMR (101 MHz, $CDCl_3$) δ 172.9 (CO), 164.8 (CO), 152.3 (*C*=CH), 148.5 (CH), 145.1 (d, *J* = 10.4 Hz, ArC), 138.0, 122.9 (d, *J* = 7.0 Hz, ArC), 113.3 (d, *J* = 23.2 Hz), 109.3, 104.8 (d, *J* = 3.2 Hz). 78.2 (C), 74.7 (CH), 52.1 (CH_2), 51.1 (*C*H_2CCH), 46.0 (CH_2), 34.6 (CH), 8.2 (CH_2). ^{19}F NMR (376 MHz, CDCl3) δ -123.3 (dd, *J* = 13.3, 7.1 Hz). HRMS (ESI) m/z calcd for $C_{20}H_{20}O_3N_3FNa$ $[M + Na]^+$, 392.1381, found 392.1397

N-((1*R*,2*R*)-3-((*tert*-Butyldiphenylsilyl)oxy)-1-hydroxy-1-(4-nitrophenyl)propan-2-yl)-2,2-dichloroacetamide (218)

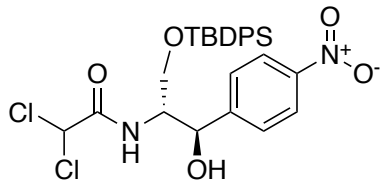

Chloramphenicol (3.00 g, 9.30 mmol) was dissolved in anhydrous DMF (50 mL). Imidazole (0.94 g, 13.90 mmol) and TBDPSCl (2.81 g, 10.20 mmol) were added sequentially and the reaction mixture was stirred at r.t. for 18 h. The reaction mixture was then diluted with H_2O (50 mL) before being extracted with EtOAc (3 × 100 mL). The combined organic layers were then sequentially washed with saturated aqueous $NaHCO_3$, H_2O and brine (100 mL). The organic layer was then dried over $MgSO_4$, filtered and concentrated under reduced pressure. Purification was performed by flash column chromatography (CH_2Cl_2/MeOH, 98:2) to yield the title compound as a dense yellow oil which crystallised upon standing (6.40 g, 82%). ^{1}H NMR (400 MHz, $CDCl_3$) δ 8.20 – 8.13 (m, 2H, ArH), 7.68 (dq, *J* = 6.7, 1.3 Hz, 4H, ArH), 7.58 – 7.36 (m, 8H, ArH), 5.79 (s, 1H, $CHCl_2$), 5.31 (d, *J* = 2.8 Hz, 1H, C*H*OH), 4.21 (dtd, *J* = 9.0, 4.6, 2.9 Hz, 1H, CH), 3.92 (d, *J* = 4.6 Hz, 2H, CH_2), 1.13 (s, 9H, $(CH_3)_3$). ^{13}C NMR (101 MHz, $CDCl_3$) δ 171.3 (NCO), 148.2 (ArC), 147.5 (ArC), 135.6 (ArC), 135.5 (ArC), 128.1 (ArC), 128.0 (ArC), 126.8 (ArC), 123.5 (ArC), 71.9 (CHOH), 66.2 ($CHCl_2$), 63.8 (CH_2), 55.9 (CH), 27.5 $(CH_3)_3$), 19.2 (C). HRMS (ESI) *m*/*z* calcd for $C_{27}H_{30}O_6N_2{}^{35}Cl_2Si$ [M + H]+, 561.1373, found 561.1377.

(1*R*,2*R*)-3-((*tert*-Butyldiphenylsilyl)oxy)-2-(2,2-dichloroacetamido)-1-(4-nitrophenyl)propyl hex-5-ynoate (219)

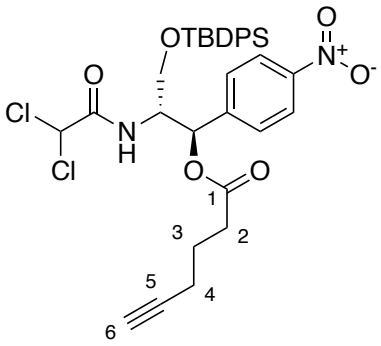

The title compound was prepared according to General Procedure J from 5-Hexynoic acid (1.07 g, 9.54 mmol), DCC (2.15 g, 10.42 mmol), **218** (5.00 g, 8.92 mmol) and DMAP (51 mg, 5 mol%). Purification was performed by flash column chromatography (CH_2Cl_2/MeOH, 98:2) to yield the title compound as a dense colourless oil (4.80 g, 83%). ^{1}H NMR (400 MHz, $CDCl_3$) δ 8.16 – 8.09 (m, 2H, ArH), 7.57 (ddd, *J* = 8.1, 3.1, 1.5 Hz, 4H, ArH), 7.49 – 7.33 (m, 8H, ArH), 6.20 (d, *J* = 7.9 Hz, 1H, C*H*OH), 5.88 (s, 1H, $CHCl_2$), 4.35 (dddd, *J* = 9.5, 7.6, 4.4, 2.8 Hz, 1H, CH), 3.67 (dd, *J* = 10.8, 4.4 Hz, 1H, CH_2'), 3.41 (dd, *J* = 10.8, 2.8 Hz, 1H, CH_2), 2.50 (td, *J* = 7.3, 1.7 Hz, 2H, H-2), 2.22 (tdd, *J* = 6.6, 2.7, 1.3 Hz, 2H, H-4), 1.95 (t, *J* = 2.7 Hz, 1H, H-6), 1.81 (p, *J* = 7.1 Hz, 2H, H-3), 1.13 (s, 9H). ^{13}C NMR (101 MHz, $CDCl_3$) δ 172.1 (NCO), 164.6 (C-1), 147.6 (ArC), 143.9 (ArC), 135.6 (ArC), 135.5 (ArC), 130.3 (ArC), 128.1 (ArC), 128.0 (ArC), 123.2 (ArC), 82.9 (C-5), 72.5 (C-6), 69.5 (CO), 65.2 ($CHCl_2$), 61.8 (CH_2), 54.3 (CH), 33.1 (C-2), 26.4 ((CH_3)$_3$), 23.2 (C-3), 17.7 (C). HRMS (ESI) *m*/*z* calcd for $C_{33}H_{36}O_7N_2{}^{35}Cl_2Si$ [M + H]+, 655.1792, found 655.1777.

(1*R*,2*R*)-2-(2,2-Dichloroacetamido)-3-hydroxy-1-(4-nitrophenyl)propyl hex-5-ynoate (220)

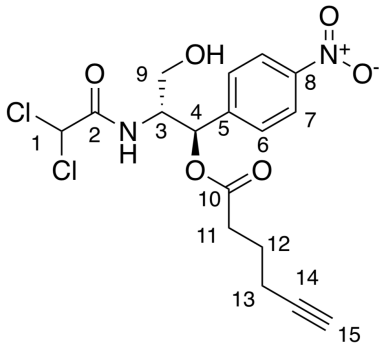

Compound **219** (4.80 g, 7.33 mmol) was dissolved in anhydrous THF. TBAF (1 M solution in THF, 10.70 mL, 10.70 mmol) was added dropwise and the reaction mixture was stirred for 18 h. The reaction mixture was then diluted with saturated aqueous NH_4Cl and Et_2O (50 mL), the layers were separated and the aqueous layer was washed with Et_2O (3 × 50 mL). The combined organic layers were dried over $MgSO_4$, filtered and concentrated under reduced pressure. Purification was performed by flash column chromatography (CH_2Cl_2/MeOH, 98:2) to yield the title compound as a dense yellow oil (1.95 g, 70%). ^{1}H NMR (400 MHz, $CDCl_3$) δ 8.27 – 8.22 (m, 2H, ArH-7), 7.61 – 7.56 (m, 2H, ArH-6), 6.89 (d, *J* = 8.9 Hz, 1H, NH), 5.79 (s, 1H, H-1), 5.11 (d, *J* = 2.4 Hz, 1H, H-4), 4.50 (dd, *J* = 10.9, 7.0 Hz, 1H, H-9), 4.47 – 4.39 (m, 1H, H-3), 4.25 (dd, *J* = 10.9, 6.1 Hz, 1H, H-9'), 2.57 (t, *J* = 7.4 Hz, 2H, H-11), 2.32 (td, *J* = 6.9, 2.7 Hz, 2H, H-13), 2.02 (t, *J* = 2.6 Hz, 1H, H-15), 1.89 (p, *J* = 7.1 Hz, 2H, H-12). ^{13}C NMR (101 MHz, $CDCl_3$) δ 173.5 (C-10), 164.4 (C-2), 147.7 (ArC), 147.0 (ArC), 126.8 (C-8), 123.8 (C-7), 82.9 (C-14), 70.8 (C-15), 69.5 (C-4), 66.0 (C-1), 62.6 (C-9), 54.1 (C-3), 32.6 (C-11), 23.3 (C-12), 17.8 (C-13). HRMS (ESI) *m/z* calcd for $C_{17}H_{18}O_6{}^{35}Cl_2N2Na$ $[M + Na]^+$, 439.0434, found 439.0432.

(2*S*,4*R*)-*N*-((1*S*,2*S*)-2-Chloro-1-((3a*S*,4*R*,6*R*,7*R*,7a*R*)-7-hydroxy-2,2-dimethyl-6-(methylthio)tetrahydro-4*H*-[1,3]dioxolo[4,5-*c*]pyran-4-yl)propyl)-1-methyl-4-propylpyrrolidine-2-carboxamide (221)

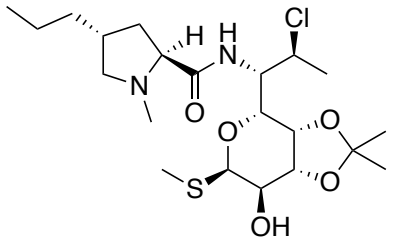

Clindamycin hydrochloride (50 mg, 0.12 mmol) was suspended in Acetone (5 mL) followed by the addition of 2,2-dimethoxypropane (24 mg, 0.2 mmol) and *p*-TsOH.H_2O (1 mg, 5 mol%). The reaction mixture was heated to 40 °C and allowed to stir for 72 h. The reaction mixture was then allowed to cool before being diluted with saturated aqueous $NaHCO_3$ (10 mL). The aqueous layer was then extracted with EtOAc (3 × 10 mL). The combined organic layers were dried over $MgSO_4$, filtered and concentrated under reduced pressure to yield the title compound as a white solid that was used without further purification (54 mg, 96%). ^{1}H NMR (400 MHz, $CDCl_3$) δ 7.70 (d, J = 10.4 Hz, 1H), 5.26 (d, J = 5.0 Hz, 1H), 4.65 – 4.53 (m, 2H), 4.46 (dd, *J* = 10.0, 2.1 Hz, 1H), 4.16 – 3.99 (m, 4H), 3.18 (q, *J* = 4.6 Hz, 1H), 3.02 (dd, *J* = 10.7, 4.7 Hz, 1H), 2.41 (s, 3H), 2.20 (s, 3H), 2.04 (s, 4H), 1.97 – 1.81 (m, 2H), 1.53 – 1.45 (m, 6H), 1.36 – 1.20 (m, 8H), 0.91 – 0.85 (m, 3H). ^{13}C NMR (101 MHz, $CDCl_3$) δ 174.14, 109.55, 86.24, 76.60, 72.75, 70.16, 68.55, 67.44, 62.77, 59.16, 52.15, 41.69, 38.23, 37.72, 35.72, 28.04, 25.87, 22.42, 21.55, 14.27, 13.31. HRMS (ESI) m/z calcd for $C_{21}H_{37}O_5N_2S^{35}ClNa$ $[M + Na]^+$, 487.2004, found 487.2001.

(3a*S*,4*R*,6*R*,7*R*,7a*S*)-4-((1*S*,2*S*)-2-Chloro-1-((2*S*,4*R*)-1-methyl-4-propylpyrrolidine-2-carboxamido)propyl)-2,2-dimethyl-6-(methylthio)tetrahydro-4*H*-[1,3]dioxolo[4,5-*c*]pyran-7-yl hex-5-ynoate (222)

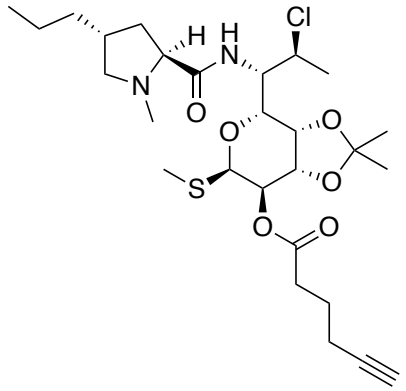

Alcohol **221** (167 mg, 0.36 mmol) was dissolved in CH_2Cl_2 (10 mL) followed by the sequential addition of 5-hexynoic Acid (81 mg, 0.72 mmol), DCC (151 mg, 0.72 mmol) and DMAP (2 mg, 5 mol %). The reaction mixture was then allowed to stir at r.t. for 18 h. The resulting precipitate was removed by filtration and filtrate was extracted once with saturated aqueous $NaHCO_3$ (10 mL). The organic layer was dried over $MgSO_4$, filtered and concentrated under reduced pressure. Purification was performed by flash column chromatography (Hexane/EtOAc, 0 -> 40%) to yield the title compound as a white solid (139 mg, 69%) ^{1}H NMR (400 MHz, $CDCl_3$) δ 7.66 (d, *J* = 10.5 Hz, 1H), 5.41 (d, *J* = 5.5 Hz, 1H), 5.02 (dd, *J* = 8.1, 5.6 Hz, 1H), 4.61 – 4.52 (m, 2H), 4.43 (dd, *J* = 10.0, 2.3 Hz, 1H), 4.17 (dd, *J* = 8.1, 5.4 Hz, 1H), 4.10 (dd, *J* = 5.4, 2.4 Hz, 1H), 3.15 (q, *J* = 4.6 Hz, 1H), 2.98 (dd, *J* = 10.5, 4.7 Hz, 1H), 2.49 (t, *J* = 7.5 Hz, 2H), 2.37 (s, 3H), 2.24 (td, *J* = 7.0, 2.6 Hz, 2H), 2.10 (s, 3H), 2.03 (d, *J* = 7.4 Hz, 1H), 1.95 (t, *J* = 2.6 Hz, 1H), 1.83 (p, *J* = 6.9 Hz, 3H), 1.47 (s, 3H), 1.44 (d, *J* = 6.8 Hz, 3H), 1.33 – 1.16 (m, 7H), 0.84 (t, *J* = 7.0 Hz, 3H). ^{13}C NMR (101 MHz, $CDCl_3$) δ 174.0, 172.3, 109.7, 83.2, 82.8, 73.4, 72.9, 71.8, 69.3, 68.6, 66.7, 62.8,

59.2, 52.1, 41.7, 38.3, 37.8, 35.7, 32.9, 27.9, 26.0, 23.5, 22.4, 21.6, 17.8, 14.3, 13.0. HRMS (ESI) m/z calcd for $C_{27}H_{43}O_6N_2S^{35}ClNa$ $[M + Na]^+$, 581.2423, found 581.2415.

Clindamycin Hexynoate (223)

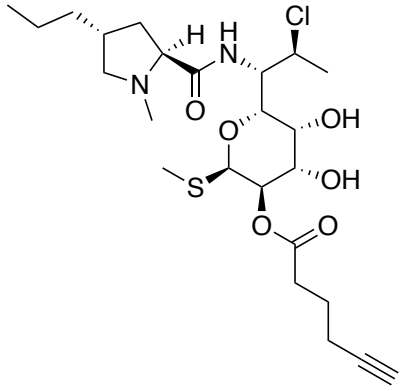

Ester **222** (139 mg, 0.24 mmol) was dissolved in a 9:1 mixture of MeOH:HCl (1 M, aq) and stirred at r.t. for 1 h, after which point the temperature was raised to 60 °C and stirring was allowed to continue for a further 2 h. The reaction mixture was then concentrated under reduced pressure. The resulting crude material was diluted with saturated aqueous $NaHCO_3$ (10 mL) before being extracted with EtOAc (3 × 15 mL). The combined organic layers were dried over $MgSO_4$, filtered and concentrated under reduced pressure. Purification was performed by flash column chromatography (Hexane/EtOAc, 0 -> 100%) to yield the title compound as a white solid (107 mg, 83%) ^1H NMR (400 MHz, $CDCl_3$) δ 8.09 (d, *J* = 9.3 Hz, 1H), 5.54 (d, *J* = 5.7 Hz, 1H), 5.15 (dd, *J* = 10.3, 5.6 Hz, 1H), 5.07 (d, *J* = 3.6 Hz, 1H), 4.70 (qd, *J* = 6.7, 1.5 Hz, 1H), 4.23 – 4.12 (m, 1H), 4.07 (d, *J* = 10.0 Hz, 1H), 3.85 (td, *J* = 9.9, 3.6 Hz, 1H), 3.67 (t, *J* = 3.6 Hz, 1H), 3.24 (s, 1H), 3.07 (dd, *J* = 11.2, 4.2 Hz, 1H), 2.79 (d, *J* = 10.2 Hz, 1H), 2.54 (td, *J* = 7.4, 1.5 Hz, 2H), 2.43 (s, 3H), 2.28 (td, *J* = 7.0, 2.6 Hz, 2H), 2.12 (s, 3H), 2.09 (s, 1H), 1.99 – 1.85 (m, 3H), 1.52 (d, *J* = 6.8 Hz, 3H), 1.40 – 1.23 (m, 4H), 0.90 (m, 3H). ^{13}C NMR (101 MHz, $CDCl_3$) δ 178.01, 172.71, 84.04, 83.32,

71.33, 69.51, 69.10, 68.33, 68.26, 67.98, 62.75, 56.72, 53.22, 42.02, 38.03, 37.89, 35.57, 32.98, 23.57, 22.58, 21.54, 17.82, 14.25, 12.92. HRMS (ESI) *m*/*z* calcd for $C_{24}H_{40}O_6N_2S^{35}Cl$ $[M + H]^+$, 519.2290, found 519.2310.

Erythromycin-2′-glutarate (224)

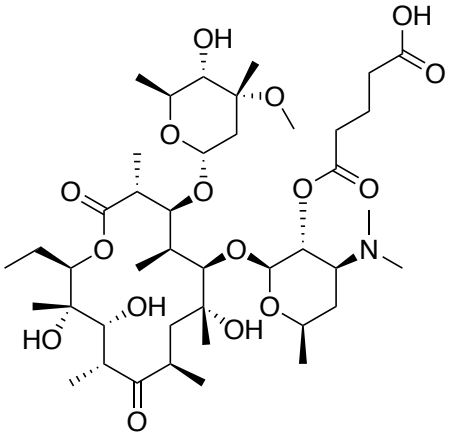

The title compound was prepared using a modified version of the procedure detailed by Bosniakovic *et al*.[187] Erythromycin (500 mg, 0.68 mmol) and glutaric anhydride (155 mg, 1.36 mmol) were dissolved in DMF (10 mL) and placed under a nitrogen atmosphere.[187] Et_3N (137 mg, 1.36 mmol) was added and the reaction mixture was allowed to stir for 72 h at r.t. before being concentrated under reduced pressure. Purification was performed by flash column chromatography (MeOH/EtOAc/Hexane, 5:2:2) to yield the title compound as a white solid (435 mg, 75%) ^{1}H NMR (400 MHz, $CDCl_3$) δ 5.02 (dd, *J* = 10.9, 2.3 Hz, 1H), 4.89 – 4.84 (m, 2H), 4.58 (d, *J* = 7.2 Hz, 1H), 3.91 (dd, *J* = 12.9, 8.0 Hz, 2H), 3.77 (s, 1H), 3.50 (ddd, *J* = 26.2, 10.5, 4.7 Hz, 2H), 3.35 (s, 3H), 3.03 (dd, *J* = 14.1, 8.0 Hz, 3H), 2.83 (td, *J* = 15.9, 13.4, 5.8 Hz, 1H), 2.64 (t, *J* = 9.1 Hz, 1H), 2.41 (s, 6H), 2.36 – 2.19 (m, 4H), 2.01 – 1.66 (m, 7H), 1.62 – 1.50 (m, 2H), 1.41 (s, 3H), 1.28 – 1.06 (m, 23H), 0.89 (d, *J* = 7.4 Hz, 3H), 0.82 (t, *J* = 7.4 Hz, 3H). ^{13}C NMR (101 MHz, $CDCl_3$) δ 175.5, 172.4, 100.4, 96.1, 83.6, 79.7, 77.9, 76.9, 74.8, 74.6, 72.8, 70.8, 69.0, 67.6, 65.7, 62.5, 49.5, 45.1, 44.8, 39.3,

39.0, 38.1, 37.9, 35.9, 35.0, 34.8, 29.0, 27.0, 21.5, 21.2, 18.7, 18.2, 16.4, 16.0, 12.0, 10.6, 9.2. HRMS (ESI) *m/z* calcd for $C_{42}H_{74}NO_{16}$ $[M + H]^+$, 848.5002, found 848.5055. Analytical data consistent with those reported in the literature.[187]

Erythromycin-2′-glutarate propargyl ester (225)

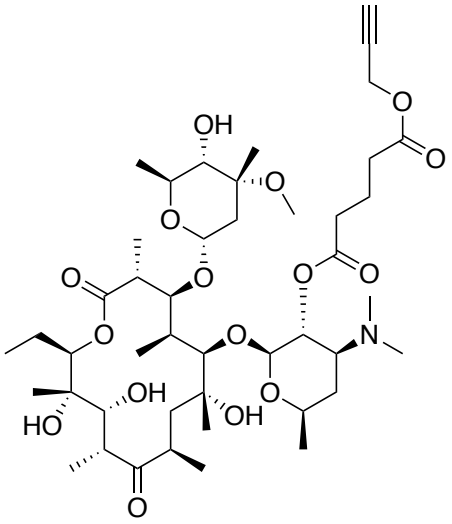

Carboxylic acid **224** (200 mg, 0.23 mmol) was dissolved in DMF (10 mL) followed by the addition of K_2CO_3 (65 mg, 0.46 mmol) and propargyl bromide (28 mg, 0.23 mmol). The reaction mixture was allowed to stir for 18 h at r.t. before being concentrated under reduced pressure. Purification was perfumed by flash column chromatography (MeOH/Hexane/EtOAc, 5:2:2) to yield the title compound as a white solid (180 mg, 88%). ^{1}H NMR (400 MHz, DMSO) δ 5.10 (dd, *J* = 10.7, 2.5 Hz, 1H), 4.78 – 4.48 (m, 4H), 4.41 (d, *J* = 7.5 Hz, 1H), 4.27 (s, 1H), 4.00 (dd, *J* = 9.4, 6.2 Hz, 1H), 3.91 (d, *J* = 9.2 Hz, 1H), 3.85 (d, *J* = 5.4 Hz, 1H), 3.72 (dt, *J* = 9.0, 4.5 Hz, 2H), 3.53 (t, J = 2.5 Hz, 1H), 3.44 (d, J = 6.5 Hz, 1H), 3.24 (s, 3H), 2.96 – 2.92 (m, 1H), 2.88 – 2.75 (m, 3H), 2.63 (td, *J* = 15.6, 15.2, 3.3 Hz, 1H), 2.46 – 2.22 (m, 6H), 2.14 (s, 5H), 1.93 – 1.65 (m, 6H), 1.63 – 1.47 (m, 2H), 1.30 – 0.96 (m, 27H), 0.84 (d, *J* = 7.4 Hz, 3H), 0.76 (t, *J* = 7.4 Hz, 3H). ^{13}C NMR (101 MHz, DMSO) δ 175.19, 172.30, 99.57, 95.18, 78.90, 77.96, 77.80, 76.22, 75.16, 73.73, 73.19, 71.82, 67.52, 65.40,

63.06, 52.00, 49.27, 44.58, 36.26, 35.33, 33.48, 32.75, 32.23, 31.25, 29.77, 26.90, 21.70, 21.59, 21.40, 20.36, 19.01, 18.75, 17.72, 15.97, 12.06, 11.14, 9.46. HRMS (ESI) *m*/*z* calcd for $C_{45}H_{76}NO_{16}$ $[M + H]^+$, 886.5159, found 886.5194.

4-(10,15,20-Triphenylporphyrin-5-yl)phenol (230)

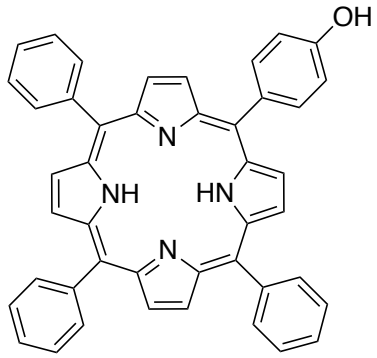

Benzaldehyde (5.74 g, 54.00 mmol) and 4-Hydroxybenzaldehyde (2.20 g, 18.00 mmol) were dissolved in propanoic acid (250 mL). The reaction mixture was heated to 120 °C before the addition of pyrrole (4.84 g, 72.00 mmol). The resulting solution was stirred at reflux for 1 h before being allowed to cool to r.t.. The reaction mixture was then concentrated under reduced pressure. The crude material was recrystallised using ethanol (120 mL) to give a purple solid which was further purified by flash column chromatography ($CHCl_3$:Acetone, 14:1) to yield the title compound as a purple solid (0.65 g, 6%). ^{1}H NMR (400 MHz, DMSO) δ 9.99 (s, 1H, OH), 8.92 (d, *J* = 4.8 Hz, 2H, ArH), 8.82 (d, *J* = 3.7 Hz, 6H. ArH), 8.24 – 8.17 (m, 6H, ArH), 8.05 – 7.98 (m, 2H, ArH), 7.84 – 7.77 (m, 9H, ArH), 7.24 – 7.19 (m, 2H, ArH), -2.89 (s, 2H, NH). ^{13}C NMR (101 MHz, DMSO) δ 158.0, 141.8, 141.7, 136.0, 134.7, 132.2, 128.5, 127.5, 121.2, 120.4, 120.1, 114.4. HRMS (ESI) *m*/*z* calcd for $C_{44}H_{31}N_4O$ $[M + H]^+$, 631.2492, found 631.2486. Analytical data consistent with those reported in the literature.[209]

5,10,15-Triphenyl-20-(4-(prop-2-yn-1-yloxy)phenyl)porphyrin (231)

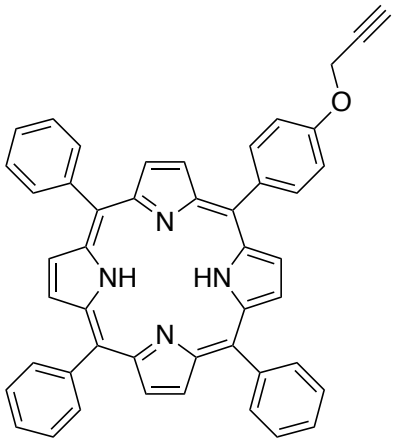

The title compound was synthesised according to General Procedure F from Porphyrin **230** (0.65 g, 1.03 mmol) and K_2CO_3 (1.42 g, 10.30 mmol) were suspended in acetone (70 mL). Propargyl bromide (0.67 g, 5.65 mmol) was added dropwise and the reaction mixture was heated to reflux and stirred for 18 h. The reaction mixture was then allowed to cool to r.t. before being concentrated under reduced pressure. The crude material was then dissolved in CH_2Cl_2 (100 mL) and washed with H_2O (3 × 100 mL) before being dried over $MgSO_4$, filtered and concentrated under reduced pressure. Purification was performance by flash column chromatography ($CHCl_3$/ Petroleum ether, 4:1) to yield the title compound as a purple solid (0.57 g, 82%). ^{1}H NMR (400 MHz, DMSO) δ 8.87 (d, *J* = 4.8 Hz, 2H, ArH), 8.83 (d, *J* = 3.9 Hz, 6H, ArH), 8.24 – 8.18 (m, 6H, ArH), 8.17 – 8.10 (m, 2H, ArH), 7.88 – 7.77 (m, 9H, ArH), 7.44 – 7.38 (m, 2H, ArH), 5.09 (d, *J* = 2.4 Hz, 2H, CH_2), 3.76 (t, *J* = 2.4 Hz, 1H, CH), -2.89 (s, 2H, NH). 13C NMR (101 MHz, DMSO) δ 157.7 (ArC), 140.2 (ArC), 135.8 (ArC), 134.7 (ArC), 134.5 (ArC), 128.5 (ArC), 127.5 (ArC), 120.4 (ArC), 120.4 (ArC), 120.3 (ArC), 113.8 (ArC), 79.9 (CH), 79.1 (C), 56.2 (CH_2). Parent ion not observed in HR-MS. Analytical data consistent with those reported in the literature.[210]

Copper (II) 5,10,15-triphenyl-20-(4-(prop-2-yn-1-yloxy)phenyl)porphyrin (226)

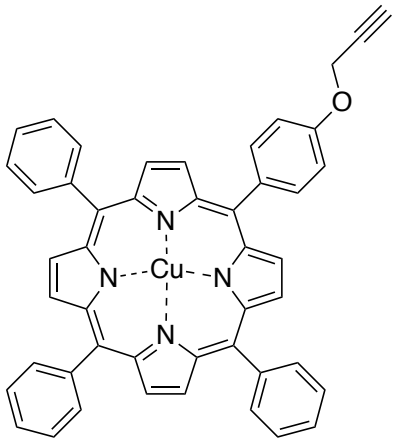

The title compound was synthesised according to General Procedure K from **231** (75 mg, 0.11 mmol) and $Cu(OAc)_2.H_2O$ (44 mg, 0.22 mmol). Purification was performed by flash column chromatography ($CHCl_3$/Petroleum ether, 4:1) to yield the title compound as a bright-blue solid (72 mg, quant.). No NMR data due to paramagnetic nature of the Cu^{2+} ion. HRMS (ESI) *m/z* calcd for $C_{47}H_{30}ON_4CuNa$ $[M + Na]^+$, 752.1608, found 752.1599.

Zinc (II) 5,10,15-triphenyl-20-(4-(prop-2-yn-1-yloxy)phenyl)porphyrin (227)

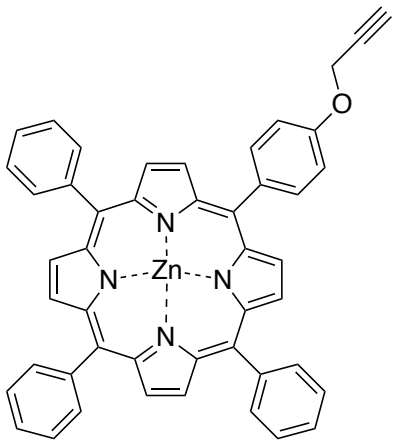

The title compound was synthesised according to General Procedure K from **231** (75 mg, 0.11 mmol) and $Zn(OAc)_2.2H_2O$ (48 mg, 0.22 mmol). Purification was performed

by flash column chromatography ($CHCl_3$/Petroleum ether, 4:1) to yield the title compound as a bright-purple solid (72 mg, quant.). ^{1}H NMR (400 MHz, $CDCl_3$) δ 9.02 – 8.94 (m, 8H), 8.30 – 8.21 (m, 6H), 8.17 (d, J = 8.1 Hz, 2H), 7.78 (d, *J* = 7.3 Hz, 9H), 7.39 (d, *J* = 8.0 Hz, 2H), 5.02 (d, *J* = 2.4 Hz, 2H), 2.72 (t, *J* = 2.4 Hz, 1H). ^{13}C NMR (101 MHz, $CDCl_3$) δ 157.3, 150.5, 150.2, 142.8, 135.4, 134.4, 132.0, 127.5, 126.6, 122.7, 121.3, 113.0, 77.2, 75.8, 56.2. HRMS (ESI) *m*/*z* calcd for $C_{47}H_{71}N_4OZn$ $[M + H]^+$, 731.1784, found 731.1759.

Iron (III) 5,10,15-triphenyl-20-(4-(prop-2-yn-1-yloxy)phenyl)porphyrin (228)

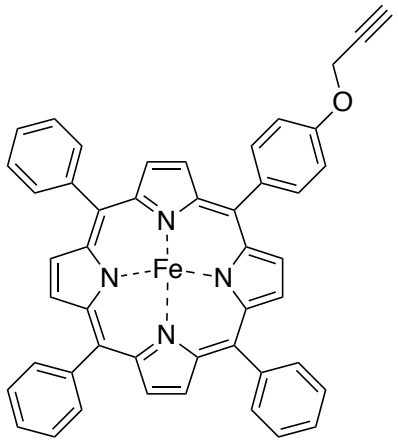

The title compound was synthesised according to General Procedure K from **231** (75 mg, 0.11 mmol) and $FeCl_2.4H_2O$ (43 mg, 0.22 mmol). Purification was performed by flash column chromatography (CH_2Cl_2/MeOH, 9:1) to yield the title compound as a dark-blue solid (72 mg, quant.). No NMR data due to paramagnetic nature of the Cu^{2+} ion. HRMS (ESI) *m*/*z* calcd for $C_{47}H_{30}N_4OFe$ $[M]^+$, 722.1764 found 722.1783.

N-(2-Ethoxy-2-oxoethyl)-N,N- dimethylprop-2-yn-1-aminium bromide (229)

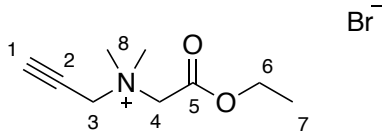

N,N-Dimethylglycine ethyl ester (3.99 g, 30.41 mmol) was dissolved in anhydrous THF (30 mL). Propargyl bromide (2.94 g, 20.00 mmol) was added dropwise over 2 min and the reaction mixture was stirred at r.t. for 18 h. The resulting solid was extracted by filtration and washed repeatedly with Hexane before being dried under reduced pressure to yield the title compound as white solid (4.78 g, 96%). ^{1}H NMR (400 MHz, DMSO) δ 4.62 (d, *J* = 2.6 Hz, 2H, H-3), 4.54 (s, 2H, H-4), 4.25 (q, *J* = 7.1 Hz, 2H, H-6), 4.16 (t, *J* = 2.5 Hz, 1H, H-1), 3.30 (s, 6H, H-8), 1.26 (t, *J* = 7.1 Hz, 3H, H-7). ^{13}C NMR (101 MHz, DMSO) δ 165.5 (CO), 83.5 (C), 72.2 (CH), 62.7 (CH_2), 60.5 (CH_2), 57.1 (CH_3), 52.3 (CH_2), 9.7 (CH_3). HRMS (ESI) *m/z* calcd for $C_9H_{16}N_1O_2$ $[M]^+$, 170.1176 found 170.1194. Analytical data consistent with those reported in the literature.[211]

3-Oxo-7-(prop-2-yn-1-yloxy)-3*H*-phenoxazine 10-oxide (235)

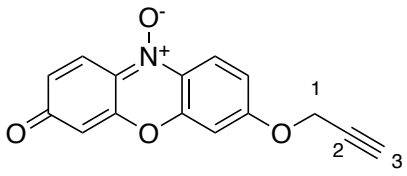

Resazurin sodium salt (0.10 g, 0.39 mmol) was dissolved in anhydrous DMF (3 mL) followed by the addition of propargyl bromide (71 mg, 0.59 mmol). The reaction mixture was placed under a nitrogen atmosphere and stirred at 60 °C for 18 h. The solvent was then removed under reduced pressure. Purification was performed by

flash column chromatography (CH_2Cl_2/MeOH, 0 -> 4%) to yield the title compound as a bright-red solid. ^{1}H NMR (400 MHz, DMSO) δ 8.11 (d, *J* = 9.3 Hz, 1H, CH), 8.00 (d, *J* = 10.0 Hz, 1H, ArH), 7.26 (d, *J* = 2.6 Hz, 1H, CH), 7.12 (dd, *J* = 9.3, 2.6 Hz, 1H, CH), 6.68 (dd, *J* = 10.2, 2.0 Hz, 1H, ArH), 6.19 (d, *J* = 1.9 Hz, 1H, ArH), 5.03 (d, *J* = 2.4 Hz, 2H, H-1), 3.72 (t, *J* = 2.4 Hz, 1H, H-3). 13C NMR (101 MHz, DMSO) δ 184.2, 162.0, 153.8, 149.0, 132.5, 131.3, 125.4, 123.5, 121.8, 114.3, 104.7, 102.4, 79.9, 78.6, 57.2. HRMS (ESI) *m*/*z* calcd for $C_{15}H_9O_4NNa$ [M + Na]$^+$, 290.0424, found 290.0430.

(4-(Prop-2-yn-1-yloxy)phenyl)methanamine (237)

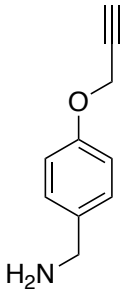

4-Hydroxybenzylamine (3.00 g, 24.40 mmol) was dissolved in DMF (30 mL) and K_2CO_3 (3.68 g, 26.70 mmol) was added in a single portion. The reaction mixture was heated to 60 ºC for 1 h before being allowed to cool to r.t. followed by the addition of propargyl bromide (2.90 g, 24.40 mmol). The reaction mixture was allowed to stir for 18 before being diluted with H2O. The aqueous phase was extracted with EtOAc (3 30 mL). The combined organic phase was the washed with saturated aqueous $NaHCO_3$, H_2O and brine (30 mL) each. The organic phase was dried over $MgSO_4$, filtered and concentrated under reduced pressure. Purification was performed by flash column chromatography (Hexane/EtOAc, 1:1) to yield the title compound as a brown oil (2.50 g, 65%). ^{1}H NMR (400 MHz, $CDCl_3$) δ 7.09 – 7.04 (m, 2H, ArH), 6.75

– 6.69 (m, 2H, ArH), 3.69 (s, 2H, CH_2NH_2), 3.31 (d, *J* = 2.4 Hz, 2H, C*H*$_2$CCH), 2.20 (t, *J* = 2.4 Hz, 1H, CH). ^{13}C NMR (101 MHz, $CDCl_3$) δ 154.1 (ArC), 129.7 (ArC), 129.6 (ArC), 115.4 (ArC), 81.9 (C), 71.6 (CH), 51.6 (CH_2NH_2), 36.9 (CH_2). HRMS (ESI) *m/z* calcd for $C_{10}H_{12}NO$ $[M + H]^+$, 162.0913, found 162.0911. Analytical data consistent with those reported in the literature.[212]

(*E*)-2-((4-(Dimethylamino)phenyl)diazenyl)-*N*-(4-(prop-2-yn-1-yloxy)benzyl)benzamid (238)

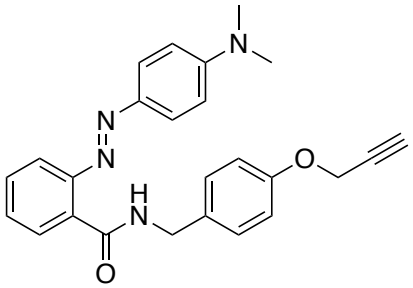

The title compound was synthesised according to General Procedure J from Methyl Red (1.00 g, 3.71 mmol), **237** (0.89 g, 5.65 mmol) and DMAP (42 mg, 0.39 mmol) were dissolved in CH_2Cl_2 (20 mL) and cooled to 0 °C. DCC (1.18 g, 5.65 mmol) was added in a single portion and the resulting suspension was allowed to warm to r.t. and stirred for 18 h. The solid was removed by filtration and washed with CH_2Cl_2 (100 mL) and the resulting filtrate was concentrated under reduced pressure. Purification was performed by flash column chromatography (Hexane/EtOAc, 0 -> 80%) to yield the title compound as a red solid (1.72 g, 74%). ^{1}H NMR (400 MHz, $CDCl_3$) δ 7.94 (dd, *J* = 7.7, 1.4 Hz, 1H, ArH), 7.92 – 7.88 (m, 2H, ArH), 7.72 (dd, *J* = 8.1, 1.3 Hz, 1H, ArH), 7.63 (td, *J* = 7.7, 1.5 Hz, 1H, ArH), 7.52 – 7.45 (m, 1H, ArH), 7.43 – 7.38 (m, 2H, ArH), 7.22 – 7.18 (m, 2H, ArH), 6.76 – 6.70 (m, 2H, ArH), 3.91 (s, 2H, CH_2), 3.45 (d, *J* = 2.4 Hz, 2H, C*H*$_2$CCH), 3.09 (s, 6H, $(CH_3)_2$), 2.29 (t, *J* = 2.4 Hz, 1H, CH). ^{13}C NMR (101 MHz, $CDCl_3$) δ 166.7 (CO), 150.2 (ArC), 143.8 (ArC), 136.8 (ArC), 132.3 (ArC), 130.0 (ArC), 129.4 (ArC), 128.4 (ArC), 125.6 (ArC), 121.7 (ArC), 119.4 (ArC),

115.5 (ArC), 111.4 (ArC), 81.3 (C), 71.7 (CH), 51.7 (CH_2), 40.3 (CH_3), 37.3 (CH_2CH). HRMS (ESI) *m/z* calcd for $C_{25}H_{25}N_5O_5$ [M + H]$^+$, 413.1972, found 413.1982.

Cyclic RGDFK(BCN) (244)

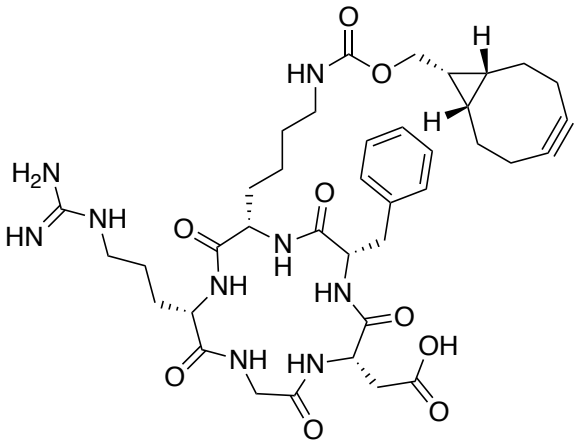

Cyclic RGDFK peptide (645 mg, 1.07 mmol) was dissolved in DMF (10 mL) followed by the addition of BCN-*p*NP (535 mg, 1.70 mmol) in DMF (5 mL). Et3N (0.44 g, 3.21 mmol) was added dropwise to the reaction mixture, resulting in the formation of a bright yellow solution. The reaction mixture was allowed to stir at r.t. for 2.5 h, after which point HR-MS indicated the complete consumption of the peptide starting material. The reaction mixture was concentrated under reduced pressure. The crude material was redissolved in ACN and a few drops of DMSO, remaining solids were removed by filtration through a Minisart syringe driven PTFE-membrane (0.45 µm). Purification was performed by semi-preparative reverse-phase high-performance liquid chromatography (Method 8) to yield the title compound as a white solid (100 mg, 13%). HRMS (ESI) *m/z* calcd for $C_{38}H_{54}O_9N_9$ [M + H]$^+$, 780.4039, found 780.4038

(BCN)Aminohexanoic YIGSR (245)

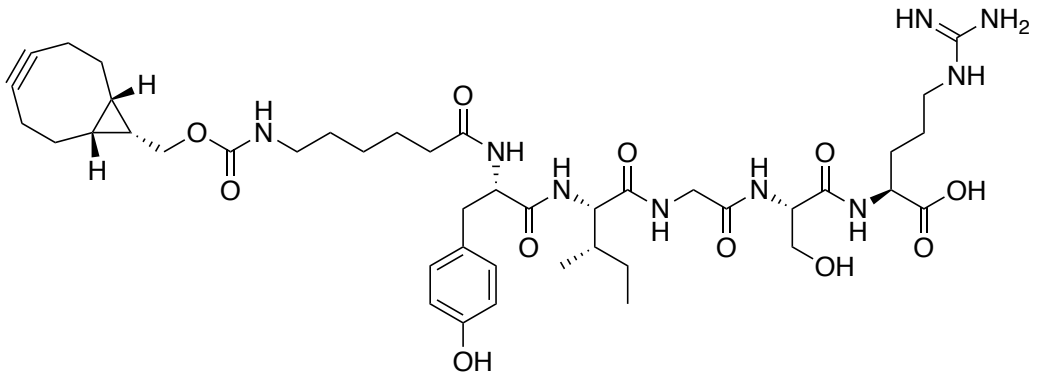

Cyclic RGDFK peptide (25 mg, 35 μmol) was dissolved in DMF (3 mL) followed by the addition of BCN-*p*NP (16 mg, 52 μmol) in DMF (1 mL). Et_3N (100 μL) was added dropwise to the reaction mixture, resulting in the formation of a bright yellow solution. The reaction mixture was allowed to stir at r.t. for 2 h, after which point HR-MS indicated the complete consumption of the peptide starting material. The reaction mixture was concentrated under reduced pressure. The crude material was redissolved in ACN and a few drops of DMSO, remaining solids were removed by filtration through a Minisart syringe driven PTFE-membrane (0.45 µm). Purification was performed by semi-preparative reverse-phase high-performance liquid chromatography (Method 8) to yield the title compound as a white solid (13 mg, 41%). LRMS (ESI) *m/z* calcd for $C_{38}H_{54}O_9N_9$ $[M + H]^+$, 884.4, found 883.9

7.6 Biological Methods

Protein Purification Buffers

Buffer	Composition
Lysis	20 mM Tris, 300 mM NaCl, pH 7.5, 20 mM Imidazole
Affinity Chromatography Binding	Same as Lysis Buffer
Affinity Chromatography Elution	20 mM Tris, 300 mM NaCl, pH 7.5, 500 mM Imidazole
Storage	30 mM PIPES, pH 6.8 (adjusted with NaOH), 10% Glycerol

Protein Expression and Purification

The InhA:pET15a construct was kindly provided by Prof. Peter Tonge.[74] A single colony from a BL21 InhA agar plate was grown overnight in 10mL LB media containing 100μg mL^{-1} ampicillin, at 37 °C with 180rpm shaking. The protein was induced with 1 mM IPTG in a Luria Bertran (LB) broth (containing ampicillin 100 μg mL^{-1}) and grown at 30 °C for 6h until the OD_{600} reached 0.6 – 0.7. The protein was isolated via cell lysis using sonication followed by centrifugation at 30,000 g for 30 min at 4 °C. Purification was performed using a Ni-affinity His-Trap 5 mL column (GE Healthcare). The column was washed with 150 mL binding buffer [Tris HCl (20 mM), NaCl (300 nM)], imidazole (500 mM), pH 7.5) and the protein was eluted with elution buffer [Tris HCl (20 mM, NaCl, (300 nM), imidazole (500 mM), pH 7.5] in a 0-100 % gradient of the elution buffer. The protein was analysed with SDS-PAGE and then exchanged to a storage buffer (PIPES, 30 mM, pH 6.8) and concentrated to 10 mg/mL using a 10 kDa Amikon centrifugal filter (Millipore). Aliquots were then mixed with 10% glycerol and stored at -80°C. The molecular weight (29.806 Da) and pI (6.10)

and extinction coefficient was determined using the ExPasy translate tool. The extinction co-efficient 37.5 $mM^{-1}cm^{-1}$ at λ_{280} was used in calculation of the protein concentration.

Enzyme Inhibition Studies

In vitro enzyme inhibition studies were carried out where the compounds were screened at a concentration of 50 µM using the thermostated UV-Vis spectrophotometer (Tecan Sunrise) at 340 nm as described below.

The assay reaction conditions were as follows for a 100 µL volume: buffer (to volume), PIPES (30 mM), Inhibitor (50 μM), OCoA (400 µM), NADH (100 µM) and InhA (150 nM). The compounds were dissolved in 1 M NaOH. It was found that 0.5% 1 M NaOH caused inhibition of 18% compared to the standard reaction. The total NaOH concentration in the reaction mixture was therefore kept constant (0.5 %).

Blank: buffer (to volume), PIPES (30 mM, pH 6.8), 1 M NaOH (0.5 %), OCoA (400 µM), NADH (100 µM) and InhA (150 nM).

To obtain the percentage of enzyme inhibition the initial velocity (v) for the 120 seconds was established and this was compared to the velocity of the blank (v_0). The initial velocity was calculated from the gradient of the absorbance vs time plots for each of the inhibitors and blanks. Inhibitory activities of the compounds were calculated as a percentage using the formula $(1 - v/v_0) \times 100$ %, where v/v_0 is the residual activity of the enzyme.

IC_{50} values were determined using the log(inhibitor) vs response — variable slope (four parameters) nonlinear regression analysis function in GraphPad Prism 8.0.

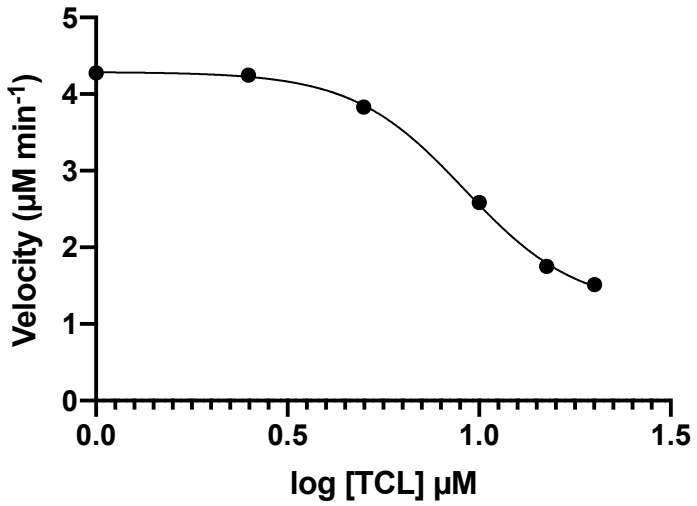

IC_{50} curve for TCL against purified InhA

Whole Cell Screening

Bacterial strains and growth conditions

Mycobacterium bovis BCG (strain Pasteur) was cultured at 37C and 5% CO_2, static, in Middlebrook 7H9 media supplemented with 0.05% Tween-80 and 10% (v/v) BBL Middlebrook OADC enrichment.

MIC_{99} determination

The measurement of the minimum inhibitory concentration (MIC_{99}) was performed in 96-well flat bottom, black polystyrene microtiter plates (Greiner) in a final volume 200 µl. Two-fold drug dilutions in neat DMSO were performed and added to the microtiter plate at a final concentration of 1% DMSO. 1% DMSO was used as a positive control and rifampicin as a negative. The inoculum was standardised at OD_{600} 0.05 in Middlebrook 7H9 medium (Difco) and added to the plate. Plates were incubated without shaking at 37°C, 5% CO_2 for 7 days. Following incubation, 42 µl of resazurin (0.02% v/v in dH_2O) was added to each well and incubated for a further 24 h.

Fluorescence was measured (Polar star omega plate reader ex 544, em 590) to determine the MIC_{99} value.

Compound activity screening

Screens were performed in 96-well flat bottom, black polystyrene microtiter plates (Greiner). Compounds in 100% DMSO were added at 20 µM and 2 µM (final concentration 1% DMSO) and made up to a final volume of 200 µl with inoculum standardised at OD_{600} 0.05. Plates were incubated for 7 days at 37°C, 5% CO_2 without shaking, and the percent inhibition calculated using the resazurin assay described above and the following equation: ((test compound – mean rifampicin negative control)/(mean positive DMSO control – mean rifampicin negative control))*100

7.7 Computational Methods

GOLD RMSD Calculations

Protein structures were individually prepared using the Maestro Protein Preparation tool. In doing so, any incorrect atom valences were corrected, water molecules were removed and the protein structures were minimised. Ligand structures were redrawn in Maestro and their structures were minimised using the LigPrep tool.

Following this each protein and ligand were loaded into the GOLD software package. The *in situ* ligand was extracted from the protein and its coordinates were used to define the active site, while the NAD^+ co-factor was left in place. The GoldScore scoring function was used for the docking calculations and the search exhaustivity was set at the default 100% setting. Each protein:ligand complex was allowed to generate up to 10 docking solutions. The docking solutions for each ligand were

exported as a Spatial Data File (SDF). The RMSD of these docking solutions was then compared to the experimentally observed binding poses using the ‘In Place Translation’ tool in Schrödinger Maestro. cLogP values were calculated using the QikProp tool in Schrödinger Maestro.6

8.0 References

1. M. R. Zimmerman, Bull. N. Y. Acad. Med., 1979, **55**, 604-608.
2. H. D. Donoghue, O. Y. Lee, D. E. Minnikin, G. S. Besra, J. H. Taylor and M. Spigelman, *Proc. Biol. Sci.*, 2010, **277**, 51-56.
3. A. Sakula, *Can. Vet. J.*, 1983, **24**, 127-131.
4. E. Cambau and M. Drancourt, *Clin. Microbiol. Infect.*, 2014, **20**, 196-201.
5. World Health Organisation, *Global Tuberculosis Report*, 2019.
6. K. A. Alexander, P. N. Laver, A. L. Michel, M. Williams, P. D. van Helden, R. M. Warren and N. C. Gey van Pittius, *Emerg. Infect. Dis.*, 2010, **16**, 1296-1299.
7. P. Sinha, A. Gupta, P. Prakash, S. Anupurba, R. Tripathi and G. N. Srivastava, *BMC Infect. Dis.*, 2016, **16**, 123.
8. G. Delogu, M. Sali and G. Fadda, *Mediterr. J. Hematol. Infect. Dis.*, 2013, **5**, e2013070.
9. J. Madacki, G. Mas Fiol and R. Brosch, *Infect. Genet. Evol.*, 2019, **72**, 67-77.
10. C. B. Beggs, C. J. Noakes, P. A. Sleigh, L. A. Fletcher and K. Siddiqi, *Int. J. Tuberc. Lung. Dis.*, 2003, **7**, 1015-1026.
11. S. Ravimohan, H. Kornfeld, D. Weissman and G. P. Bisson, *Eur. Respir. Rev.*, 2018, **27**, 170077.
12. J. Y. Lee, Tuberc. Respir. Dis. (Seoul), 2015, **78**, 47-55.
13. F. Byarugaba, E. M. Charles-Etter, S. Godreuil and P. Grimaud, *Emerg. Infect. Dis.*, 2009, **15**, 124-125.
14. S. Kiazyk and T. B. Ball, *Can. Commun. Dis. Rep.*, 2017, **43**, 62-66.
15. G. Manina, N. Dhar and John D. McKinney, *Cell Host & Microbe*, 2015, **17**, 32-46.
16. R. M. G. J. Houben and P. J. Dodd, *PLOS Medicine*, 2016, **13**, e1002152.
17. S. Luca and T. Mihaescu, *Maedica (Buchar)*, 2013, **8**, 53-58.
18. L. C. Rodrigues, V. K. Diwan and J. G. Wheeler, *Int. J. Epidemiol.*, 1993, **22**, 1154-1158.
19. H. M. Dockrell and S. G. Smith, *Front. Immunol.*, 2017, **8**, 1134.
20. G. Sotgiu, R. Centis, L. D'Ambrosio and G. B. Migliori, *Cold Spring Harb. Perspect. Med.*, 2015, **5**, a017822.
21. M. L. Bastos, Z. Lan and D. Menzies, *Eur. Respir. J.*, 2017, **49**, 1600803.
22. M. F. Rabahi, J. Silva Júnior, A. C. G. Ferreira, D. G. S. Tannus-Silva and M. B. Conde, *J. Bras. Pneumol.*, 2017, **43**, 472-486.
23. P. Sensi, Rev. Infect. Dis., 1983, **5 Suppl 3**, S402-406.
24. W. Mahatthanatrakul, T. Nontaput, W. Ridtitid, M. Wongnawa and M. Sunbhanich, *J. Clin. Pharm. Ther.*, 2007, **32**, 161-167.
25. H. M. Bolt, *Drug Metab. Rev.*, 2004, **36**, 497-509.
26. J. F. Murray, D. E. Schraufnagel and P. C. Hopewell, *Ann. Am. Thorac. Soc.*, 2015, **12**, 1749-1759.
27. G. F. d. S. Fernandes, H. R. N. Salgado and J. L. d. Santos, *Crit. Rev. Anal. Chem.*, 2017, **47**, 298-308.
28. B. Rubin, G. L. H. Jr., B. G. H. Thomas and J. C. Burke, *Am. Rev. Tuberc.*, 1952, **65**, 392-401.
29. D. F. E. Jr., W. D. Cawthon, C. Muschenheim and W. McDermott, *Am. Rev. Tuberc.*, 1952, **65**, 429-442.
30. E. H. Robitzek and I. J. Selikoff, *Am. Rev. Tuberc.*, 1952, **65**, 402-428.
31. W. M. Benson, P. L. Stefko and M. D. Roe, *Am. Rev. Tuberc.*, 1952, **65**, 376-391.
32. W. S. Jr. and E. Wolinsky, *Am. Rev. Tuberc.*, 1952, **65**, 365-375.

33. R. L. Yeager, W. G. Munroe and F. I. Dessau, *Am Rev Tuberc*, 1952, **65**, 523-546.
34. M. Solotorovsky, F. J. Gregory, E. J. Ironson, E. J. Bugie, R. C. O'Neill and R. Pfister, 3rd, *Proc. Soc. Exp. Biol. Med.*, 1952, **79**, 563-565.
35. R. M. McCune , Jr. and R. Tompsett *J. Exp. Med.*, 1956, **104**, 737-762.
36. W. Fox, G. A. Ellard and D. A. Mitchison, *Int. J. Tuberc. Lung Dis.*, 1999, **3**, S231-279.
37. Y. Zhang, W. Shi, W. Zhang and D. Mitchison, *Microbiol. Spectr.*, 2013, **2**, 1-12.
38. Y. Zhang, S. Permar and Z. Sun, *J. Med. Microbiol.*, 2002, **51**, 42-49.
39. N. D. Peterson, B. C. Rosen, N. A. Dillon and A. D. Baughn, *Antimicrob. Agents Chemother.*, 2015, **59**, 7320-7326.
40. W. Shi, J. Chen, J. Feng, P. Cui, S. Zhang, X. Weng, W. Zhang and Y. Zhang, *Emerg. Microbes. Infect.*, 2014, **3**, e58.
41. P. Gopal, W. Nartey, P. Ragunathan, J. Sarathy, F. Kaya, M. Yee, C. Setzer, M. S. S. Manimekalai, V. Dartois, G. Grüber and T. Dick, *ACS Infect. Dis.*, 2017, **3**, 807-819.
42. R. Goude, A. G. Amin, D. Chatterjee and T. Parish, *Antimicrob. Agents Chemother.*, 2009, **53**, 4138-4146.
43. L. Deng, K. Mikusová, K. G. Robuck, M. Scherman, P. J. Brennan and M. R. McNeil, *Antimicrob. Agents Chemother.*, 1995, **39**, 694-701.
44. J. O. Kilburn and J. Greenberg, *Antimicrob. Agents Chemother.*, 1977, **11**, 534-540.
45. A. Rendon, S. Tiberi, A. Scardigli, L. D'Ambrosio, R. Centis, J. A. Caminero and G. B. Migliori, *J. Thorac. Dis.*, 2016, **8**, 2666-2671.
46. G. Günther, Clin. Med. (Lond.), 2014, **14**, 279-285.
47. N. Ndjeka, K. Schnippel, I. Master, G. Meintjes, G. Maartens, R. Romero, X. Padanilam, M. Enwerem, S. Chotoo, N. Singh, J. Hughes, E. Variava, H. Ferreira, J. te Riele, N. Ismail, E. Mohr, N. Bantubani and F. Conradie, *Eur. Respir. J.*, 2018, **52**, 1801528.
48. J. Karumbi and P. Garner, *Cochrane Database Syst. Rev.*, 2015, **2015**, Cd003343.
49. World Health Organisation, Treatment Guidelines for Drug-Resistant Tuberculosis, 2016.
50. G. B. Migliori, G. De Iaco, G. Besozzi, R. Centis and D. M. Cirillo, *Euro. Surveill.*, 2007, **12**, E070517.070511.
51. A. A. Velayati, M. R. Masjedi, P. Farnia, P. Tabarsi, J. Ghanavi, A. H. ZiaZarifi and S. E. Hoffner, *Chest*, 2009, **136**, 420-425.
52. Z. F. Udwadia, R. A. Amale, K. K. Ajbani and C. Rodrigues, *Clin. Infect. Dis.*, 2012, **54**, 579-581.
53. C. M. Nathanson, L. E. Cuevas, J. Cunningham, M. D. Perkins, R. W. Peeling, M. Guillerm, F. Moussy and A. Ramsay, *Int. J. Tuberc. Lung Dis.*, 2010, **14**, 1461-1467.
54. K. J. Kieser and E. J. Rubin, *Nat. Rev. Microbiol.*, 2014, **12**, 550-562.
55. L. J. Alderwick, J. Harrison, G. S. Lloyd and H. L. Birch, *Cold Spring Harb. Perspect. Med.*, 2015, **5**, a021113.
56. A. T. Vincent, S. Nyongesa, I. Morneau, M. B. Reed, E. I. Tocheva and F. J. Veyrier, *Front. Microbiol.*, 2018, **9**.
57. V. Dubée, S. Triboulet, J.-L. Mainardi, M. Ethève-Quelquejeu, L. Gutmann, A. Marie, L. Dubost, J.-E. Hugonnet and M. Arthur, *Antimicrob. Agents Chemother.*, 2012, **56**, 4189-4195.

58. S. G. Kurz and R. A. Bonomo, *Expert Rev. Anti Infect. Ther.*, 2012, **10**, 999-1006.
59. V. Nataraj, C. Varela, A. Javid, A. Singh, G. S. Besra and A. Bhatt, *Mol. Microbiol.*, 2015, **98**, 7-16.
60. K. Takayama, C. Wang and G. S. Besra, *Clin. Microbiol. Rev.*, 2005, **18**, 81-101.
61. Z. S. Bhat, M. A. Rather, M. Maqbool, H. U. Lah, S. K. Yousuf and Z. Ahmad, *Biomed. Pharmacother.*, 2017, **95**, 1520-1534.
62. S. Deoghare, Indian J. Pharmacol., 2013, **45**, 536-537.
63. K. Hards, J. R. Robson, M. Berney, L. Shaw, D. Bald, A. Koul, K. Andries and G. M. Cook, *J. Antimicrob. Chemother.*, 2015, **70**, 2028-2037.
64. E. Pontali, G. Sotgiu, L. D'Ambrosio, R. Centis and G. B. Migliori, *Eur. Respir. J.*, 2016, **47**, 394-402.
65. A. Xavier and M. Lakshmanan, *J. Pharmacol. Pharmacother.*, 2014, **5**, 222-224.
66. V. Skripconoka, M. Danilovits, L. Pehme, T. Tomson, G. Skenders, T. Kummik, A. Cirule, V. Leimane, A. Kurve, K. Levina, L. J. Geiter, D. Manissero and C. D. Wells, *Eur. Respir. J.*, 2013, **41**, 1393-1400.
67. S. J. Keam, *Drugs*, 2019, **79**, 1797-1803.
68. C. K. Stover, P. Warrener, D. R. VanDevanter, D. R. Sherman, T. M. Arain, M. H. Langhorne, S. W. Anderson, J. A. Towell, Y. Yuan, D. N. McMurray, B. N. Kreiswirth, C. E. Barry and W. R. Baker, *Nature*, 2000, **405**, 962-966.
69. U. Manjunatha, H. I. Boshoff and C. E. Barry, *Commun. Integr. Biol.*, 2009, **2**, 215-218.
70. F. Conradie, A. H. Diacon, N. Ngubane, P. Howell, D. Everitt, A. M. Crook, C. M. Mendel, E. Egizi, J. Moreira, J. Timm, T. D. McHugh, G. H. Wills, A. Bateson, R. Hunt, C. Van Niekerk, M. Li, M. Olugbosi and M. Spigelman, *N. Engl. J. Med.*, 2020, **382**, 893-902.
71. H. Marrakchi, M.-A. Lanéelle and M. Daffé, *Chem. Biol.*, 2014, **21**, 67-85.
72. K. A. Abrahams and G. S. Besra, *Parasitology*, 2018, **145**, 116-133.
73. N. Tahiri, P. Fodran, D. Jayaraman, J. Buter, M. D. Witte, T. A. Ocampo, D. B. Moody, I. Van Rhijn and A. J. Minnaard, *Angew. Chem., Int. Ed.*, 2020, **59**, 7555-7560.
74. S. Parikh, D. P. Moynihan, G. Xiao and P. J. Tonge, *Biochemistry*, 1999, **38**, 13623-13634.
75. A. Chollet, L. Mourey, C. Lherbet, A. Delbot, S. Julien, M. Baltas, J. Bernadou, G. Pratviel, L. Maveyraud and V. Bernardes-Génisson, *J. Struct. Biol.*, 2015, **190**, 328-337.
76. D. A. Rozwarski, C. Vilchèze, M. Sugantino, R. Bittman and J. C. Sacchettini, *J. Biol. Chem.*, 1999, **274**, 15582-15589.
77. A. Banerjee, E. Dubnau, A. Quemard, V. Balasubramanian, K. S. Um, T. Wilson, D. Collins, G. de Lisle and W. R. Jacobs, Jr., *Science*, 1994, **263**, 227-230.
78. G. S. Timmins and V. Deretic, *Mol. Microbiol.*, 2006, **62**, 1220-1227.
79. C. Metcalfe, I. K. Macdonald, E. J. Murphy, K. A. Brown, E. L. Raven and P. C. Moody, *J. Biol. Chem.*, 2008, **283**, 6193-6200.
80. D. A. Rozwarski, G. A. Grant, D. H. R. Barton, W. R. Jacobs and J. C. Sacchettini, *Science*, 1998, **279**, 98-102.
81. R. S. Magliozzo and J. A. Marcinkeviciene, *J. Biol. Chem.*, 1997, **272**, 8867-8870.
82. R. Rawat, A. Whitty and P. J. Tonge, *PNAS*, 2003, **100**, 13881-13886.

83. S. Ducasse-Cabanot, M. Cohen-Gonsaud, H. Marrakchi, M. Nguyen, D. Zerbib, J. Bernadou, M. Daffe, G. Labesse and A. Quemard, *Antimicrob. Agents Chemother.*, 2004, **48**, 242-249.
84. A. Argyrou, M. W. Vetting, B. Aladegbami and J. S. Blanchard, *Nat. Struct. Mol. Biol.*, 2006, **13**, 408-413.
85. F. Wang, P. Jain, G. Gulten, Z. Liu, Y. Feng, K. Ganesula, A. S. Motiwala, T. R. Ioerger, D. Alland, C. Vilcheze, W. R. Jacobs, Jr. and J. C. Sacchettini, *Antimicrob. Agents Chemother.*, 2010, **54**, 3776-3782.
86. N. L. Wengenack, J. R. Uhl, A. L. St Amand, A. J. Tomlinson, L. M. Benson, S. Naylor, B. C. Kline, F. R. Cockerill, 3rd and F. Rusnak, *J. Infect. Dis.*, 1997, **176**, 722-727.
87. E. R. Dalla Costa, M. O. Ribeiro, M. S. N. Silva, L. S. Arnold, D. C. Rostirolla, P. I. Cafrune, R. C. Espinoza, M. Palaci, M. A. Telles, V. Ritacco, P. N. Suffys, M. L. Lopes, C. L. Campelo, S. S. Miranda, K. Kremer, P. E. A. da Silva, L. d. S. Fonseca, J. L. Ho, A. L. Kritski and M. L. R. Rossetti, *BMC Microbiology*, 2009, **9**, 39.
88. H. Ando, Y. Kondo, T. Suetake, E. Toyota, S. Kato, T. Mori and T. Kirikae, *Antimicrob. Agents Chemother.*, 2010, **54**, 1793-1799.
89. C. E. Cade, A. C. Dlouhy, K. F. Medzihradszky, S. P. Salas-Castillo and R. A. Ghiladi, *Protein Sci*, 2010, **19**, 458-474.
90. J. N. Torres, L. V. Paul, T. C. Rodwell, T. C. Victor, A. M. Amallraja, A. Elghraoui, A. P. Goodmanson, S. M. Ramirez-Busby, A. Chawla, V. Zadorozhny, E. M. Streicher, F. A. Sirgel, D. Catanzaro, C. Rodrigues, M. T. Gler, V. Crudu, A. Catanzaro and F. Valafar, *Emerg. Microbes Infect.*, 2015, **4**, e42.
91. X. Zhao, H. Yu, S. Yu, F. Wang, J. C. Sacchettini and R. S. Magliozzo, *Biochemistry*, 2006, **45**, 4131-4140.
92. C. Vilcheze, F. Wang, M. Arai, M. H. Hazbon, R. Colangeli, L. Kremer, T. R. Weisbrod, D. Alland, J. C. Sacchettini and W. R. Jacobs, Jr., *Nat. Med.*, 2006, **12**, 1027-1029.
93. M. Seifert, D. Catanzaro, A. Catanzaro and T. C. Rodwell, *PLoS One*, 2015, **10**, e0119628.
94. C. Baldock, J. B. Rafferty, S. E. Sedelnikova, P. J. Baker, A. R. Stuitje, A. R. Slabas, T. R. Hawkes and D. W. Rice, *Science*, 1996, **274**, 2107-2110.
95. M. C. Davis, S. G. Franzblau and A. R. Martin, *Bioorg. Med. Chem. Lett.*, 1998, **8**, 843-846.
96. S. Broussy, V. Bernardes-Génisson, A. Quémard, B. Meunier and J. Bernadou, *J. Org. Chem.*, 2005, **70**, 10502-10510.
97. L. Bonnac, G.-Y. Gao, L. Chen, K. Felczak, E. M. Bennett, H. Xu, T. Kim, N. Liu, H. Oh, P. J. Tonge and K. W. Pankiewicz, *Bioorg. Med. Chem. Lett.*, 2007, **17**, 4588-4591.
98. K. Rozman, I. Sosic, R. Fernandez, R. J. Young, A. Mendoza, S. Gobec and L. Encinas, *Drug Discov. Today*, 2017, **22**, 492-502.
99. M. R. Kuo, H. R. Morbidoni, D. Alland, S. F. Sneddon, B. B. Gourlie, M. M. Staveski, M. Leonard, J. S. Gregory, A. D. Janjigian, C. Yee, J. M. Musser, B. Kreiswirth, H. Iwamoto, R. Perozzo, W. R. Jacobs, Jr., J. C. Sacchettini and D. A. Fidock, *J. Biol. Chem.*, 2003, **278**, 20851-20859.
100. X. He, A. Alian and P. R. Ortiz de Montellano, *Bioorg. Med. Chem.*, 2007, **15**, 6649-6658.
101. X. He, A. Alian, R. Stroud and P. R. Ortiz de Montellano, *J. Med. Chem.*, 2006, **49**, 6308-6323.
102. S. L. Parikh, G. Xiao and P. J. Tonge, *Biochemistry*, 2000, **39**, 7645-7650.
103. R. J. Heath, J. R. Rubin, D. R. Holland, E. Zhang, M. E. Snow and C. O. Rock, *J. Biol. Chem.*, 1999, **274**, 11110-11114.

104. S. Sivaraman, T. J. Sullivan, F. Johnson, P. Novichenok, G. Cui, C. Simmerling and P. J. Tonge, *J. Med. Chem.*, 2004, **47**, 509-518.
105. T. J. Sullivan, J. J. Truglio, M. E. Boyne, P. Novichenok, X. Zhang, C. F. Stratton, H. J. Li, T. Kaur, A. Amin, F. Johnson, R. A. Slayden, C. Kisker and P. J. Tonge, *ACS Chem. Biol.*, 2006, **1**, 43-53.
106. R. Vosatka, M. Kratky and J. Vinsova, *Eur. J. Pharm. Sci.*, 2018, **114**, 318-331.
107. S. R. Luckner, N. Liu, C. W. am Ende, P. J. Tonge and C. Kisker, *J. Biol. Chem.*, 2010, **285**, 14330-14337.
108. L. C. P. Ballell Pages, J.; Fernandez Menendez, R.; Fernandez Velando, E. P.; Gonzalez Del Valle, S.; Mendoza Osana, A.; Wolfendale, M. J., *(Pyrazol-3-yl)-1,3,4-thiadiazole-2-amine and (Pyrazol-3-yl)-1,3,4-thiazole-2-amine Compounds.*, PCT publication No. WO 2010/118852 A1, 2010.
109. J. F. M. Castro-Pichel, R.; Fenandez Velando, E. P.; Gonzelz Del Valle, S.; Mallo-Rubio, A., *3-Amino-Pyrazole Derivatives Useful Against Tuberculosis*, PCT publication No. WO 2012/049161, 2012.
110. P. S. Shirude, P. Madhavapeddi, M. Naik, K. Murugan, V. Shinde, R. Nandishaiah, J. Bhat, A. Kumar, S. Hameed, G. Holdgate, G. Davies, H. McMiken, N. Hegde, A. Ambady, J. Venkatraman, M. Panda, B. Bandodkar, V. K. Sambandamurthy and J. A. Read, *J. Med. Chem.*, 2013, **56**, 8533-8542.
111. M. Martínez-Hoyos, E. Perez-Herran, G. Gulten, L. Encinas, D. Álvarez-Gómez, E. Alvarez, S. Ferrer-Bazaga, A. García-Pérez, F. Ortega, I. Angulo-Barturen, J. Rullas-Trincado, D. Blanco Ruano, P. Torres, P. Castañeda, S. Huss, R. Fernández Menéndez, S. González del Valle, L. Ballell, D. Barros, S. Modha, N. Dhar, F. Signorino-Gelo, J. D. McKinney, J. F. García-Bustos, J. L. Lavandera, J. C. Sacchettini, M. S. Jimenez, N. Martín-Casabona, J. Castro-Pichel and A. Mendoza-Losana, *EBioMedicine*, 2016, **8**, 291-301.
112. U. H. Manjunatha, S. P. S Rao, R. R. Kondreddi, C. G. Noble, L. R. Camacho, B. H. Tan, S. H. Ng, P. S. Ng, N. L. Ma, S. B. Lakshminarayana, M. Herve, S. W. Barnes, W. Yu, K. Kuhen, F. Blasco, D. Beer, J. R. Walker, P. J. Tonge, R. Glynne, P. W. Smith and T. T. Diagana, *Sci. Transl. Med.*, 2015, **7**, 269ra263-269ra263.
113. L. Slepikas, G. Chiriano, R. Perozzo, S. Tardy, A. Kranjc, O. Patthey-Vuadens, H. Ouertatani-Sakouhi, S. Kicka, C. F. Harrison, T. Scrignari, K. Perron, H. Hilbi, T. Soldati, P. Cosson, E. Tarasevicius and L. Scapozza, *J. Med. Chem.*, 2016, **59**, 10917-10928.
114. M. M. Sim, S. B. Ng, A. D. Buss, S. C. Crasta, K. L. Goh and S. K. Lee, *Bioorg. Med. Chem. Lett.*, 2002, **12**, 697-699.
115. A. Zervosen, W. P. Lu, Z. Chen, R. E. White, T. P. Demuth, Jr. and J. M. Frere, *Antimicrob. Agents Chemother.*, 2004, **48**, 961-969.
116. E. E. Carlson, J. F. May and L. L. Kiessling, *Chem. Biol.*, 2006, **13**, 825-837.
117. D. C. Rees, M. Congreve, C. W. Murray and R. Carr, *Nat. Rev. Drug Discov.*, 2004, **3**, 660-672.
118. B. Lamoree and R. E. Hubbard, *Essays Biochem.*, 2017, **61**, 453-464.
119. C. Jacquemard and E. Kellenberger, *Expert Opin. Drug Discov.*, 2019, **14**, 413-416.
120. F. Prati, F. Zuccotto, D. Fletcher, M. A. Convery, R. Fernandez-Menendez, R. Bates, L. Encinas, J. Zeng, C. W. Chung, P. De Dios Anton, A. Mendoza-Losana, C. Mackenzie, S. R. Green, M. Huggett, D. Barros, P. G. Wyatt and P. C. Ray, *ChemMedChem*, 2018, **13**, 672-677.
121. M. Sabbah, V. Mendes, R. G. Vistal, D. M. G. Dias, M. Záhorszká, K. Mikušová, J. Korduláková, A. G. Coyne, T. L. Blundell and C. Abell, *J. Med. Chem.*, 2020, **63**, 4749-4761.

122. R. A. Goodnow, C. E. Dumelin and A. D. Keefe, *Nat. Rev. Drug Discov.*, 2017, **16**, 131-147.
123. N. Favalli, G. Bassi, J. Scheuermann and D. Neri, *FEBS Lett*, 2018, **592**, 2168-2180.
124. M. A. Clark, R. A. Acharya, C. C. Arico-Muendel, S. L. Belyanskaya, D. R. Benjamin, N. R. Carlson, P. A. Centrella, C. H. Chiu, S. P. Creaser, J. W. Cuozzo, C. P. Davie, Y. Ding, G. J. Franklin, K. D. Franzen, M. L. Gefter, S. P. Hale, N. J. V. Hansen, D. I. Israel, J. Jiang, M. J. Kavarana, M. S. Kelley, C. S. Kollmann, F. Li, K. Lind, S. Mataruse, P. F. Medeiros, J. A. Messer, P. Myers, H. O'Keefe, M. C. Oliff, C. E. Rise, A. L. Satz, S. R. Skinner, J. L. Svendsen, L. Tang, K. van Vloten, R. W. Wagner, G. Yao, B. Zhao and B. A. Morgan, *Nat. Chem. Biol.*, 2009, **5**, 647-654.
125. F. Buller, Y. Zhang, J. Scheuermann, J. Schäfer, P. Bühlmann and D. Neri, *Chemistry & Biology*, 2009, **16**, 1075-1086.
126. L. H. Yuen, S. Dana, Y. Liu, S. I. Bloom, A.-G. Thorsell, D. Neri, A. J. Donato, D. Kireev, H. Schüler and R. M. Franzini, *J. Am. Chem. Soc.*, 2019, **141**, 5169-5181.
127. S. Dawadi, N. Simmons, G. Miklossy, K. M. Bohren, J. C. Faver, M. N. Ucisik, P. Nyshadham, Z. Yu and M. M. Matzuk, *PNAS*, 2020, **117**, 16782-16789.
128. L. Encinas, H. O'Keefe, M. Neu, M. J. Remuiñán, A. M. Patel, A. Guardia, C. P. Davie, N. Pérez-Macías, H. Yang, M. A. Convery, J. A. Messer, E. Pérez-Herrán, P. A. Centrella, D. Álvarez-Gómez, M. A. Clark, S. Huss, G. K. O'Donovan, F. Ortega-Muro, W. McDowell, P. Castañeda, C. C. Arico-Muendel, S. Pajk, J. Rullás, I. Angulo-Barturen, E. Álvarez-Ruíz, A. Mendoza-Losana, L. Ballell Pages, J. Castro-Pichel and G. Evindar, *J. Med. Chem.*, 2014, **57**, 1276-1288.
129. R. C. Hartkoorn, C. Sala, J. Neres, F. Pojer, S. Magnet, R. Mukherjee, S. Uplekar, S. Boy-Röttger, K. H. Altmann and S. T. Cole, *EMBO Mol. Med.*, 2012, **4**, 1032-1042.
130. R. C. Hartkoorn, F. Pojer, J. A. Read, H. Gingell, J. Neres, O. P. Horlacher, K.-H. Altmann and S. T. Cole, *Nat. Chem. Biol.*, 2014, **10**, 96-98.
131. R. R. Schaller, *IEEE Spectrum*, 1997, **34**, 52-59.
132. J. R. Helliwell, *Biosci. Rep.*, 2017, **37**.
133. G. Sliwoski, S. Kothiwale, J. Meiler and E. W. Lowe, Jr., *Pharmacol. Rev.*, 2014, **66**, 334-395.
134. S. P. Leelananda and S. Lindert, *Beilstein J. Org. Chem.*, 2016, **12**, 2694-2718.
135. G. Jones, P. Willett, R. C. Glen, A. R. Leach and R. Taylor, *J. Mol. Biol.*, 1997, **267**, 727-748.
136. L. Olsen, S. Jost, H.-W. Adolph, I. Pettersson, L. Hemmingsen and F. S. Jørgensen, *Bioorg. Med. Chem.*, 2006, **14**, 2627-2635.
137. S. Yan, T. Appleby, G. Larson, J. Z. Wu, R. Hamatake, Z. Hong and N. Yao, *Bioorg. Med. Chem. Lett.*, 2006, **16**, 5888-5891.
138. S. John, S. Thangapandian, S. Sakkiah and K. W. Lee, *BMC Bioinformatics*, 2011, **12**, S28.
139. M. Arooj, S. Sakkiah, G. Cao and K. W. Lee, *PLoS One*, 2013, **8**, e60470.
140. A. Perdih, M. Hrast, H. Barreteau, S. Gobec, G. Wolber and T. Solmajer, *J. Chem. Inf. Model.*, 2014, **54**, 1451-1466.
141. E. Sarukhanyan, S. Shityakov and T. Dandekar, *Front. Chem.*, 2020, **7**.
142. G. Kleywegt, Acta Crystallogr. D, 2000, **56**, 249-265.
143. G. M. Sastry, S. L. Dixon and W. Sherman, *J. Chem. Inf. Model.*, 2011, **51**, 2455-2466.
144. E. Harder, W. Damm, J. Maple, C. Wu, M. Reboul, J. Y. Xiang, L. Wang, D. Lupyan, M. K. Dahlgren, J. L. Knight, J. W. Kaus, D. S. Cerutti, G. Krilov, W. L. Jorgensen, R. Abel and R. A. Friesner, *J. Chem. Theory Comput.*, 2016, **12**, 281-296.

145. W. H. J. Ward, G. A. Holdgate, S. Rowsell, E. G. McLean, R. A. Pauptit, E. Clayton, W. W. Nichols, J. G. Colls, C. A. Minshull, D. A. Jude, A. Mistry, D. Timms, R. Camble, N. J. Hales, C. J. Britton and I. W. F. Taylor, *Biochemistry*, 1999, **38**, 12514-12525.
146. A. Priyadarshi, E. E. Kim and K. Y. Hwang, *Proteins*, 2010, **78**, 480-486.
147. H. T. Kim, S. Kim, B. K. Na, J. Chung, E. Hwang and K. Y. Hwang, *Biochem. Bioph. Res. Co.*, 2017, **493**, 28-33.
148. E. F. V. Scriven and K. Turnbull, *Chem. Rev.*, 1988, **88**, 297-368.
149. K. Barral, A. D. Moorhouse and J. E. Moses, *Org. Lett.*, 2007, **9**, 1809-1811.
150. F. L. Benton and T. E. Dillon, *J. Am. Chem. Soc.*, 1942, **64**, 1128-1129.
151. J. M. Lansinger and R. C. Ronald, *Synth. Commun.*, 1979, **9**, 341-349.
152. A. K. Chakraborti, L. Sharma and M. K. Nayak, *J. Org. Chem.*, 2002, **67**, 6406-6414.
153. J. Chae, Arch. Pharm. Res., 2008, **31**, 305-309.
154. L. Zuo, S. Yao, W. Wang and W. Duan, *Tetrahedron Lett.*, 2008, **49**, 4054-4056.
155. C. R. Schmid, C. A. Beck, J. S. Cronin and M. A. Staszak, *Org. Process Res. Dev.*, 2004, **8**, 670-673.
156. T. A. Cinu, S. K. Sidhartha, B. Indira, B. G. Varadaraj, P. S. Vishnu and G. G. Shenoy, *Arab. J. Chem.*, 2019, **12**, 3316-3323.
157. in Greene's Protective Groups in Organic Synthesis, DOI: 10.1002/9780470053485.ch3, pp. 367-430.
158. V. V. Rostovtsev, L. G. Green, V. V. Fokin and K. B. Sharpless, *Angew. Chem., Int. Ed.*, 2002, **41**, 2596-2599.
159. C. W. Tornøe, C. Christensen and M. Meldal, *J. Org. Chem.*, 2002, **67**, 3057-3064.
160. L. Liang and D. Astruc, *Coord. Chem. Rev.*, 2011, **255**, 2933-2945.
161. E. Haldón, M. C. Nicasio and P. J. Pérez, *Org. Biomol. Chem.*, 2015, **13**, 9528-9550.
162. L. Zhang, X. Chen, P. Xue, H. H. Y. Sun, I. D. Williams, K. B. Sharpless, V. V. Fokin and G. Jia, *J. Am. Chem. Soc.*, 2005, **127**, 15998-15999.
163. L. K. Rasmussen, B. C. Boren and V. V. Fokin, *Org. Lett.*, 2007, **9**, 5337-5339.
164. J. R. Johansson, T. Beke-Somfai, A. Said Stålsmeden and N. Kann, *Chem. Rev.*, 2016, **116**, 14726-14768.
165. B. C. Boren, S. Narayan, L. K. Rasmussen, L. Zhang, H. Zhao, Z. Lin, G. Jia and V. V. Fokin, *J. Am. Chem. Soc.*, 2008, **130**, 8923-8930.
166. X. Creary, A. Anderson, C. Brophy, F. Crowell and Z. Funk, *J. Org. Chem.*, 2012, **77**, 8756-8761.
167. K. Takasu, T. Azuma and Y. Takemoto, *Tetrahedron Lett.*, 2010, **51**, 2737-2740.
168. I. Dreier, S. Kumar, H. Søndergaard, M. L. Rasmussen, L. H. Hansen, N. H. List, J. Kongsted, B. Vester and P. Nielsen, *J. Med. Chem.*, 2012, **55**, 2067-2077.
169. M. Corredor, J. Bujons, À. Messeguer and I. Alfonso, *Org. Biomol. Chem.*, 2013, **11**, 7318-7325.
170. V. R. Sirivolu, S. K. V. Vernekar, T. Ilina, N. S. Myshakina, M. A. Parniak and Z. Wang, *J. Med. Chem.*, 2013, **56**, 8765-8780.
171. S. Chetty, PhD, University of Nottingham, 2015.
172. R. Appel, Angew. Chem., Int. Ed., 1975, **14**, 801-811.
173. Y. Peng, C. Ji, Y. Chen, C. Huang and Y. Jiang, *Synth. Commun.*, 2004, **34**, 4325-4330.
174. H.-W. Kim and H.-J. Lee, T. A. Lee Dong-Soo, T. A. Chung Kyoo-Hyun, *B. Korean Chem. Soc.*, 2010, **31**, 3434–3436.

175. F. Kopp, U. Linne, M. Oberthür and M. A. Marahiel, *J. Am. Chem. Soc.*, 2008, **130**, 2656-2666.
176. J. M. Odriozola, J. A. Ramos and K. Bloch, *Biochim. Biophys. Acta*, 1977, **488**, 207-217.
177. J. M. Odriozola and K. Bloch, Biochim. Biophys. Acta, Lipids Lipid Metab., 1977, **488**, 198-206.
178. S. S. Kharkwal, PhD, University of Nottingham, 2011.
179. L. Olotu-Umoren, PhD, University of Nottingham, 2012.
180. F. Rodriguez, N. Saffon, J. C. Sammartino, G. Degiacomi, M. R. Pasca and C. Lherbet, *Bioorg. Chem.*, 2020, **95**, 103498.
181. J. S. Freundlich, F. Wang, C. Vilchèze, G. Gulten, R. Langley, G. A. Schiehser, D. P. Jacobus, W. R. Jacobs Jr. and J. C. Sacchettini, *ChemMedChem*, 2009, **4**, 241-248.
182. J. A. Kluge, O. Rabotyagova, G. G. Leisk and D. L. Kaplan, *Trends Biotechnol.*, 2008, **26**, 244-251.
183. L. Römer and T. Scheibel, *Prion*, 2008, **2**, 154-161.
184. D. Harvey, P. Bardelang, S. L. Goodacre, A. Cockayne and N. R. Thomas, *Adv. Mater.*, 2017, **29**.
185. L. D. Lavis, *ACS Chem. Biol.*, 2008, **3**, 203-206.
186. A. S. M. Bapat, M.; Gokhale, R. S.; Shah, S. S.; Sengupta, S.; Prasad, S.; Ghosh, S.; Chawrai, S. R.; Arora, N.; Reddy, D. S.; Mishra, M.; Bajaj, K., *Conjugate-based Antifungal And Antibacterial Prodrugs*, PCT publication No. WO US2014/364595, 2014.
187. A. Bosnjakovic, M. K. Mishra, W. Ren, Y. E. Kurtoglu, T. Shi, D. Fan and R. M. Kannan, *Nanomedicine*, 2011, **7**, 284-294.
188. F. D'Souza, S. Gadde, M. E. Zandler, K. Arkady, M. E. El-Khouly, M. Fujitsuka and O. Ito, *J. Phys. Chem. A*, 2002, **106**, 12393-12404.
189. B. Boëns, P.-A. Faugeras, J. Vergnaud, R. Lucas, K. Teste and R. Zerrouki, *Tetrahedron*, 2010, **66**, 1994-1996.
190. R. M. K. Calderon, J. Valero, B. Grimm, J. de Mendoza and D. M. Guldi, *J. Am. Chem. Soc.*, 2014, **136**, 11436-11443.
191. T. Maeda, K. Titani and K. Sekiguchi, *J. Biochem.*, 1994, **115**, 182-189.
192. S. Ali, J. E. Saik, D. J. Gould, M. E. Dickinson and J. L. West, *Biores. Open Access*, 2013, **2**, 241-249.
193. D. Pallarola, A. Bochen, H. Boehm, F. Rechenmacher, T. R. Sobahi, J. P. Spatz and H. Kessler, *Adv. Funct. Mater.*, 2014, **24**, 943-956.
194. T. G. Kapp, F. Rechenmacher, S. Neubauer, O. V. Maltsev, E. A. Cavalcanti-Adam, R. Zarka, U. Reuning, J. Notni, H. J. Wester, C. Mas-Moruno, J. Spatz, B. Geiger and H. Kessler, *Sci. Rep.*, 2017, **7**, 39805.
195. M. Nakagawa and D. G. Crosby, *J. Agric. Food Chem.*, 1974, **22**, 849-853.
196. S. Buchan and H. A. Scarborough, *J. Am. Chem. Soc.*, 1934, DOI: 10.1039/JR9340000705, 705-708.
197. S. K. Tipparaju, D. C. Mulhearn, G. M. Klein, Y. Chen, S. Tapadar, M. H. Bishop, S. Yang, J. Chen, M. Ghassemi, B. D. Santarsiero, J. L. Cook, M. Johlfs, A. D. Mesecar, M. E. Johnson and A. P. Kozikowski, *ChemMedChem*, 2008, **3**, 1250-1268.
198. G. Cheng, S. P. Muench, Y. Zhou, G. A. Afanador, E. J. Mui, A. Fomovska, B. S. Lai, S. T. Prigge, S. Woods, C. W. Roberts, M. R. Hickman, P. J. Lee, S. E. Leed, J. M. Auschwitz, D. W. Rice and R. McLeod, *Bioorg. Med. Chem. Lett.*, 2013, **23**, 2035-2043.
199. H. Yoneyama, M. Numata, K. Uemura, Y. Usami and S. Harusawa, *J. Org. Chem.*, 2017, **82**, 5538-5556.

200. Z. Xu, H. Chen, Z. Wang, A. Ying and L. Zhang, *J. Am. Chem. Soc.*, 2016, **138**, 5515-5518.
201. M. Irfan, B. Aneja, U. Yadava, S. I. Khan, N. Manzoor, C. G. Daniliuc and M. Abid, *Eur. J. Med. Chem.*, 2015, **93**, 246-254.
202. K. Muranaka, S. Ichikawa and A. Matsuda, *J. Org. Chem.*, 2011, **76**, 9278-9293.
203. S. A. Nuñez, K. Yeung, N. S. Fox and S. T. Phillips, *J. Org. Chem.*, 2011, **76**, 10099-10113.
204. F. Zhang, S. Zaidi, K. M. Haney, G. E. Kellogg and Y. Zhang, *J. Org. Chem.*, 2011, **76**, 7945-7952.
205. P. C. Montevecchi and M. L. Navacchia, *J. Org. Chem.*, 1998, **63**, 537-542.
206. A. E. G. Lindgren, C. T. Öberg, J. M. Hillgren and M. Elofsson, *Eur. J. Org. Chem.*, 2016, **2016**, 426-429.
207. S. Gupta, M. Chhibber, S. Sinha and A. Surolia, *J. Med. Chem.*, 2007, **50**, 5589-5599.
208. C. Ji, P. A. Miller and M. J. Miller, *ACS Med. Chem. Lett.*, 2015, **6**, 707-710.
209. F. Liu, Y. Zhang, L. Xu and W. Zhang, *Chem. Eur. J.*, 2015, **21**, 5540-5547.
210. O. Rezazgui, P. Trouillas, S.-h. Qiu, B. Siegler, J. Gierschner and S. Leroy-Lhez, *New J. Chem.*, 2016, **40**, 3843-3856.
211. W. Z. Xu, G. Gao and J. F. Kadla, *Cellulose*, 2013, **20**, 1187-1199.
212. V. Hugenberg, S. Wagner, K. Kopka, M. Schäfers, R. C. Schuit, A. D. Windhorst and S. Hermann, *J. Med. Chem.*, 2017, **60**, 307-321.

9.0 Characterisation Data

9.1 NMR Spectra

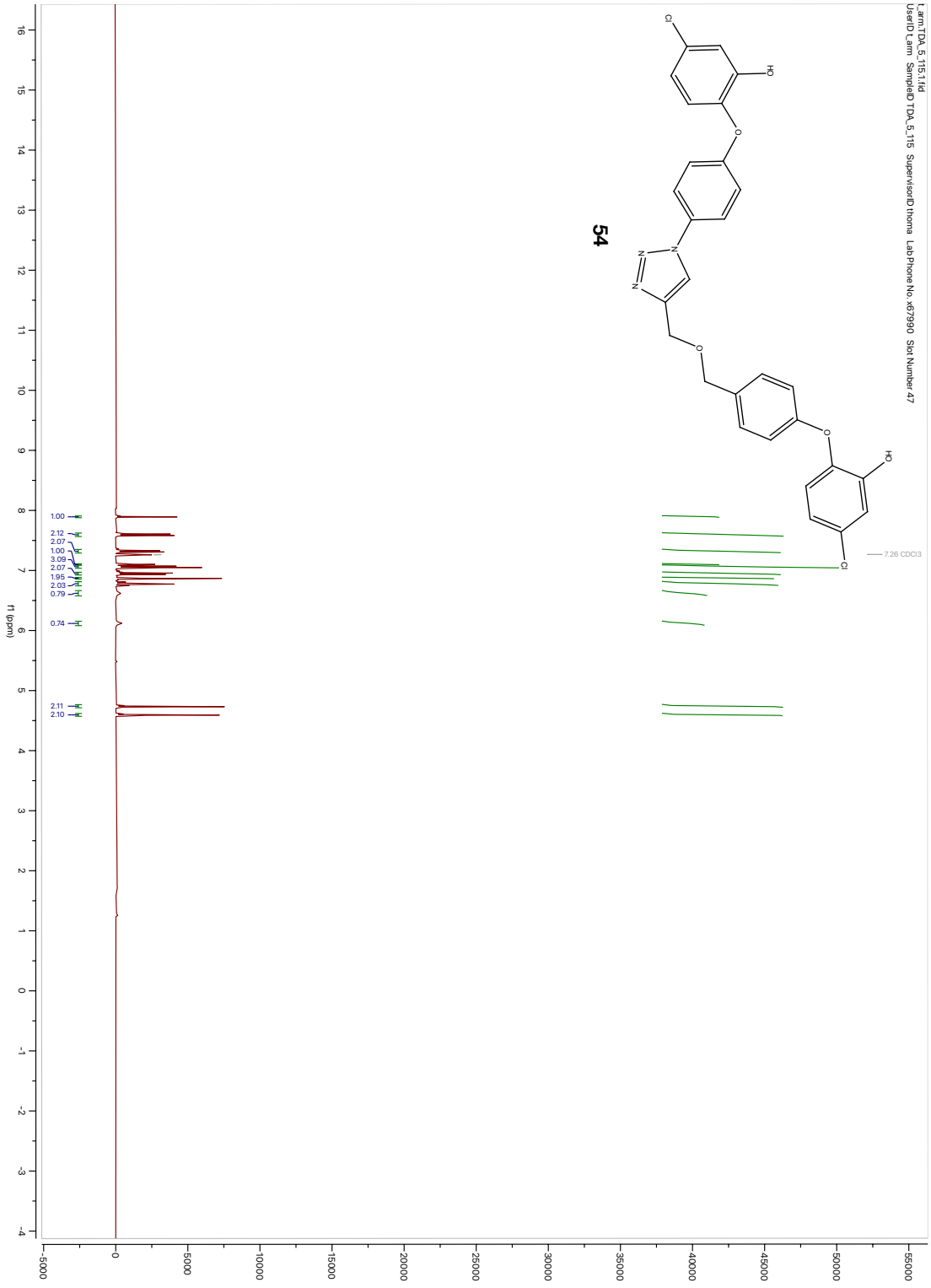

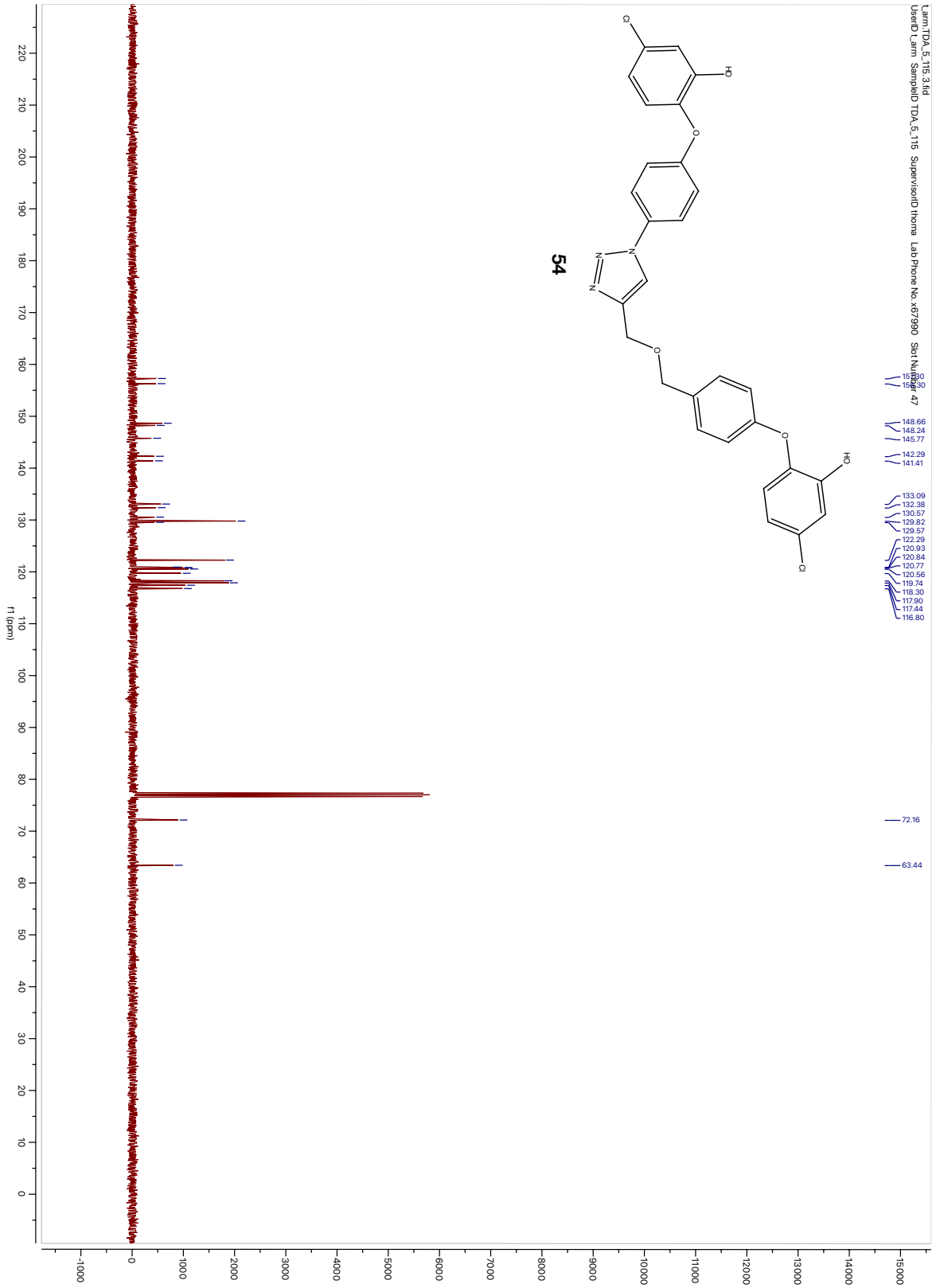
t_arm:TDA_5_115.3.fid
UserID t_arm SampleID TDA_5_115 SupervisorID thoma Lab Phone No.x67990 Slot Number 47
54
152.80
150.90
148.66
148.24
145.77
142.29
141.41
133.09
132.38
130.57
129.82
129.57
122.29
120.93
120.84
120.77
120.56
119.74
118.30
117.90
117.44
116.80
72.16
63.44
f1 (ppm)

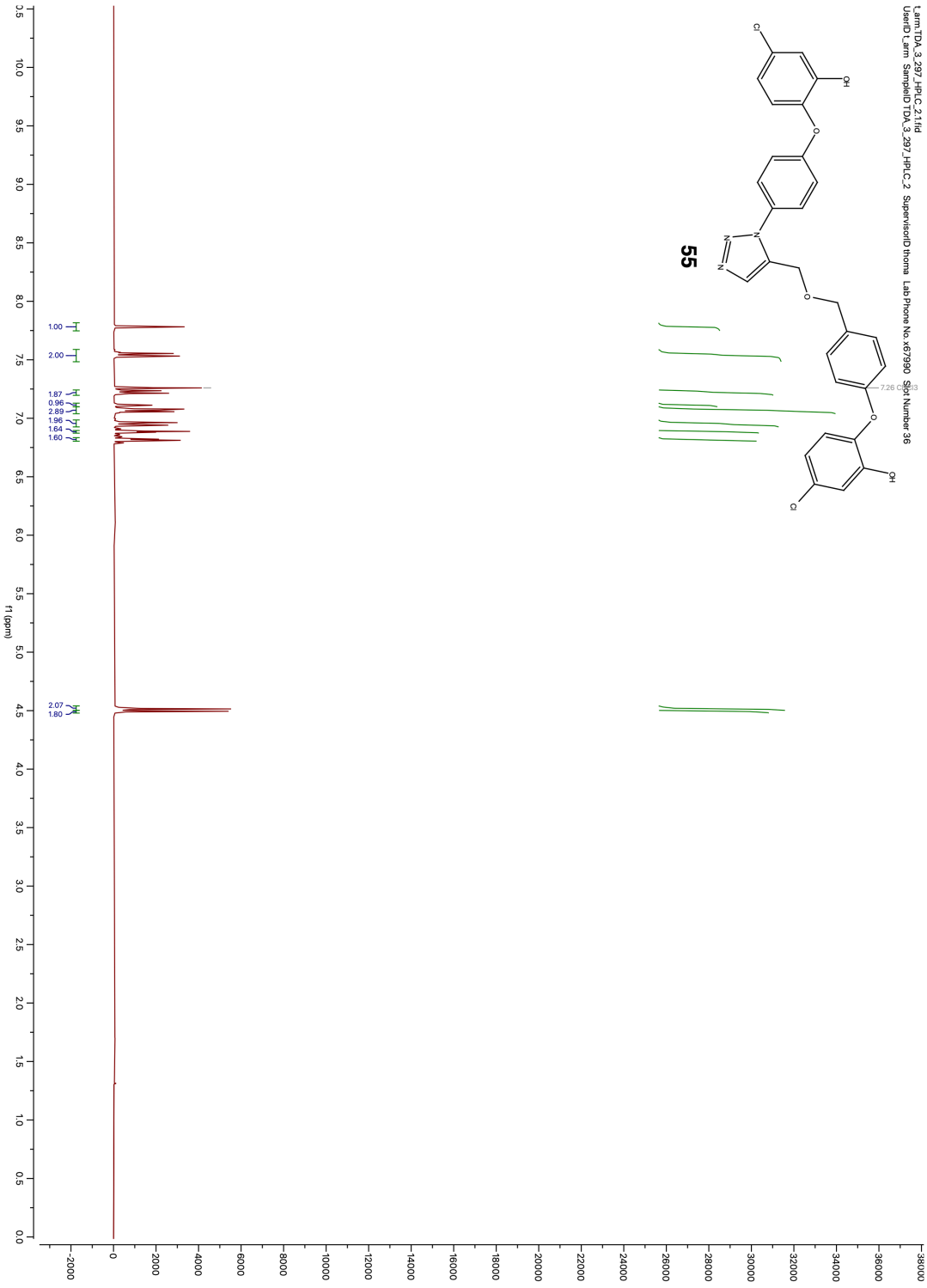
t_arm_TDA_3_297_HPLC_2.1.fid
UserID t_arm SampleID TDA_3_297_HPLC_2 SupervisorID thoma Lab Phone No. x67990 Slot Number 36
55
7.26 CDCl3
1.00
2.00
1.87
0.96
2.89
1.96
1.64
1.60
2.07
1.80
f1 (ppm)

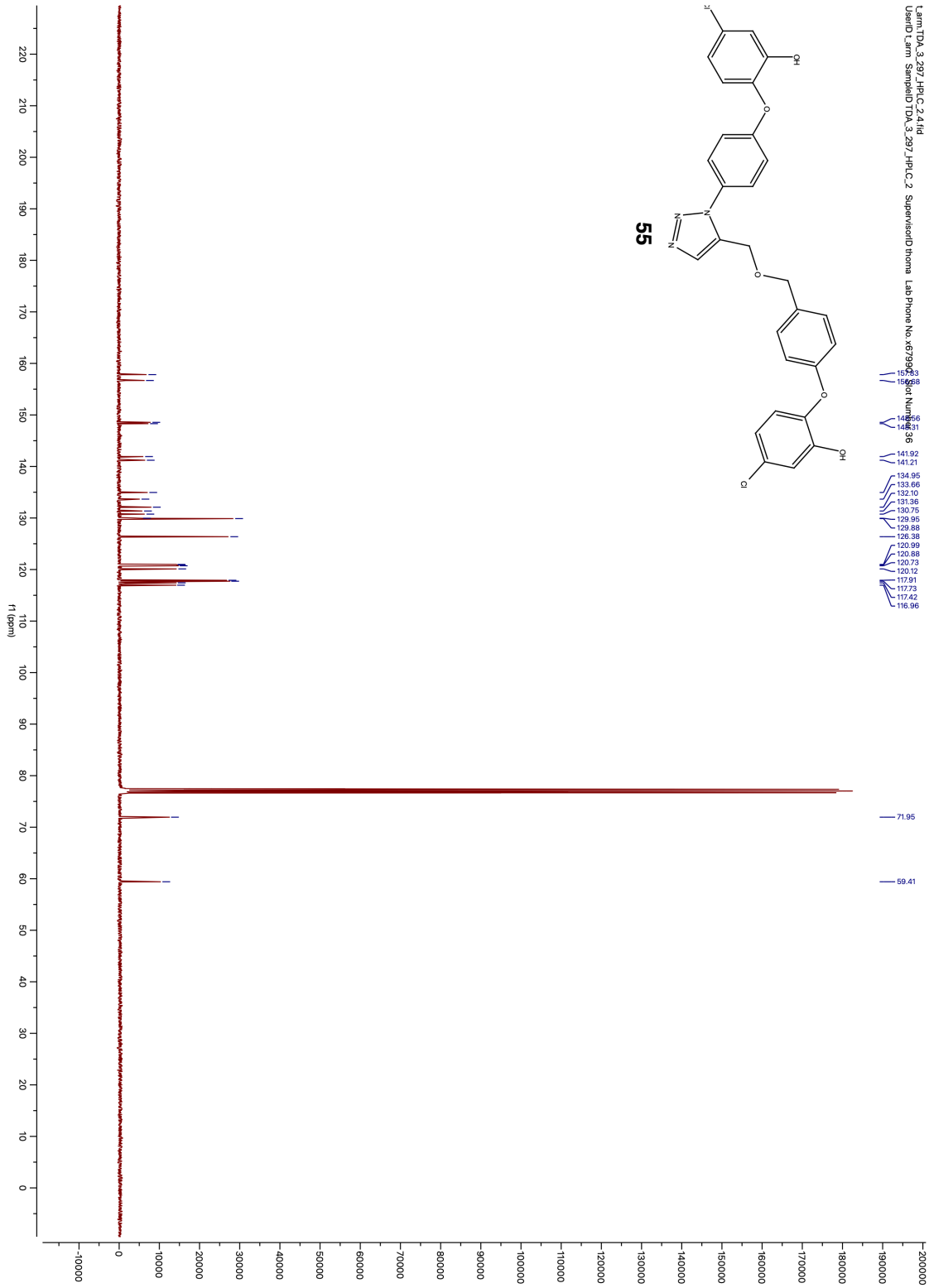
t_arm.TDA_3_297_HPLC_2.4.fid
UserID t_arm SampleID TDA_3_297_HPLC_2 SupervisorID thoma Lab Phone No. x6799
Serial Number 36
55
157.33
156.68
148.66
148.21
141.92
141.21
134.95
133.66
132.10
131.36
130.75
129.95
129.88
126.38
120.99
120.88
120.73
120.12
117.91
117.73
117.42
116.96
71.95
59.41
f1 (ppm)

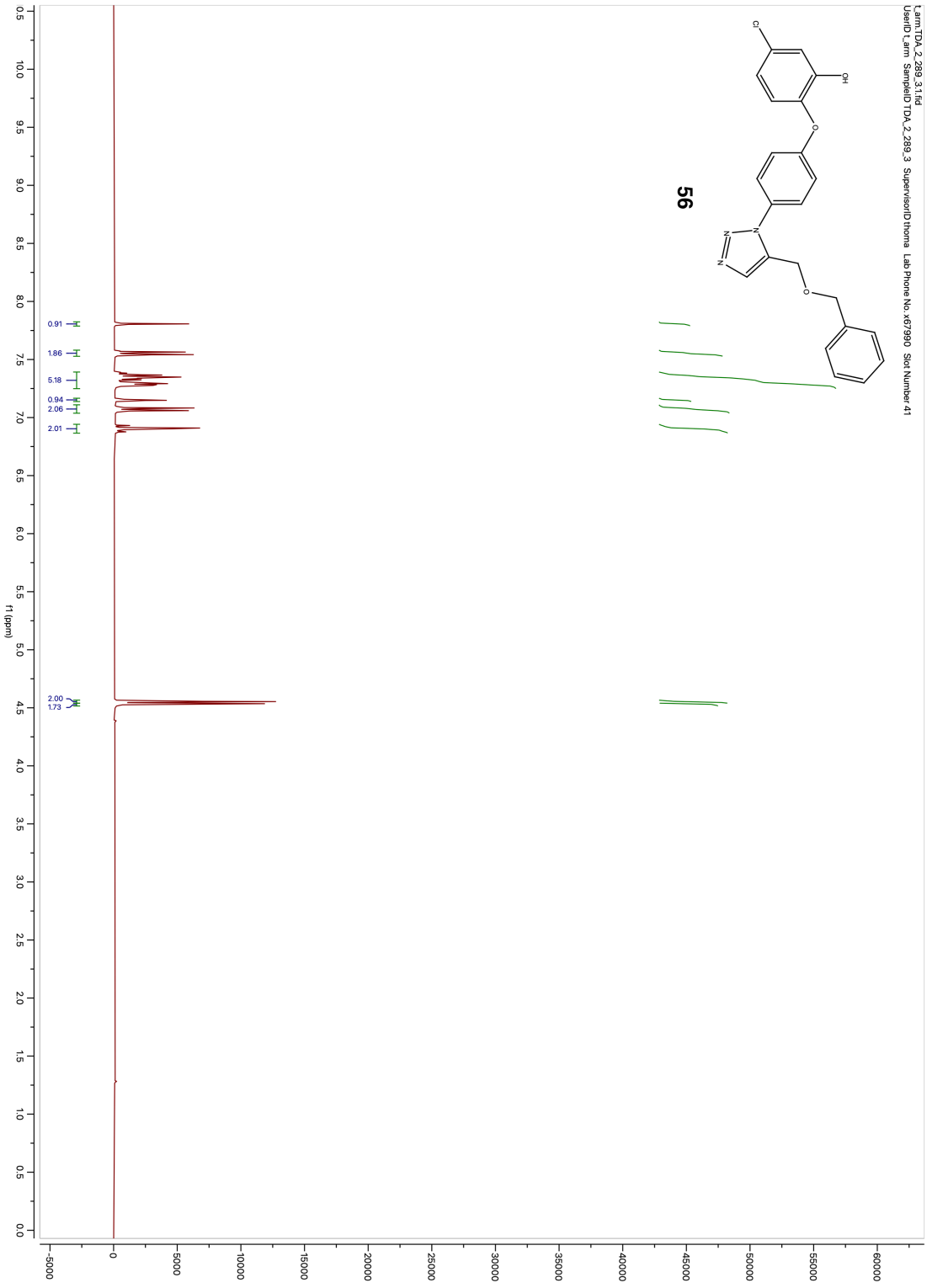
t_arm:TDA_2_289_3.1.fid
UserID t_arm SampleID TDA_2_289_3 Supervisor/ID thoma Lab Phone No. x67990 Slot Number 41
56
Cl
OH
O
N
N
O
0.91
1.86
5.18
0.94
2.06
2.01
2.00
1.73
f1 (ppm)

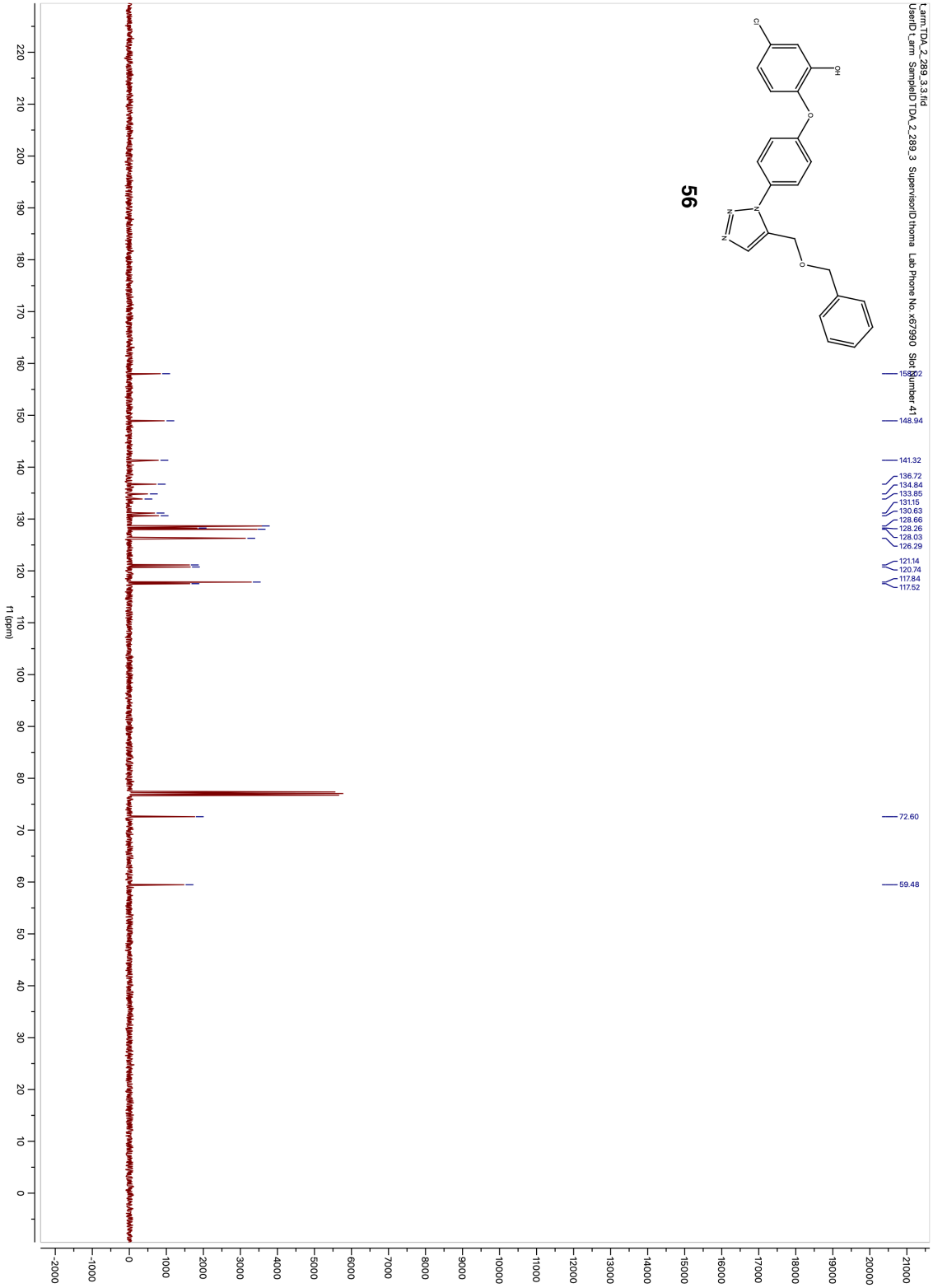
t_arm.TDA_2_289_3.3.fid
UserID t_arm SampleID TDA_2_289_3 SupervisorID thoma Lab Phone No. x67990 Slot Number 41
56
158.22
148.94
141.32
136.72
134.84
133.85
131.15
130.63
128.66
128.26
128.03
126.29
121.14
120.74
117.84
117.52
72.60
59.48
f1 (ppm)

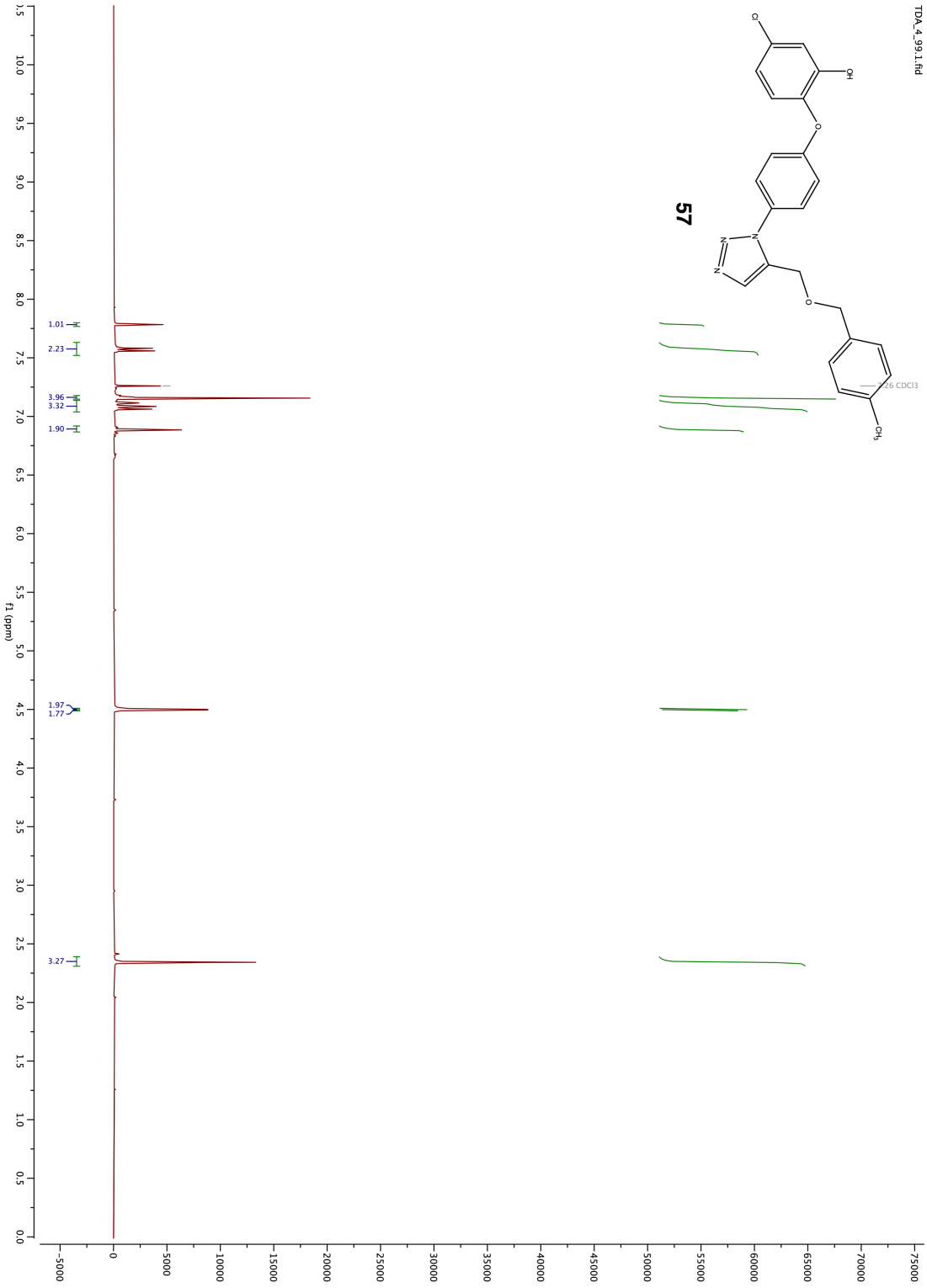
TDA_4_99_1.fid
57
1.01
2.23
3.96
3.32
1.90
1.97
1.77
3.27
f1 (ppm)

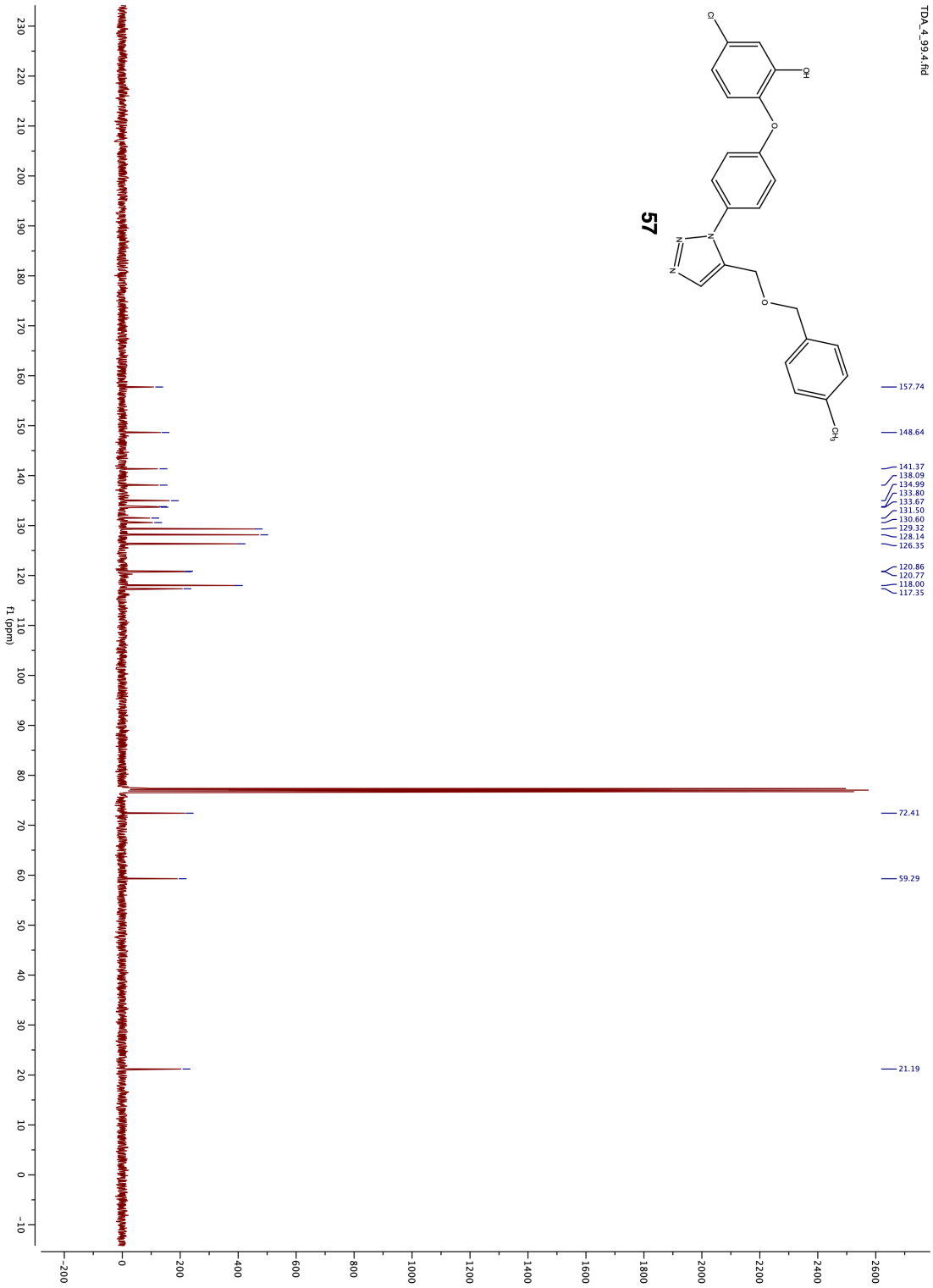
TDA_4_99.4.fid
57
157.74
148.64
141.37
138.09
134.99
133.80
133.67
131.50
130.60
129.32
128.14
126.35
120.86
120.77
118.00
117.35
72.41
59.29
21.19
f1 (ppm)

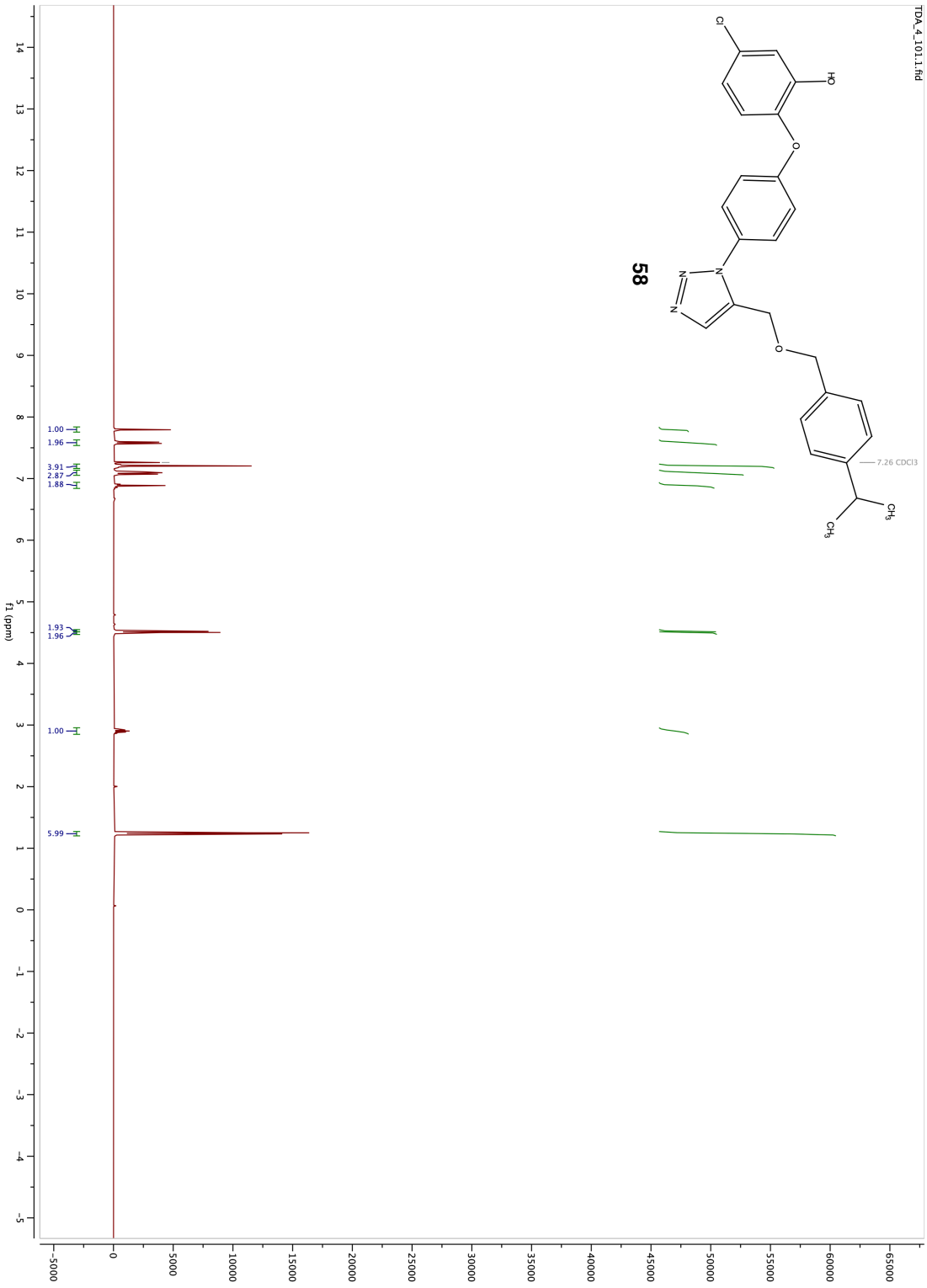
TDA_4_101.1.fid
58
7.26 CDCl3
1.00
1.96
3.91
2.87
1.88
1.93
1.96
1.00
5.99
f1 (ppm)

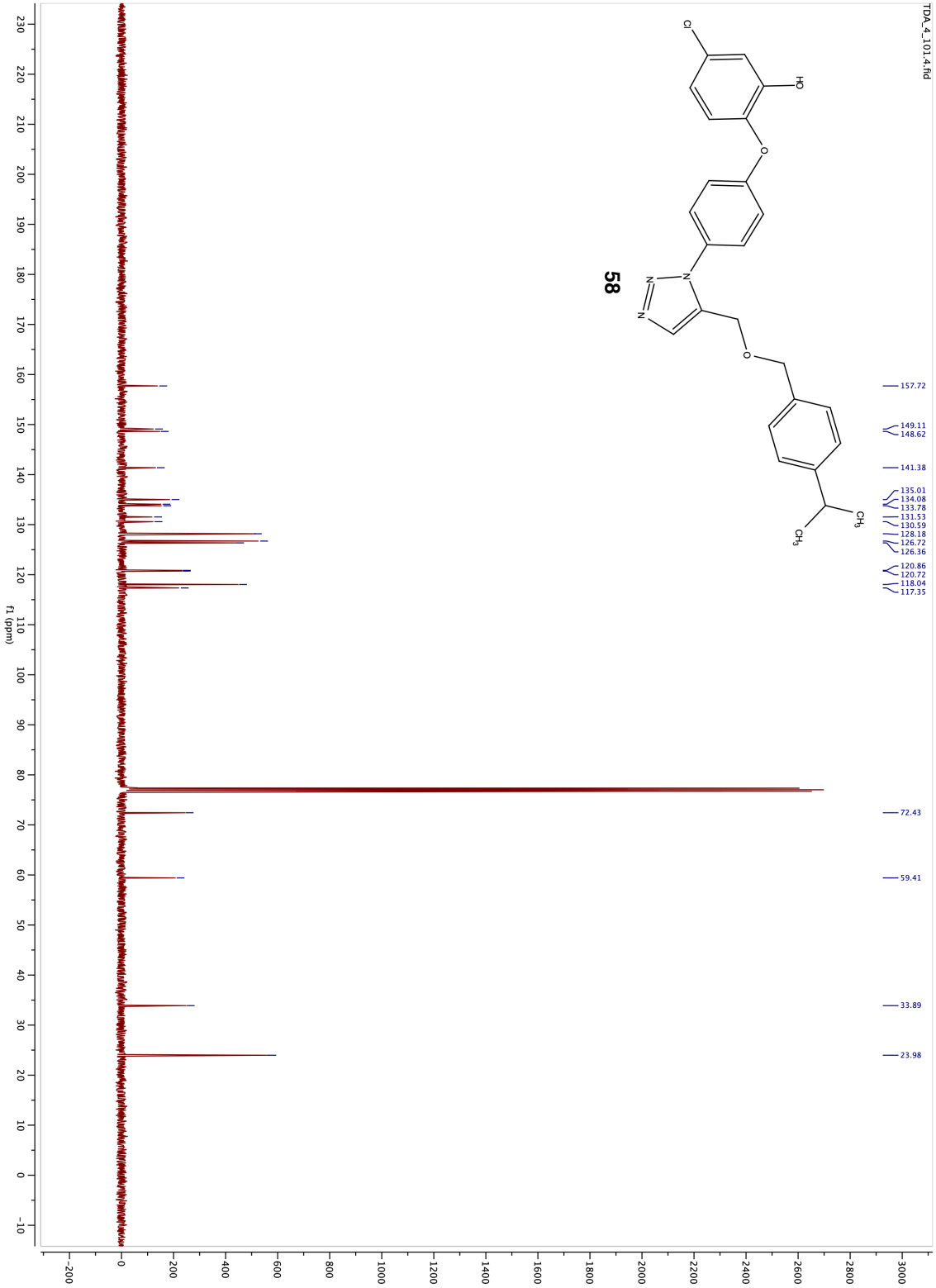
TDA_4_101.4.fid
58
Cl
HO
O
N
N
N
O
CH3
CH3
157.72
149.11
148.62
141.38
135.01
134.08
133.78
131.53
130.59
128.18
126.72
126.36
120.86
120.72
118.04
117.35
72.43
59.41
33.89
23.98
f1 (ppm)

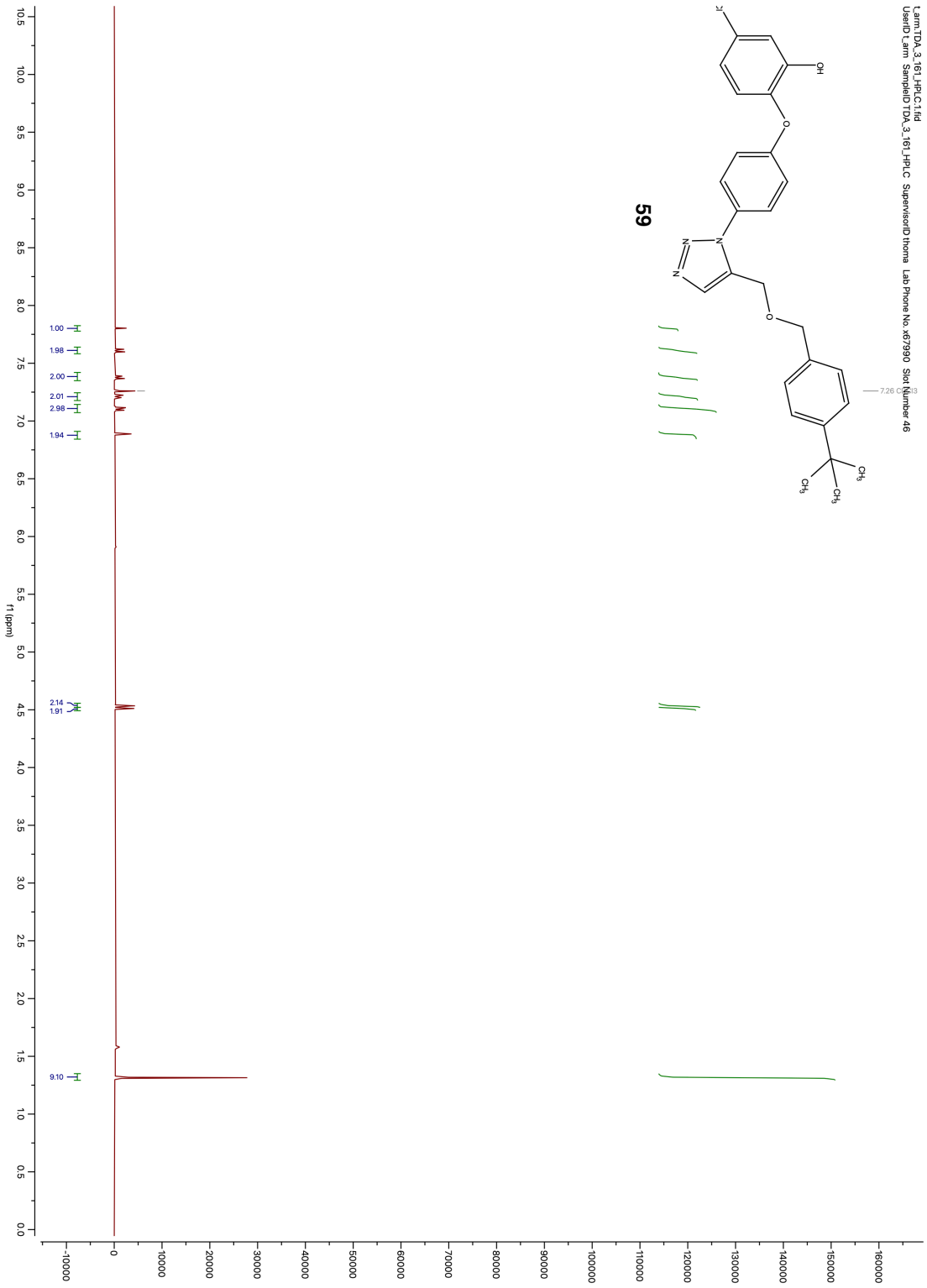
L_arm.TDA_3_161_HPLC.1.fid
UserID L_arm SampleID TDA_3_161_HPLC SupervisorID thoma Lab Phone No. x67990 Slot Number 46
59
OH
N
N
N
O
O
CH3
CH3
CH3
7.26
1.00
1.98
2.00
2.01
2.98
1.94
2.14
1.91
9.10
f1 (ppm)

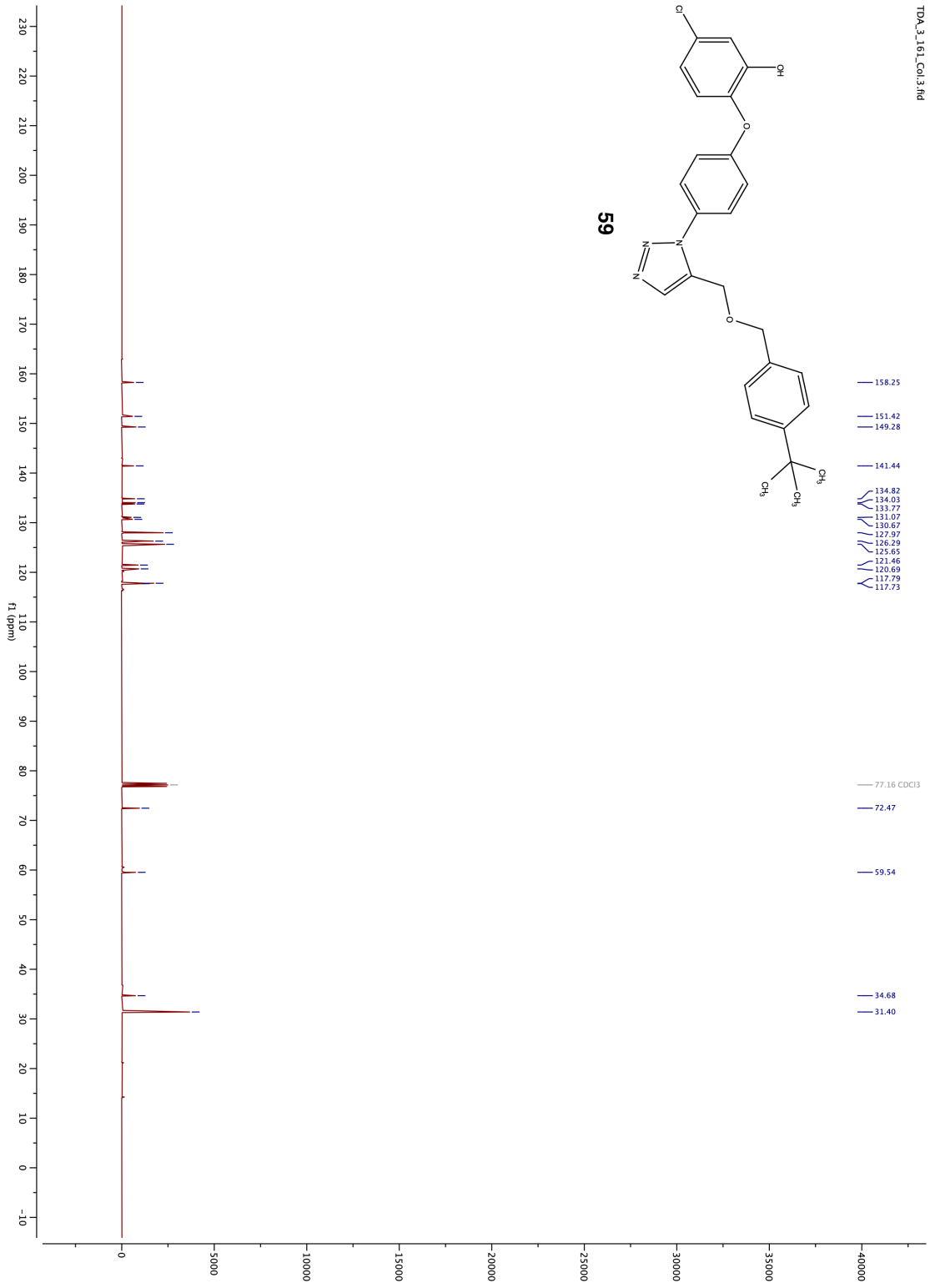
TDA_3_161_Col.3.fid
59
158.25
151.42
149.28
141.44
134.82
134.03
133.77
131.07
130.67
127.97
126.29
125.65
121.46
120.69
117.79
117.73
77.16 CDCl3
72.47
59.54
34.68
31.40
f1 (ppm)

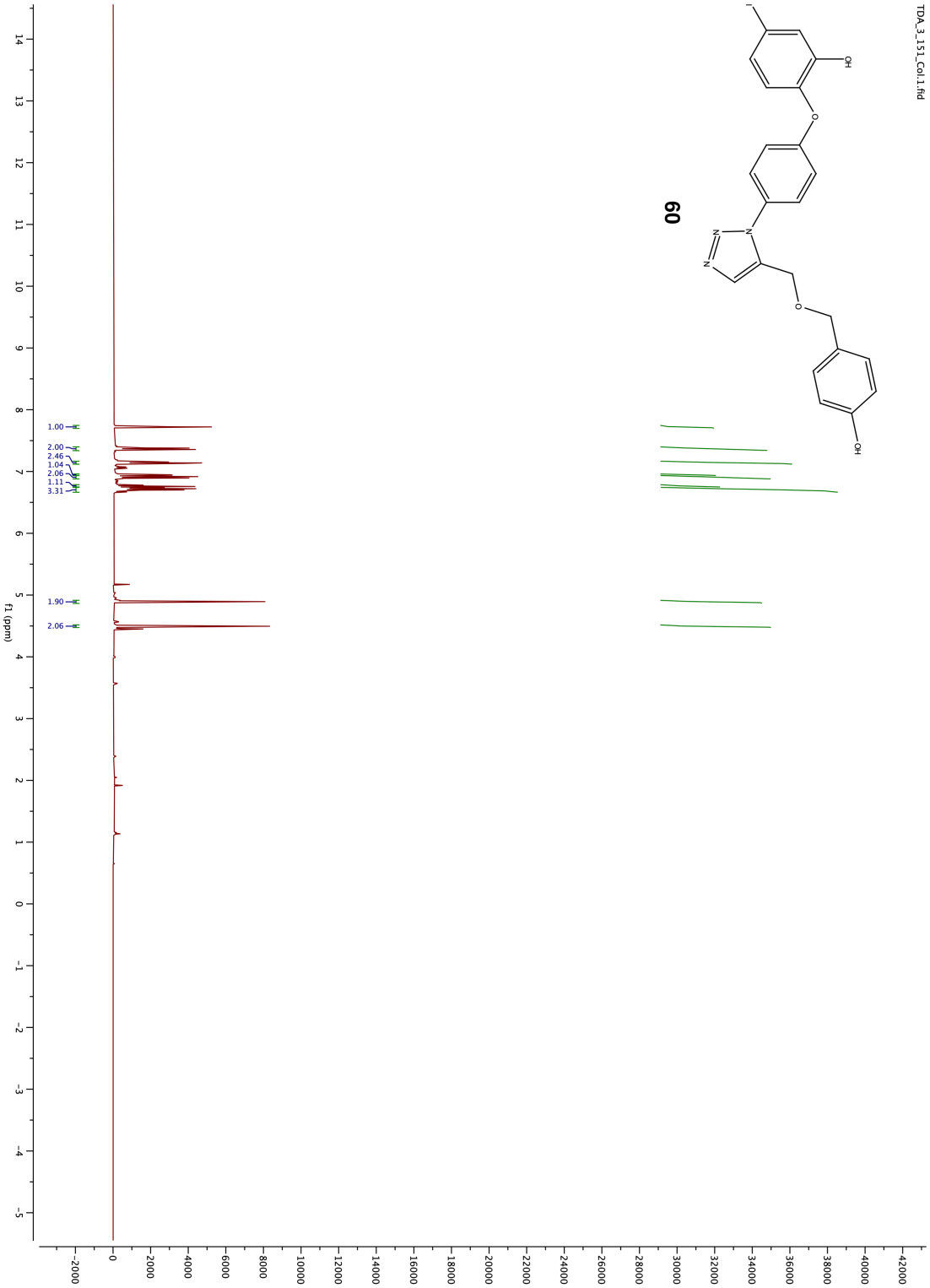
TDA_3_151_Col.1.fid
60
OH
O
N
N
N
O
OH
1.00
2.00
2.46
1.04
2.06
1.11
3.31
1.90
2.06
f1 (ppm)

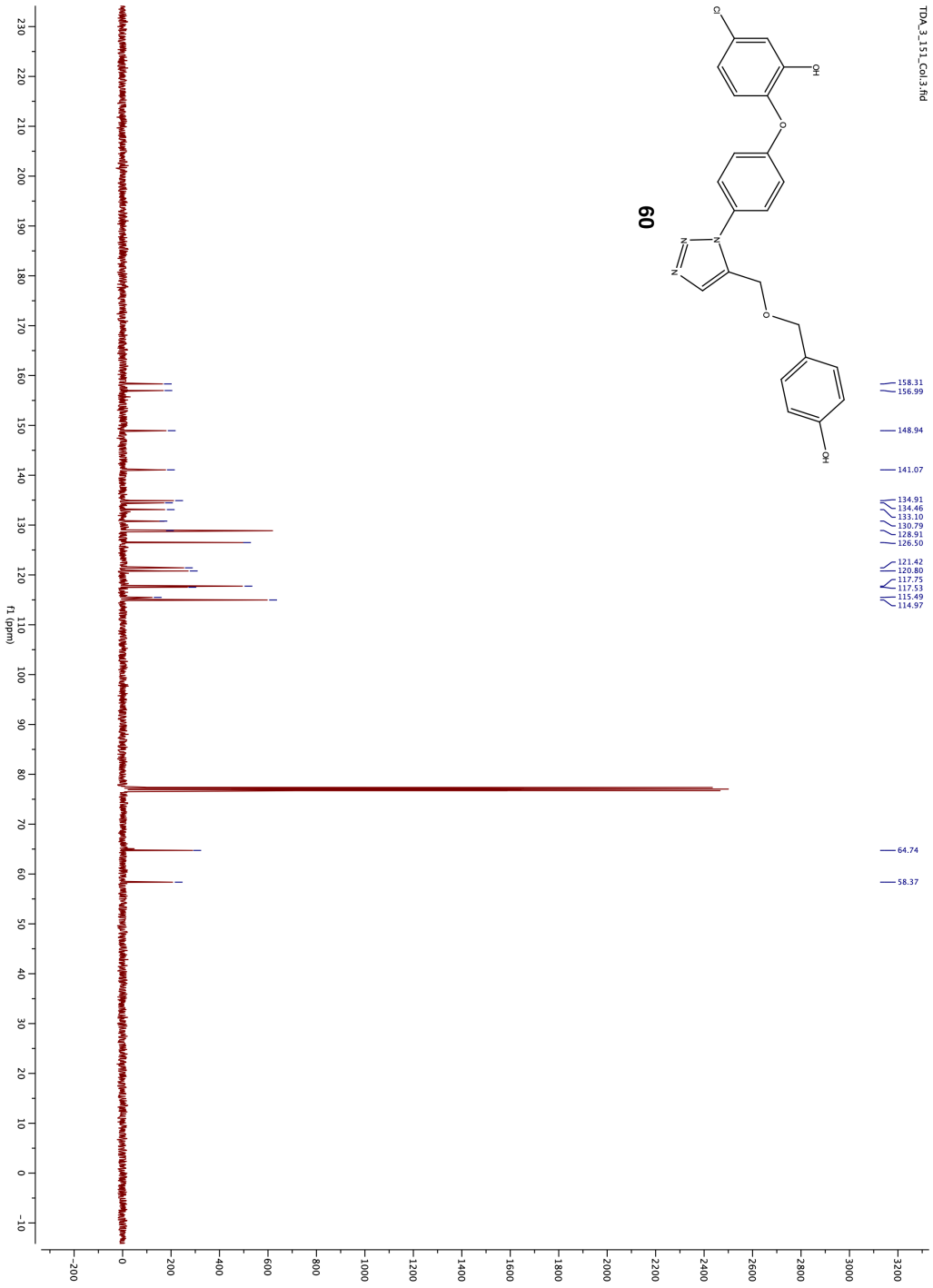
60
TDA_3_151_Col.3.fid
158.31
156.99
148.94
141.07
134.91
134.46
133.10
130.79
128.91
126.50
121.42
120.80
117.75
117.53
115.49
114.97
64.74
58.37
f1 (ppm)

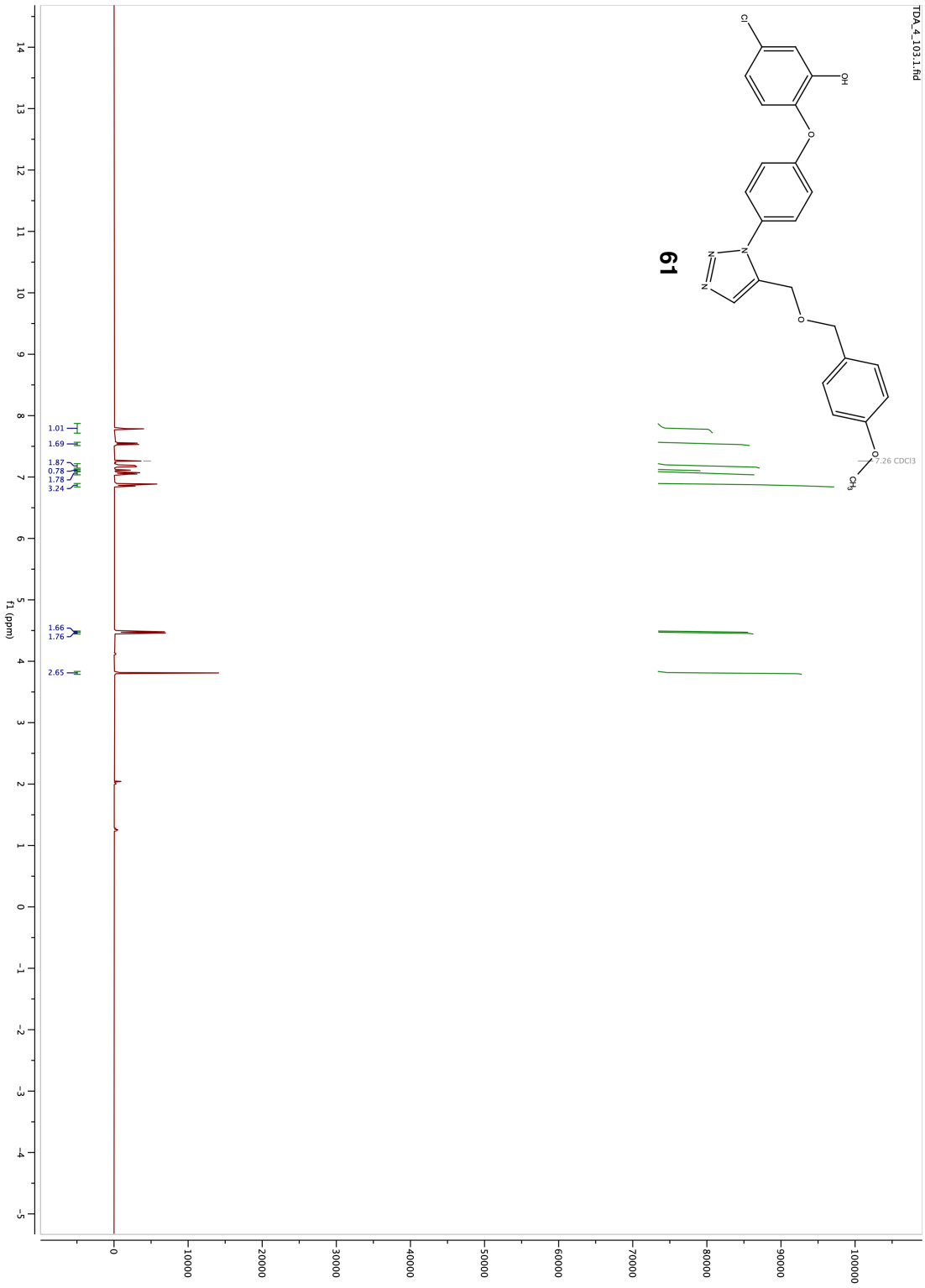
TDA_4_103.1.fid
61
1.01
1.69
1.87
0.78
1.78
3.24
1.66
1.76
2.65
7.26 CDCl3
F1 (ppm)

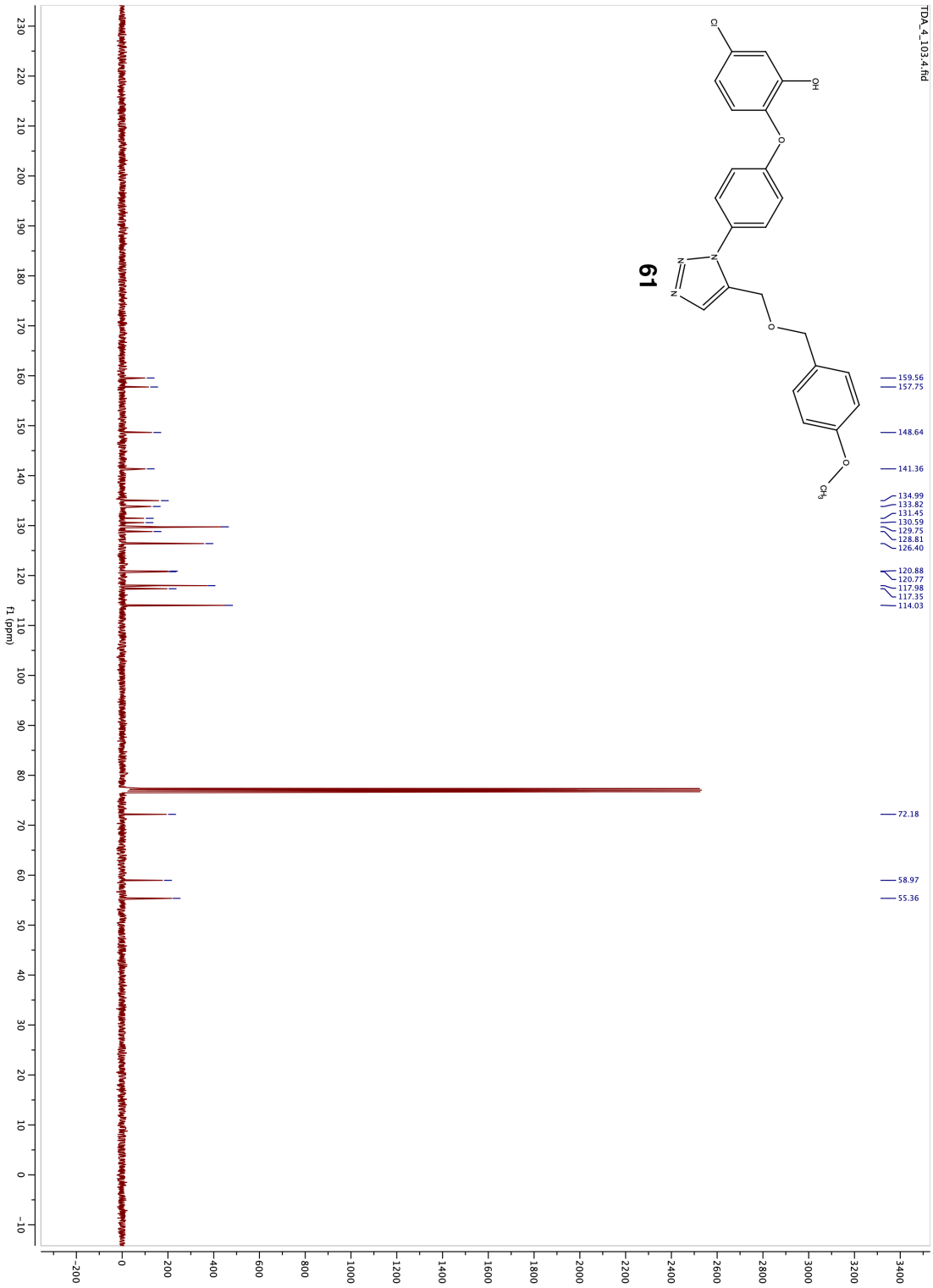
TDA_4_103.4.fid
61
159.56
157.75
148.64
141.36
134.99
133.82
131.45
130.59
129.75
128.81
126.40
120.88
120.77
117.98
117.35
114.03
72.18
58.97
55.36
f1 (ppm)

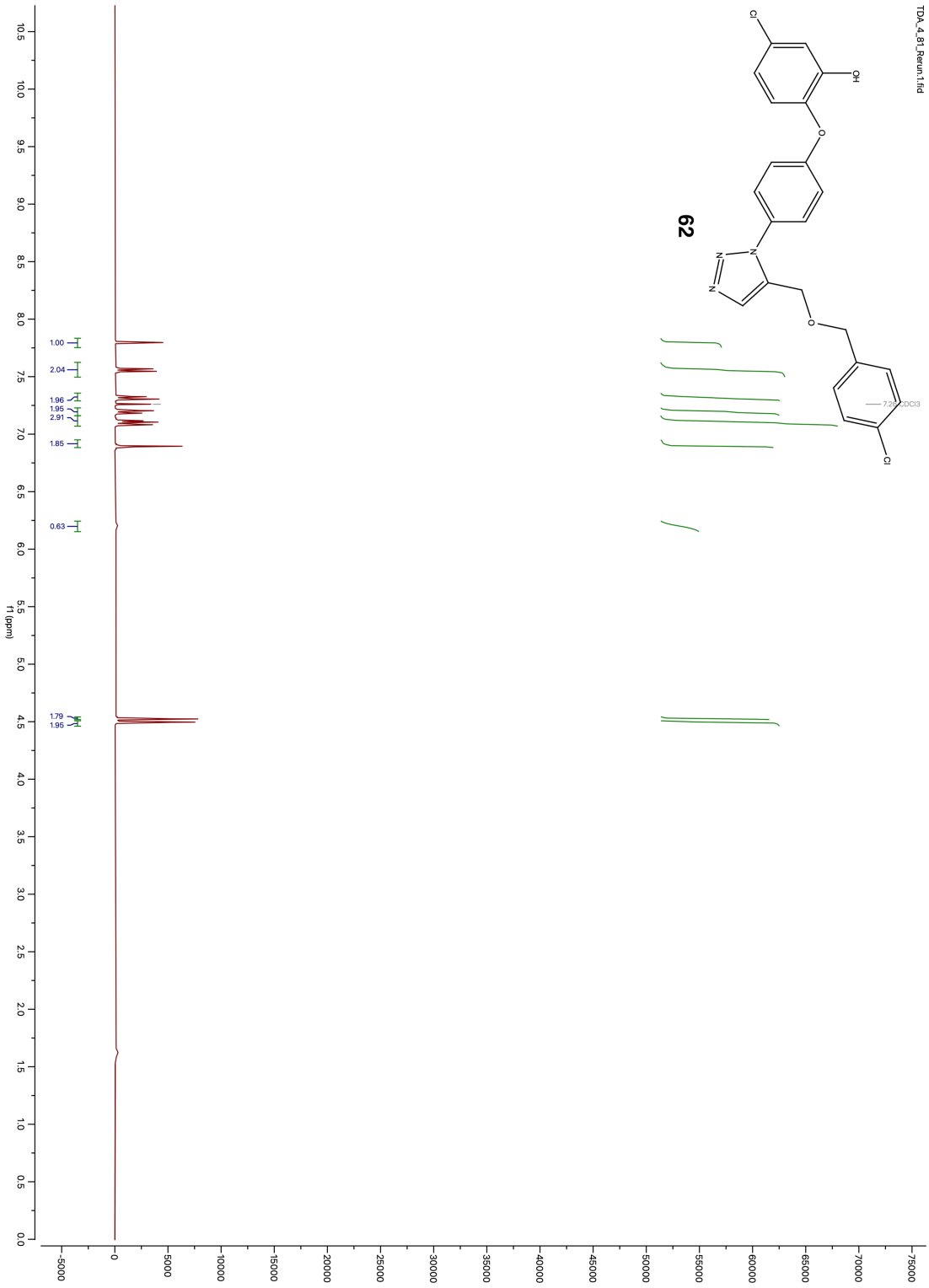
TDA_4_81_Rerun.1.fid
62
Cl
OH
O
N
N
N
O
Cl
7.26 CDCl3
1.00
2.04
1.96
1.95
2.91
1.85
0.63
1.79
1.95
f1 (ppm)

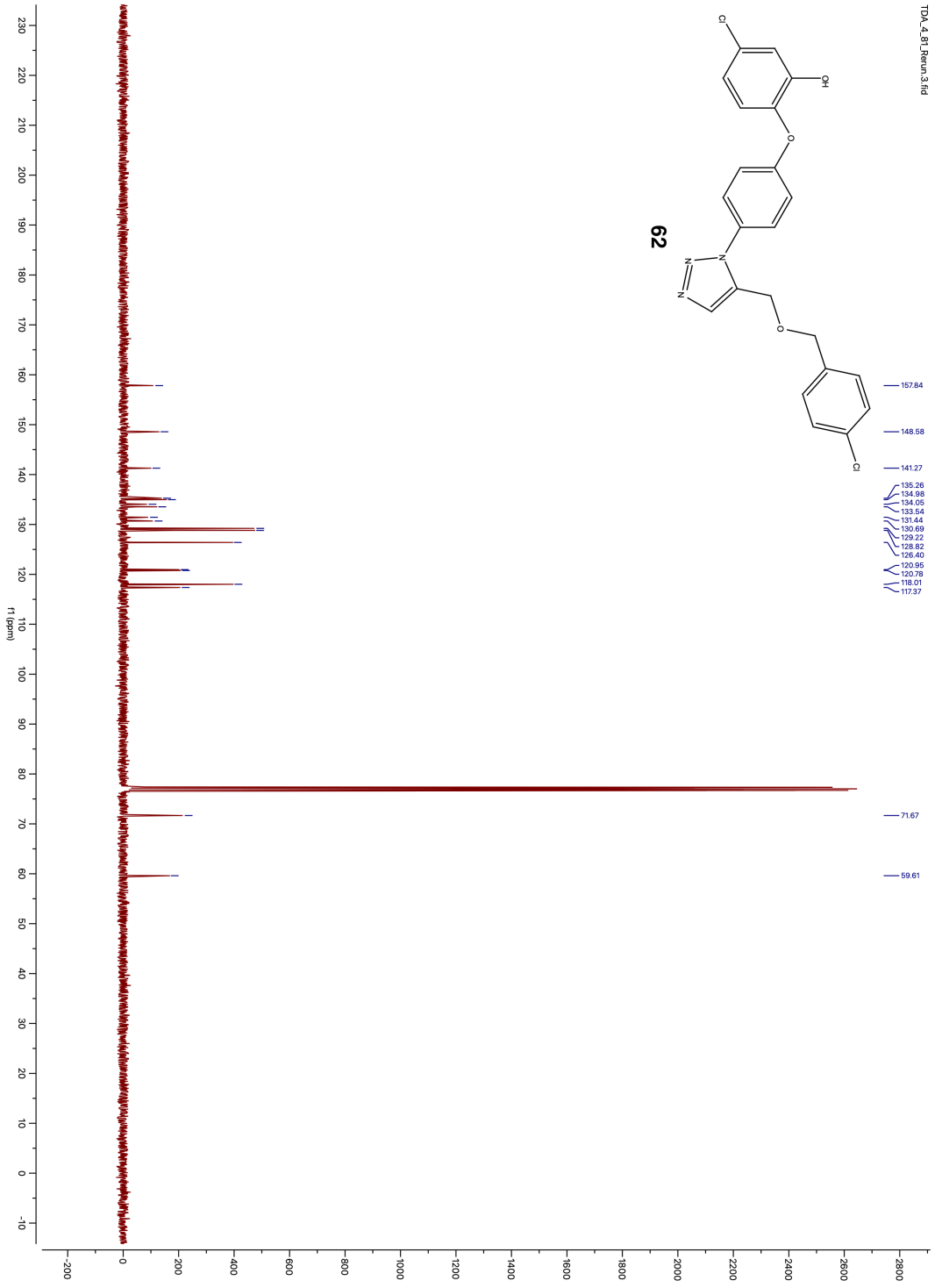
TDA_4_81_Rerun_3.fid
62
Cl
OH
O
N
N
N
O
Cl
157.84
148.58
141.27
135.26
134.98
134.05
133.54
131.44
130.69
129.22
128.82
126.40
120.95
120.78
118.01
117.37
71.67
59.61
f1 (ppm)

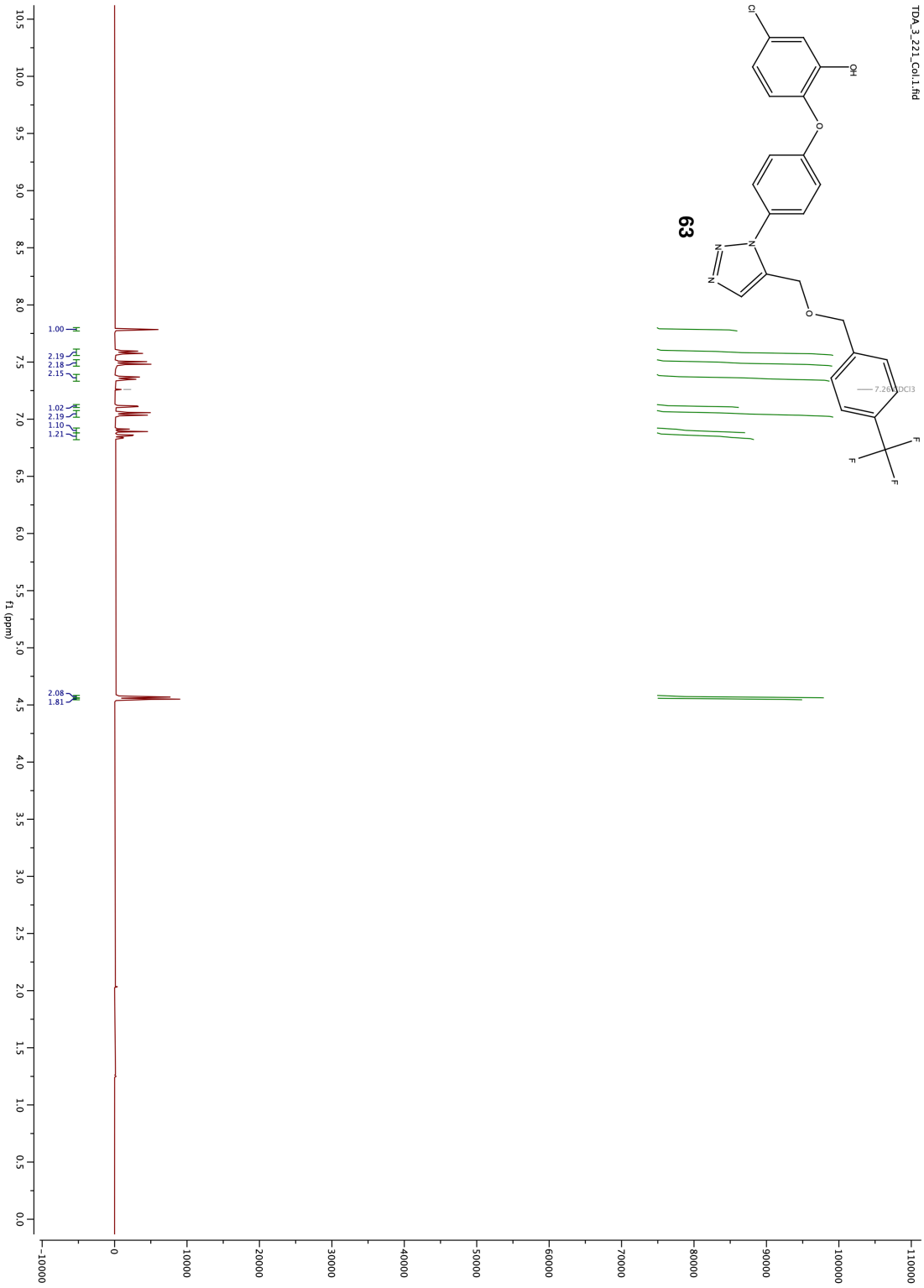
TDA_3_221_Col_1.fid
63
Cl
OH
O
N
N
O
F
F
F
7.26 CDCl3
1.00
2.19
2.18
2.15
1.02
2.19
1.10
1.21
2.08
1.81
f1 (ppm)

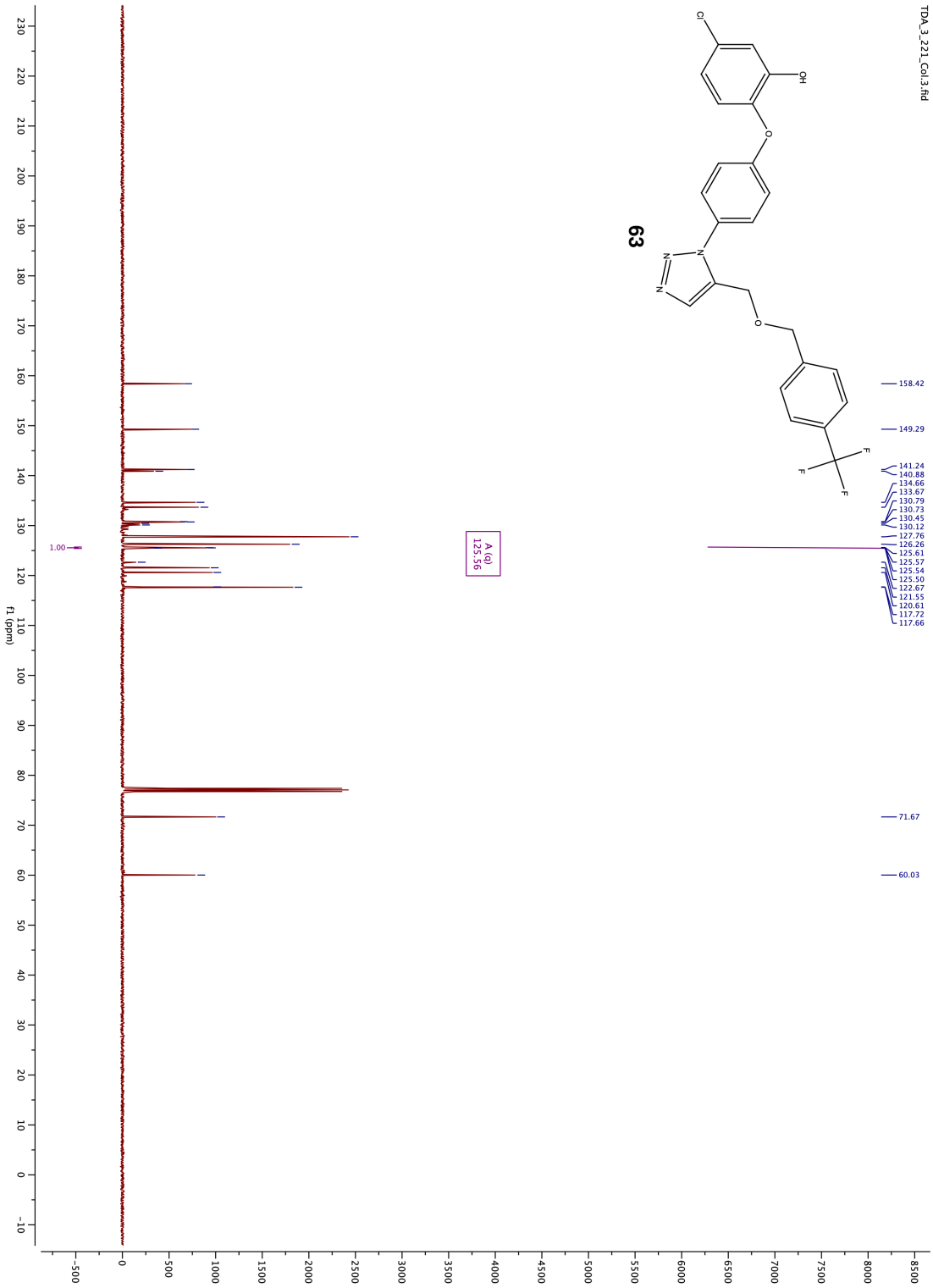
TDA_3_221_Col3.fid
63
Cl
OH
O
N
N
N
O
F
F
F
158.42
149.29
141.24
140.88
134.66
133.67
130.79
130.73
130.45
130.12
127.76
126.26
125.61
125.57
125.54
125.50
122.67
121.55
120.61
117.72
117.66
71.67
60.03
1.00
A (q)
125.56
f1 (ppm)

t_arm.TDA_3_221_Col_2.3.fid
UserID t_arm SampleID TDA_3_221_Col_2 SupervisorID thoma Lab Phone No. x67990 Slot Number 28
Processed with back linear prediction to eliminate baseline artefacts: broad peaks may be attenuated. Standard data in file 100003

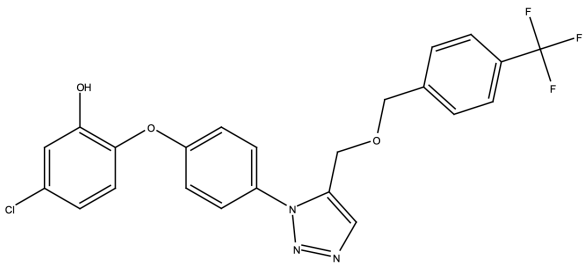

63

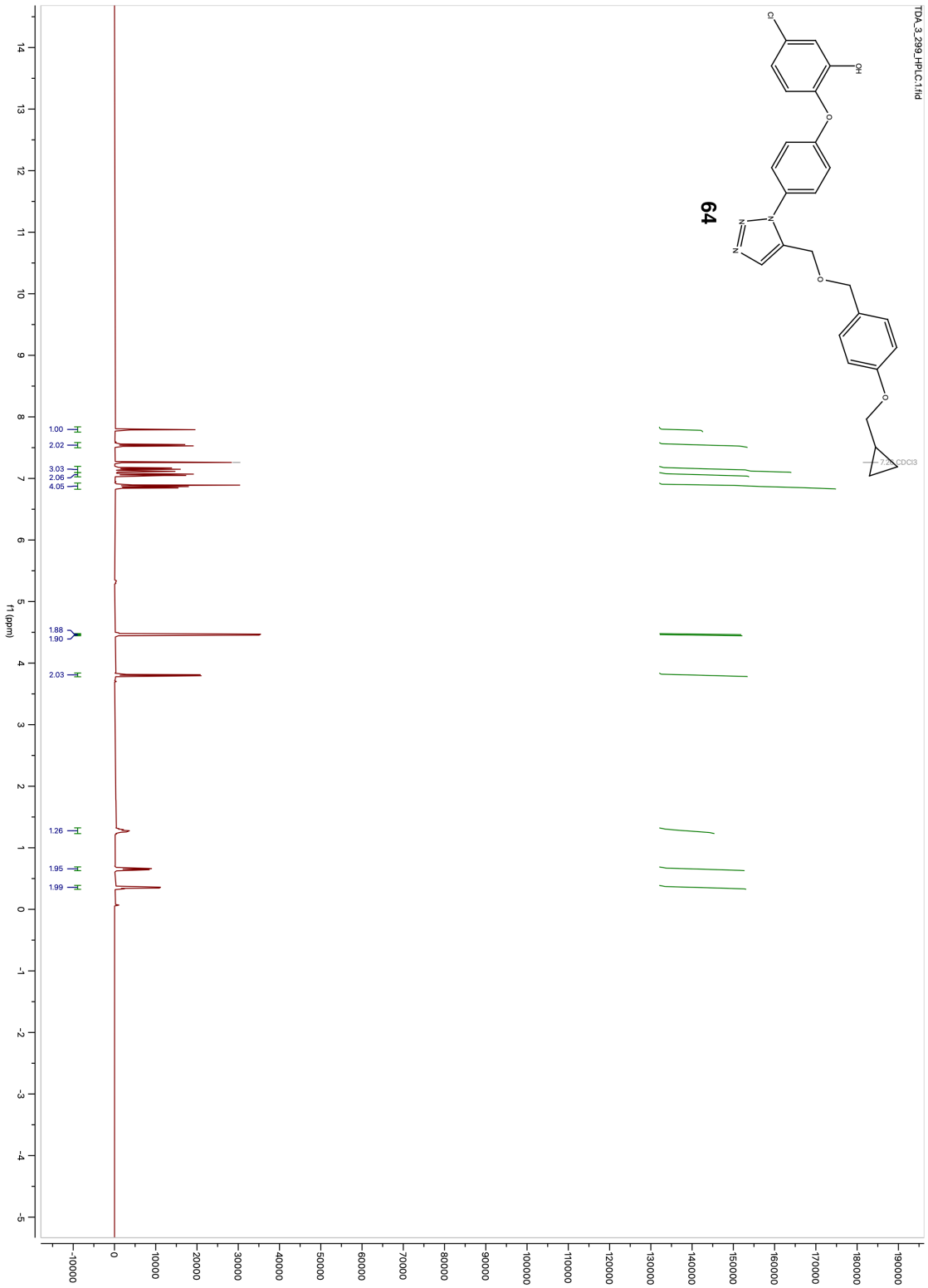
TDA_3_299_HPLC.1.fid
64
1.00
2.02
3.03
2.06
4.05
1.88
1.90
2.03
1.26
1.95
1.99
f1 (ppm)

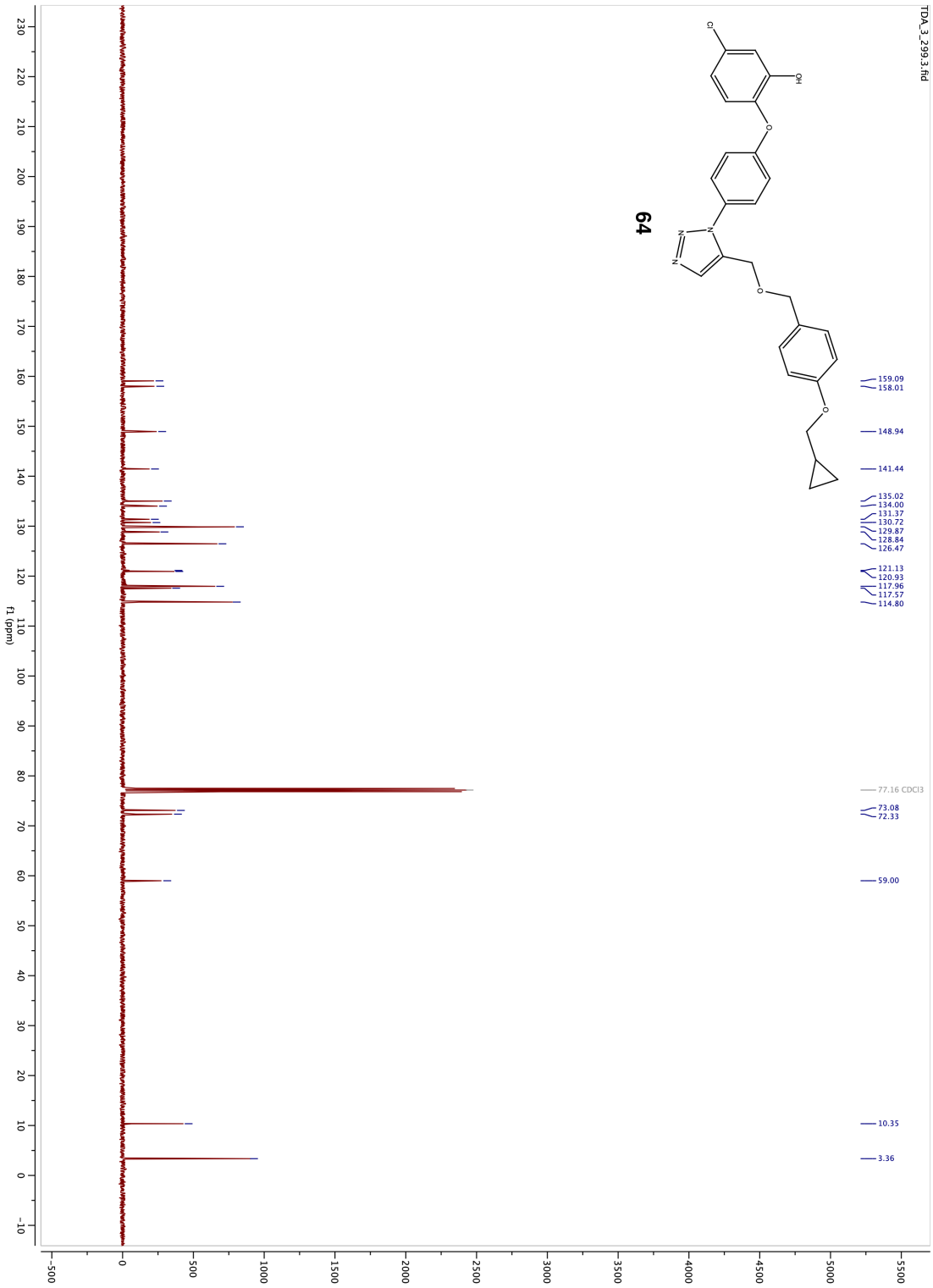
TDA_3_299.3.fid
64
159.09
158.01
148.94
141.44
135.02
134.00
131.37
130.72
129.87
128.84
126.47
121.13
120.93
117.96
117.57
114.80
77.16 CDCl3
73.08
72.33
59.00
10.35
3.36
f1 (ppm)

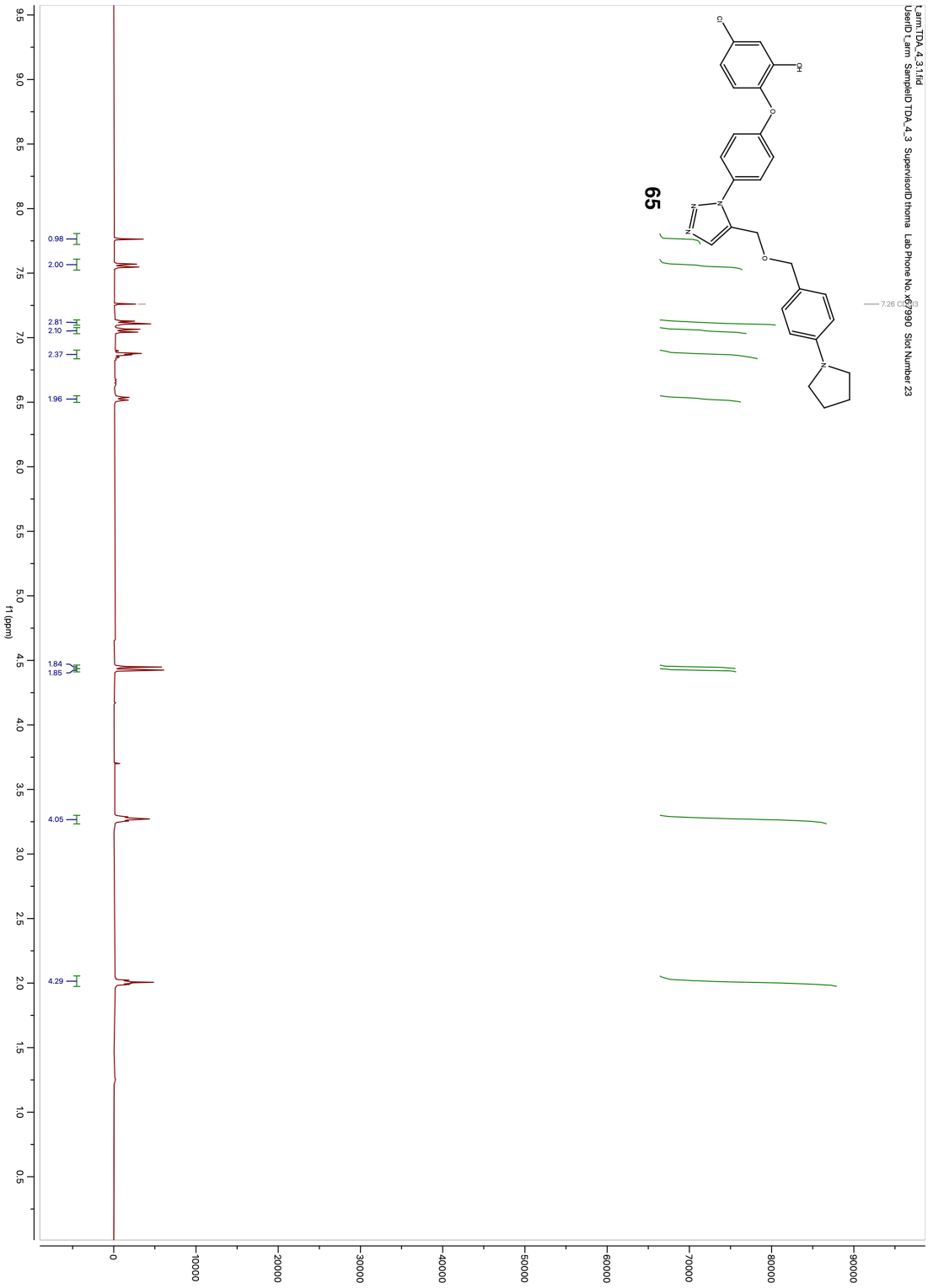
t_arm:TDA_4_3.1.fid
UserID t_arm SampleID TDA_4_3 SupervisorID thoma Lab Phone No. x67990 Slot Number 23
65
0.98
2.00
2.81
2.10
2.37
1.96
1.84
1.85
4.05
4.29
f1 (ppm)

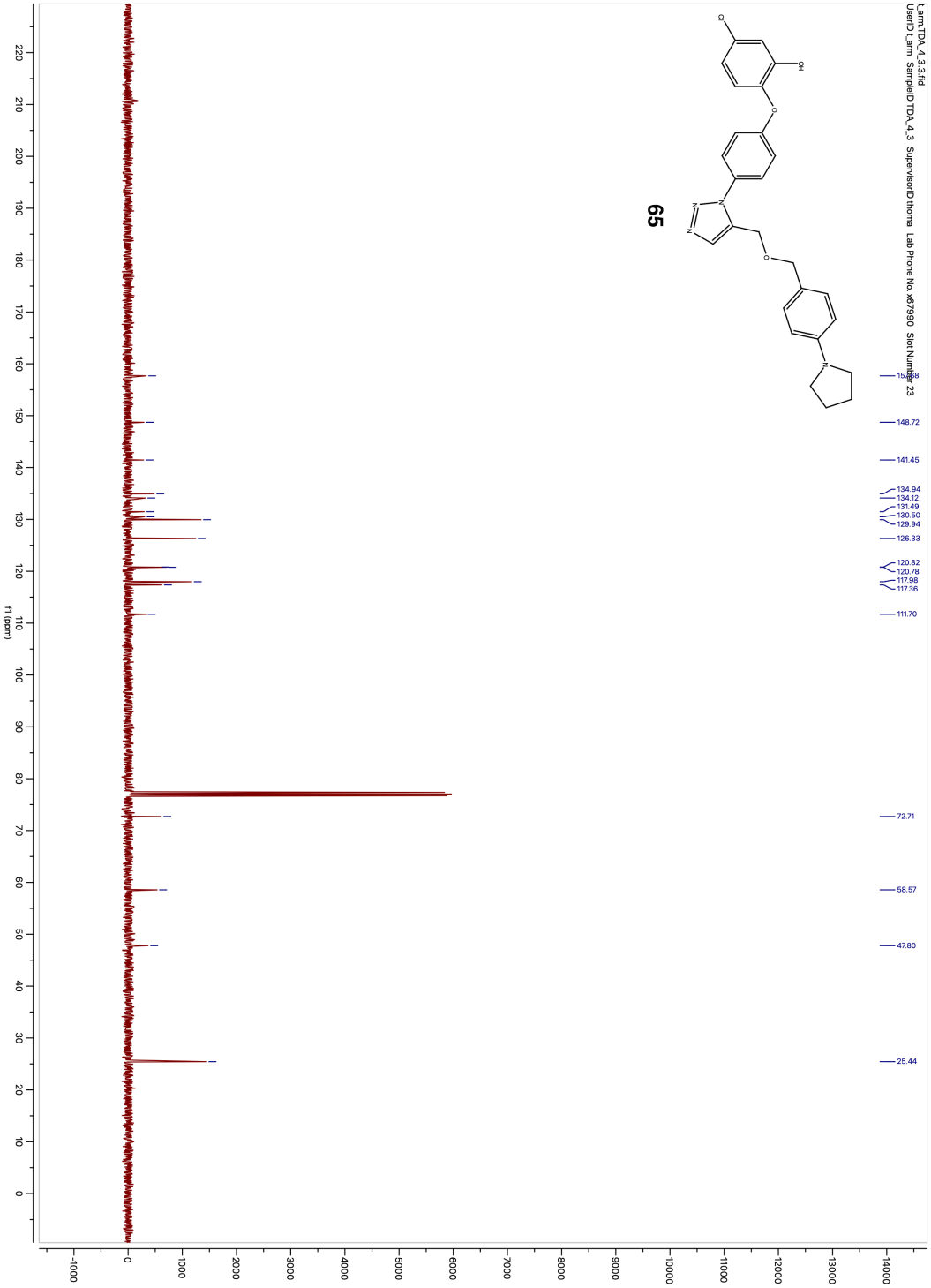
t_arm.TDA_4_3.3.fid
UserID t_arm SampleID TDA_4_3 SupervisorID thoma Lab Phone No. x67990 Slot Number 23
65
153.38
148.72
141.45
134.94
134.12
131.49
130.50
129.94
126.33
120.82
120.78
117.98
117.36
111.70
72.71
58.57
47.80
25.44
f1 (ppm)

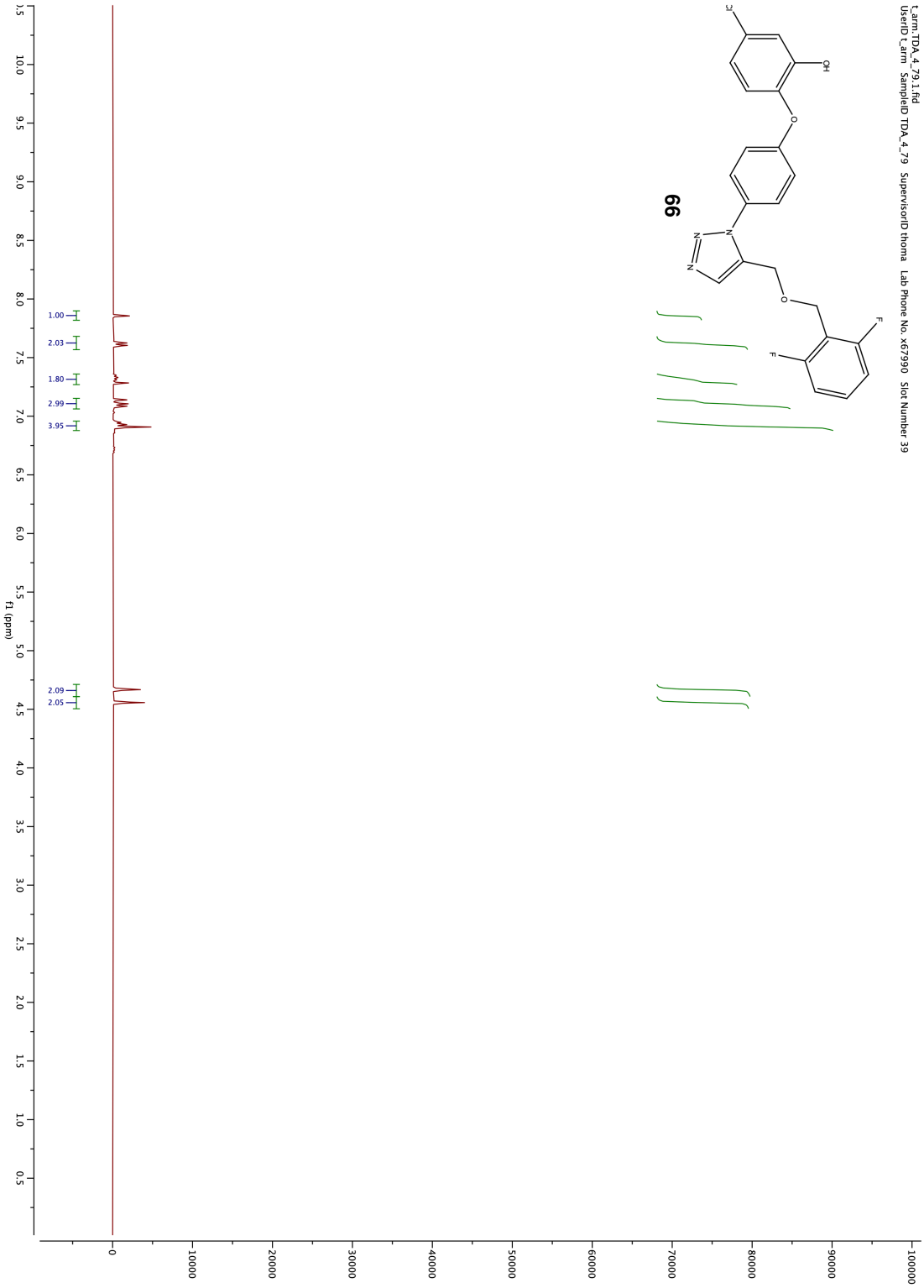
t_arm_TDA_4_79_1.fid
UserID t_arm SampleID TDA_4_79 SupervisorID thoma Lab Phone No. x67990 Slot Number 39
66
1.00
2.03
1.80
2.99
3.95
2.09
2.05
f1 (ppm)

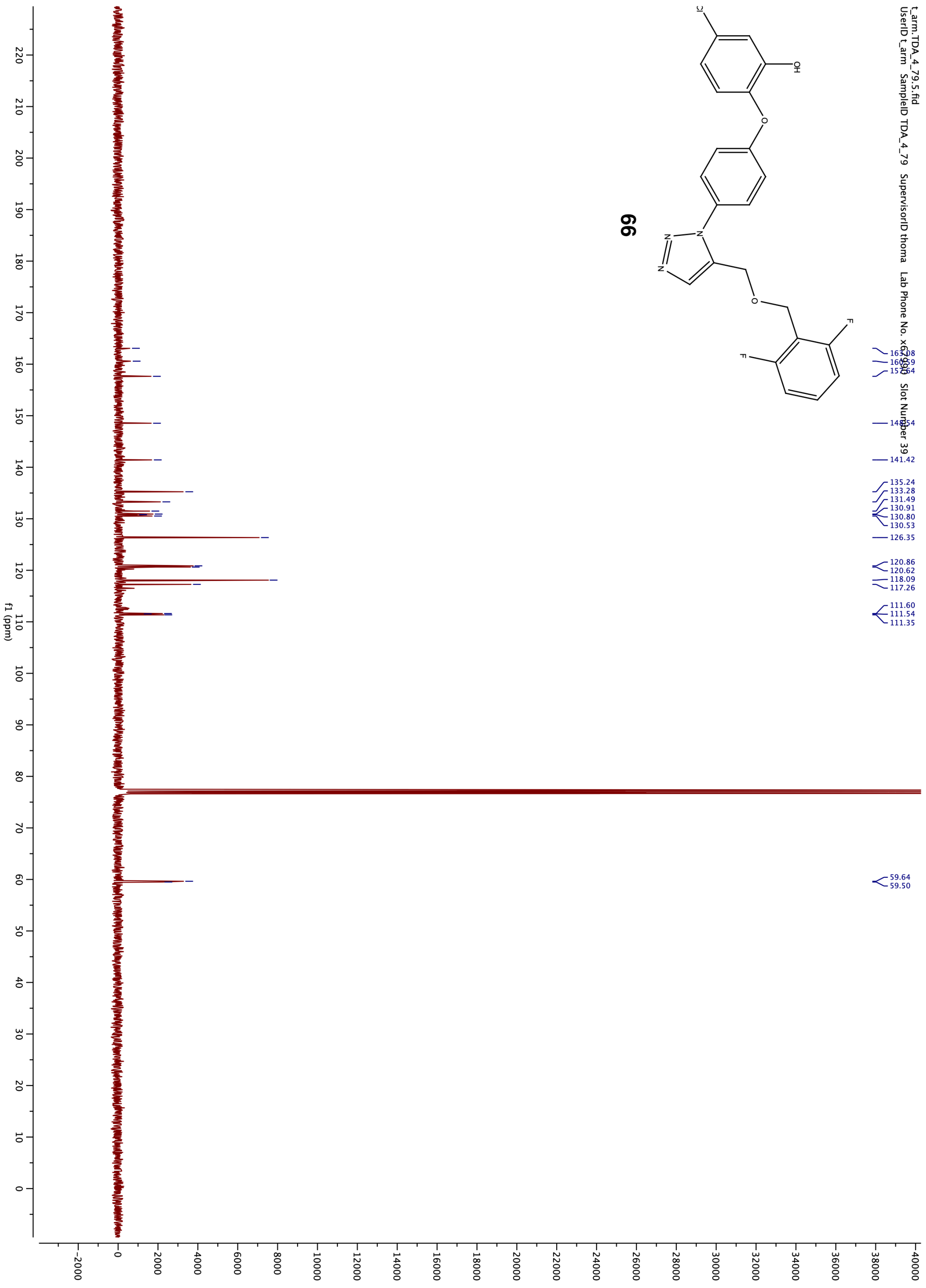
t_arm.TDA_4_79.5.fid
UserID t_arm SampleID TDA_4_79 SupervisorID thoma Lab Phone No. x Slot Number 39
66
148.54
141.42
135.24
133.28
131.49
130.91
130.80
130.53
126.35
120.86
120.62
118.09
117.26
111.60
111.54
111.35
59.64
59.50
f1 (ppm)

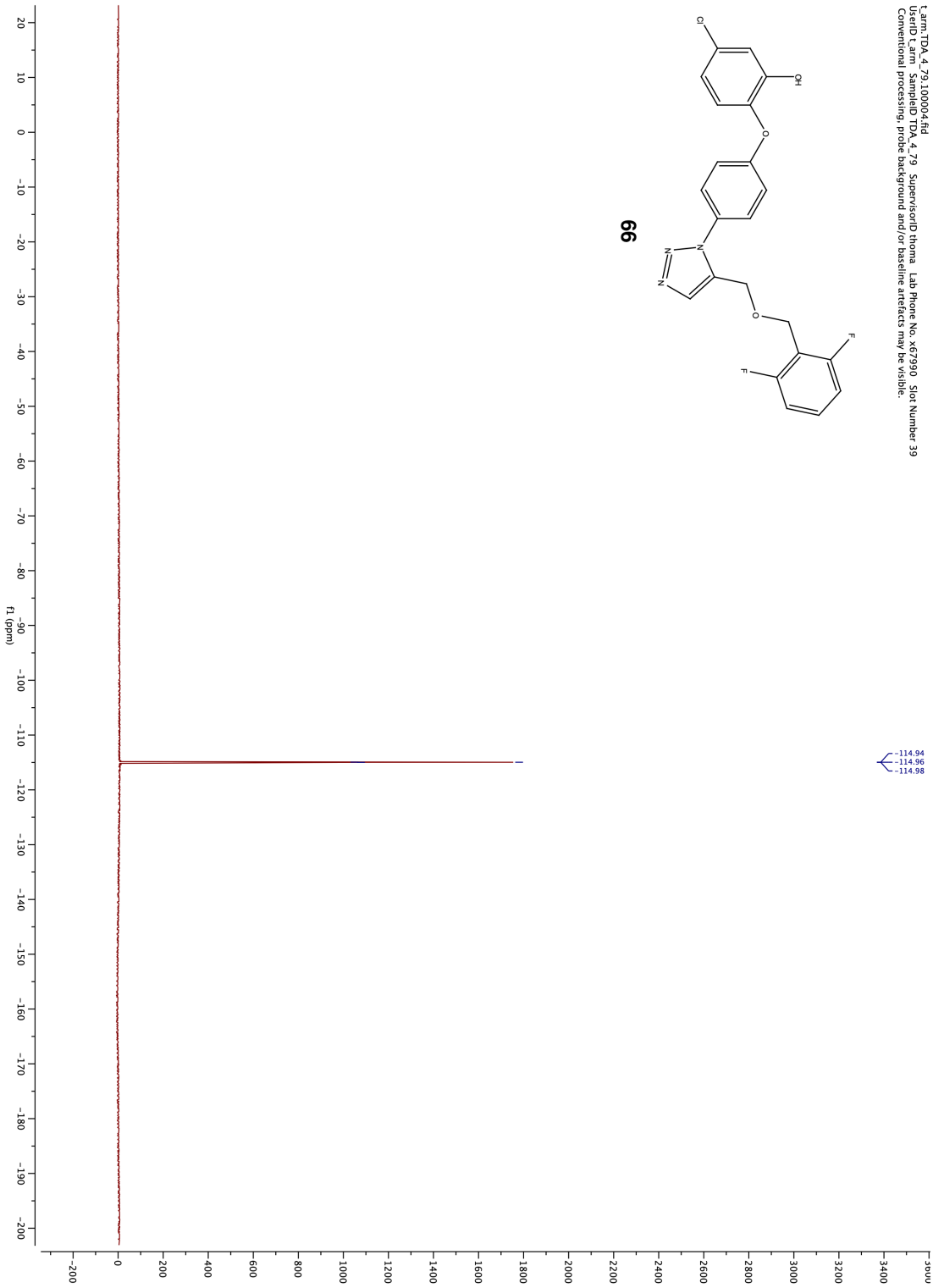
t_arm.TDA_4_79.100004.fid
UserID t_arm SampleID TDA_4_79 SupervisorID thoma Lab Phone No. x67990 Slot Number 39
Conventional processing, probe background and/or baseline artefacts may be visible.
66
Cl
OH
O
N
N
N
O
F
F
-114.94
-114.96
-114.98
f1 (ppm)

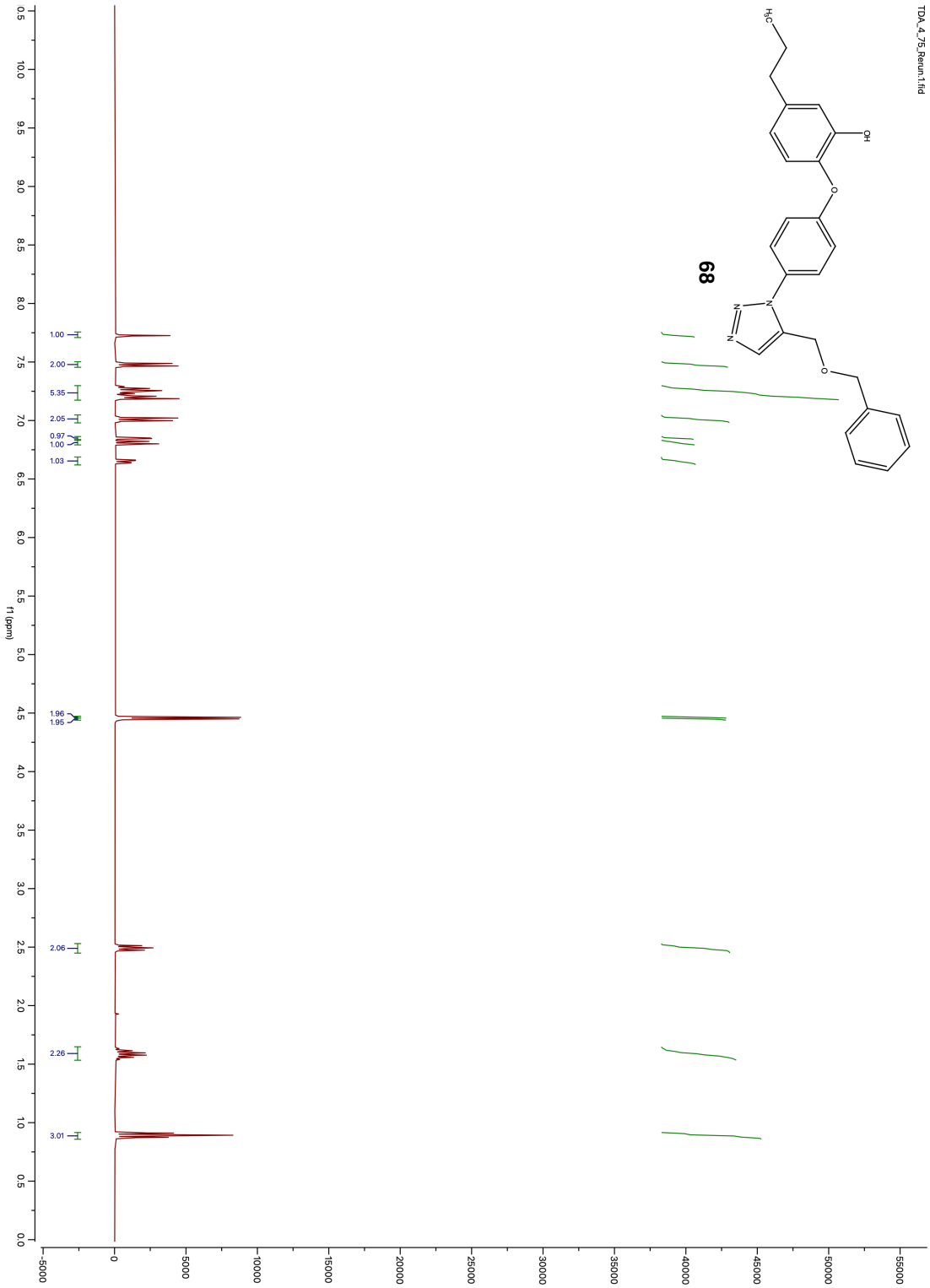
TDA_4_75_Rerun.1.fid
69
1.00
2.00
5.35
2.05
0.97
1.00
1.03
1.96
1.95
2.06
2.26
3.01
f1 (ppm)

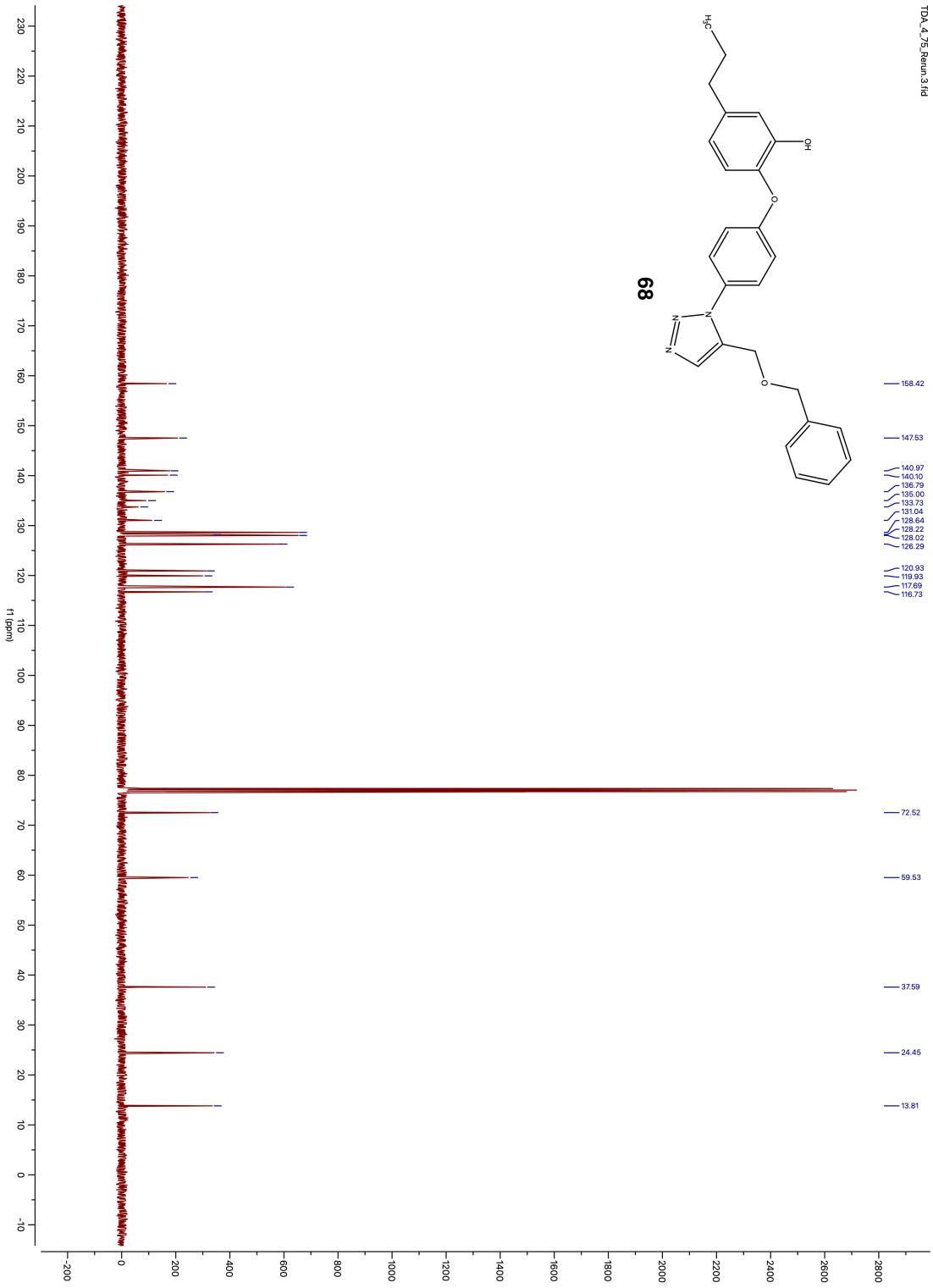
TDA_4_75_Rerun.3.fid
68
158.42
147.53
140.97
140.10
136.79
135.00
133.73
131.04
128.64
128.22
128.02
126.29
120.93
119.93
117.69
116.73
72.52
59.53
37.59
24.45
13.81
f1 (ppm)

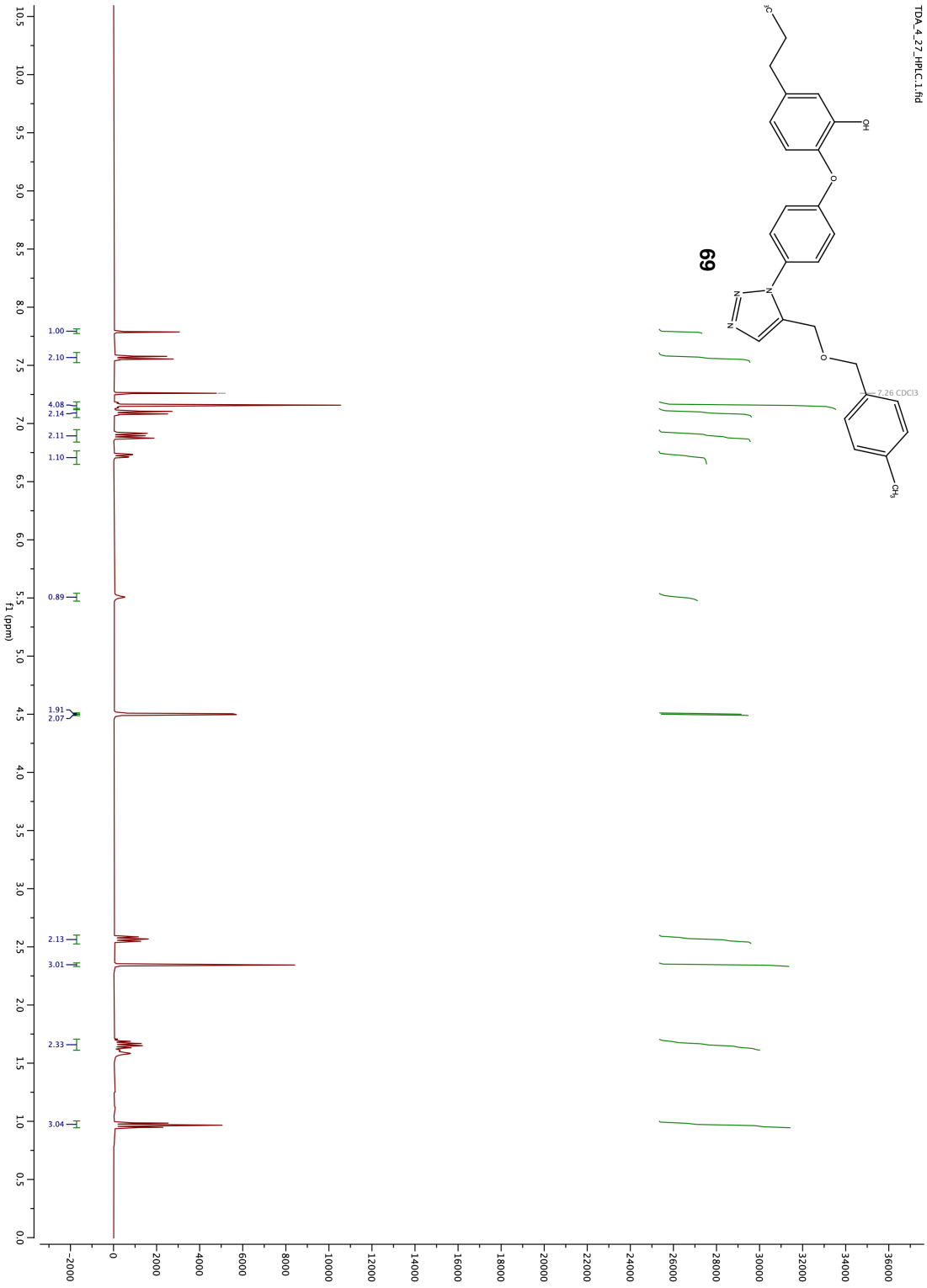
TDA_4_27_HPLC.1.fid
69
7.26 CDCl3
1.00
2.10
4.08
2.14
2.11
1.10
0.89
1.91
2.07
2.13
3.01
2.33
3.04
f1 (ppm)

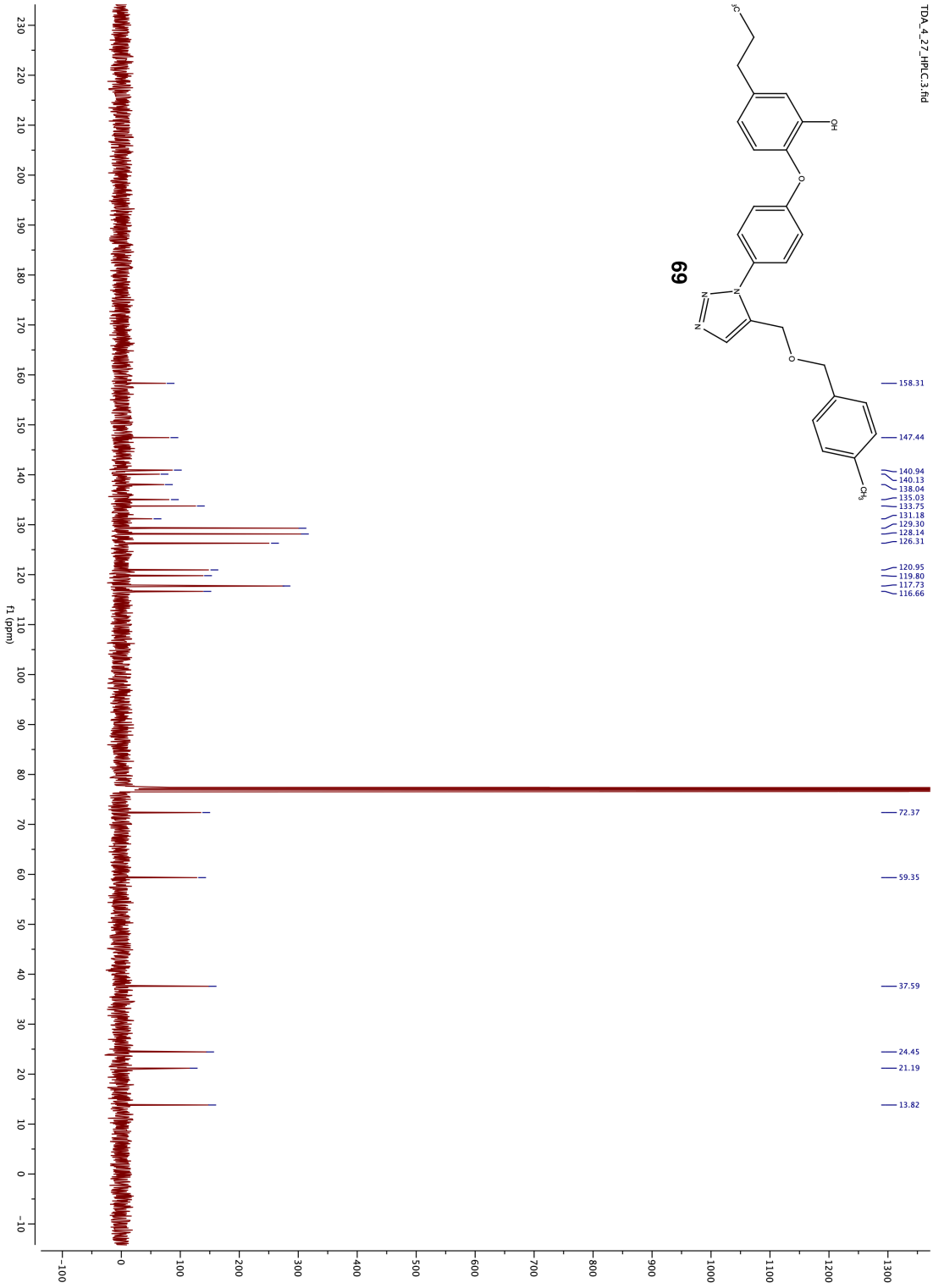
TDA_4_27_HPLC_3.fid
69
158.31
147.44
140.94
140.13
138.04
135.03
133.75
131.18
129.30
128.14
126.31
120.95
119.80
117.73
116.66
72.37
59.35
37.59
24.45
21.19
13.82
f1 (ppm)

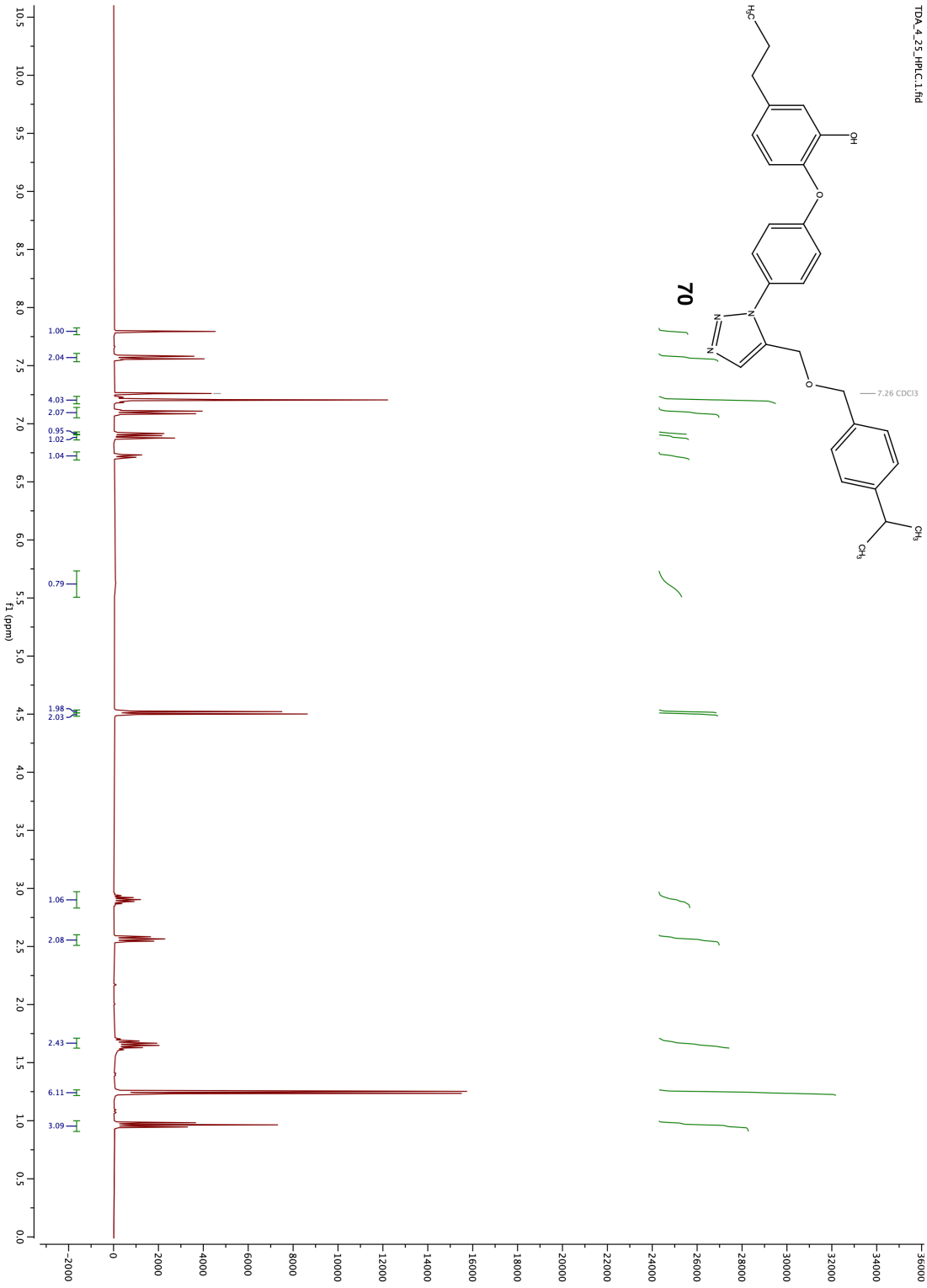
TDA_4_25_HPLC.1.fid
70
7.26 CDCl3
1.00
2.04
4.03
2.07
0.95
1.02
1.04
0.79
1.98
2.03
1.06
2.08
2.43
6.11
3.09
f1 (ppm)

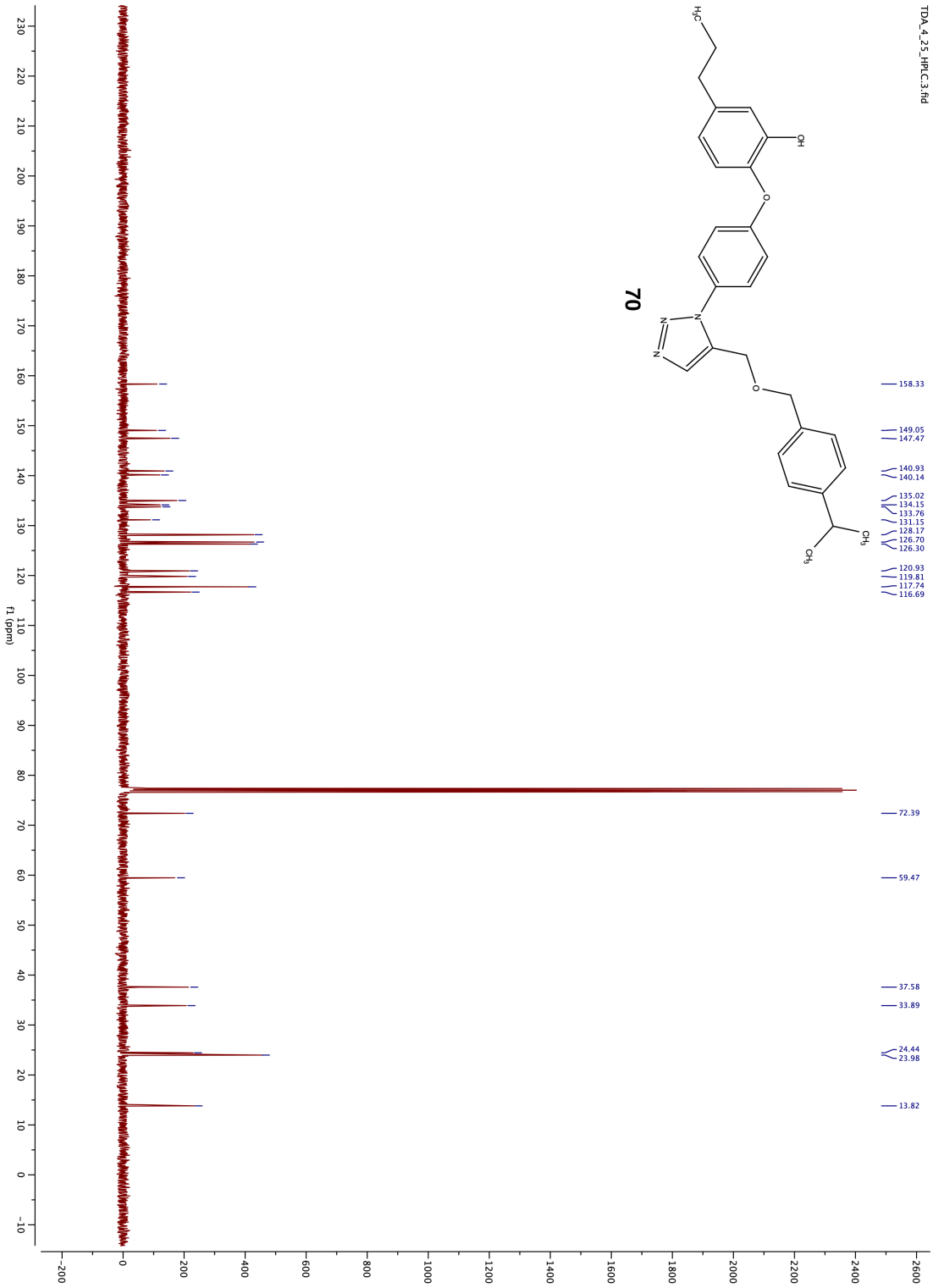
TDA_4_25_HPLC.3.fid
70
158.33
149.05
147.47
140.93
140.14
135.02
134.15
133.76
131.15
128.17
126.70
126.30
120.93
119.81
117.74
116.69
72.39
59.47
37.58
33.89
24.44
23.98
13.82
f1 (ppm)

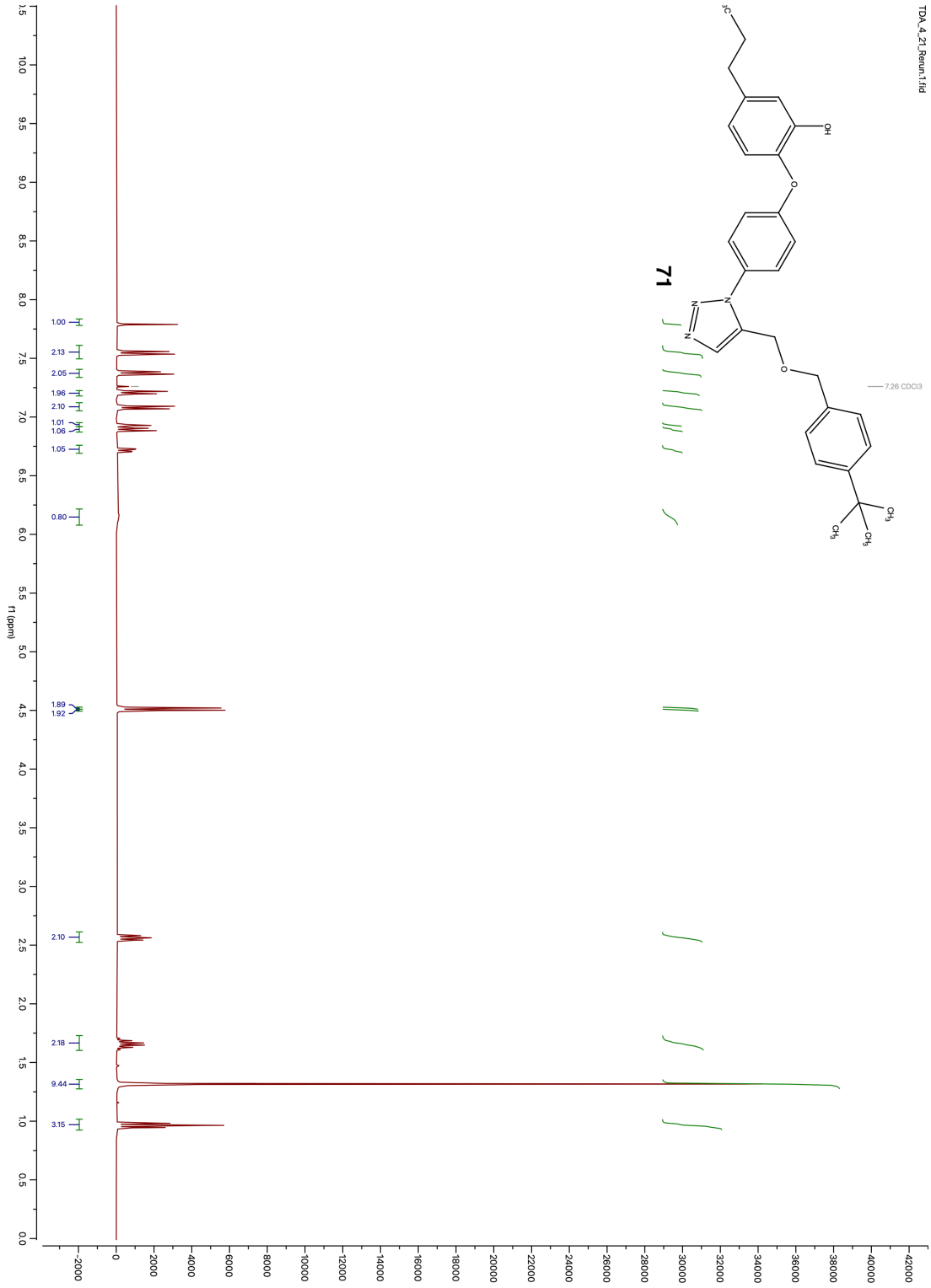
TDA_4_21_Rerun.1.fid
71
7.26 CDCl3
1.00
2.13
2.05
1.96
2.10
1.01
1.06
1.05
0.80
1.89
1.92
2.10
2.18
9.44
3.15
f1 (ppm)

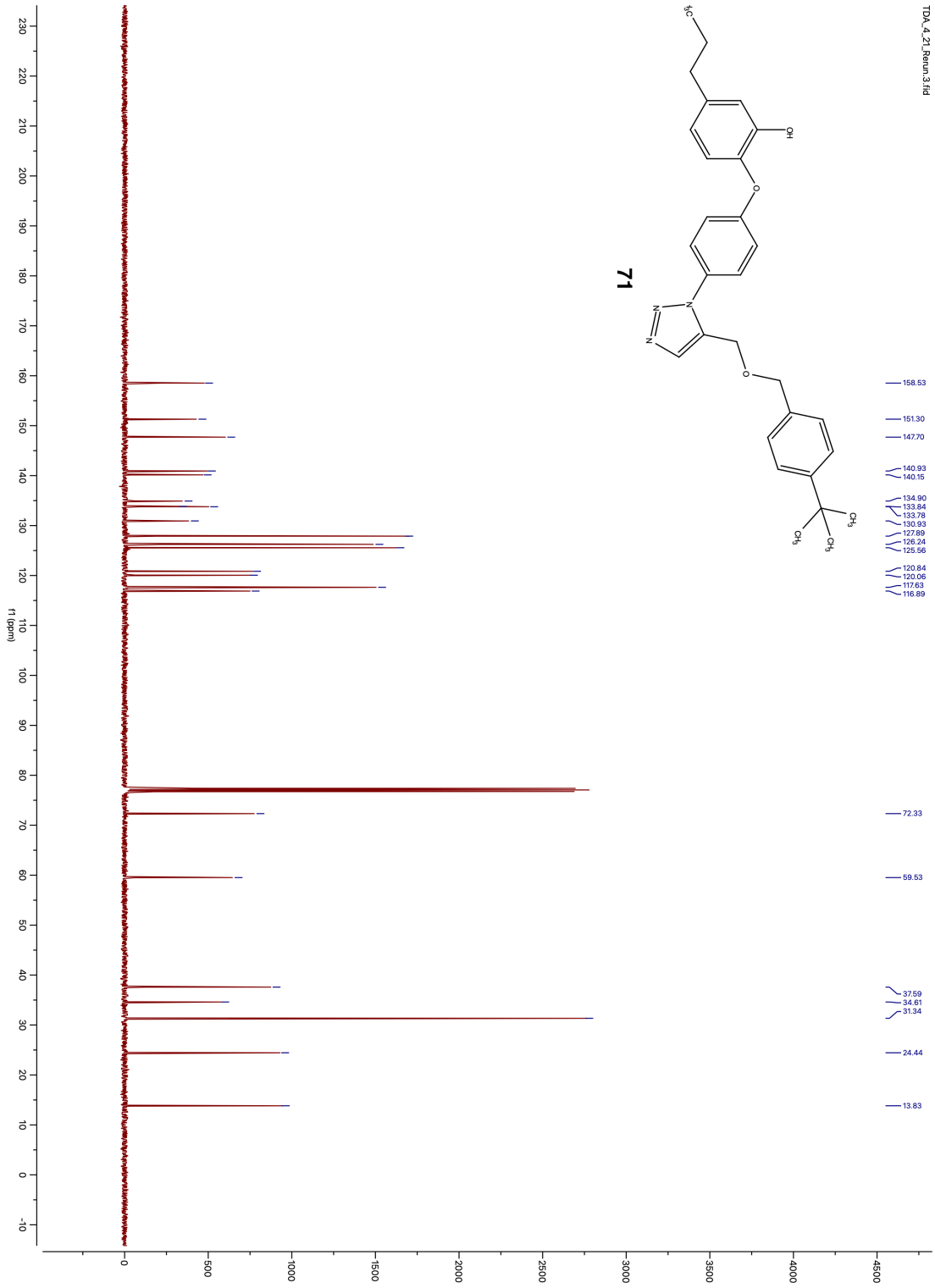
TDA_4_21_Rerun.3.fid
71
158.53
151.30
147.70
140.93
140.15
134.90
133.84
133.78
130.93
127.89
126.24
125.56
120.84
120.06
117.63
116.89
72.33
59.53
37.59
34.61
31.34
24.44
13.83
f1 (ppm)

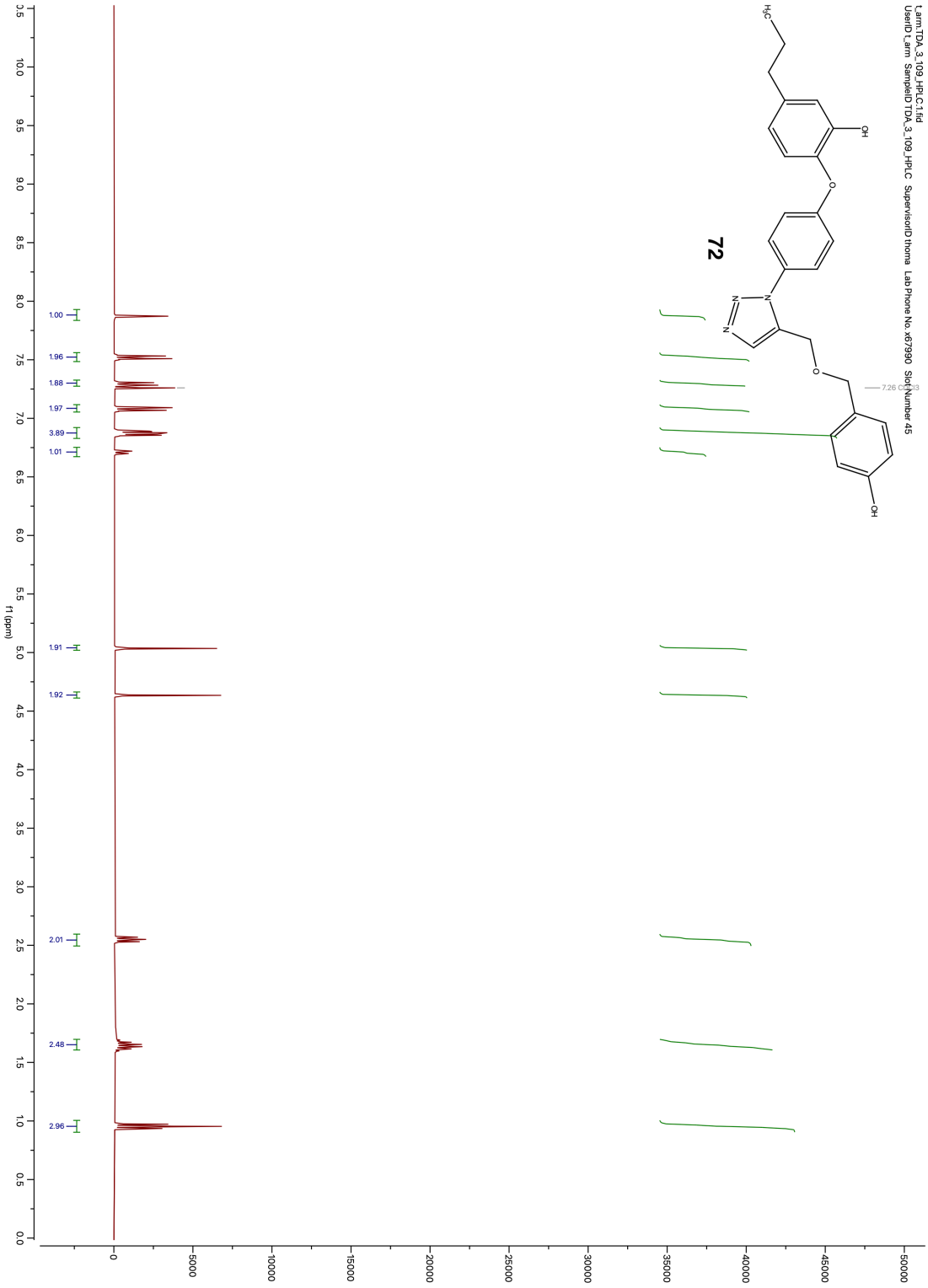
t_arm:TDA_3_109_HPLC.1.fid
UserID t_arm SampleID TDA_3_109_HPLC SupervisorID thoma Lab Phone No. x67990 SlotNumber 45
72
7.26 CDCl3
f1 (ppm)
1.00
1.96
1.88
1.97
3.89
1.01
1.91
1.92
2.01
2.48
2.96

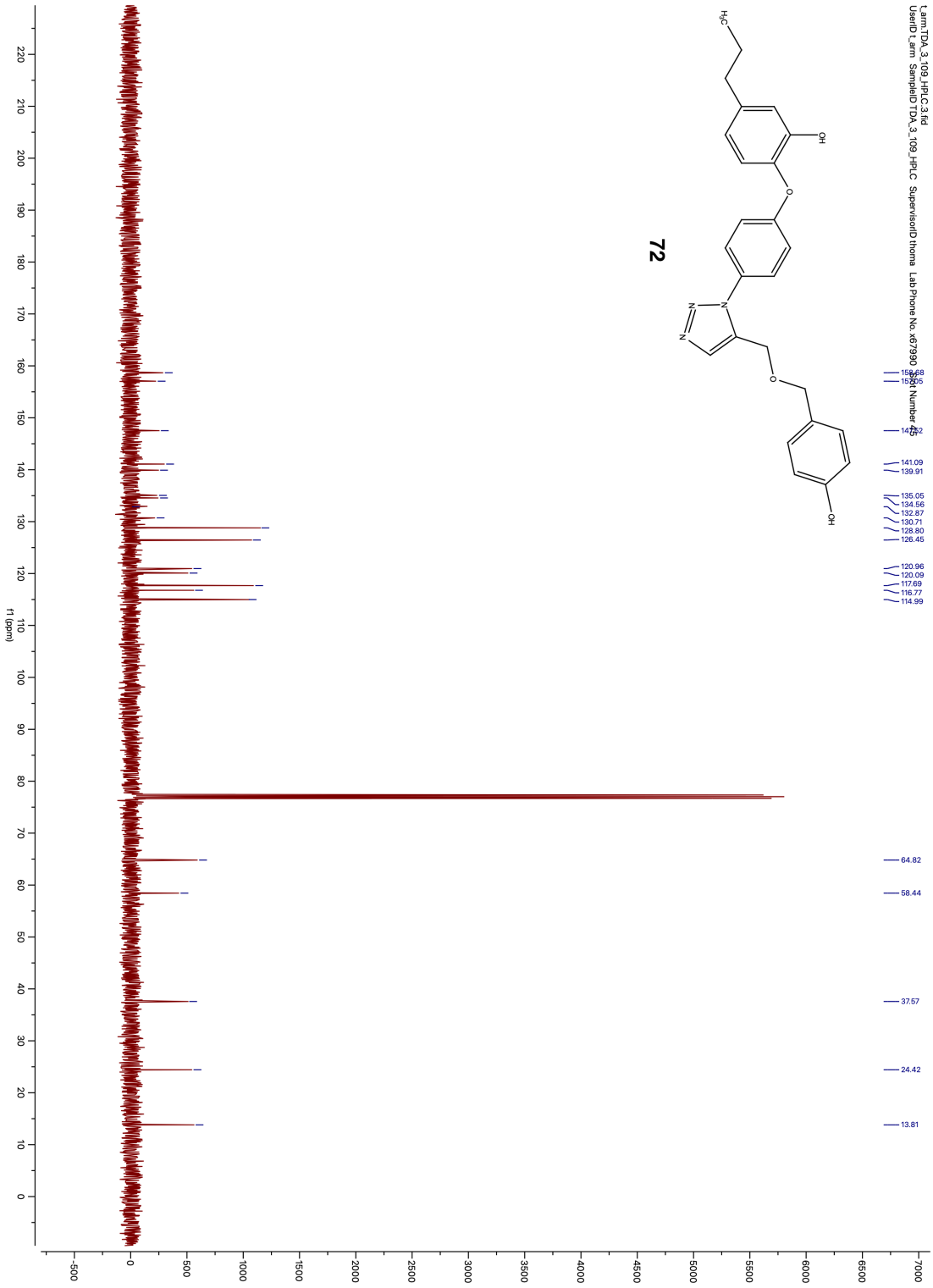
t_arm:TDA_3_109_HPLC_3.fid
UserID t_arm SampleID TDA_3_109_HPLC SupervisorID thoma Lab Phone No. x67990
Acquisition Number 17
72
H3C
OH
O
N
N
N
O
OH
158.68
157.95
147.52
141.09
139.91
135.05
134.56
132.87
130.71
128.80
126.45
120.96
120.09
117.69
116.77
114.99
64.82
58.44
37.57
24.42
13.81
f1 (ppm)

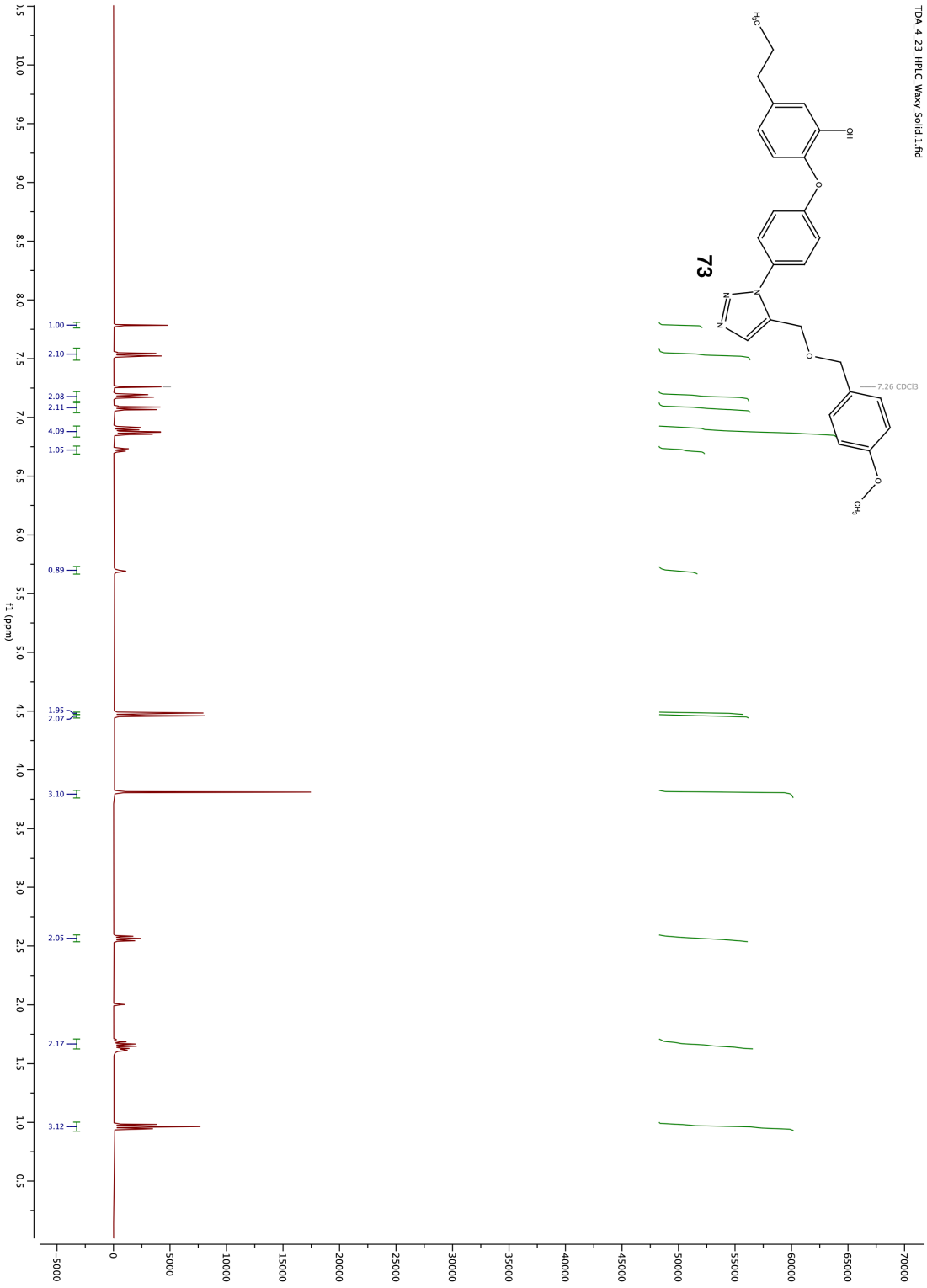
TDA_4_23_HPLC_Waxy_Solid.1.fid
73
7.26 CDCl3
1.00
2.10
2.08
2.11
4.09
1.05
0.89
1.95
2.07
3.10
2.05
2.17
3.12
f1 (ppm)

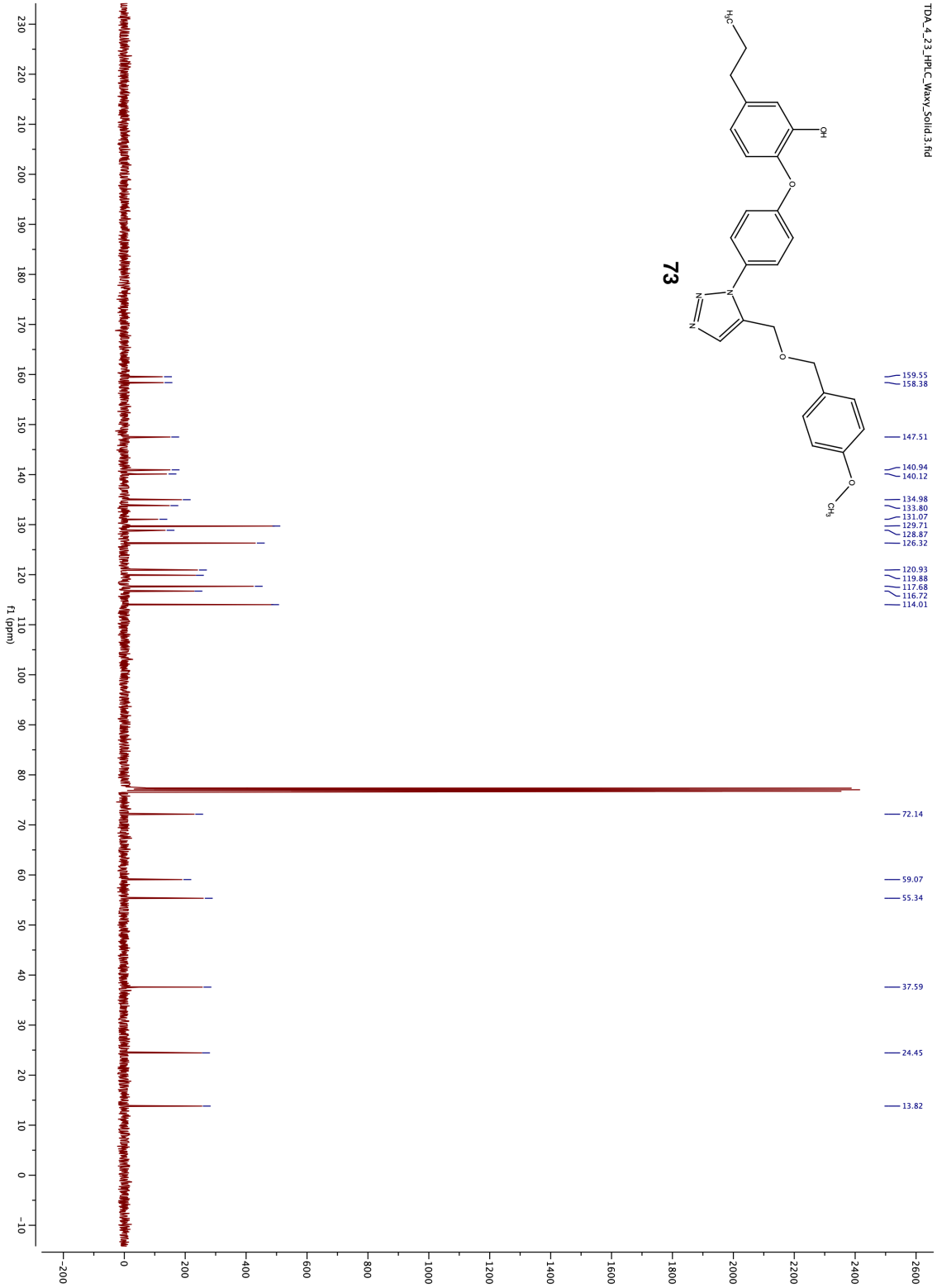
TDA_4_23_HPLC_Waxy_Solid.3.fid
73
159.55
158.38
147.51
140.94
140.12
134.98
133.80
131.07
129.71
128.87
126.32
120.93
119.88
117.68
116.72
114.01
72.14
59.07
55.34
37.59
24.45
13.82
f1 (ppm)

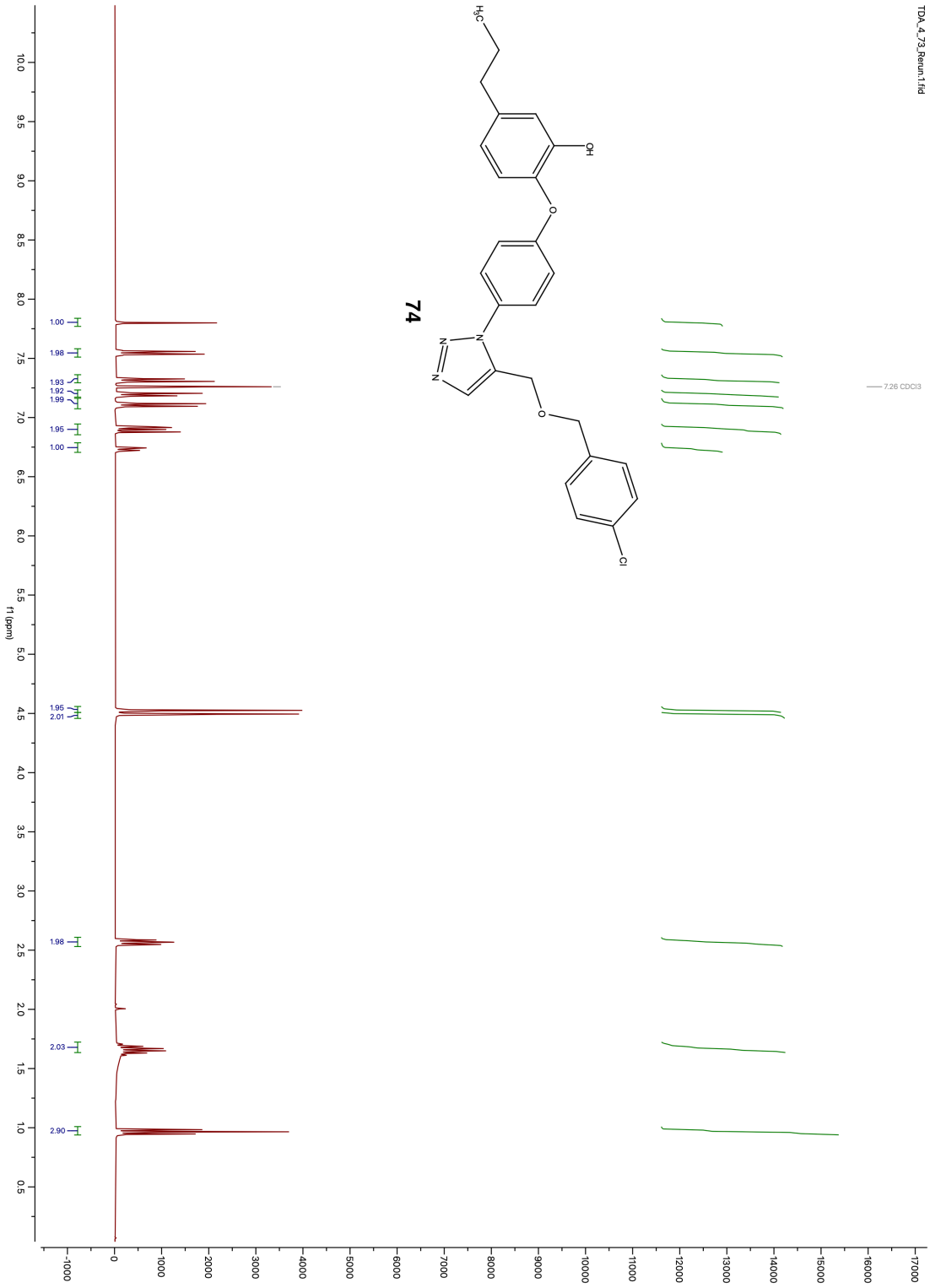
TDA_4_73_Rerun.1.fid
74
OH
Cl
7.26 CDCl3
1.00
1.98
1.93
1.92
1.99
1.95
1.00
1.95
2.01
1.98
2.03
2.90
f1 (ppm)

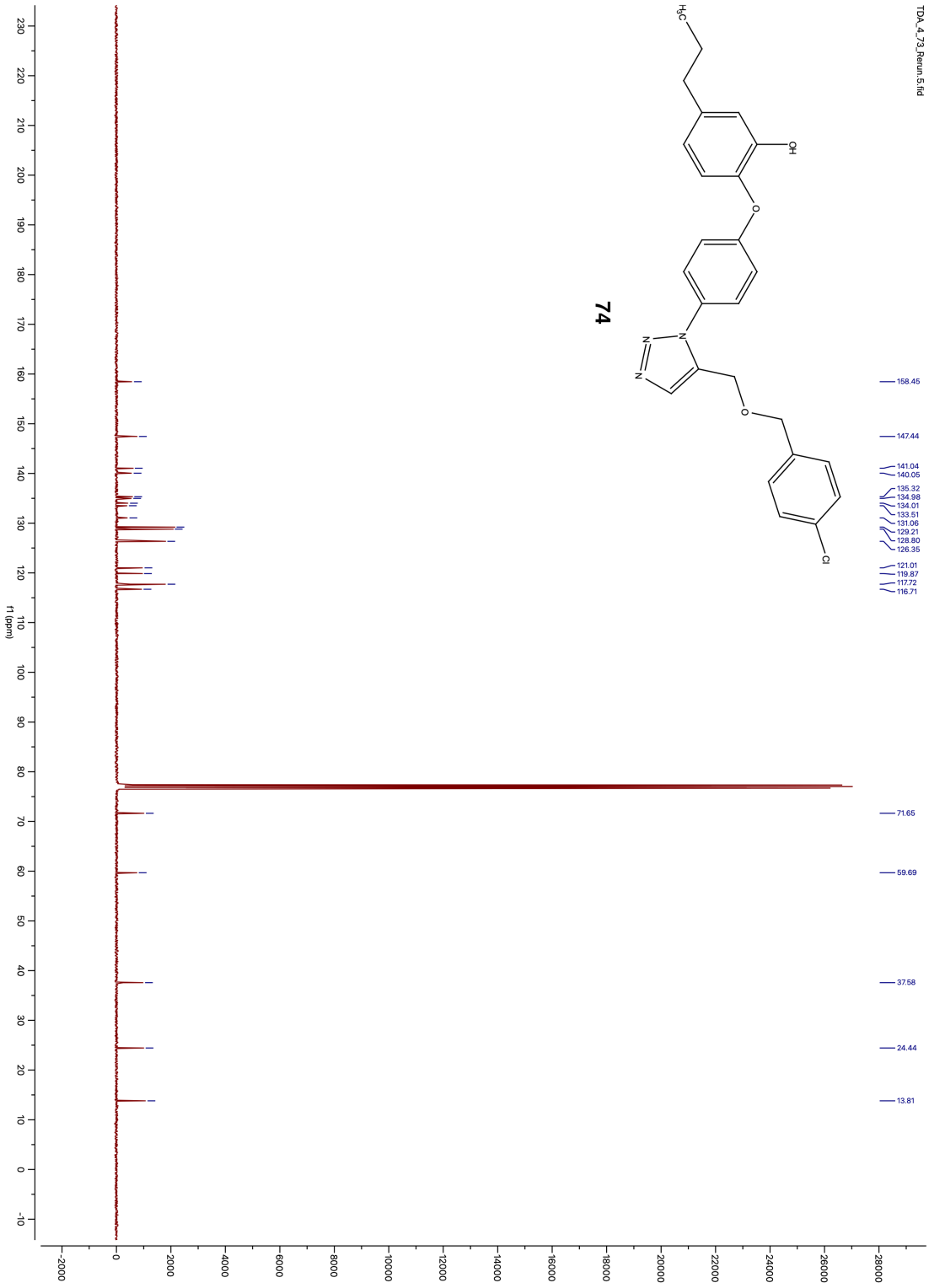
TDA_4_73_Rerun.5.fid
74
158.45
147.44
141.04
140.05
135.32
134.98
134.01
133.51
131.06
129.21
128.80
126.35
121.01
119.87
117.72
116.71
71.65
59.69
37.58
24.44
13.81
f1 (ppm)

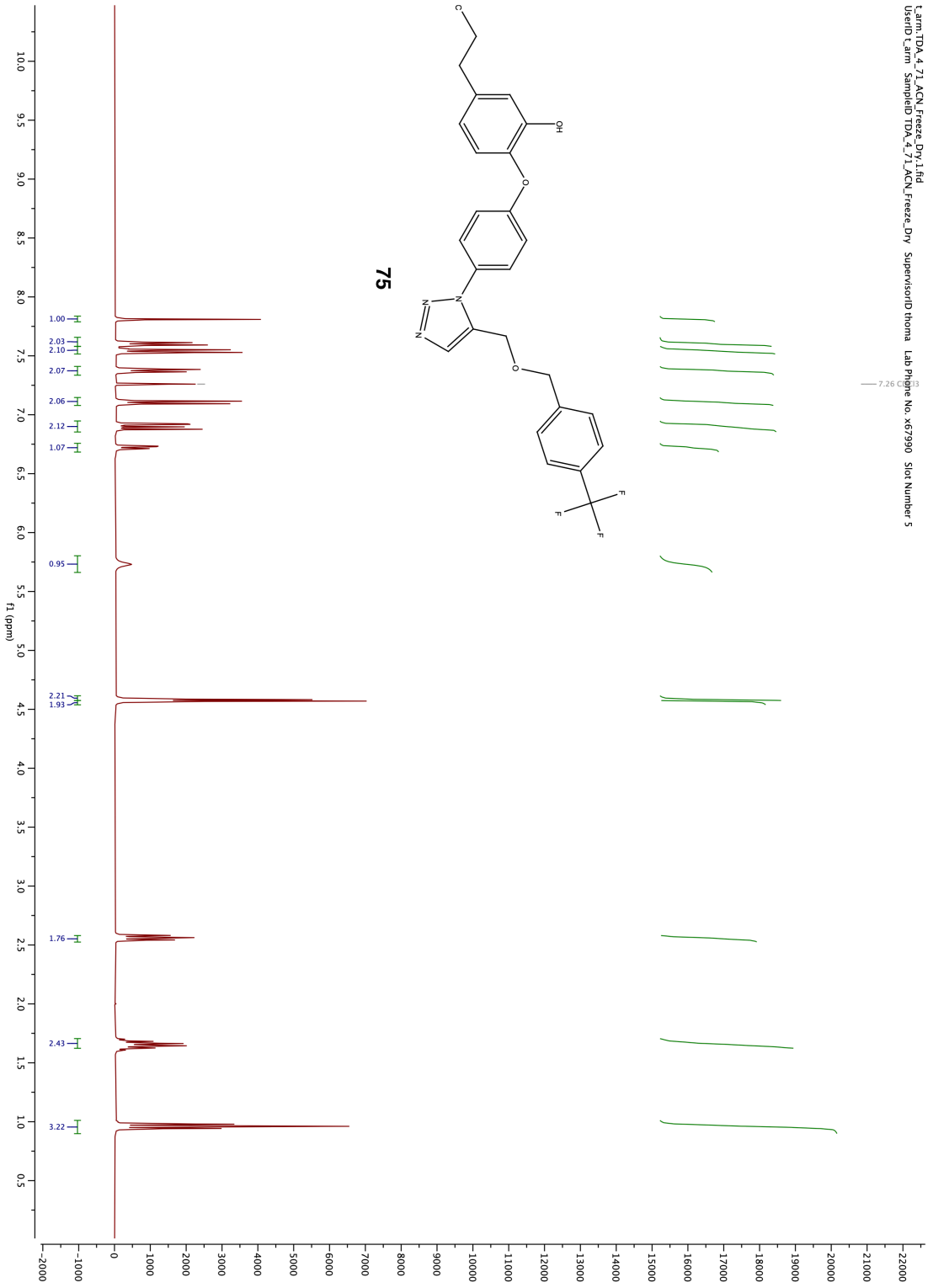
t_arm.TDA_4_71_ACN_Freeze_Dry.1.fid
UserID t_arm SampleID TDA_4_71_ACN_Freeze_Dry SupervisorID thoma Lab Phone No. x67990 Slot Number 5
7.26 CDCl3
75
OH
O
N
N
N
O
F
F
F
f1 (ppm)
1.00
2.03
2.10
2.07
2.06
2.12
1.07
0.95
2.21
1.93
1.76
2.43
3.22

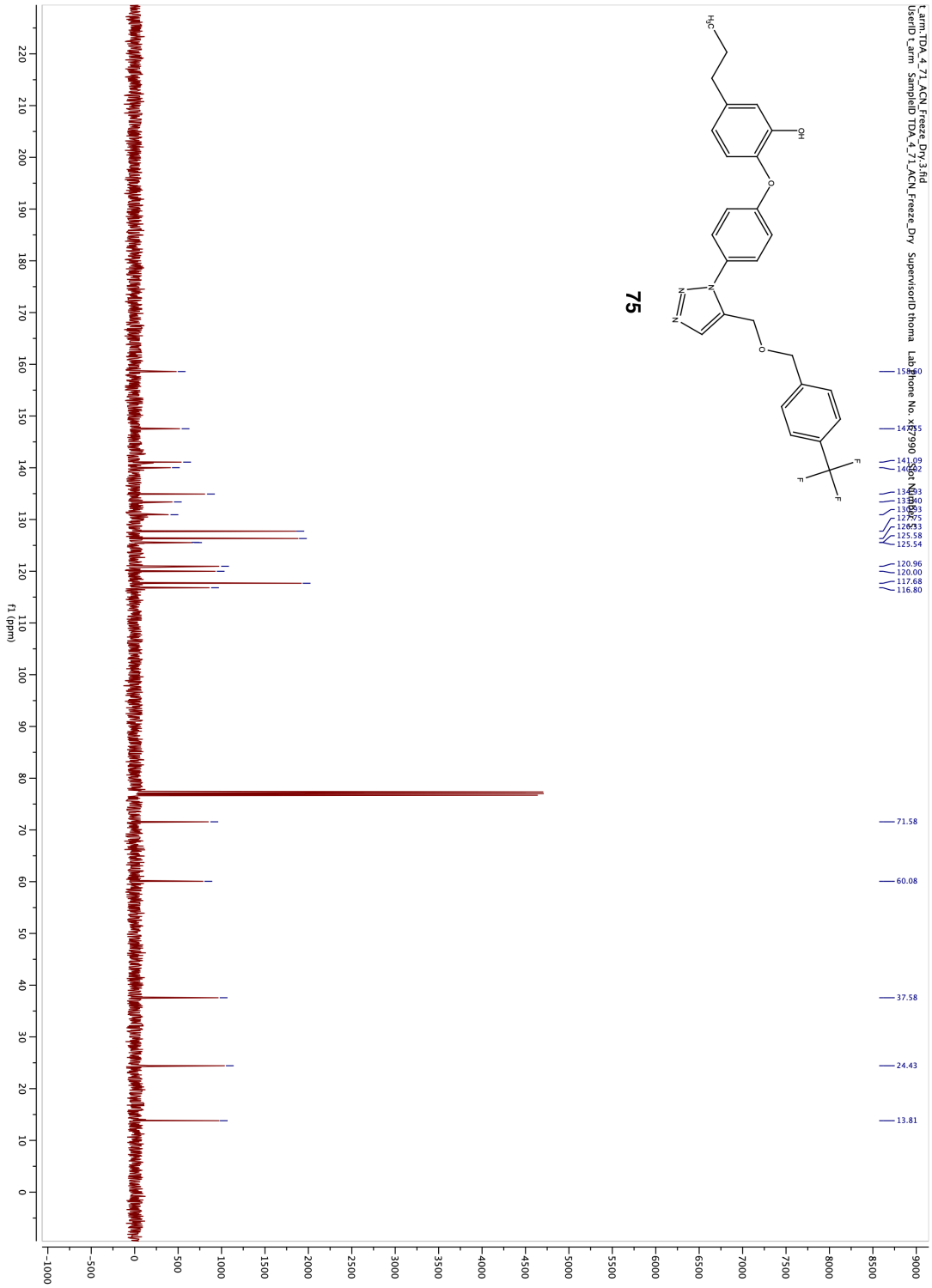
t_arm-TDA_4_71_ACN_Freeze_Dry_3.fid
UserID t_arm SampleID TDA_4_71_ACN_Freeze_Dry SupervisorID thoma Lab Notebook No. :27990
75
158.60
142.55
141.09
140.62
133.93
133.40
130.93
127.75
126.53
125.58
125.54
120.96
120.00
117.68
116.80
71.58
60.08
37.58
24.43
13.81
f1 (ppm)

t_arm.TDA_4_71_ACN_Freeze_Dry.4.fid
UserID t_arm SampleID TDA_4_71_ACN_Freeze_Dry SupervisorID thoma Lab Phone No. x67990 Slot Number 5
Processed with back linear prediction to eliminate baseline artefacts: broad peaks may be attenuated. Standard data in file 100004

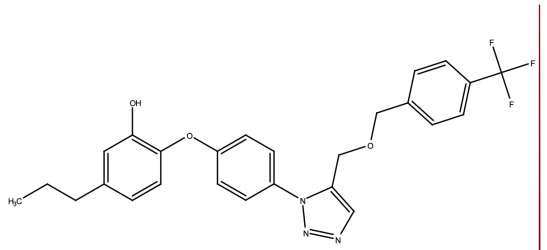

75

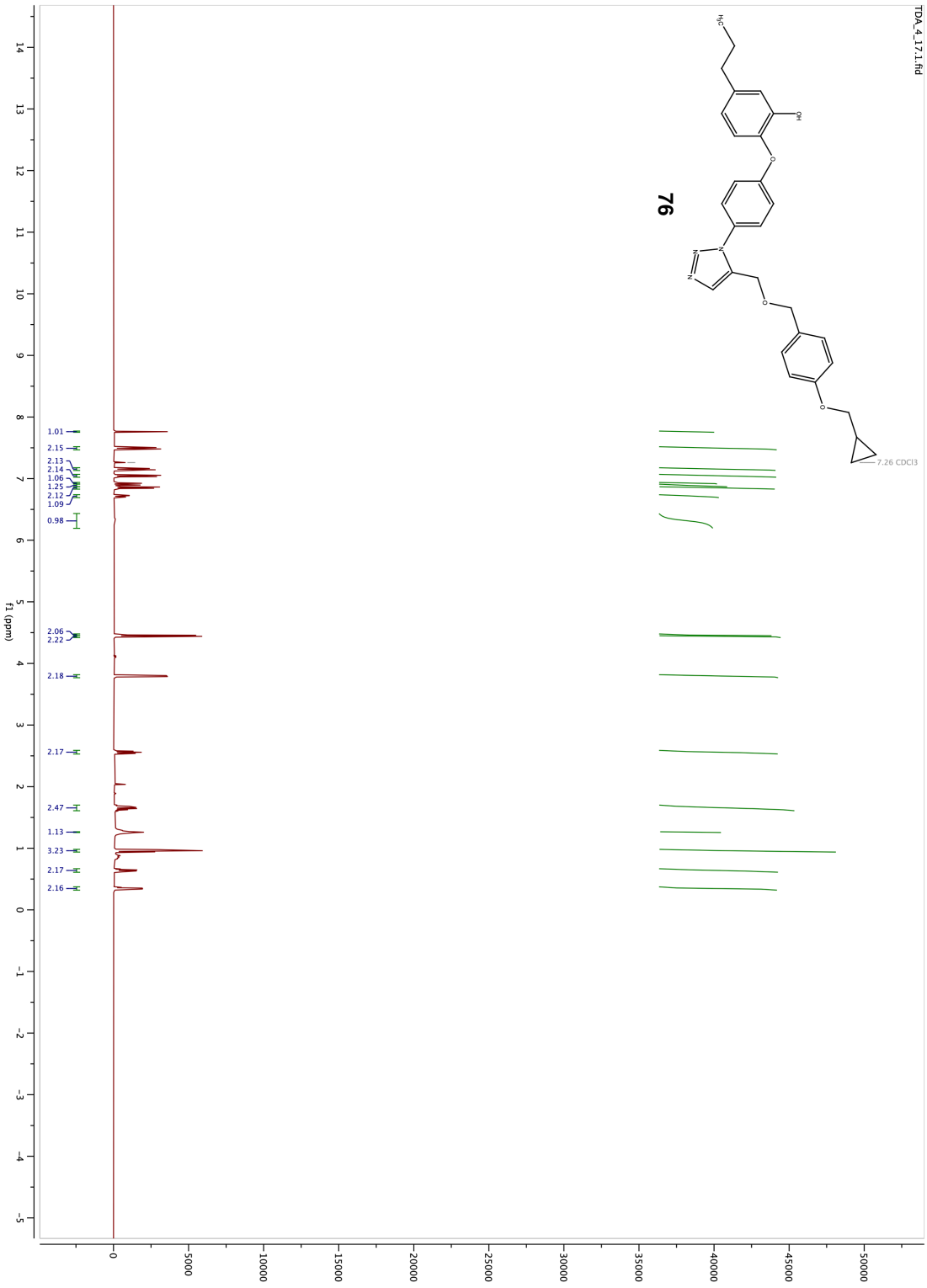
TDA_4_17.1.fid
76
7.26 CDCl3
1.01
2.15
2.13
2.14
1.06
1.25
2.12
1.09
0.98
2.06
2.22
2.18
2.17
2.47
1.13
3.23
2.17
2.16
f1 (ppm)

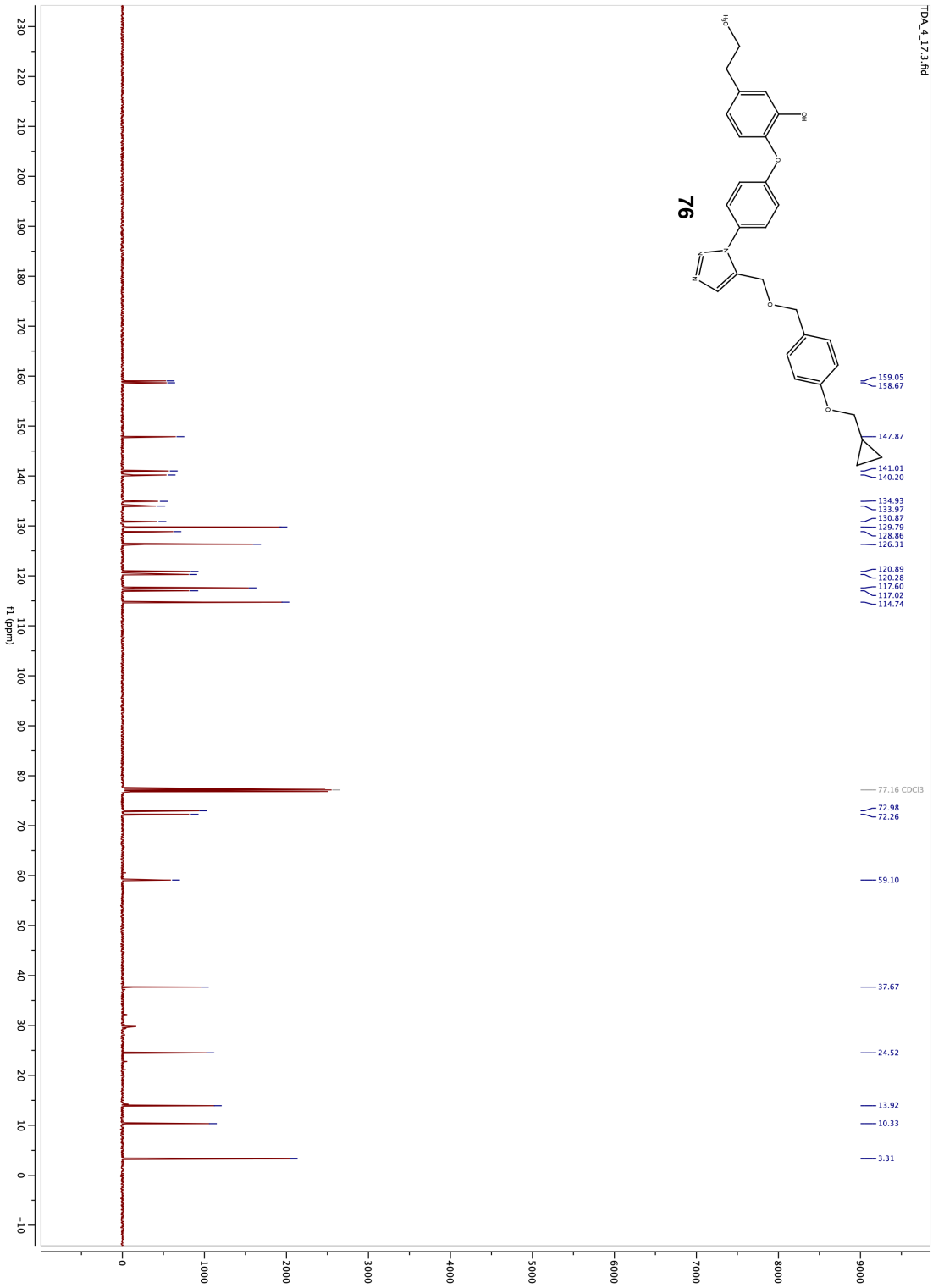
TDA_4_17.3.fid
76
159.05
158.67
147.87
141.01
140.20
134.93
133.97
130.87
129.79
128.86
126.31
120.89
120.28
117.60
117.02
114.74
77.16 CDCl3
72.98
72.26
59.10
37.67
24.52
13.92
10.33
3.31
f1 (ppm)

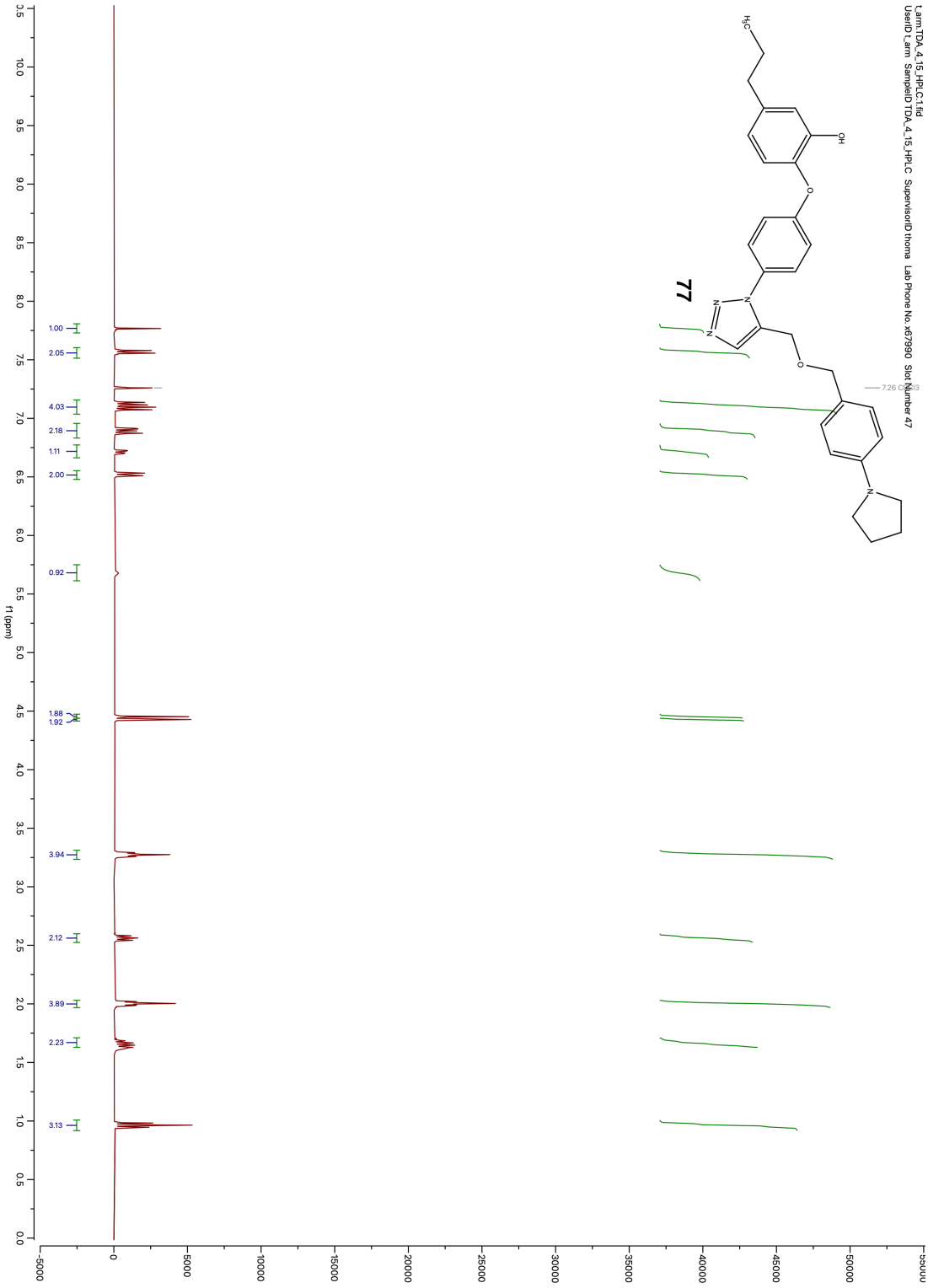
t_arm:TDA_4.15_HPLC.1.fid
UserID t_arm SampleID TDA_4.15_HPLC SupervisorID thoma Lab Phone No. x67990 Slot Number 47
77
7.26 CDCl3
1.00
2.05
4.03
2.18
1.11
2.00
0.92
1.88
1.92
3.94
2.12
3.89
2.23
3.13
f1 (ppm)

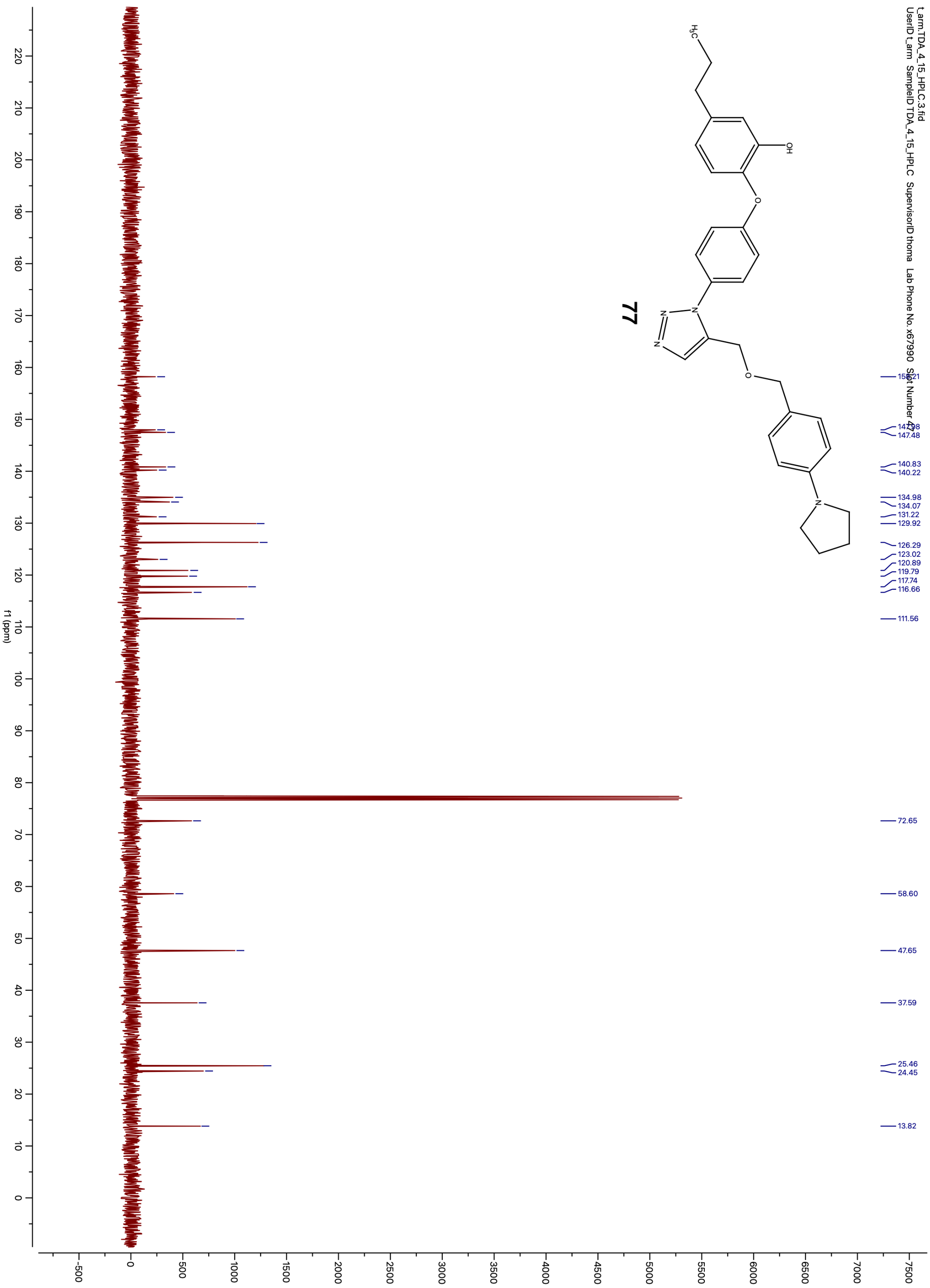
Larm.TDA_4_15_HPLC.3.fid
77
OH
O
N
H3C
147.48
140.83
140.22
134.98
134.07
131.22
129.92
126.29
123.02
120.89
119.79
117.74
116.66
111.56
72.65
58.60
47.65
37.59
25.46
24.45
13.82
f1 (ppm)

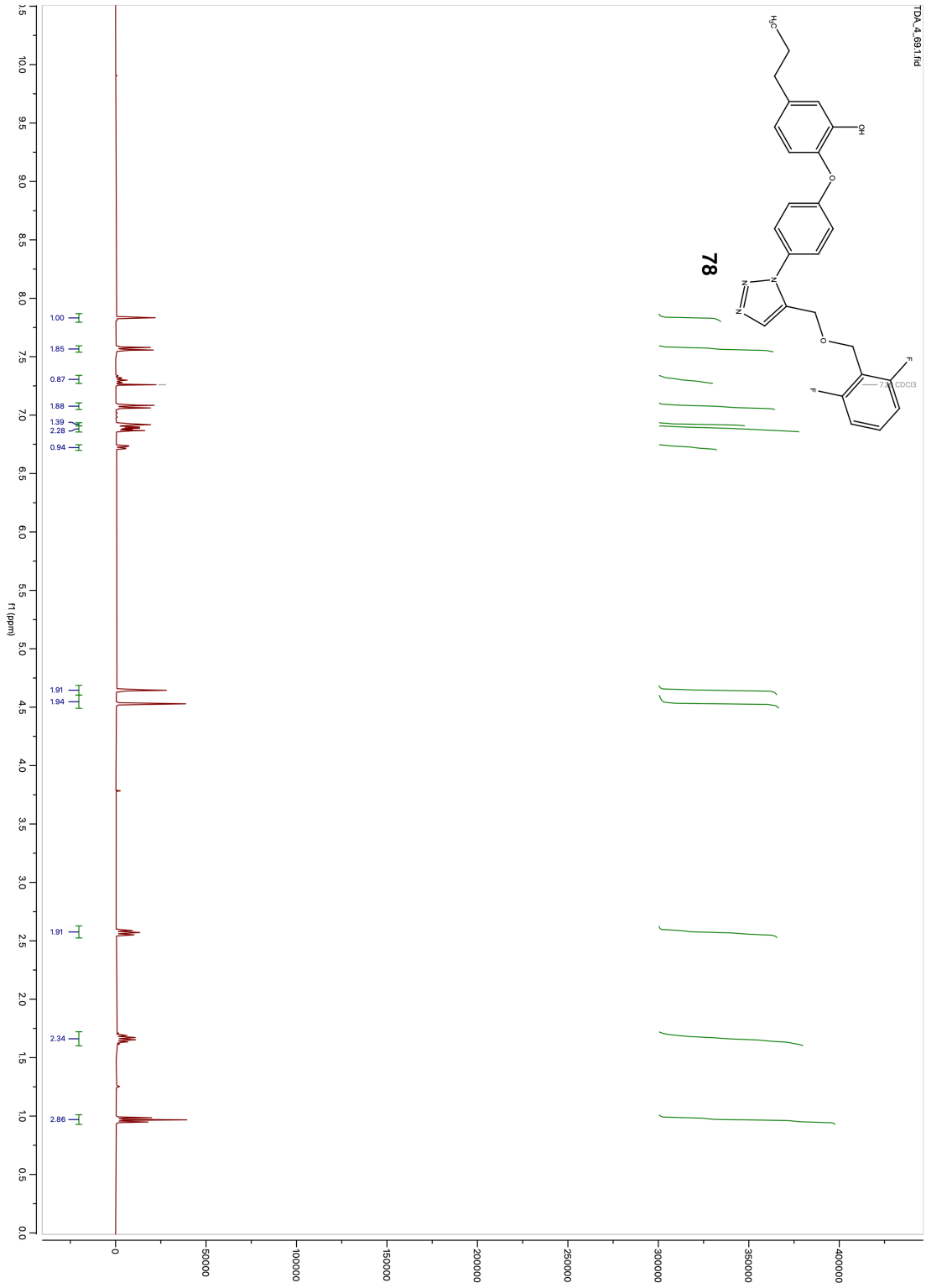
TDA_4_69.1.fid
78
CDCl3
1.00
1.85
0.87
1.88
1.39
2.28
0.94
1.91
1.94
1.91
2.34
2.86
f1 (ppm)

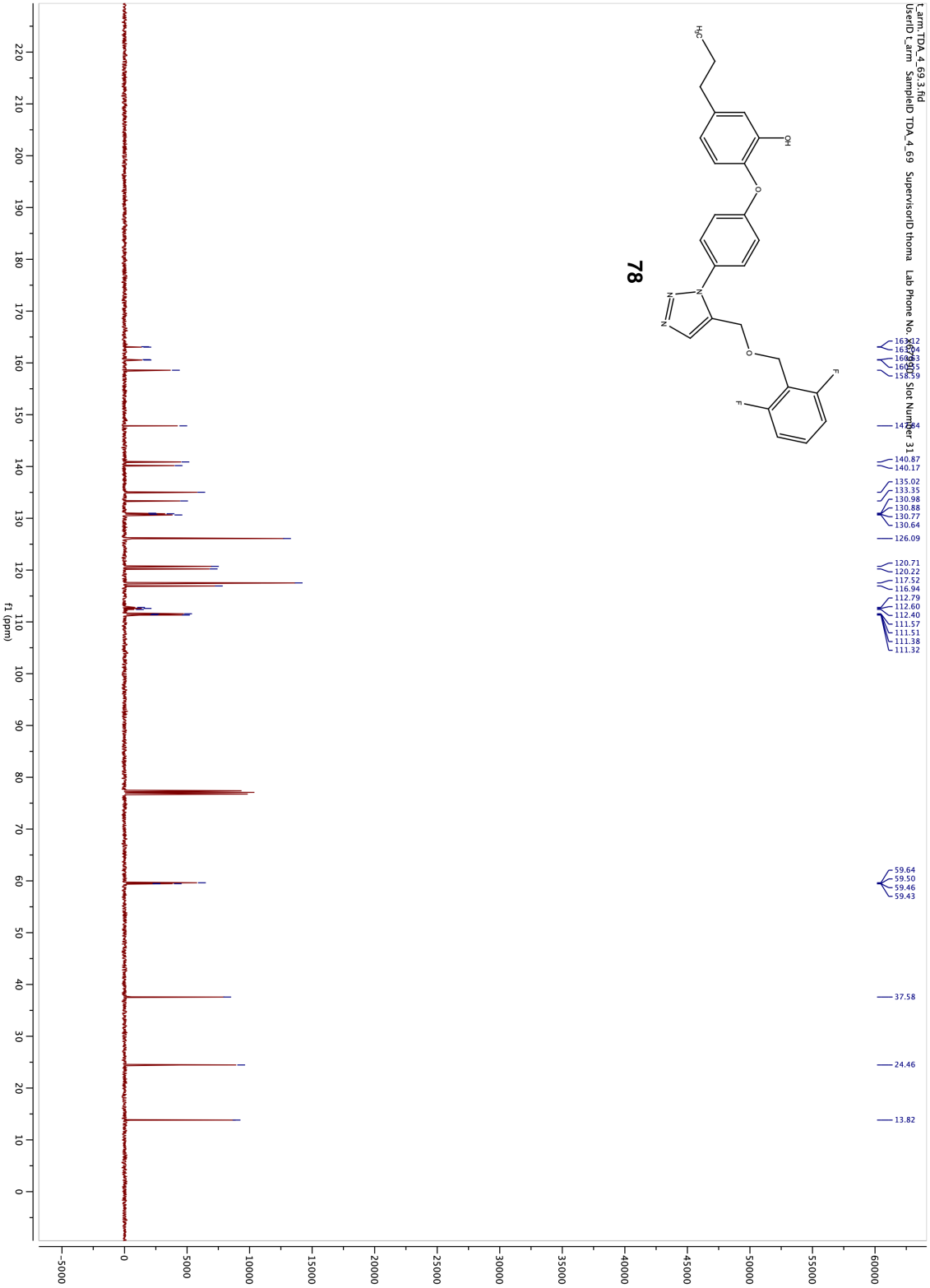
t_arm.TDA_4_69.3.fid
UserID t_arm SampleID TDA_4_69 SupervisorID thoma Lab Phone No. Slot Number 31
78
163.12
162.74
160.93
160.55
154.59
140.84
140.87
140.17
135.02
133.35
130.98
130.88
130.77
130.64
126.09
120.71
120.22
117.52
116.94
112.79
112.60
112.40
111.57
111.51
111.38
111.32
59.64
59.50
59.46
59.43
37.58
24.46
13.82
f1 (ppm)

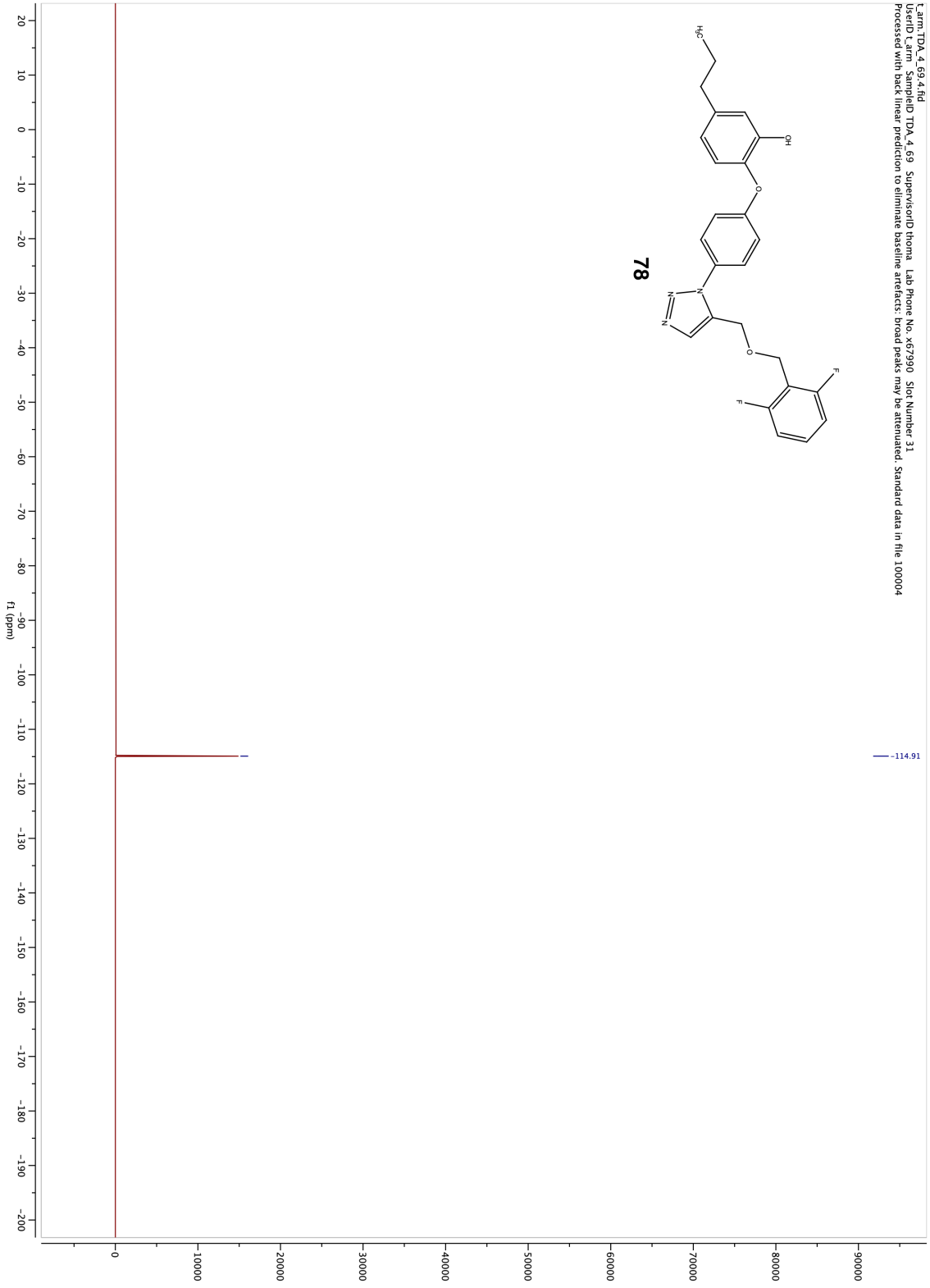
t_arm.TDA_4_69.4.fid
UserID t_arm SampleID TDA_4_69 SupervisorID thoma Lab Phone No. x67990 Slot Number 31
Processed with back linear prediction to eliminate baseline artefacts: broad peaks may be attenuated. Standard data in file 100004
78
-114.91
f1 (ppm)

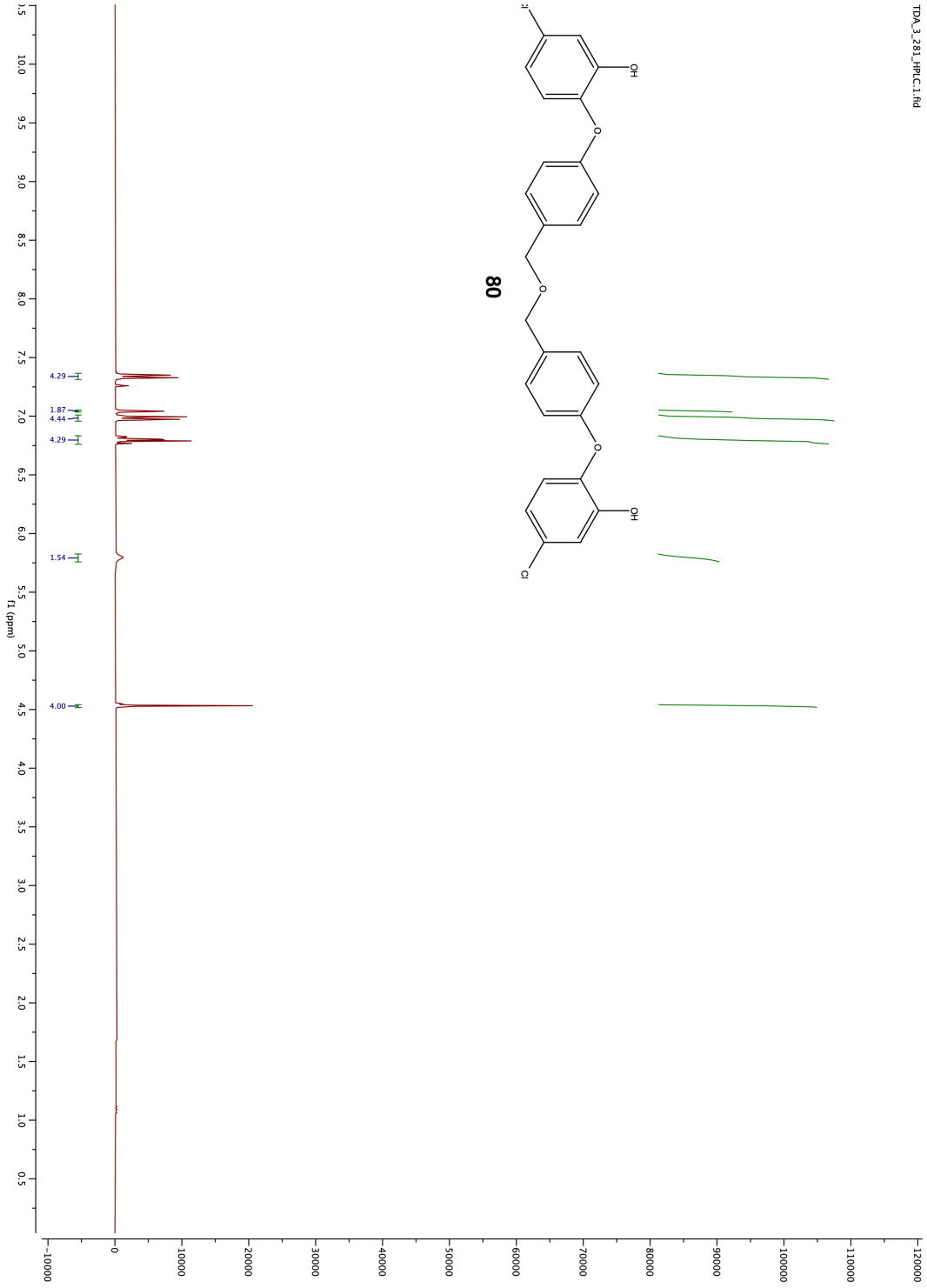
TDA_3_281_HPLC_1.fid
80
OH
O
O
O
OH
Cl
4.29
1.87
4.44
4.29
1.54
4.00
f1 (ppm)

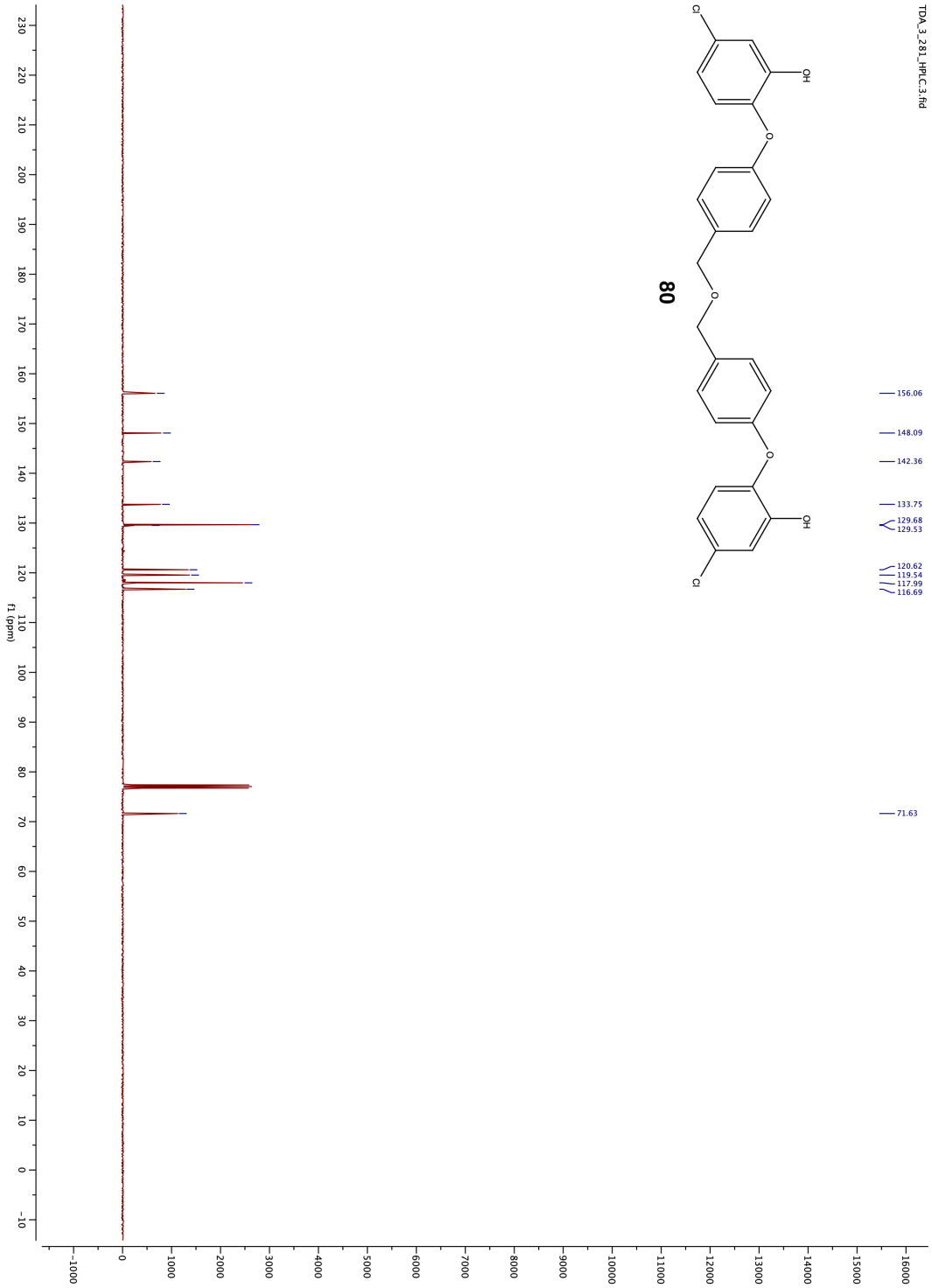
TDA_3_281_HPLC3.fid
80
Cl
OH
O
O
O
OH
Cl
156.06
148.09
142.36
133.75
129.68
129.53
120.62
119.54
117.99
116.69
71.63
f1 (ppm)

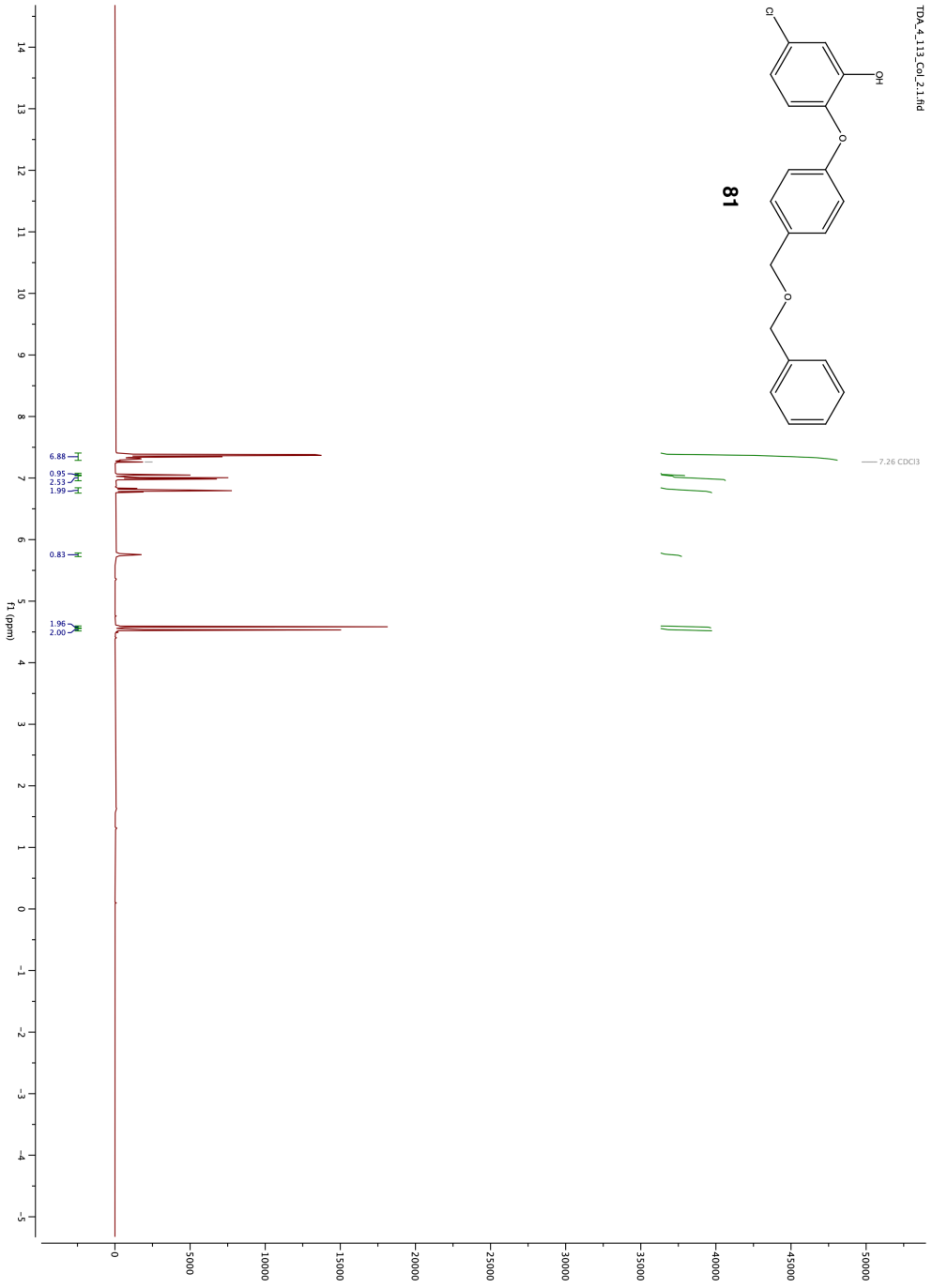
TDA_4_113_Col_2.1.fid
Cl
OH
O
O
81
7.26 CDCl3
6.88
0.95
2.53
1.99
0.83
1.96
2.00
f1 (ppm)

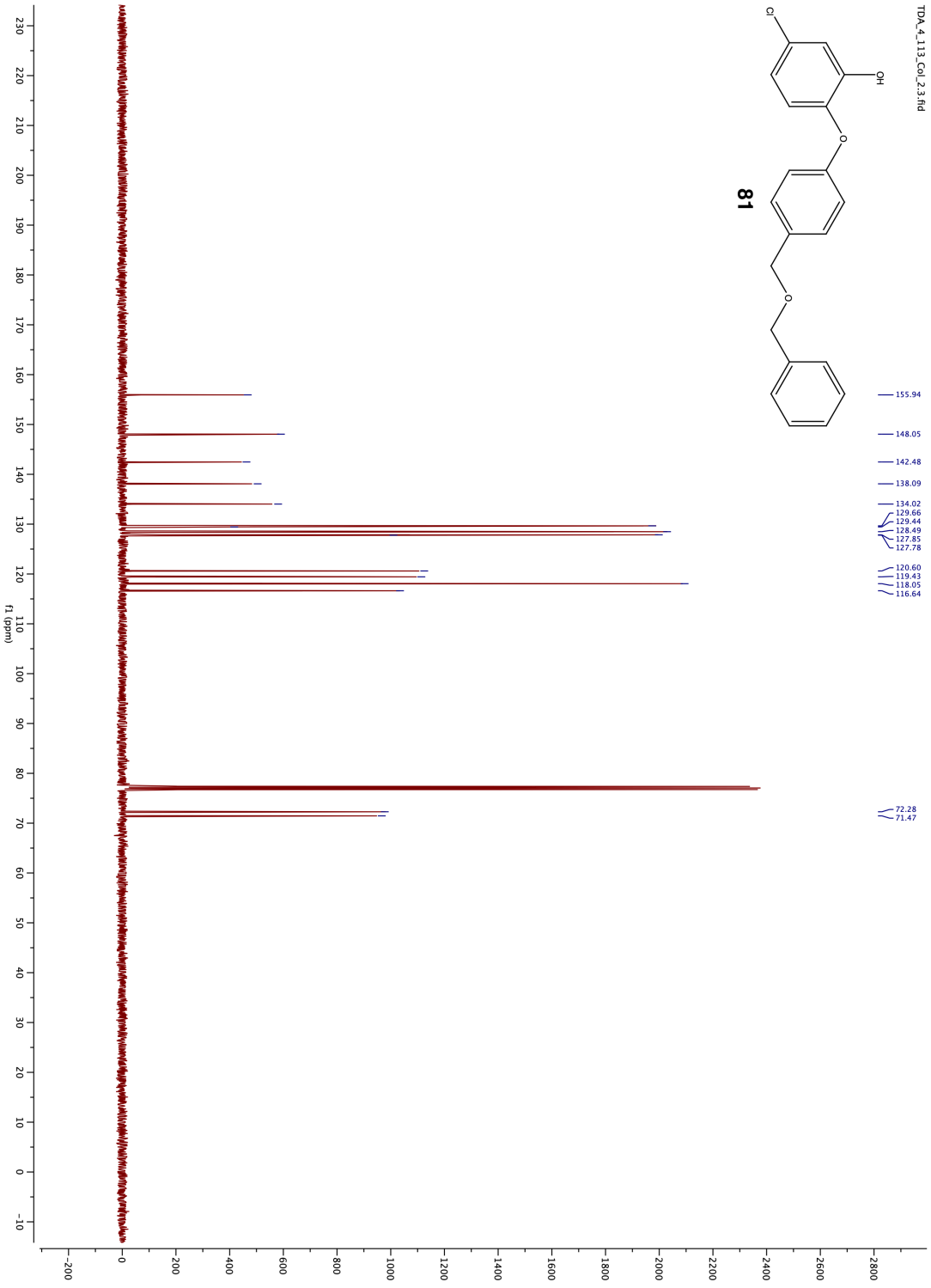
TDA_4_113_Col_2,3.fid
81
Cl
OH
O
O
155.94
148.05
142.48
138.09
134.02
129.66
129.44
128.49
127.85
127.78
120.60
119.43
118.05
116.64
72.28
71.47
f1 (ppm)

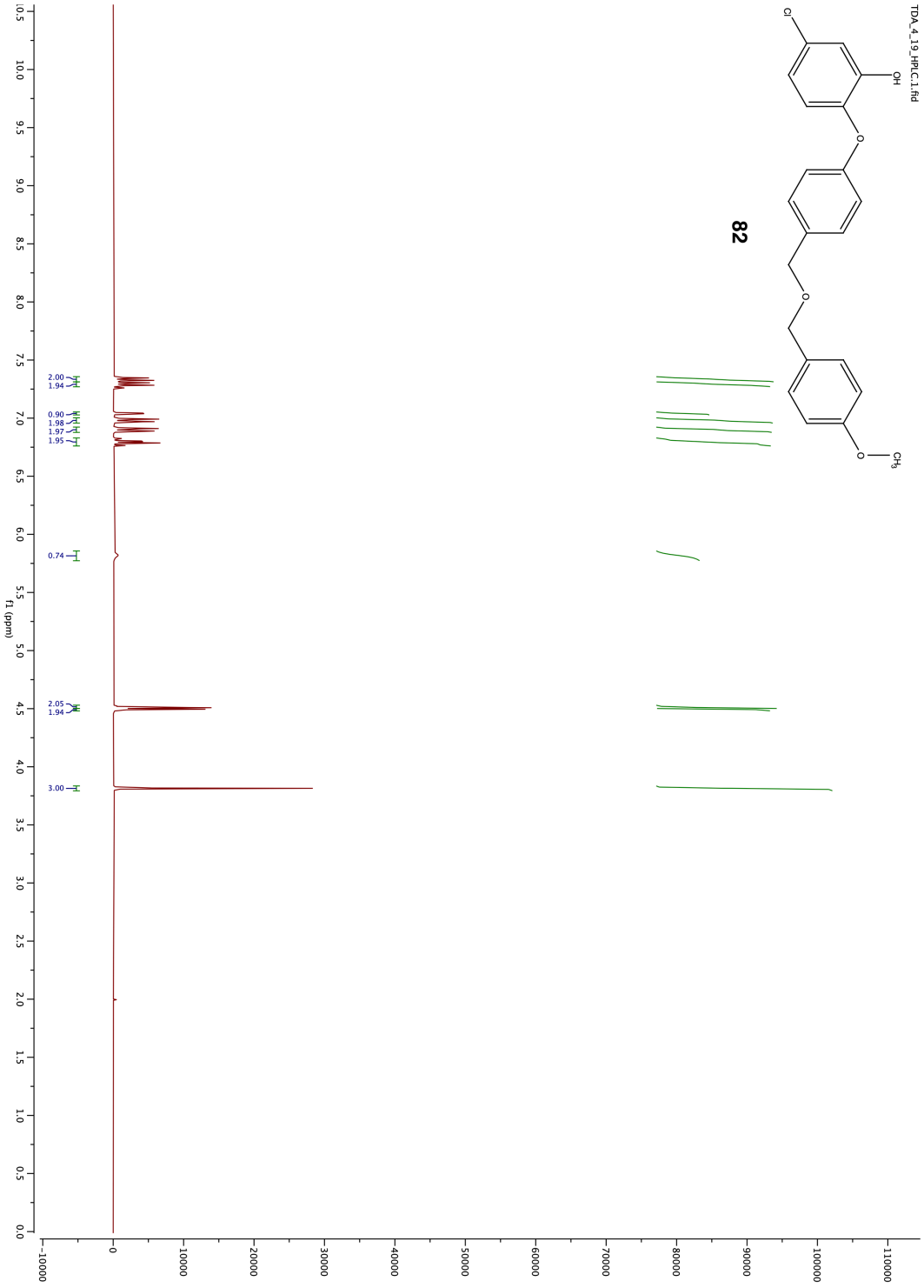
TDA_4_19_HPLC_1.fid
82
2.00
1.94
0.90
1.98
1.97
1.95
0.74
2.05
1.94
3.00
f1 (ppm)

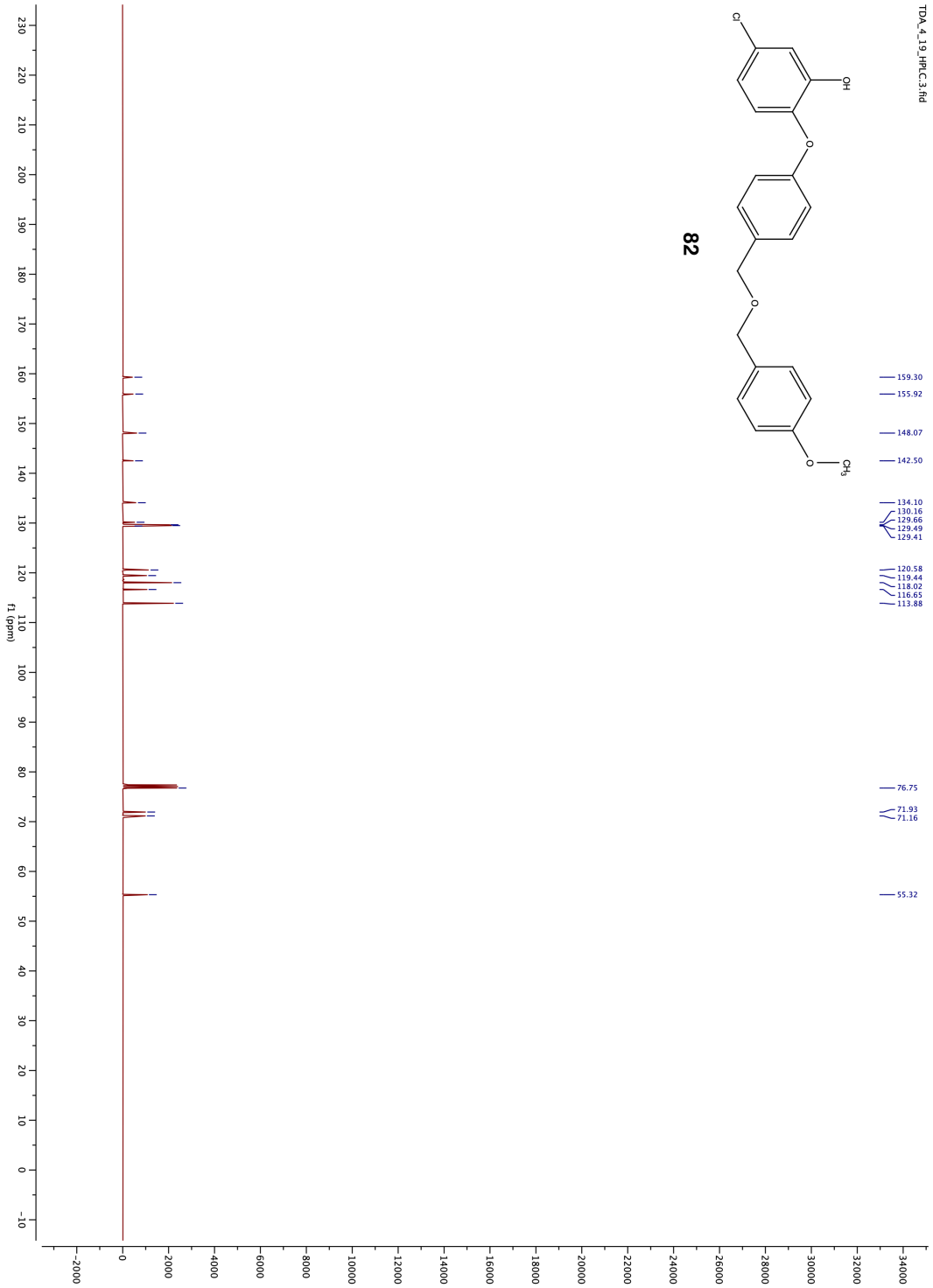
TDA_4_19_HPLC_3.fid
82
Cl
OH
O
O
O
CH3
159.30
155.92
148.07
142.50
134.10
130.16
129.66
129.49
129.41
120.58
119.44
118.02
116.65
113.88
76.75
71.93
71.16
55.32
f1 (ppm)

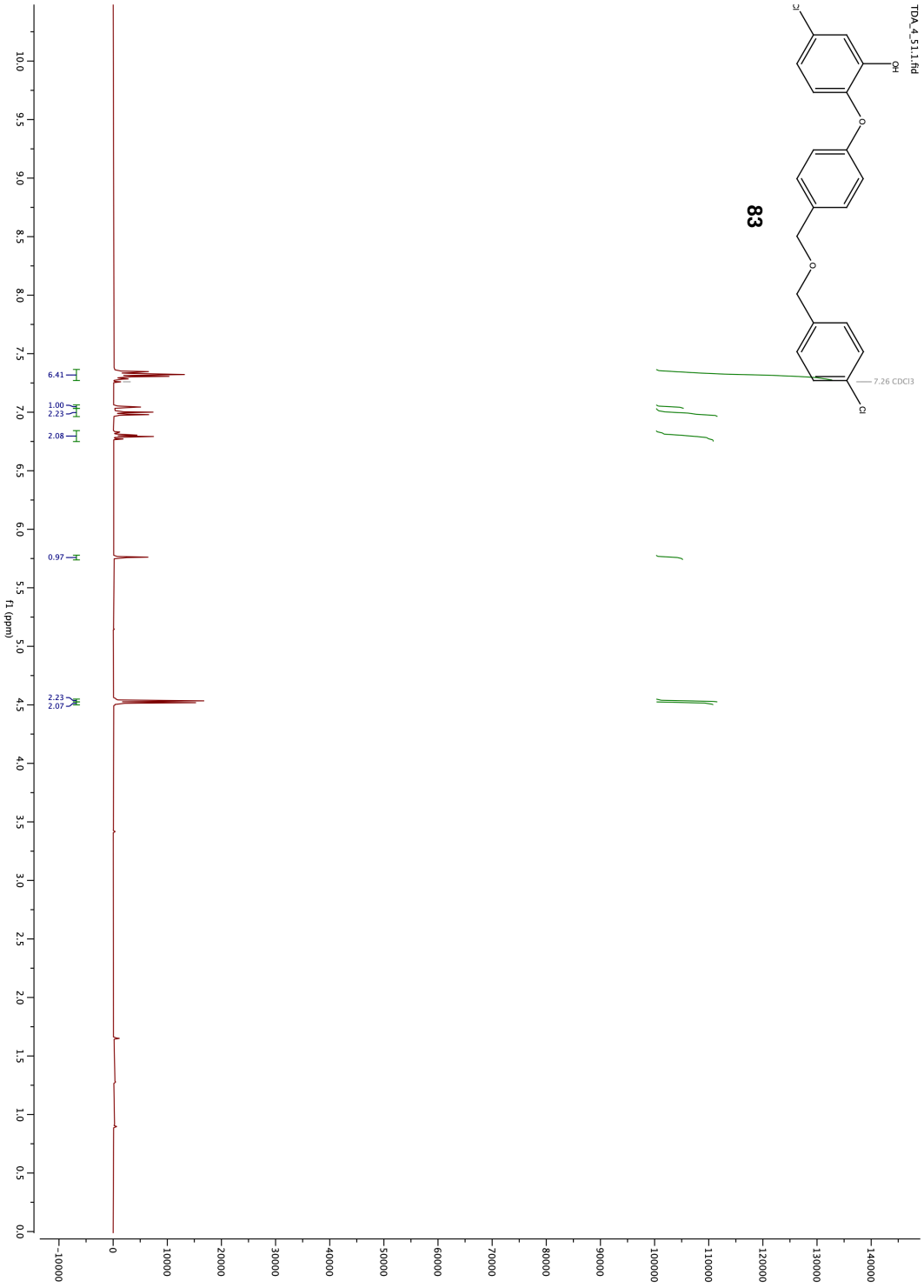
TDA_4_51_1.fid
83
7.26 CDCl3
6.41
1.00
2.23
2.08
0.97
2.23
2.07
f1 (ppm)

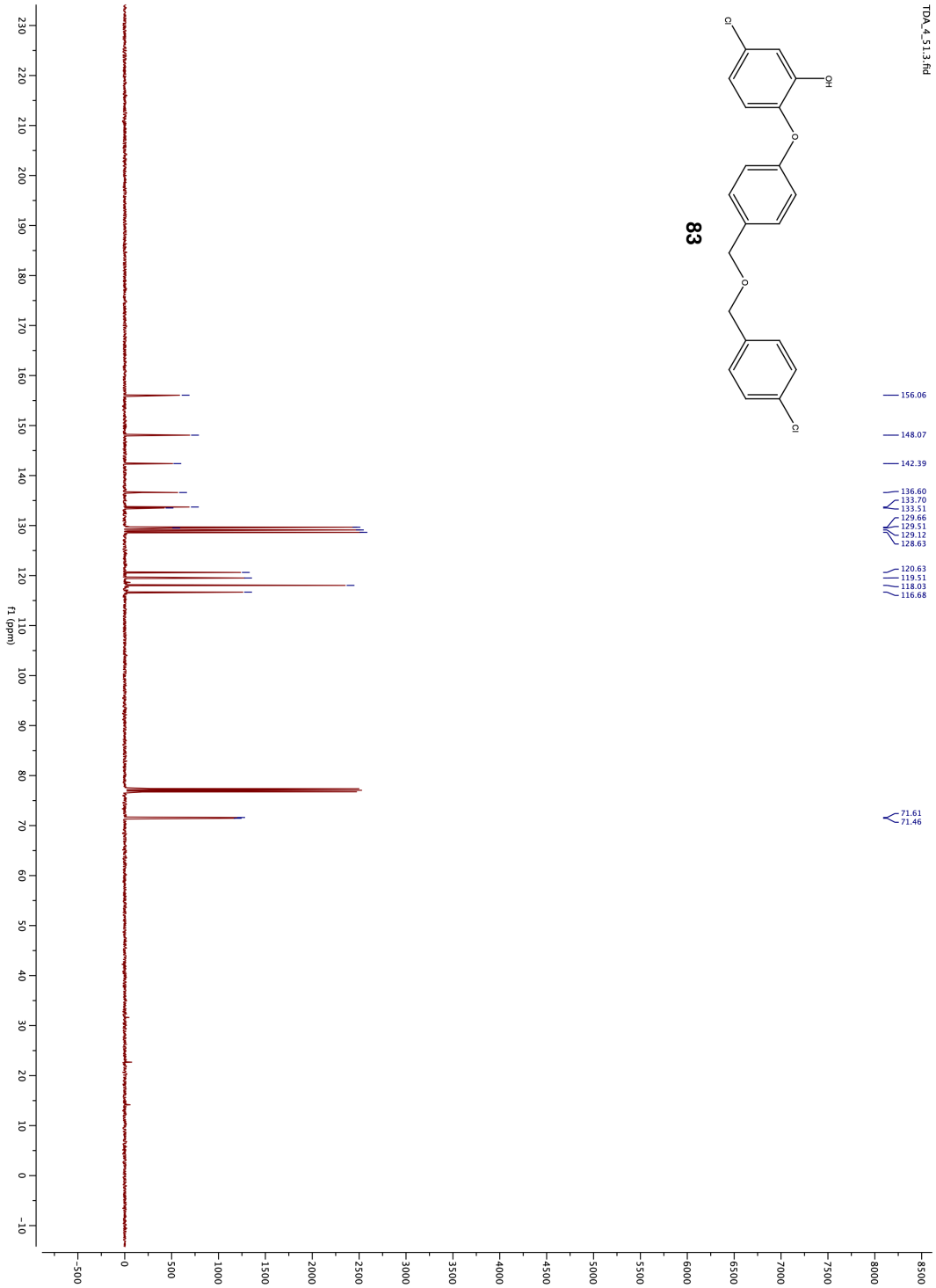
TDA_4_51_3.fid
83
Cl
OH
O
O
Cl
156.06
148.07
142.39
136.60
133.70
133.51
129.66
129.51
129.12
128.63
120.63
119.51
118.03
116.68
71.61
71.46
f1 (ppm)

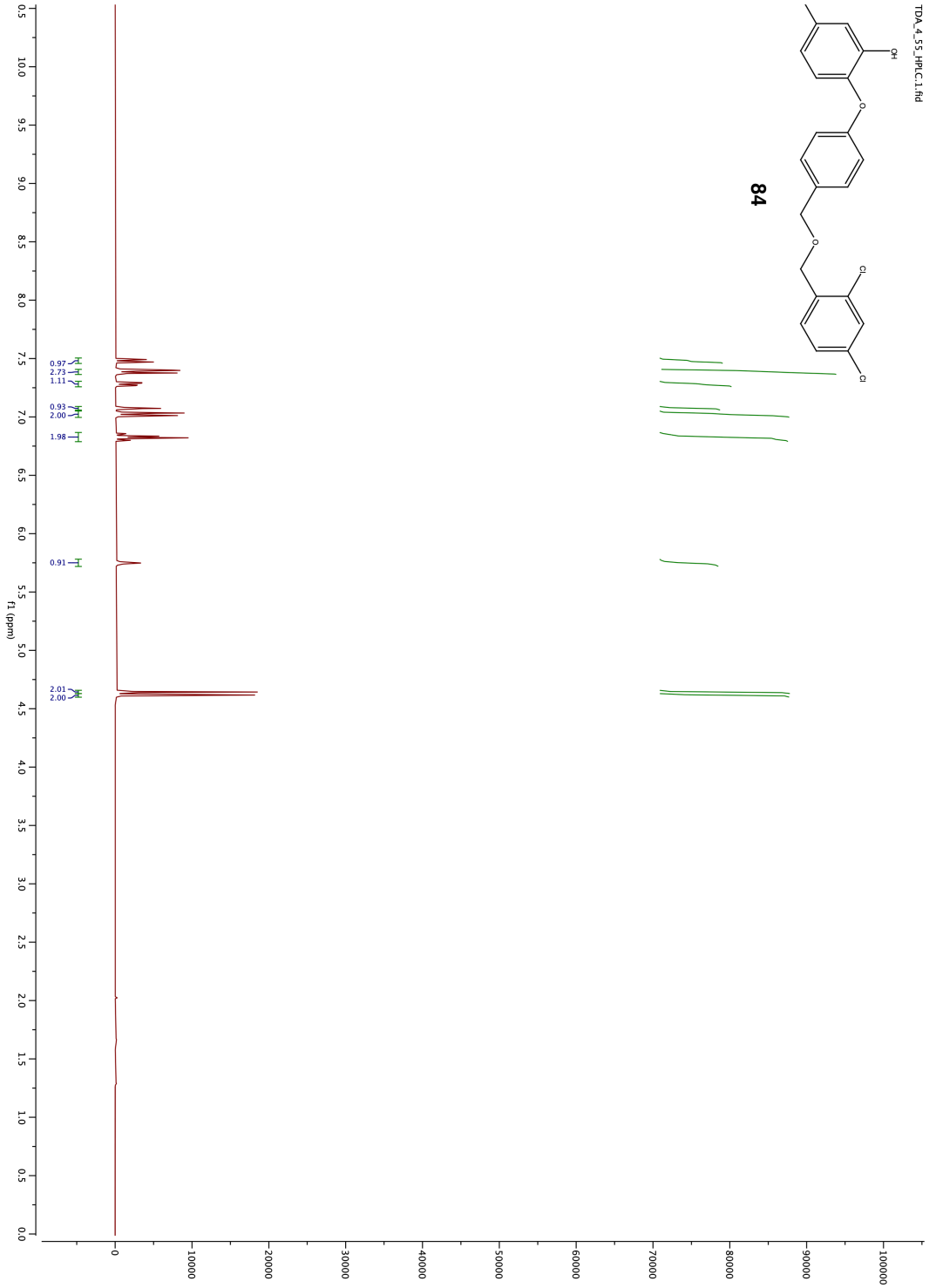
TDA_4_55_HPLC_1.fid
84
0.97
2.73
1.11
0.93
2.00
1.98
0.91
2.01
2.00
f1 (ppm)

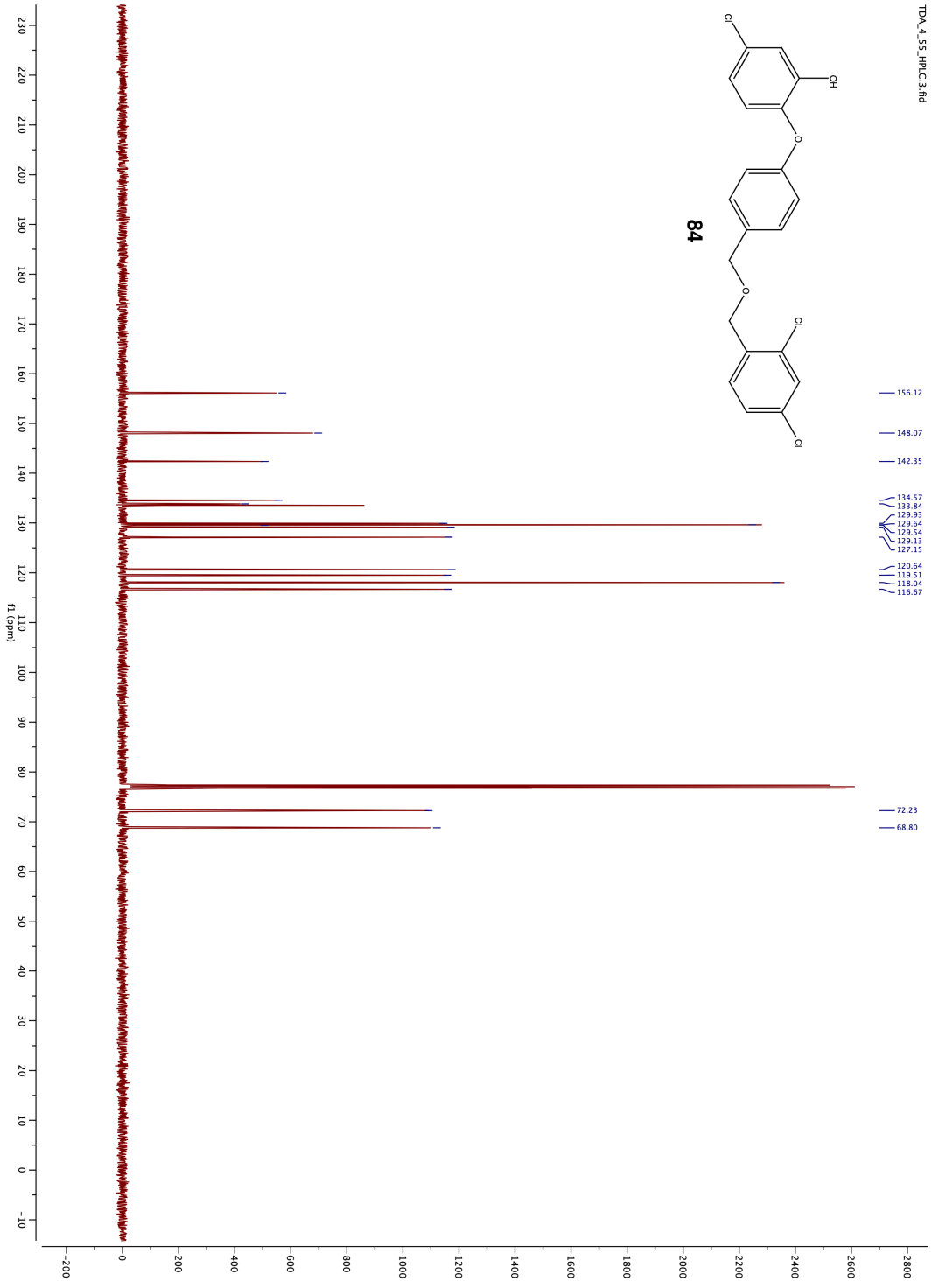
TDA_4_55_HPLC_3.fid
84
Cl
OH
O
O
Cl
Cl
156.12
148.07
142.35
134.57
133.84
129.93
129.64
129.54
129.13
127.15
120.64
119.51
118.04
116.67
72.23
68.80
f1 (ppm)

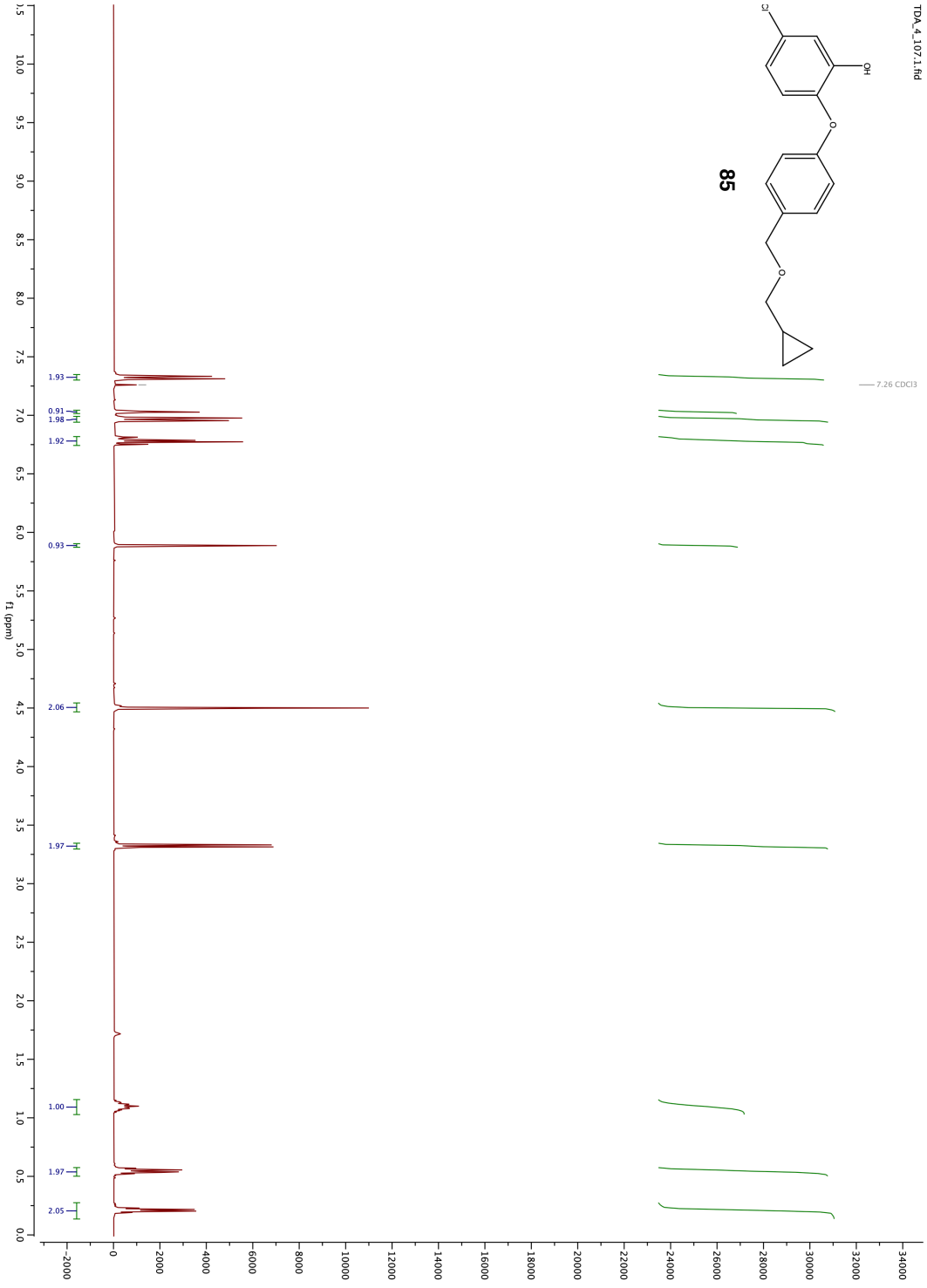
TDA_4_107_1.fid
85
7.26 CDCl3
1.93
0.91
1.98
1.92
0.93
2.06
1.97
1.00
1.97
2.05
f1 (ppm)

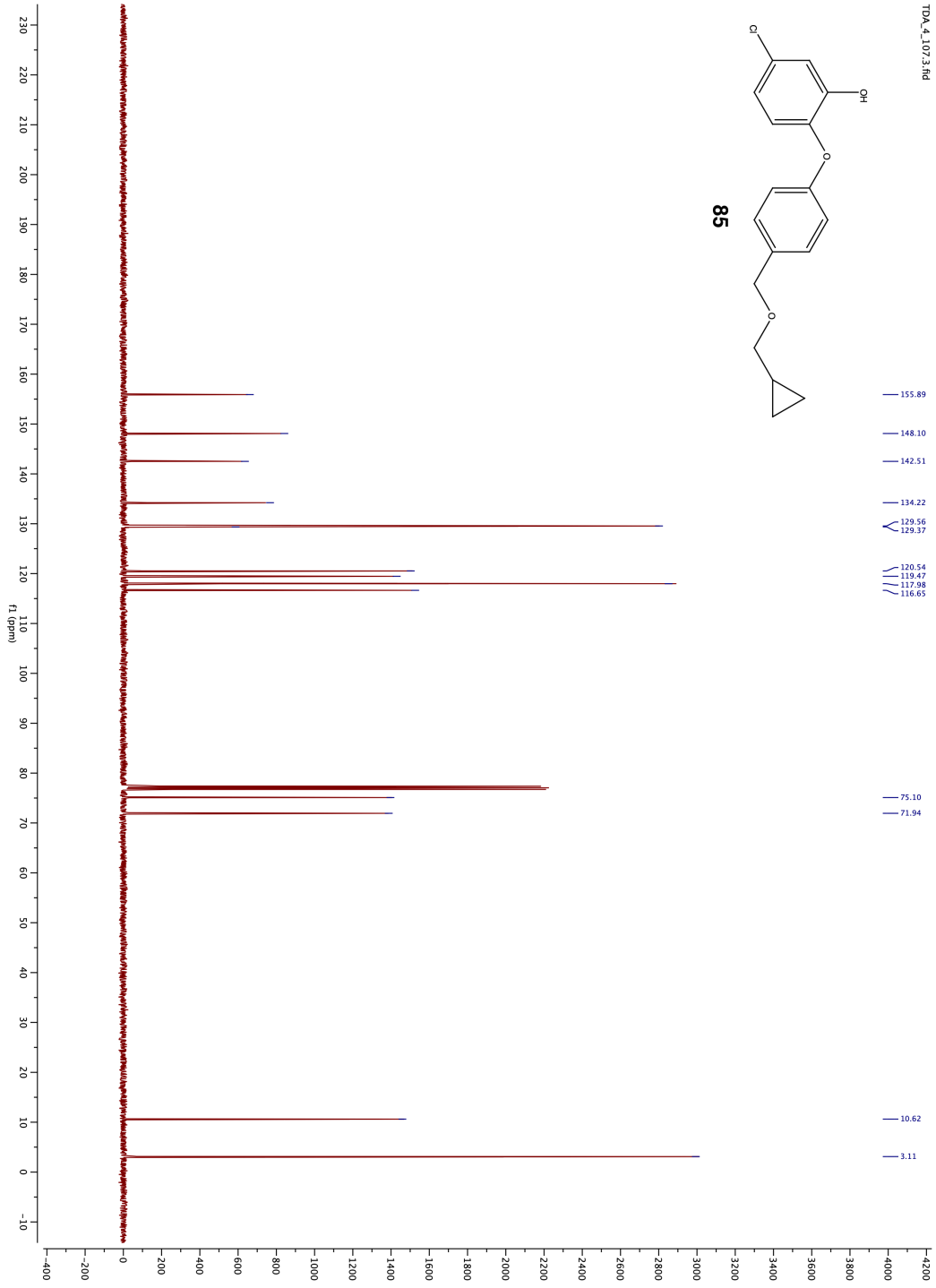
TDA_4_107.3.fid
85
Cl
OH
O
O
155.89
148.10
142.51
134.22
129.56
129.37
120.54
119.47
117.98
116.65
75.10
71.94
10.62
3.11
f1 (ppm)

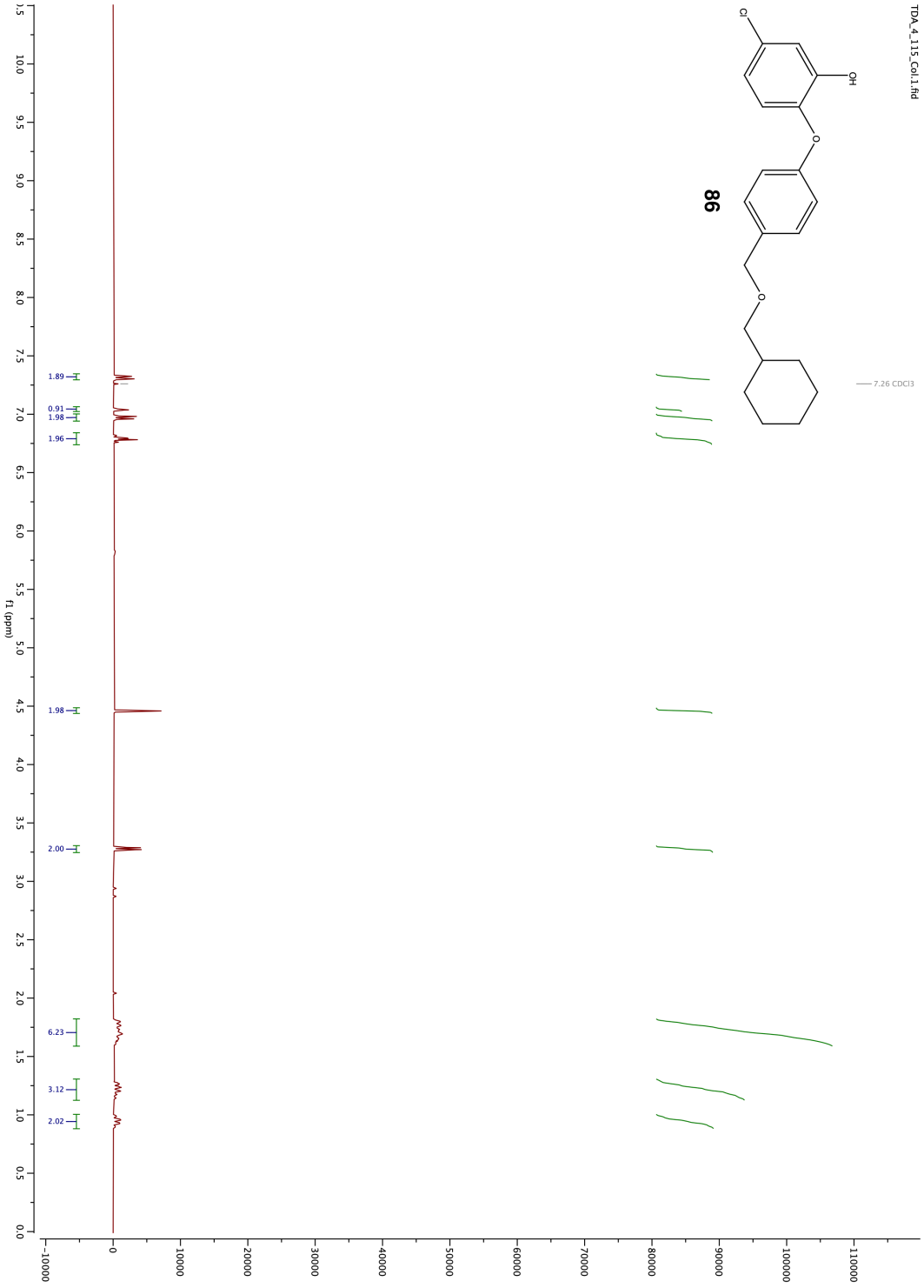
TDA_4_115_Co1.1.fid
98
7.26 CDCl3
1.89
0.91
1.98
1.96
1.98
2.00
6.23
3.12
2.02
f1 (ppm)

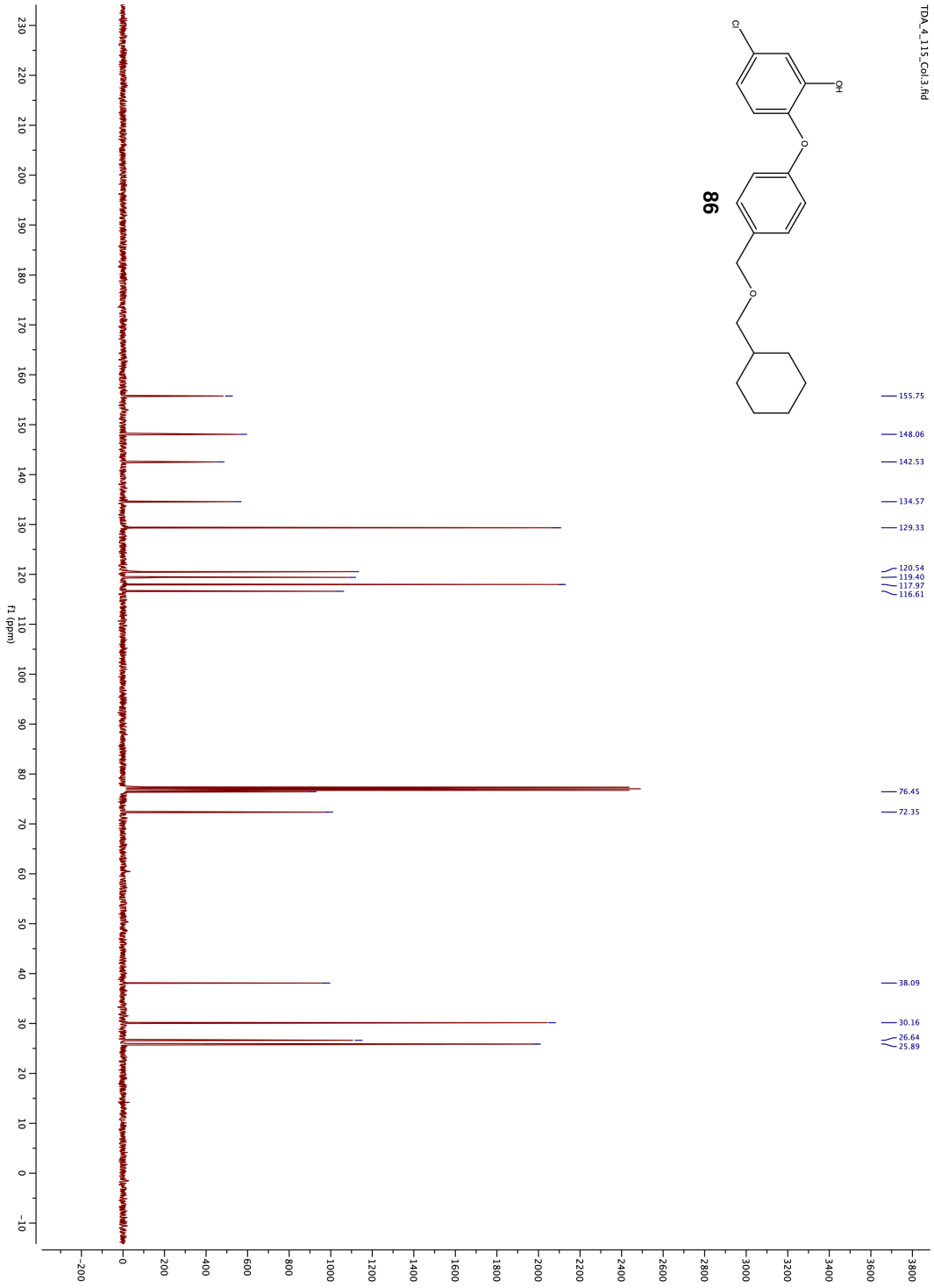
TDA_4_115_Col3.fid
98
Cl
OH
O
O
155.75
148.06
142.53
134.57
129.33
120.54
119.40
117.97
116.61
76.45
72.35
38.09
30.16
26.64
25.89
f1 (ppm)

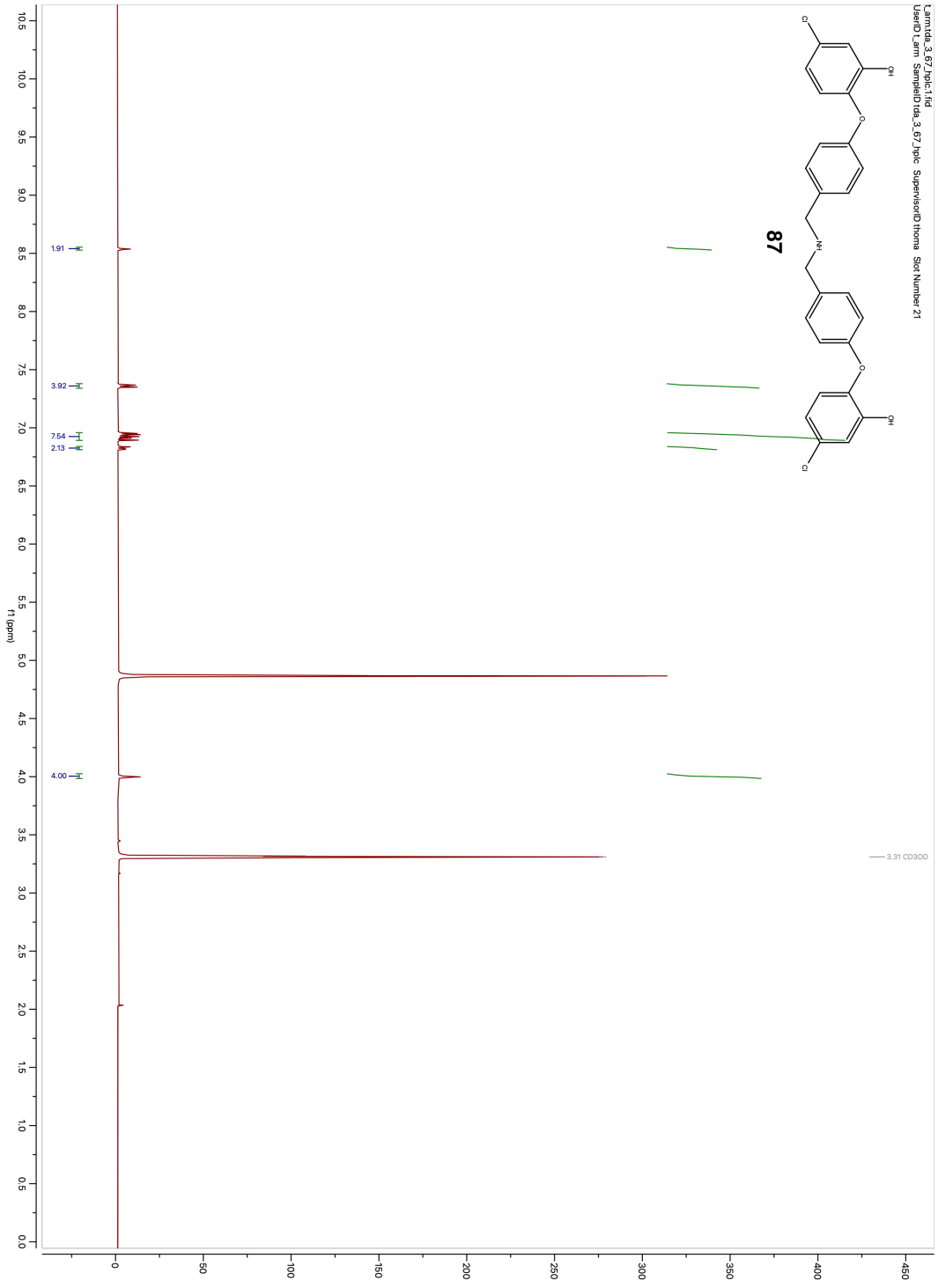
L_arm.1da_3.67_hplc.1.fid
UserID L_arm SampleID 1da_3.67_hplc SupervisorID thoma Slot Number 21
87
1.91
3.92
7.54
2.13
4.00
3.31 CD3OD
f1 (ppm)

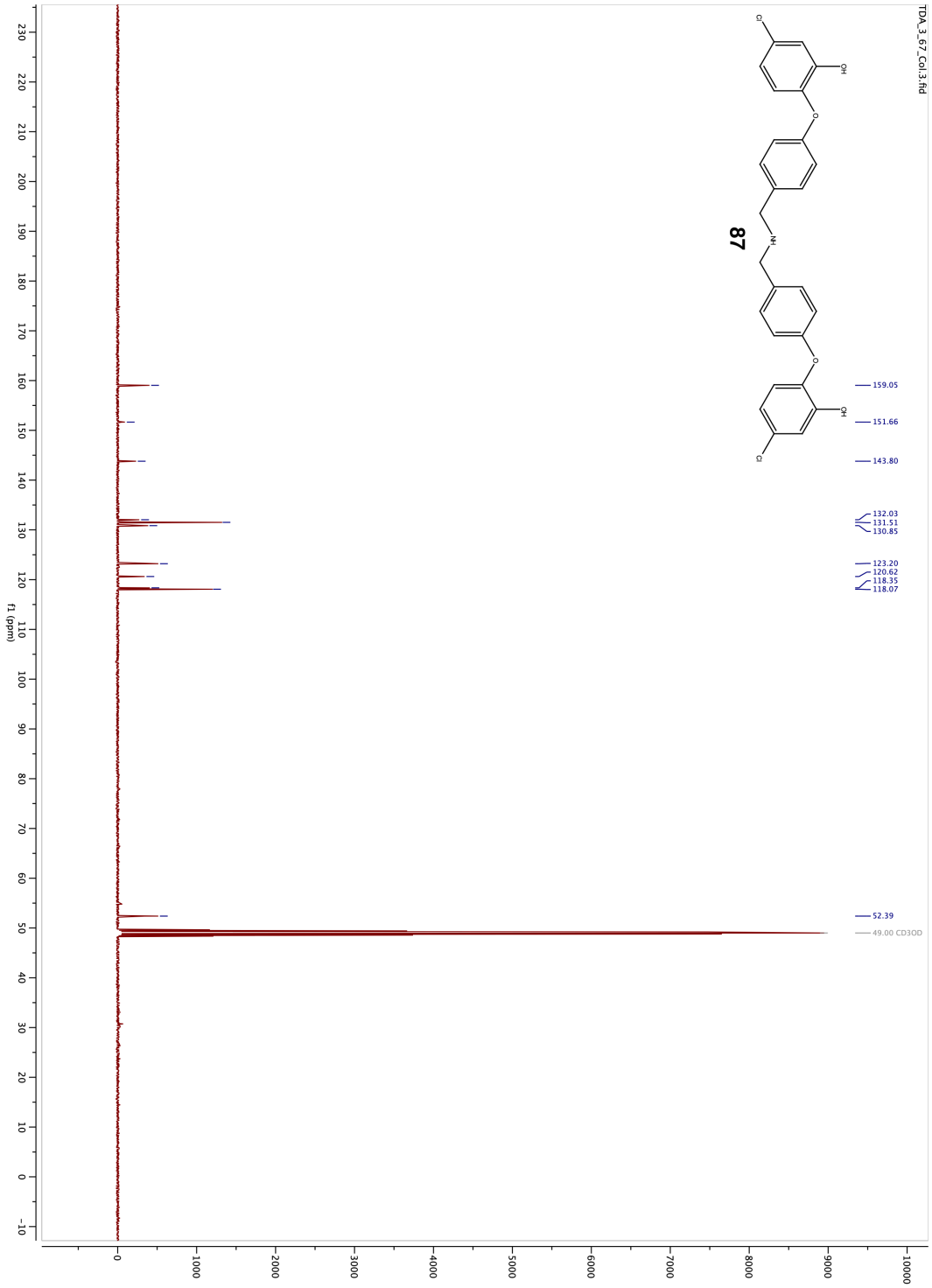
TDA_3_67_Col3.fid
87
159.05
151.66
143.80
132.03
131.51
130.85
123.20
120.62
118.35
118.07
52.39
49.00 CD3OD
f1 (ppm)

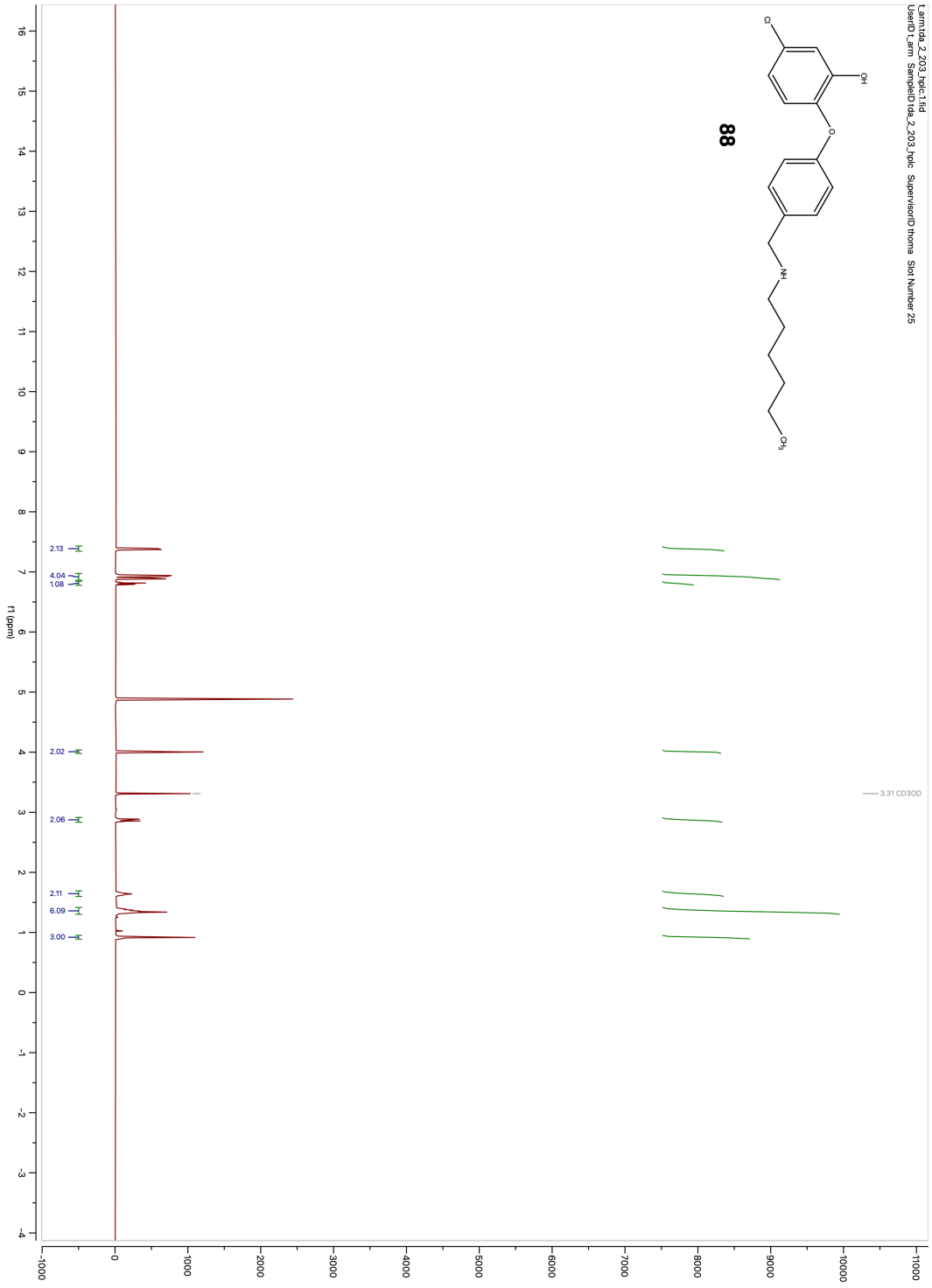
L_arm.1.da_2.203_hpic.1.fid
UserID L_arm SampleID rda_2.203_hpic SupervisorID thoma Slot Number 25
88
Cl
OH
O
NH
CH3
2.13
4.04
1.08
2.02
2.06
2.11
6.09
3.00
3.31 CD3OD
f1 (ppm)

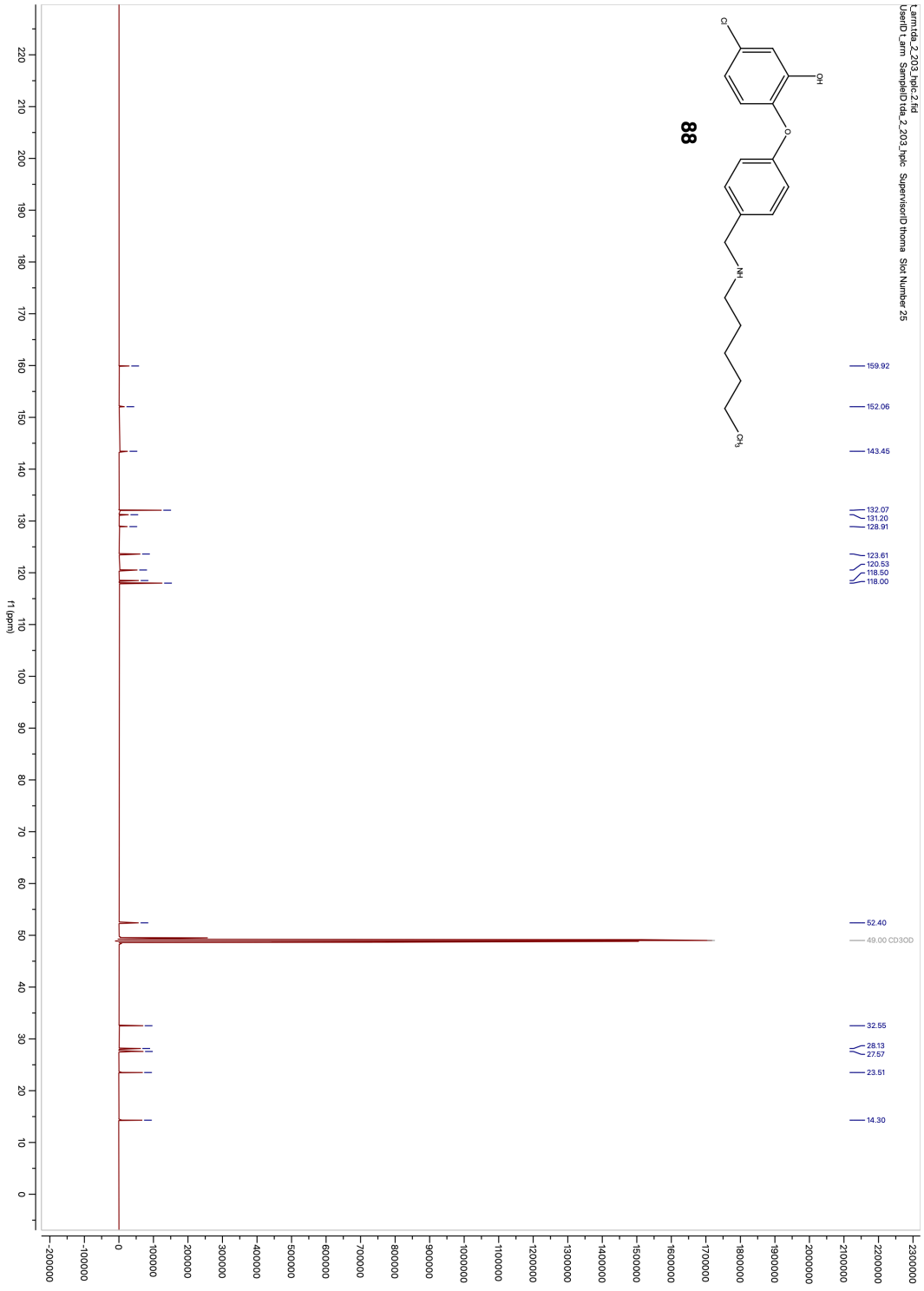
88
159.92
152.06
143.45
132.07
131.20
128.91
123.61
120.53
118.50
118.00
52.40
49.00 CD3OD
32.55
28.13
27.57
23.51
14.30
f1 (ppm)

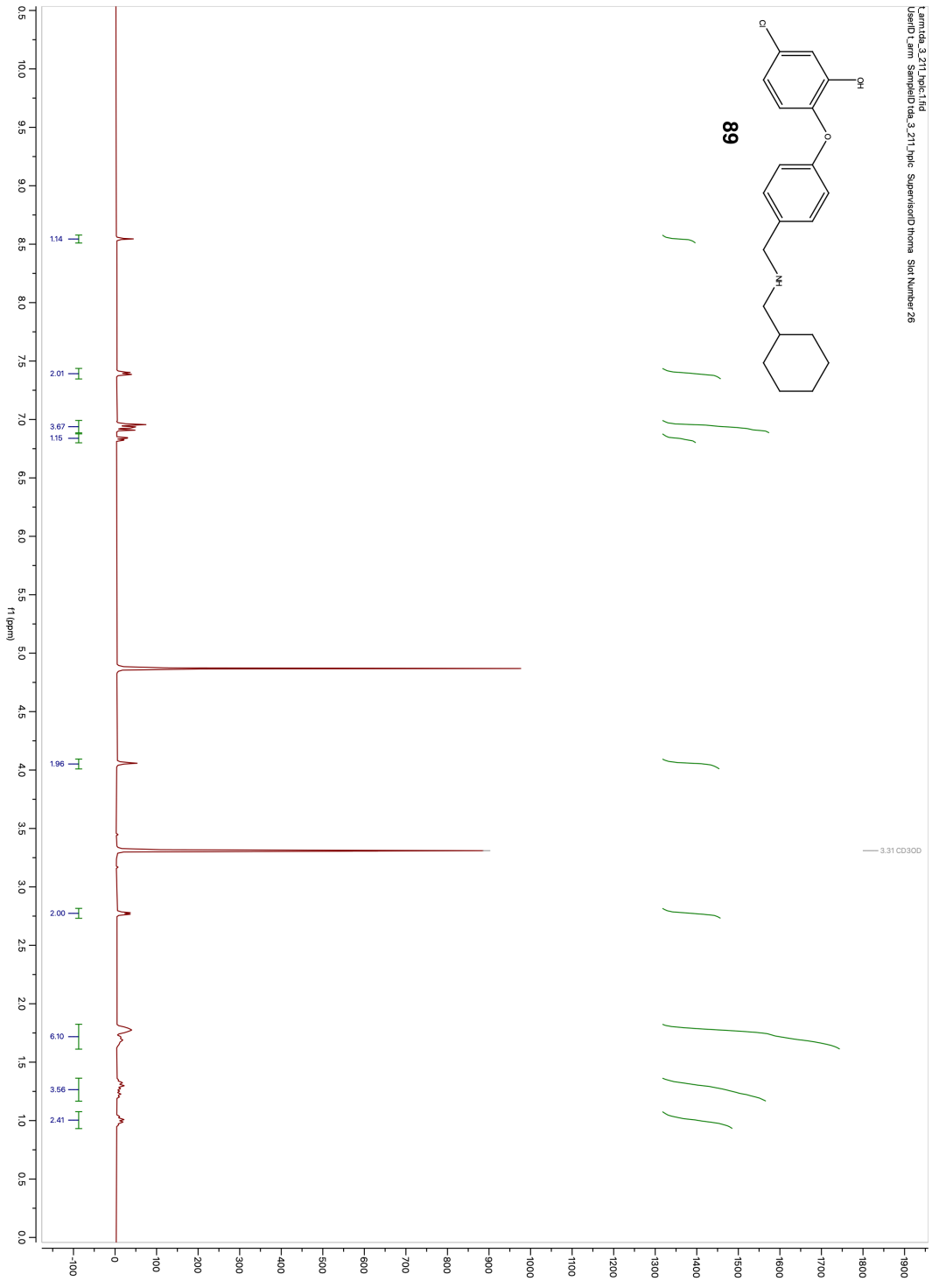
L:arm:rda_3_211_hpic:1.fid
UserID L:arm SampleID rda_3_211_hpic SupervisorID tnoma Slot Number 26
68
Cl
OH
O
NH
1.14
2.01
3.67
1.15
1.96
2.00
6.10
3.56
2.41
3.31 CD3OD
f1 (ppm)

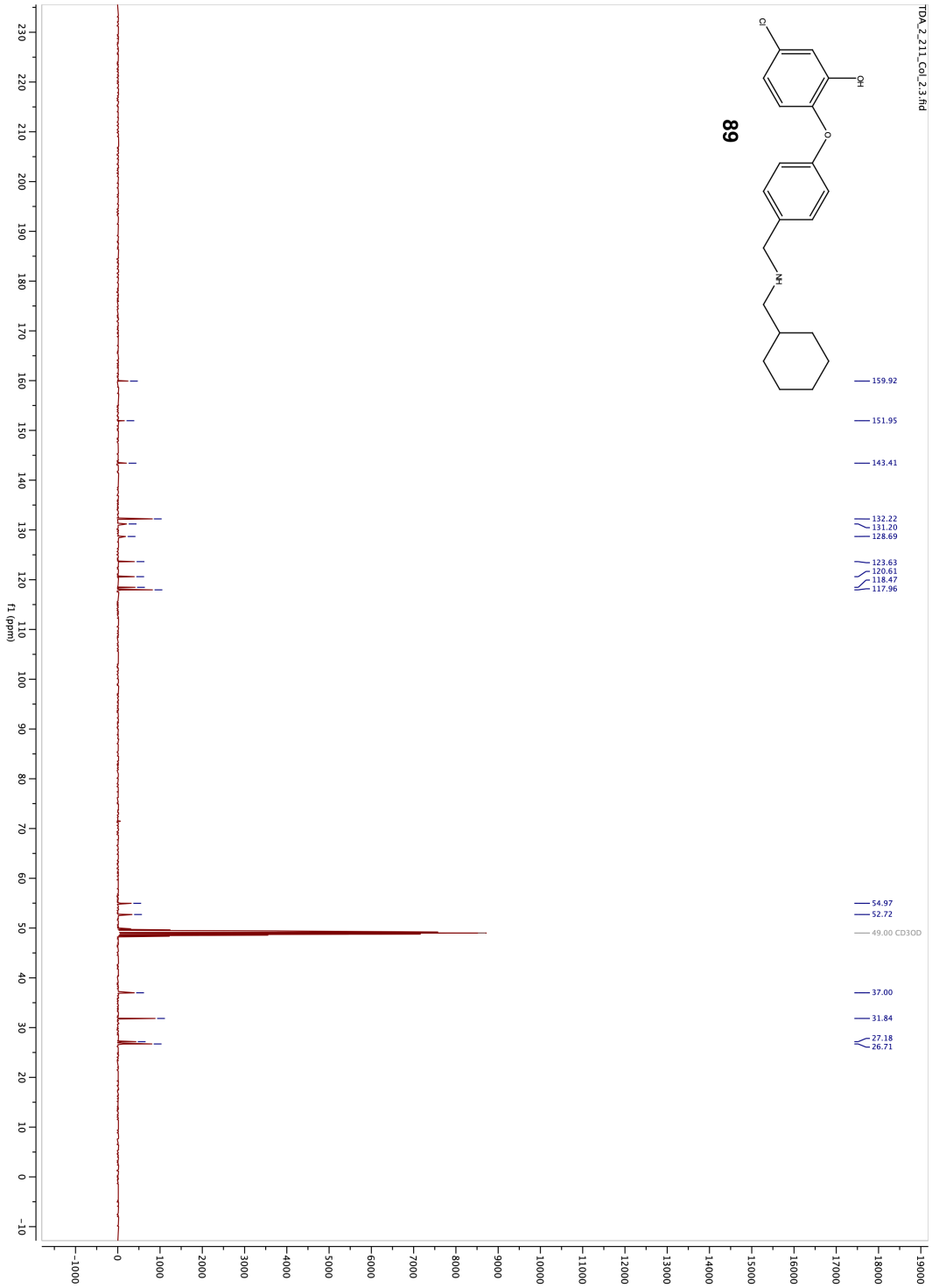
TDA_2_211_Col_2_3.fid
68
Cl
OH
O
NH
159.92
151.95
143.41
132.22
131.20
128.69
123.63
120.61
118.47
117.96
54.97
52.72
49.00 CD3OD
37.00
31.84
27.18
26.71
f1 (ppm)

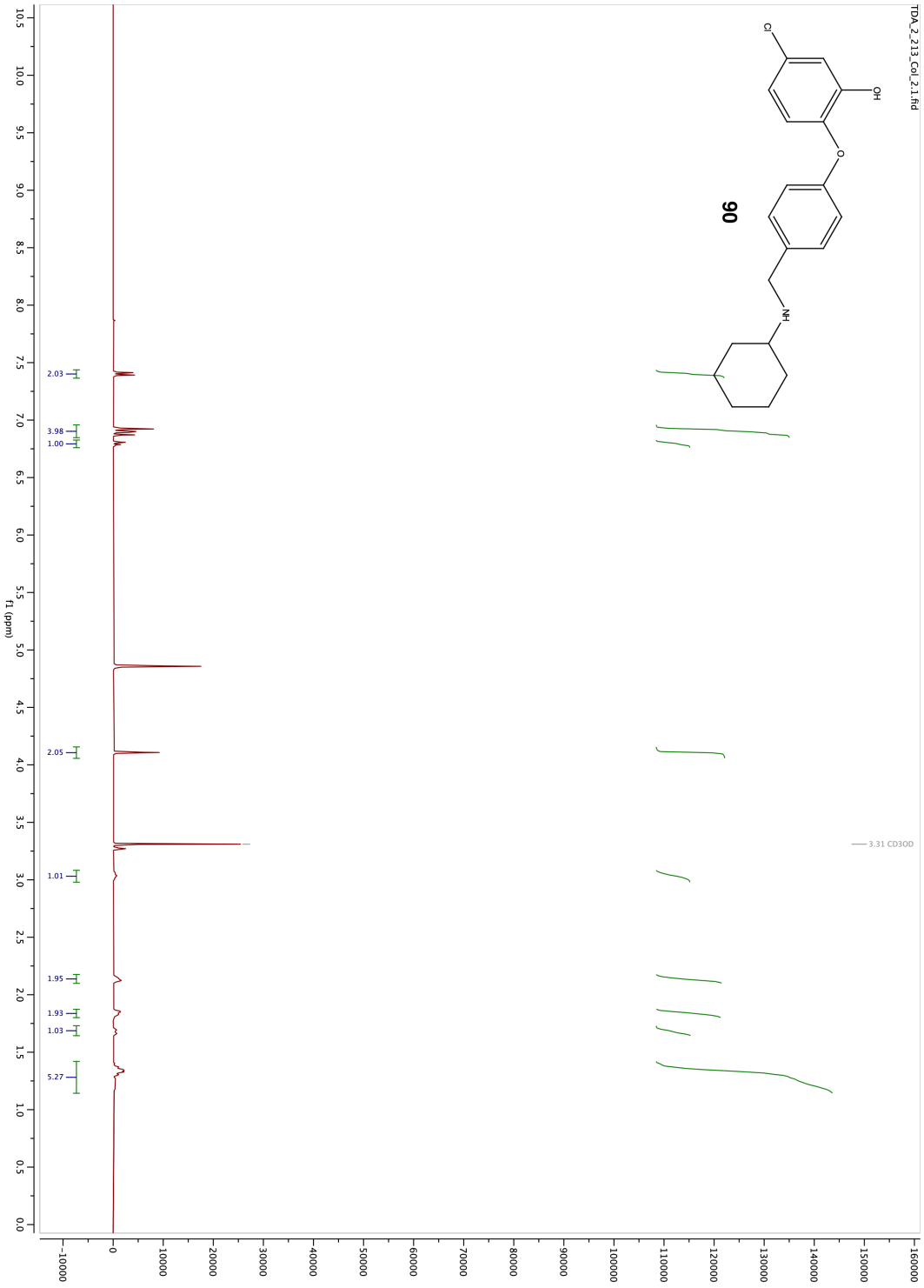
TDA_2_213_Col_2_1.fid
90
Cl
OH
O
NH
2.03
3.98
1.00
2.05
1.01
1.95
1.93
1.03
5.27
3.31 CD3OD
f1 (ppm)

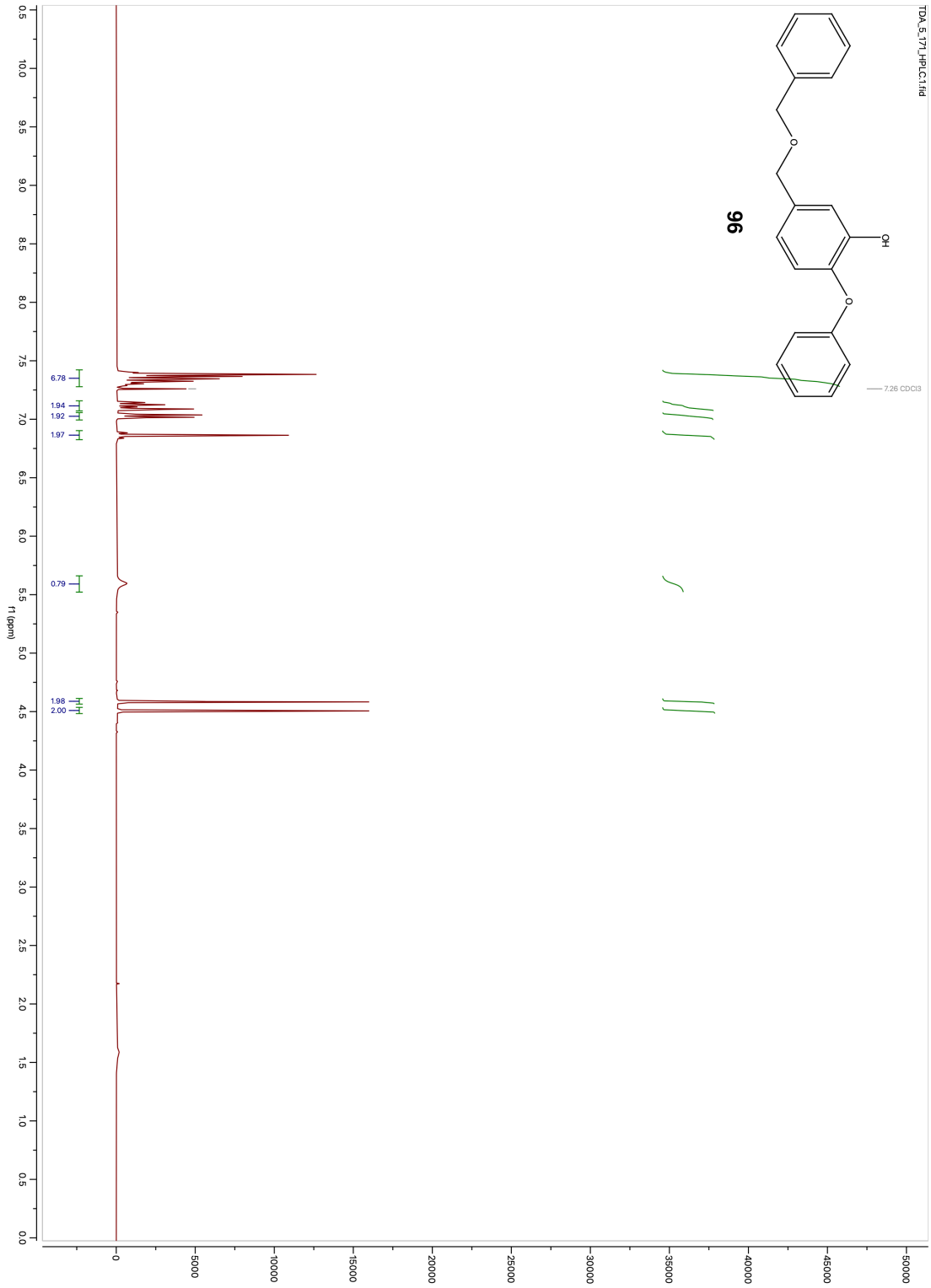
TDA_5_171_HPLC.1.fid
96
OH
O
O
7.26 CDCl3
6.78
1.94
1.92
1.97
0.79
1.98
2.00
f1 (ppm)

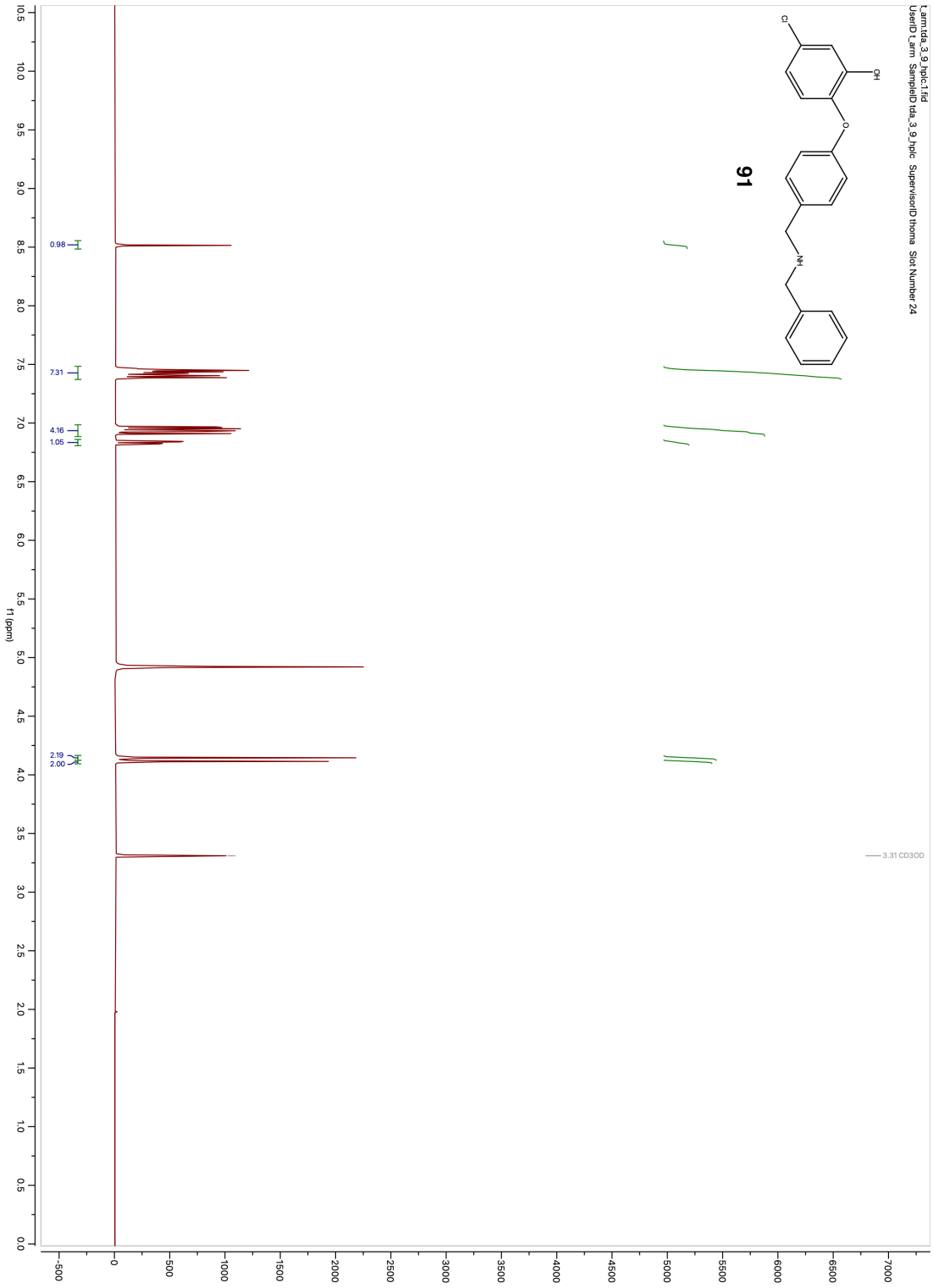
t_arm:tda_3_9_hplc_1.fid
UserID t_arm SampleID tda_3_9_hplc SupervisorID thoma Slot Number 24
91
Cl
OH
O
NH
0.98
7.31
4.16
1.05
2.19
2.00
3.31 CD3OD
f1 (ppm)

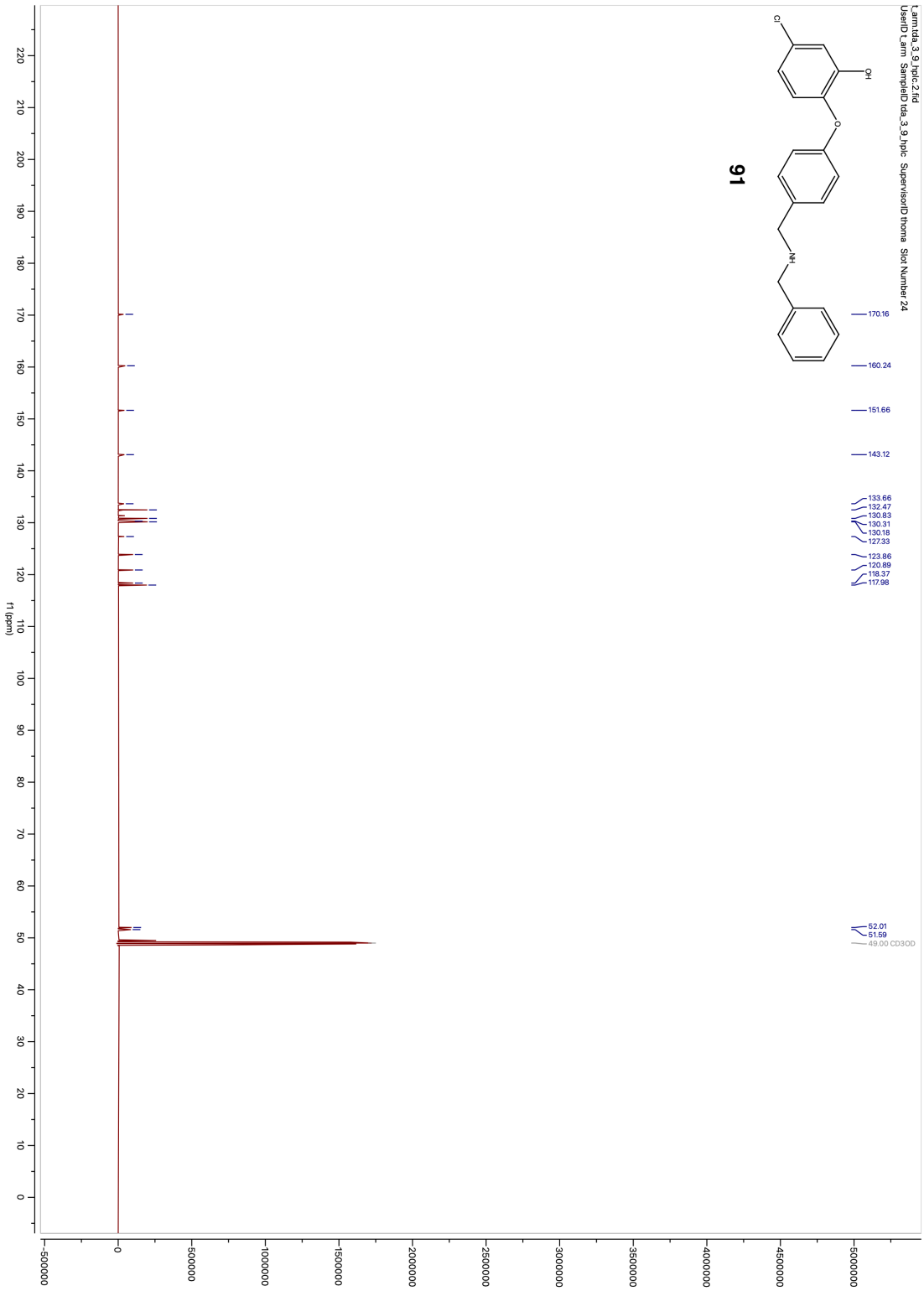
t_arm:tda_3_9_hplc_2.fid
UserID t_arm SampleID tda_3_9_hplc SupervisorID thoma Slot Number 24
91
Cl
OH
O
NH
170.16
160.24
151.66
143.12
133.66
132.47
130.83
130.31
130.18
127.33
123.86
120.89
118.37
117.98
52.01
51.59
49.00 CD3OD
f1 (ppm)

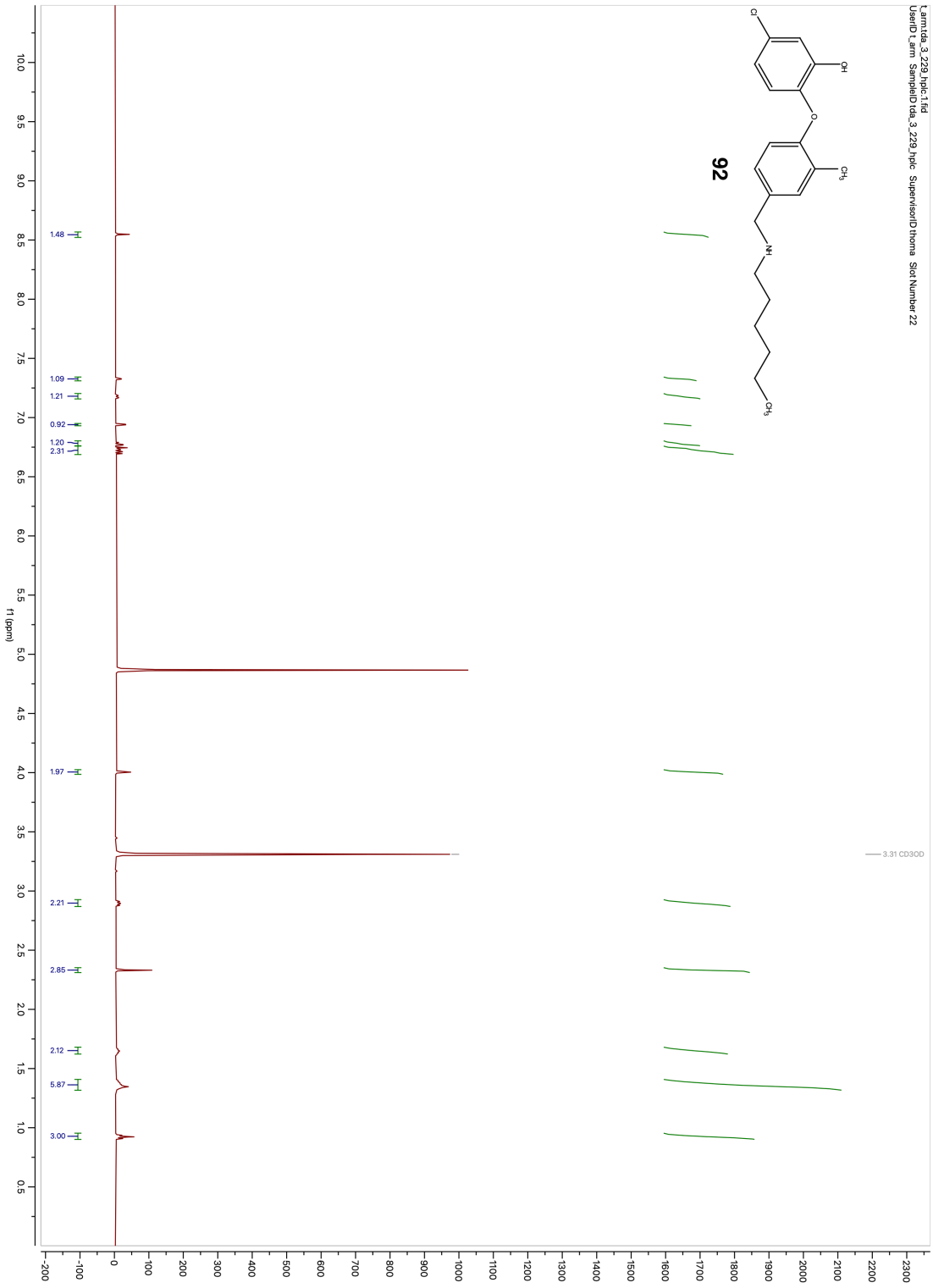
t_arm:1da_3_229_hplc_1.fid
UserID t_arm SampleID 1da_3_229_hplc SupervisorID thoma Slot Number 22
92
Cl
OH
O
CH3
NH
CH3
1.48
1.09
1.21
0.92
1.20
2.31
1.97
2.21
2.85
2.12
5.87
3.00
3.31 CD3OD
f1 (ppm)

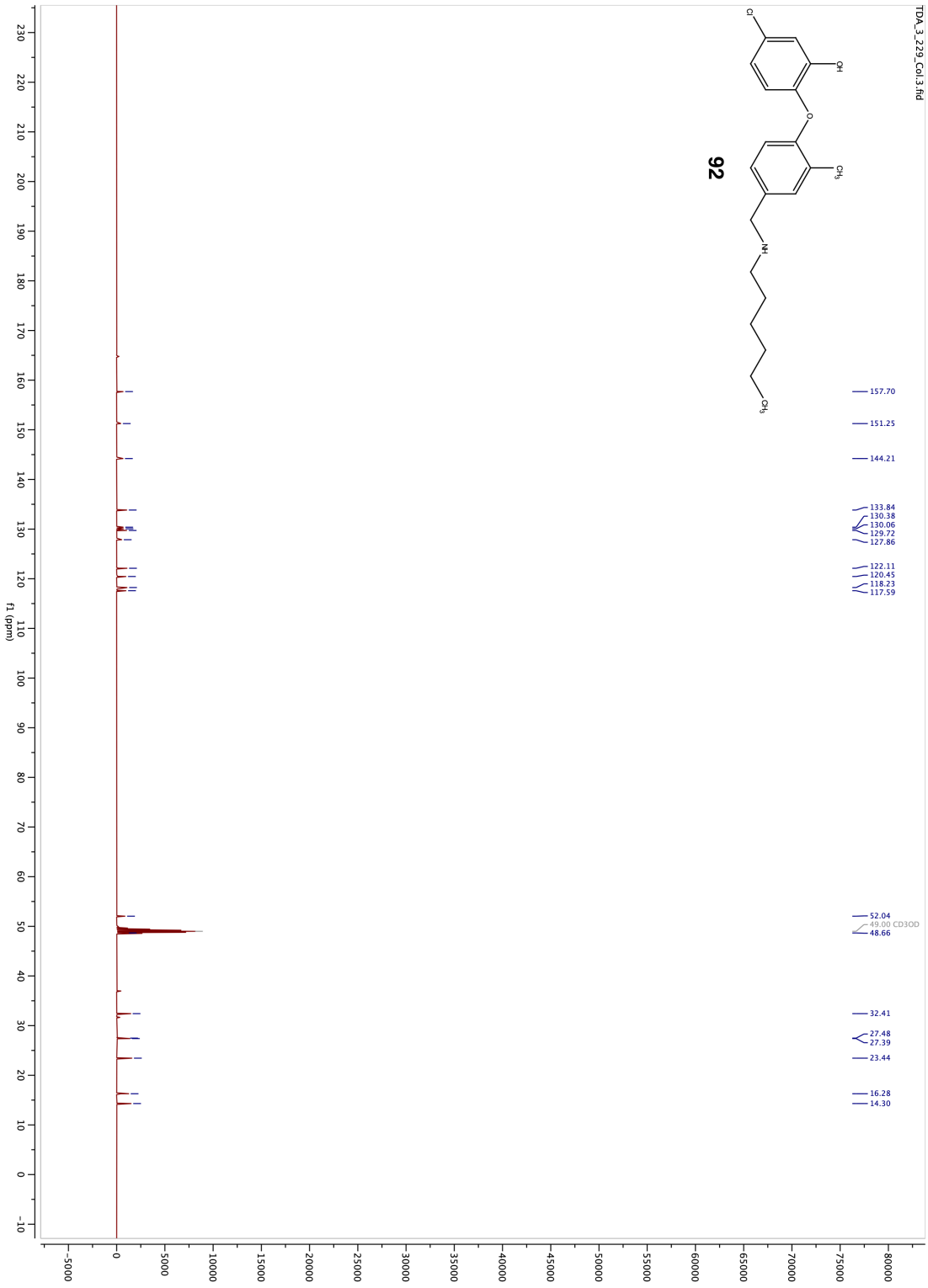
TDA_3_229_Col_3.fid
92
Cl
OH
O
CH3
NH
CH3
157.70
151.25
144.21
133.84
130.38
130.06
129.72
127.86
122.11
120.45
118.23
117.59
52.04
49.00 CD3OD
48.66
32.41
27.48
27.39
23.44
16.28
14.30
f1 (ppm)

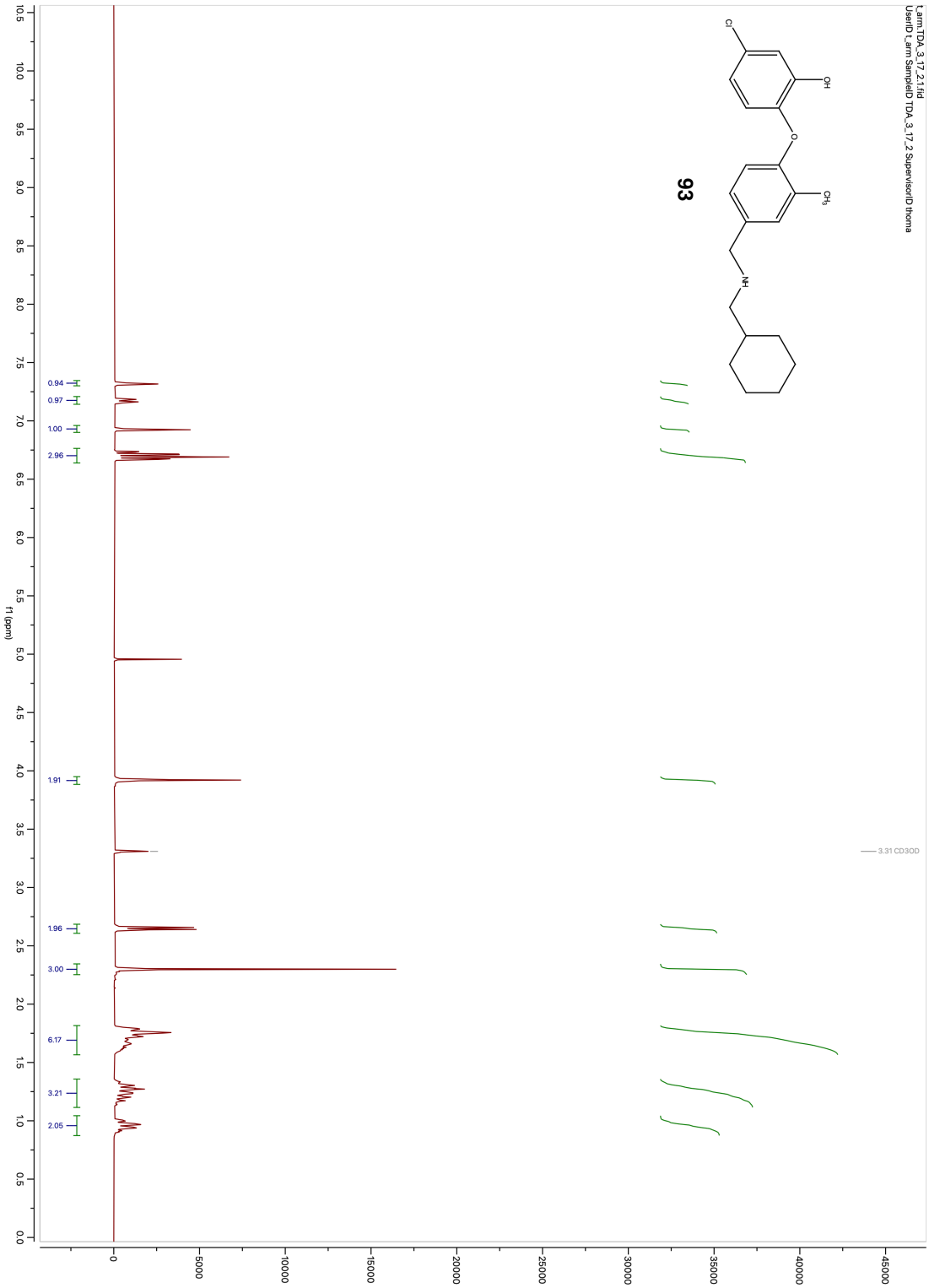
t_arm:TDA_3_17_2:1.fid
UserID t_arm SampleID TDA_3_17_2 SupervisorID thoma
93
Cl
OH
O
CH3
NH
0.94
0.97
1.00
2.96
1.91
1.96
3.00
6.17
3.21
2.05
3.31 CD3OD
f1 (ppm)

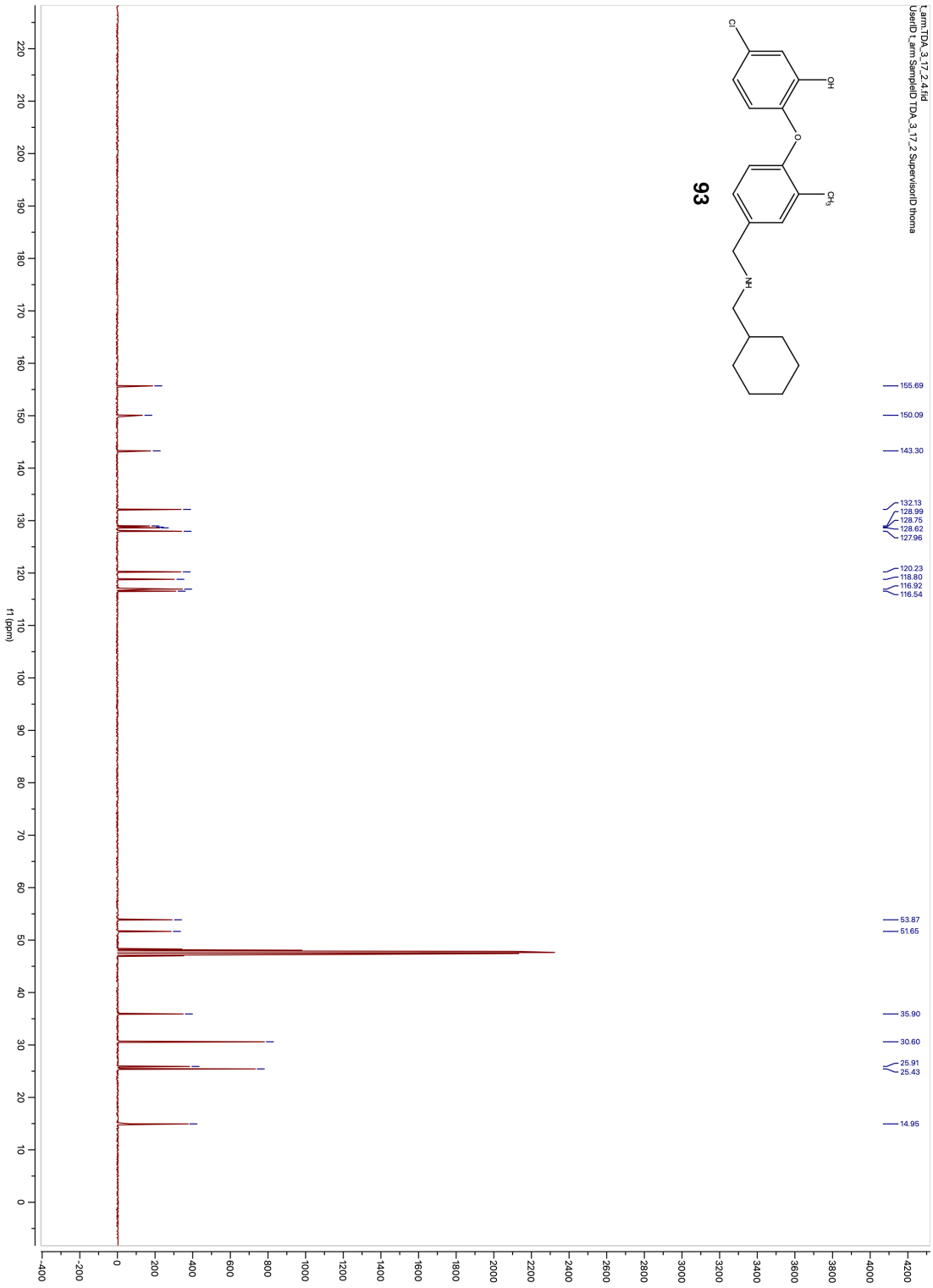
t_arm:TDA_3_17_2_4.fid
UserID t_arm SampleID TDA_3_17_2 SupervisorID thoma
93
Cl
OH
O
CH3
NH
155.69
150.09
143.30
132.13
128.99
128.75
128.62
127.96
120.23
118.80
116.92
116.54
53.87
51.65
35.90
30.60
25.91
25.43
14.95
f1 (ppm)

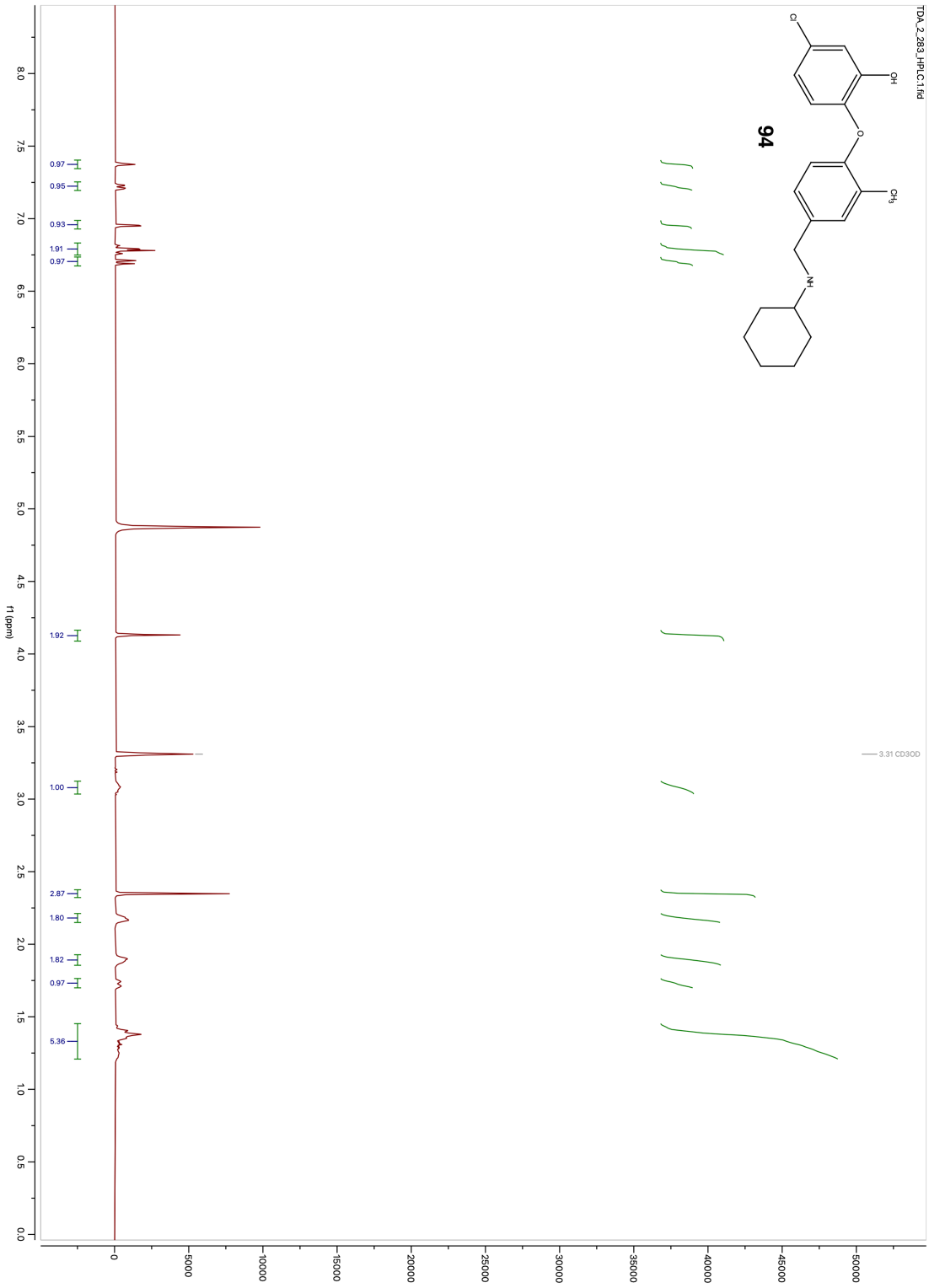
TDA_2.283_HPLC.1.fid
94
Cl
OH
O
CH3
NH
0.97
0.95
0.93
1.91
0.97
1.92
1.00
2.87
1.80
1.82
0.97
5.36
3.31 CD3OD
f1 (ppm)

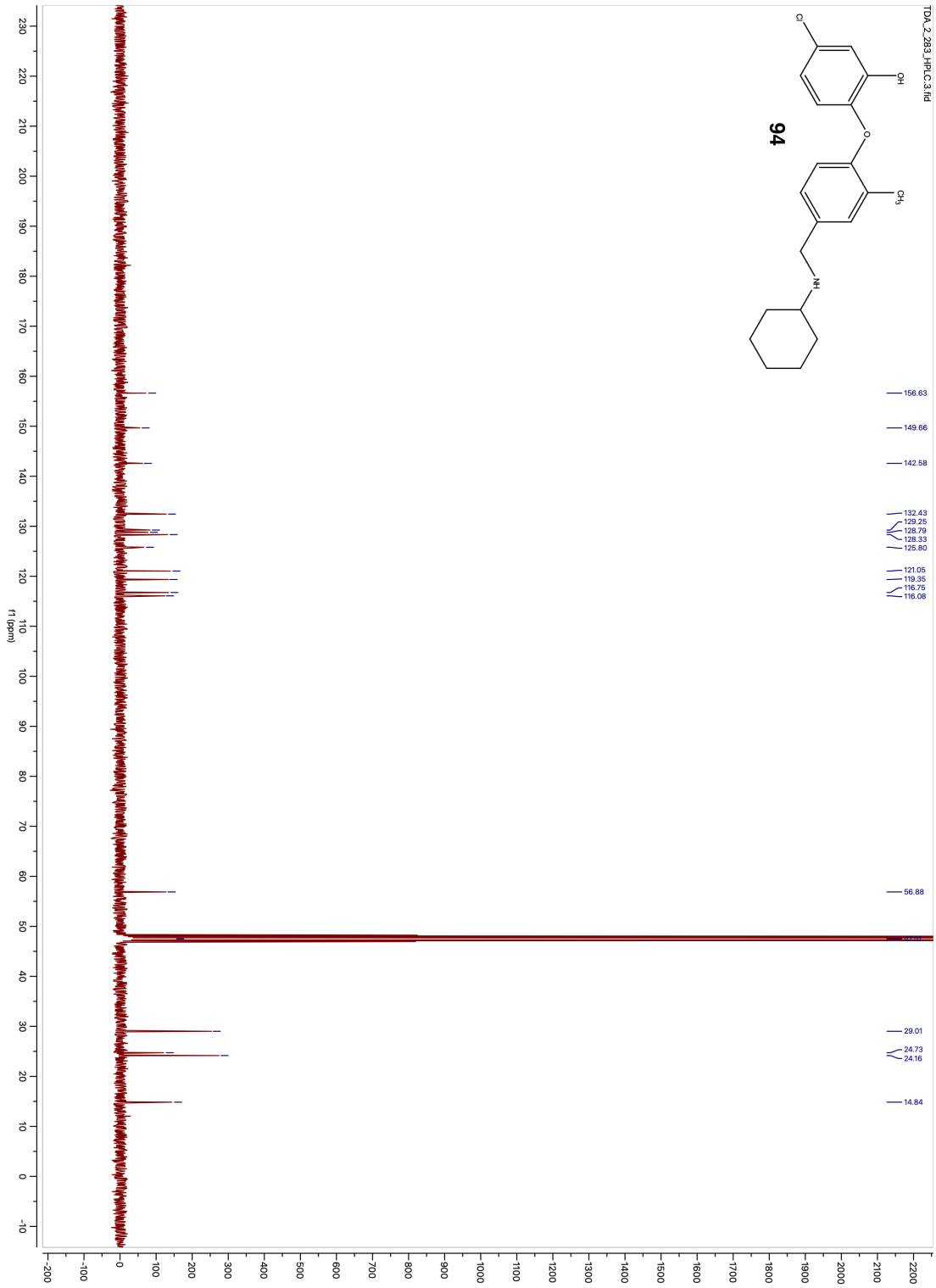
TDA_2.283_HPLC.3.fid
94
Cl
OH
O
CH3
NH
156.63
149.66
142.58
132.43
129.25
128.79
128.33
125.80
121.05
119.35
116.75
116.08
56.88
29.01
24.73
24.16
14.84
f1 (ppm)

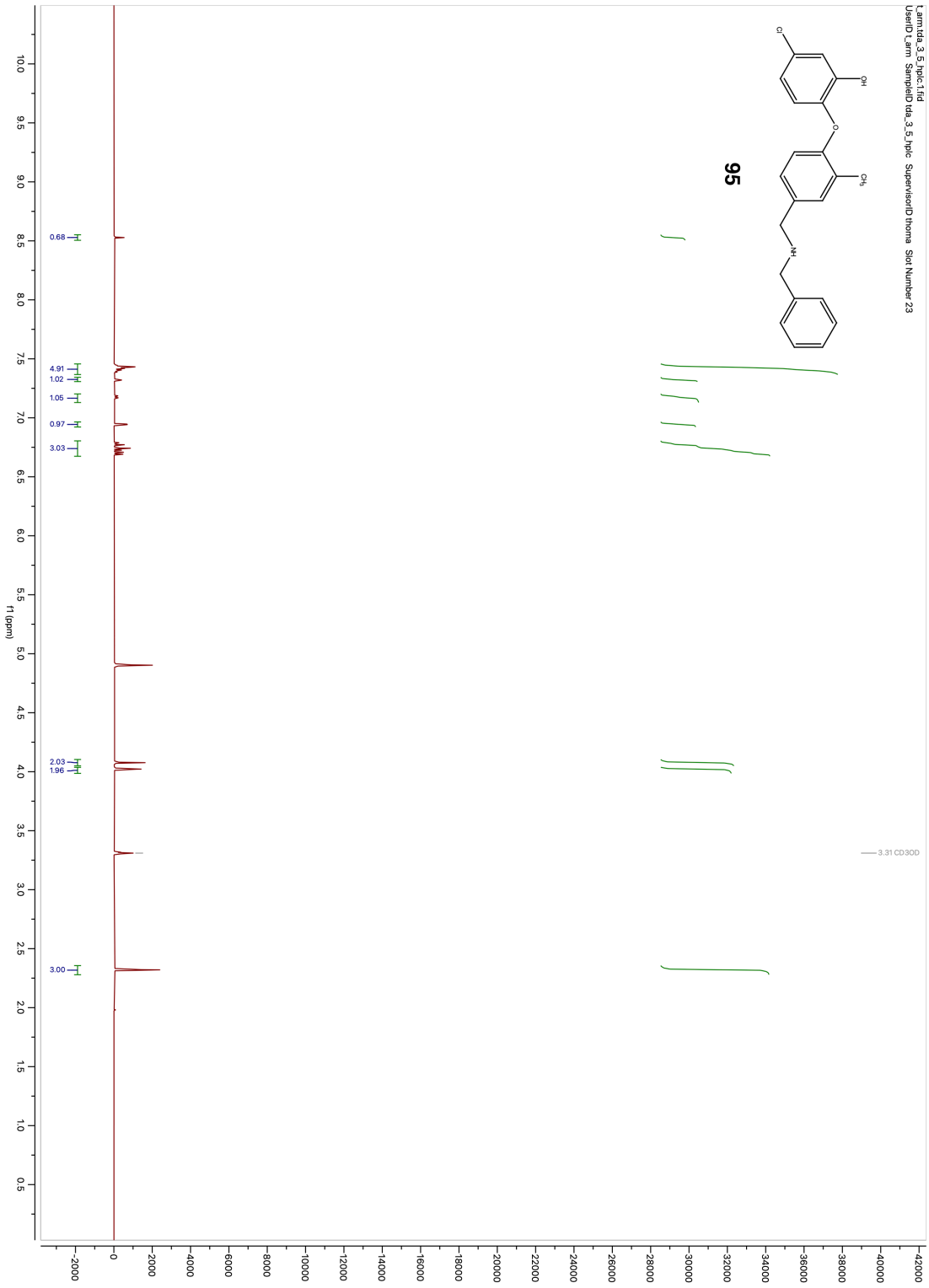
t_arm:1da_3_5_hplc_1.fid
UserID t_arm SampleID 1da_3_5_hplc SupervisorID thoma Slot Number 23
95
Cl
OH
O
CH3
NH
0.68
4.91
1.02
1.05
0.97
3.03
2.03
1.96
3.00
3.31 CD3OD
f1 (ppm)

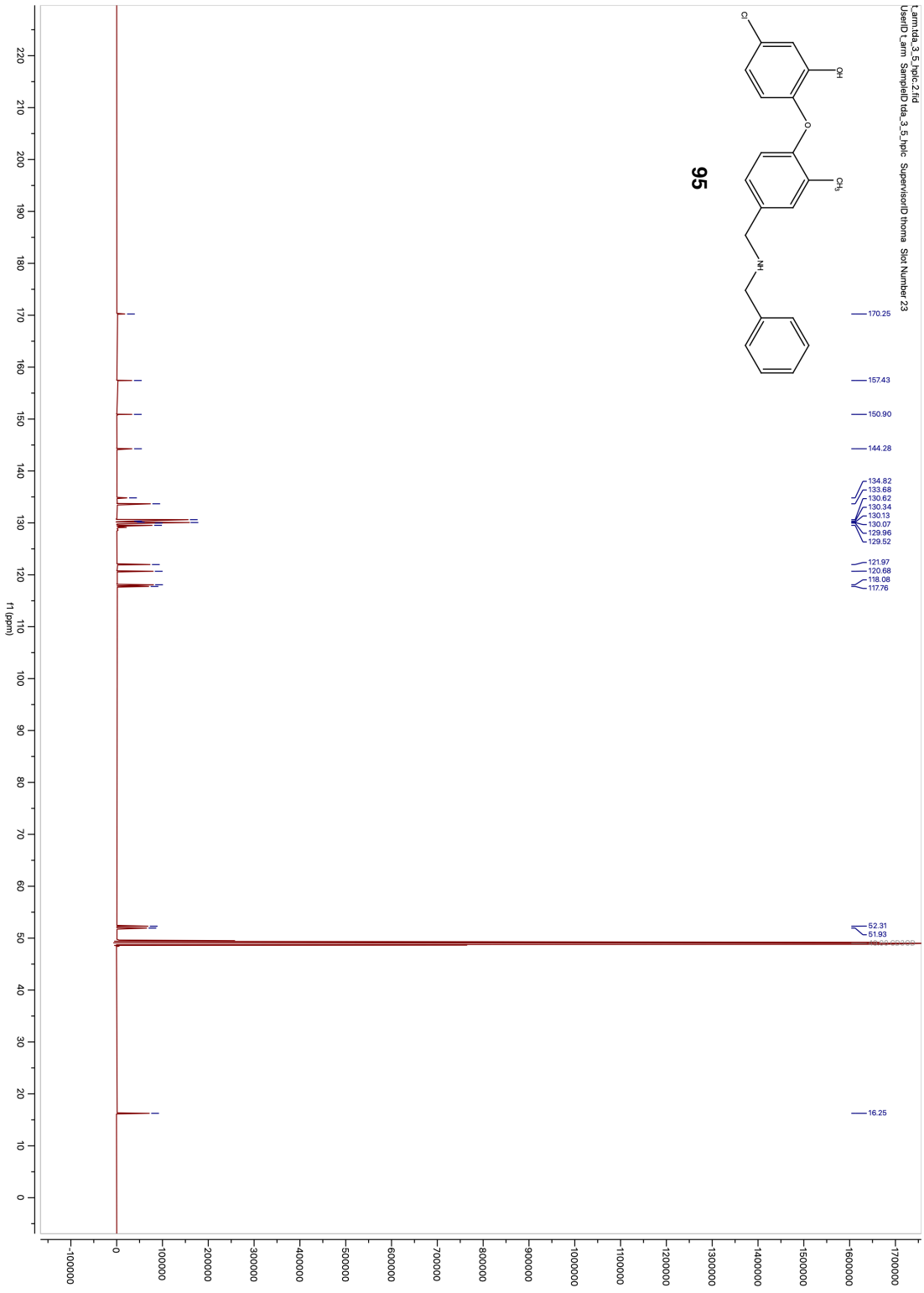
t_arm:tda_3_5_hplc_2.fid
UserID t_arm SampleID tda_3_5_hplc SupervisorID thoma Slot Number 23
95
Cl
OH
O
CH3
NH
170.25
157.43
150.90
144.28
134.82
133.68
130.62
130.34
130.13
130.07
129.96
129.52
121.97
120.68
118.08
117.76
52.31
51.93
16.25
f1 (ppm)

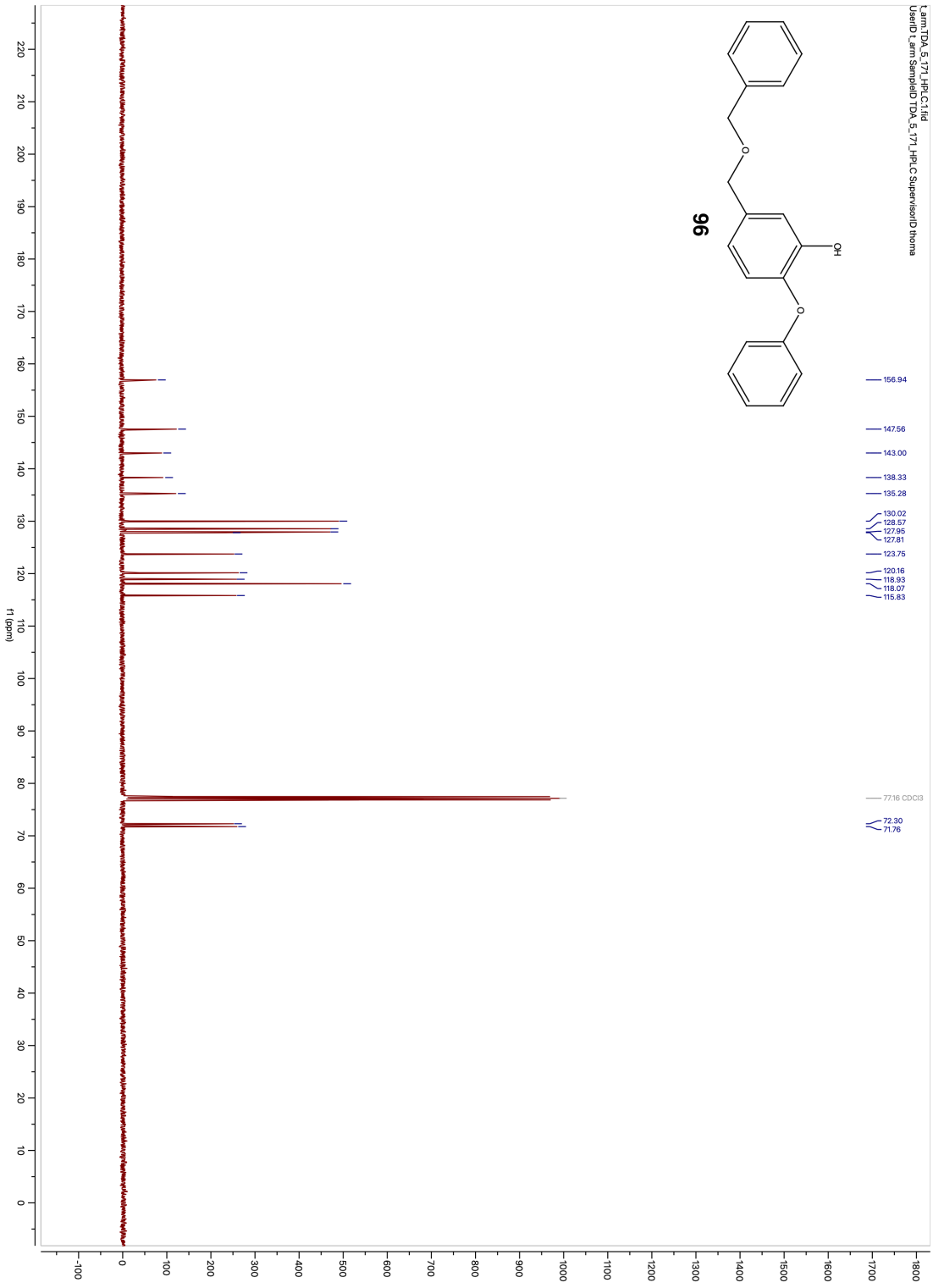
t_arm:TDA_5_171_HPLC:1:fid
UserID t_arm SampleID TDA_5_171_HPLC SupervisorID thoma
96
OH
O
O
156.94
147.56
143.00
138.33
135.28
130.02
128.57
127.95
127.81
123.75
120.16
118.93
118.07
115.83
77.16 CDCl3
72.30
71.76
f1 (ppm)

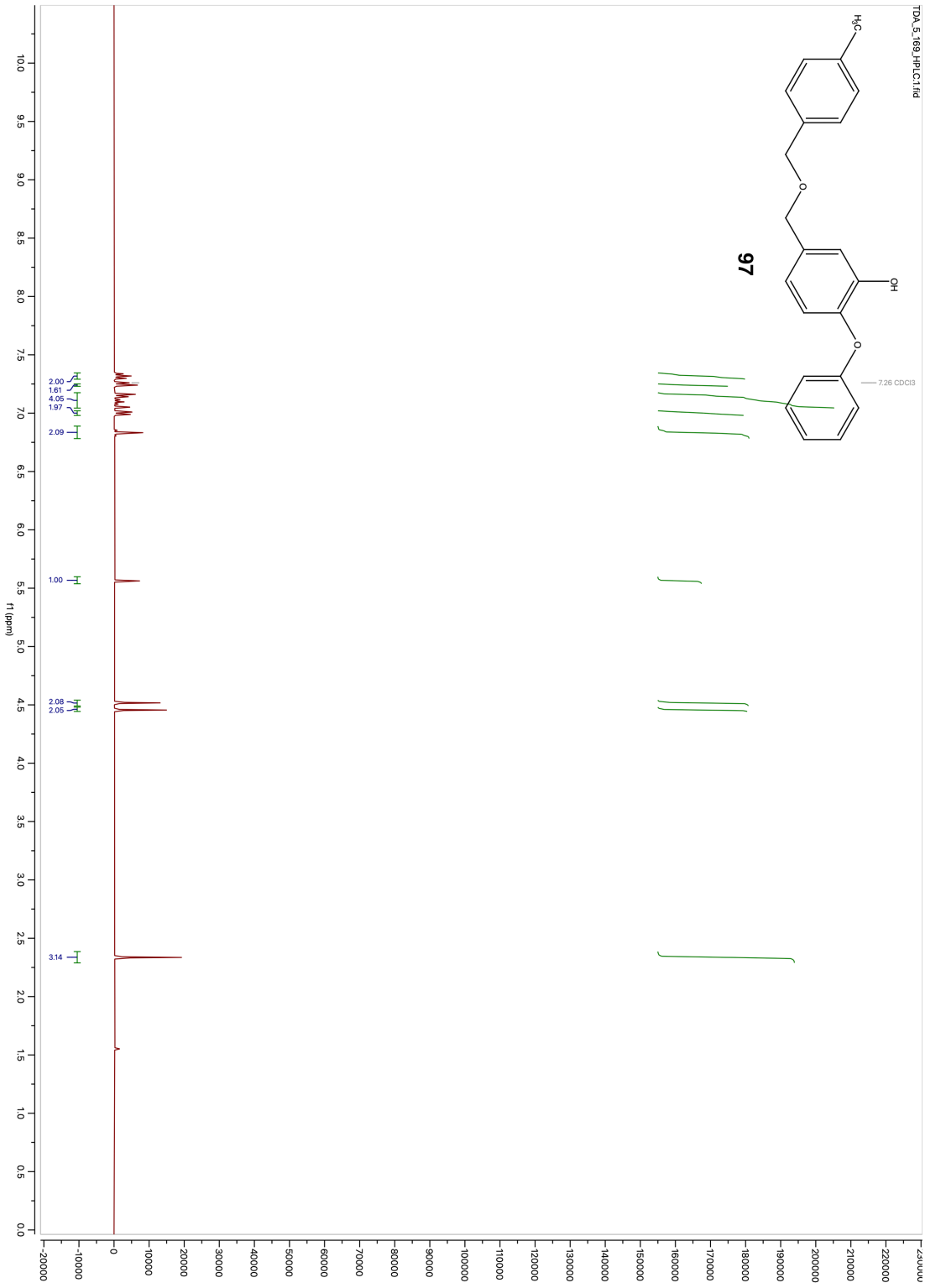
TDA_5.169_HPLC.1.fid
97
7.26 CDCl3
2.00
1.61
4.05
1.97
2.09
1.00
2.08
2.05
3.14
f1 (ppm)

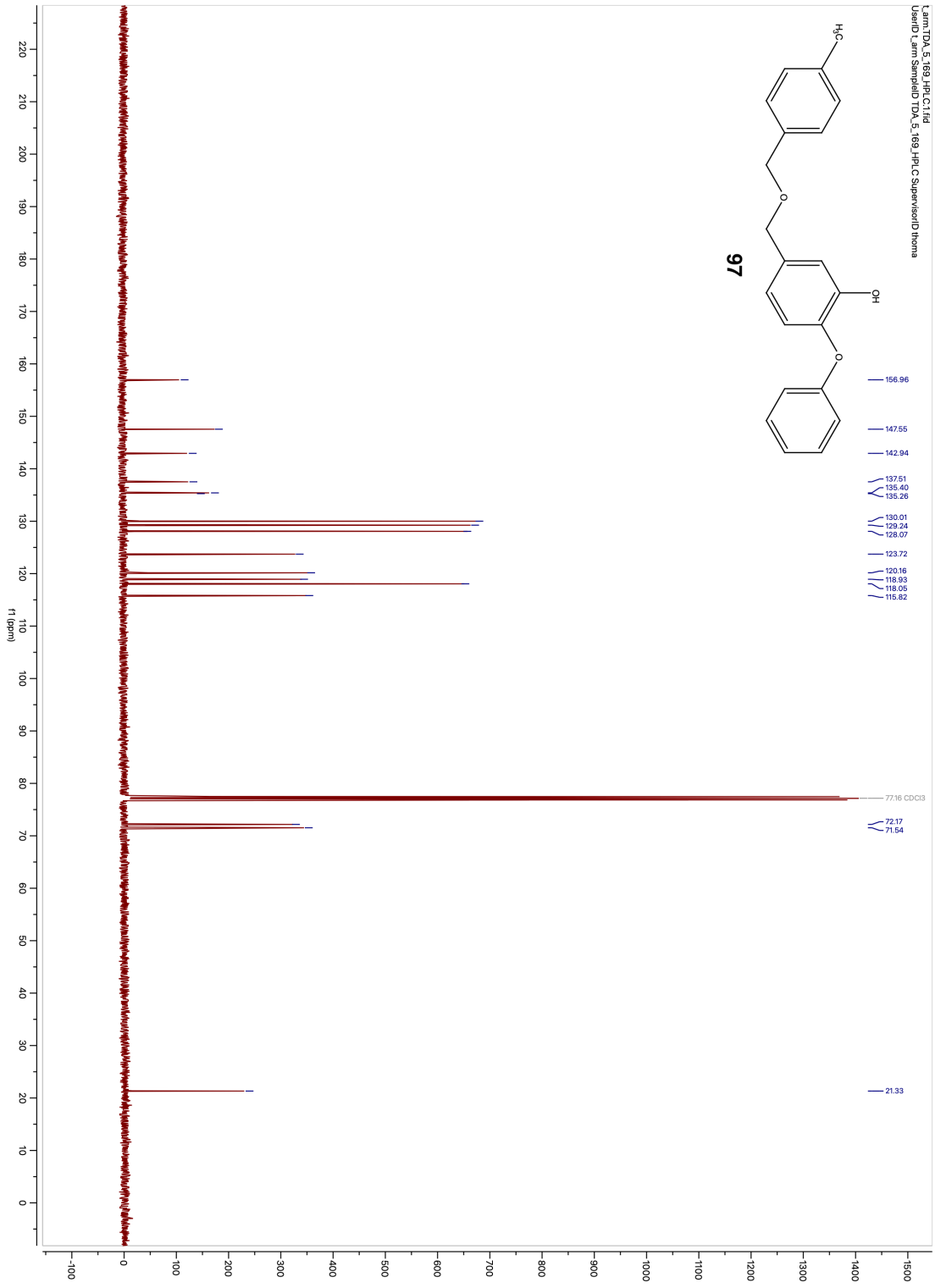
t_arm:TDA_5_169_HPLC.1.fid
UserID t_arm SampleID TDA_5_169_HPLC SupervisorID thoma
97
H3C
O
OH
O
156.96
147.55
142.94
137.51
135.40
135.26
130.01
129.24
128.07
123.72
120.16
118.93
118.05
115.82
77.16 CDCl3
72.17
71.54
21.33
f1 (ppm)

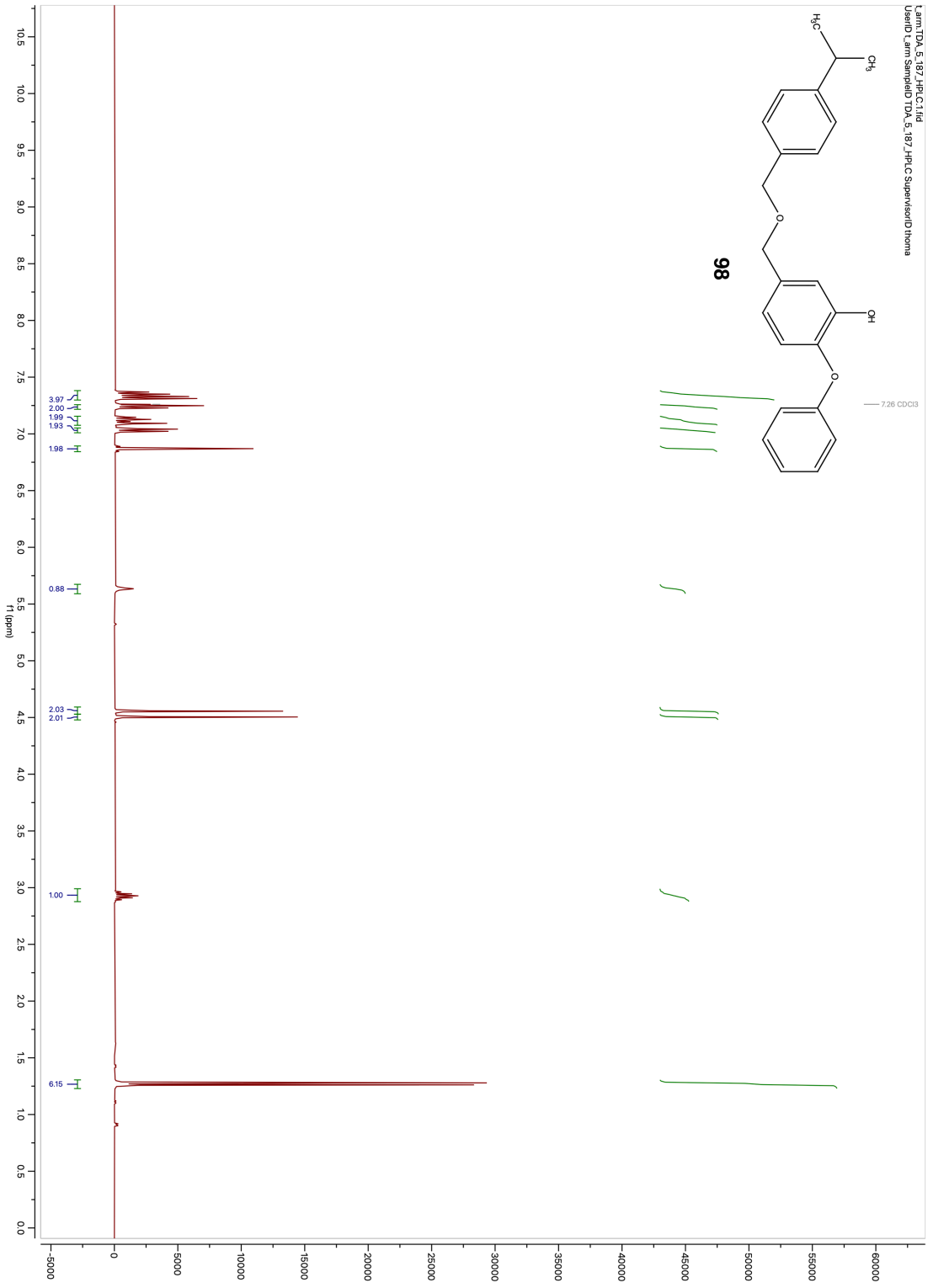
t_arm:TDA_5_187_HPLC:1:fid
UserID t_arm SampleID TDA_5_187_HPLC SupervisorID thoma
98
7.26 CDCl3
3.97
2.00
1.99
1.93
1.98
0.88
2.03
2.01
1.00
6.15
f1 (ppm)

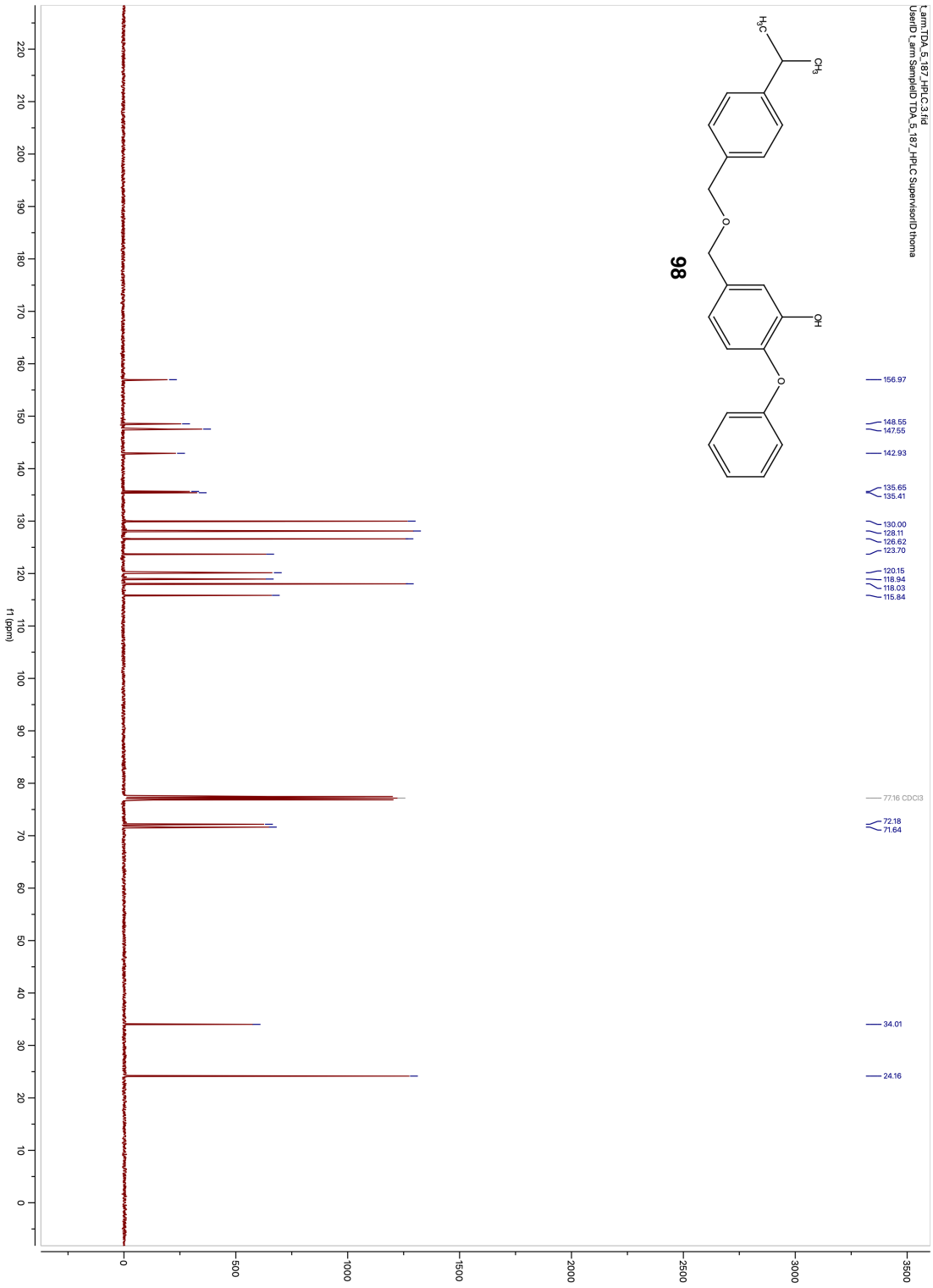
t_arm:TDA_5_187_HPLC.3.fid
UserID t_arm SampleID TDA_5_187_HPLC SupervisorID thoma
98
H3C
CH3
OH
O
O
156.97
148.55
147.55
142.93
135.65
135.41
130.00
128.11
126.62
123.70
120.15
118.94
118.03
115.84
77.16 CDCl3
72.18
71.64
34.01
24.16
f1 (ppm)

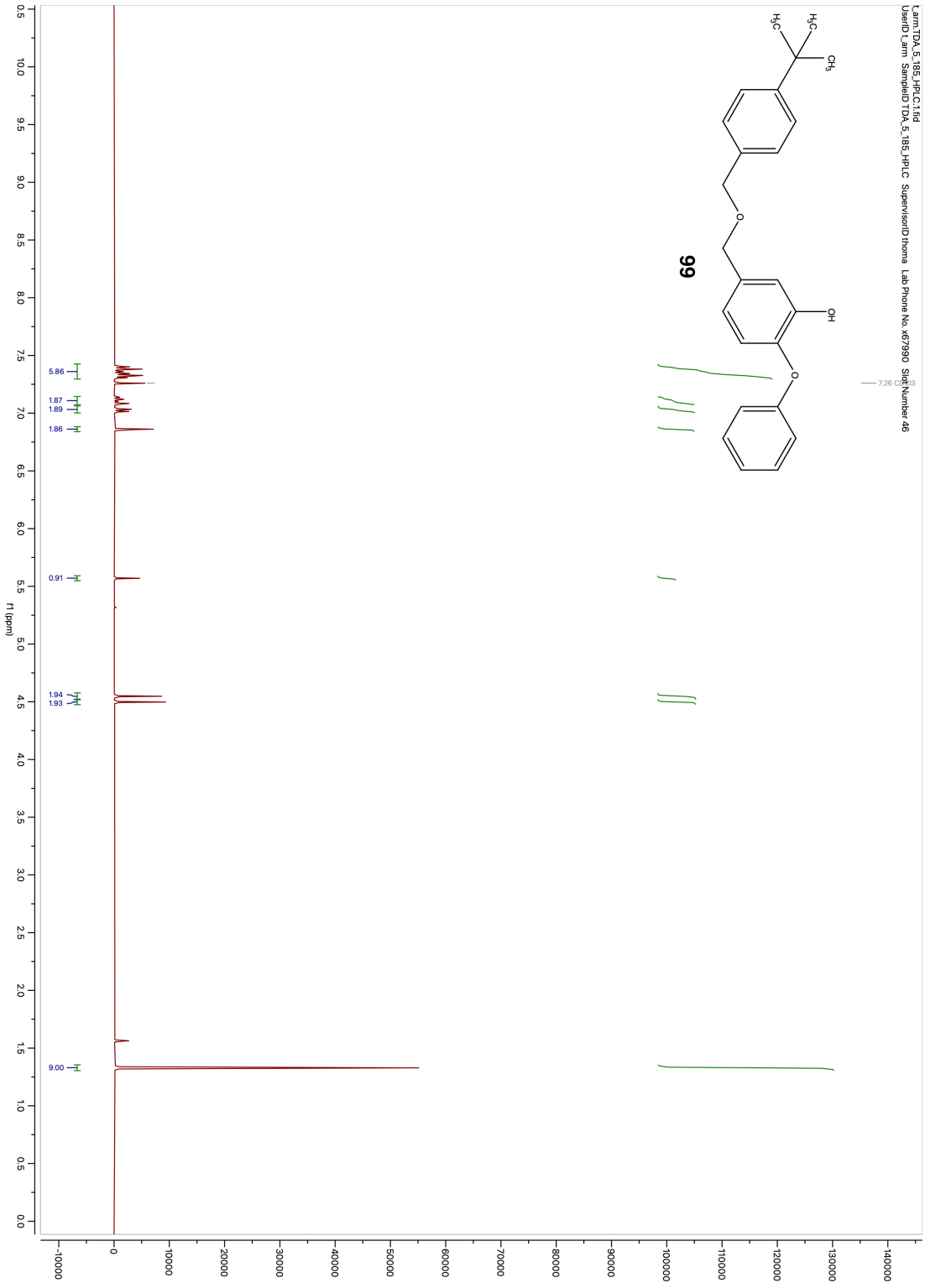
t_arm:TDA_5_185_HPLC.1.fid
UserID t_arm SampleID TDA_5_185_HPLC SupervisorID thoma Lab Phone No. x67990 Slot Number 46
99
OH
5.86
1.87
1.89
1.86
0.91
1.94
1.93
9.00
f1 (ppm)

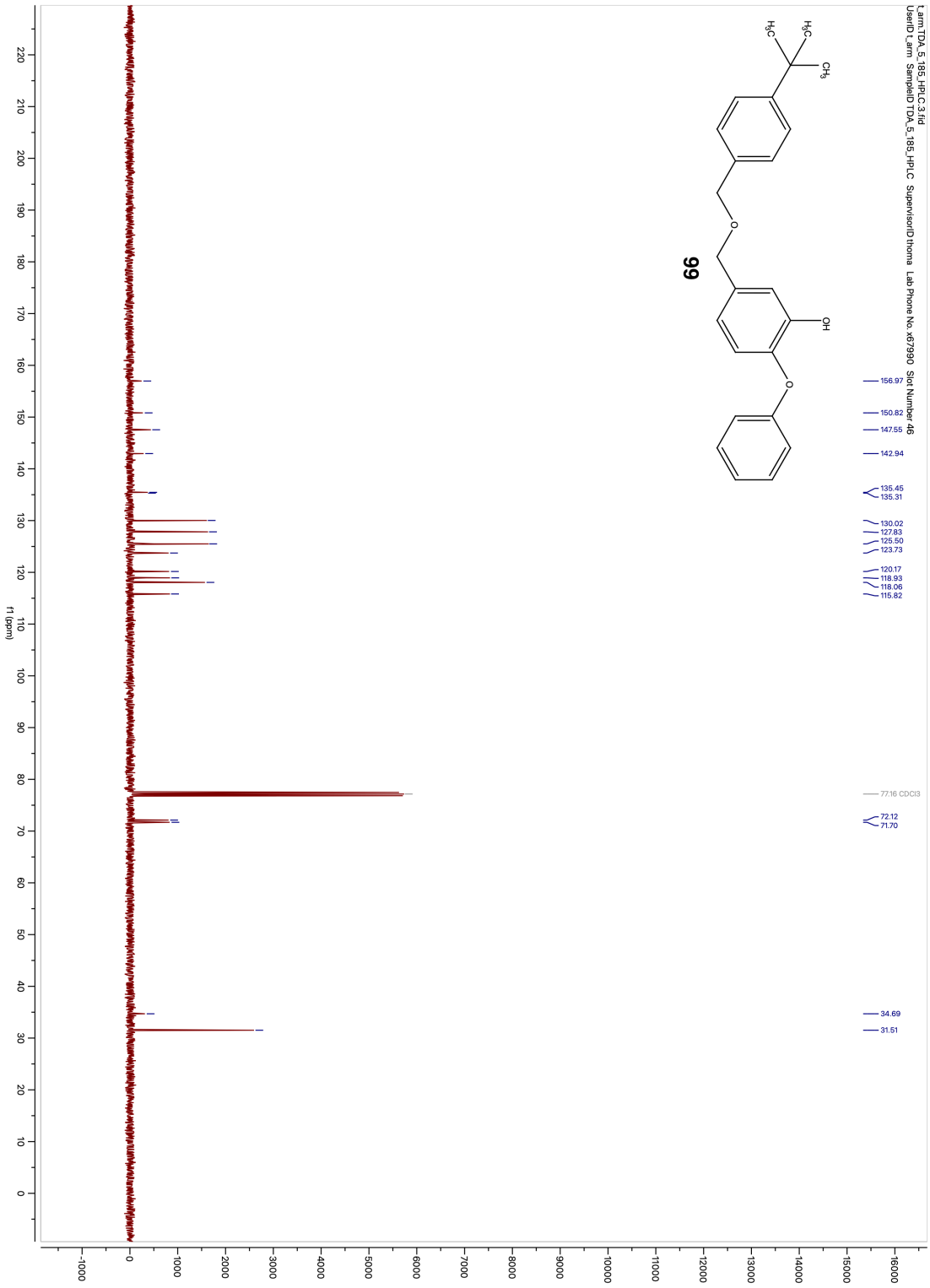
t_arm:TDA_5_185_HPLC_3.fid
UserID t_arm SampleID TDA_5_185_HPLC SupervisorID thoma Lab Phone No. x67990 Slot Number 46
99
H3C
H3C
CH3
O
OH
O
156.97
150.82
147.55
142.94
135.45
135.31
130.02
127.83
125.50
123.73
120.17
118.93
118.06
115.82
77.16 CDCl3
72.12
71.70
34.69
31.51
f1 (ppm)

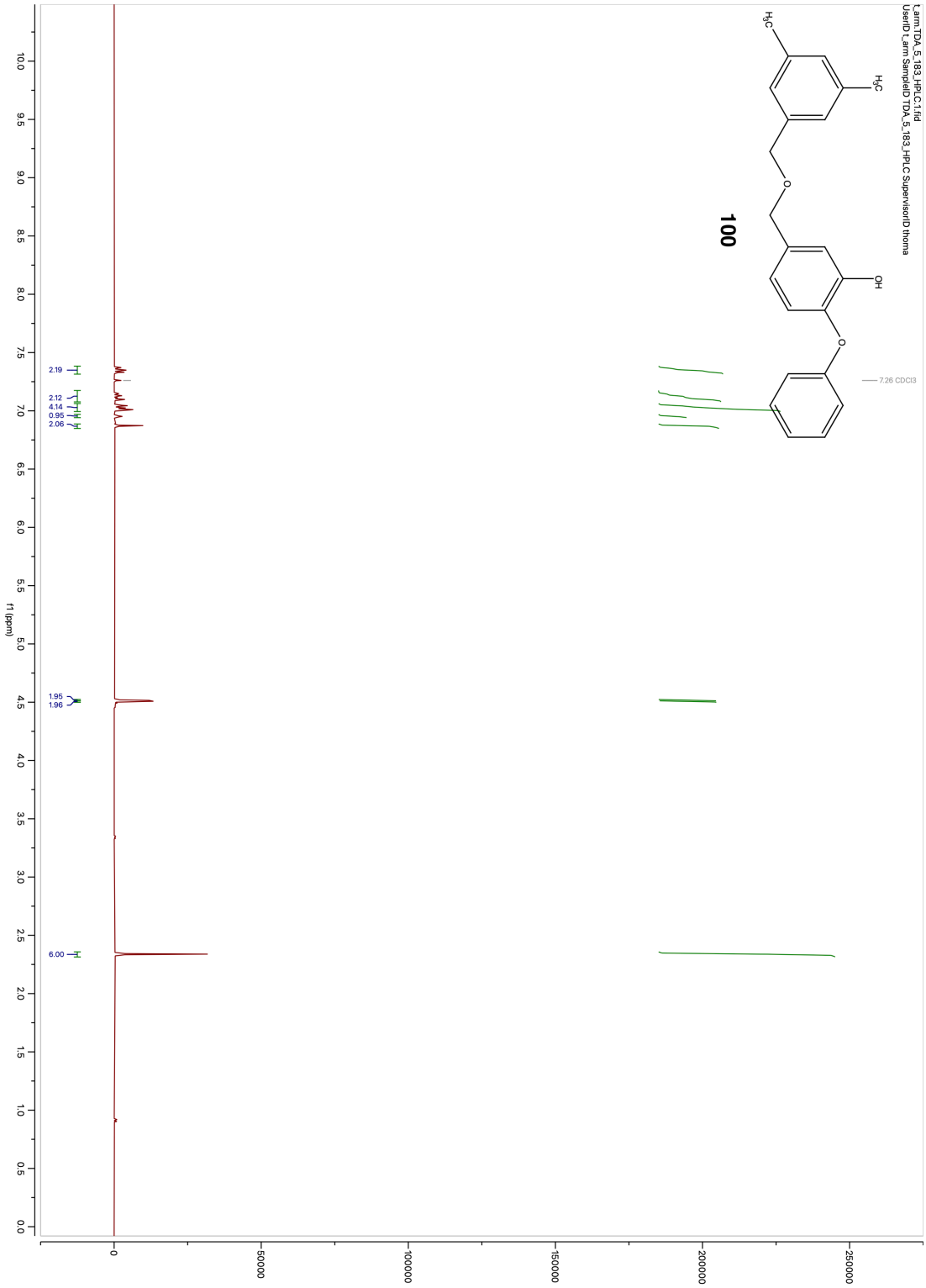
L_arm TDA_5_183_HPLC_1.fid
UserID L_arm SampleID TDA_5_183_HPLC SupervisorID thoma
100
H3C
H3C
O
O
OH
7.26 CDCl3
2.19
2.12
4.14
0.95
2.06
1.95
1.96
6.00
f1 (ppm)
10.0
9.5
9.0
8.5
8.0
7.5
7.0
6.5
6.0
5.5
5.0
4.5
4.0
3.5
3.0
2.5
2.0
1.5
1.0
0.5
0.0
0
50000
100000
150000
200000
250000

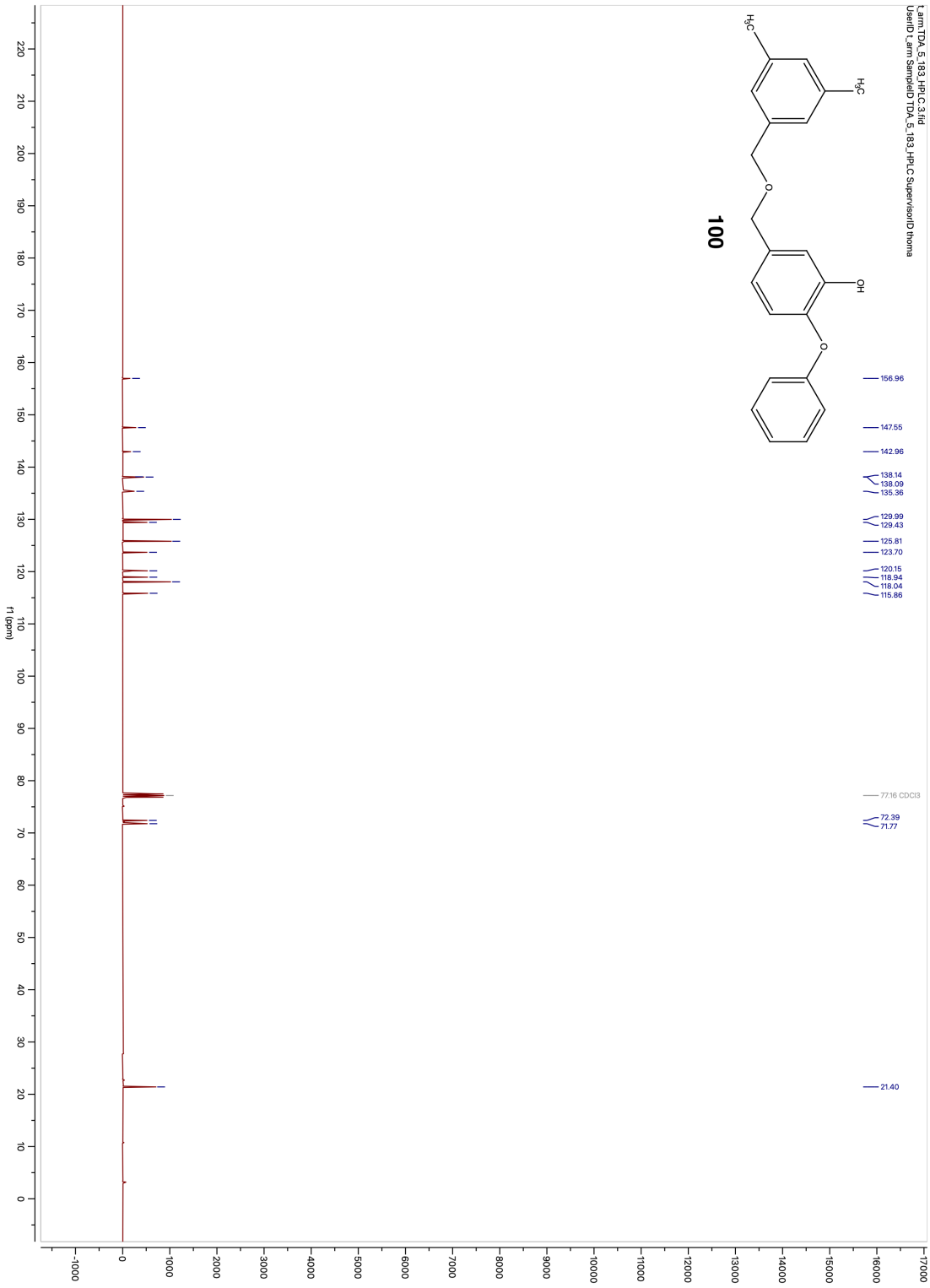
t_arm:TDA_5_183_HPLC.3.fid
UserID t_arm SampleID TDA_5_183_HPLC SupervisorID thoma
100
H3C
H3C
O
O
OH
156.96
147.55
142.96
138.14
138.09
135.36
129.99
129.43
125.81
123.70
120.15
118.94
118.04
115.86
77.16 CDCl3
72.39
71.77
21.40
f1 (ppm)

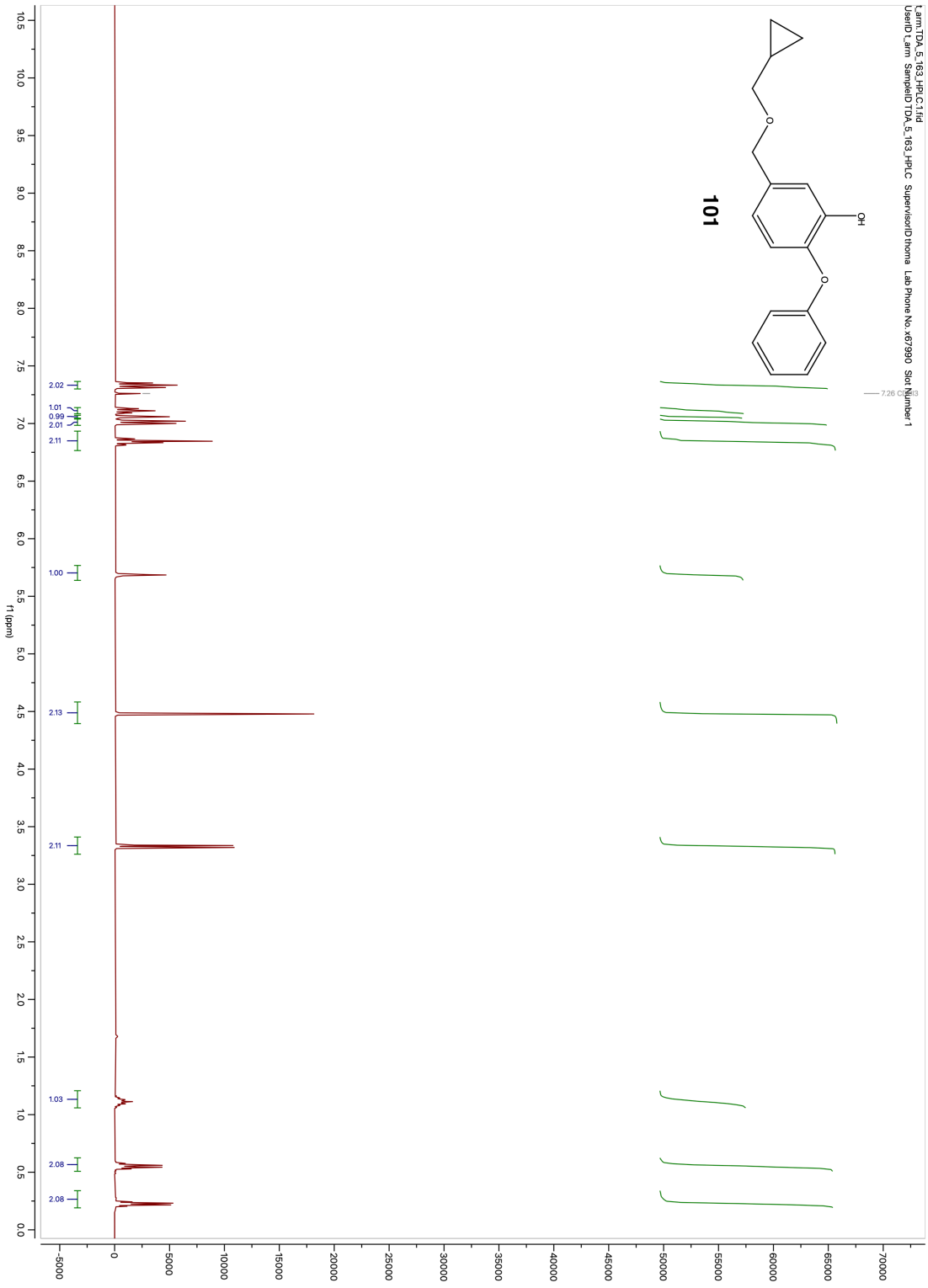
t_arm:TDA_5_163_HPLC.1.fid
UserID t_arm SampleID TDA_5_163_HPLC SupervisorID thoma Lab Phone No. x67990 Slot Number 1
101
OH
O
O
7.26 CDCl3
2.02
1.01
0.99
2.01
2.11
1.00
2.13
2.11
1.03
2.08
2.08
f1 (ppm)

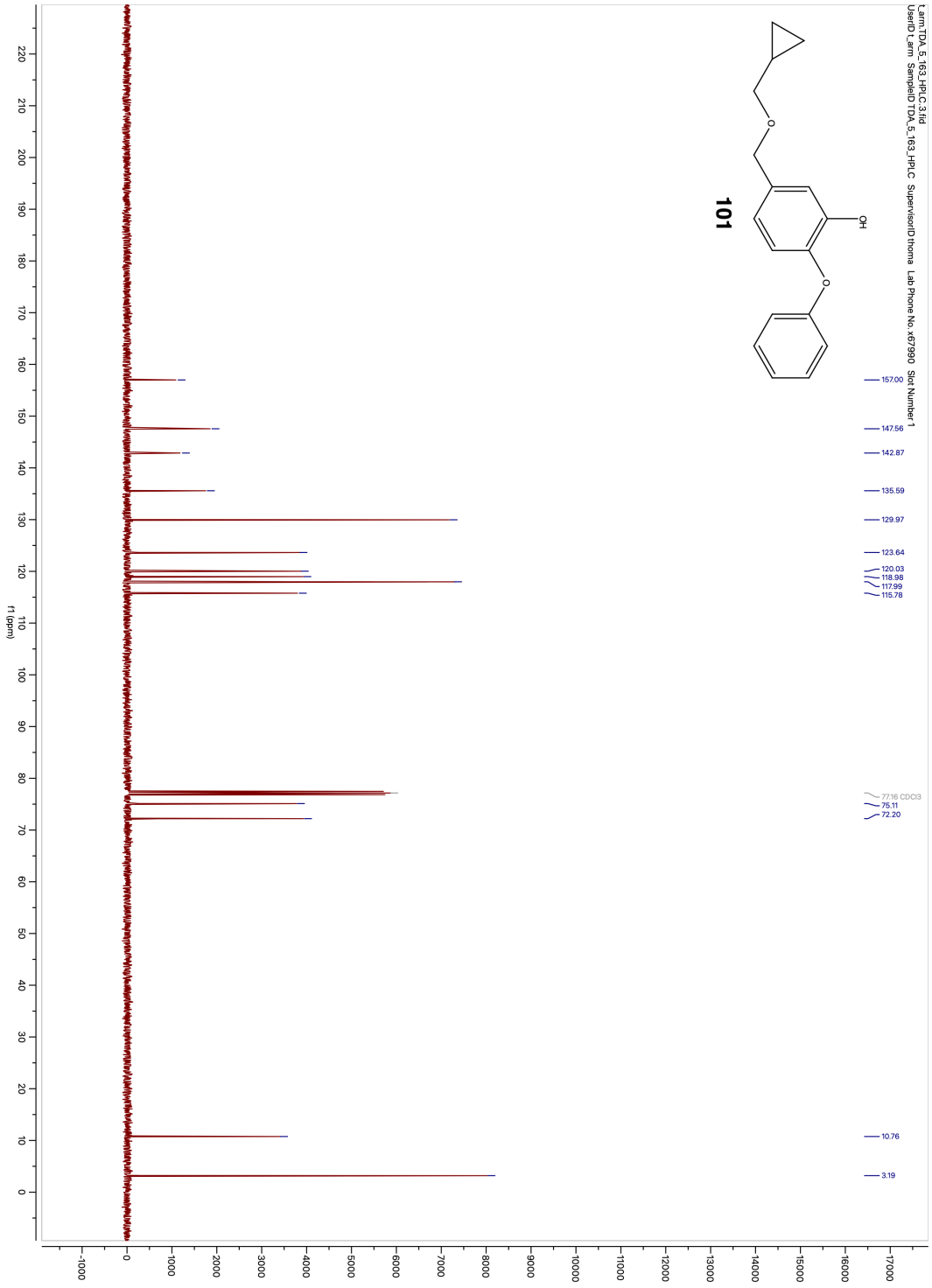
L:arm,TDA_5_163_HPLC_3.fid
UserID L:arm SampleID TDA_5_163_HPLC SupervisorID thoma Lab Phone No. x67990 Slot Number 1
101
OH
157.00
147.56
142.87
135.59
129.97
123.64
120.03
118.98
117.99
115.78
77.16 CDCl3
75.11
72.20
10.76
3.19
f1 (ppm)

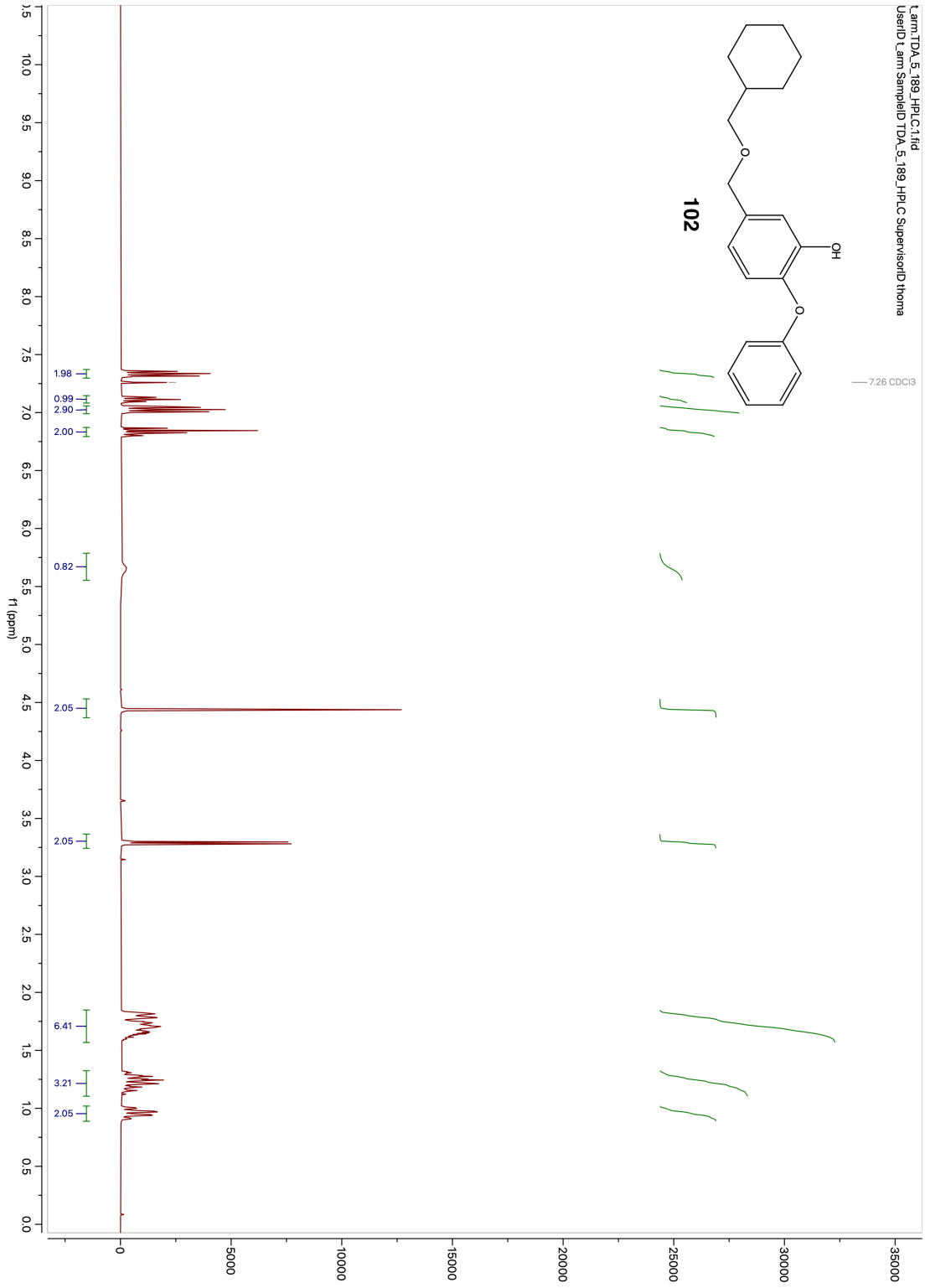
t_arm.TDA_5_189_HPLC.1.fid
UserID t_arm SampleID TDA_5_189_HPLC SupervisorID thorna
102
OH
O
O
7.26 CDCl3
1.98
0.99
2.90
2.00
0.82
2.05
2.05
6.41
3.21
2.05
f1 (ppm)
10.5
10.0
9.5
9.0
8.5
8.0
7.5
7.0
6.5
6.0
5.5
5.0
4.5
4.0
3.5
3.0
2.5
2.0
1.5
1.0
0.5
0.0
0
5000
10000
15000
20000
25000
30000
35000

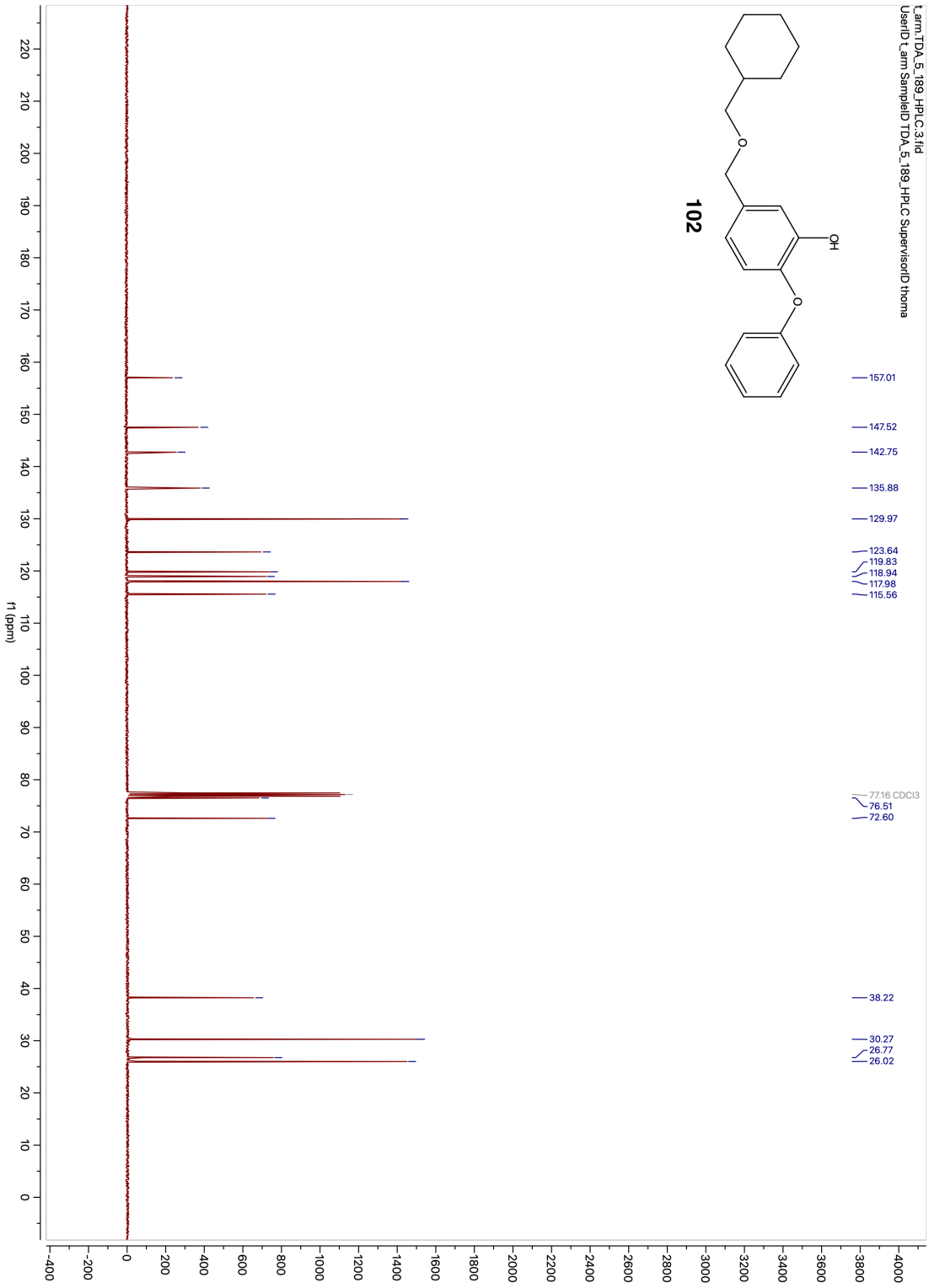
t_arm TDA_5_189_HPLC.3.fid
UserID t_arm SampleID TDA_5_189_HPLC SupervisorID thorna
102
OH
O
O
157.01
147.52
142.75
135.88
129.97
123.64
119.83
118.94
117.98
115.56
77.16 CDCl3
76.51
72.60
38.22
30.27
26.77
26.02
f1 (ppm)

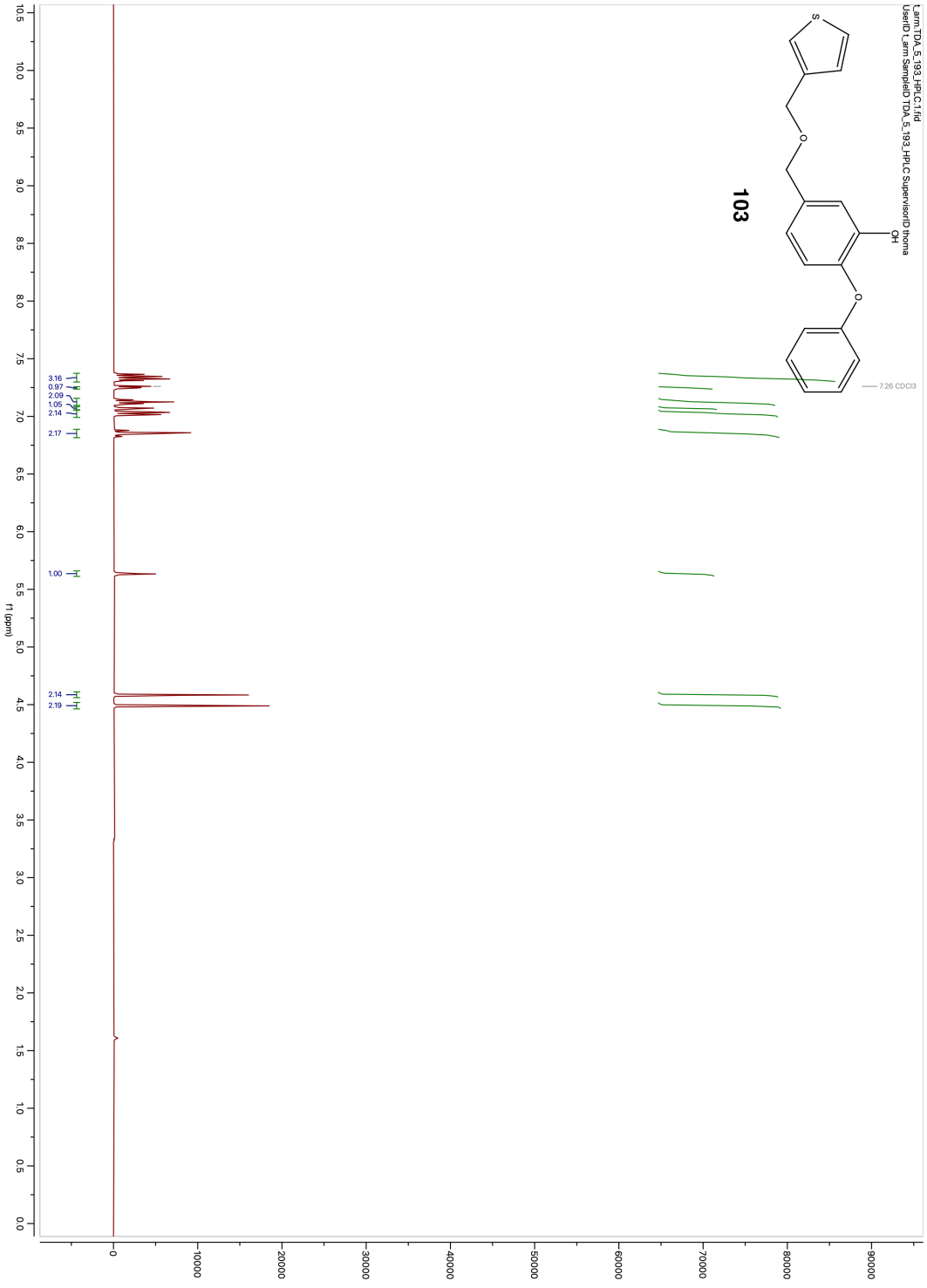
L:arm:TDA_5-193_HPLC:1.fid
UserID L:arm SampleID TDA_5-193_HPLC SupervisorID thoma
103
OH
S
O
O
7.26 CDCl3
3.16
0.97
2.09
1.05
2.14
2.17
1.00
2.14
2.19
f1 (ppm)

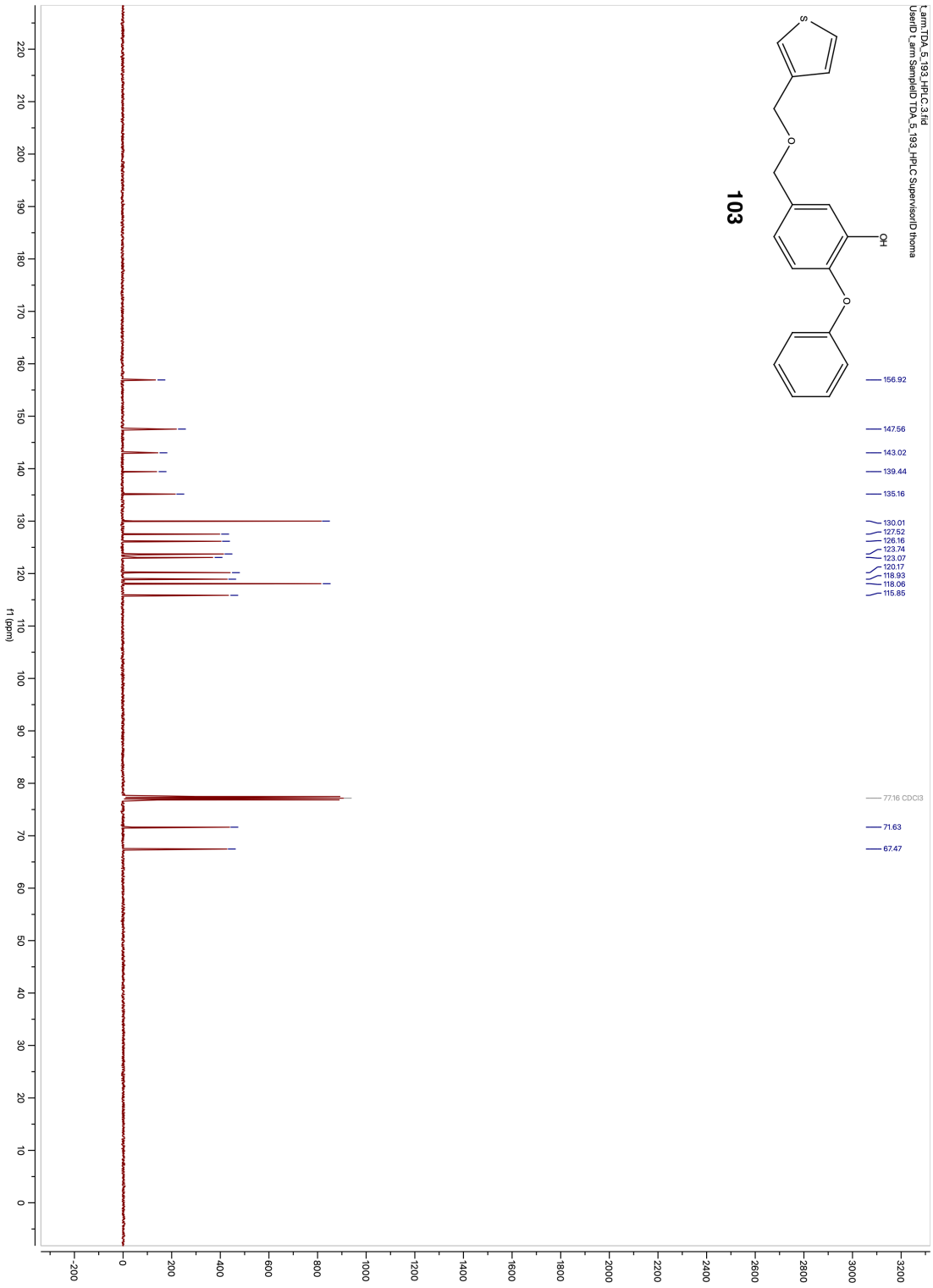
t_arm:TDA_5_193_HPLC.3.fid
UserID t_arm SampleID TDA_5_193_HPLC SupervisorID thoma
103
S
O
OH
O
156.92
147.56
143.02
139.44
135.16
130.01
127.52
126.16
123.74
123.07
120.17
118.93
118.06
115.85
77.16 CDCl3
71.63
67.47
f1 (ppm)

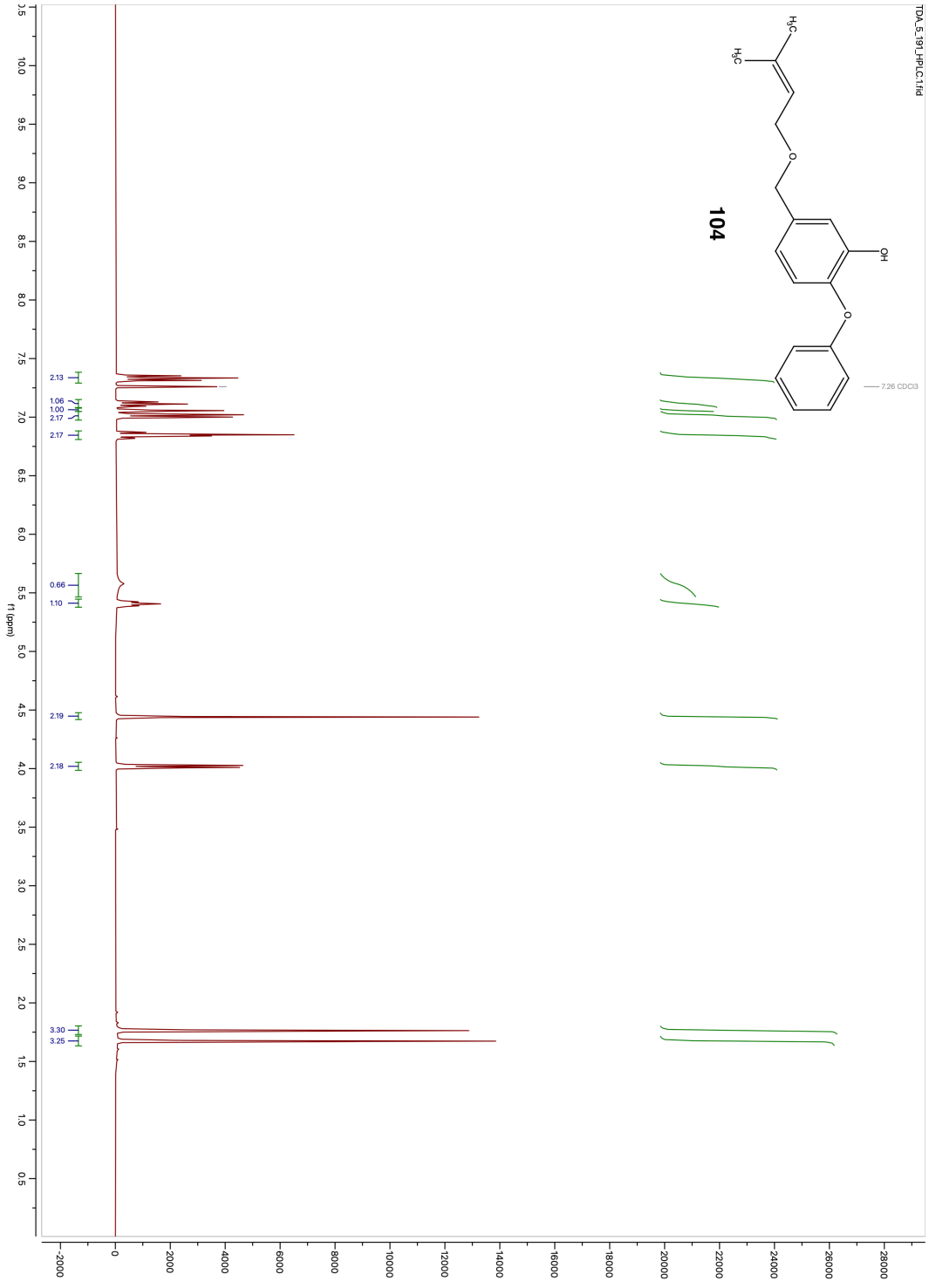
TDA_5_191_HPLC.1fid
104
OH
O
O
H3C
H3C
7.26 CDCl3
2.13
1.06
1.00
2.17
2.17
0.66
1.10
2.19
2.18
3.30
3.25
f1 (ppm)

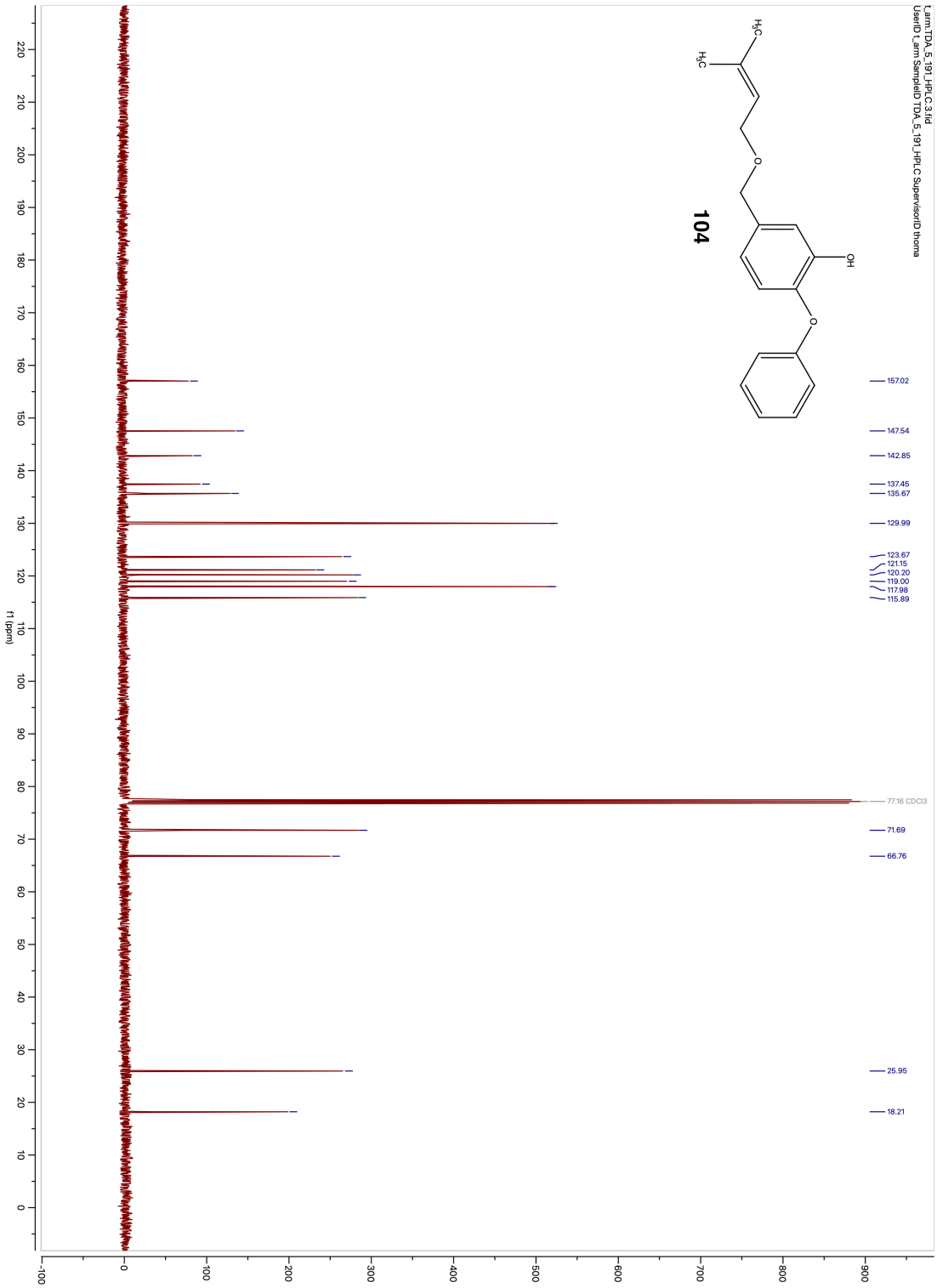
t_arm:TDA_5_191_HPLC.3.fid
UserID t_arm SampleID TDA_5_191_HPLC SupervisorID thoma
104
157.02
147.54
142.85
137.45
135.67
129.99
123.67
121.15
120.20
119.00
117.98
115.89
77.16 CDCl3
71.69
66.76
25.95
18.21
f1 (ppm)

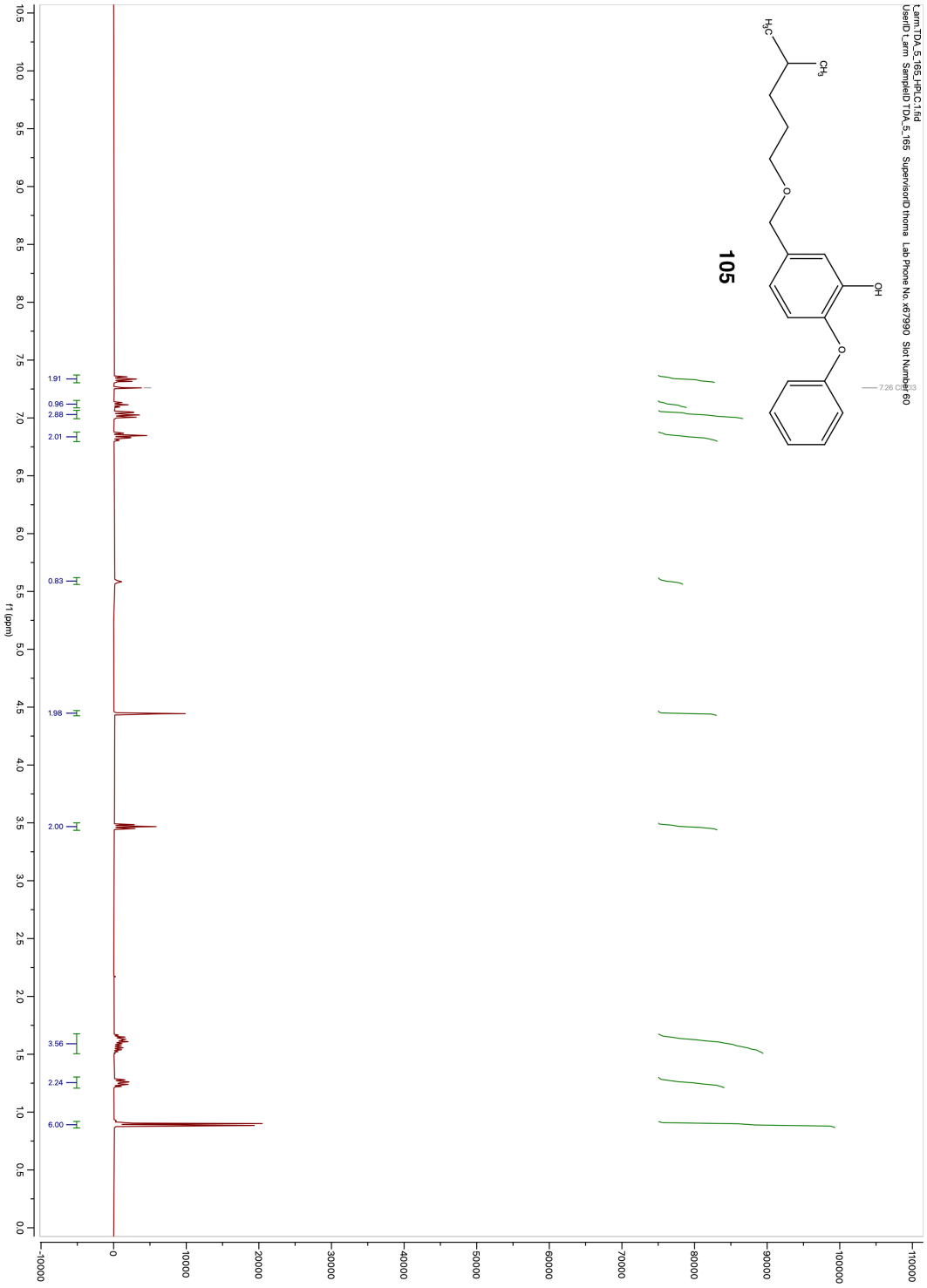
L:arm,TDA_5-165_HPLC-1.fid
UserID L:arm SampleID TDA_5-165 SupervisorID thoma Lab Phone No. x67990 Slot Number 60
105
OH
7.26 CHCl3
1.91
0.96
2.88
2.01
0.83
1.98
2.00
3.56
2.24
6.00
f1 (ppm)

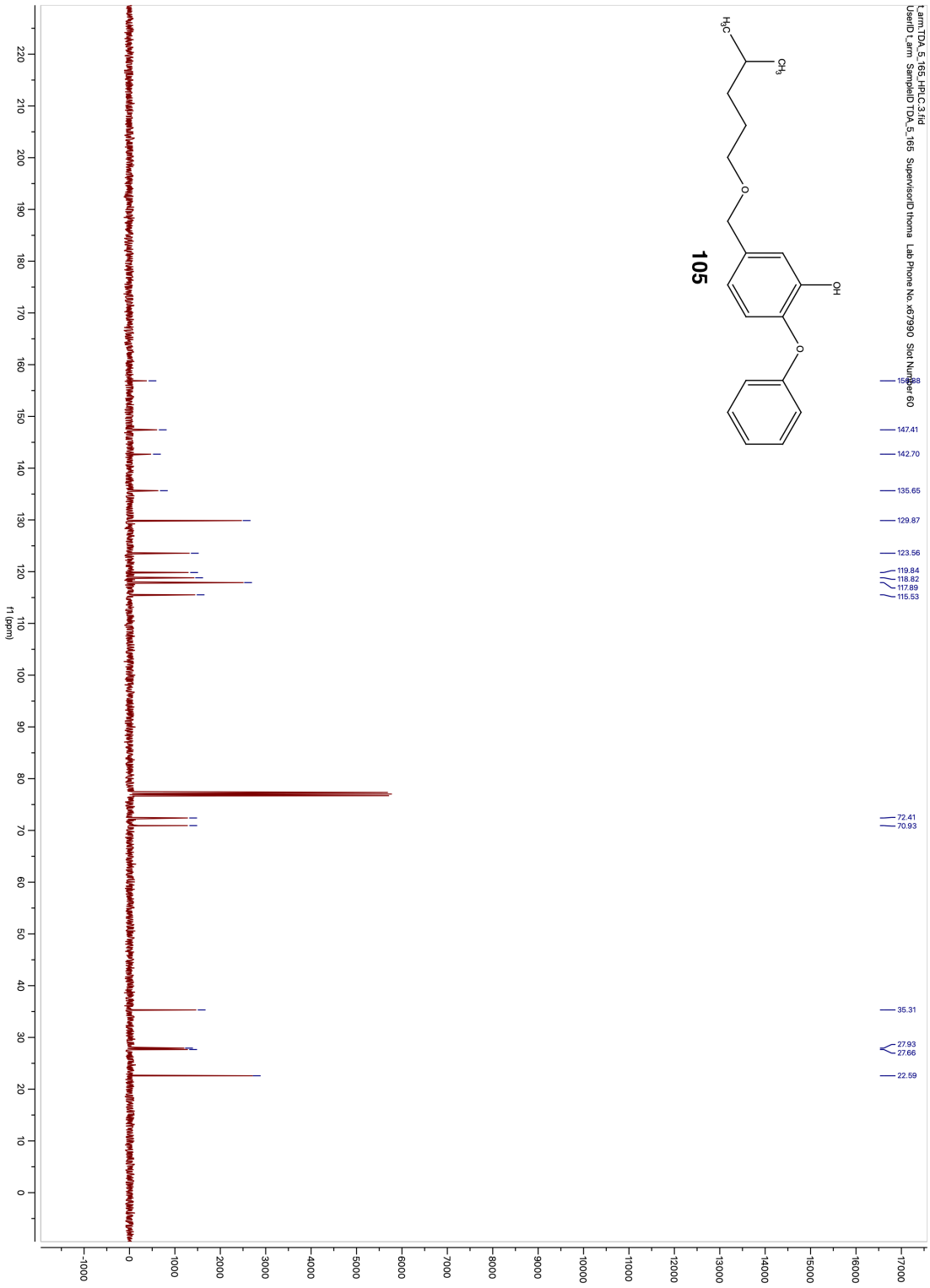
t_arm:TDA_5.165_HPLC.3.fid
UserID t_arm SampleID TDA_5.165 SupervisorID thoma Lab Phone No. x67990 Slot Number 60
105
OH
156.88
147.41
142.70
135.65
129.87
123.56
119.84
118.82
117.89
115.53
72.41
70.93
35.31
27.93
27.66
22.59
f1 (ppm)

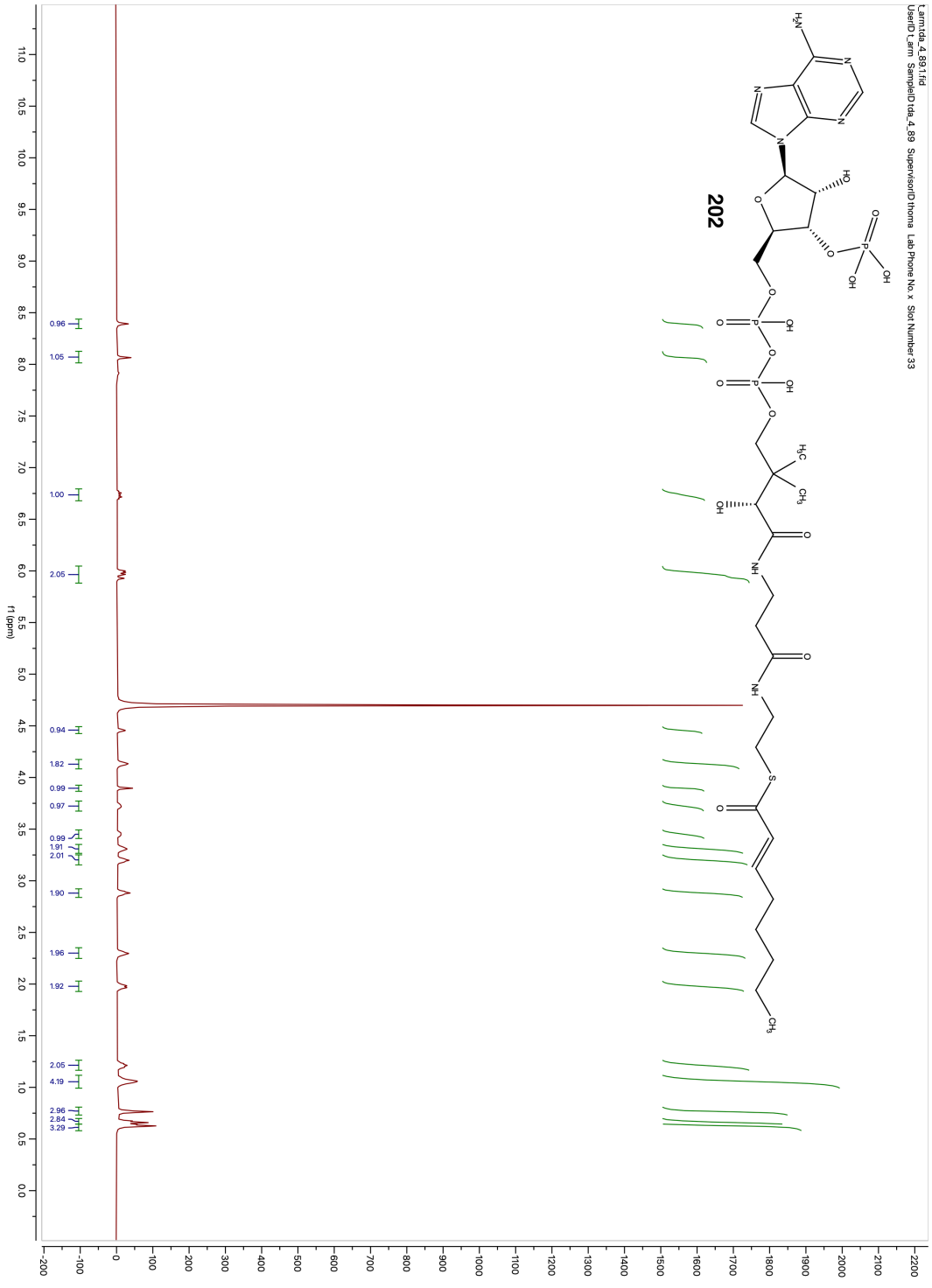
L:\arm\tda_4.89.1.fid
UserID:L_arm SampleID:tda_4.89 SupervisorID:thoma Lab Phone No.: x Slot Number:33
202
f1 (ppm)
0.96
1.05
1.00
2.05
0.94
1.82
0.99
0.97
0.99
1.91
2.01
1.90
1.96
1.92
2.05
4.19
2.96
2.84
3.29

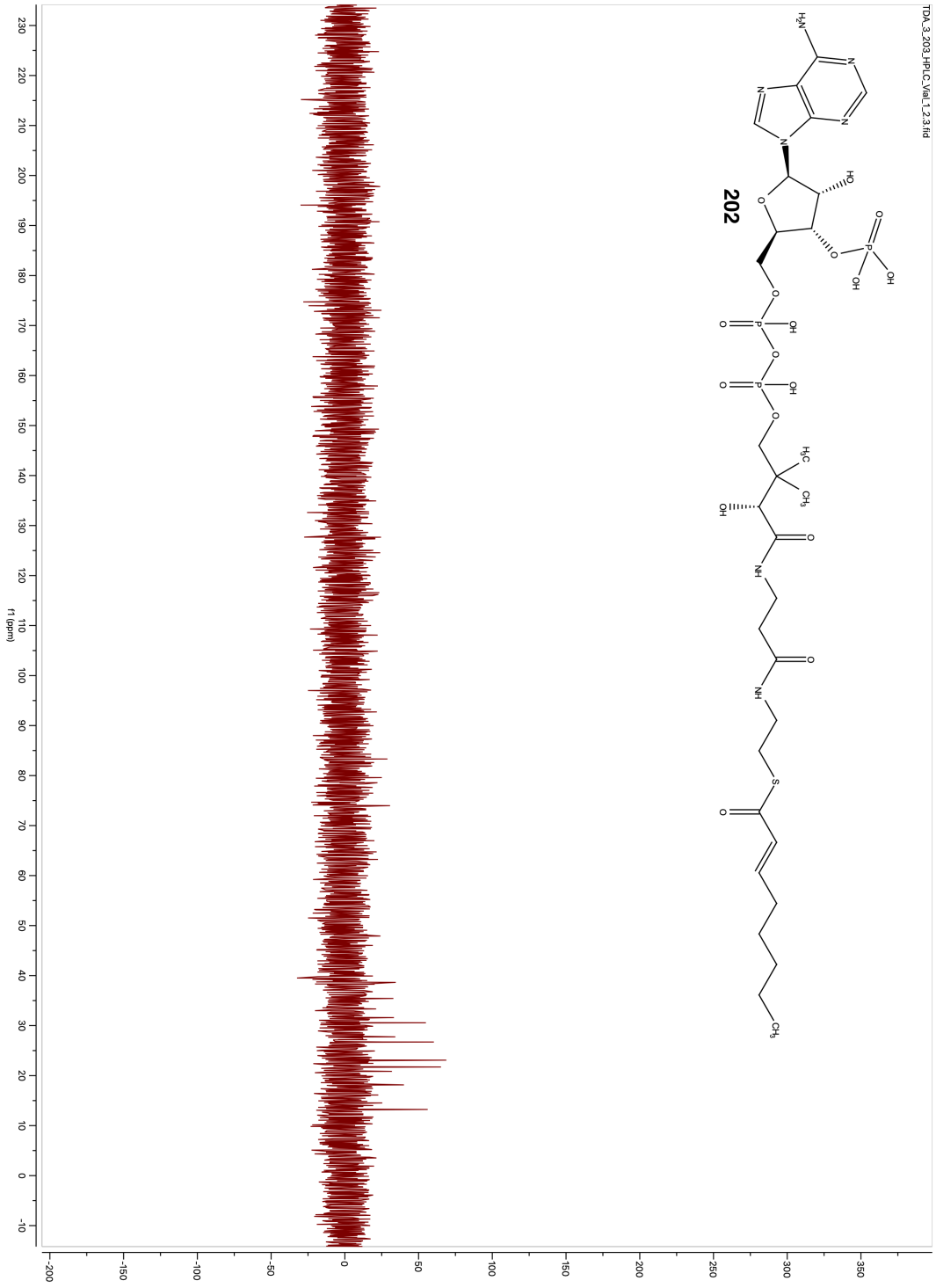
TDA_3_203_HPLC_Vial_1_2_3.fid
202
f1 (ppm)

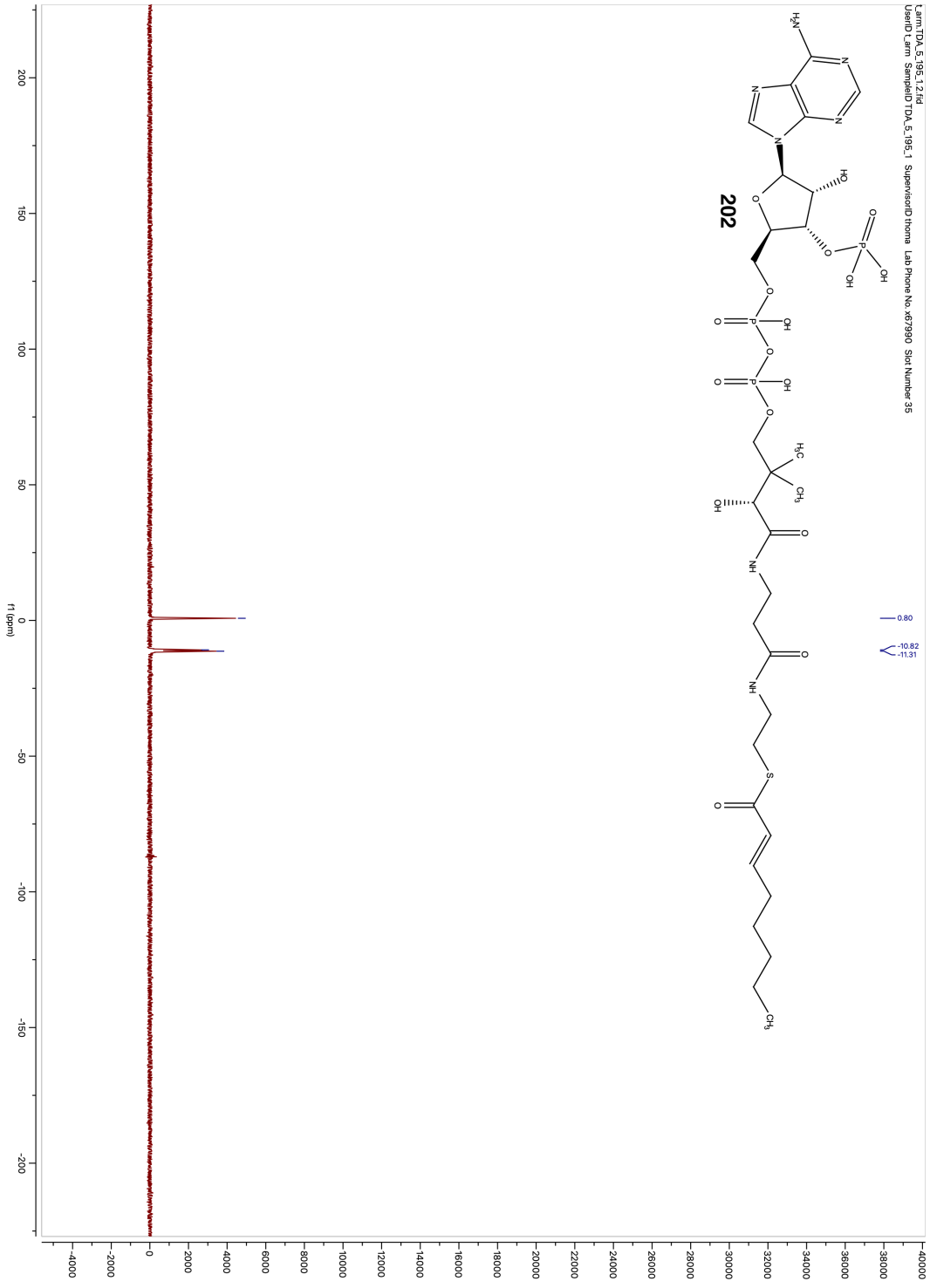
202
0.80
-10.82
-11.31
f1 (ppm)

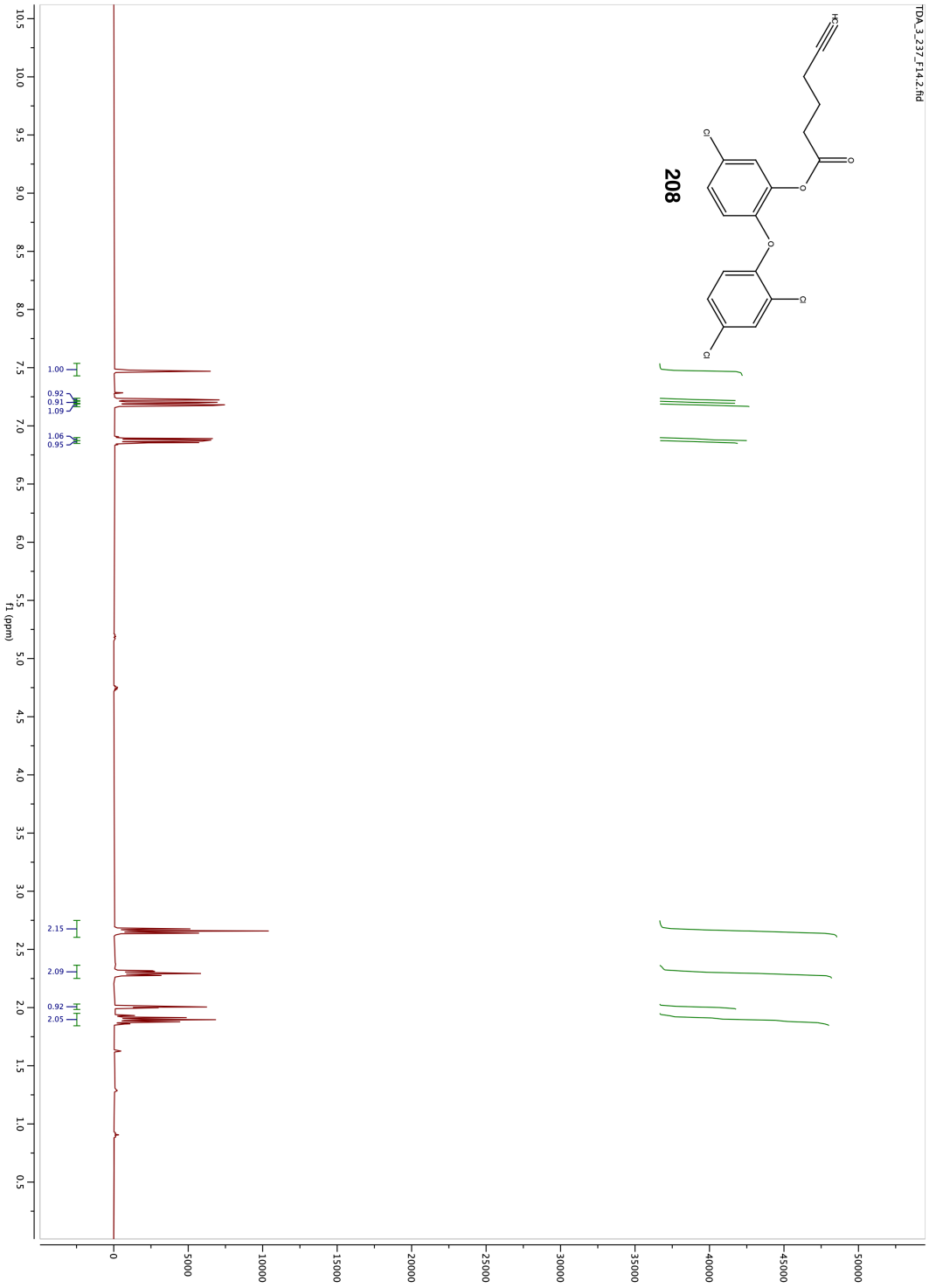
TDA_3_237_F14.2.fid
208
1.00
0.92
0.91
1.09
1.06
0.95
2.15
2.09
0.92
2.05
f1 (ppm)

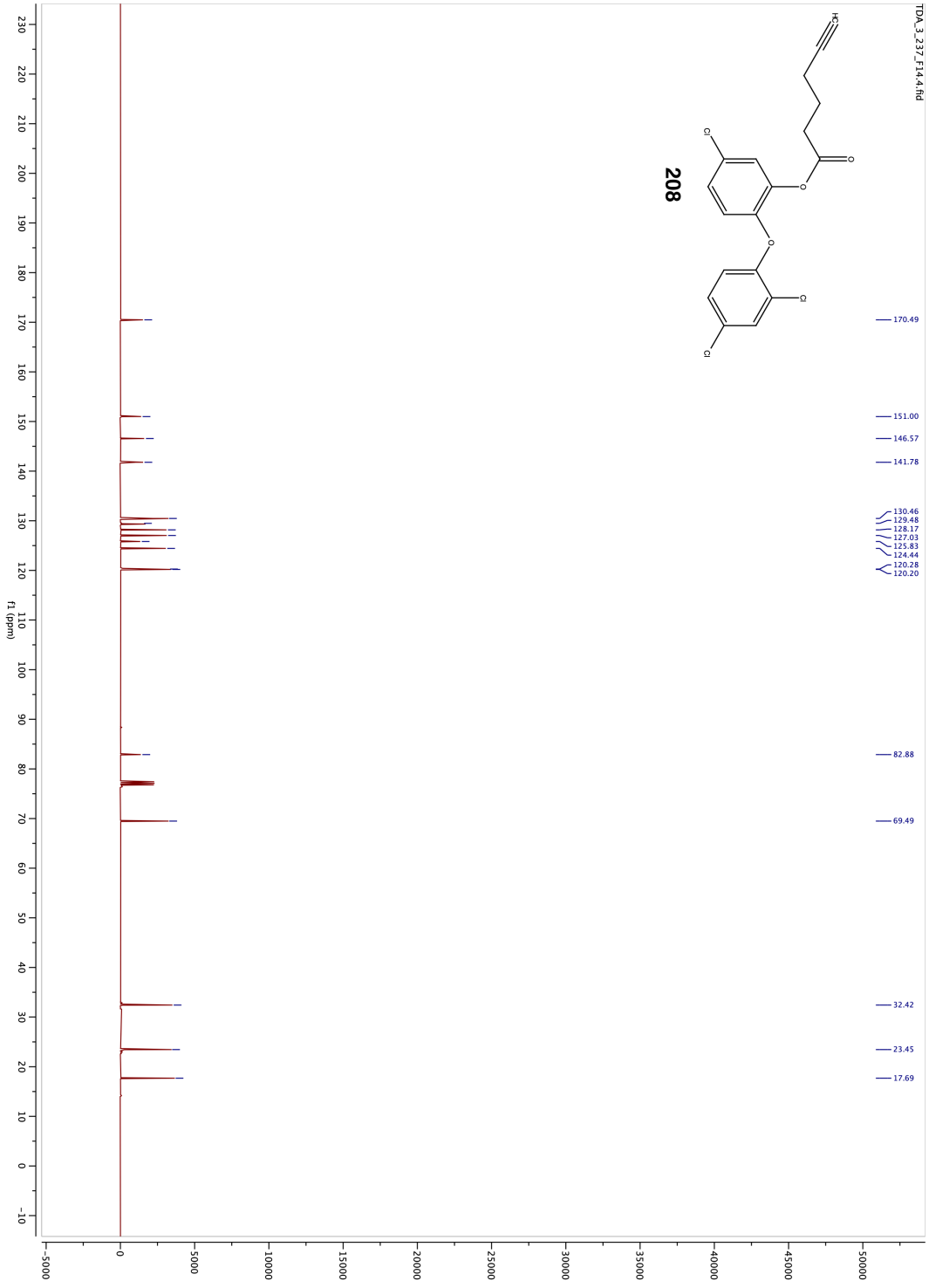
TDA_3_237_F14.4.fid
208
170.49
151.00
146.57
141.78
130.46
129.48
128.17
127.03
125.83
124.44
120.28
120.20
82.88
69.49
32.42
23.45
17.69
f1 (ppm)

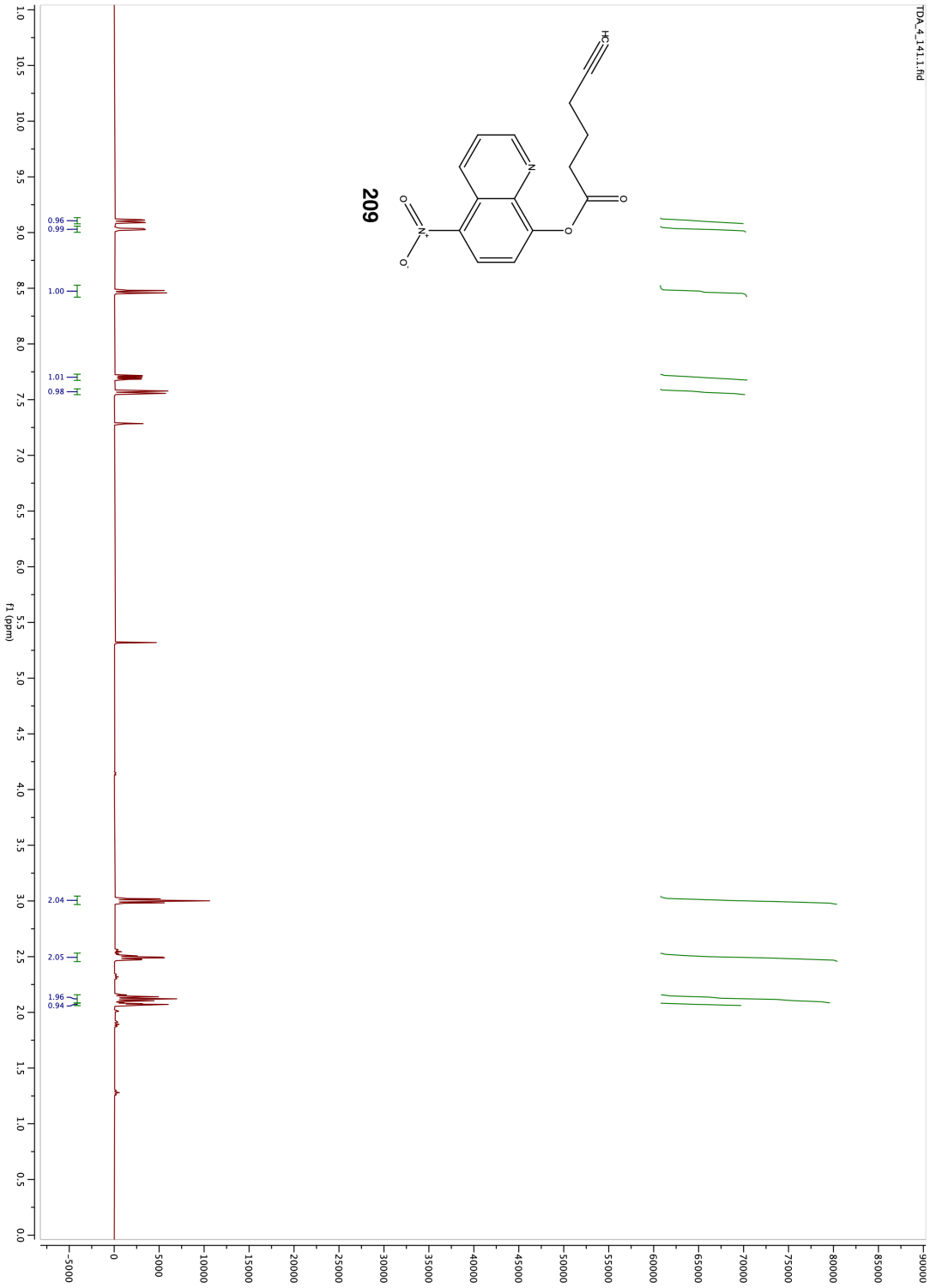
209
TDA_4_141.1.fid
f1 (ppm)
0.96
0.99
1.00
1.01
0.98
2.04
2.05
1.96
0.94

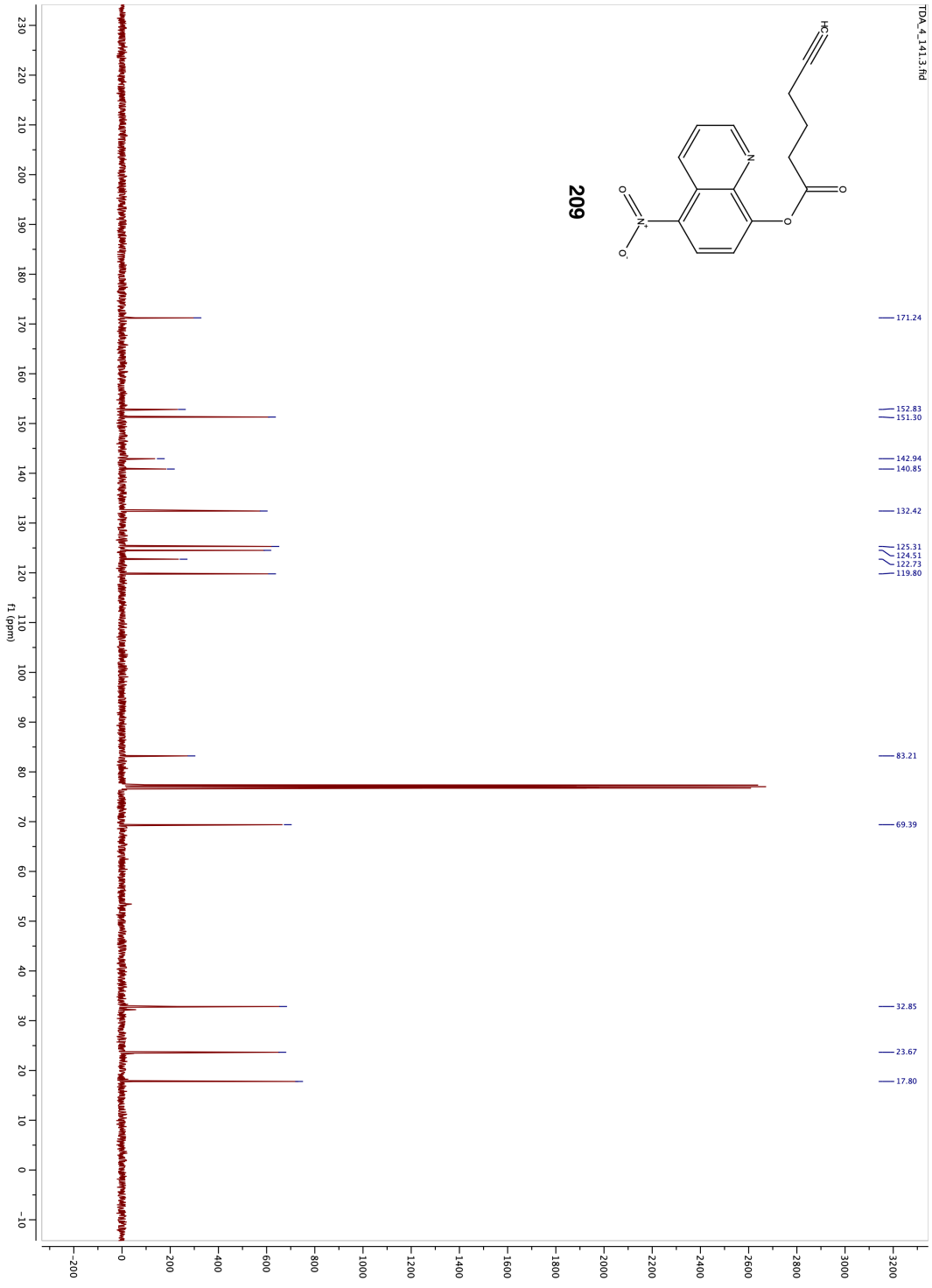
TDA_4_141.3.fid
209
171.24
152.83
151.30
142.94
140.85
132.42
125.31
124.51
122.73
119.80
83.21
69.39
32.85
23.67
17.80
f1 (ppm)

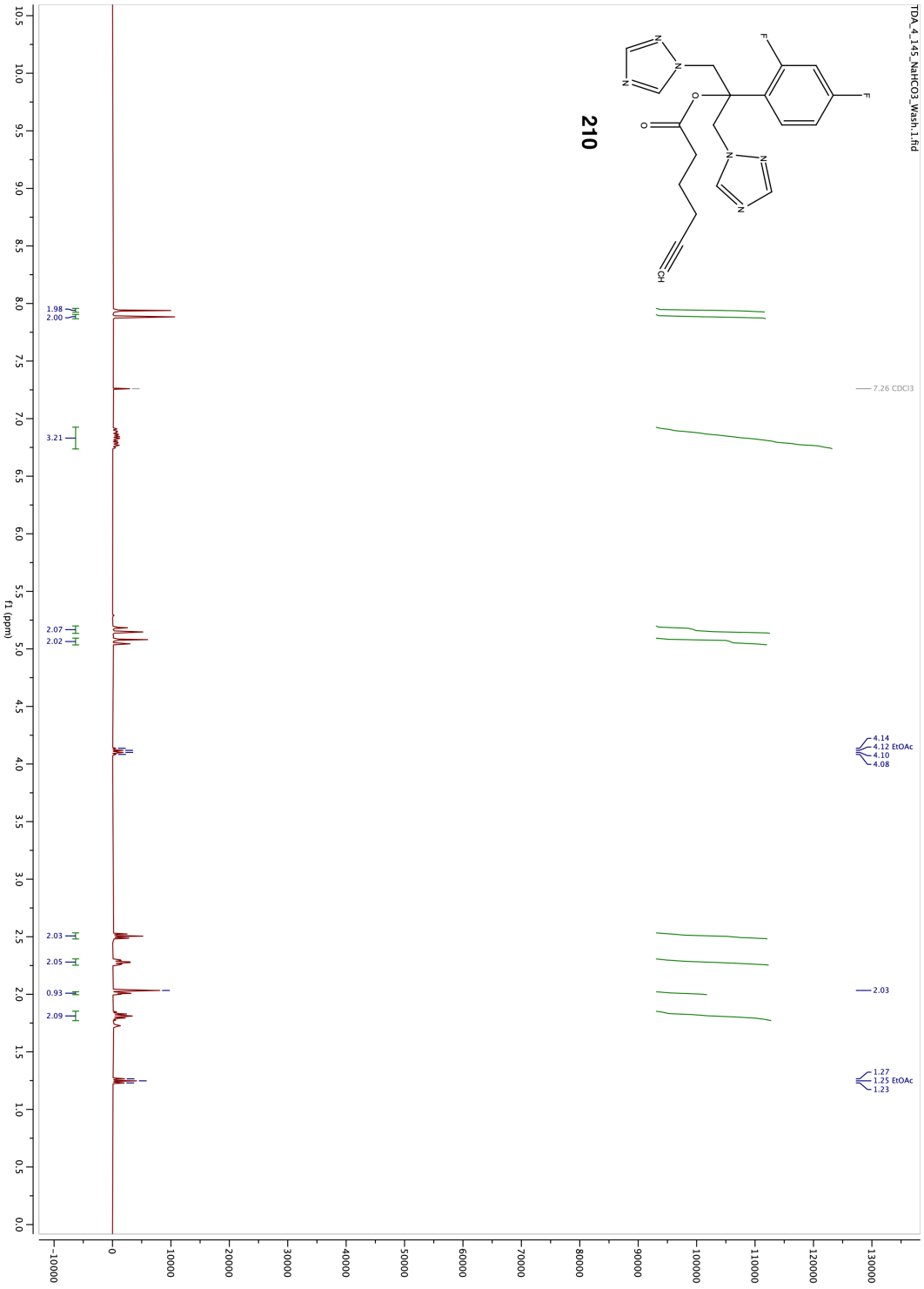
TDA_4_145_NaHCO3_Wash.1.fid
210
7.26 CDCl3
4.14
4.12 EtOAc
4.10
4.08
2.03
1.27
1.25 EtOAc
1.23
1.98
2.00
3.21
2.07
2.02
2.03
2.05
0.93
2.09
f1 (ppm)

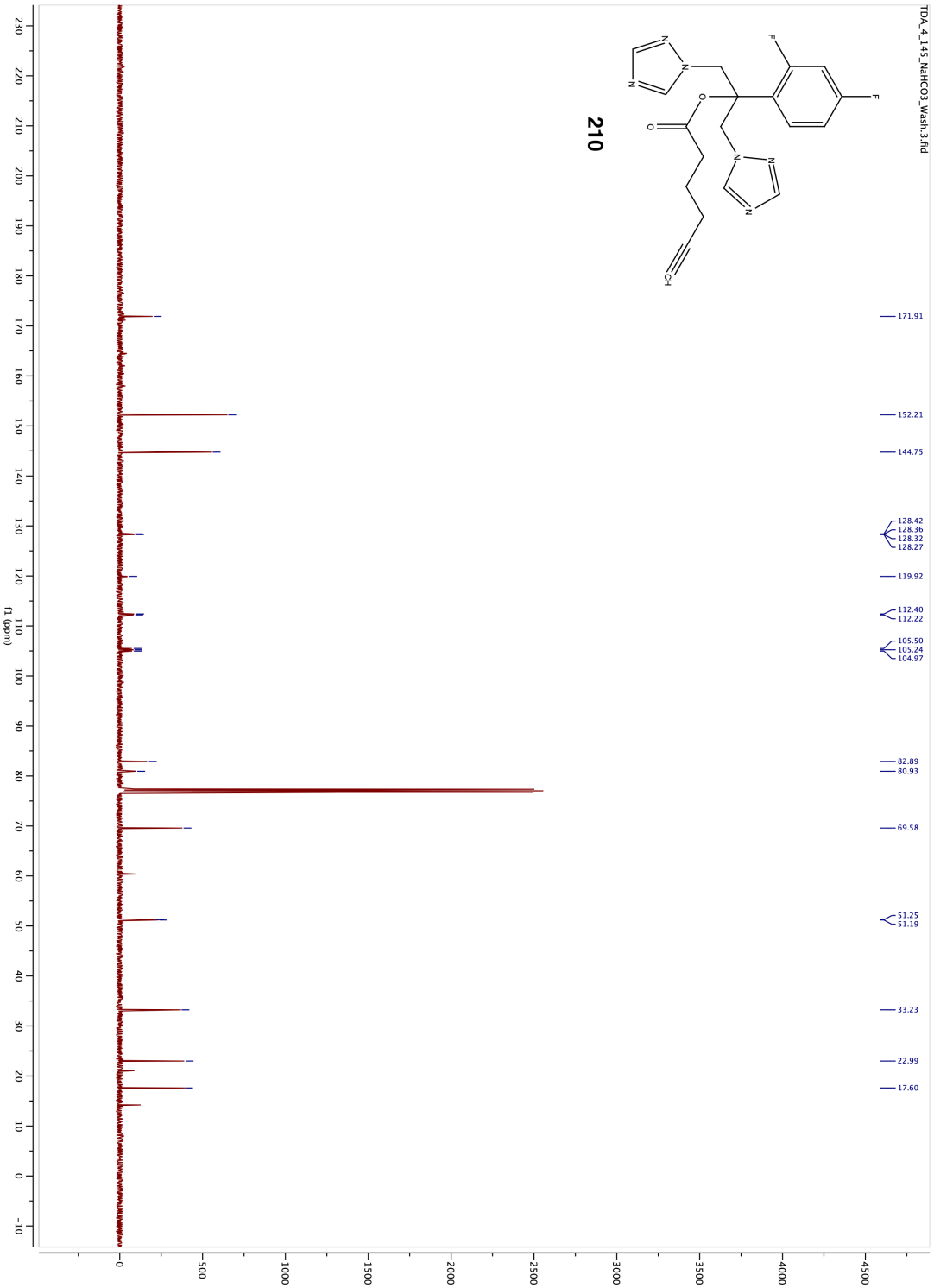
TDA_4_145_NaHCO3_Wash.3.fid
210
171.91
152.21
144.75
128.42
128.36
128.32
128.27
119.92
112.40
112.22
105.50
105.24
104.97
82.89
80.93
69.58
51.25
51.19
33.23
22.99
17.60
f1 (ppm)

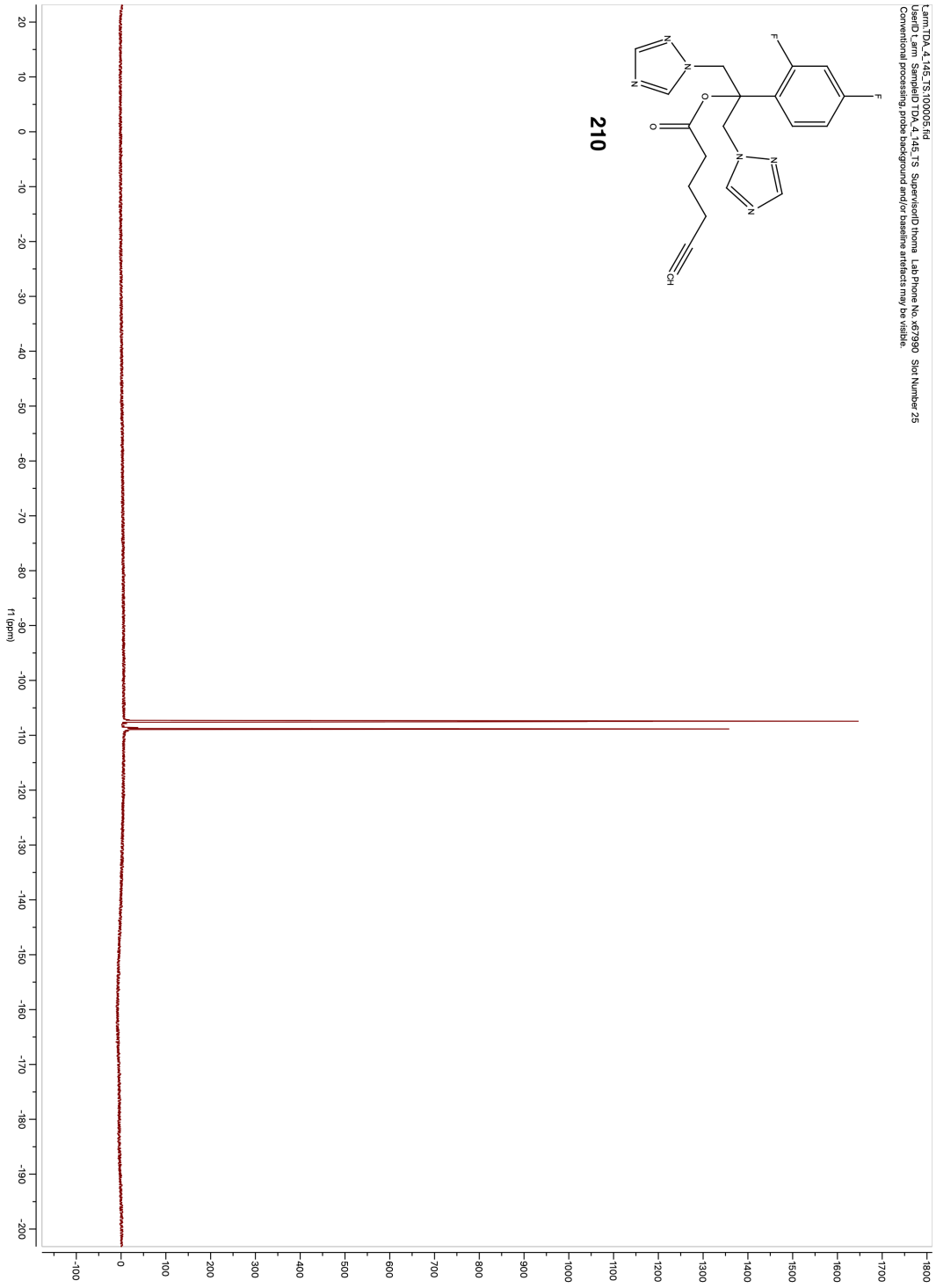
210
F
F
O
O
N
N
N
N
N
CH
f1 (ppm)

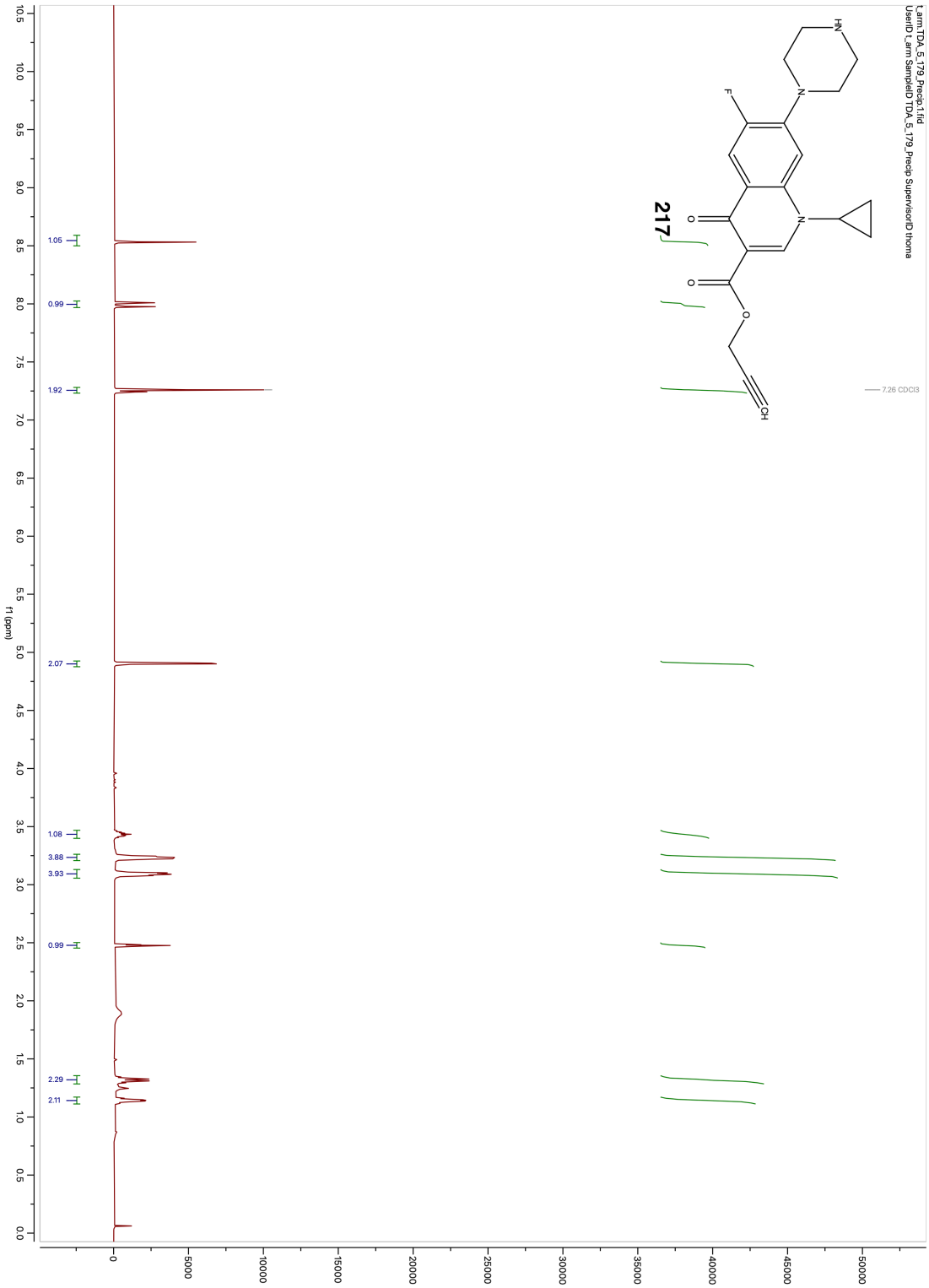
t_arm:TDA_5_179_Precip.1.fid
UserID t_arm SampleID TDA_5_179_Precip SupervisorID thoma
217
HN
F
N
O
O
O
N
CH
7.26 CDCl3
f1 (ppm)
1.05
0.99
1.92
2.07
1.08
3.88
3.93
0.99
2.29
2.11

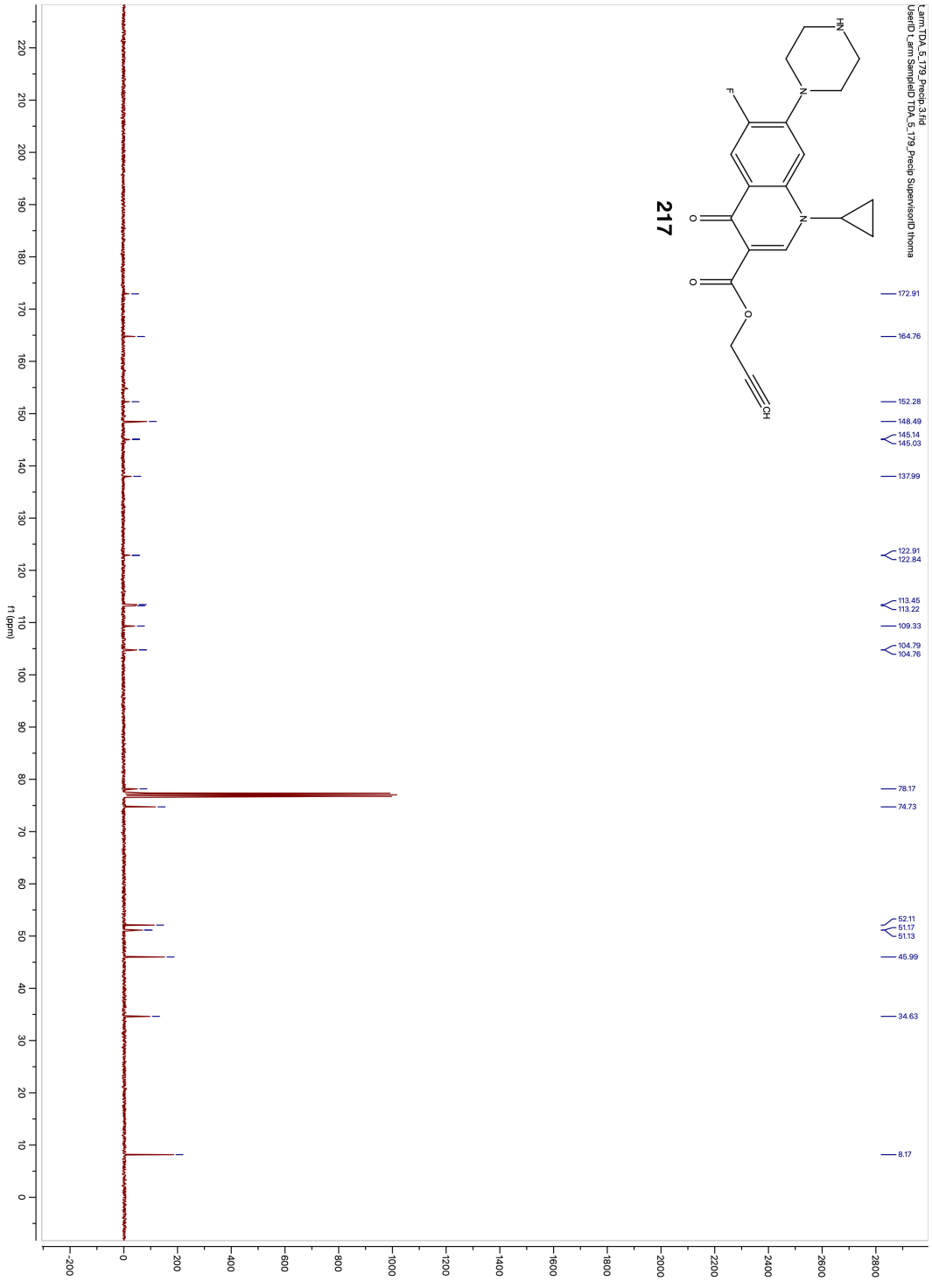
217
F
HN
N
O
O
O
N
CH
172.91
164.76
152.28
148.49
145.14
145.03
137.99
122.91
122.84
113.45
113.22
109.33
104.79
104.76
78.17
74.73
52.11
51.17
51.13
45.99
34.63
8.17
f1 (ppm)

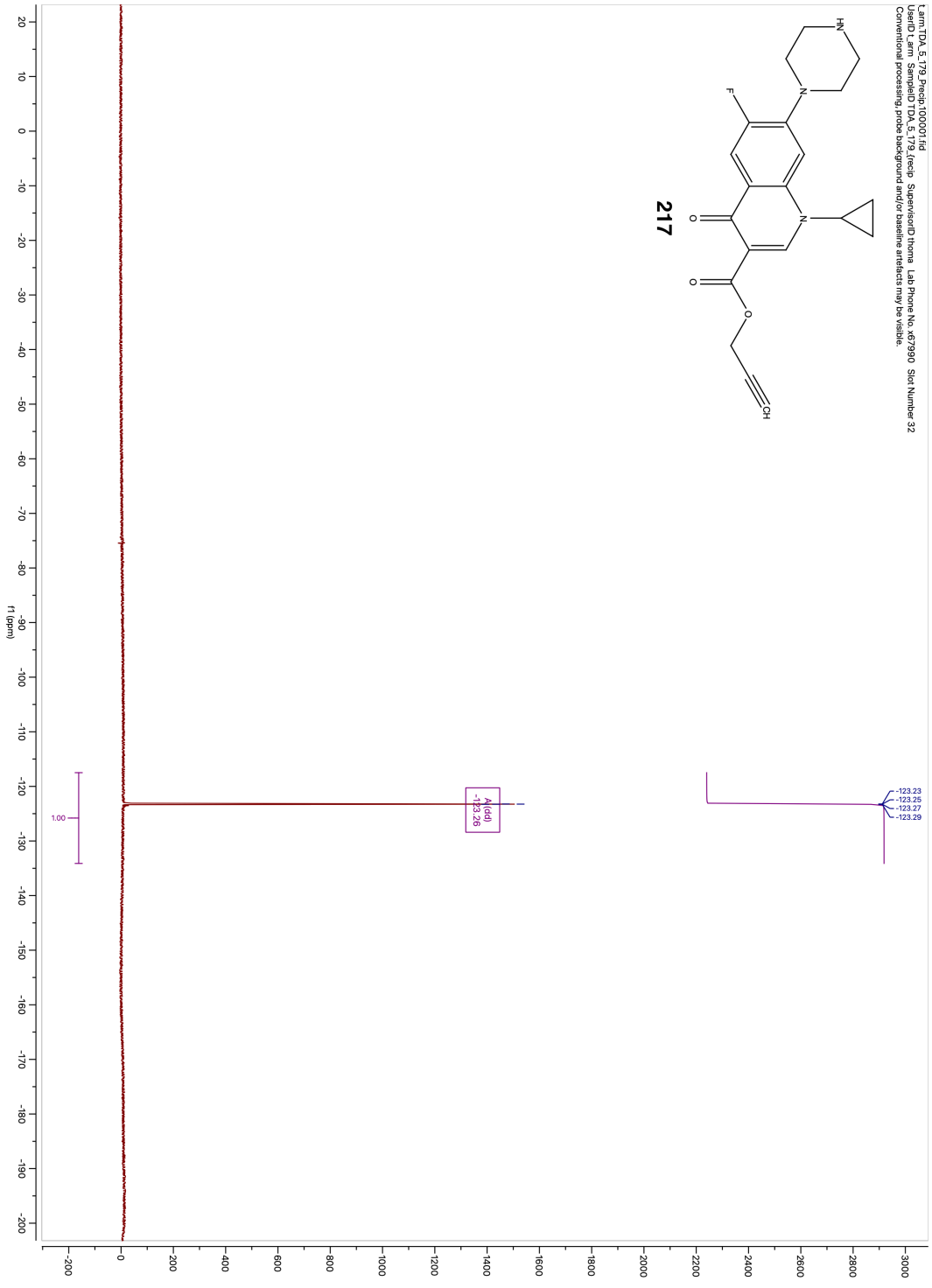
L.arm.TDA_5_179_Precip.10000.1.fid
UserID L.arm SampleID TDA_5_179_(recip SupervisorID thoma Lab Phone No. x67990 Slot Number 32
Conventional processing, probe background and/or baseline artefacts may be visible.
217
HN
N
F
O
N
O
O
CH
1.00
A (dd)
-123.26
-123.23
-123.25
-123.27
-123.29
f1 (ppm)

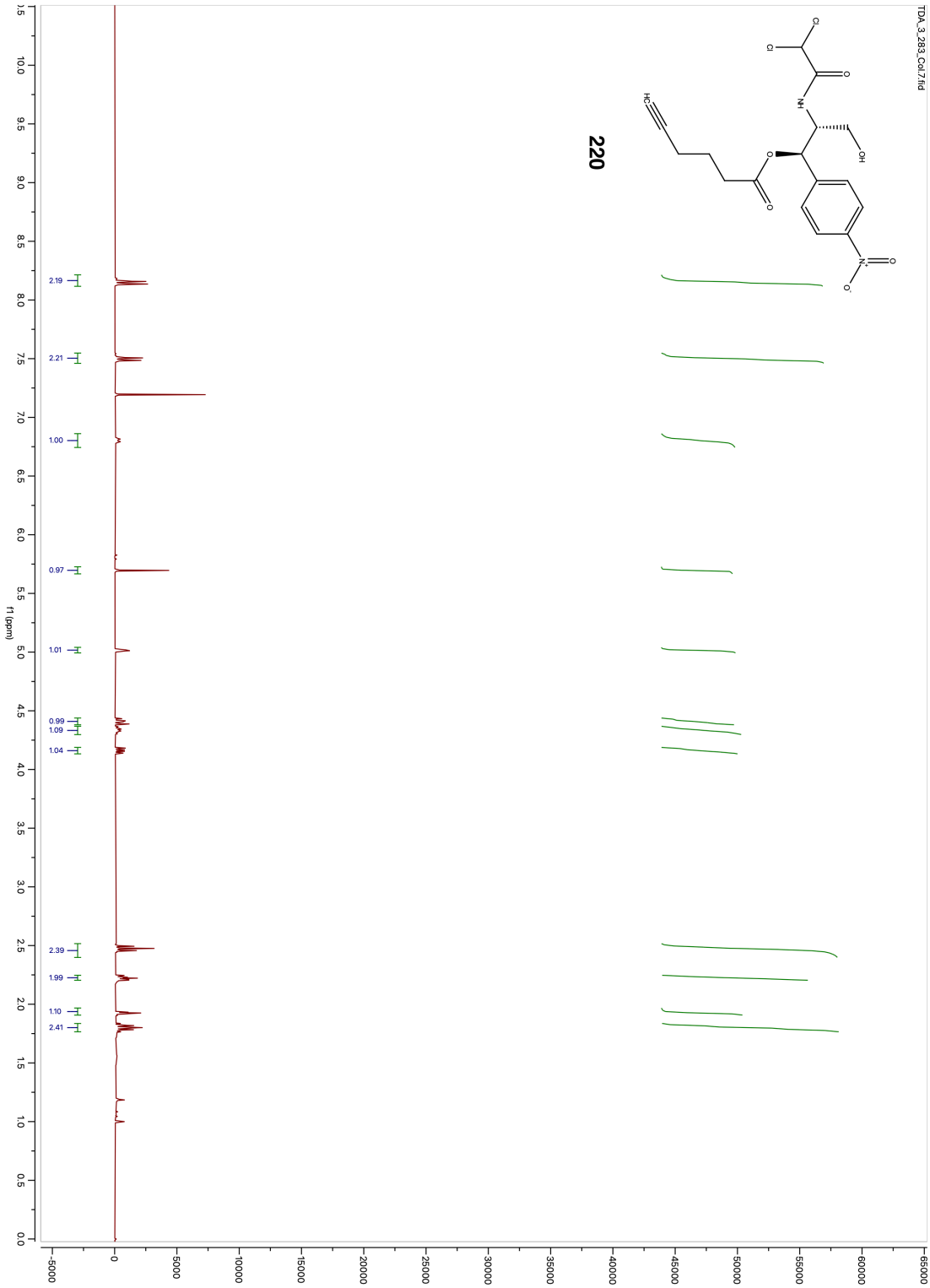
220
TDA_3_283_Col7.fid
f1 (ppm)
2.19
2.21
1.00
0.97
1.01
0.99
1.09
1.04
2.39
1.99
1.10
2.41

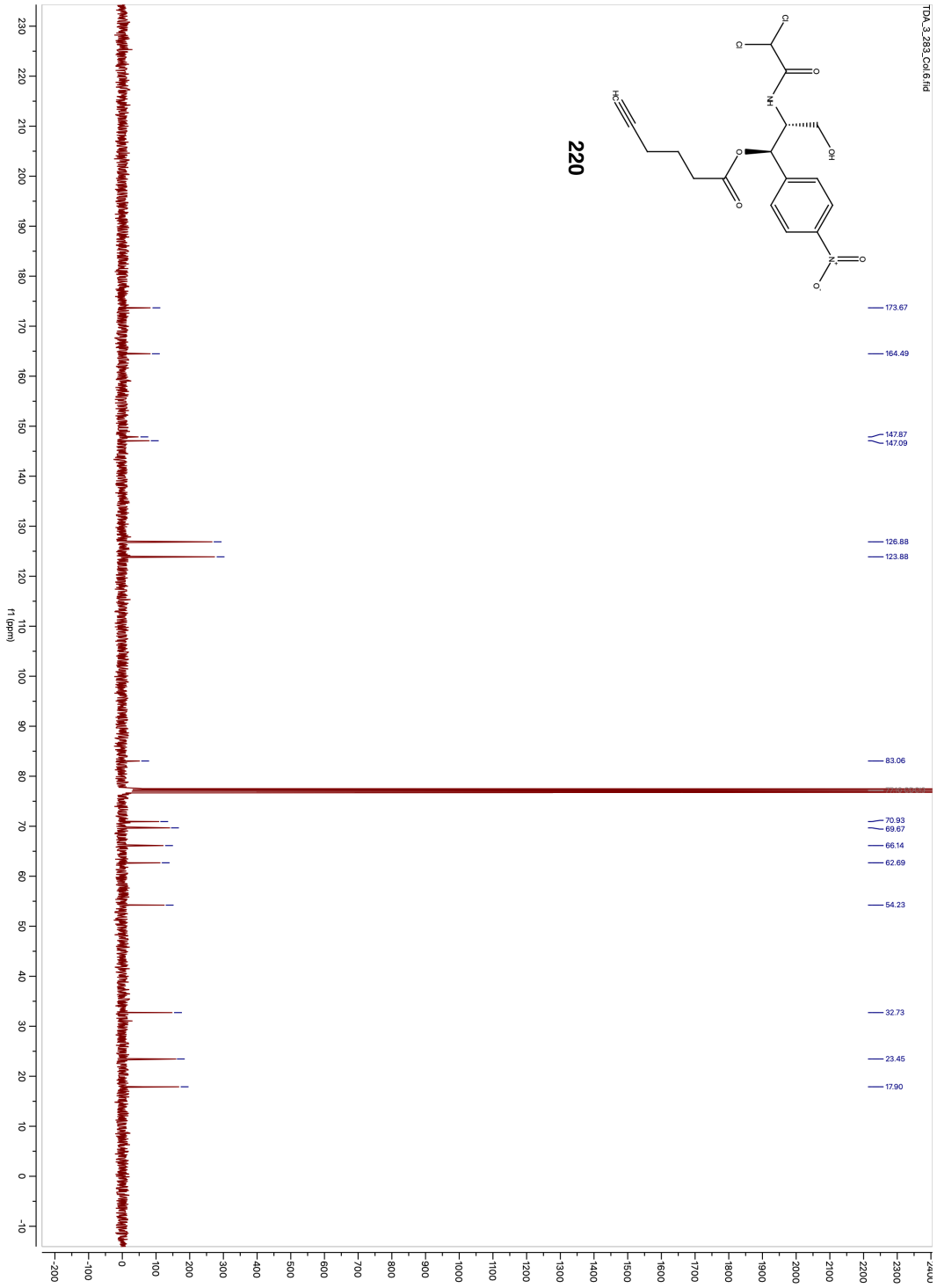
TDA_3_283_Col 6.fid
220
173.67
164.49
147.87
147.09
126.88
123.88
83.06
70.93
69.67
66.14
62.69
54.23
32.73
23.45
17.90
f1 (ppm)

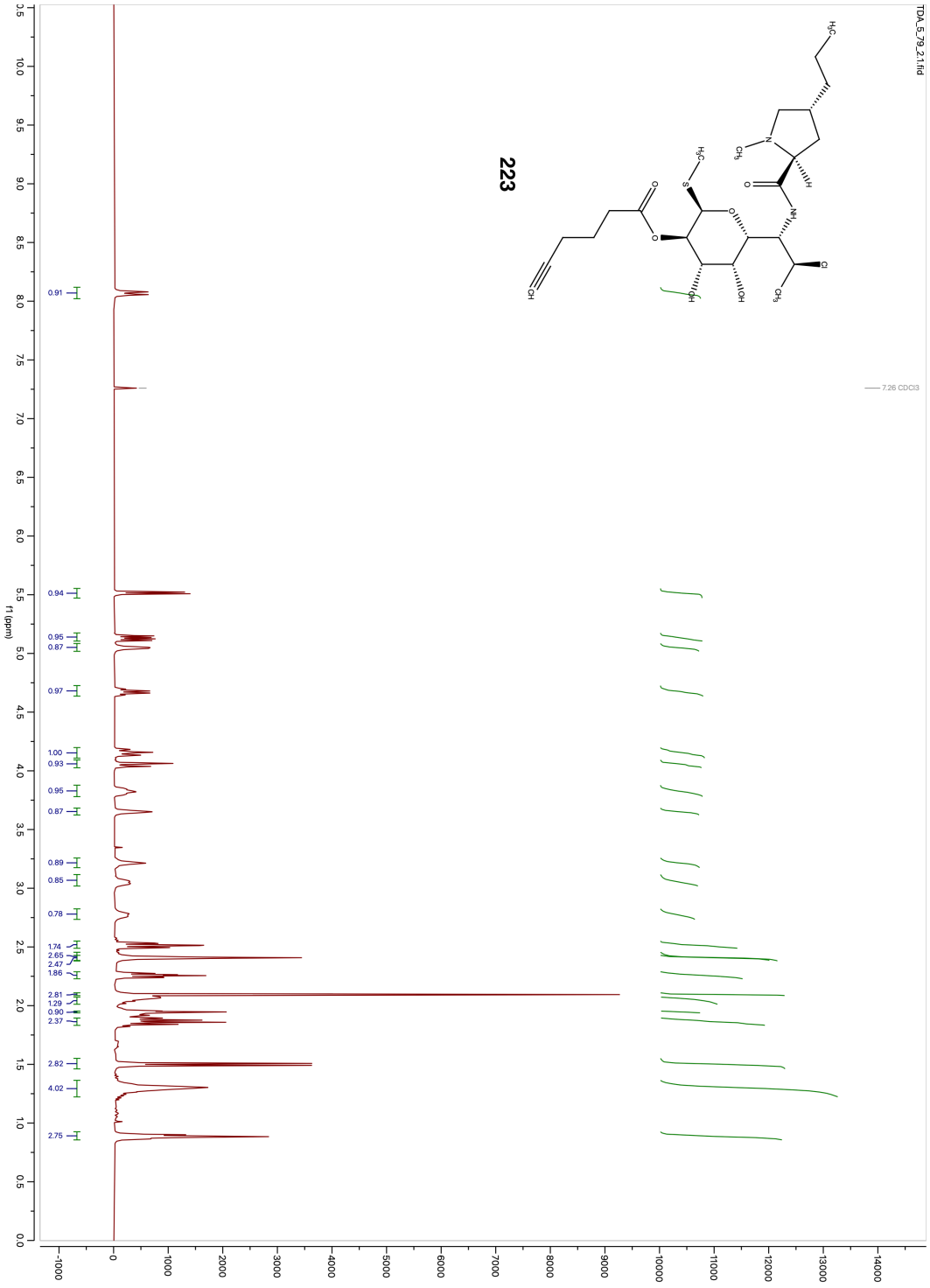
223
TDA_5_79_2.1.fid
7.26 CDCl3
f1 (ppm)
0.91
0.94
0.95
0.87
0.97
1.00
0.93
0.95
0.87
0.89
0.85
0.78
1.74
2.65
2.47
1.86
2.81
1.29
0.90
2.37
2.82
4.02
2.75

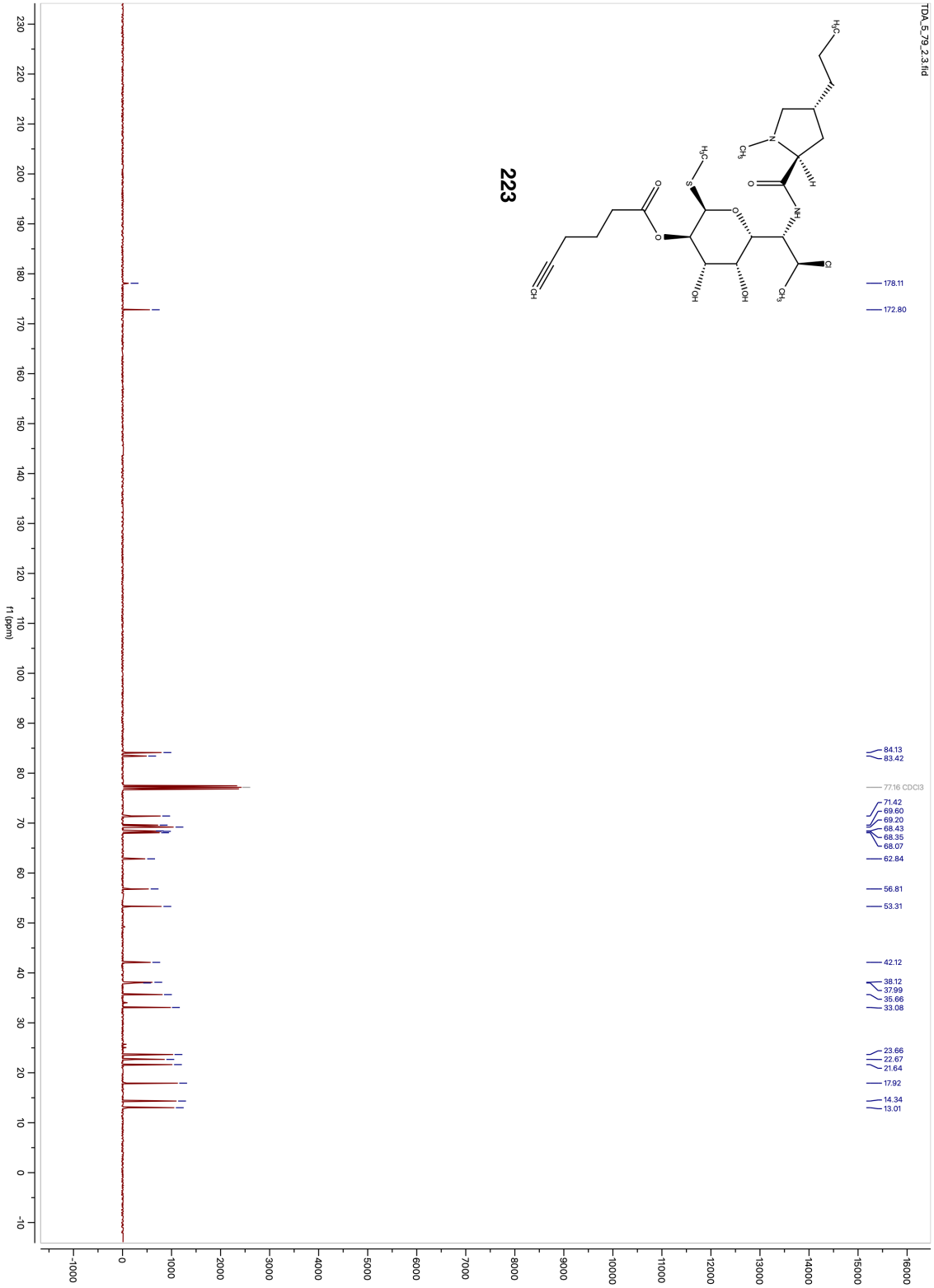
TDA_5_79_2_3.fid
223
178.11
172.80
84.13
83.42
77.16 CDCl3
71.42
69.60
69.20
68.43
68.35
68.07
62.84
56.81
53.31
42.12
38.12
37.99
35.66
33.08
23.66
22.67
21.64
17.92
14.34
13.01
f1 (ppm)

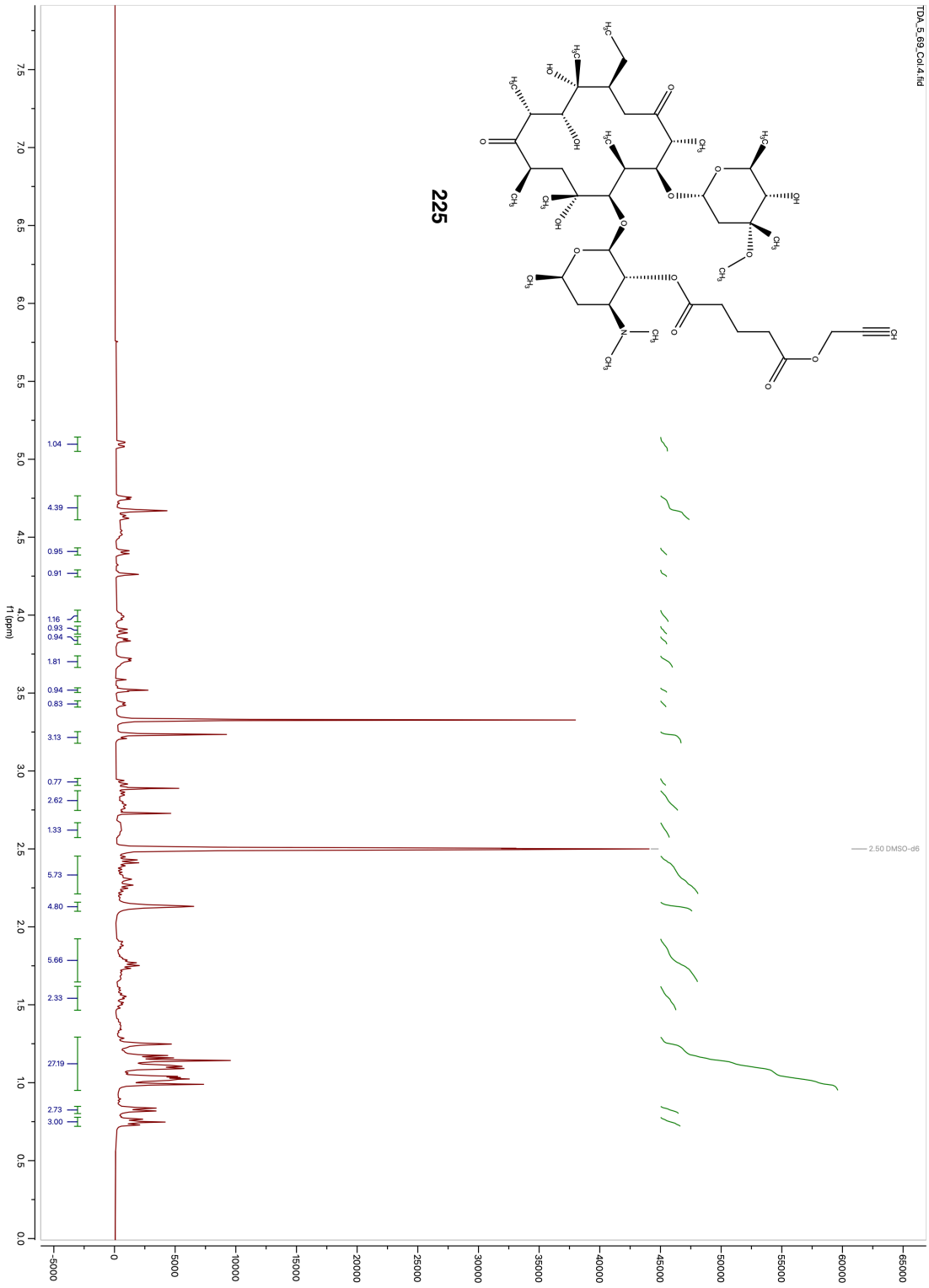
TDA_5_69_Col.4.fid
225
2.50 DMSO-d6
f1 (ppm)
1.04
4.39
0.95
0.91
1.16
0.93
0.94
1.81
0.94
0.83
3.13
0.77
2.62
1.33
5.73
4.80
5.66
2.33
27.19
2.73
3.00

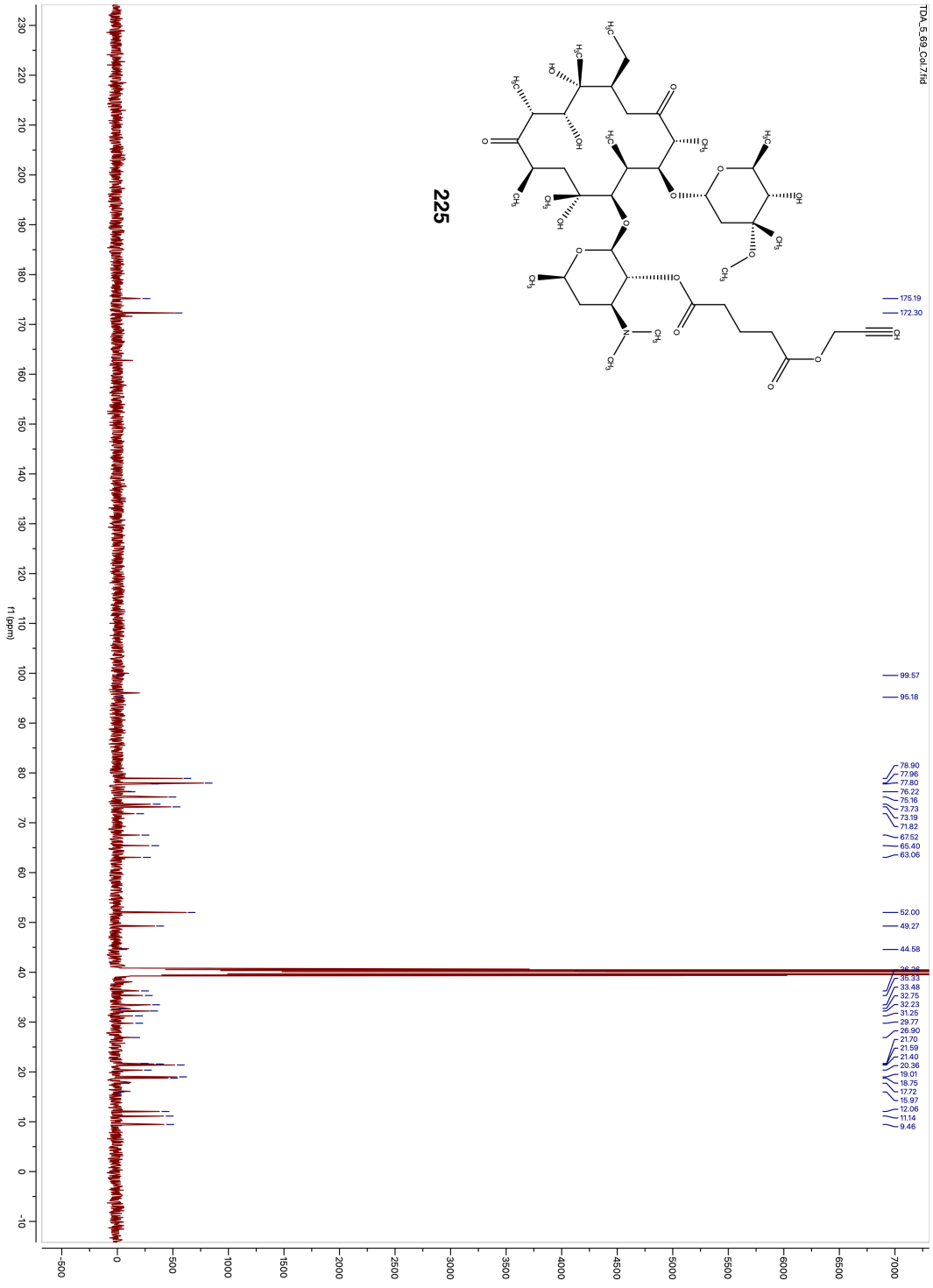
225
TDA_5_69_Col_7.fid
f1 (ppm)
175.19
172.30
99.57
95.18
78.90
77.96
77.80
76.22
75.16
73.73
73.19
71.82
67.52
65.40
63.06
52.00
49.27
44.58
38.33
33.48
32.75
32.23
31.25
29.77
26.90
21.70
21.59
21.40
20.36
19.01
18.75
17.72
15.97
12.06
11.14
9.46

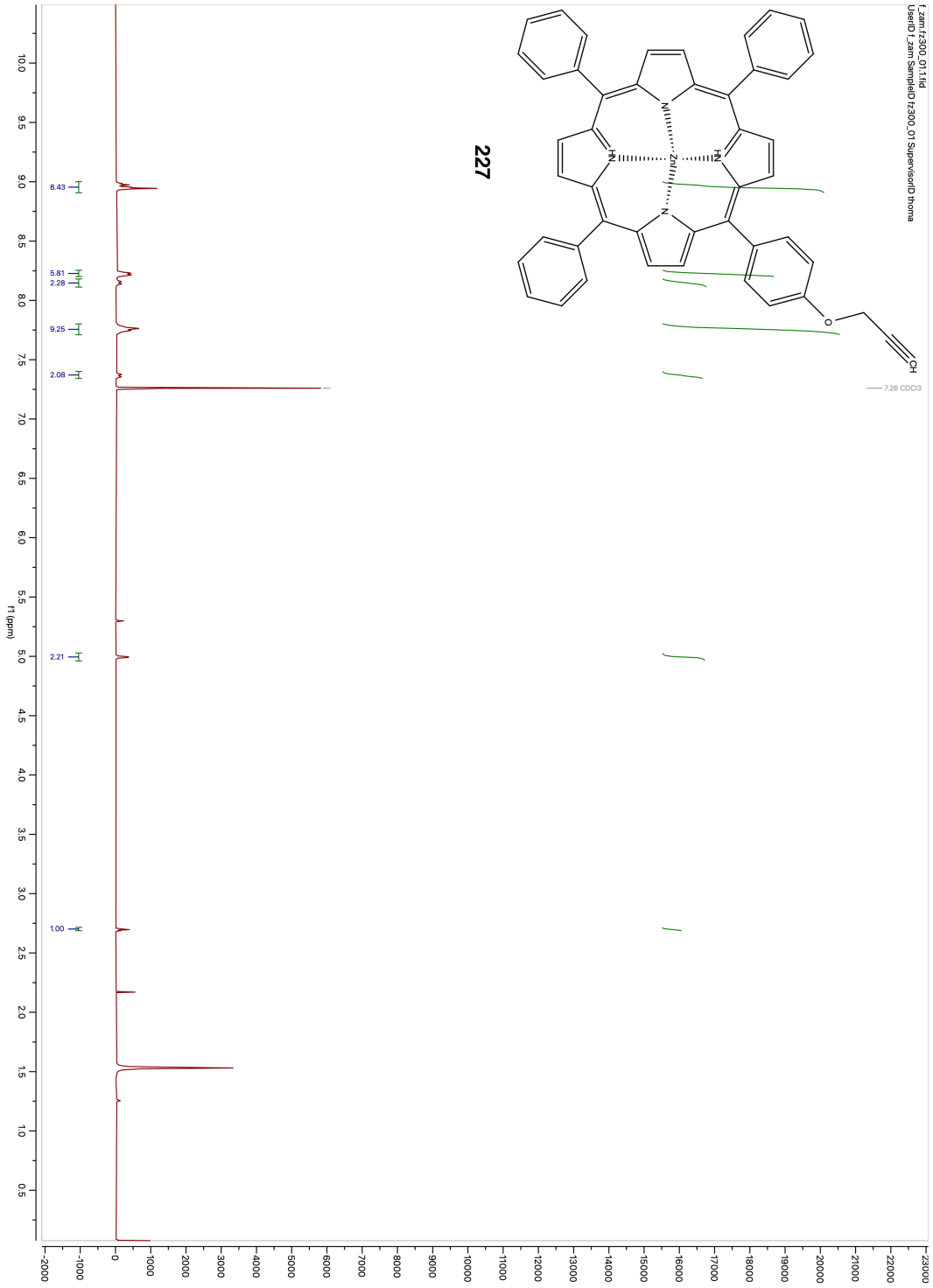
f_zam.fz300_01.1.fid
UserID f_zam SampleID fz300_01 SupervisorID thoma
227
N
Zn
HN
NH
O
CH
7.26 CDCl3
8.43
5.81
2.28
9.25
2.08
2.21
1.00
f1 (ppm)

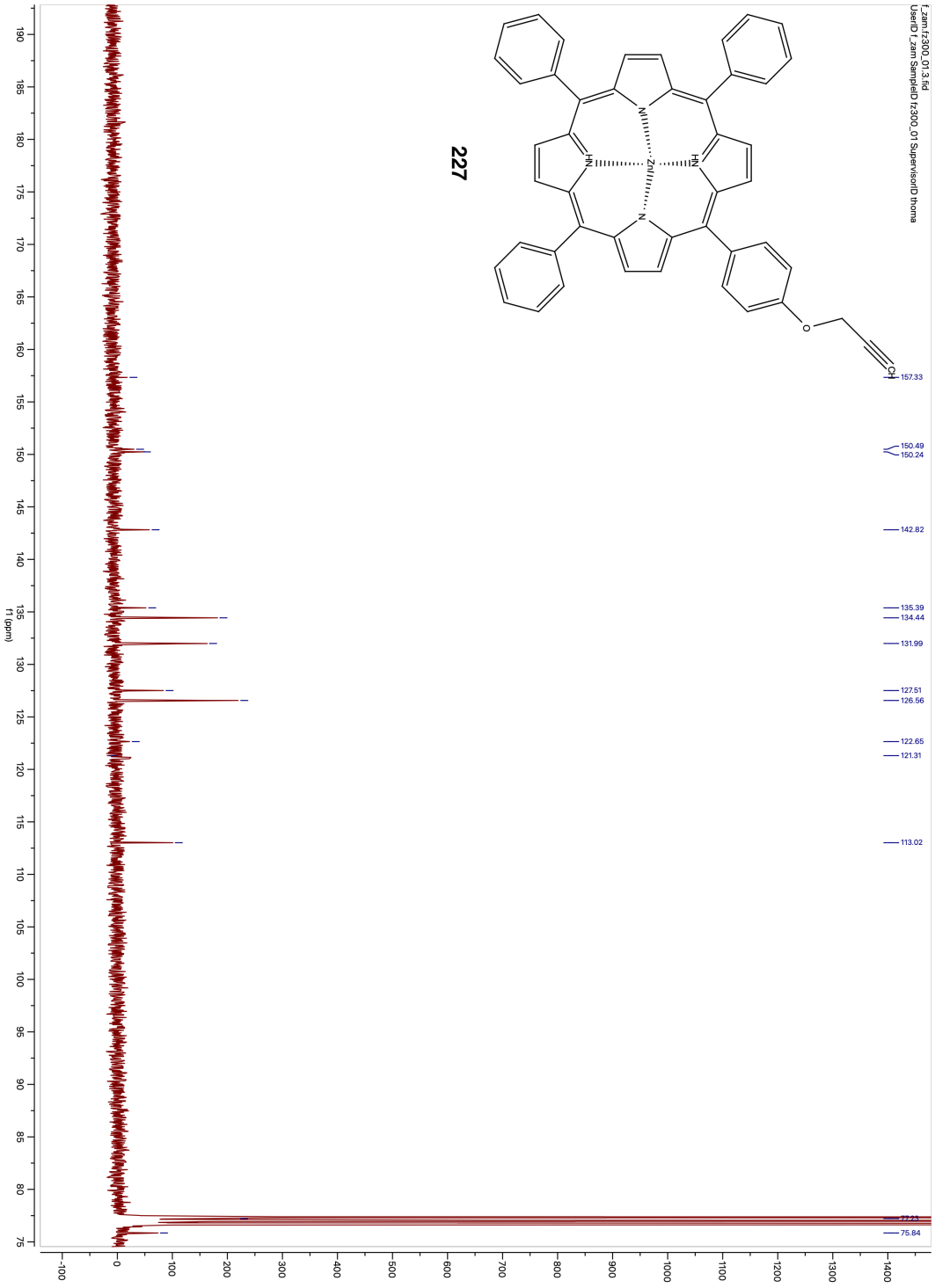
227
f_zam.fz300_01.3.fid
UserID f_zam SampleID fz300_01 SupervisorID thoma
157.33
150.49
150.24
142.82
135.39
134.44
131.99
127.51
126.56
122.65
121.31
113.02
77.23
75.84
f1 (ppm)

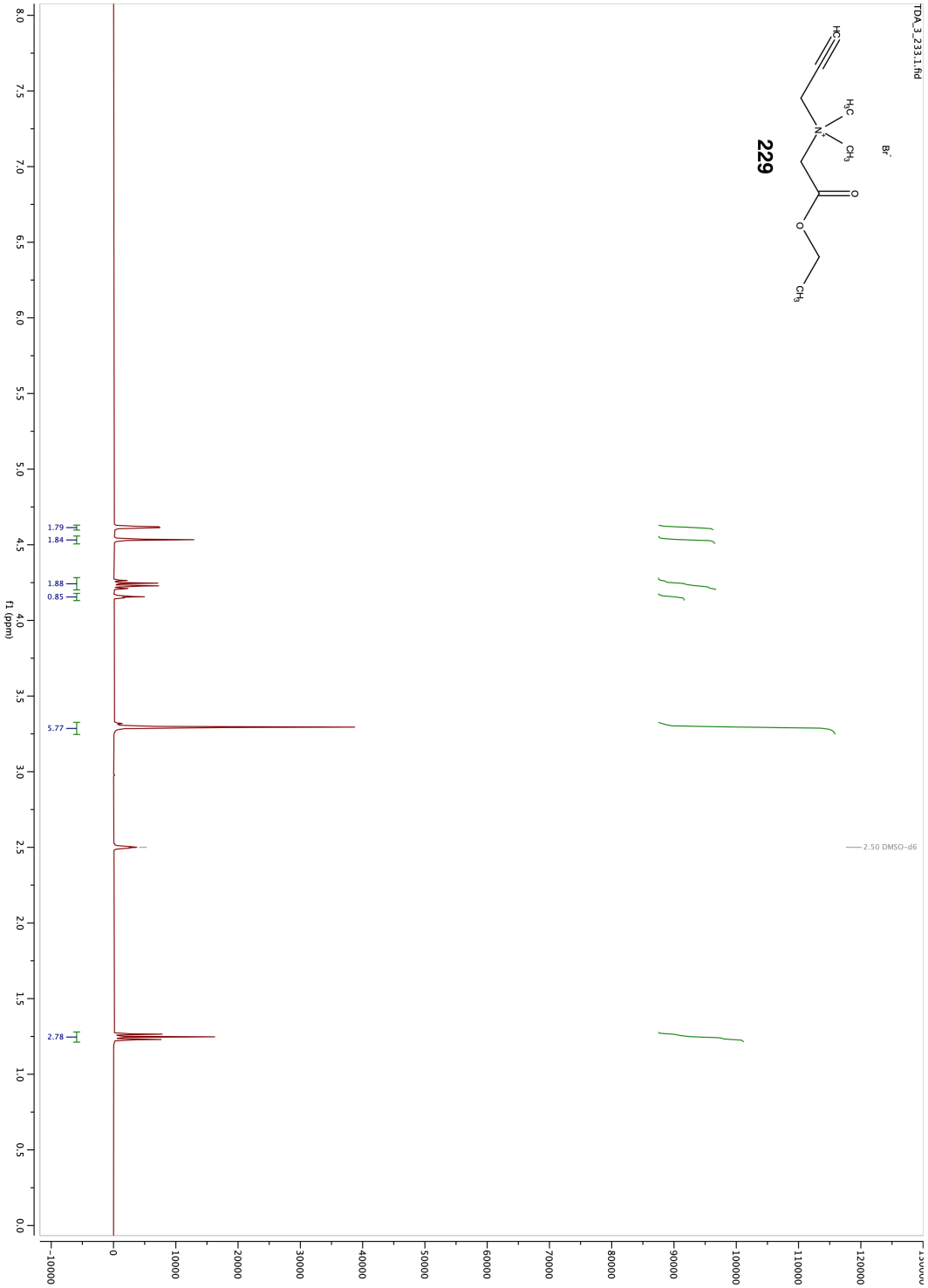
TDA_3_233.1.fid
229
Br⁻
2.50 DMSO-d6
1.79
1.84
1.88
0.85
5.77
2.78
f1 (ppm)

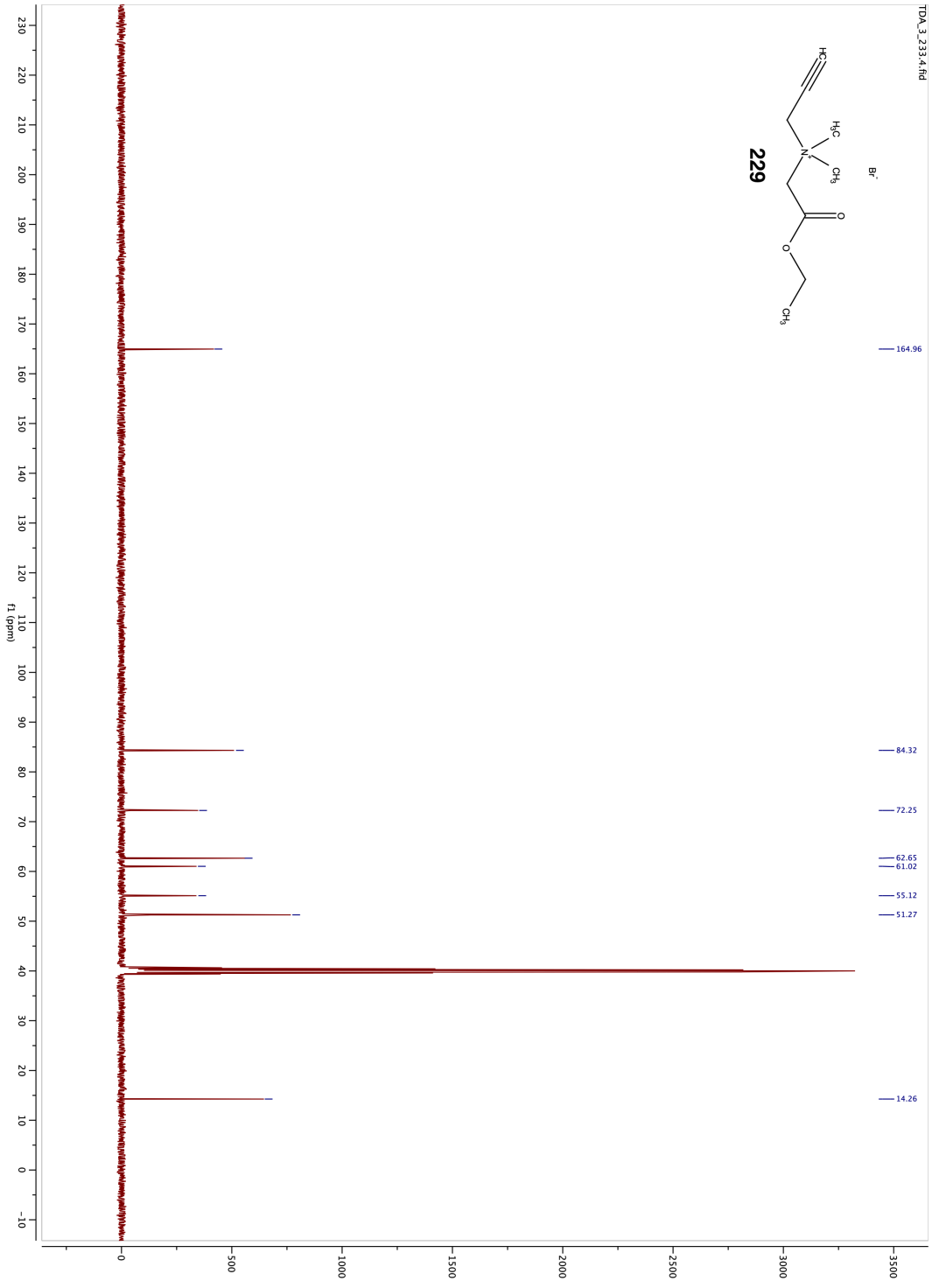
TDA_3_233.4.fid
229
Br⁻
164.96
84.32
72.25
62.65
61.02
55.12
51.27
14.26
f1 (ppm)

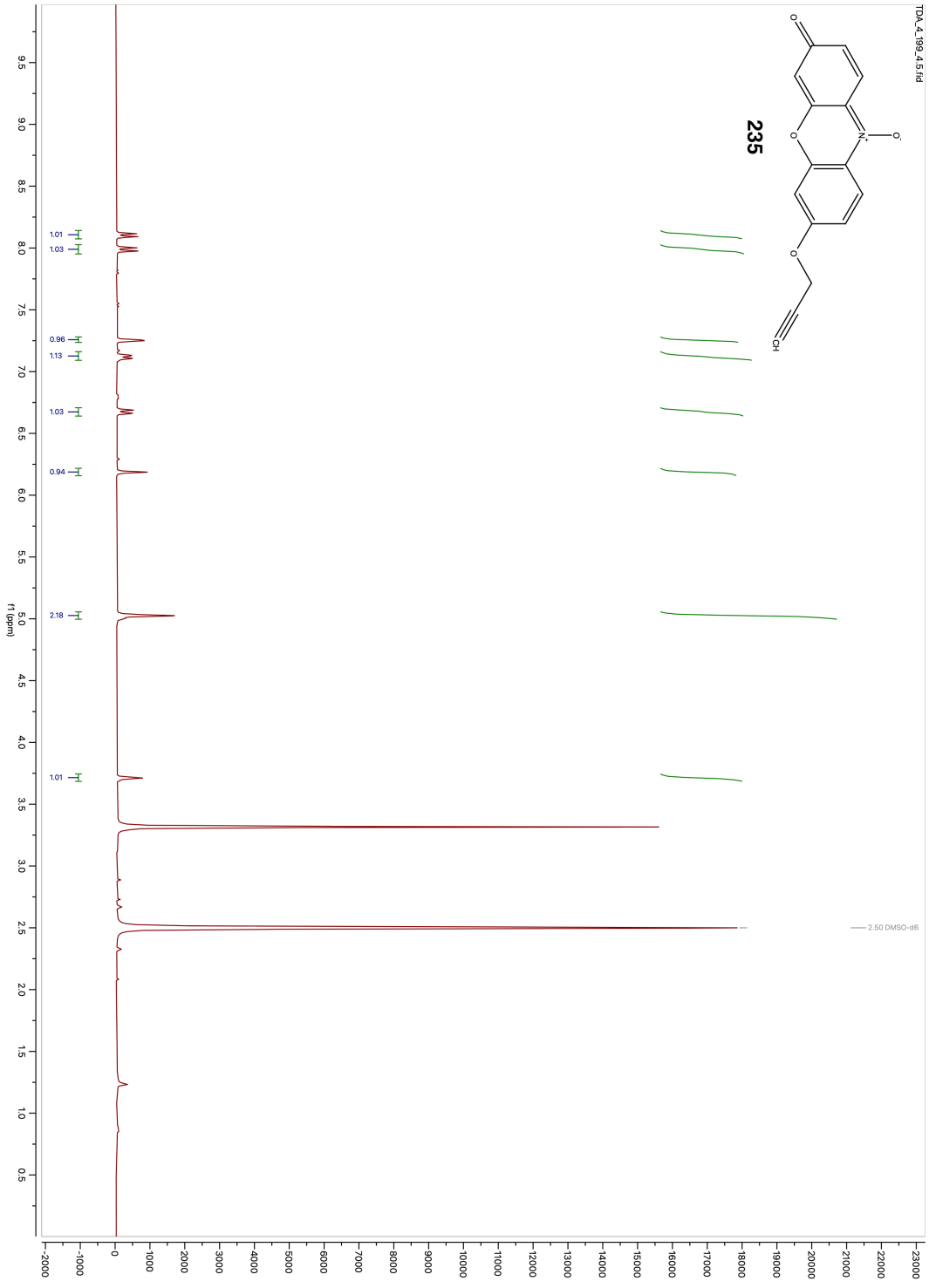
TDA_4-199_4.5.fid
235
1.01
1.03
0.96
1.13
1.03
0.94
2.18
1.01
2.50 DMSO-d6
f1 (ppm)

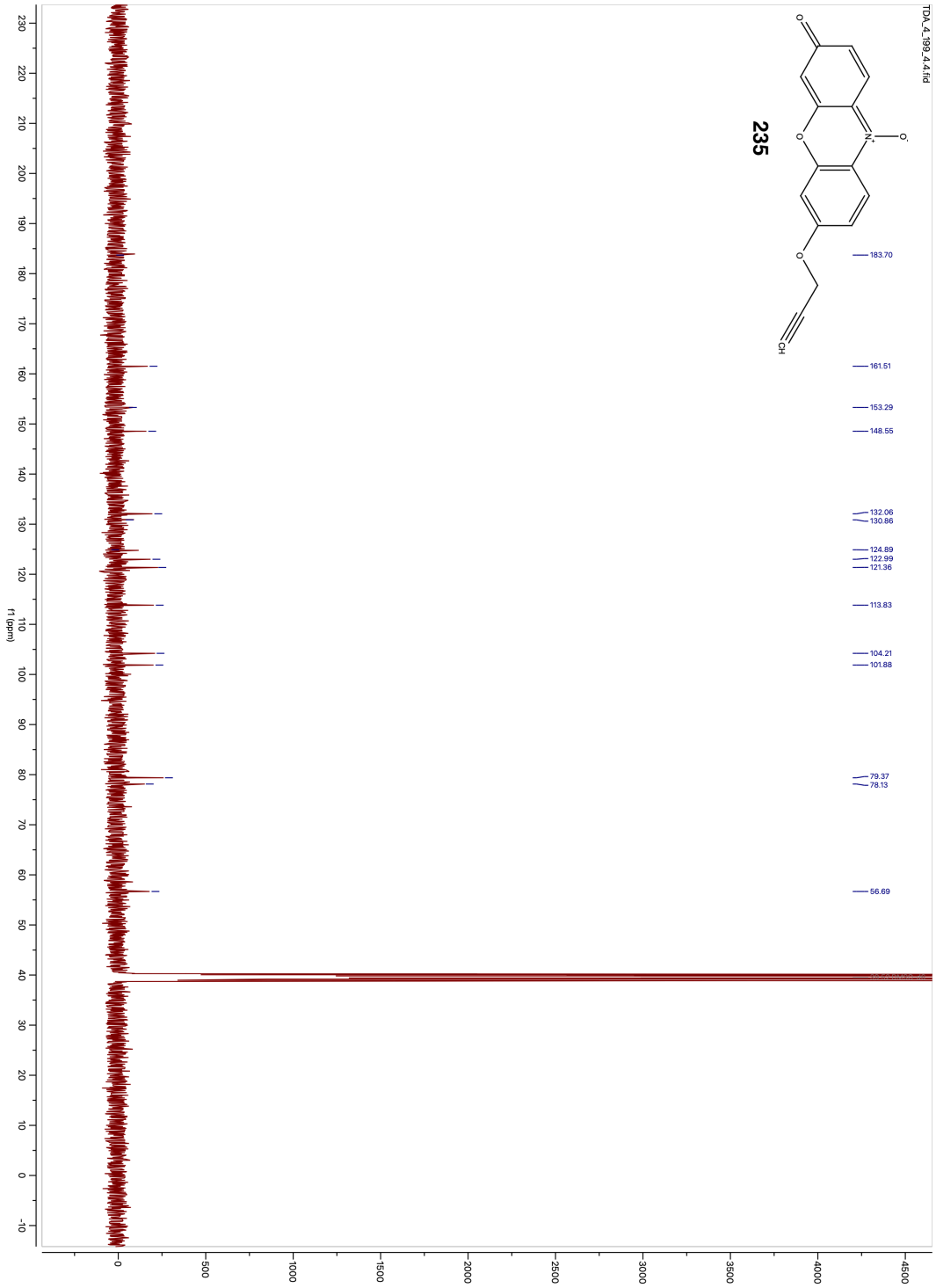
TDA_4-199_4.4.fid
235
183.70
161.51
153.29
148.55
132.06
130.86
124.89
122.99
121.36
113.83
104.21
101.88
79.37
78.13
56.69
f1 (ppm)

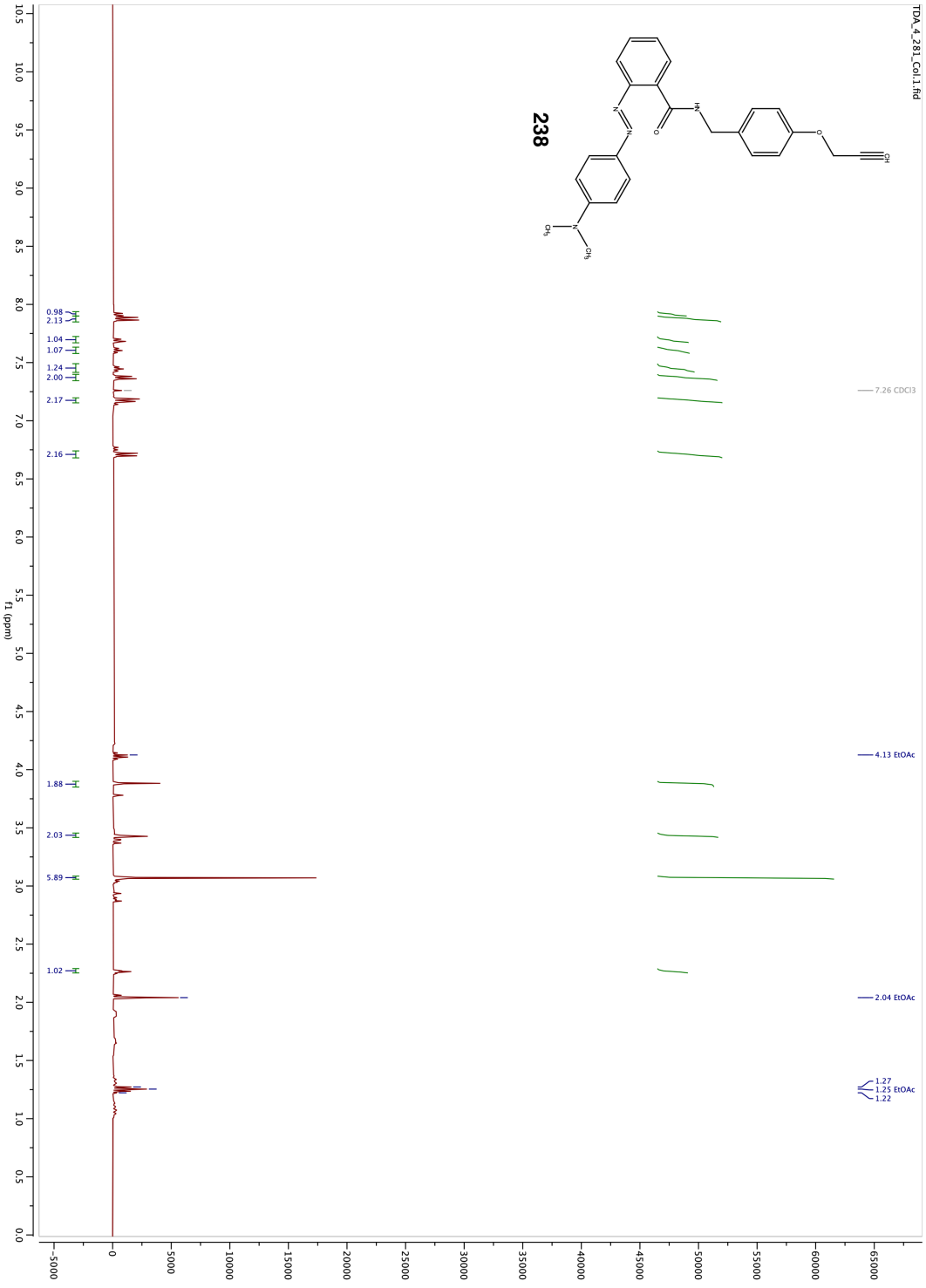
TDA_4_281_Co1.1.fid
238
0.98
2.13
1.04
1.07
1.24
2.00
2.17
2.16
1.88
2.03
5.89
1.02
7.26 CDCl3
4.13 EtOAc
2.04 EtOAc
1.27
1.25 EtOAc
1.22
f1 (ppm)

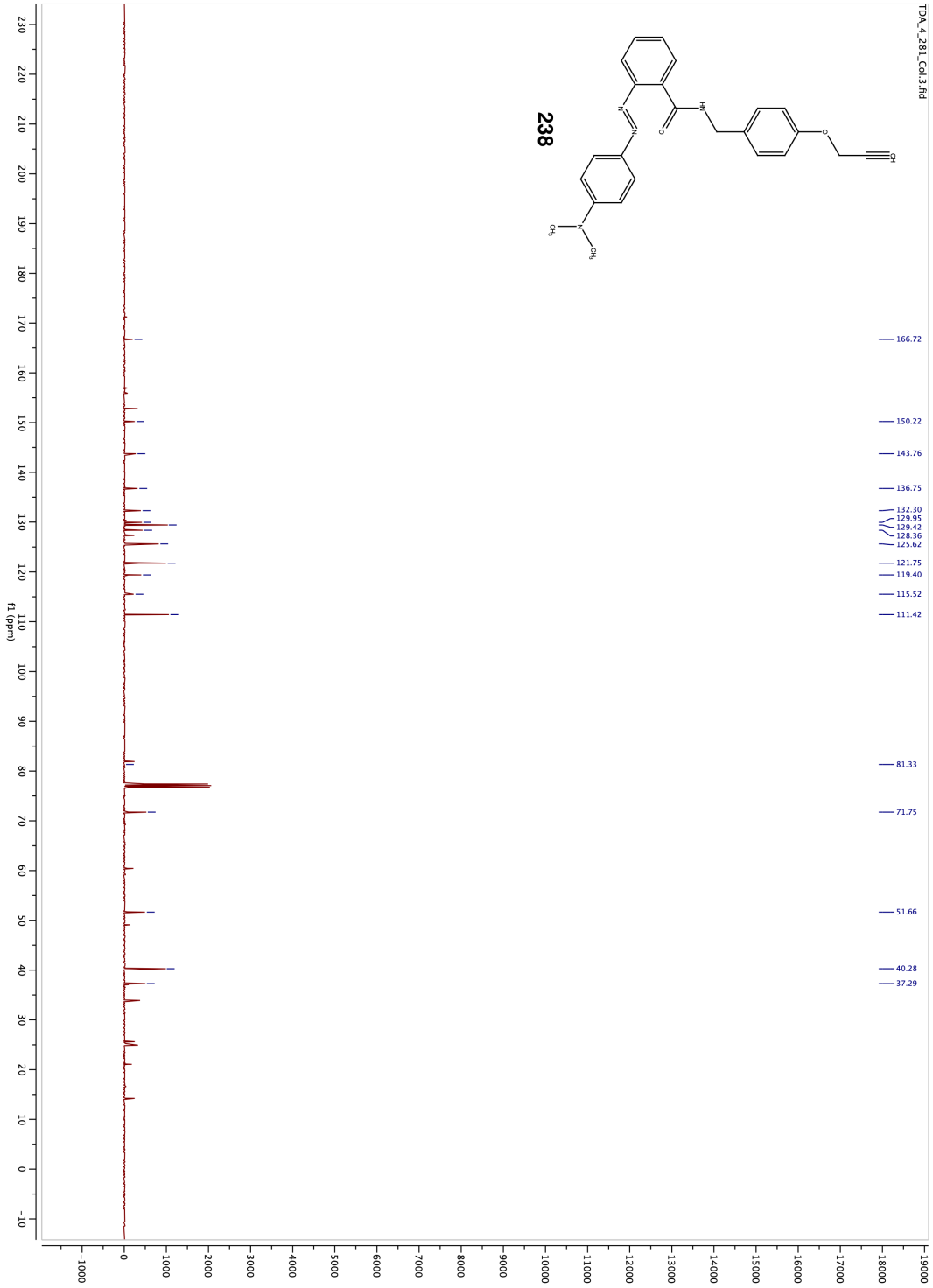
238
TDA_4_281_Col3.fid
166.72
150.22
143.76
136.75
132.30
129.95
129.42
128.36
125.62
121.75
119.40
115.52
111.42
81.33
71.75
51.66
40.28
37.29
f1 (ppm)

9.2 HR-MS Spectra

Mass Spectrometry
Analytical Services
School of Chemistry

The University of Nottingham

Sample-ID	t_arm_TDA_5_115	Lab	C13
Submitter	Tom Armstrong	Supervisor	Neil Thomas
Analysis Name	t_arm_TDA_5_115_597023_20_01_84726.d	Acquisition Date	1/6/2020 12:04:37 PM
Ionisation Mode	ESI Positive	Instrument	Bruker MicroTOF

+MS, 0.6-0.8min #50-66

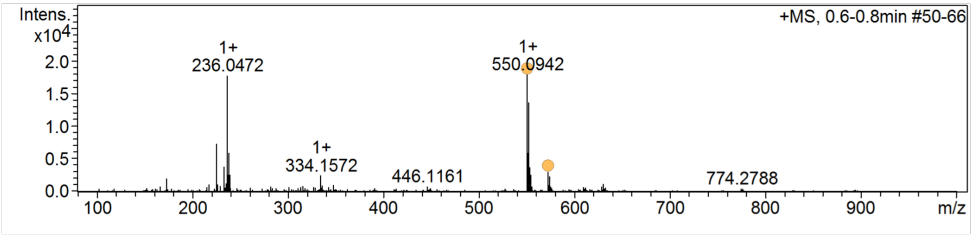

#	m/z	I %
1	173.0782	11.2
2	217.1052	5.9
3	225.1963	41.1
4	226.1984	5.9
5	233.0359	21.3
6	235.0344	6.9
7	236.0472	99.3
8	237.0506	14.0
9	238.0446	33.3
10	239.2094	14.1
11	334.1572	13.9
12	550.0942	100.0
13	551.0988	33.1
14	552.0919	76.3
15	553.0947	21.2
16	554.0916	14.4
17	572.0762	16.9
18	573.0795	5.5
19	574.0743	12.6
20	630.0022	6.5

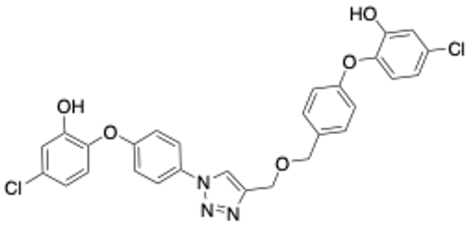

54

Generate Molecular Formula Parameters

Charge	Tolerance	sigma limit	H/C Ratio	Electron Conf.	Nitrogen Rule	Chrom.BackGround	Calibration
+1	6 ppm	0.08	3 - 0	both	false	false	TRUE

Expected Formula C28 H21 Cl2 N3 O5 **Adduct(s):** H, Na, NH4, C3H5N2, radical

#	meas. m/z	theo. m/z	|Err|[ppm]	Sigma	Formula	Adduct	Adduct Mass
1	550.0942	550.0931	2.10	0.0267	C28H22Cl2N3O5	M+H	1.0078
1	572.0762	572.0750	2.00	0.0294	C28H21Cl2N3NaO5	M+Na	22.9898

Note: Sigma fits < 0.05 indicates high probability of correct MF

Mass Spectrometry
Analytical Services
School of Chemistry

The University of Nottingham

Sample-ID	t_arm_TDA_3_297_F21	Lab	C13
Submitter	Tom Armstrong	Supervisor	Neil Thomas
Analysis Name	t_arm_TDA_3_297_F21_579838_12_01_71462.d	Acquisition Date	2/4/2019 11:47:26 AM
Ionisation Mode	ESI Negative	Instrument	Bruker MicroTOF

-MS, 0.6-0.8min #51-66

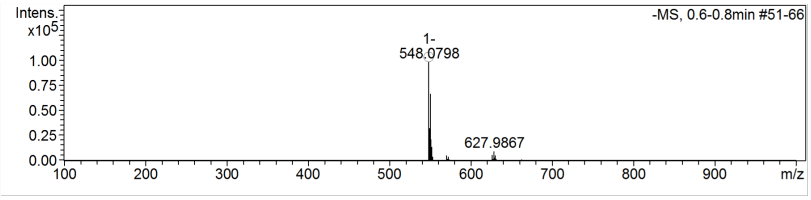

#	m/z	I %
1	548.0798	100.0
2	549.0807	33.1
3	549.7197	0.9
4	550.0764	67.8
5	551.0789	21.7
6	552.0747	13.9
7	553.0761	4.0
8	554.0745	0.8
9	570.0601	5.6
10	571.0626	1.9
11	572.0557	4.1
12	573.0587	1.2
13	625.9873	5.7
14	626.9907	1.8
15	627.9867	9.7
16	628.9895	3.1
17	629.9874	5.3
18	630.9908	1.6
19	631.9909	1.0
20	662.0689	1.4

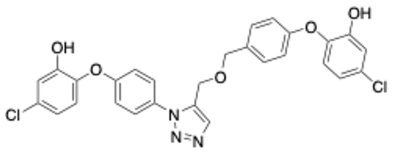

55

Generate Molecular Formula Parameters

Charge	Tolerance	sigma limit	H/C Ratio	Electron Conf.	Nitrogen Rule	Chrom.BackGround	Calibration
-1	6 ppm	0.08	3 - 0	both	false	false	TRUE

Expected Formula C28 H21 Cl2 N3 O5 **Adduct(s):** H, radical

#	meas. m/z	theo. m/z	|Err|[ppm]	Sigma	Formula	Adduct	Adduct Mass
1	548.0798	548.0785	2.30	0.0105	C28H20Cl2N3O5	M- H	1.0078

Note: Sigma fits < 0.05 indicates high probability of correct MF

Mass Spectrometry
Analytical Services
School of Chemistry

The University of Nottingham

Sample-ID	t_arm_TDA_2_289_HPLC	Lab	C13
Submitter	Tom Armstrong	Supervisor	Neil Thomas
Analysis Name	t_arm_TDA_2_289_HPLC_585135_18_01_75713.d	Acquisition Date	4/25/2019 9:51:25 AM
Ionisation Mode	ESI Negative	Instrument	Bruker MicroTOF

-MS, 0.6-0.8min #51-66

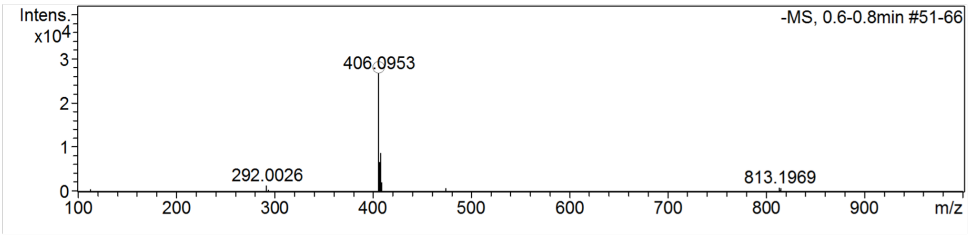

#	m/z	I %
1	112.9857	2.3
2	292.0026	5.3
3	293.0034	0.4
4	293.9990	2.0
5	406.0953	100.0
6	407.0994	25.4
7	408.0926	32.8
8	409.0942	8.1
9	410.1038	0.4
10	412.3909	0.5
11	474.0828	3.2
12	476.0817	0.4
13	813.1969	3.6
14	814.1981	1.3
15	815.1932	3.1
16	816.1902	0.9
17	817.1929	0.4
18	835.1716	0.4

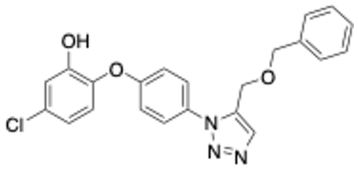

56

Generate Molecular Formula Parameters

Charge	Tolerance	sigma limit	H/C Ratio	Electron Conf.	Nitrogen Rule	Chrom.BackGround	Calibration
-1	6 ppm	0.08	3 - 0	both	false	false	TRUE

Expected Formula C22 H18 Cl1 N3 O3 **Adduct(s):** H, radical

#	meas. m/z	theo. m/z	|Err|[ppm]	Sigma	Formula	Adduct	Adduct Mass
1	406.0953	406.0964	2.60	0.0134	C22H17ClN3O3	M- H	1.0078

Note: Sigma fits < 0.05 indicates high probability of correct MF

Mass Spectrometry
Analytical Services
School of Chemistry

The University of Nottingham

Sample-ID	t_arm_TDA_4_99_HPLC_Peak_2	Lab	C13
Submitter	Tom Armstrong	Supervisor	Neil Thomas
Analysis Name	t_arm_TDA_4_99_HPLC_Peak_2_5851_4_01_75683.d	Acquisition Date	4/24/2019 10:28:21 AM
Ionisation Mode	ESI – Negative	Instrument	Bruker MicroTOF

-MS, 0.6-0.8min #50-66

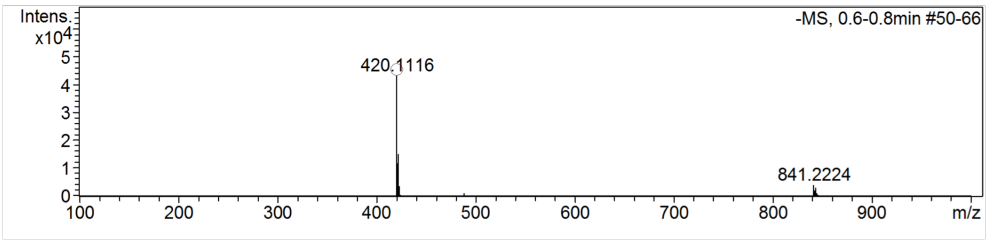

#	m/z	I %
1	112.9852	1.0
2	227.3274	0.2
3	419.8538	0.4
4	420.1116	100.0
5	421.1126	27.6
6	422.1100	35.0
7	423.1111	8.5
8	424.1157	1.3
9	456.0884	0.8
10	458.0814	0.2
11	478.0710	0.7
12	488.0978	2.8
13	841.2224	9.7
14	842.2251	4.9
15	843.2241	7.4
16	844.2272	2.8
17	845.2215	1.5
18	863.2003	0.9
19	865.2048	0.6
20	942.2125	0.7

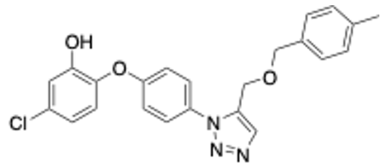

57

Generate Molecular Formula Parameters

Charge	Tolerance	sigma limit	H/C Ratio	Electron Conf.	Nitrogen Rule	Chrom.BackGround	Calibration
-1	6 ppm	0.08	3 - 0	both	false	false	TRUE

Expected Formula C23 H20 Cl1 N3 O3 **Adduct(s):** H, radical

#	meas. m/z	theo. m/z	|Err|[ppm]	Sigma	Formula	Adduct	Adduct Mass
1	420.1116	420.1120	1.00	0.0074	C23H19ClN3O3	M- H	1.0078

Note: Sigma fits < 0.05 indicates high probability of correct MF

Mass Spectrometry
Analytical Services
School of Chemistry

The University of Nottingham

Sample-ID	t_arm_TDA_4_101	Lab	C13
Submitter	Tom Armstrong	Supervisor	Neil Thomas
Analysis Name	t_arm_TDA_4_101_583280_82_01_74231.d	Acquisition Date	3/25/2019 2:38:46 PM
Ionisation Mode	ESI Negative	Instrument	Bruker MicroTOF

-MS, 0.6-0.8min #51-66

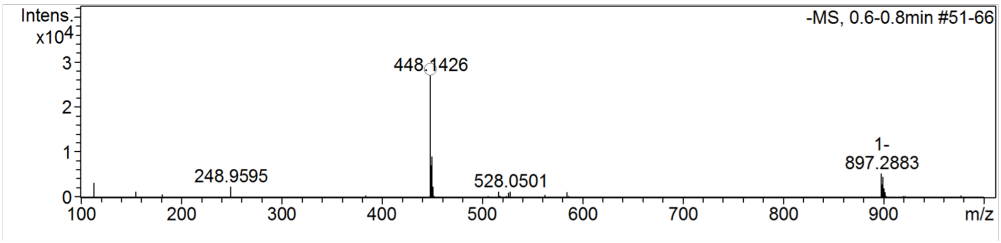

#	m/z	I %
1	112.9855	12.3
2	154.9729	4.9
3	180.9721	2.5
4	248.9595	8.8
5	384.0749	2.0
6	448.1426	100.0
7	449.1442	26.6
8	450.1401	33.7
9	451.1428	9.0
10	516.1293	5.1
11	526.0520	3.9
12	528.0501	5.2
13	562.1340	2.2
14	584.1165	4.4
15	897.2883	19.7
16	898.2893	10.6
17	899.2852	17.0
18	900.2889	7.6
19	901.2863	4.5
20	977.1955	1.8

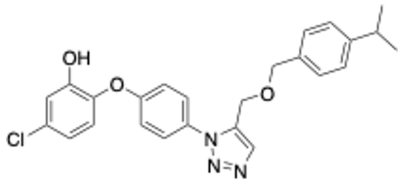

58

Generate Molecular Formula Parameters

Charge	Tolerance	sigma limit	H/C Ratio	Electron Conf.	Nitrogen Rule	Chrom.BackGround	Calibration
-1	6 ppm	0.08	3 - 0	both	false	false	TRUE

Expected Formula C25 H24 Cl1 N3 O3 **Adduct(s):** H, radical

#	meas. m/z	theo. m/z	|Err|[ppm]	Sigma	Formula	Adduct	Adduct Mass
1	448.1426	448.1433	1.70	0.0154	C25H23ClN3O3	M- H	1.0078

Note: Sigma fits < 0.05 indicates high probability of correct MF

Mass Spectrometry
Analytical Services
School of Chemistry

The University of Nottingham

Sample-ID	t_arm_TDA_3_161_HPLC	Lab	C13
Submitter	Tom Armstrong	Supervisor	Neil Thomas
Analysis Name	t_arm_TDA_3_161_HPLC_585731_37_01_76116.d	Acquisition Date	5/7/2019 8:31:05 AM
Ionisation Mode	ESI Negative	Instrument	Bruker MicroTOF

-MS, 0.6-0.8min #50-66

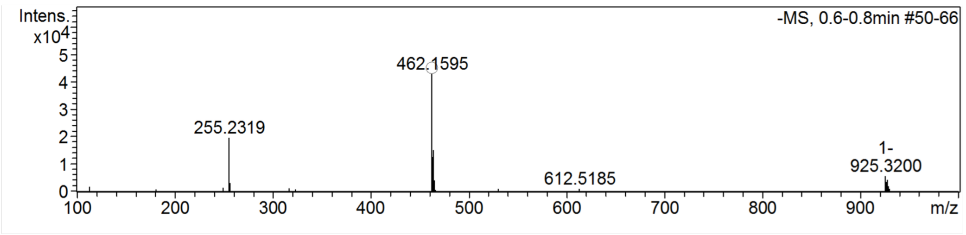

#	m/z	I %
1	112.9856	4.4
2	180.9734	2.3
3	248.9611	3.6
4	255.2319	46.0
5	256.2365	7.6
6	316.9473	3.1
7	323.2184	2.4
8	384.9359	1.1
9	462.1595	100.0
10	463.1617	29.9
11	464.1559	35.5
12	465.1569	10.0
13	466.1579	1.7
14	530.1427	2.6
15	612.5185	2.6
16	925.3200	13.7
17	926.3265	8.5
18	927.3199	10.4
19	928.3237	5.0
20	929.3158	2.9

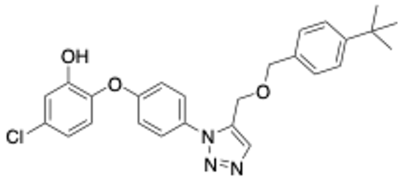

59

Generate Molecular Formula Parameters

Charge	Tolerance	sigma limit	H/C Ratio	Electron Conf.	Nitrogen Rule	Chrom.BackGround	Calibration
-1	6 ppm	0.08	3 - 0	both	false	false	TRUE

Expected Formula C26 H26 Cl1 N3 O3 **Adduct(s):** H, radical

#	meas. m/z	theo. m/z	|Err|[ppm]	Sigma	Formula	Adduct	Adduct Mass
1	462.1595	462.1590	1.20	0.0061	C26H25ClN3O3	M- H	1.0078

Note: Sigma fits < 0.05 indicates high probability of correct MF

Mass Spectrometry
Analytical Services
School of Chemistry

The University of Nottingham

Sample-ID	t_arm_TDA_3_151_Col	Lab	C13
Submitter	Tom Armstrong	Supervisor	Neil Thomas
Analysis Name	t_arm_TDA_3_151_Col_576274_53_01_68491.d	Acquisition Date	11/21/2018 4:11:57 PM
Ionisation Mode	ESI Positive	Instrument	Bruker MicroTOF

+MS, 0.6-0.8min #51-67

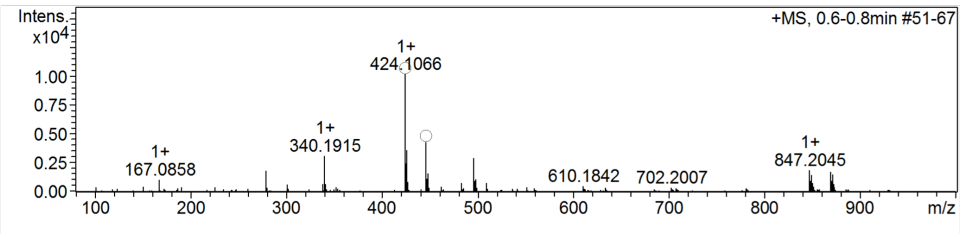

#	m/z	I %
1	167.0858	10.5
2	279.0934	17.8
3	340.1915	30.6
4	424.1066	100.0
5	425.1095	24.6
6	426.1044	35.8
7	427.1054	8.5
8	446.0875	42.4
9	447.0905	11.1
10	448.0862	15.6
11	483.1799	7.8
12	496.1231	29.0
13	497.1265	9.5
14	498.1227	10.9
15	847.2045	18.5
16	848.2071	9.6
17	849.2028	14.6
18	869.1856	17.1
19	870.1870	9.5
20	871.1839	15.1

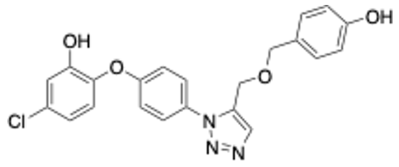

60

Generate Molecular Formula Parameters

Charge	Tolerance	sigma limit	H/C Ratio	Electron Conf.	Nitrogen Rule	Chrom.BackGround	Calibration
+1	6 ppm	0.08	3 - 0	both	false	false	TRUE

Expected Formula C22 H18 Cl1 N3 O4 **Adduct(s):** H, Na, NH4, C3H5N2, radical

#	meas. m/z	theo. m/z	|Err|[ppm]	Sigma	Formula	Adduct	Adduct Mass
1	424.1066	424.1059	1.70	0.0034	C22H19ClN3O4	M+H	1.0078
1	446.0875	446.0878	0.70	0.0069	C22H18ClN3NaO4	M+Na	22.9898

Note: Sigma fits < 0.05 indicates high probability of correct MF

Mass Spectrometry
Analytical Services
School of Chemistry

The University of Nottingham

Sample-ID	t_arm_TDA_4_103	Lab	C13
Submitter	Tom Armstrong	Supervisor	Neil Thomas
Analysis Name	t_arm_TDA_4_103_583281_83_01_74232.d	Acquisition Date	3/25/2019 2:41:18 PM
Ionisation Mode	ESI Negative	Instrument	Bruker MicroTOF

-MS, 0.6-0.8min #51-67

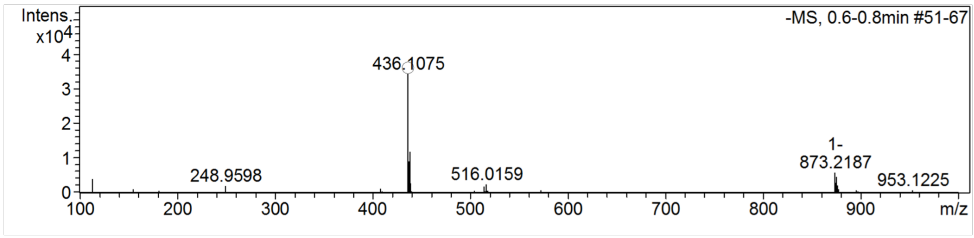

#	m/z	I %
1	112.9856	11.6
2	154.9738	3.0
3	180.9726	1.8
4	248.9598	6.0
5	408.0757	3.8
6	436.1075	100.0
7	437.1105	26.5
8	438.1049	34.5
9	439.1075	8.3
10	504.0947	1.9
11	514.0173	5.5
12	516.0159	7.2
13	572.0787	2.3
14	873.2187	16.9
15	874.2208	8.4
16	875.2160	13.7
17	876.2200	6.2
18	877.2151	3.1
19	895.1976	2.0
20	953.1225	2.4

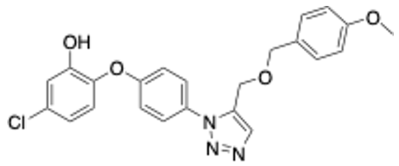

61

Generate Molecular Formula Parameters

Charge	Tolerance	sigma limit	H/C Ratio	Electron Conf.	Nitrogen Rule	Chrom.BackGround	Calibration
-1	6 ppm	0.08	3 - 0	both	false	false	TRUE

Expected Formula C23 H20 Cl1 N3 O4 **Adduct(s):** H, radical

#	meas. m/z	theo. m/z	|Err|[ppm]	Sigma	Formula	Adduct	Adduct Mass
1	436.1075	436.1070	1.30	0.0081	C23H19ClN3O4	M- H	1.0078

Note: Sigma fits < 0.05 indicates high probability of correct MF

Mass Spectrometry
Analytical Services
School of Chemistry

The University of Nottingham

Sample-ID	t_arm_TDA_4_81_Col	Lab	C13
Submitter	Tom Armstrong	Supervisor	Neil Thomas
Analysis Name	t_arm_TDA_4_81_Col_582866_87_01_73909.d	Acquisition Date	3/18/2019 5:25:21 PM
Ionisation Mode	ESI Negative	Instrument	Bruker MicroTOF

-MS, 0.6-0.8min #50-66

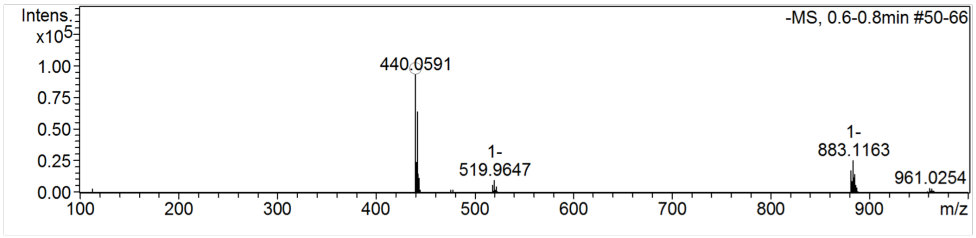

#	m/z	I %
1	112.9857	3.5
2	440.0591	100.0
3	441.0611	26.4
4	442.0559	68.6
5	443.0587	16.1
6	444.0535	12.6
7	445.0552	2.9
8	517.9658	6.6
9	519.9647	10.8
10	520.9675	2.9
11	521.9633	5.2
12	881.1170	18.8
13	882.1204	9.8
14	883.1163	27.4
15	884.1159	13.2
16	885.1145	15.6
17	886.1152	6.8
18	887.1106	4.4
19	961.0254	3.9
20	963.0214	3.5

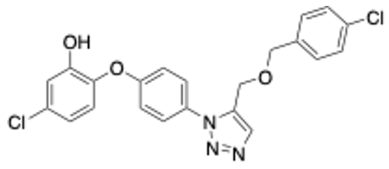

62

Generate Molecular Formula Parameters

Charge	Tolerance	sigma limit	H/C Ratio	Electron Conf.	Nitrogen Rule	Chrom.BackGround	Calibration
-1	6 ppm	0.08	3 - 0	both	false	false	TRUE

Expected Formula C22 H17 Cl2 N3 O3 **Adduct(s):** H, radical

#	meas. m/z	theo. m/z	|Err|[ppm]	Sigma	Formula	Adduct	Adduct Mass
1	440.0591	440.0574	3.80	0.0064	C22H16Cl2N3O3	M- H	1.0078

Note: Sigma fits < 0.05 indicates high probability of correct MF

Mass Spectrometry
Analytical Services
School of Chemistry

The University of Nottingham

Sample-ID	t_arm_TDA_3_221_F15	Lab	C13
Submitter	Tom Armstrong	Supervisor	Neil Thomas
Analysis Name	t_arm_TDA_3_221_F15_577851_11_01_69894.d	Acquisition Date	12/13/2018 10:30:25 AM
Ionisation Mode	ESI Negative	Instrument	Bruker MicroTOF

-MS, 0.6-0.8min #51-67

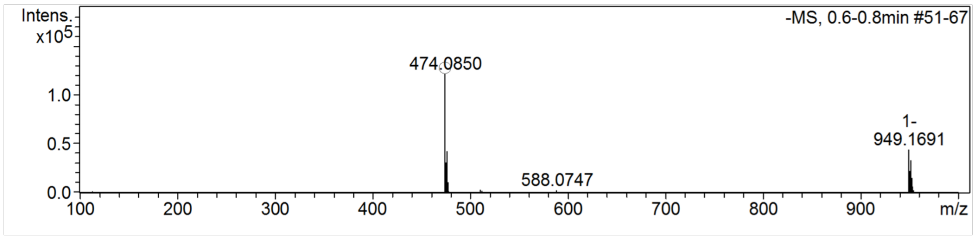

#	m/z	I %
1	112.9853	1.1
2	473.5698	0.8
3	473.6900	0.7
4	474.0850	100.0
5	474.5697	0.8
6	475.0869	25.6
7	476.0811	35.2
8	477.0845	9.1
9	478.0890	1.4
10	510.0607	2.6
11	512.0566	2.0
12	588.0747	2.4
13	590.0722	0.8
14	949.1691	36.7
15	950.1678	18.4
16	951.1702	27.4
17	952.1702	12.5
18	953.1655	5.5
19	954.1690	2.2
20	955.1684	0.8

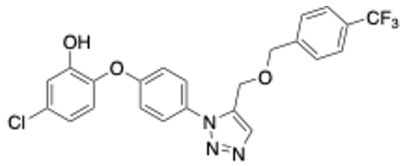

63

Generate Molecular Formula Parameters

Charge	Tolerance	sigma limit	H/C Ratio	Electron Conf.	Nitrogen Rule	Chrom.BackGround	Calibration
-1	6 ppm	0.08	3 - 0	both	false	false	TRUE

Expected Formula C23 H17 Cl1 F3 N3 O3 **Adduct(s):** H, radical

#	meas. m/z	theo. m/z	|Err|[ppm]	Sigma	Formula	Adduct	Adduct Mass
1	474.0850	474.0838	2.50	0.0045	C23H16ClF3N3O3	M- H	1.0078

Note: Sigma fits < 0.05 indicates high probability of correct MF

Mass Spectrometry
Analytical Services
School of Chemistry

The University of Nottingham

Sample-ID	t_arm_TDA_3_299_F15	Lab	C13
Submitter	Tom Armstrong	Supervisor	Neil Thomas
Analysis Name	t_arm_TDA_3_299_F15_579968_40_01_71537.d	Acquisition Date	2/5/2019 3:05:08 PM
Ionisation Mode	ESI Negative	Instrument	Bruker MicroTOF

-MS, 0.6-0.8min #50-66

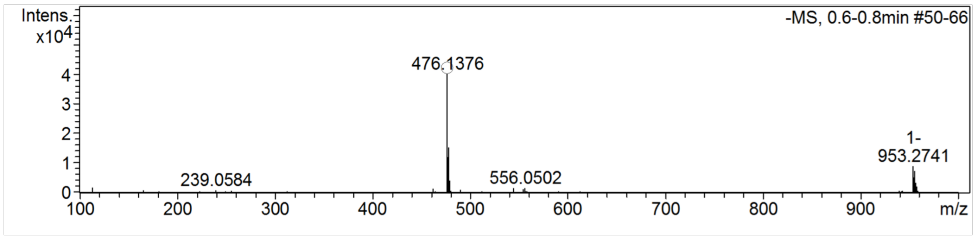

#	m/z	I %
1	112.9855	4.4
2	165.0394	2.2
3	239.0584	2.1
4	255.2312	1.8
5	462.1206	3.6
6	476.1376	100.0
7	477.1392	30.3
8	478.1348	38.1
9	479.1382	10.3
10	490.1165	2.5
11	544.1254	4.0
12	554.0465	2.9
13	556.0502	4.1
14	942.2609	1.8
15	953.2741	22.6
16	954.2806	13.1
17	955.2755	18.3
18	956.2741	8.7
19	957.2748	5.4
20	958.2759	2.0

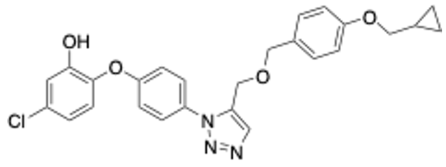

64

Generate Molecular Formula Parameters

Charge	Tolerance	sigma limit	H/C Ratio	Electron Conf.	Nitrogen Rule	Chrom.BackGround	Calibration
-1	6 ppm	0.08	3 - 0	both	false	false	TRUE

Expected Formula C26 H24 Cl1 N3 O4 **Adduct(s):** H, radical

#	meas. m/z	theo. m/z	|Err|[ppm]	Sigma	Formula	Adduct	Adduct Mass
1	476.1376	476.1383	1.40	0.0056	C26H23ClN3O4	M- H	1.0078

Note: Sigma fits < 0.05 indicates high probability of correct MF

Mass Spectrometry
Analytical Services
School of Chemistry

The University of Nottingham

Sample-ID	t_arm_TDA_4_1_Col	Lab	C13
Submitter	Tom Armstrong	Supervisor	Neil Thomas
Analysis Name	t_arm_TDA_4_1_Col_580035_15_01_71580.d	Acquisition Date	2/6/2019 1:52:27 PM
Ionisation Mode	ESI Positive	Instrument	Bruker MicroTOF

+MS, 0.6-0.8min #50-66

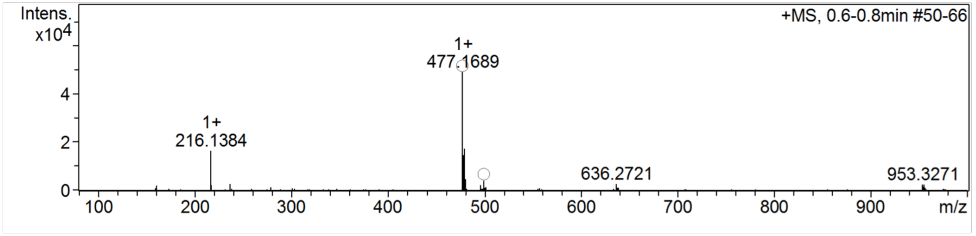

#	m/z	I %
1	160.1114	4.5
2	216.1384	33.6
3	217.1370	5.0
4	236.0481	5.8
5	279.0937	3.1
6	477.1689	100.0
7	478.1716	30.1
8	479.1680	35.6
9	480.1681	9.8
10	496.1221	4.9
11	499.1483	8.6
12	500.1523	2.6
13	501.1473	3.0
14	636.2721	6.1
15	637.2749	2.7
16	638.2717	2.8
17	953.3271	5.6
18	954.3293	3.8
19	955.3255	5.4
20	956.3299	2.6

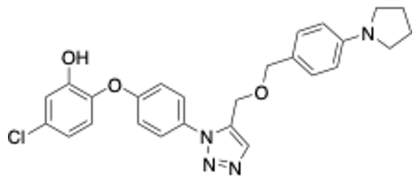

65

Generate Molecular Formula Parameters

Charge	Tolerance	sigma limit	H/C Ratio	Electron Conf.	Nitrogen Rule	Chrom.BackGround	Calibration
+1	6 ppm	0.08	3 - 0	both	false	false	TRUE

Expected Formula C26 H25 Cl1 N4 O3 **Adduct(s):** H, Na, NH4, C3H5N2, radical

#	meas. m/z	theo. m/z	|Err|[ppm]	Sigma	Formula	Adduct	Adduct Mass
1	477.1689	477.1688	0.30	0.0065	C26H26ClN4O3	M+H	1.0078
1	499.1483	499.1507	5.00	0.0112	C26H25ClN4NaO3	M+Na	22.9898

Note: Sigma fits < 0.05 indicates high probability of correct MF

Mass Spectrometry
Analytical Services
School of Chemistry

The University of Nottingham

Sample-ID	t_arm_TDA_4_79_2_Col	Lab	C13
Submitter	Tom Armstrong	Supervisor	Neil Thomas
Analysis Name	t_arm_TDA_4_79_2_Col_582771_13_01_73811.d	Acquisition Date	3/18/2019 10:36:42 AM
Ionisation Mode	ESI Negative	Instrument	Bruker MicroTOF

-MS, 0.6-0.8min #51-66

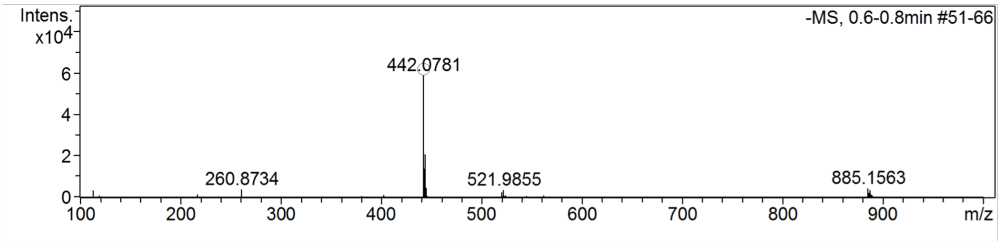

#	m/z	I %
1	112.9856	5.7
2	118.9410	1.9
3	216.9094	2.7
4	260.8734	6.6
5	402.8059	2.5
6	442.0781	100.0
7	443.0812	23.9
8	444.0756	35.7
9	445.0768	8.2
10	519.9869	4.5
11	521.9855	6.3
12	522.9866	1.4
13	523.9841	1.7
14	544.7373	1.5
15	562.0263	2.0
16	885.1563	7.7
17	886.1580	3.9
18	887.1539	6.2
19	888.1567	2.6
20	889.1536	1.7

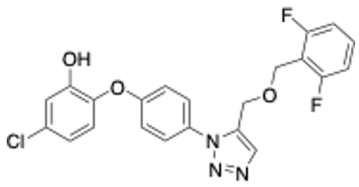

66

Generate Molecular Formula Parameters

Charge	Tolerance	sigma limit	H/C Ratio	Electron Conf.	Nitrogen Rule	Chrom.BackGround	Calibration
-1	6 ppm	0.08	3 - 0	both	false	false	TRUE

Expected Formula C22 H16 Cl1 F2 N3 O3 **Adduct(s):** H, radical

#	meas. m/z	theo. m/z	|Err|[ppm]	Sigma	Formula	Adduct	Adduct Mass
1	442.0781	442.0775	1.30	0.0058	C22H15ClF2N3O3	M- H	1.0078

Note: Sigma fits < 0.05 indicates high probability of correct MF

Mass Spectrometry
Analytical Services
School of Chemistry

The University of Nottingham

Sample-ID	t_arm_TDA_4_75	Lab	C13
Submitter	Tom Armstrong	Supervisor	Neil Thomas
Analysis Name	t_arm_TDA_4_75_583284_85_01_74236.d	Acquisition Date	3/25/2019 3:05:52 PM
Ionisation Mode	ESI Negative	Instrument	Bruker MicroTOF

-MS, 0.6-0.8min #51-67

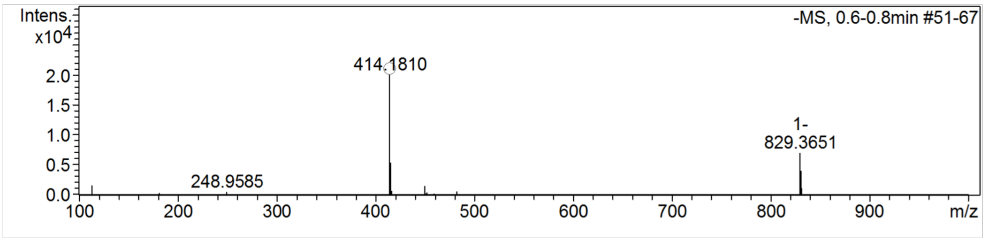

#	m/z	I %
1	112.9856	8.0
2	154.9734	0.8
3	180.9718	1.6
4	248.9585	2.9
5	413.8760	0.2
6	413.9286	0.2
7	414.1810	100.0
8	415.1839	26.9
9	416.1886	3.4
10	450.1586	7.8
11	451.1613	1.3
12	452.1550	2.2
13	459.1662	1.2
14	482.1668	2.9
15	483.1702	0.7
16	550.1564	0.7
17	829.3651	35.0
18	830.3691	20.1
19	831.3733	5.8
20	851.3456	0.6

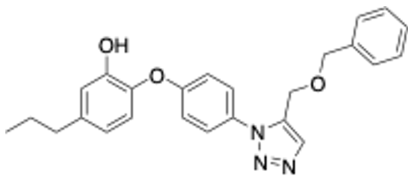

68

Generate Molecular Formula Parameters

Charge	Tolerance	sigma limit	H/C Ratio	Electron Conf.	Nitrogen Rule	Chrom.BackGround	Calibration
-1	6 ppm	0.08	3 - 0	both	false	false	TRUE

Expected Formula C25 H25 N3 O3 **Adduct(s):** H, radical

#	meas. m/z	theo. m/z	|Err|[ppm]	Sigma	Formula	Adduct	Adduct Mass
1	414.1810	414.1823	3.10	0.0114	C25H24N3O3	M- H	1.0078

Note: Sigma fits < 0.05 indicates high probability of correct MF

Mass Spectrometry
Analytical Services
School of Chemistry

The University of Nottingham

Sample-ID	t_arm_TDA_4_27	Lab	C13
Submitter	Tom Armstrong	Supervisor	Neil Thomas
Analysis Name	t_arm_TDA_4_27_580720_29_01_72129.d	Acquisition Date	2/18/2019 3:15:38 PM
Ionisation Mode	ESI Negative	Instrument	Bruker MicroTOF

-MS, 0.6-0.8min #50-66

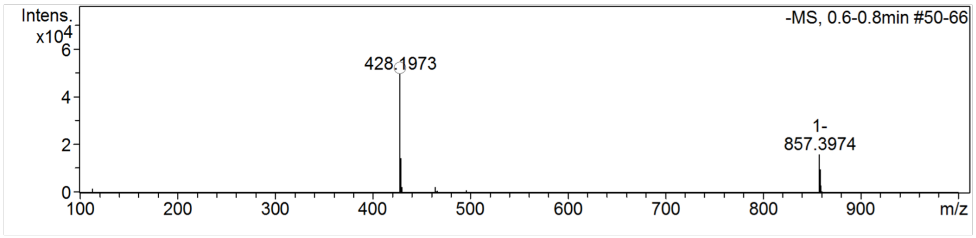

#	m/z	I %
1	112.9854	3.8
2	180.9724	0.9
3	248.9591	0.8
4	414.1783	0.5
5	427.9203	0.5
6	428.1973	100.0
7	429.1998	29.3
8	430.2022	4.9
9	464.1726	4.7
10	465.1744	1.3
11	466.1720	1.7
12	496.1840	2.0
13	497.1864	0.5
14	564.1721	0.4
15	857.3974	32.4
16	858.3986	19.6
17	859.4028	6.4
18	860.4044	1.5
19	879.3762	0.7
20	880.3819	0.5

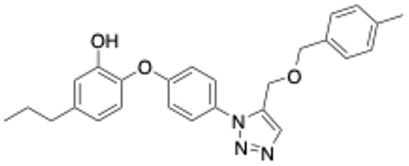

69

Generate Molecular Formula Parameters

Charge	Tolerance	sigma limit	H/C Ratio	Electron Conf.	Nitrogen Rule	Chrom.BackGround	Calibration
-1	6 ppm	0.08	3 - 0	both	false	false	TRUE

Expected Formula C26 H27 N3 O3 **Adduct(s):** H, radical

#	meas. m/z	theo. m/z	|Err|[ppm]	Sigma	Formula	Adduct	Adduct Mass
1	428.1973	428.1980	1.40	0.0019	C26H26N3O3	M- H	1.0078

Note: Sigma fits < 0.05 indicates high probability of correct MF

Mass Spectrometry
Analytical Services
School of Chemistry

The University of Nottingham

Sample-ID	t_arm_TDA_4_25_Cr	Lab	C13
Submitter	Tom Armstrong	Supervisor	Neil Thomas
Analysis Name	t_arm_TDA_4_25_Cr_580576_35_01_72003.d	Acquisition Date	2/15/2019 8:35:03 AM
Ionisation Mode	ESI Negative	Instrument	Bruker MicroTOF

-MS, 0.6-0.8min #51-66

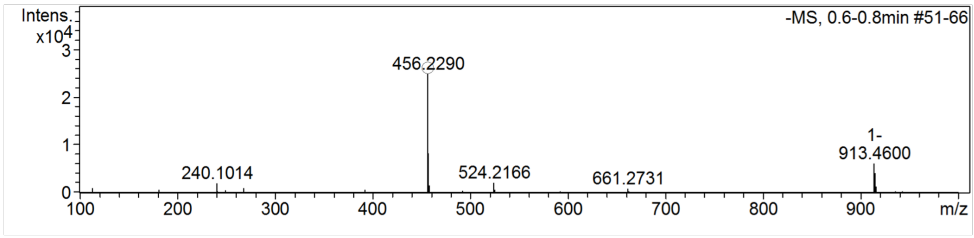

#	m/z	I %
1	112.9856	4.2
2	180.9725	2.5
3	240.1014	8.0
4	241.1051	1.3
5	248.9596	2.3
6	268.1081	4.0
7	392.1602	2.9
8	456.2290	100.0
9	457.2314	33.4
10	458.2329	6.2
11	492.2060	1.6
12	524.2166	8.7
13	525.2197	2.8
14	661.2731	3.7
15	662.2785	1.3
16	913.4600	24.8
17	914.4611	16.8
18	915.4647	5.4
19	935.4399	1.3
20	942.3214	1.4

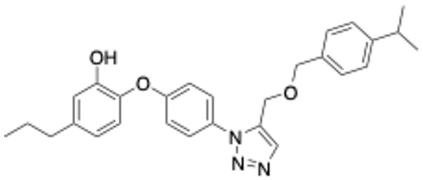

70

Generate Molecular Formula Parameters

Charge	Tolerance	sigma limit	H/C Ratio	Electron Conf.	Nitrogen Rule	Chrom.BackGround	Calibration
-1	6 ppm	0.08	3 - 0	both	false	false	TRUE

Expected Formula C28 H31 N3 O3 **Adduct(s):** H, radical

#	meas. m/z	theo. m/z	|Err|[ppm]	Sigma	Formula	Adduct	Adduct Mass
1	456.2290	456.2293	0.50	0.0097	C28H30N3O3	M- H	1.0078

Note: Sigma fits < 0.05 indicates high probability of correct MF

Mass Spectrometry
Analytical Services
School of Chemistry

The University of Nottingham

Sample-ID	t_arm_TDA_4_21_F14	Lab	C13
Submitter	Tom Armstrong	Supervisor	Neil Thomas
Analysis Name	t_arm_TDA_4_21_F14_580466_10_01_71929.d	Acquisition Date	2/13/2019 11:23:18 AM
Ionisation Mode	ESI Negative	Instrument	Bruker MicroTOF

-MS, 0.6-0.8min #51-66

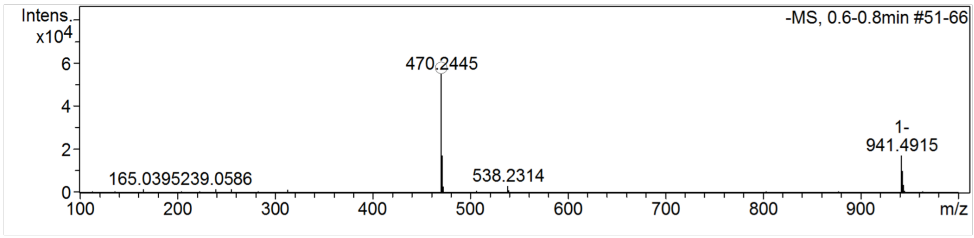

#	m/z	I %
1	112.9855	1.4
2	136.0401	1.4
3	165.0395	3.2
4	223.0268	1.2
5	239.0586	3.3
6	255.2305	3.1
7	313.0772	2.6
8	470.2445	100.0
9	471.2469	31.3
10	472.2481	5.6
11	506.2200	1.9
12	538.2314	6.0
13	539.2341	2.0
14	803.1915	1.2
15	877.2091	1.2
16	941.4915	31.5
17	942.4945	18.6
18	943.4956	6.8
19	944.4969	1.6
20	963.4706	1.2

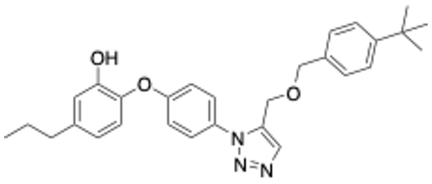

71

Generate Molecular Formula Parameters

Charge	Tolerance	sigma limit	H/C Ratio	Electron Conf.	Nitrogen Rule	Chrom.BackGround	Calibration
-1	6 ppm	0.08	3 - 0	both	false	false	TRUE

Expected Formula C29 H33 N3 O3 **Adduct(s):** H, radical

#	meas. m/z	theo. m/z	|Err|[ppm]	Sigma	Formula	Adduct	Adduct Mass
1	470.2445	470.2449	0.90	0.0084	C29H32N3O3	M- H	1.0078

Note: Sigma fits < 0.05 indicates high probability of correct MF

Mass Spectrometry
Analytical Services
School of Chemistry

The University of Nottingham

Sample-ID	t_arm_TDA_3_109_F33	Lab	C13
Submitter	Tom Armstrong	Supervisor	Neil Thomas
Analysis Name	t_arm_TDA_3_109_F33_575154_48_01_67478.d	Acquisition Date	11/6/2018 3:01:23 PM
Ionisation Mode	ESI Negative	Instrument	Bruker MicroTOF

-MS, 0.6-0.8min #50-66

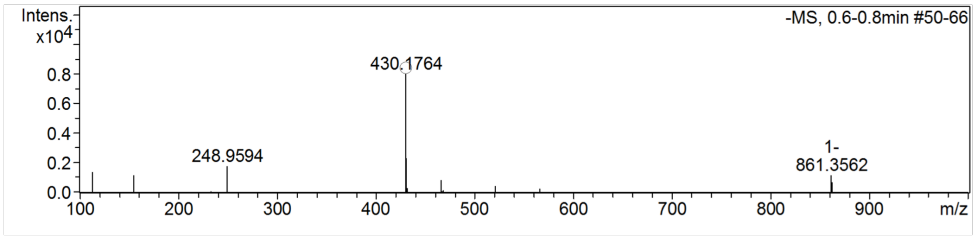

#	m/z	I %
1	112.9854	17.8
2	154.9727	14.7
3	232.9862	1.1
4	248.9594	22.4
5	430.1764	100.0
6	431.1791	29.2
7	432.1807	4.1
8	466.1539	10.8
9	467.1578	1.3
10	468.1548	2.0
11	520.9100	6.0
12	566.1505	3.4
13	861.3562	14.7
14	862.3592	8.9

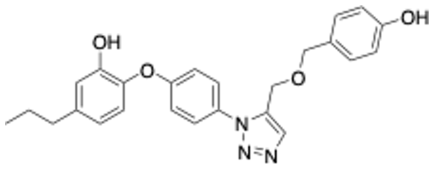

72

Generate Molecular Formula Parameters

Charge	Tolerance	sigma limit	H/C Ratio	Electron Conf.	Nitrogen Rule	Chrom.BackGround	Calibration
-1	6 ppm	0.08	3 - 0	both	false	false	TRUE

Expected Formula C25 H25 N3 O4 **Adduct(s):** H, radical

#	meas. m/z	theo. m/z	|Err|[ppm]	Sigma	Formula	Adduct	Adduct Mass
1	430.1764	430.1772	2.00	0.0052	C25H24N3O4	M- H	1.0078

Note: Sigma fits < 0.05 indicates high probability of correct MF

Mass Spectrometry
Analytical Services
School of Chemistry

The University of Nottingham

Sample-ID	t_arm_TDA_4_23_Main_HPLC_Peak	Lab	C13
Submitter	Tom Armstrong	Supervisor	Neil Thomas
Analysis Name	t_arm_TDA_4_23_Main_HPLC_Peak_5_43_01_75916.d	Acquisition Date	4/30/2019 1:41:57 PM
Ionisation Mode	ESI – Negative	Instrument	Bruker MicroTOF

-MS, 0.6-0.8min #50-66

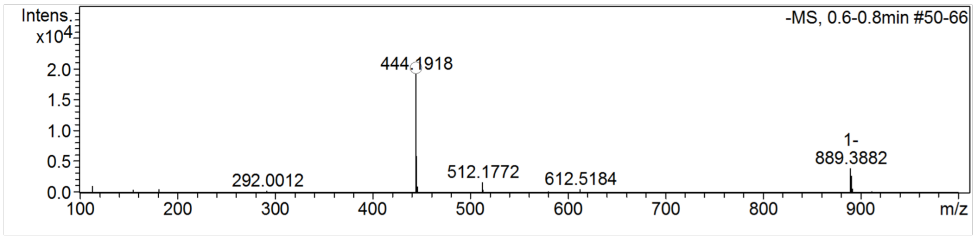

#	m/z	I %
1	112.9854	6.0
2	154.9889	2.8
3	180.9729	3.1
4	248.9593	0.9
5	255.2313	1.1
6	292.0012	1.6
7	443.9198	0.6
8	444.1918	100.0
9	445.1947	31.0
10	446.1961	5.2
11	480.1747	0.4
12	512.1772	9.1
13	513.1793	2.6
14	580.1638	1.3
15	612.5184	3.1
16	889.3882	20.6
17	890.3894	14.3
18	891.3971	3.4
19	911.3696	1.4
20	912.3690	0.5

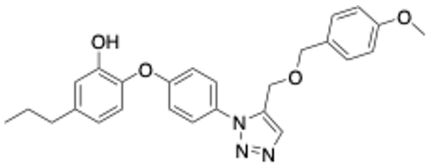

73

Generate Molecular Formula Parameters

Charge	Tolerance	sigma limit	H/C Ratio	Electron Conf.	Nitrogen Rule	Chrom.BackGround	Calibration
-1	6 ppm	0.08	3 - 0	both	false	false	TRUE

Expected Formula C26 H27 N3 O4 **Adduct(s):** H, radical

#	meas. m/z	theo. m/z	|Err|[ppm]	Sigma	Formula	Adduct	Adduct Mass
1	444.1918	444.1929	2.50	0.0077	C26H26N3O4	M- H	1.0078

Note: Sigma fits < 0.05 indicates high probability of correct MF

Mass Spectrometry
Analytical Services
School of Chemistry

The University of Nottingham

Sample-ID	t_arm_TDA_4_73_Cr	Lab	C13
Submitter	Tom Armstrong	Supervisor	Neil Thomas
Analysis Name	t_arm_TDA_4_73_Cr_582149_57_01_73352.d	Acquisition Date	3/8/2019 8:45:05 AM
Ionisation Mode	ESI Negative	Instrument	Bruker MicroTOF

-MS, 0.6-0.8min #51-66

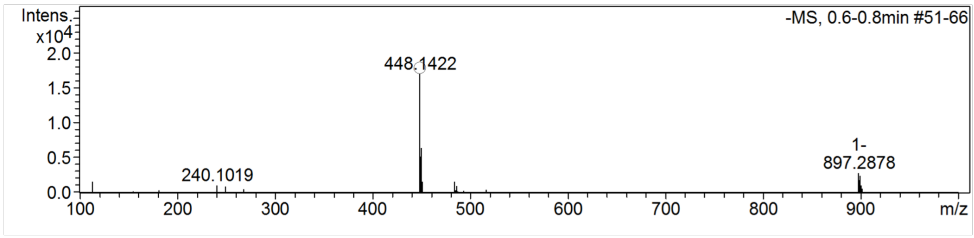

#	m/z	I %
1	112.9854	9.6
2	154.9721	1.5
3	180.9719	2.1
4	240.1019	6.1
5	248.9595	5.3
6	268.1085	3.3
7	448.1422	100.0
8	449.1444	30.6
9	450.1395	37.9
10	451.1428	9.5
11	484.1187	9.5
12	485.1242	2.4
13	486.1154	5.9
14	493.1273	2.0
15	516.1268	2.8
16	897.2878	16.5
17	898.2887	10.8
18	899.2875	14.2
19	900.2888	6.3
20	901.2873	3.6

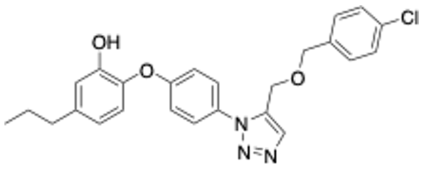

74

Generate Molecular Formula Parameters

Charge	Tolerance	sigma limit	H/C Ratio	Electron Conf.	Nitrogen Rule	Chrom.BackGround	Calibration
-1	6 ppm	0.08	3 - 0	both	false	false	TRUE

Expected Formula C25 H24 Cl1 N3 O3 **Adduct(s):** H, radical

#	meas. m/z	theo. m/z	|Err|[ppm]	Sigma	Formula	Adduct	Adduct Mass
1	448.1422	448.1433	2.50	0.0129	C25H23ClN3O3	M- H	1.0078

Note: Sigma fits < 0.05 indicates high probability of correct MF

Mass Spectrometry
Analytical Services
School of Chemistry

The University of Nottingham

Sample-ID	t_arm_TDA_4_73_Cr	Lab	C13
Submitter	Tom Armstrong	Supervisor	Neil Thomas
Analysis Name	t_arm_TDA_4_73_Cr_582149_57_01_73352.d	Acquisition Date	3/8/2019 8:45:05 AM
Ionisation Mode	ESI Negative	Instrument	Bruker MicroTOF

-MS, 0.6-0.8min #51-66

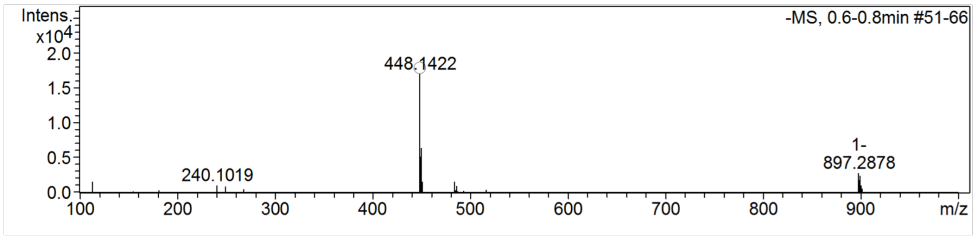

#	m/z	I %
1	112.9854	9.6
2	154.9721	1.5
3	180.9719	2.1
4	240.1019	6.1
5	248.9595	5.3
6	268.1085	3.3
7	448.1422	100.0
8	449.1444	30.6
9	450.1395	37.9
10	451.1428	9.5
11	484.1187	9.5
12	485.1242	2.4
13	486.1154	5.9
14	493.1273	2.0
15	516.1268	2.8
16	897.2878	16.5
17	898.2887	10.8
18	899.2875	14.2
19	900.2888	6.3
20	901.2873	3.6

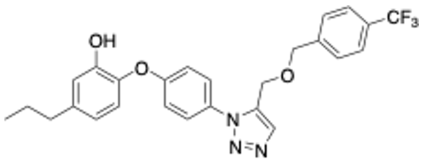

75

Generate Molecular Formula Parameters

Charge	Tolerance	sigma limit	H/C Ratio	Electron Conf.	Nitrogen Rule	Chrom.BackGround	Calibration
-1	6 ppm	0.08	3 - 0	both	false	false	TRUE

Expected Formula C25 H24 Cl1 N3 O3 **Adduct(s):** H, radical

#	meas. m/z	theo. m/z	|Err|[ppm]	Sigma	Formula	Adduct	Adduct Mass
1	448.1422	448.1433	2.50	0.0129	C25H23ClN3O3	M- H	1.0078

Note: Sigma fits < 0.05 indicates high probability of correct MF

Mass Spectrometry
Analytical Services
School of Chemistry

The University of Nottingham

Sample-ID	t_arm_TDA_4_17_HPLC_Main_Peak	Lab	C13
Submitter	Tom Armstrong	Supervisor	Neil Thomas
Analysis Name	t_arm_TDA_4_17_HPLC_Main_Peak_5_4_01_75873.d	Acquisition Date	4/30/2019 9:56:40 AM
Ionisation Mode	ESI– Negative	Instrument	Bruker MicroTOF

-MS, 0.6-0.8min #51-67

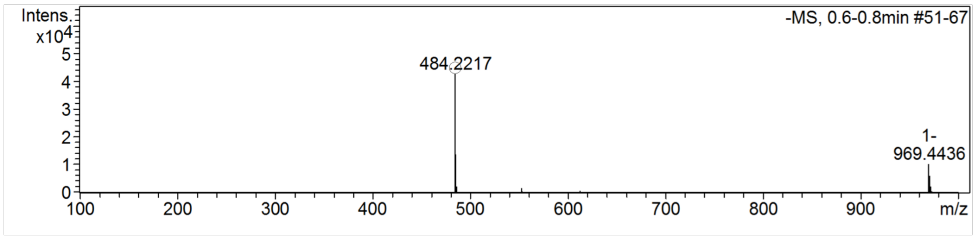

#	m/z	I %
1	154.9914	0.4
2	411.3817	0.3
3	483.7694	0.3
4	483.9072	0.4
5	484.2217	100.0
6	484.6491	0.1
7	484.7787	0.1
8	485.2250	32.5
9	486.2282	5.6
10	487.2330	0.5
11	520.1996	1.0
12	552.2095	3.9
13	553.2094	1.2
14	612.5185	1.7
15	613.5173	0.2
16	969.4436	24.3
17	970.4492	14.2
18	971.4573	5.2
19	972.4529	1.1
20	991.4276	0.3

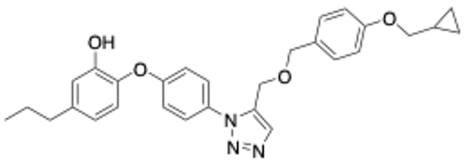

76

Generate Molecular Formula Parameters

Charge	Tolerance	sigma limit	H/C Ratio	Electron Conf.	Nitrogen Rule	Chrom.BackGround	Calibration
-1	6 ppm	0.08	3 - 0	both	false	false	TRUE

Expected Formula C29 H31 N3 O4 **Adduct(s):** H, radical

#	meas. m/z	theo. m/z	|Err|[ppm]	Sigma	Formula	Adduct	Adduct Mass
1	484.2217	484.2242	5.00	0.0037	C29H30N3O4	M- H	1.0078

Note: Sigma fits < 0.05 indicates high probability of correct MF

Mass Spectrometry
Analytical Services
School of Chemistry

The University of Nottingham

Sample-ID	t_arm_TDA_4_15_Col	Lab	C13
Submitter	Tom Armstrong	Supervisor	Neil Thomas
Analysis Name	t_arm_TDA_4_15_Col_580364_21_01_71846.d	Acquisition Date	2/11/2019 4:11:04 PM
Ionisation Mode	ESI Negative	Instrument	Bruker MicroTOF

-MS, 0.6-0.8min #51-67

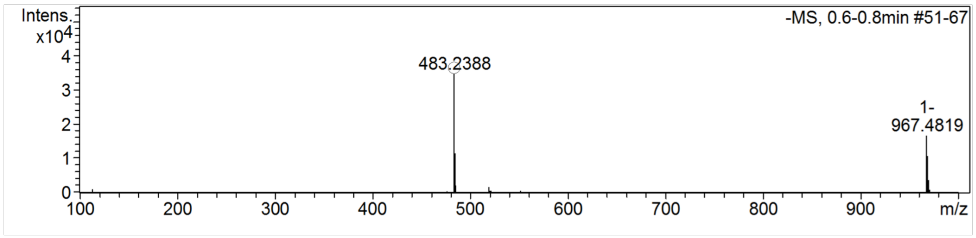

#	m/z	I %
1	112.9854	2.9
2	180.9730	1.0
3	248.9599	0.8
4	316.9468	0.5
5	476.1383	1.3
6	482.8955	0.5
7	483.2388	100.0
8	484.2407	33.5
9	485.2444	6.4
10	519.2151	5.0
11	520.2176	1.6
12	521.2138	1.6
13	551.2264	2.0
14	552.2303	0.6
15	942.2433	1.0
16	967.4819	48.0
17	968.4826	30.9
18	969.4823	11.0
19	970.4879	2.7
20	989.4580	0.3

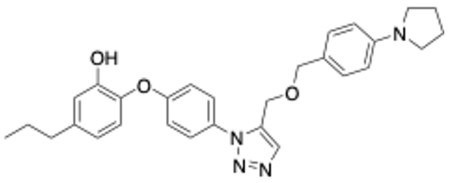

77

Generate Molecular Formula Parameters

Charge	Tolerance	sigma limit	H/C Ratio	Electron Conf.	Nitrogen Rule	Chrom.BackGround	Calibration
-1	6 ppm	0.08	3 - 0	both	false	false	TRUE

Expected Formula C29 H32 N4 O3 **Adduct(s):** H, radical

#	meas. m/z	theo. m/z	|Err|[ppm]	Sigma	Formula	Adduct	Adduct Mass
1	483.2388	483.2402	2.70	0.0040	C29H31N4O3	M- H	1.0078

Note: Sigma fits < 0.05 indicates high probability of correct MF

Mass Spectrometry
Analytical Services
School of Chemistry

The University of Nottingham

Sample-ID	t_arm_TDA_4_69	Lab	C13
Submitter	Tom Armstrong	Supervisor	Neil Thomas
Analysis Name	t_arm_TDA_4_69_582046_1_01_73257.d	Acquisition Date	3/7/2019 9:29:35 AM
Ionisation Mode	ESI Negative	Instrument	Bruker MicroTOF

-MS, 0.6-0.8min #51-66

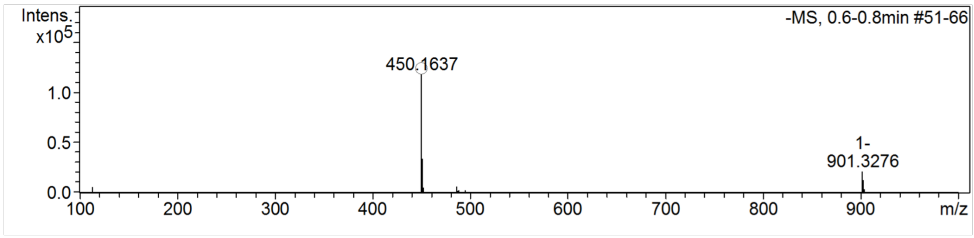

#	m/z	I %
1	112.9854	5.1
2	148.9512	0.5
3	151.0747	0.9
4	448.7122	0.6
5	450.1637	100.0
6	450.8586	0.5
7	451.1663	28.7
8	452.1666	4.7
9	453.1677	0.6
10	486.1397	5.4
11	487.1412	1.6
12	488.1367	2.1
13	495.1489	2.2
14	496.1503	0.6
15	528.0711	0.6
16	530.0702	0.6
17	901.3276	18.2
18	902.3315	10.9
19	903.3340	3.0
20	904.3381	0.7

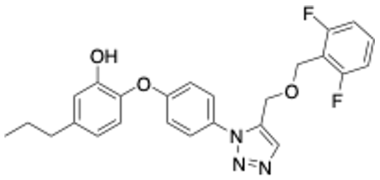

78

Generate Molecular Formula Parameters

Charge	Tolerance	sigma limit	H/C Ratio	Electron Conf.	Nitrogen Rule	Chrom.BackGround	Calibration
-1	6 ppm	0.08	3 - 0	both	false	false	TRUE

Expected Formula C25 H23 F2 N3 O3 **Adduct(s):** H, radical

#	meas. m/z	theo. m/z	|Err|[ppm]	Sigma	Formula	Adduct	Adduct Mass
1	450.1637	450.1635	0.50	0.0016	C25H22F2N3O3	M- H	1.0078

Note: Sigma fits < 0.05 indicates high probability of correct MF

Mass Spectrometry
Analytical Services
School of Chemistry

The University of Nottingham

Sample-ID	t_arm_TDA_3_281_HPLC_Solid	Lab	C13
Submitter	Tom Armstrong	Supervisor	Neil Thomas
Analysis Name	t_arm_TDA_3_281_HPLC_Solid_5855_55_01_76013.d	Acquisition Date	5/2/2019 8:18:56 AM
Ionisation Mode	ESI– Negative	Instrument	Bruker MicroTOF

-MS, 0.6-0.8min #51-67

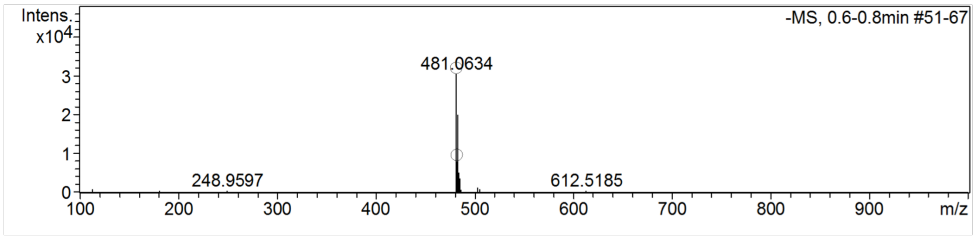

#	m/z	I %
1	112.9859	3.3
2	180.9726	1.6
3	248.9597	1.7
4	316.9493	0.8
5	480.6549	0.6
6	481.0634	100.0
7	481.5297	0.5
8	482.0666	26.3
9	483.0592	65.5
10	483.7865	0.3
11	484.0613	17.3
12	485.0587	12.1
13	486.0583	2.9
14	503.0427	4.4
15	504.0474	1.1
16	505.0402	3.2
17	506.0443	0.8
18	507.0405	0.4
19	612.5185	1.6
20	987.1046	0.4

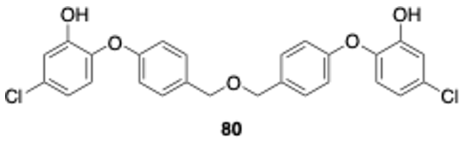

80

Generate Molecular Formula Parameters

Charge	Tolerance	sigma limit	H/C Ratio	Electron Conf.	Nitrogen Rule	Chrom.BackGround	Calibration
-1	6 ppm	0.08	3 - 0	both	false	false	TRUE

Expected Formula C26 H20 Cl2 O5 **Adduct(s):** H, radical

#	meas. m/z	theo. m/z	|Err|[ppm]	Sigma	Formula	Adduct	Adduct Mass
1	481.0634	481.0615	4.00	0.0189	C26H19Cl2O5	M- H	1.0078

Note: Sigma fits < 0.05 indicates high probability of correct MF

Mass Spectrometry
Analytical Services
School of Chemistry

The University of Nottingham

Sample-ID	t_arm_TDA_4_113_HPLC	Lab	C13
Submitter	Tom Armstrong	Supervisor	Neil Thomas
Analysis Name	t_arm_TDA_4_113_HPLC_585673_13_01_76091.d	Acquisition Date	5/3/2019 12:42:17 PM
Ionisation Mode	ESI Negative	Instrument	Bruker MicroTOF

-MS, 0.6-0.8min #50-66

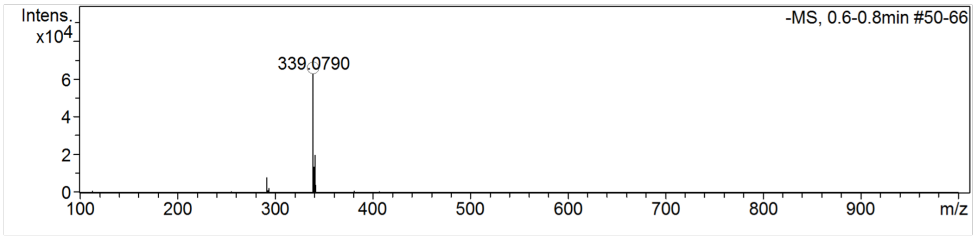

#	m/z	I %
1	112.9853	1.8
2	132.8673	0.8
3	134.8644	0.8
4	180.9727	0.9
5	184.0763	1.0
6	210.0549	0.6
7	248.9596	0.8
8	255.2301	1.4
9	283.2616	1.0
10	292.0009	13.1
11	293.0023	2.0
12	293.9993	4.2
13	339.0790	100.0
14	340.0810	22.0
15	341.0767	31.8
16	342.0778	6.8
17	343.0822	1.0
18	381.0628	1.7
19	383.0652	0.6
20	407.0647	1.3

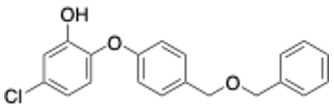

81

Generate Molecular Formula Parameters

Charge	Tolerance	sigma limit	H/C Ratio	Electron Conf.	Nitrogen Rule	Chrom.BackGround	Calibration
-1	6 ppm	0.08	3 - 0	both	false	false	TRUE

Expected Formula C20 H17 Cl1 O3 **Adduct(s):** H, radical

#	meas. m/z	theo. m/z	|Err|[ppm]	Sigma	Formula	Adduct	Adduct Mass
1	339.0790	339.0793	0.90	0.0141	C20H16ClO3	M- H	1.0078

Note: Sigma fits < 0.05 indicates high probability of correct MF

Mass Spectrometry
Analytical Services
School of Chemistry

The University of Nottingham

Sample-ID	t_arm_TDA_4_19_F10	Lab	C13
Submitter	Tom Armstrong	Supervisor	Neil Thomas
Analysis Name	t_arm_TDA_4_19_F10_580486_18_01_71943.d	Acquisition Date	2/13/2019 2:57:23 PM
Ionisation Mode	ESI Negative	Instrument	Bruker MicroTOF

-MS, 0.6-0.8min #51-67

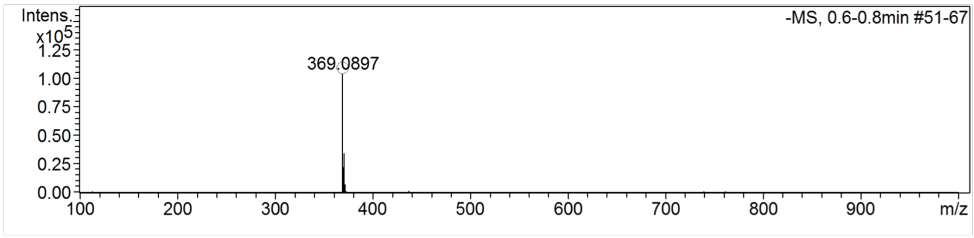

#	m/z	I %
1	112.9856	1.2
2	180.9726	0.6
3	255.2306	1.0
4	293.0564	0.7
5	369.0897	100.0
6	369.7565	0.5
7	369.8936	0.5
8	370.0932	21.8
9	371.0867	33.3
10	372.0895	7.3
11	373.0923	1.3
12	437.0752	1.8
13	446.9998	0.6
14	448.9966	0.9
15	739.1818	1.2
16	740.1867	0.5
17	741.1806	0.8
18	761.1647	1.6
19	762.1655	0.8
20	763.1627	1.1

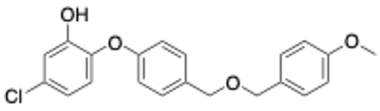

82

Generate Molecular Formula Parameters

Charge	Tolerance	sigma limit	H/C Ratio	Electron Conf.	Nitrogen Rule	Chrom.BackGround	Calibration
-1	6 ppm	0.08	3 - 0	both	false	false	TRUE

Expected Formula C21 H19 Cl1 O4 **Adduct(s):** H, radical

#	meas. m/z	theo. m/z	|Err|[ppm]	Sigma	Formula	Adduct	Adduct Mass
1	369.0897	369.0899	0.50	0.0111	C21H18ClO4	M- H	1.0078

Note: Sigma fits < 0.05 indicates high probability of correct MF

Mass Spectrometry
Analytical Services
School of Chemistry

The University of Nottingham

Sample-ID	t_arm_TDA_4_51_Cr	Lab	C13
Submitter	Tom Armstrong	Supervisor	Neil Thomas
Analysis Name	t_arm_TDA_4_51_Cr_581505_68_01_72795.d	Acquisition Date	2/28/2019 8:42:19 AM
Ionisation Mode	ESI Negative	Instrument	Bruker MicroTOF

-MS, 0.6-0.8min #51-67

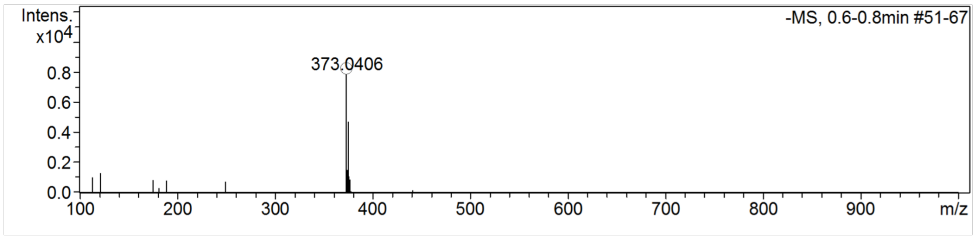

#	m/z	I %
1	112.9857	13.1
2	121.0284	16.8
3	174.9556	10.7
4	180.9737	4.1
5	189.0168	10.2
6	248.9607	9.6
7	373.0406	100.0
8	374.0422	19.5
9	375.0363	60.1
10	376.0413	13.9
11	377.0343	11.1
12	378.0389	1.5
13	441.0233	2.2
14	452.9466	0.7

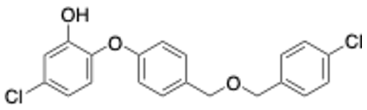

83

Generate Molecular Formula Parameters

Charge	Tolerance	sigma limit	H/C Ratio	Electron Conf.	Nitrogen Rule	Chrom.BackGround	Calibration
-1	6 ppm	0.08	3 - 0	both	false	false	TRUE

Expected Formula C20 H16 Cl2 O3 **Adduct(s):** H, radical

#	meas. m/z	theo. m/z	|Err|[ppm]	Sigma	Formula	Adduct	Adduct Mass
1	373.0406	373.0404	0.70	0.0300	C20H15Cl2O3	M- H	1.0078

Note: Sigma fits < 0.05 indicates high probability of correct MF

Mass Spectrometry
Analytical Services
School of Chemistry

The University of Nottingham

Sample-ID	t_arm_VDA_2_283_HPLC	Lab	C13
Submitter	Tom Armstrong	Supervisor	Neil Thomas
Analysis Name	t_arm_VDA_2_283_HPLC_01_82325.d	Acquisition Date	30/10/2019 4:03:02 PM
Ionisation Mode	ESI Negative	Instrument	Bruker MicroTOF

+MS, 0.6-0.8min #51-67

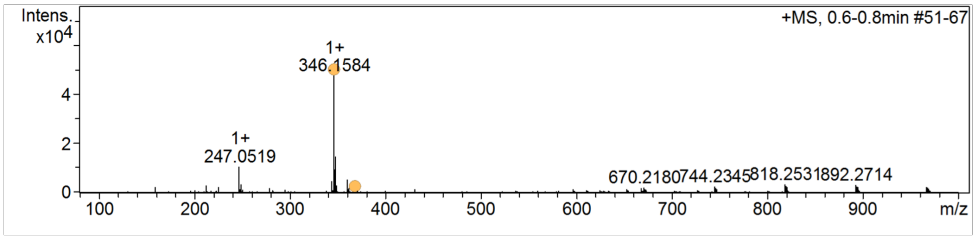

#	m/z	I %
1	152.9616	14.0
2	163.0595	5.0
3	186.9930	6.2
4	247.0519	23.2
5	249.0499	6.0
6	343.0478	9.8
7	346.9584	100.0
8	347.0606	20.2
9	348.0638	21.6
10	349.9980	106.0
11	360.0025	20.8
12	740.2960	35.0
13	818.2931	6.0
14	819.2937	5.3
15	820.2764	3.0
16	892.2887	6.3
17	895.2860	3.7
18	894.2702	3.9
19	966.2908	8.3
20	968.2900	5.5

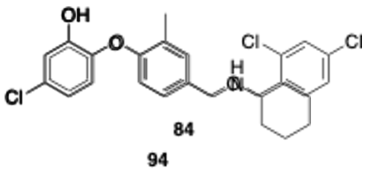

84

94

Generate Molecular Formula Parameters

Charge	Tolerance	sigma limit	H/C Ratio	Electron Conf.	Nitrogen Rule	Chrom.BackGround	Calibration
+1	6 ppm	0.08	3 - 0	both	false	false	TRUE

Expected Formula C20 H25 Cl3 N3 O2 **Adduct(s):** H, Na, NH4, C3H5N2, radical

#	meas. m/z	theo. m/z	|Err|[ppm]	Sigma	Formula	Adduct	Adduct Mass
1	346.0636	346.0638	0.50	0.0289	C20H25Cl3N3O2	M+H	1.0078

Note: Sigma fits < 0.05 indicates high probability of correct MF

Mass Spectrometry
Analytical Services
School of Chemistry

The University of Nottingham

Sample-ID	t_arm_TDA_4_107	Lab	C13
Submitter	Tom Armstrong	Supervisor	Neil Thomas
Analysis Name	t_arm_TDA_4_107_583167_9_01_74144.d	Acquisition Date	3/22/2019 10:47:24 AM
Ionisation Mode	ESI Negative	Instrument	Bruker MicroTOF

-MS, 0.6-0.8min #51-67

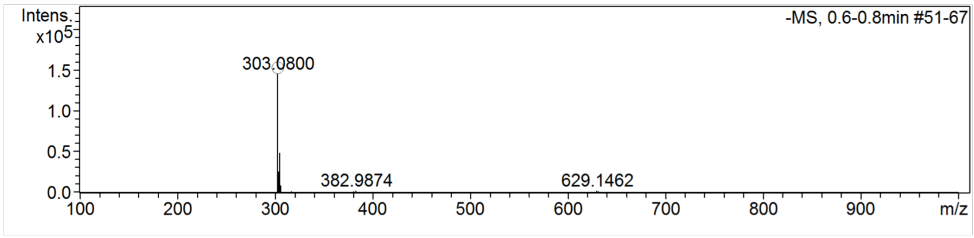

#	m/z	I %
1	112.9853	0.6
2	302.1224	0.5
3	303.0800	100.0
4	304.0827	18.1
5	305.0772	33.9
6	306.0794	6.2
7	307.0829	0.9
8	317.0576	1.5
9	319.0557	0.5
10	371.0658	0.6
11	380.9893	1.4
12	382.9874	1.9
13	629.1462	1.7
14	630.1485	0.7
15	631.1438	1.2
16	979.2313	0.8
17	980.2374	0.6
18	981.2325	1.0
19	982.2319	0.6
20	983.2298	0.7

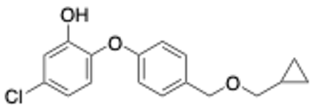

85

Generate Molecular Formula Parameters

Charge	Tolerance	sigma limit	H/C Ratio	Electron Conf.	Nitrogen Rule	Chrom.BackGround	Calibration
-1	6 ppm	0.08	3 - 0	both	false	false	TRUE

Expected Formula C17 H17 Cl1 O3 **Adduct(s):** H, radical

#	meas. m/z	theo. m/z	|Err|[ppm]	Sigma	Formula	Adduct	Adduct Mass
1	303.0800	303.0793	2.10	0.0032	C17H16ClO3	M- H	1.0078

Note: Sigma fits < 0.05 indicates high probability of correct MF

Mass Spectrometry
Analytical Services
School of Chemistry

The University of Nottingham

Sample-ID	t_arm_TDA_4_115	Lab	C13
Submitter	Tom Armstrong	Supervisor	Neil Thomas
Analysis Name	t_arm_TDA_4_115_583374_47_01_74317.d	Acquisition Date	3/26/2019 3:57:08 PM
Ionisation Mode	ESI Negative	Instrument	Bruker MicroTOF

-MS, 0.6-0.8min #51-66

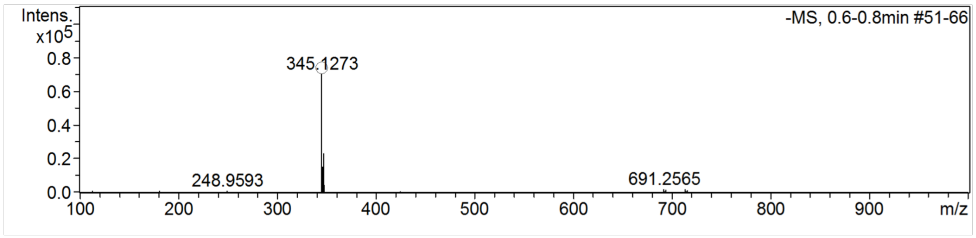

#	m/z	I %
1	112.9857	2.0
2	180.9724	1.6
3	248.9593	1.7
4	345.1273	100.0
5	346.1292	22.3
6	347.1244	33.6
7	348.1247	6.7
8	349.1281	0.9
9	413.1104	0.8
10	423.0349	1.0
11	425.0333	1.3
12	481.0993	0.8
13	691.2565	3.2
14	692.2598	1.4
15	693.2527	2.5
16	694.2583	1.0
17	713.2370	3.0
18	714.2431	1.2
19	715.2336	2.1
20	716.2392	0.8

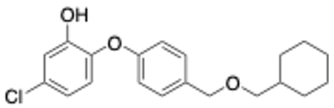

86

Generate Molecular Formula Parameters

Charge	Tolerance	sigma limit	H/C Ratio	Electron Conf.	Nitrogen Rule	Chrom.BackGround	Calibration
-1	6 ppm	0.08	3 - 0	both	false	false	TRUE

Expected Formula C20 H23 Cl1 O3 **Adduct(s):** H, radical

#	meas. m/z	theo. m/z	|Err|[ppm]	Sigma	Formula	Adduct	Adduct Mass
1	345.1273	345.1263	3.00	0.0068	C20H22ClO3	M- H	1.0078

Note: Sigma fits < 0.05 indicates high probability of correct MF

Mass Spectrometry
Analytical Services
School of Chemistry

The University of Nottingham

Sample-ID	t_arm_TDA_3_67_F17	Lab	C13
Submitter	Tom Armstrong	Supervisor	Neil Thomas
Analysis Name	t_arm_TDA_3_67_F17_578076_5_01_70040.d	Acquisition Date	12/17/2018 12:21:24 PM
Ionisation Mode	ESI Positive	Instrument	Bruker MicroTOF

+MS, 0.6-0.8min #50-66

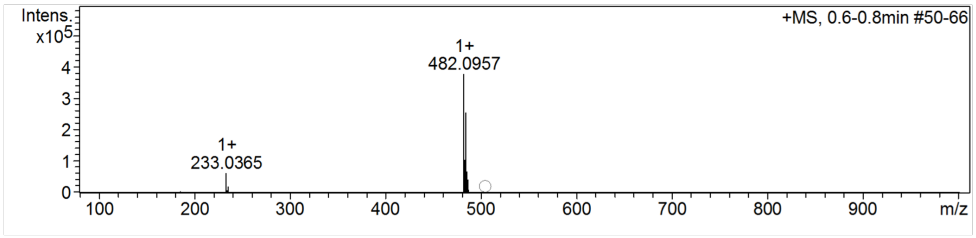

#	m/z	I %
1	132.9588	1.0
2	185.1156	1.1
3	233.0365	16.6
4	234.0398	2.2
5	235.0339	5.4
6	236.0379	0.7
7	482.0957	100.0
8	483.0980	28.0
9	484.0928	67.4
10	485.0945	18.2
11	486.0903	11.1
12	487.0906	2.6
13	488.0899	0.5
14	644.2148	0.5
15	646.2135	0.5
16	963.1798	0.8
17	964.1800	0.5
18	965.1718	0.9
19	966.1761	0.5
20	967.1723	0.7

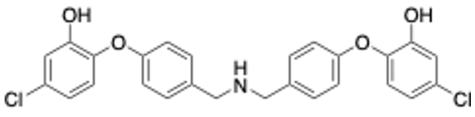

87

Generate Molecular Formula Parameters

Charge	Tolerance	sigma limit	H/C Ratio	Electron Conf.	Nitrogen Rule	Chrom.BackGround	Calibration
+1	6 ppm	0.08	3 - 0	both	false	false	TRUE

Expected Formula C26 H21 Cl2 N1 O4 **Adduct(s):** H, Na, NH4, C3H5N2, radical

#	meas. m/z	theo. m/z	|Err|[ppm]	Sigma	Formula	Adduct	Adduct Mass
1	504.0724	504.0740	3.20	0.0545	C26H21Cl2NNaO4	M+Na	22.9898

Note: Sigma fits < 0.05 indicates high probability of correct MF

Mass Spectrometry
Analytical Services
School of Chemistry

The University of Nottingham

Sample-ID	t_arm_TDA_2_203_Cr	Lab	C13
Submitter	Tom Armstrong	Supervisor	Neil Thomas
Analysis Name	t_arm_TDA_2_203_Cr_571524_21_01_64389.d	Acquisition Date	8/20/2018 2:36:41 PM
Ionisation Mode	ESI Positive	Instrument	Bruker MicroTOF

+MS, 0.6-0.8min #51-67

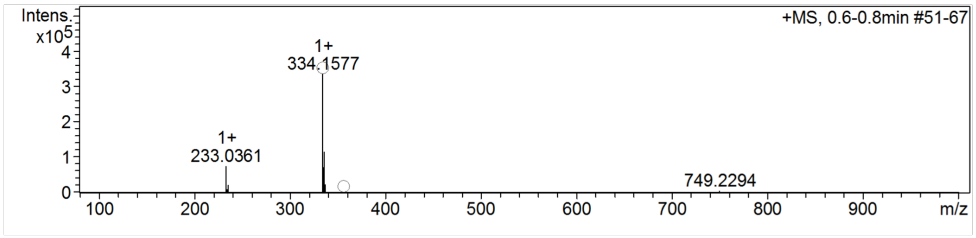

#	m/z	I %
1	144.1383	1.1
2	233.0361	22.7
3	234.0391	3.3
4	235.0337	7.0
5	236.0362	1.0
6	334.1577	100.0
7	334.5898	0.6
8	335.1609	21.5
9	336.1553	34.7
10	337.1575	7.2
11	338.1604	0.9
12	473.1557	0.5
13	475.1542	0.7
14	477.2864	0.5
15	612.3055	0.5
16	724.4330	0.6
17	747.2314	1.0
18	749.2294	1.7
19	750.2317	0.8
20	751.2263	0.9

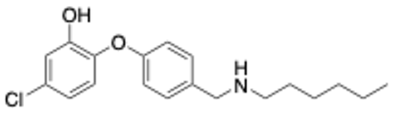

88

Generate Molecular Formula Parameters

Charge	Tolerance	sigma limit	H/C Ratio	Electron Conf.	Nitrogen Rule	Chrom.BackGround	Calibration
+1	6 ppm	0.08	3 - 0	both	false	false	TRUE

Expected Formula C19 H24 Cl1 N1 O2 **Adduct(s):** H, Na, NH4, C3H5N2, radical

#	meas. m/z	theo. m/z	|Err|[ppm]	Sigma	Formula	Adduct	Adduct Mass
1	334.1577	334.1568	2.50	0.0015	C19H25ClNO2	M+H	1.0078

Note: Sigma fits < 0.05 indicates high probability of correct MF

Mass Spectrometry
Analytical Services
School of Chemistry

The University of Nottingham

Sample-ID	t_arm_TDA_2_211_Pure_Sample	Lab	C13
Submitter	Tom Armstrong	Supervisor	Neil Thomas
Analysis Name	t_arm_TDA_2_211_Pure_Sample_597_15_01_85117.d	Acquisition Date	1/15/2020 1:12:32 PM
Ionisation Mode	ESI – Positive	Instrument	Bruker MicroTOF

+MS, 0.6-0.8min #51-67

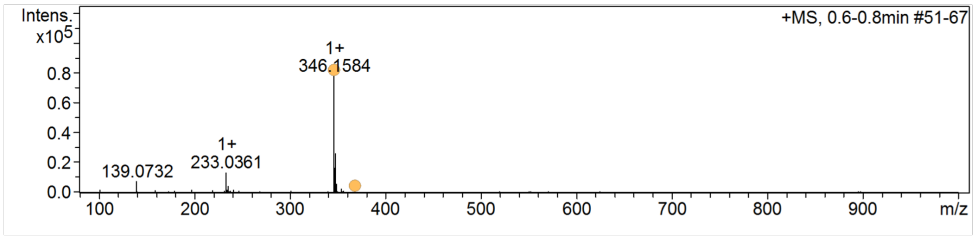

#	m/z	I %
1	101.0028	2.1
2	139.0732	9.8
3	158.9649	1.9
4	179.1020	1.2
5	197.1133	2.2
6	219.1860	1.7
7	231.1194	1.3
8	233.0361	17.5
9	234.0389	2.4
10	235.0337	5.5
11	237.2328	1.6
12	241.1682	2.1
13	247.0524	1.5
14	301.1391	1.6
15	346.1584	100.0
16	347.1609	21.6
17	348.1549	34.0
18	349.1584	7.1
19	354.1259	3.0
20	356.1235	1.2

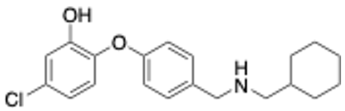

89

Generate Molecular Formula Parameters

Charge	Tolerance	sigma limit	H/C Ratio	Electron Conf.	Nitrogen Rule	Chrom.BackGround	Calibration
+1	6 ppm	0.08	3 - 0	both	false	false	TRUE

Expected Formula C20 H24 Cl1 N1 O2 **Adduct(s):** H, Na, NH4, C3H5N2, radical

#	meas. m/z	theo. m/z	|Err|[ppm]	Sigma	Formula	Adduct	Adduct Mass
1	346.1584	346.1568	4.50	0.0051	C20H25ClNO2	M+H	1.0078

Note: Sigma fits < 0.05 indicates high probability of correct MF

Mass Spectrometry
Analytical Services
School of Chemistry

The University of Nottingham

Sample-ID	t_arm_Org	Lab	C13
Submitter	Tom Armstrong	Supervisor	Neil Thomas
Analysis Name	t_arm_Org_571806_51_01_64642.d	Acquisition Date	8/24/2018 4:19:42 PM
Ionisation Mode	ESI Positive	Instrument	Bruker MicroTOF

+MS, 0.6-0.8min #51-67

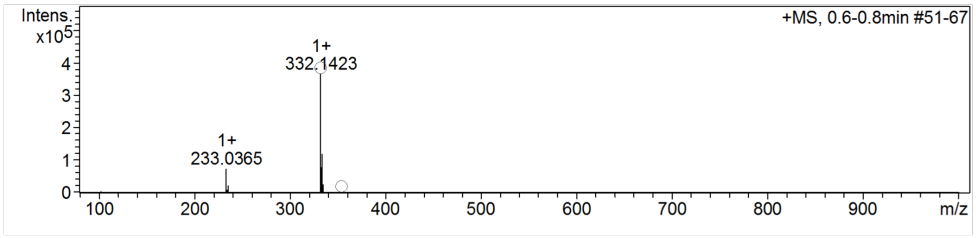

#	m/z	I %
1	102.1279	1.5
2	160.1326	0.8
3	184.9723	0.4
4	215.1301	0.8
5	233.0365	20.0
6	234.0399	2.7
7	235.0338	6.4
8	236.0366	0.9
9	332.1423	100.0
10	332.6113	0.4
11	332.7450	0.4
12	333.1450	21.5
13	334.1393	32.9
14	335.1421	7.0
15	336.1442	0.9
16	722.4172	0.8
17	723.4224	0.4
18	724.4169	0.4
19	745.2080	0.6
20	777.2610	0.5

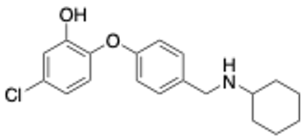

90

Generate Molecular Formula Parameters

Charge	Tolerance	sigma limit	H/C Ratio	Electron Conf.	Nitrogen Rule	Chrom.BackGround	Calibration
+1	6 ppm	0.08	3 - 0	both	false	false	TRUE

Expected Formula C19 H22 Cl1 N1 O2 **Adduct(s):** H, Na, NH4, C3H5N2, radical

#	meas. m/z	theo. m/z	|Err|[ppm]	Sigma	Formula	Adduct	Adduct Mass
1	332.1423	332.1412	3.50	0.0073	C19H23ClNO2	M+H	1.0078
1	354.1218	354.1231	3.80	0.0394	C19H22ClNNaO2	M+Na	22.9898

Note: Sigma fits < 0.05 indicates high probability of correct MF

Mass Spectrometry
Analytical Services
School of Chemistry

The University of Nottingham

Sample-ID	t_arm_TDA_3_9_Cr	Lab	C13
Submitter	Tom Armstrong	Supervisor	Neil Thomas
Analysis Name	t_arm_TDA_3_9_Cr_573375_2_01_66096.d	Acquisition Date	10/4/2018 8:55:04 AM
Ionisation Mode	ESI Positive	Instrument	Bruker MicroTOF

+MS, 0.6-0.8min #51-67

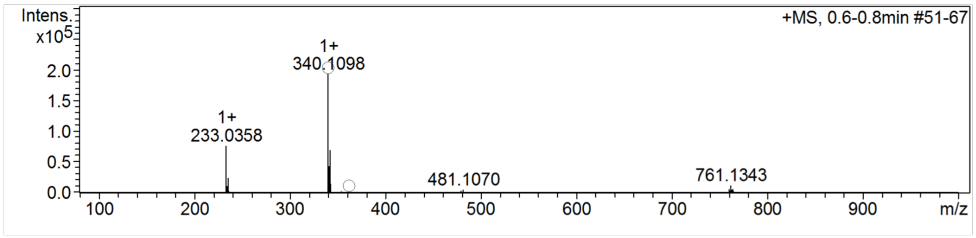

#	m/z	I %
1	233.0358	39.5
2	234.0393	5.8
3	235.0333	12.5
4	236.0360	1.8
5	258.1717	1.0
6	274.1504	1.0
7	340.1098	100.0
8	341.1125	22.6
9	342.1071	35.9
10	343.1103	7.5
11	354.1238	1.4
12	382.1201	1.0
13	479.1087	1.9
14	481.1070	2.5
15	759.1382	3.4
16	760.1399	1.6
17	761.1343	6.1
18	762.1377	2.7
19	763.1323	3.2
20	764.1344	1.2

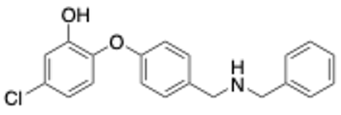

91

Generate Molecular Formula Parameters

Charge	Tolerance	sigma limit	H/C Ratio	Electron Conf.	Nitrogen Rule	Chrom.BackGround	Calibration
+1	6 ppm	0.08	3 - 0	both	false	false	TRUE

Expected Formula C20 H18 Cl1 N1 O2 **Adduct(s):** H, Na, NH4, C3H5N2, radical

#	meas. m/z	theo. m/z	|Err|[ppm]	Sigma	Formula	Adduct	Adduct Mass
1	340.1098	340.1099	0.30	0.0054	C20H19ClNO2	M+H	1.0078
1	362.0937	362.0918	5.30	0.0514	C20H18ClNNaO2	M+Na	22.9898

Note: Sigma fits < 0.05 indicates high probability of correct MF

Mass Spectrometry
Analytical Services
School of Chemistry

The University of Nottingham

Sample-ID	t_arm_TDA_3_229_Cr	Lab	C13
Submitter	Tom Armstrong	Supervisor	Neil Thomas
Analysis Name	t_arm_TDA_3_229_Cr_578221_4_01_70180.d	Acquisition Date	12/19/2018 10:15:07 AM
Ionisation Mode	ESI Negative	Instrument	Bruker MicroTOF

-MS, 0.6-0.8min #50-66

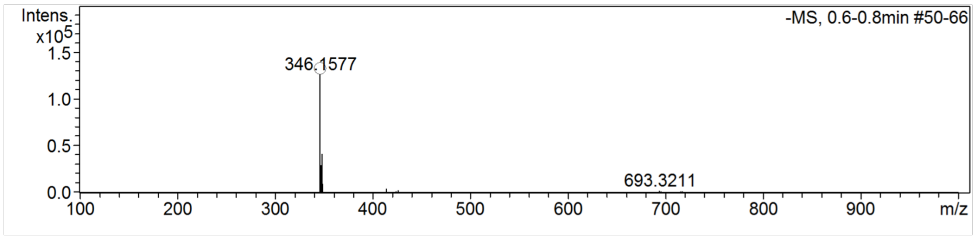

#	m/z	I %
1	261.0310	0.9
2	346.1577	100.0
3	347.1607	23.6
4	348.1560	33.0
5	349.1577	7.5
6	350.1621	0.9
7	380.1184	0.9
8	382.1148	0.7
9	414.1451	3.5
10	415.1463	0.6
11	416.1404	1.0
12	424.0652	1.5
13	426.0654	2.2
14	693.3211	1.8
15	694.3210	0.9
16	695.3198	1.2
17	696.3188	0.6
18	715.3031	1.3
19	716.3032	0.7
20	717.2982	1.2

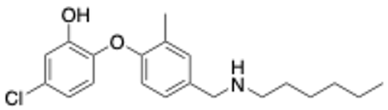

92

Generate Molecular Formula Parameters

Charge	Tolerance	sigma limit	H/C Ratio	Electron Conf.	Nitrogen Rule	Chrom.BackGround	Calibration
-1	6 ppm	0.08	3 - 0	both	false	false	TRUE

Expected Formula C20 H26 Cl1 N1 O2 **Adduct(s):** H, radical

#	meas. m/z	theo. m/z	|Err|[ppm]	Sigma	Formula	Adduct	Adduct Mass
1	346.1577	346.1579	0.60	0.0098	C20H25ClNO2	M- H	1.0078

Note: Sigma fits < 0.05 indicates high probability of correct MF

Mass Spectrometry
Analytical Services
School of Chemistry

The University of Nottingham

Sample-ID	t_arm_TDA_3_17	Lab	C13
Submitter	Tom Armstrong	Supervisor	Neil Thomas
Analysis Name	t_arm_TDA_3_17_594047_11_01_82285.d	Acquisition Date	10/31/2019 12:18:09 PM
Ionisation Mode	ESI Negative	Instrument	Bruker MicroTOF

-MS, 0.6-0.8min #51-66

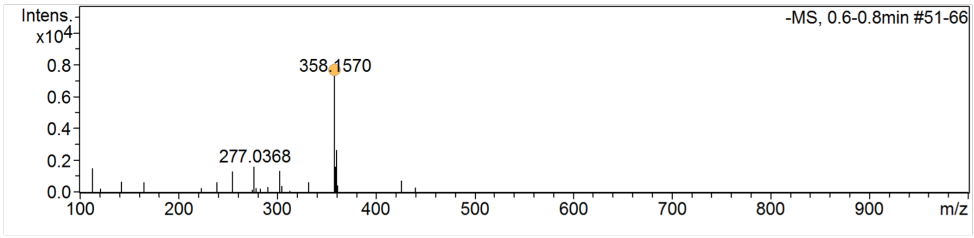

#	m/z	I %
1	112.9853	21.1
2	121.0293	3.4
3	142.0053	9.4
4	165.0397	8.7
5	223.0272	3.6
6	239.0590	8.7
7	255.2320	18.5
8	277.0368	22.5
9	279.0348	3.8
10	283.2624	3.1
11	291.0176	4.6
12	303.0787	18.7
13	305.0756	5.3
14	332.1422	8.9
15	358.1570	100.0
16	359.1612	22.5
17	360.1554	36.9
18	361.1581	5.9
19	426.1445	10.1
20	440.0582	3.9

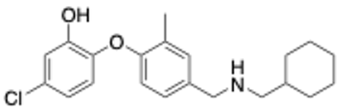

93

Generate Molecular Formula Parameters

Charge	Tolerance	sigma limit	H/C Ratio	Electron Conf.	Nitrogen Rule	Chrom.BackGround	Calibration
-1	6 ppm	0.08	3 - 0	both	false	false	TRUE

Expected Formula C21 H26 Cl1 N1 O2 **Adduct(s):** H, radical

#	meas. m/z	theo. m/z	|Err|[ppm]	Sigma	Formula	Adduct	Adduct Mass
1	358.1570	358.1579	2.70	0.0133	C21H25ClNO2	M- H	1.0078

Note: Sigma fits < 0.05 indicates high probability of correct MF

Mass Spectrometry
Analytical Services
School of Chemistry

The University of Nottingham

Sample-ID	t_arm_TDA_3_5_Col	Lab	C13
Submitter	Tom Armstrong	Supervisor	Neil Thomas
Analysis Name	t_arm_TDA_3_5_Col_573355_29_01_66083.d	Acquisition Date	10/3/2018 4:40:01 PM
Ionisation Mode	ESI Positive	Instrument	Bruker MicroTOF

+MS, 0.6-0.8min #50-66

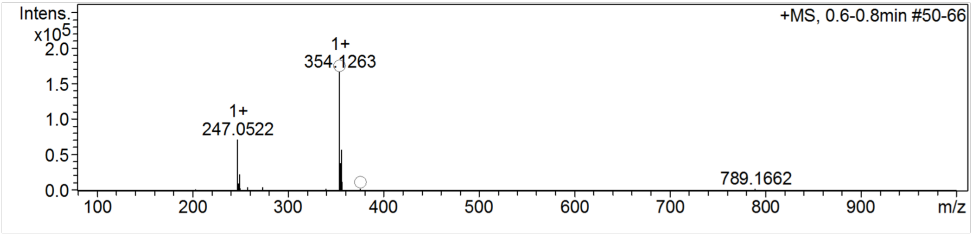

#	m/z	I %
1	203.0757	1.5
2	242.2840	0.8
3	244.2082	1.1
4	247.0522	43.0
5	248.0546	6.4
6	249.0494	14.0
7	250.0525	2.2
8	258.1726	3.4
9	274.1502	3.0
10	340.1091	1.6
11	354.1263	100.0
12	355.1283	23.4
13	356.1236	34.7
14	357.1256	7.5
15	358.1293	1.0
16	376.1069	1.8
17	787.1673	1.0
18	789.1662	1.7
19	790.1690	0.8
20	791.1648	0.9

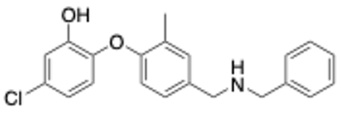

95

Generate Molecular Formula Parameters

Charge	Tolerance	sigma limit	H/C Ratio	Electron Conf.	Nitrogen Rule	Chrom.BackGround	Calibration
+1	6 ppm	0.08	3 - 0	both	false	false	TRUE

Expected Formula C21 H20 Cl1 N1 O2 **Adduct(s):** H, Na, NH4, C3H5N2, radical

#	meas. m/z	theo. m/z	|Err|[ppm]	Sigma	Formula	Adduct	Adduct Mass
1	354.1263	354.1255	2.20	0.0017	C21H21ClNO2	M+H	1.0078
1	376.1069	376.1075	1.60	0.0119	C21H20ClNNaO2	M+Na	22.9898

Note: Sigma fits < 0.05 indicates high probability of correct MF

Mass Spectrometry
Analytical Services
School of Chemistry

The University of Nottingham

Sample-ID	t_arm_TDA_5_171	Lab	C13
Submitter	Tom Armstrong	Supervisor	Neil Thomas
Analysis Name	t_arm_TDA_5_171_601213_31_01_87867.d	Acquisition Date	3/5/2020 4:02:13 PM
Ionisation Mode	ESI Negative	Instrument	Bruker MicroTOF

-MS, 0.6-0.8min #51-67

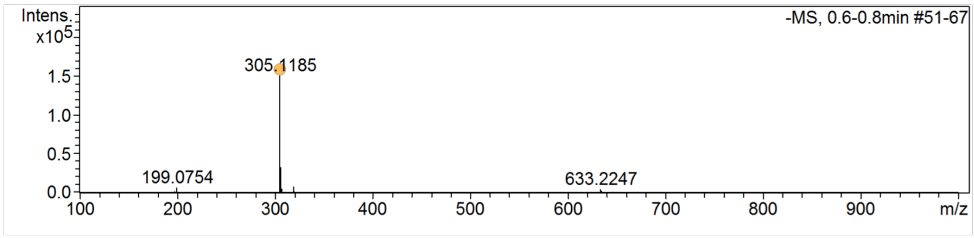

#	m/z	I %
1	197.0594	0.7
2	199.0754	4.2
3	200.0794	0.7
4	304.1496	0.6
5	304.5035	0.1
6	304.7750	0.1
7	305.1185	100.0
8	305.5199	0.0
9	305.5635	0.0
10	305.9373	0.2
11	306.1219	21.9
12	307.1244	3.1
13	308.1253	0.3
14	319.0974	4.9
15	320.1008	1.0
16	373.1048	0.5
17	611.2453	0.1
18	633.2247	2.9
19	634.2290	1.2
20	647.2031	0.3

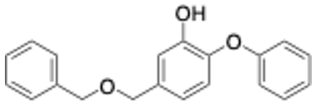

96

Generate Molecular Formula Parameters

Charge	Tolerance	sigma limit	H/C Ratio	Electron Conf.	Nitrogen Rule	Chrom.BackGround	Calibration
-1	6 ppm	0.08	3 - 0	both	false	false	TRUE

Expected Formula C20 H18 O3 **Adduct(s):** H, radical

#	meas. m/z	theo. m/z	|Err|[ppm]	Sigma	Formula	Adduct	Adduct Mass
1	305.1185	305.1183	0.50	0.0011	C20H17O3	M- H	1.0078

Note: Sigma fits < 0.05 indicates high probability of correct MF

Mass Spectrometry
Analytical Services
School of Chemistry

The University of Nottingham

Sample-ID	t_arm_TDA_5_169_8min	Lab	C13
Submitter	Tom Armstrong	Supervisor	Neil Thomas
Analysis Name	t_arm_TDA_5_169_8min_600425_25_01_87274.d	Acquisition Date	2/26/2020 12:51:26 PM
Ionisation Mode	ESI Negative	Instrument	Bruker MicroTOF

-MS, 0.6-0.8min #51-66

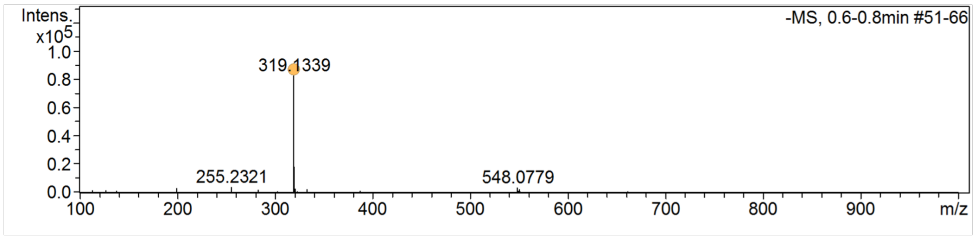

#	m/z	I %
1	112.9857	2.0
2	126.9043	1.9
3	138.0194	1.5
4	199.0757	3.6
5	255.2321	4.5
6	256.2352	0.6
7	283.2632	2.2
8	303.0788	0.9
9	319.1339	100.0
10	320.1369	22.2
11	321.1398	3.2
12	323.2200	0.9
13	333.1131	2.9
14	352.1099	0.6
15	387.1208	1.1
16	548.0779	3.9
17	549.0793	1.2
18	550.0747	2.7
19	551.0775	0.7
20	661.2549	1.1

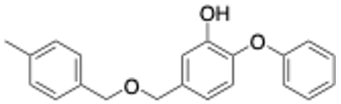

97

Generate Molecular Formula Parameters

Charge	Tolerance	sigma limit	H/C Ratio	Electron Conf.	Nitrogen Rule	Chrom.BackGround	Calibration
-1	6 ppm	0.08	3 - 0	both	false	false	TRUE

Expected Formula C21 H20 O3 **Adduct(s):** H, radical

#	meas. m/z	theo. m/z	|Err|[ppm]	Sigma	Formula	Adduct	Adduct Mass
1	319.1339	319.1340	0.30	0.0052	C21H19O3	M- H	1.0078

Note: Sigma fits < 0.05 indicates high probability of correct MF

Mass Spectrometry
Analytical Services
School of Chemistry

The University of Nottingham

Sample-ID	t_arm_TDA_5_187	Lab	C13
Submitter	Tom Armstrong	Supervisor	Neil Thomas
Analysis Name	t_arm_TDA_5_187_601181_14_01_87846.d	Acquisition Date	3/5/2020 12:17:02 PM
Ionisation Mode	ESI Negative	Instrument	Bruker MicroTOF

-MS, 0.6-0.8min #50-66

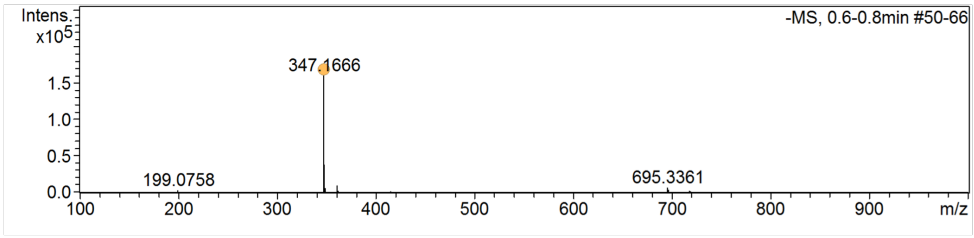

#	m/z	I %
1	112.9848	0.1
2	149.0963	0.5
3	165.0394	0.1
4	199.0758	1.8
5	239.0589	0.2
6	255.2337	0.2
7	299.1777	0.4
8	346.0532	0.6
9	347.1666	100.0
10	348.1689	24.0
11	349.1714	3.6
12	350.1719	0.5
13	361.1439	5.9
14	362.1466	1.5
15	415.1520	0.8
16	695.3361	4.3
17	696.3390	2.3
18	697.3429	0.6
19	717.3182	1.6
20	718.3194	0.8

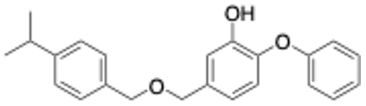

98

Generate Molecular Formula Parameters

Charge	Tolerance	sigma limit	H/C Ratio	Electron Conf.	Nitrogen Rule	Chrom.BackGround	Calibration
-1	6 ppm	0.08	3 - 0	both	false	false	TRUE

Expected Formula C23 H24 O3 **Adduct(s):** H, radical

#	meas. m/z	theo. m/z	|Err|[ppm]	Sigma	Formula	Adduct	Adduct Mass
1	347.1666	347.1653	3.80	0.0072	C23H23O3	M- H	1.0078

Note: Sigma fits < 0.05 indicates high probability of correct MF

Mass Spectrometry
Analytical Services
School of Chemistry

The University of Nottingham

Sample-ID	t_arm_TDA_5_185	Lab	C13
Submitter	Tom Armstrong	Supervisor	Neil Thomas
Analysis Name	t_arm_TDA_5_185_601204_21_01_87853.d	Acquisition Date	3/5/2020 2:14:08 PM
Ionisation Mode	ESI Negative	Instrument	Bruker MicroTOF

-MS, 0.6-0.8min #51-67

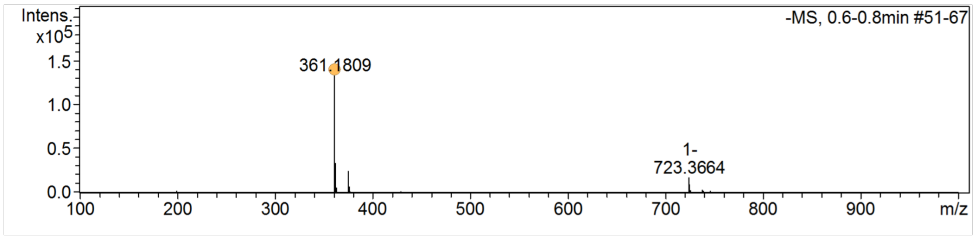

#	m/z	I %
1	163.1115	0.4
2	199.0746	1.2
3	239.0578	0.3
4	360.0252	0.6
5	361.1809	100.0
6	362.1835	25.5
7	363.1855	4.2
8	364.1872	0.5
9	375.1588	18.6
10	376.1628	5.2
11	377.1651	0.7
12	429.1667	0.9
13	723.3664	12.6
14	724.3686	6.7
15	725.3727	2.0
16	737.3448	2.4
17	738.3476	1.2
18	745.3464	1.2
19	746.3500	0.6
20	759.3260	0.5

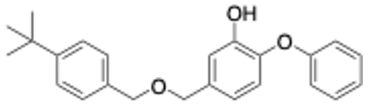

99

Generate Molecular Formula Parameters

Charge	Tolerance	sigma limit	H/C Ratio	Electron Conf.	Nitrogen Rule	Chrom.BackGround	Calibration
-1	6 ppm	0.08	3 - 0	both	false	false	TRUE

Expected Formula C24 H26 O3 **Adduct(s):** H, radical

#	meas. m/z	theo. m/z	|Err|[ppm]	Sigma	Formula	Adduct	Adduct Mass
1	361.1809	361.1809	0.00	0.0049	C24H25O3	M- H	1.0078

Note: Sigma fits < 0.05 indicates high probability of correct MF

Mass Spectrometry
Analytical Services
School of Chemistry

The University of Nottingham

Sample-ID	t_arm_TDA_5_183_HPLC	Lab	C13
Submitter	Tom Armstrong	Supervisor	Neil Thomas
Analysis Name	t_arm_TDA_5_183_HPLC_600886_30_01_87617.d	Acquisition Date	3/2/2020 4:18:48 PM
Ionisation Mode	ESI Negative	Instrument	Bruker MicroTOF

-MS, 0.6-0.8min #51-66

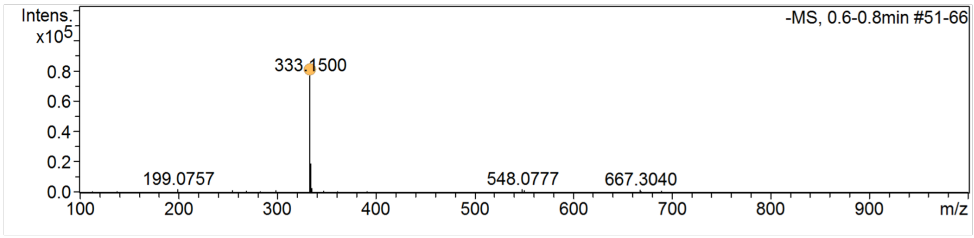

#	m/z	I %
1	112.9851	0.8
2	138.0193	0.8
3	199.0757	2.7
4	255.2324	1.9
5	269.1178	1.4
6	283.2630	0.9
7	299.1656	1.7
8	311.0751	0.6
9	333.1500	100.0
10	334.1523	24.9
11	335.1553	3.7
12	347.1650	1.6
13	361.1789	0.9
14	391.1080	0.8
15	401.1373	0.6
16	548.0777	2.7
17	550.0741	1.8
18	667.3040	2.2
19	668.3081	1.0
20	689.2854	1.3

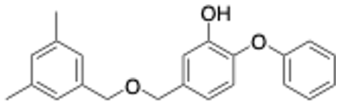

100

Generate Molecular Formula Parameters

Charge	Tolerance	sigma limit	H/C Ratio	Electron Conf.	Nitrogen Rule	Chrom.BackGround	Calibration
-1	6 ppm	0.08	3 - 0	both	false	false	TRUE

Expected Formula C22 H22 O3 **Adduct(s):** H, radical

#	meas. m/z	theo. m/z	|Err|[ppm]	Sigma	Formula	Adduct	Adduct Mass
1	333.1500	333.1496	1.20	0.0047	C22H21O3	M- H	1.0078

Note: Sigma fits < 0.05 indicates high probability of correct MF

Mass Spectrometry
Analytical Services
School of Chemistry

The University of Nottingham

Sample-ID	t_arm_TDA_5_163_2	Lab	C13
Submitter	Tom Armstrong	Supervisor	Neil Thomas
Analysis Name	t_arm_TDA_5_163_2_601212_30_01_87866.d	Acquisition Date	3/5/2020 3:59:38 PM
Ionisation Mode	ESI Negative	Instrument	Bruker MicroTOF

-MS, 0.6-0.8min #51-66

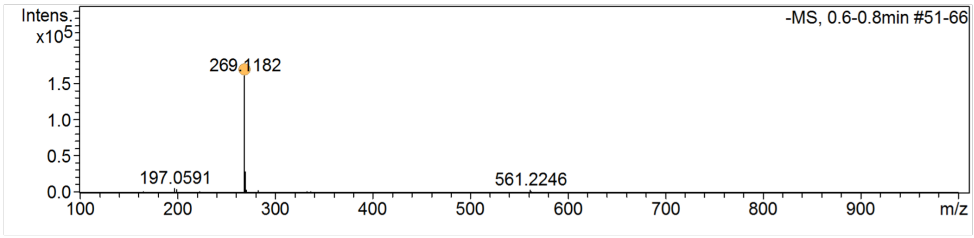

#	m/z	I %
1	165.0398	1.0
2	197.0591	3.8
3	198.0635	0.5
4	199.0751	2.6
5	200.0782	0.3
6	223.0275	0.9
7	239.0579	0.4
8	268.2681	0.7
9	269.1182	100.0
10	269.7626	0.1
11	269.9361	0.1
12	270.1211	18.1
13	271.1230	2.3
14	283.1016	1.7
15	287.0479	0.4
16	313.0787	0.2
17	333.1485	0.8
18	337.1089	0.7
19	561.2246	2.4
20	562.2273	0.9

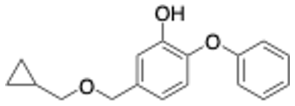

101

Generate Molecular Formula Parameters

Charge	Tolerance	sigma limit	H/C Ratio	Electron Conf.	Nitrogen Rule	Chrom.BackGround	Calibration
-1	6 ppm	0.08	3 - 0	both	false	false	TRUE

Expected Formula C17 H18 O3 **Adduct(s):** H, radical

#	meas. m/z	theo. m/z	|Err|[ppm]	Sigma	Formula	Adduct	Adduct Mass
1	269.1182	269.1183	0.40	0.0037	C17H17O3	M- H	1.0078

Note: Sigma fits < 0.05 indicates high probability of correct MF

Mass Spectrometry
Analytical Services
School of Chemistry

The University of Nottingham

Sample-ID	t_arm_TDA_5_189_R_T_18min	Lab	C13
Submitter	Tom Armstrong	Supervisor	Neil Thomas
Analysis Name	t_arm_TDA_5_189_R_T_18min_60035_62_01_87199.d	Acquisition Date	2/25/2020 5:07:48 PM
Ionisation Mode	ESI – Negative	Instrument	Bruker MicroTOF

-MS, 0.6-0.8min #51-66

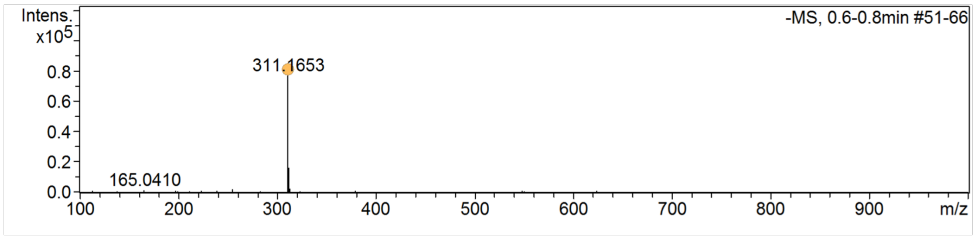

#	m/z	I %
1	112.9853	1.3
2	138.0193	0.8
3	165.0410	1.7
4	197.0597	1.2
5	199.0756	1.0
6	211.0961	1.1
7	223.0285	1.5
8	239.0588	1.4
9	255.2320	2.6
10	283.2639	1.1
11	303.0789	0.7
12	311.1653	100.0
13	312.1685	21.5
14	313.0832	1.2
15	313.1711	3.0
16	323.2197	0.7
17	379.1525	1.4
18	548.0788	1.5
19	550.0747	1.0
20	623.3370	1.4

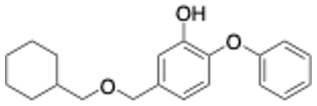

102

Generate Molecular Formula Parameters

Charge	Tolerance	sigma limit	H/C Ratio	Electron Conf.	Nitrogen Rule	Chrom.BackGround	Calibration
-1	6 ppm	0.08	3 - 0	both	false	false	TRUE

Expected Formula C20 H24 O3 **Adduct(s):** H, radical

#	meas. m/z	theo. m/z	|Err|[ppm]	Sigma	Formula	Adduct	Adduct Mass
1	311.1653	311.1653	0.10	0.0032	C20H23O3	M- H	1.0078

Note: Sigma fits < 0.05 indicates high probability of correct MF

Mass Spectrometry
Analytical Services
School of Chemistry

The University of Nottingham

Sample-ID	t_arm_TDA_5_193	Lab	C13
Submitter	Tom Armstrong	Supervisor	Neil Thomas
Analysis Name	t_arm_TDA_5_193_601182_13_01_87845.d	Acquisition Date	3/5/2020 12:14:27 PM
Ionisation Mode	ESI Negative	Instrument	Bruker MicroTOF

-MS, 0.6-0.8min #50-66

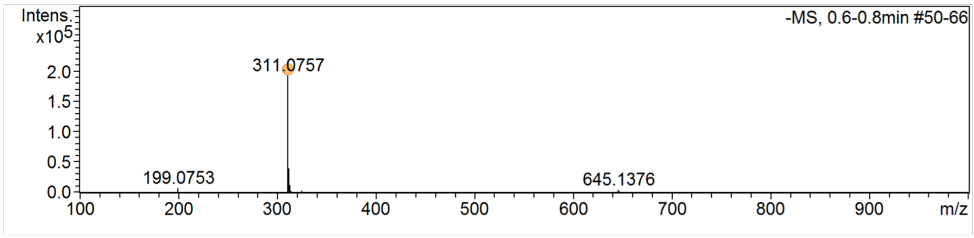

#	m/z	I %
1	112.9985	0.1
2	197.0594	0.6
3	199.0753	3.7
4	200.0788	0.6
5	310.0838	0.6
6	311.0757	100.0
7	311.5228	0.2
8	311.6817	0.1
9	312.0778	21.1
10	313.0742	6.6
11	314.0752	1.2
12	325.0537	1.3
13	326.0564	0.1
14	355.0645	0.5
15	379.0625	0.2
16	431.0247	0.3
17	623.1575	0.6
18	645.1376	2.2
19	646.1398	0.9
20	647.1392	0.4

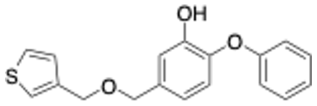

103

Generate Molecular Formula Parameters

Charge	Tolerance	sigma limit	H/C Ratio	Electron Conf.	Nitrogen Rule	Chrom.BackGround	Calibration
-1	6 ppm	0.08	3 - 0	both	false	false	TRUE

Expected Formula C18 H16 O3 S1 **Adduct(s):** H, radical

#	meas. m/z	theo. m/z	|Err|[ppm]	Sigma	Formula	Adduct	Adduct Mass
1	311.0757	311.0747	3.00	0.0038	C18H15O3S	M- H	1.0078

Note: Sigma fits < 0.05 indicates high probability of correct MF

Mass Spectrometry
Analytical Services
School of Chemistry

The University of Nottingham

Sample-ID	t_arm_TDA_5_191_HPLC	Lab	C13
Submitter	Tom Armstrong	Supervisor	Neil Thomas
Analysis Name	t_arm_TDA_5_191_HPLC_601136_66_01_87820.d	Acquisition Date	3/4/2020 4:33:32 PM
Ionisation Mode	ESI Negative	Instrument	Bruker MicroTOF

-MS, 0.6-0.8min #50-66

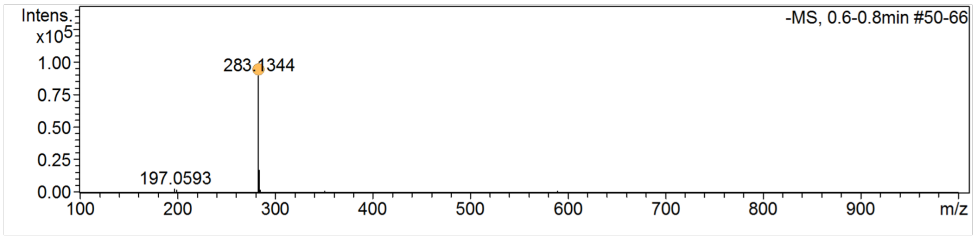

#	m/z	I %
1	112.9854	0.4
2	197.0593	3.0
3	198.0643	0.2
4	199.0753	2.5
5	248.9625	0.1
6	282.2353	0.4
7	283.1344	100.0
8	283.7626	0.1
9	283.9470	0.1
10	284.1369	19.7
11	285.1397	2.4
12	297.1130	0.7
13	341.0923	0.2
14	351.1206	1.3
15	368.1099	0.2
16	589.2546	1.2
17	590.2568	0.4

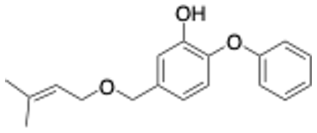

104

Generate Molecular Formula Parameters

Charge	Tolerance	sigma limit	H/C Ratio	Electron Conf.	Nitrogen Rule	Chrom.BackGround	Calibration
-1	6 ppm	0.08	3 - 0	both	false	false	TRUE

Expected Formula C18 H20 O3 **Adduct(s):** H, radical

#	meas. m/z	theo. m/z	|Err|[ppm]	Sigma	Formula	Adduct	Adduct Mass
1	283.1344	283.1340	1.50	0.0010	C18H19O3	M- H	1.0078

Note: Sigma fits < 0.05 indicates high probability of correct MF

Mass Spectrometry
Analytical Services
School of Chemistry

The University of Nottingham

Sample-ID	t_arm_TDA_5_165	Lab	C13
Submitter	Tom Armstrong	Supervisor	Neil Thomas
Analysis Name	t_arm_TDA_5_165_601183_12_01_87844.d	Acquisition Date	3/5/2020 11:54:42 AM
Ionisation Mode	ESI Negative	Instrument	Bruker MicroTOF

-MS, 0.6-0.8min #51-66

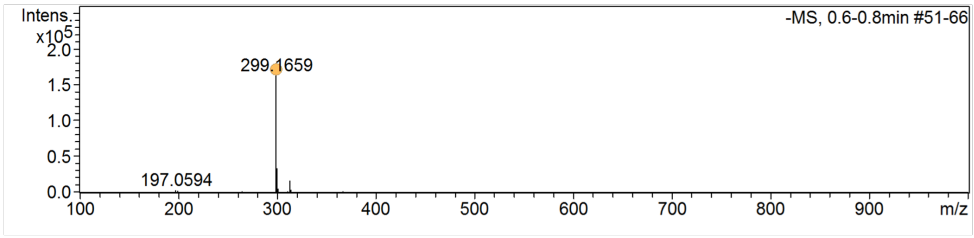

#	m/z	I %
1	197.0594	1.9
2	199.0748	1.2
3	255.2320	0.5
4	265.1466	0.7
5	283.2631	0.5
6	293.1789	0.4
7	298.2139	0.5
8	299.1659	100.0
9	300.1682	21.0
10	301.1700	3.0
11	302.1721	0.3
12	311.1679	0.8
13	313.1439	10.1
14	314.1473	2.1
15	325.1848	0.5
16	339.1934	0.4
17	357.1244	0.3
18	367.1518	1.0
19	599.3359	0.5
20	621.3183	0.3

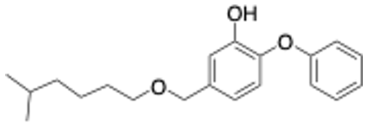

105

Generate Molecular Formula Parameters

Charge	Tolerance	sigma limit	H/C Ratio	Electron Conf.	Nitrogen Rule	Chrom.BackGround	Calibration
-1	6 ppm	0.08	3 - 0	both	false	false	TRUE

Expected Formula C19 H24 O3 **Adduct(s):** H, radical

#	meas. m/z	theo. m/z	|Err|[ppm]	Sigma	Formula	Adduct	Adduct Mass
1	299.1659	299.1653	2.30	0.0019	C19H23O3	M- H	1.0078

Note: Sigma fits < 0.05 indicates high probability of correct MF

Mass Spectrometry
Analytical Services
School of Chemistry

The University of Nottingham

Sample-ID	t_arm_TDA_CoA_Impure	Lab	C13
Submitter	Tom Armstrong	Supervisor	Neil Thomas
Analysis Name	t_arm_TDA_CoA_58748.d	Acquisition Date	3/23/2018 4:24:23 PM
Ionisation Mode	ESI Negative	Instrument	Bruker MicroTOF

-MS, 0.6-0.8min #50-66

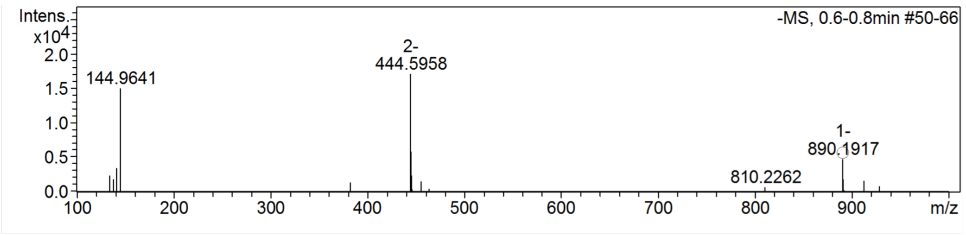

#	m/z	I %
1	134.0428	13.9
2	138.0190	10.7
3	141.0914	20.2
4	144.9641	87.8
5	382.5513	8.0
6	444.5958	100.0
7	445.0975	34.3
8	445.5970	13.9
9	446.0971	2.2
10	455.5871	9.0
11	463.5752	2.8
12	810.2262	3.9
13	890.1917	28.1
14	891.1955	10.7
15	892.1942	1.2
16	912.1735	9.5
17	913.1747	0.7
18	928.1494	4.9
19	934.1584	1.1
20	950.1294	0.6

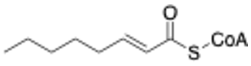

202

Generate Molecular Formula Parameters

Charge	Tolerance	sigma limit	H/C Ratio	Electron Conf.	Nitrogen Rule	Chrom.BackGround	Calibration
-1	6 ppm	0.08	3 - 0	both	false	false	TRUE

Expected Formula C29 H48 N7 O17 P3 S1 **Adduct(s):** H, radical

#	meas. m/z	theo. m/z	|Err|[ppm]	Sigma	Formula	Adduct	Adduct Mass
1	890.1917	890.1967	5.70	0.0478	C29H47N7O17P3S	M- H	1.0078

Note: Sigma fits < 0.05 indicates high probability of correct MF

Mass Spectrometry
Analytical Services
School of Chemistry

The University of Nottingham

Sample-ID	t_arm_TDA_3_237_F14	Lab	C13
Submitter	Tom Armstrong	Supervisor	Neil Thomas
Analysis Name	t_arm_TDA_3_237_F14_578536_5_01_70437.d	Acquisition Date	1/7/2019 1:16:55 PM
Ionisation Mode	ESI Positive	Instrument	Bruker MicroTOF

+MS, 0.6-0.8min #50-66

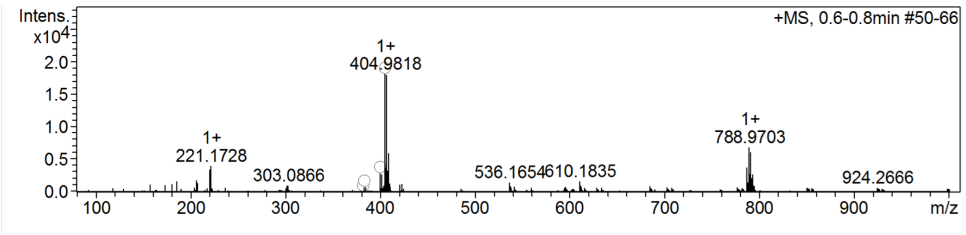

#	m/z	I %
1	185.1142	8.9
2	206.1427	10.1
3	220.1440	19.0
4	221.1728	21.9
5	400.0275	15.8
6	402.0217	14.6
7	404.9818	100.0
8	405.9851	20.8
9	406.9788	98.8
10	407.9822	18.0
11	408.9763	33.0
12	536.1654	8.3
13	610.1835	8.9
14	786.9718	20.7
15	787.9724	8.3
16	788.9703	37.6
17	789.9722	15.5
18	790.9667	33.8
19	791.9684	11.6
20	792.9646	14.7

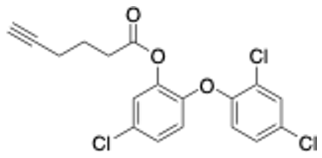

208

Generate Molecular Formula Parameters

Charge	Tolerance	sigma limit	H/C Ratio	Electron Conf.	Nitrogen Rule	Chrom.BackGround	Calibration
+1	6 ppm	0.08	3 - 0	both	false	false	TRUE

Expected Formula C18 H13 Cl3 O3 **Adduct(s):** H, Na, NH4, C3H5N2, radical

#	meas. m/z	theo. m/z	|Err|[ppm]	Sigma	Formula	Adduct	Adduct Mass
1	383.0001	383.0003	0.50	0.0282	C18H14Cl3O3	M+H	1.0078
1	404.9818	404.9822	1.10	0.0075	C18H13Cl3NaO3	M+Na	22.9898

Note: Sigma fits < 0.05 indicates high probability of correct MF

Mass Spectrometry
Analytical Services
School of Chemistry

The University of Nottingham

Sample-ID	t_arm_TDA_4_141_Cr	Lab	C13
Submitter	Tom Armstrong	Supervisor	Neil Thomas
Analysis Name	t_arm_TDA_4_141_Cr_584233_1_01_75030.d	Acquisition Date	4/5/2019 8:54:40 AM
Ionisation Mode	ESI Positive	Instrument	Bruker MicroTOF

+MS, 0.6-0.8min #51-67

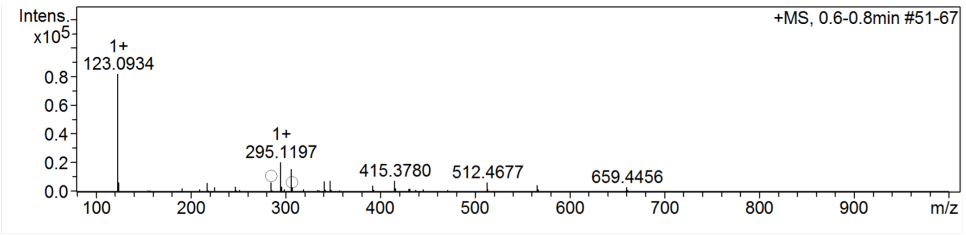

#	m/z	I %
1	123.0934	100.0
2	124.0953	8.0
3	191.0446	3.2
4	217.1324	7.9
5	225.1949	3.9
6	247.1474	4.6
7	285.0876	8.3
8	295.1197	25.2
9	296.1205	4.7
10	306.2899	19.2
11	307.2928	4.2
12	341.2193	8.8
13	347.2795	9.3
14	392.2492	5.4
15	415.3780	9.7
16	416.3815	3.0
17	512.4677	8.3
18	513.4703	2.8
19	565.4081	5.9
20	659.4456	3.9

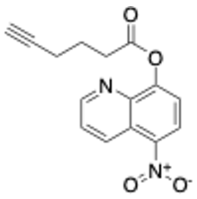

209

Generate Molecular Formula Parameters

Charge	Tolerance	sigma limit	H/C Ratio	Electron Conf.	Nitrogen Rule	Chrom.BackGround	Calibration
+1	6 ppm	0.08	3 - 0	both	false	false	TRUE

Expected Formula C15 H12 N2 O4 **Adduct(s):** H, Na, NH4, C3H5N2, radical

#	meas. m/z	theo. m/z	|Err|[ppm]	Sigma	Formula	Adduct	Adduct Mass
1	285.0876	285.0870	2.20	0.0042	C15H13N2O4	M+H	1.0078
1	307.0675	307.0689	4.60	0.0053	C15H12N2NaO4	M+Na	22.9898

Note: Sigma fits < 0.05 indicates high probability of correct MF

Mass Spectrometry
Analytical Services
School of Chemistry

The University of Nottingham

Sample-ID	t_arm_TDA_4_145_F15	Lab	C13
Submitter	Tom Armstrong	Supervisor	Neil Thomas
Analysis Name	t_arm_TDA_4_145_F15_584370_27_01_75144.d	Acquisition Date	4/8/2019 12:32:13 PM
Ionisation Mode	ESI Positive	Instrument	Bruker MicroTOF

+MS, 0.6-0.8min #51-67

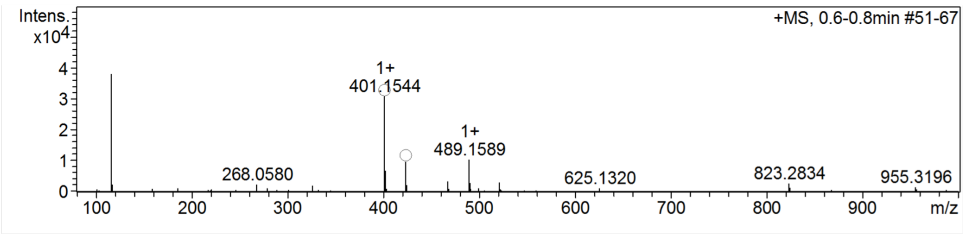

#	m/z	I %
1	116.1195	100.0
2	117.1209	6.4
3	185.1080	3.2
4	268.0580	6.4
5	279.0933	3.1
6	326.0998	5.6
7	401.1544	81.2
8	402.1568	18.1
9	423.1368	25.7
10	424.1376	5.8
11	467.1757	9.1
12	468.1774	2.8
13	489.1589	27.5
14	490.1612	7.6
15	499.1501	3.0
16	521.1334	8.0
17	625.1320	3.0
18	823.2834	7.1
19	824.2838	3.5
20	955.3196	4.1

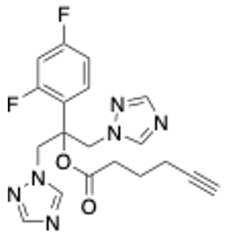

210

Generate Molecular Formula Parameters

Charge	Tolerance	sigma limit	H/C Ratio	Electron Conf.	Nitrogen Rule	Chrom.BackGround	Calibration
+1	6 ppm	0.08	3 - 0	both	false	false	TRUE

Expected Formula C19 H18 F2 N6 O2 **Adduct(s):** H, Na, NH4, C3H5N2, radical

#	meas. m/z	theo. m/z	|Err|[ppm]	Sigma	Formula	Adduct	Adduct Mass
1	401.1544	401.1532	2.90	0.0046	C19H19F2N6O2	M+H	1.0078
1	423.1368	423.1352	4.00	0.0026	C19H18F2N6NaO2	M+Na	22.9898

Note: Sigma fits < 0.05 indicates high probability of correct MF

Mass Spectrometry
Analytical Services
School of Chemistry

The University of Nottingham

Sample-ID	t_arm_TDA_5_179_Precip	Lab	C13
Submitter	Tom Armstrong	Supervisor	Neil Thomas
Analysis Name	t_arm_TDA_5_179_Precip_600039_41_01_86988.d	Acquisition Date	2/20/2020 3:32:18 PM
Ionisation Mode	ESI Positive	Instrument	Bruker MicroTOF

+MS, 0.6-0.8min #50-66

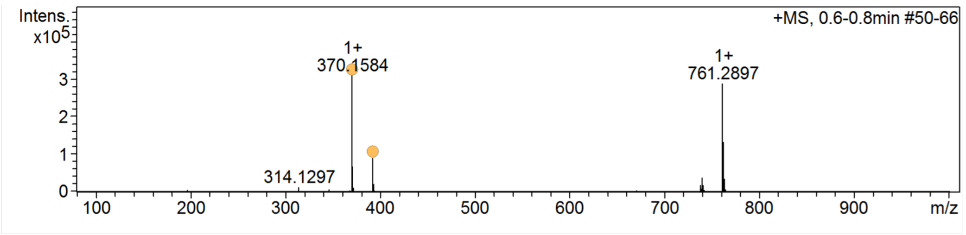

#	m/z	I %
1	196.5733	1.3
2	314.1297	3.7
3	346.1560	1.9
4	368.1415	0.9
5	370.1584	100.0
6	371.1601	22.0
7	372.1612	3.1
8	392.1397	29.0
9	393.1421	6.3
10	394.1439	0.9
11	670.2239	0.9
12	737.2875	5.5
13	738.2891	2.4
14	739.3061	12.0
15	740.3080	5.5
16	741.3106	1.3
17	761.2897	92.9
18	762.2927	42.8
19	763.2948	10.9
20	764.2925	1.9

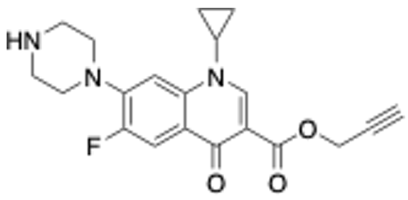

217

Generate Molecular Formula Parameters

Charge	Tolerance	sigma limit	H/C Ratio	Electron Conf.	Nitrogen Rule	Chrom.BackGround	Calibration
+1	6 ppm	0.08	3 - 0	both	false	false	TRUE

Expected Formula C20 H20 F1 N3 O3 **Adduct(s):** H, Na, NH4, C3H5N2, radical

#	meas. m/z	theo. m/z	|Err|[ppm]	Sigma	Formula	Adduct	Adduct Mass
1	370.1584	370.1561	6.10	0.0060	C20H21FN3O3	M+H	1.0078
1	392.1397	392.1381	4.10	0.0068	C20H20FN3NaO3	M+Na	22.9898

Note: Sigma fits < 0.05 indicates high probability of correct MF

Mass Spectrometry
Analytical Services
School of Chemistry

The University of Nottingham

Sample-ID	t_arm_TDA_3_283_Col	Lab	C13
Submitter	Tom Armstrong	Supervisor	Neil Thomas
Analysis Name	t_arm_TDA_3_283_Col_579377_21_01_71088.d	Acquisition Date	1/25/2019 2:30:39 PM
Ionisation Mode	ESI Positive	Instrument	Bruker MicroTOF

+MS, 0.6-0.8min #51-67

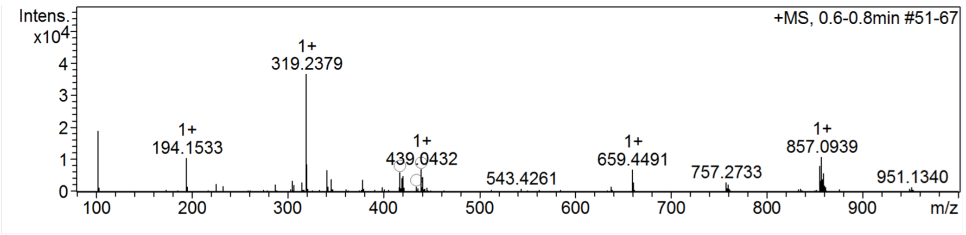

#	m/z	I %
1	102.1284	51.8
2	194.1533	28.7
3	305.0091	9.4
4	319.2379	100.0
5	320.2400	23.3
6	341.2203	18.6
7	345.3096	10.9
8	378.3108	10.3
9	417.0605	16.8
10	419.0597	11.9
11	420.3570	13.4
12	439.0432	19.2
13	441.0398	12.8
14	659.4491	19.0
15	660.4543	8.1
16	855.0963	22.0
17	856.0991	9.3
18	857.0939	29.7
19	858.0946	11.0
20	859.0896	15.9

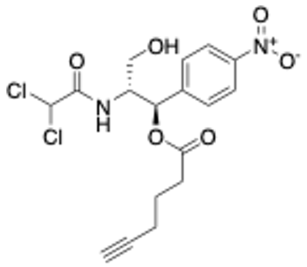

220

Generate Molecular Formula Parameters

Charge	Tolerance	sigma limit	H/C Ratio	Electron Conf.	Nitrogen Rule	Chrom.BackGround	Calibration
+1	6 ppm	0.08	3 - 0	both	false	false	TRUE

Expected Formula C17 H18 Cl2 N2 O6 **Adduct(s):** H, Na, NH4, C3H5N2, radical

#	meas. m/z	theo. m/z	|Err|[ppm]	Sigma	Formula	Adduct	Adduct Mass
1	417.0605	417.0615	2.20	0.0162	C17H19Cl2N2O6	M+H	1.0078
1	439.0432	439.0434	0.50	0.0063	C17H18Cl2N2NaO6	M+Na	22.9898
1	434.0879	434.0880	0.30	0.0207	C17H22Cl2N3O6	M+H4N	18.0344

Note: Sigma fits < 0.05 indicates high probability of correct MF

Mass Spectrometry
Analytical Services
School of Chemistry

The University of Nottingham

Sample-ID	t_arm_TDA_5_79_WU	Lab	C13
Submitter	Tom Armstrong	Supervisor	Neil Thomas
Analysis Name	t_arm_TDA_5_79_WU_594936_36_01_82931.d	Acquisition Date	11/18/2019 3:26:43 PM
Ionisation Mode	ESI Positive	Instrument	Bruker MicroTOF

+MS, 0.6-0.8min #50-66

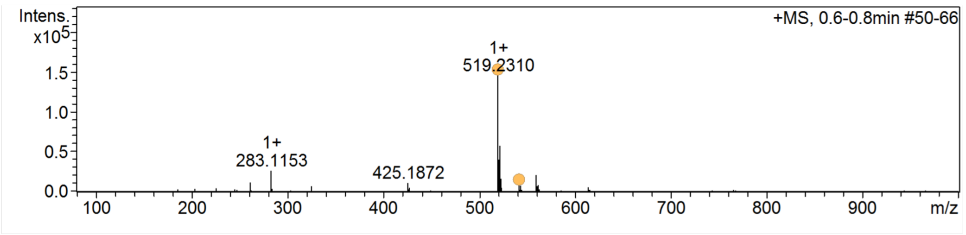

#	m/z	I %
1	203.0908	2.4
2	225.1956	2.8
3	245.1022	1.8
4	261.1333	7.8
5	283.1153	18.1
6	284.1180	2.5
7	325.1256	4.4
8	425.1872	7.5
9	427.1838	3.1
10	519.2310	100.0
11	520.2331	27.9
12	521.2282	39.9
13	522.2300	10.8
14	523.2276	3.2
15	541.2100	5.0
16	543.2264	5.2
17	559.2600	14.2
18	560.2614	4.4
19	561.2577	5.5
20	613.2700	3.7

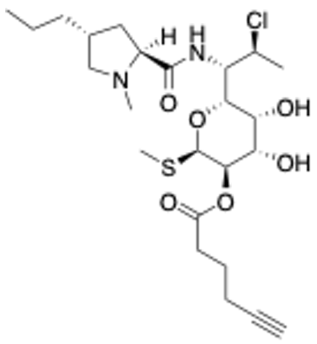

223

Generate Molecular Formula Parameters

Charge	Tolerance	sigma limit	H/C Ratio	Electron Conf.	Nitrogen Rule	Chrom.BackGround	Calibration
+1	6 ppm	0.08	3 - 0	both	false	false	TRUE

Expected Formula C24 H39 Cl1 N2 O6 S1 **Adduct(s):** H, Na, NH4, C3H5N2, radical

#	meas. m/z	theo. m/z	|Err|[ppm]	Sigma	Formula	Adduct	Adduct Mass
1	519.2310	519.2290	3.80	0.0074	C24H40ClN2O6S	M+H	1.0078

Note: Sigma fits < 0.05 indicates high probability of correct MF

Mass Spectrometry
Analytical Services
School of Chemistry

The University of Nottingham

Sample-ID	t_arm_TDA_5_69_TLC	Lab	C13
Submitter	Tom Armstrong	Supervisor	Neil Thomas
Analysis Name	t_arm_TDA_5_69_TLC_594624_9_01_82702.d	Acquisition Date	11/12/2019 1:25:25 PM
Ionisation Mode	ESI Positive	Instrument	Bruker MicroTOF

+MS, 0.6-0.8min #44-58

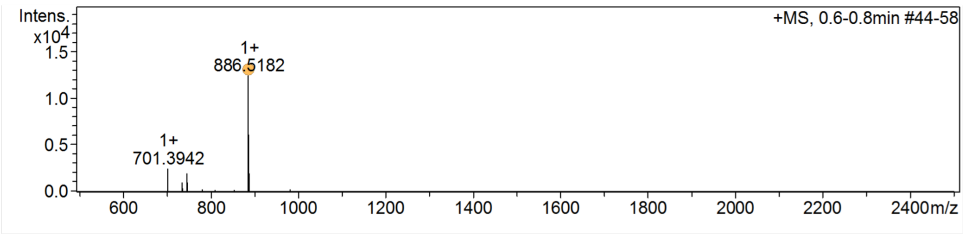

#	m/z	I %
1	701.3942	20.0
2	702.4001	7.4
3	707.1634	0.3
4	734.4678	7.9
5	735.4709	2.5
6	745.5029	15.8
7	746.5062	7.7
8	781.1848	1.6
9	782.1809	0.3
10	809.7827	1.2
11	855.2051	1.2
12	856.2065	0.6
13	886.5182	100.0
14	887.5193	49.3
15	888.5227	16.2
16	889.5276	2.9
17	930.2204	0.3
18	982.6673	2.0

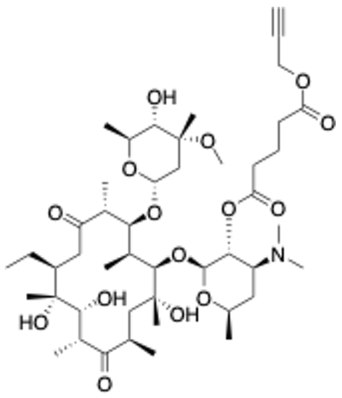

Generate Molecular Formula Parameters

225

Charge	Tolerance	sigma limit	H/C Ratio	Electron Conf.	Nitrogen Rule	Chrom.BackGround	Calibration
+1	6 ppm	0.08	3 - 0	both	false	false	TRUE

Expected Formula C45 H75 N1 O16 **Adduct(s):** H, Na, NH4, C3H5N2, radical

#	meas. m/z	theo. m/z	|Err|[ppm]	Sigma	Formula	Adduct	Adduct Mass
1	886.5182	886.5159	2.60	0.0073	C45H76NO16	M+H	1.0078

Note: Sigma fits < 0.05 indicates high probability of correct MF

Mass Spectrometry
Analytical Services
School of Chemistry

The University of Nottingham

Sample-ID	t_arm_TDA_4_235	Lab	C13
Submitter	Tom Armstrong	Supervisor	Neil Thomas
Analysis Name	t_arm_TDA_4_235_589807_46_01_79192.d	Acquisition Date	7/18/2019 4:56:40 PM
Ionisation Mode	ESI Positive	Instrument	Bruker MicroTOF

+MS, 0.6-0.8min #51-67

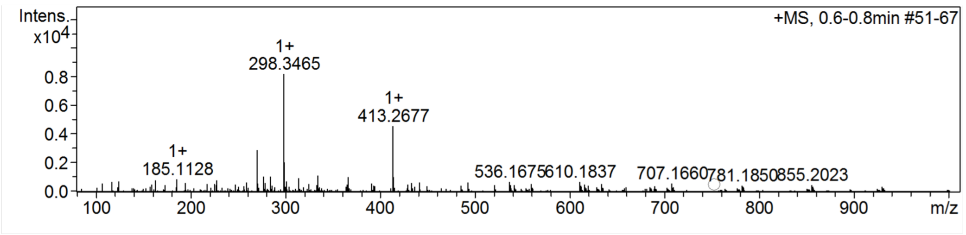

#	m/z	I %
1	116.9839	8.5
2	124.0744	9.1
3	163.0181	9.8
4	185.1128	10.9
5	227.1150	9.8
6	259.0653	8.0
7	270.3149	35.8
8	277.1249	12.9
9	284.3306	13.0
10	298.3465	100.0
11	299.3504	25.4
12	301.1276	9.0
13	314.3401	11.6
14	334.1573	13.9
15	366.2982	12.7
16	413.2677	55.9
17	414.2681	12.4
18	441.2984	8.2
19	536.1675	8.4
20	610.1837	8.6

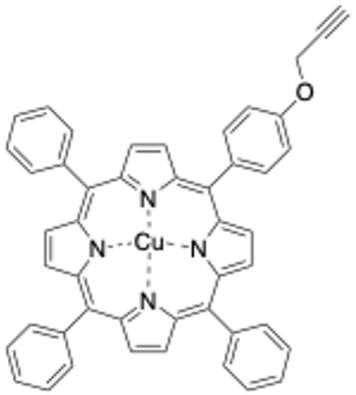

226

Generate Molecular Formula Parameters

Charge	Tolerance	sigma limit	H/C Ratio	Electron Conf.	Nitrogen Rule	Chrom.BackGround	Calibration
+1	6 ppm	0.08	3 - 0	both	false	false	TRUE

Expected Formula C47 H30 Cu1 N4 O1 **Adduct(s):** H, Na, NH4, C3H5N2, radical

#	meas. m/z	theo. m/z	|Err|[ppm]	Sigma	Formula	Adduct	Adduct Mass
1	752.1599	752.1608	1.10	0.0603	C47H30CuN4NaO	M+Na	22.9898

Note: Sigma fits < 0.05 indicates high probability of correct MF

Mass Spectrometry
Analytical Services
School of Chemistry

The University of Nottingham

Sample-ID	f_zam_fz300_final	Lab	C13
Submitter	Francesco Zamberlan	Supervisor	Neil Thomas
Analysis Name	f_zam_fz300_final_589879_41_01_79256.d	Acquisition Date	7/19/2019 3:28:59 PM
Ionisation Mode	ESI Positive	Instrument	Bruker MicroTOF

+MS, 0.6-0.8min #50-66

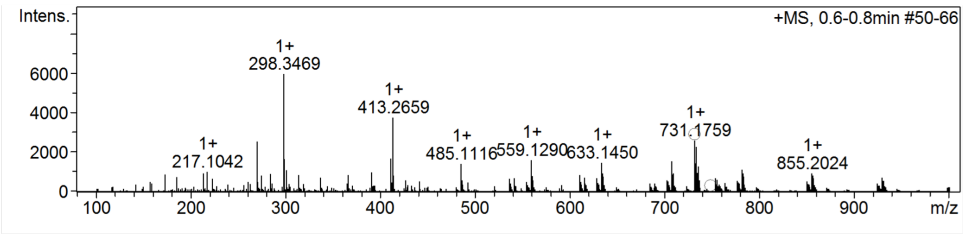

#	m/z	I %
1	217.1042	16.9
2	270.3146	42.5
3	298.3469	100.0
4	299.3496	27.9
5	301.1369	18.6
6	391.2822	16.6
7	411.1083	28.2
8	413.2659	63.0
9	485.1116	24.0
10	559.1290	27.0
11	633.1450	24.7
12	707.1647	26.3
13	731.1759	43.8
14	732.1808	24.4
15	733.1729	38.1
16	734.1730	16.4
17	735.1750	21.6
18	781.1878	18.9
19	782.1881	15.8
20	855.2024	15.9

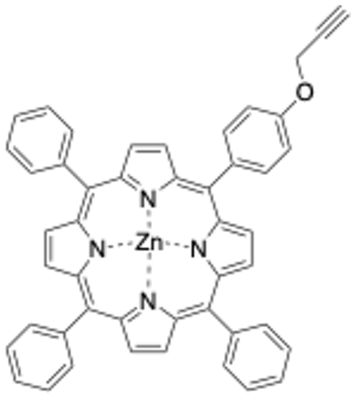

227

Generate Molecular Formula Parameters

Charge	Tolerance	sigma limit	H/C Ratio	Electron Conf.	Nitrogen Rule	Chrom.BackGround	Calibration
+1	6 ppm	0.08	3 - 0	both	false	false	TRUE

Expected Formula C47 H30 N4 O1 Zn1 **Adduct(s):** H, Na, NH4, C3H5N2, radical

#	meas. m/z	theo. m/z	|Err|[ppm]	Sigma	Formula	Adduct	Adduct Mass
1	731.1759	731.1784	3.40	0.0578	C47H31N4OZn	M+H	1.0078

Note: Sigma fits < 0.05 indicates high probability of correct MF

Mass Spectrometry
Analytical Services
School of Chemistry

The University of Nottingham

Sample-ID	t_arm_TDA_4_253_Col	Lab	C13
Submitter	Tom Armstrong	Supervisor	Neil Thomas
Analysis Name	t_arm_TDA_4_253_Col_590331_16_01_79623.d	Acquisition Date	7/31/2019 10:59:26 AM
Ionisation Mode	ESI Positive	Instrument	Bruker MicroTOF

+MS, 0.6-0.8min #51-67

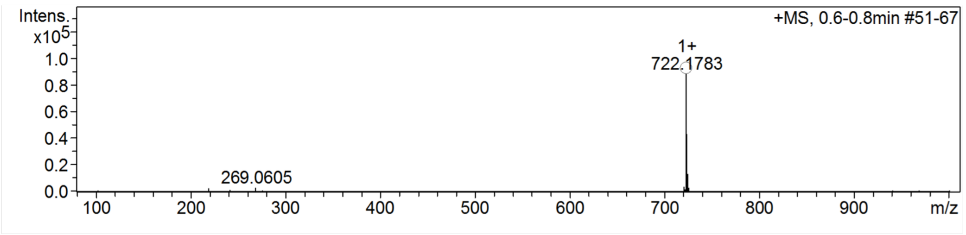

#	m/z	I %
1	102.0924	1.4
2	173.0781	0.8
3	217.1035	0.8
4	219.1878	3.4
5	241.1682	1.8
6	269.0605	3.5
7	276.1204	1.5
8	279.0932	1.1
9	720.1792	4.4
10	721.1820	2.2
11	722.1783	100.0
12	723.1780	49.1
13	724.1845	15.1
14	725.1866	3.7
15	726.1899	0.8
16	940.3530	1.3
17	941.3560	0.8
18	968.2450	1.4
19	969.2477	1.0
20	1000.2735	1.3

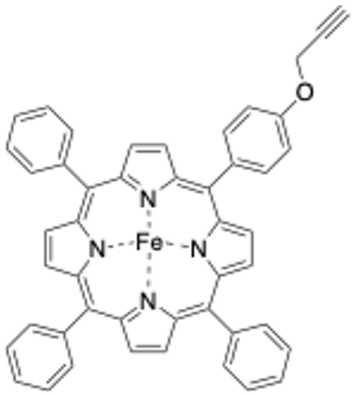

228

Generate Molecular Formula Parameters

Charge	Tolerance	sigma limit	H/C Ratio	Electron Conf.	Nitrogen Rule	Chrom.BackGround	Calibration
+1	6 ppm	0.08	3 - 0	both	false	false	TRUE

Expected Formula C47 H30 Fe1 N4 O1 **Adduct(s):** H, Na, NH4, C3H5N2, radical

#	meas. m/z	theo. m/z	|Err|[ppm]	Sigma	Formula	Adduct	Adduct Mass
1	722.1783	722.1764	2.60	0.0245	C47H30FeN4O	M+	-0.0005

Note: Sigma fits < 0.05 indicates high probability of correct MF

Mass Spectrometry
Analytical Services
School of Chemistry

The University of Nottingham

Sample-ID	t_arm_TDA_3_233	Lab	C13
Submitter	Tom Armstrong	Supervisor	Neil Thomas
Analysis Name	t_arm_TDA_3_233_578404_57_01_70347.d	Acquisition Date	1/3/2019 10:18:36 AM
Ionisation Mode	ESI Positive	Instrument	Bruker MicroTOF

+MS, 0.6-0.8min #50-66

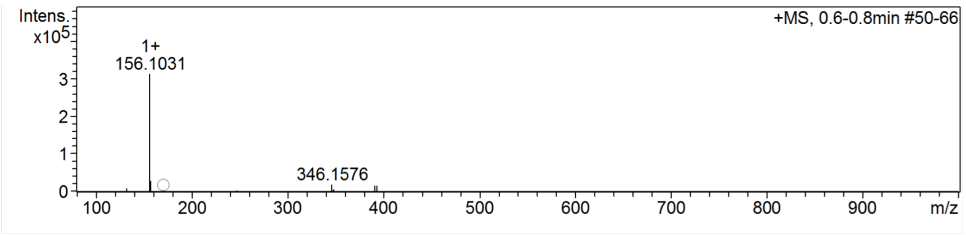

#	m/z	I %
1	116.0712	1.1
2	132.1028	3.0
3	156.1031	100.0
4	157.1055	9.3
5	158.1067	0.9
6	169.1331	0.6
7	170.1194	0.5
8	173.0780	0.6
9	247.0517	1.4
10	249.0499	0.5
11	288.1232	0.6
12	310.1054	0.9
13	346.1576	6.5
14	347.1623	1.6
15	348.1548	2.3
16	349.1587	0.5
17	391.1237	5.3
18	392.1246	0.9
19	393.1221	5.3
20	394.1233	1.0

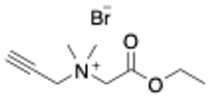

229

Generate Molecular Formula Parameters

Charge	Tolerance	sigma limit	H/C Ratio	Electron Conf.	Nitrogen Rule	Chrom.BackGround	Calibration
+1	12 ppm	0.08	3 - 0	both	false	false	TRUE

Expected Formula C9 H16 N1 O2 **Adduct(s):** H, Na, NH4, C3H5N2, radical

#	meas. m/z	theo. m/z	|Err|[ppm]	Sigma	Formula	Adduct	Adduct Mass
1	170.1194	170.1176	11.10	0.0053	C9H16NO2	M+	-0.0005

Note: Sigma fits < 0.05 indicates high probability of correct MF

Mass Spectrometry
Analytical Services
School of Chemistry

The University of Nottingham

Sample-ID	t_arm_TDA_4_199_Col	Lab	C13
Submitter	Tom Armstrong	Supervisor	Neil Thomas
Analysis Name	t_arm_TDA_4_199_Col_586797_12_01_76897.d	Acquisition Date	5/24/2019 1:38:42 PM
Ionisation Mode	ESI Positive	Instrument	Bruker MicroTOF

+MS, 0.6-0.8min #50-66

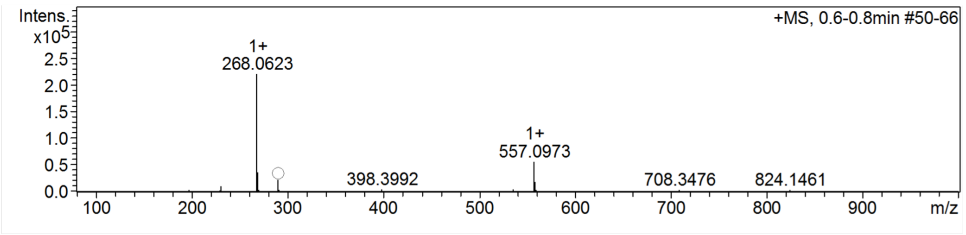

#	m/z	I %
1	197.0783	2.0
2	198.1252	1.0
3	201.0458	1.1
4	229.0381	1.2
5	230.1546	4.9
6	252.0656	1.1
7	268.0623	100.0
8	269.0643	16.4
9	270.0661	2.0
10	290.0430	10.2
11	291.0458	1.6
12	398.3992	2.4
13	535.1135	2.1
14	541.1020	1.1
15	557.0973	25.6
16	558.0990	8.3
17	559.1040	1.8
18	708.3476	1.8
19	824.1461	1.9
20	825.1496	1.0

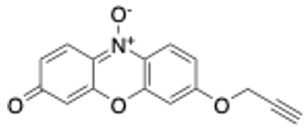

235

Generate Molecular Formula Parameters

Charge	Tolerance	sigma limit	H/C Ratio	Electron Conf.	Nitrogen Rule	Chrom.BackGround	Calibration
+1	6 ppm	0.08	3 - 0	both	false	false	TRUE

Expected Formula C15 H9 N1 O4 **Adduct(s):** H, Na, NH4, C3H5N2, radical

#	meas. m/z	theo. m/z	|Err|[ppm]	Sigma	Formula	Adduct	Adduct Mass
1	290.0430	290.0424	2.00	0.0075	C15H9NNaO4	M+Na	22.9898

Note: Sigma fits < 0.05 indicates high probability of correct MF

Mass Spectrometry
Analytical Services
School of Chemistry

The University of Nottingham

Sample-ID	t_arm_TDA_4_281_Cr	Lab	C13
Submitter	Tom Armstrong	Supervisor	Neil Thomas
Analysis Name	t_arm_TDA_4_281_Cr_591307_60_01_80266.d	Acquisition Date	8/14/2019 2:35:47 PM
Ionisation Mode	ESI Positive	Instrument	Bruker MicroTOF

+MS, 0.6-0.8min #51-67

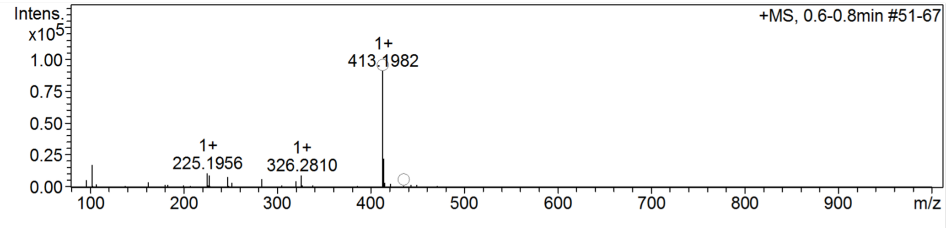

#	m/z	I %
1	96.0406	6.5
2	102.0907	19.6
3	107.0472	2.8
4	162.0903	4.6
5	180.0381	2.0
6	183.0870	2.3
7	225.1956	12.1
8	227.1134	10.2
9	247.1778	9.2
10	252.1128	4.2
11	284.1422	7.0
12	305.1562	2.0
13	320.2306	5.3
14	326.2810	10.2
15	413.1982	100.0
16	414.2015	24.8
17	415.2032	3.9
18	421.2442	3.2
19	443.2276	2.4
20	449.3848	2.4

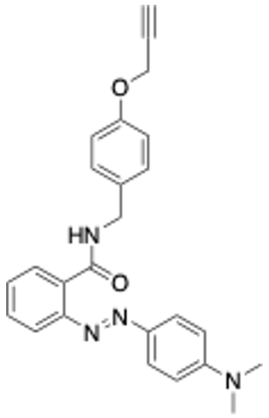

238

Generate Molecular Formula Parameters

Charge	Tolerance	sigma limit	H/C Ratio	Electron Conf.	Nitrogen Rule	Chrom.BackGround	Calibration
+1	6 ppm	0.08	3 - 0	both	false	false	TRUE

Expected Formula C25 H24 N4 O2 **Adduct(s):** H, Na, NH4, C3H5N2, radical

#	meas. m/z	theo. m/z	|Err|[ppm]	Sigma	Formula	Adduct	Adduct Mass
1	413.1982	413.1972	2.40	0.0239	C25H25N4O2	M+H	1.0078
1	435.1776	435.1791	3.60	0.0262	C25H24N4NaO2	M+Na	22.9898

Note: Sigma fits < 0.05 indicates high probability of correct MF

Mass Spectrometry
Analytical Services
School of Chemistry

The University of Nottingham

Sample-ID	t_arm_TDA_5_87_White_solid_MeOH	Lab	C13
Submitter	Tom Armstrong	Supervisor	Neil Thomas
Analysis Name	t_arm_TDA_5_87_White_solid_MeOH_53_01_83482.d	Acquisition Date	11/27/2019 5:18:18 PM
Ionisation Mode	ESI– Positive	Instrument	Bruker MicroTOF

+MS, 0.6-0.8min #44-58

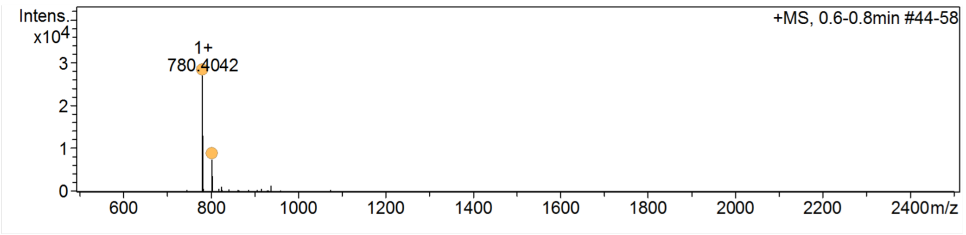

#	m/z	I %
1	745.5012	1.2
2	780.4042	100.0
3	781.4051	48.2
4	782.4087	11.5
5	783.4123	2.5
6	802.3839	28.0
7	803.3892	13.0
8	804.3911	3.6
9	818.3571	2.2
10	824.3643	4.1
11	825.3672	1.3
12	842.3272	1.9
13	863.5221	1.2
14	865.3745	1.0
15	887.3607	1.3
16	907.6274	1.2
17	916.3740	2.4
18	938.3569	4.9
19	939.3577	2.3
20	1074.3325	1.4

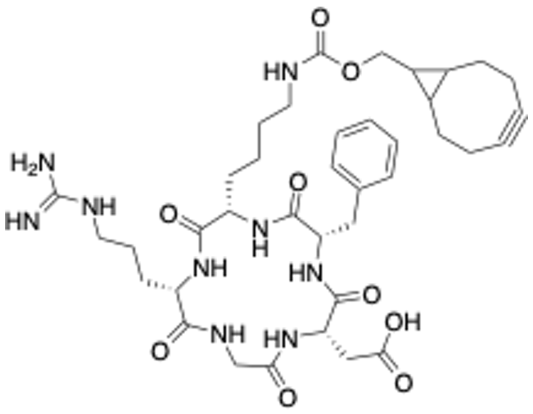

244

Generate Molecular Formula Parameters

Charge	Tolerance	sigma limit	H/C Ratio	Electron Conf.	Nitrogen Rule	Chrom.BackGround	Calibration
+1	6 ppm	0.08	3 - 0	both	false	false	TRUE

Expected Formula C38 H53 N9 O9 **Adduct(s):** H, Na, NH4, C3H5N2, radical

#	meas. m/z	theo. m/z	|Err|[ppm]	Sigma	Formula	Adduct	Adduct Mass
1	780.4042	780.4039	0.40	0.0146	C38H54N9O9	M+H	1.0078
1	802.3839	802.3858	2.40	0.0119	C38H53N9NaO9	M+Na	22.9898

Note: Sigma fits < 0.05 indicates high probability of correct MF

9.3 Representative Analytical HPLC Trace

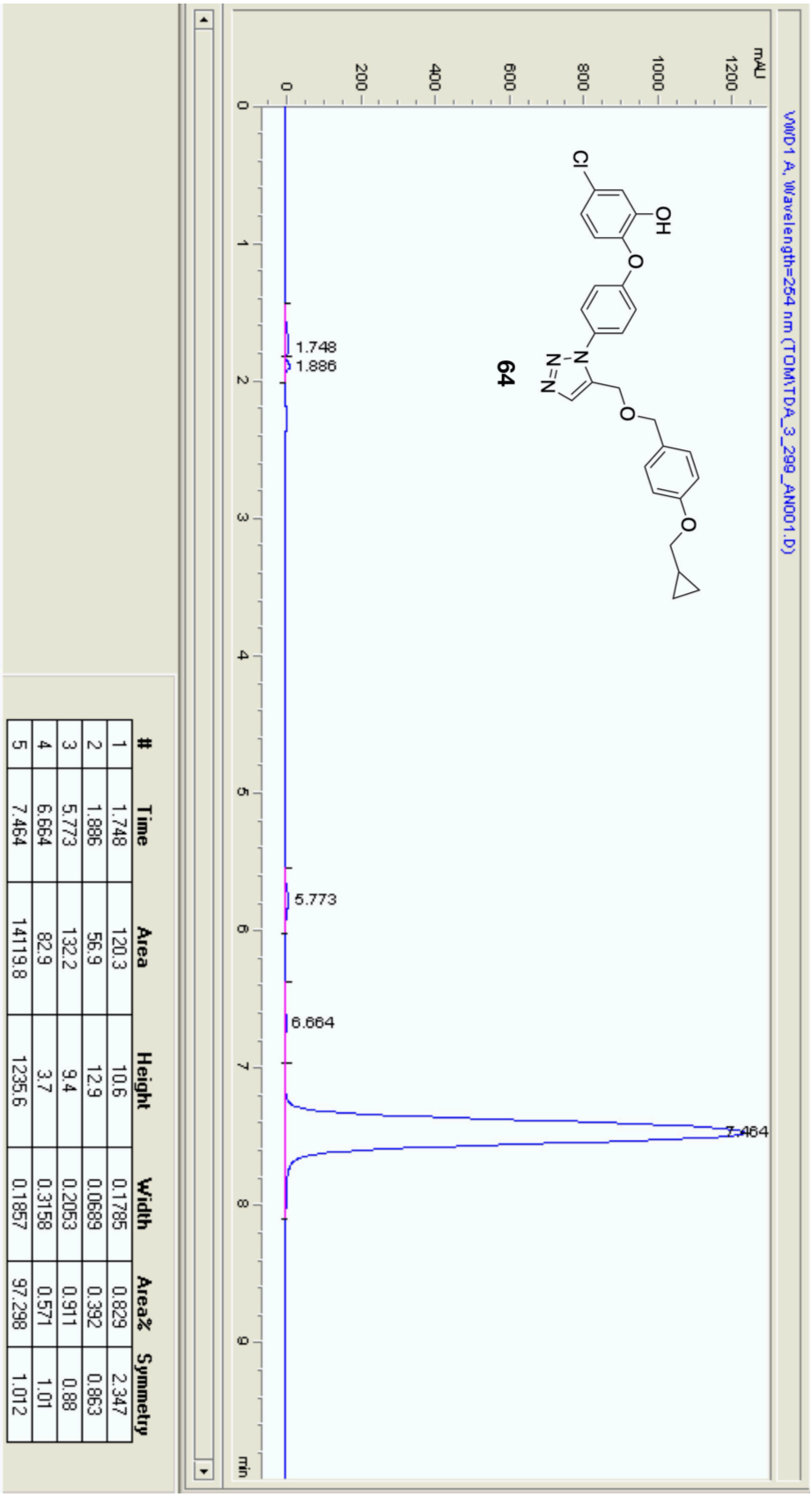

#	Time	Area	Height	Width	Area%	Symmetry
1	1.748	120.3	10.6	0.1785	0.829	2.347
2	1.886	56.9	12.9	0.0689	0.392	0.863
3	5.773	132.2	9.4	0.2053	0.911	0.88
4	6.664	82.9	3.7	0.3158	0.571	1.01
5	7.464	14119.8	1235.6	0.1857	97.298	1.012

10. Publications Based On This Work

Bioorganic & Medicinal Chemistry 28 (2020) 115744

Contents lists available at ScienceDirect

Bioorganic & Medicinal Chemistry

journal homepage: www.elsevier.com/locate/bmc

Inhibition of *Mycobacterium tuberculosis* InhA: Design, synthesis and evaluation of new di-triclosan derivatives

Tom Armstrong[a], Malcolm Lamont[a], Alice Lanne[b], Luke J. Alderwick[b], Neil R. Thomas[a,*]

[a] Biodiscovery Institute, School of Chemistry, University of Nottingham, University Park, Nottingham NG7 2RD, United Kingdom
[b] Institute of Microbiology and Infection, School of Bioscience, University of Birmingham, Birmingham B15 2TT, United Kingdom

ARTICLE INFO

Keywords:
InhA
Triclosan
Triazole
Isoniazid
Mycobacterium tuberculosis
TB

ABSTRACT

Multi-drug resistant tuberculosis (MDR-TB) represents a growing problem for global healthcare systems. In addition to 1.3 million deaths in 2018, the World Health Organisation reported 484,000 new cases of MDR-TB. Isoniazid is a key anti-TB drug that inhibits InhA, a crucial enzyme in the cell wall biosynthesis pathway and identical in *Mycobacterium tuberculosis* and *M. bovis*. Isoniazid is a pro-drug which requires activation by the enzyme KatG, mutations in KatG prevent activation and confer INH-resistance. 'Direct inhibitors' of InhA are attractive as they would circumvent the main clinically observed resistance mechanisms. A library of new 1,5-triazoles, designed to mimic the structures of both triclosan molecules uniquely bound to InhA have been synthesised. The inhibitory activity of these compounds was evaluated using isolated enzyme assays with **2** (5-chloro-2-(4-(5-(((4-(4-chloro-2-hydroxyphenoxy)benzyl)oxy)methyl)-1H-1,2,3-triazol-1-yl)phenoxy)phenol) exhibiting an IC_{50} of 5.6 μM. Whole-cell evaluation was also performed, with **11** (5-chloro-2-(4-(5-(((4-(cyclopropylmethoxy)benzyl)oxy)methyl)-1H-1,2,3-triazol-1-yl)phenoxy)phenol) showing the greatest potency, with an MIC_{99} of 12.9 μM against *M. bovis*.

1. Introduction

Tuberculosis (TB) is one the leading global causes of mortality and is currently the world's deadliest infectious disease. In addition to the estimated 1.3 million deaths from TB in 2018, a further 0.25 million Human Immunodeficiency Virus-positive (HIV) individuals died as a result of co-infection with *Mycobacterium tuberculosis*.[1]

The current anti-TB treatment course relies on four drugs: isoniazid (INH), rifampicin (RIF), ethambutol (ETH) and pyrazinamide (PZA). The increasing prevalence of multi-drug resistant TB (MDR-TB) threatens to undermine the efficacy of this treatment regimen. MDR-TB infections are characterised as those displaying resistance to INH and RIF. In 2018, the WHO reported over 484,000 new MDR-TB infections. Additionally, 13,000 were classified as extensively drug resistant (XDR-TB) meaning they were also insensitive to any fluoroquinolone and at least one of the second-line injectable drugs.[2–4] This emerging resistance is further exacerbated by the lack of novel drugs coming through the pipeline, with only three new drugs entering the clinic in the last 40 years (delamanid, pretomanid and bedaquiline).[5,6]

Mycobacteria's dense and complex cell wall represents one of the main reasons for the hardiness of the bacteria. The relative impermeability of the Mycobacterial cell wall can primarily be attributed to its mycolic acid component. This waxy layer consists of long chain ($\sim C_{50\text{-}90}$) α-branched, β-hydroxylated fatty acids. This barrier not only hinders the passage of small molecules into the cell, but also provides protection from the host's immune response.[7]

The frontline drug INH elicits its biological effects through disruption of the mycolic acid biosynthetic pathway, *via* inhibition of the enzyme InhA.[8] InhA is a nicotinamide adenine dinucleotide (NADH)-dependent enoyl acyl carrier reductase which catalyses the chemoselective reduction of its 2-*trans*-enoyl-ACP substrate. The enzyme has an identical amino acid sequence (and hence structure) in *M. tuberculosis* and *M. bovis*, the main causative agents of tuberculosis in humans and dairy cattle respectively. INH is actually a pro-drug which requires activation before it can inhibit mycolic acid biosynthesis (Fig. 1).

Initially, the catalase peroxidase enzyme, KatG converts INH to its

Abbreviations: ETH, ethambutol; GOLD, Genetic Optimisation for Ligand Docking; HIV, human immunodeficiency virus; HPLC, high-performance liquid chromatography; INH, isoniazid; MDR-TB, multi-drug resistant tuberculosis; NAD, nicotinamide adenine dinucleotide (oxidised form); NADH, nicotinamide adenine dinucleotide (reduced form); PZA, pyrazinamide; RIF, rifampicin; RuAAC, ruthenium-catalysed azide alkyne cycloaddition, TB, tuberculosis; TCS, triclosan; XDR-TB, extensively drug-resistant tuberculosis

* Corresponding author.
E-mail address: neil.thomas@nottingham.ac.uk (N.R. Thomas).

https://doi.org/10.1016/j.bmc.2020.115744
Received 10 July 2020; Received in revised form 24 August 2020; Accepted 27 August 2020
Available online 08 September 2020
0968-0896/ © 2020 Published by Elsevier Ltd.

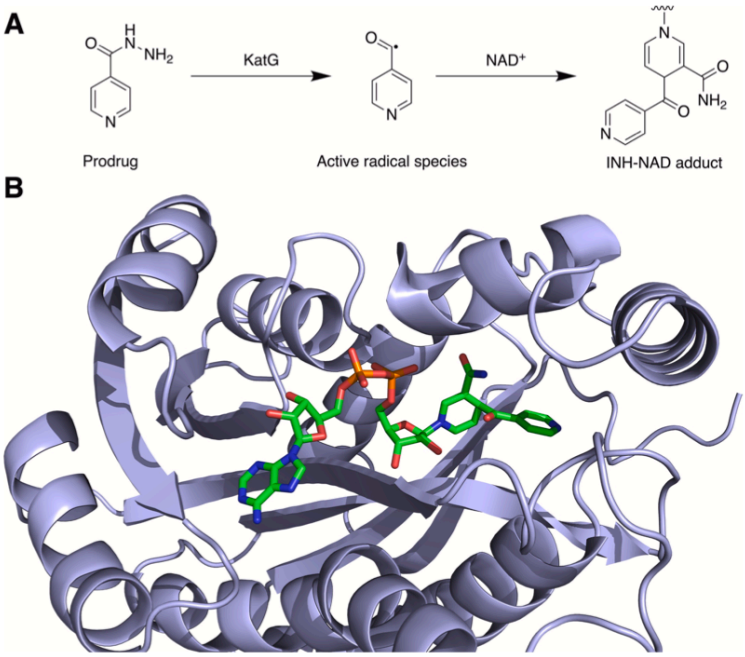

Fig. 1. (A) The structure of key anti-TB drug INH and the pathway through which it elicits its biological effects. (B) Crystal structure of the INH-NAD adduct bound to InhA showing how the adduct blocks the substrate binding cavity (PDB: 1ZID).

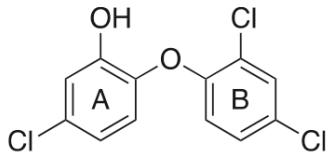

Fig. 2. The structure of TCS and the denotation of the A and B rings.

corresponding isonicotinyl radical species. Upon activation, INH forms a covalent adduct with the InhA co-factor which in turn blocks the active site, preventing substrate binding.[9,10] A single KatG point mutation, S315T, is sufficient to render INH inactive and has been implicated in up to 95% of INH resistant clinical isolates examined.[11,12] With this in mind, the development of 'direct InhA inhibitors' represents a compelling approach for the discovery of new anti-TB drugs.[13–16] Direct inhibitors refer to compounds which, unlike INH, do not require prior activation to exert their inhibitory effects. These inhibitors would circumvent the current resistance mechanisms and could be used to treat resistant infections. One such direct inhibitor is the small molecule, broad spectrum antibiotic triclosan (TCS, Fig. 2). TCS is a moderate, reversible inhibitor of InhA and has formed the basis of a number of studies, using its scaffold in the development of more potent inhibitors.[17,18]

Crystallographic studies have highlighted an unusual binding trait for the TCS:InhA complex. Two molecules of TCS are able to occupy the InhA active site (PDB: 1P45, Fig. 3), something not replicated in homologous proteins from other bacteria.[19] Inspection of the crystal structure reveals that the **TCS2** molecule lies only ~4.2 Å away from the **TCS1** moiety (Fig. 3). This suggests that through modification of the B-ring, it may be possible to obtain TCS derivatives which are capable of occupying both binding sites through a single molecule, potentially producing a more potent and selective inhibitor for InhA, that also benefits from a lower entropic cost to binding.

In this article, we report the *in silico* design, synthesis and characterization of a series of novel TCS derivatives bearing a 1,5-triazole group attached to the B-ring. These compounds were designed to occupy both of the TCS binding sites observed in the 1P45 crystal structure. Biological evaluation was performed using an isolated InhA enzyme assay and whole-cell screening against *M. bovis*.

The first step in designing TCS analogues which could anchor into both binding sites was identifying a suitable linker to connect the two fragments. It was vital that the linker did not disrupt the experimentally observed binding mode for **TCS1**, while at the same time the linker geometry had to direct the attached fragment back into the **TCS2** binding region. To this end, it was thought that a disubstituted 1,2,3-triazole ring would be an appropriate motif. It was hoped that the rigid nature of the triazole scaffold would direct any substituent group back into the **TCS2** binding site. This notion was explored using the **G**enetic **O**ptimisation for **L**igand **D**ocking (GOLD) platform.[20] Two test compounds, a 1,4 and a 1,5-triazole, were designed and both were docked into the InhA active site (PDB: 1P45). The binding poses obtained are shown below in Fig. 4.

As demonstrated in Fig. 4, when the two fragments are connected through a 1,5-triazole unit (**2**), the TCS-like binding mode is retained, and the secondary fragment occupies the same space as the **TCS2**

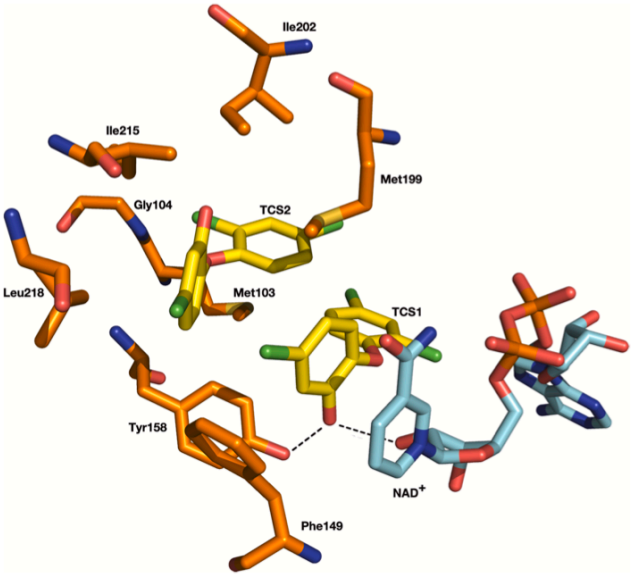

Fig. 3. X-ray structure showing two TCS molecules bound to the InhA active site. Residues are shown with orange carbons, NAD^+ is shown with teal carbons, TCS are shown with yellow carbons. H-bonds are shown by dashed-black lines. (PDB: 1P45).

moiety. The 1,4-triazole (**1**) did not generate a suitable structure and the B-ring modification resulted in a perturbation of the TCS binding mode, including loss of the key hydrogen bonding network shown in Fig. 3. This is of particular importance as this H-bonding network is conserved amongst all potent direct InhA inhibitors, with the exception of the methyl-thiazole compound class.[19,21–23]

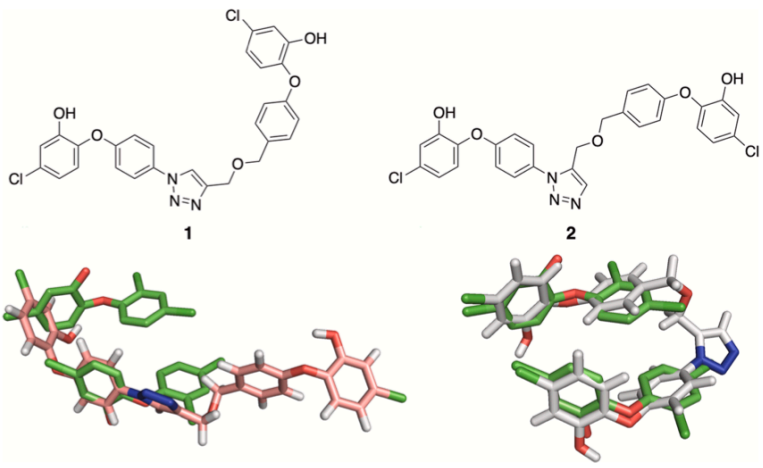

Fig. 4. The structures of two basic TCS-triazole compounds and their docking poses generated by GOLD, this shows the overlap between the designed compounds and the two TCS moieties found in the active site. (PDB: 1P45).

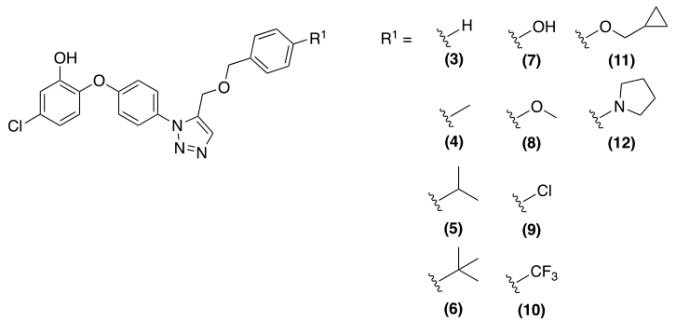

Fig. 5. Design strategy for novel TCS-based InhA inhibitors.

With this information in hand, a range of compounds bearing a single aromatic ring attached through the 1,5-triazole motif were also designed (Fig. 5). Previous studies have demonstrated that the B-ring Cl atoms are not required for potent InhA inhibition and so they were removed in an attempt to control the lipophilicity of the target compounds.[18,24]

The synthesis of biaryl azide **16** is shown in Scheme 1. The initial biaryl scaffold was assembled through an S_NAr reaction using 1-fluoro-4-nitrobenzene and 4-chloro-2-methoxyphenol, furnishing **13** in near quantitative yields. Sequential BBr_3 mediated ether demethylation and nitro reduction with Zn/NH_4Cl gave amine **15** in a good yield over two steps. Finally, functional group interconversion under the mild conditions first reported by Barral *et al.* provided the target azide **16** in a good yield.[25]

The synthesis of alkyne-bearing TCS fragment **22** is shown in Scheme 2. The biphenyl scaffold **17** was assembled in a similar fashion to the corresponding nitro compound **13**, in a good yield. Cleavage of the methyl ether was performed using AcOH and HBr at elevated temperatures, generating **18** in a modest yield. This method was used due to the instability of the benzaldehyde group that was observed when demethylation was attempted with BBr_3. The newly exposed phenol was then reprotected using MOMCl in a good yield. Benzaldehyde **19** was reduced to its corresponding benzyl alcohol using $NaBH_4$ before etherification using NaH and propargyl bromide, giving ether **21** in good yield over two steps. The phenol functionality was then unmasked using 6 M HCl to furnish the alkyne-bearing TCS fragment **22** in a near quantitative yield.

The selective formation of 1,5-triazoles can be achieved through the use of a ruthenium catalysed azide-alkyne cycloaddition (RuAAC), this methodology has seen an increasing numbers of examples in the literature over the last decade.[26,27] With **22** and **16** in hand, the 1,5-triazole motif was assembled *via* a RuACC, using $Cp^*RuCl(PPh_3)_2$ in 1,4-dioxane (Scheme 3).

The RuAAC reaction furnished **2** in an acceptable yield, following reverse phase high performance liquid chromatography (HPLC) purification. The identity of the product was confirmed as a 1,5-triazole using the NMR methods previously discussed by Creary *et al.*[28] Following the synthesis of **2**, the aforementioned truncated analogues were synthesised from the azide **16** and alkyne fragments (**23–32**, synthesis detailed in supplementary information), using the same RuAAC conditions, giving the desired 1,5-triazoles in moderate yields after HPLC (Scheme 4).

An isolated enzyme assay was used to assess the inhibitory properties of the compounds synthesised. Initial screening was performed at 50 μM with 150 nM of InhA from *M. tuberculosis* using a standard UV absorbance assay that has been widely used in the identification of

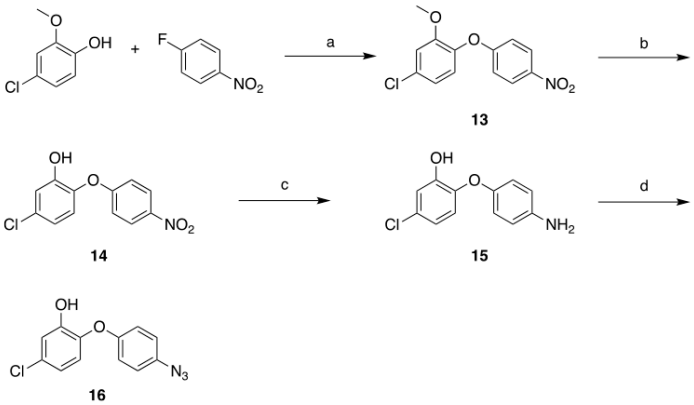

Scheme 1. Reagents and conditions: (a) K_2CO_3, DMF, 130 °C, 18 h, 95%; (b) BBr_3, CH_2Cl_2, 0 °C - > r.t., N_2, 3 h, 89%; (c) Zn, NH_4Cl, MeOH, r.t., 18 h, 75%; (d) ^tBuONO, $TMSN_3$, ACN, 0 °C - > r.t., 3 h, 80%.

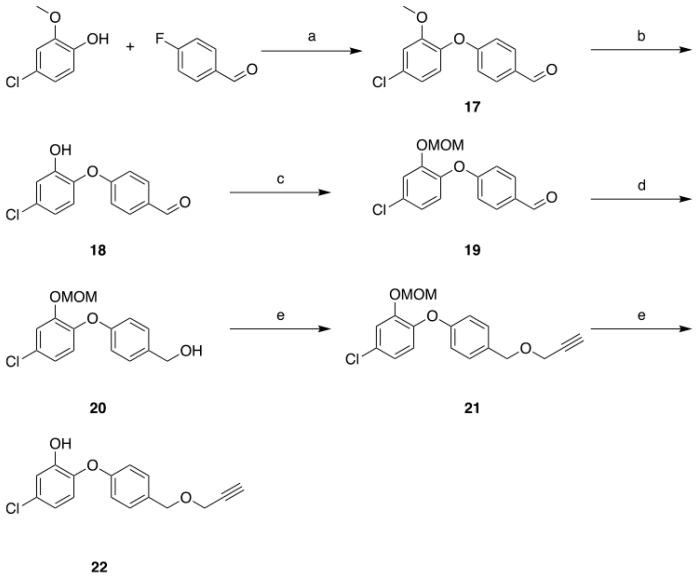

Scheme 2. Reagents and conditions: (a) K_2CO_3, DMF, 130 °C, 18 h, 92%; (b) AcOH, HBr, 140 °C, 18 h, 38%; (c) MOMCl, DIPEA, CH_2Cl_2, r.t., 18 h, 86%; (d) $NaBH_4$, MeOH, 0 °C - > r.t., 4 h, quant.; (e) NaH, propargyl bromide, DMF, 0 °C - > r.t., 18 h, 79%; (f) 6 M HCl (aq), MeOH, 70 °C, 2 h, 90%.

novel InhA inhibitors. Assays were performed using 2-*trans*-octenoyl CoA as a mimic for the enzyme's natural substrate.[29] All compounds evaluated were of above 90% purity as determined by analytical HPLC.

The inhibitory activity observed for compounds **2–12** is summarised in Table 1, these results indicate a number of the compounds tested showed moderate inhibition of InhA at 50 μM. Moving from H- > Me- > ^{i}Pr (**3**- > **5**) results in increased inhibition, however, the introduction of a ^{t}Bu (**6**) leads to a significant reduction in enzyme inhibition, suggesting that such a bulky group results in major clashes with the protein. This loosely correlates with the fitness scores, with compound **6** showing a lower fitness score than **5**. The possibility that this region is size sensitive is further supported by the fact that compounds **8**, **10** and **12**, all of which bear relatively small R groups, show moderate inhibition. The most potent compound was **2** which showed a total reduction in enzyme activity at 50 μM.

The predicted binding mode for **2** is shown in Fig. 6. This binding pose shows how the 'front' TCS fragment is able to engage the NAD^+ co-factor and Tyr158 through the key hydrogen bonding network. The 1,5-triazole architecture directs the second TCS fragment back towards the substrate binding loop, where a number of hydrophobic contacts are made. Further evaluation of **2** showed it exhibits an IC_{50} of 5.6 ± 0.8 μM (n = 3). This represents a modest improvement on TCS (IC_{50} = 9.2 ± 1.3 μM, n = 3) recorded in experiments conducted in parallel and widely reported in the literature.[30]

Whole-cell evaluation of all 12 compounds was undertaken to investigate the correlation between isolated enzyme activity and whole-cell potency. Compounds were initially assessed for growth inhibition against *Mycobacterium bovis* at a fixed concentration of 40 μM. Results are shown in Table 2.

Disappointingly, the isolated assay potency of **2** towards InhA did not correlate to whole-cell potency. This could possibly be attributed to inability to pass through the dense mycobacterial cell wall, or other factors such as efficient transport by efflux pumps.[31,32] It is possible that reintroducing the *ortho* Cl atom to the B-ring (giving a compound with a cLogP 6.61) could result in greater whole-cell potency, although the previous QSAR study by Sivaraman *et al.*[24] indicate that this chlorine is not critical, this is something that will be explored going forward. Of the 12 compounds tested, **11** showed the greatest potency, with 99% growth inhibition at 40 μM. This compound was subject to further evaluation to determine its MIC_{99} (Fig. 7).

Compound **11** displayed an MIC_{99} of 12.9 ± 5.0 μM (6.2 μg mL^{-1}, n. = 3). Clearly there is a disconnect between the activity of **11** in

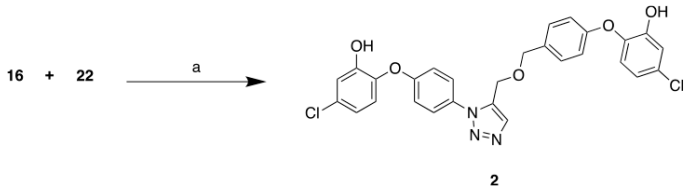

Scheme 3. Reagents and conditions: (a) Cp*RuCl(PPh_3)$_2$, 1,4-dioxane, 60 °C, N_2, 18 h, 17%.

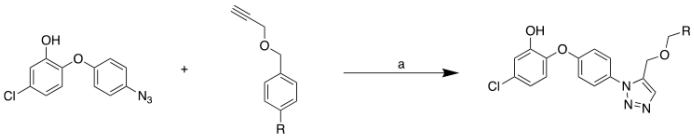

16 23 - 32 3-12

Scheme 4. Reagents and conditions: (a) Cp*RuCl(PPh_3)$_2$, 1,4-dioxane, 60 °C, N_2, 18 h, 5–33%.

Table 1
Inhibitory data for compounds tested using an isolated enzyme assay, conducted at 50 μM. GOLD fitness scores are also included for each compound. Inhibition values are an average of duplicate assays.

Compound	GOLD Fitness Score	Inhibition/%
2	87.7	100
3	65.2	12
4	73.5	38
5	77.8	72
6	74.0	6
7	69.0	13
8	76.7	44
9	73.2	0
10	75.6	47
11	80.7	11
12	83.6	42
TCS	70.8	92

Table 2
Inhibition data for all compounds tested against Mycobacterium bovis at 40 μM, results are shown as an average of 3 assays.

Compound	Inhibition/%	cLogP
2	20	5.80
3	3	5.11
4	−6	5.43
5	15	5.89
6	20	6.11
7	0	4.37
8	40	5.03
9	4	5.61
10	19	6.09
11	99	6.07
12	23	5.95
TCS	70	4.98[38]

isolated enzyme assays and its performance in the whole-cell screening tests. This suggests that **11** has other off-target sites within the bacteria which result in significant potency. At high concentrations TCS has been reported to act as a mitochondrial uncoupling, cell membrane permeator and to cause disruption to both lipid and protein biosynthesis.[18] Further work will be required to elucidate the main biological target(s) of **11**.

As previously mentioned, TCS has formed the basis for a number of SAR studies towards potent inhibitors of InhA. The most common

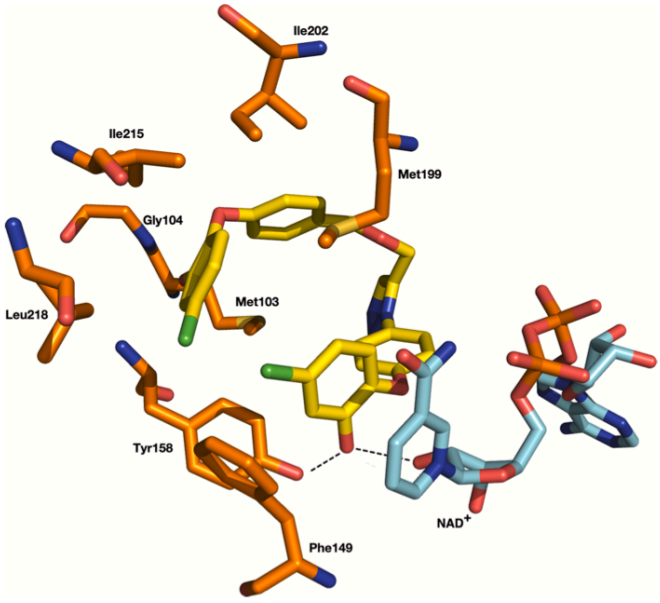

Fig. 6. Predicted binding mode for **2**. Residues are shown with orange carbons, NAD^+ is shown with teal carbons, **2** is shown with yellow carbons. H-bonds are shown by dashed-black lines. (PDB: 1P45).

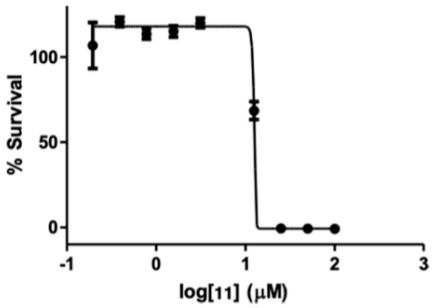

Fig. 7. MIC_{99} curve for **11**.

modification is replacement of the A-ring Cl atom with various hydrophobic groups. Comprehensive B-ring modifications remain relatively unexplored.[33–35] Two examples of previously disclosed direct InhA inhibitors are shown in Fig 8.[35,36] Compound **2** is similar in concept to **33**, recently reported by Rodriguez *et al.*, which sought to merge two TCS molecules in a macrocyclic arrangement. Compounds **33** and **2** have similar IC_{50} values, which would be expected as they both target the same binding sites.

In terms of MIC_{99} data, in this study, **11** showed significant potency in whole-cell assays with an MIC_{99} value of 12.9 μM, this value is approaching the MIC_{99} of **34** (6.6 μM). It is possible that, following the elucidation of **11**'s target, its potency could be further improved to the match or exceed the activity of **34**.

The rational *in silico* design, synthesis and characterization of a novel series of triazole-bearing TCS derivatives is reported. These compounds were designed to exploit the large volume of the InhA active site and occupy both TCS binding sites observed in the PDB: 1P45 crystal structure. Docking results suggested that these compounds would be able to occupy both of the TCS binding regions, possibly giving a direct inhibitor of Mycobacterial InhA with higher affinity and selectivity than TCS. Enzyme assays on purified *M. tuberculosis* InhA were used to evaluate the compounds synthesised, with the most potent showing an IC_{50} of 5.6 ± 0.8 μM which is similar to that of TCS. Whole-cell evaluation against *M. bovis* showed the most potent compound was **11** which displayed an MIC of 12.9 ± 5.0 μM, despite only showing 11% inhibition at 50 μM in isolated enzyme assays.

Author Contributions

T.A. synthesised all compounds, performed enzyme assays, analysed data and wrote the manuscript. M.L. expressed & purified InhA and performed enzyme assays. A.L. performed whole-cell screening assays and analysed data. L.J.A. supervised the whole-cell screening assays. N.R.T. came up with the initial drug design concept, supervised the synthetic research, contributed to writing and editing the manuscript.

Funding

T.A. is supported by the Wellcome Trust Antimicrobials and Antimicrobial Resistance (AAMR) doctoral training programme Birmingham/Nottingham [203974/Z/17/A].

M.L. is supported by a Biotechnology and Biological Sciences Research Council doctoral training studentship [Grant Number BB/M008770/1].

A.L. is supported by the Wellcome Trust Antimicrobials and Antimicrobial Resistance (AAMR) doctoral training programme Birmingham/Nottingham [215154/Z/18/Z].

Declaration of Competing Interest

The authors declare that they have no known competing financial interests or personal relationships that could have appeared to influence the work reported in this paper.

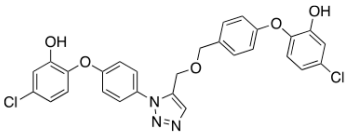

2
M.W: 550.39 g mol^{-1}
Mtb_{InhA} IC_{50} (μM): 5.6 ± 0.8
MIC_{99} (μM): >80

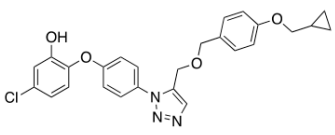

11
M.W: 477.95 g mol^{-1}
Mtb_{InhA} IC_{50} (μM): >50
MIC_{99} (μM): 12.9 ± 5.0

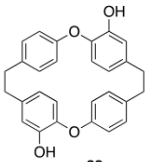

33
M.W: 424.50 g mol^{-1}
Mtb_{InhA} IC_{50} (μM): 4.7 ± 0.4
MIC_{99} (μM): 94.2*

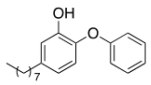

34
M.W: 289.43 g mol^{-1}
Mtb_{InhA} IC_{50} (μM): 0.005 ± 0.0003
MIC_{99} (μM): 6.6 ± 1.7

*Standard deviation not reported by authors

Fig. 8. The structures of previously disclosed TCS-based inhibitors of InhA and their biological activities.

Acknowledgements

The InhA:pET15a construct was kindly provided by Prof. Peter Tonge (SUNY, Stonybrook, NY, USA).[37]

Appendix A. Supplementary material

Experimental details are reported including: full synthetic procedures and characterization data for all compounds. NMR spectra and analytical HPLC traces of key compounds **2** and **11** are included. Methods for protein expression, purification, isolated enzyme activity assay conditions, IC_{50} curve for compound **2** and whole-cell screening methods are also included.

Supplementary data to this article can be found online at https://doi.org/10.1016/j.bmc.2020.115744.

References

1. World Health Organisation. Global Tuberculosis Report; 2019.
2. Bastos ML, Lan Z, Menzies D. An updated systematic review and meta-analysis for treatment of multidrug-resistant tuberculosis. *Eur Respir J.* 2017;49:1600803.
3. Günther G. Multidrug-resistant and extensively drug-resistant tuberculosis: a review of current concepts and future challenges. *Clin Med (Lond).* 2014;14:279–285.
4. Pontali E, D'Ambrosio L, Centis R, Sotgiu G, Migliori GB. Multidrug-resistant tuberculosis and beyond: an updated analysis of the current evidence on bedaquiline. *Eur Respir J.* 2017;49:1700146.
5. Deoghare S. Bedaquiline: a new drug approved for treatment of multidrug-resistant tuberculosis. *Indian J. Pharmacol.* 2013;45:536–537.
6. Xavier A, Lakshmanan M. Delamanid: A new armor in combating drug-resistant tuberculosis. *J Pharmacol Pharmacother.* 2014;5:222–224.
7. Zhai W, Wu F, Zhang Y, Fu Y, Liu Z. The immune escape mechanisms of mycobacterium tuberculosis. *Int J Mol Sci.* 2019;20:340.
8. Marrakchi H, Laneelle G, Quemard AK. InhA, a target of the antituberculous drug isoniazid, is involved in a mycobacterial fatty acid elongation system, FAS-II. *Microbiology.* 2000;146:289–296.
9. Rozwarski DA, Grant GA, Barton DH, Jacobs Jr WR, Sacchettini JC. Modification of the NADH of the isoniazid target (InhA) from Mycobacterium tuberculosis. *Science.* 1998;279:98–102.
10. Timmins GS, Deretic V. Mechanisms of action of isoniazid. *Mol Microbiol.* 2006;62:1220–1227.
11. Zhang Y, Heym B, Allen B, Young D, Cole S. The catalase—peroxidase gene and isoniazid resistance of Mycobacterium tuberculosis. *Nature.* 1992;358:591–593.
12. Zhao X, Yu H, Yu S, Wang F, Sacchettini JC, Magliozzo RS. Hydrogen peroxide-mediated isoniazid activation catalyzed by mycobacterium tuberculosis catalase–-peroxidase (KatG) and Its S315T Mutant. *Biochemistry.* 2006;45:4131–4140.
13. Manjunatha UH, Rao SP, Kondreddi RR, et al. Direct inhibitors of InhA are active against Mycobacterium tuberculosis. *Sci Transl Med.* 2015;7:269ra3.
14. Martínez-Hoyos M, Perez-Herran E, Gulten G, et al. Antitubercular drugs for an old target: GSK693 as a promising InhA direct inhibitor. *EBioMedicine.* 2016;8:291–301.
15. Rozman K, Sosic I, Fernandez R, et al. A new 'golden age' for the antitubercular target InhA. *Drug Discov Today.* 2017;22:492–502.
16. Chetty S, Ramesh M, Singh-Pillay A, Soliman ME. Recent advancements in the development of anti-tuberculosis drugs. *Bioorg Med Chem Lett.* 2017;27:370–386.
17. Parikh SL, Xiao G, Tonge PJ. Inhibition of InhA, the Enoyl Reductase from Mycobacterium tuberculosis, by Triclosan and Isoniazid. *Biochemistry.* 2000;39:7645–7650.
18. Vosatka R, Kratky M, Vinsova J. Triclosan and its derivatives as antimycobacterial active agents. *Eur J Pharm Sci.* 2018;114:318–331.
19. Kuo MR, Morbidoni HR, Alland D, et al. Targeting tuberculosis and malaria through inhibition of Enoyl reductase: compound activity and structural data. *J Biol Chem.* 2003;278:20851–20859.
20. Jones G, Willett P, Glen RC, Leach AR, Taylor R. Development and validation of a genetic algorithm for flexible docking. *J Mol Biol.* 1997;267:727–748.
21. Shirude PS, Madhavapeddi P, Naik M, et al. Methyl-thiazoles: a novel mode of inhibition with the potential to develop novel inhibitors targeting InhA in Mycobacterium tuberculosis. *J Med Chem.* 2013;56:8533–8542.
22. Ng PS, Manjunatha UH, Rao SPS, et al. Structure activity relationships of 4-hydroxy-2-pyridones: A novel class of antituberculosis agents. *Eur J Med Chem.* 2015;106:144–156.
23. Encinas L, O'Keefe H, Neu M, et al. Encoded library technology as a source of hits for the discovery and lead optimization of a potent and selective class of bactericidal direct inhibitors of mycobacterium tuberculosis InhA. *J Med Chem.* 2014;57:1276–1288.
24. Sivaraman S, Sullivan TJ, Johnson F, et al. Inhibition of the bacterial enoyl reductase FabI by triclosan: a structure-reactivity analysis of FabI inhibition by triclosan analogues. *J Med Chem.* 2004;47:509–518.
25. Barral K, Moorhouse AD, Moses JE. Efficient conversion of aromatic amines into azides: a one-pot synthesis of triazole linkages. *Org Lett.* 2007;9:1809–1811.
26. Boren BC, Narayan S, Rasmussen LK, et al. Ruthenium-catalyzed azide–alkyne cycloaddition: scope and mechanism. *J Am Chem Soc.* 2008;130:8923–8930.
27. Johansson JR, Beke-Somfai T, Said Stålsmeden A, Kann N. Ruthenium-catalyzed azide alkyne cycloaddition reaction: scope, mechanism, and applications. *Chem Rev.* 2016;116:14726–14768.
28. Creary X, Anderson A, Brophy C, Crowell F, Funk Z. Method for assigning structure of 1,2,3-triazoles. *J Org Chem.* 2012;77:8756–8761.
29. He X, Alian A, Stroud R, Ortiz de Montellano PR. Pyrrolidine carboxamides as a novel class of inhibitors of enoyl acyl carrier protein reductase from Mycobacterium tuberculosis. *J Med Chem.* 2006;49:6308–6323.
30. Slepikas L, Chiriano G, Perozzo R, et al. In silico driven design and synthesis of rhodanine derivatives as novel antibacterials targeting the enoyl reductase InhA. *J Med Chem.* 2016;59:10917–10928.
31. Szumowski JD, Adams KN, Edelstein PH, Ramakrishnan L. Antimicrobial efflux pumps and Mycobacterium tuberculosis drug tolerance: evolutionary considerations. *Curr Top Microbiol Immunol.* 2013;374:81–108.
32. Balganesh M, Dinesh N, Sharma S, Kuruppath S, Nair AV, Sharma U. Efflux pumps of mycobacterium tuberculosis play a significant role in antituberculosis activity of potential drug candidates. *Antimicrob Agents Chemother.* 2012;56:2643–2651.
33. He X, Alian A, Ortiz de Montellano PR. Inhibition of the Mycobacterium tuberculosis enoyl acyl carrier protein reductase InhA by arylamides. *Bioorg Med Chem.* 2007;15:6649–6658.
34. Stec J, Vilchèze C, Lun S, et al. Biological evaluation of potent triclosan-derived inhibitors of the enoyl-acyl carrier protein reductase InhA in drug-sensitive and drug-resistant strains of mycobacterium tuberculosis. *ChemMedChem.* 2014;9:2528–2537.
35. Sullivan TJ, Truglio JJ, Boyne ME, et al. High affinity InhA inhibitors with activity against drug-resistant strains of Mycobacterium tuberculosis. *ACS Chem Biol.* 2006;1:43–53.
36. Rodriguez F, Saffon N, Sammartino JC, Degiacomi G, Pasca MR, Lherbet C. First triclosan-based macrocyclic inhibitors of InhA enzyme. *Bioorg Chem.* 2020;95:103498.
37. Parikh S, Moynihan DP, Xiao G, Tonge PJ. Roles of tyrosine 158 and lysine 165 in the catalytic mechanism of InhA, the enoyl-ACP reductase from Mycobacterium tuberculosis. *Biochemistry.* 1999;38:13623–13634.
38. Han J, Cao Z, Gao W. Remarkable sorption properties of polyamide 12 microspheres for a broad-spectrum antibacterial (triclosan) in water. *J Mater Chem A.* 2013;1(16):4941–4944.